A BIFURCATION ANALYSIS OF A MULTI COMPARTMENT PLANKTON-ZOOPLANKTON-NUTRIENT INTERACTION

A thesis
Submitted in partial fulfilment of
the requirements for the Degree
of
Doctor of Philosophy
in
Computational and Applied Mathematics
in the
University of Canterbury
by

NORHAYATI HAMZAH

University of Canterbury

2004

Acknowledgements

First of all, I would like to convey my sincere thanks to Pehin Abu Bakar Apong, former Vice-chancellor of Universiti Brunei Darussalam, for giving me the opportunity to undertake PHD studies.

My sincere gratitude also goes to our Prime Minister of Education, YB Pehin Orang Kaya Laila Wijaya Dato Seri Setia Awg Hj Abd Aziz B Begawan Pehin Udana Khatib Dato Seri Padula Awang Hj Omar, who has supported me through our changeable and inconsistent scholarship system. Thank you for your understanding and trust.

Next I must mention my father, who always gave me the encouragement to pursue my study. I would have chased my dream and love for Art.

I acknowledge my supervisor at University of Canterbury Professor G.C. Wake, who has taught me Mathematics and Research since 1995, for his continual helpful comments and personal understanding and also my thanks to his wife Elizabeth, for her advice and encouragement.

My thanks to Dr Alex Ross, my second supervisor at the New Zealand National Institute of Water and Atmosphere (NIWA) who first taught me to explore the program XPP and AUTO. Thank you also for your understanding, support and personal advices.

Special and uncountable thanks to Professor Roger Hosking, who helped me with editing and by making things easier for me. Thank you very much for your comment and suggestions. You are the best colleague and teacher.

Thanks also go to two computer geniuses, the first is Mohd Budiman Hamzah, for helping put together the graphs from postscript file to editable format and who has taught me lots of "cool" tools available in Microsoft PowerPoint. And the second is Abdul

Ghani,Hj Naim, who has always been available to help me reinstall the major programs XPP and AUTO, whenever the hard disk was spoiled.

Dr Peter Tritscher, who has taught me the computer software MATHEMATICA.

Dr. Hillary Ockendon of OCIAM of University of Oxford, for her suggestions and giving the important tools to get the mathematics going.

Lastly, to God for getting me back on my feet after years of illness, for the happenings and helped me get through all barriers to finally complete this work. I love you

Preface

This thesis concentrates on understanding the long term behaviour of a multi-compartment phytoplankton-zooplankton-nutrient interaction. A *variable-yield* model is considered, in which the rate of carbon uptake by phytoplankton necessary for its growth is governed by cell quota i.e. the ratio of external nutrient (nitrogen) and the internal nutrient (carbon). The internal and external nutrient of the phytoplankton are governed by separate equations. The work addresses the question 'How complex should a model be?', besides attempting to understand analytical and qualitative model behaviour. The simplest model considered consists of *four* ordinary differential equations relating to one pool or compartment, and is then extended to *eight* ordinary differential equations: (four equations for each pool) of the two compartments, and finally to *twelve* ordinary differential equations: (four equations in each of the three compartments).

Chapter 1 introduces the basic mathematical model, and critiques its formulation based on various ecological studies on phytoplankton-zooplankton-nutrient interactions. Local stability analysis necessary to investigate stability of our model is discussed, together with an introductory explanation of bifurcation theory, which is used by modelers to tune and adjust the dynamical system. Thus by altering system parameters the behaviour of the system may change gradually or even abruptly. Abrupt changes occur at bifurcating values of the parameter. Chapter 1 also includes a manual for running the software XPP and also AUTO, sophisticated software to study bifurcation and hence important model behaviour.

Chapter 2 provides a complete analysis of the behaviour of the one compartment model. It includes local stability analysis for all the solutions and a global analysis for the null solution. A detailed study of this simplest model includes a complete profile of bifurcation diagrams executed by the software AUTO, with information on the behaviour of the steady state and periodic solutions for comparison with and extension of the analytical results.

Chapter 3 presents analytical as well as numerical studies of the two-compartment model. Two cases are considered, one with an equal growth parameter of the phytoplankton and the other where the growth parameter in each compartment is different. Stability analysis for the first case is examined by both local stability analysis and bifurcation analysis, but other case can only be done numerically via a complete profile of bifurcation diagrams using the software AUTO.

Chapter 4 presents stability analysis for the three compartment model via bifurcation diagrams generated numerically using AUTO. This chapter considers 3 cases: the equal growth parameter of phytoplankton, different growth parameters of phytoplankton and both different growth parameters and different diffusion parameters.

Chapter 5 presents the various conclusions drawn from all of three models considered.

Table of Contents

Chapter 1

Mathematical models and solutions methodology

Chapter 1: The Models and solution methodology

1.0 Introduction

The main objective of this first chapter is to introduce the mathematical modeling, beginning with a survey of related previous work. The model adopted in this thesis is based on previously studies undertaken by a phytoplankton ecologist and appropriate assumptions. Some of the procedures that are needed to run the useful software, notably XPP and AUTO are also discussed. These programs can be obtained and downloaded free from their respective websides [51, 52]. The numerical software efficiently execute bifurcations diagrams that are needed to confirm stability in the models adopted, and in particular their qualitative behaviour. The software support the analytical results obtained, and identify certain facets that are not obtained analytically.

1.1 What is Plankton?

Plankton are tiny open-water plants, animals or bacteria. The name, like the word *planet*, is derived from a Greek root that means, "wanderer." These organisms range in size from microscopic bacteria and plants to larger animals, such as jellyfish. Plankton generally have limited or no swimming ability and are transported through the water by currents and tides. Plankton communities serve as a base for the food chain that supports the commercial fisheries.

Plankton can be divided into three major size classes:

- **phytoplankton**–microscopic plants and bacteria
- **zooplankton**–microscopic animals
- **macrozooplankton**–larger fish eggs and larvae and pelagic invertebrates

Plankton is often used as indicators of environmental and aquatic health because of their high sensitivity to environmental change and short life span. Phytoplankton is useful indicators of high nutrient conditions due to their propensity to multiply rapidly in the right conditions. Zooplankton is useful indicators of future fisheries health because they are a food source for organisms at higher trophic levels, such as finfish.

1.1.1 Phytoplankton

In shallow coastal areas marine plants may include large algae and flowering plants such as sea grasses, but in the open sea primary productivity is carried out by microscopic plants (golden brown algae, green algae and blue green algae), coccolithophores, diatoms and dinoflagellates, collectively called phytoplankton. The phytoplankton, the largest individuals of which are less than 1mm in length, float and drift in the photic zone, the sunlit surface layers of the sea. Here photosynthesis involves the taking up of carbon dioxide and nutrients, particularly phosphates and nitrates. Under favourable conditions, phytoplankton can quickly multiply by cell division to form dense 'blooms'. In some areas, and at particular times of the year, some dinoflagellates multiply to such densities that they change the colour of the sea, a phenomenum known as 'red tides', and a few species produce toxins which are passed on to humans eating plankivorous molluscs. The

sea covers approximately 71 percent of the planet's surface, and the total biomass of phytoplankton is perhaps five times larger than that of all terrestrial vegetation. However, the distribution of nutrients across the world's seas, and therefore the distribution of marine plants, is far from even [28].

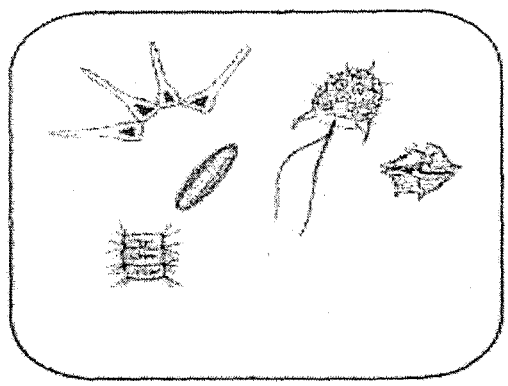

Figure 1.1: Phytoplankton species

1.1.2 Zooplankton

The major consumers of phytoplankton are the zooplankton, small animals which drift in the sea. Zooplankton are planktonic animals that range in size from microscopic rotifers to macroscopic jellyfish. Some species, particularly copepods, are the most abundant animals in the world, and remain planktonic for their entire lives as the holoplankton. The larvae of most marine invertebrates and fish also form part of the plankton, if only temporarily, as the meroplankton. Zooplankton are not capable of moving against surface currents, many species are capable of making vertical migrations in the water column. Zooplankton organisms move up into the surface areas of the sea during the night to graze on the phytoplankton. During the hours of the daylight, they move below the photic

zone, allowing the phytoplankton to photosynthesis and increase their numbers by cell division in the absence of grazing.

Their distribution is governed by salinity, temperature and food availability. The smallest zooplankton can be characterized as recyclers of water-column nutrients and often are closely tied to measures of nutrient enrichment. Larger zooplankton are important food for forage fish species and larval stages of all fish. They also link the primary producers (phytoplankton) with larger or higher trophic-level organisms. The zooplankton community is composed of both primary consumers, which eat phytoplankton, and secondary consumers, which feed on other zooplankton.

Zooplankton can be classified into three size classes:

- **Microzooplankton**–(protozoans and rotifers) are usually less than 200 microcrons in size.
- **Mesozooplankton**–(including copepods and invertebrate larvae) are between 200 microns and 2 millimeters in size.
- **Macrozooplankton**–(including amphipods, shrimp, fish larvae and gelatinous zooplankton or jelly fish) are greater than 2 millimeters in size.

Zooplankton, like phytoplankton, make excellent indicators of environmental conditions, because they are sensitive to changes in water quality. They respond to low dissolved oxygen, high nutrient levels, toxic contaminants, poor food quality or abundance and predation. A condition of quality of the conditions in a river can be derived by looking at zooplankton indicators such as their biomass, abundance and species diversity [28].

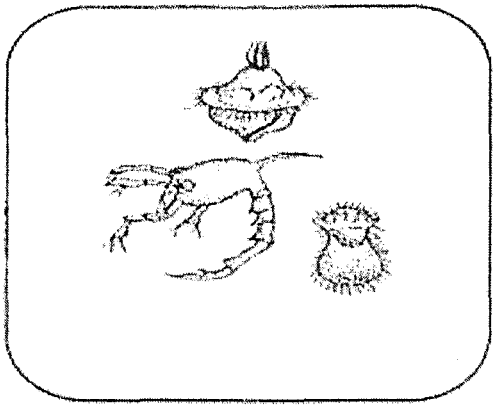

Figure 1.2: Zooplankton species

1.1.3 The planktonic food chains

The connection between trophic levels- algae, herbivores and carnivores- is referred to as a food chain, in which material or energy accumulated at each step by either plants and animals is transferred as food to the next trophic level. The first or lowest trophic level consists of plant material, and the highest trophic level consists of high-levels carnivores [28].

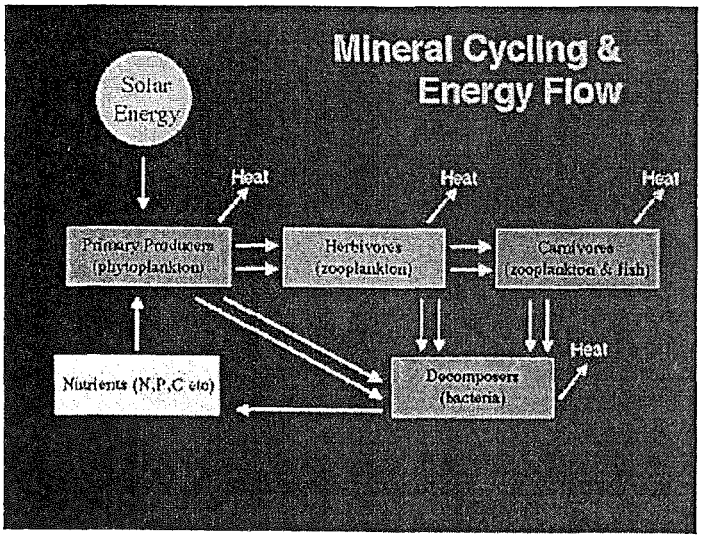

Figure 1.3: The planktonic food chain

1.2 Constant yield versus variable yield [20]

The growth of a microorganism in a chemostat was earlier studied by Monod [34], when he assumed that the rate of organism is limited by the availability of a single nutrient. He assumed that the specific growth rate of the organisms is directly proportional to the external nutrient level. This is termed **constant yield** model.

Monod [34] described the microbial populations growing in continuous cultures to be

$$\frac{dx}{xdt} = \mu - D$$

$$\frac{dN}{dt} = D(N^0 - N) - \left(\frac{x\mu}{Y}\right) \tag{1.1}$$

where x is the population density and N is the resource availability. μ is a function of N and is the per capita reproduction rate depend on quota rather than resource availability, D is the turnover rate of the habitat representing both the density-independent loss rate for the population and the rate at which unconsumed resource enters and leaves the habitat, N^0 is the concentration at which unconsumed resource enters the habitat, N is the abiotic resource i.e. one that does not itself reproduce and Y is the yield coefficient.

The Droop model also known as the **variable yield** model subdivided the nutrient into internal and external cellular pool. Only the internal nutrient is available for cell growth and metabolism. Passage of nutrient from outside to inside the cells introduces inevitable time delays which is absent in the **constant yield** model. In other words, we can described the **variable yield** model to considered both the "functional" and the "numerical" responses. The "functional" response describes the dependence of the per

capita rate of resource consumption on resource availability; while the "numerical" response describes the dependence of the per capita rate of the reproduction on the amount of resource consumed. In contrast with the **constant yield** model, the variable yield model uses the functional as well as the numerical responses to explicitly describe the acquisition of scarce resources and their conversion to reproduction, whereas the **constant yield** model does not attempt to describe separately the processes of resource consumption and reproduction, and uses a single function to describe both.

The variable yield model can be described as follows:

$$\frac{dx}{xdt} = \mu' - D$$

$$\frac{dN}{dt} = D(N^0 - N) - x\rho \qquad \textbf{(1.2)}$$

$$\frac{dQ}{dt} = \rho - \mu' Q$$

where ρ is the rate of resource consumption assumed to be functions of N. By defining $\mu(N) = \rho(N)/Q$, the **variable yield** equation **(1.2)** becomes the **constant yield** equation **(1.1)**. The yield coefficient is then defined as $Y = 1/Q$.

1.3 TYPE 1, TYPE 2 and TYPE 3 FUNCTIONS

There are three types of function which is used to describe most ecological models depending on the data fitting and requirements. In this section, examples from Grover [20] shall be discussed. The first one is the **TYPE I** function which is also known as the **Holling TYPE I** functional response. With respect to **section 1.2**, this type of functions

corresponds to the constant yield model which is linear. The following is the **TYPE I** relations:

i) the **TYPE I** rate of resource consumption $\rho = aN$ such that $N \le N^*_{\max}$

ii) the **TYPE I** population growth can be written as $\mu = \dfrac{\mu'_{\max} N}{\left(\dfrac{\mu'_{\max} Q_{\min}}{a}\right) + N}$ such that $N \le N^*_{\max}$

iii) the **TYPE I** resource consumption given by $N^* = \dfrac{D\mu'_{\max} Q_{\min}}{a(\mu'_{\max} - D)}$

iv) other relations of **TYPE I** is $N^*_{\max} = \dfrac{\mu'_{\max}(Q_{\max} - Q_{\min})}{a}$ such that $\rho_{\max} = aN^*_{\max}$.

The **TYPE II** is also known as **the Michelis Menten** saturating function or the **Holling TYPE II** functional response. The saturating effect have the property such that the rate of growth increases with nutrient availability only to some limiting value $K_{\max}$. The following is the **TYPE II** relations:

i) the **TYPE II** rate of resource consumption $\rho = \dfrac{\rho_{\max} N}{K_\rho + N}$.

ii) the **TYPE II** population growth can be written as $\mu = \dfrac{\mu_{\max} N}{K_\mu + N}$.

iii) the **TYPE II** resource consumption given by $N^* = \dfrac{DK_\mu}{\mu_{\max} - D}$.

iv) other relations of **TYPE II** is $K_\mu = K_\rho \left(\dfrac{Q_{\max}}{Q_{\min}}\right)$ such that $\mu_{\max} = \dfrac{\rho_{\max}}{Q_{\max}}$.

The **TYPE III** is also known as the **sigmoidal** or the **Holling Type III** functional response. It has the rectangular hyperbola function such that for the linear relation $\rho = aN$, a has a relations $a = \dfrac{bN^2}{1+cN+b\tau N^2}$. Thus the following is the **TYPE III** relations:

i) the **TYPE III** rate of resource consumption $\rho = \dfrac{bN^2}{1+cN+b\tau N^2}$.

iv) the **TYPE III** population growth can be written as $\mu = \dfrac{\left(\dfrac{b}{Q_{\min}}\right)N^2}{1+cN+b\tau\left(\dfrac{Q_{\max}}{Q_{\min}}\right)N^2}$.

v) the **TYPE III** resource consumption given by

$$N^* = \frac{cD + \sqrt{c^2D^2 + \dfrac{4bD(\mu_{\max} - D)}{\mu_{\max}Q_{\min}}}}{2b(\mu_{\max} - D)/\mu_{\max}Q_{\min}}.$$

iv) other relations of **TYPE III** is $\rho_{\max} = \dfrac{1}{\tau}$ such that $\mu_{\max} = \dfrac{1}{\tau Q_{\max}}$.

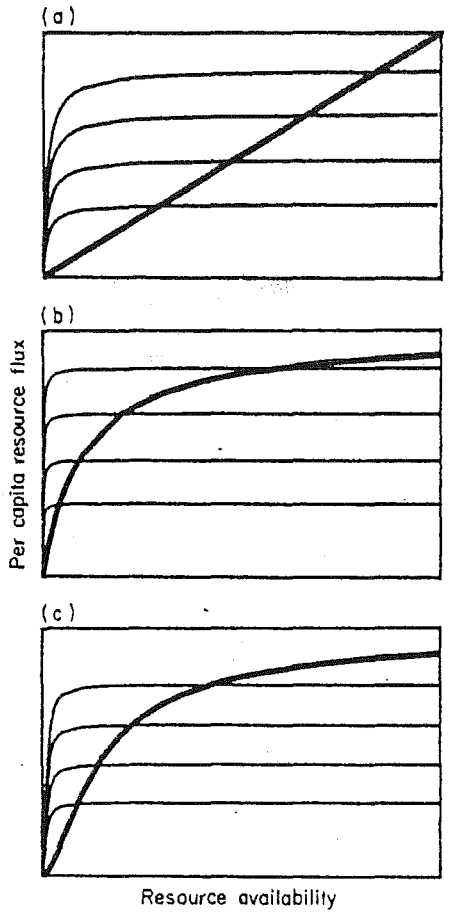

Figure 1.4: The graph showing the resource fluxes predicted by variable yield based on Droop's equation and constant yield models. The heavy lines shows $\rho(N)$, the resource flux determined by the organism's functional response, which is combined with the Droop's equation to give a variable yield model. The light lines show the resources fluxes predicted by constant yield models a) shows the linear, or Holling TYPE I functional response, b) Michelis Menten saturating function or the Holling TYPE II functional response and c) sigmoidal functional response or the Holling TYPE III functional response [20].

1.4 The biological background of various plankton models

A simple early diffusion model to describe the dynamics of phytoplankton was constructed by Riley [40], mathematical models of increasing complexity have been constructed ever since. The interaction between phytoplankton and herbivore was considered by Steele [44], Steele and Frost [45] and Steele and Henderson [46, 47], while Evans and Parlow [16], Frost [17], Taylor [48] and Wroblewski et.al. [50] modelled nutrient concentrations, in addition to the rate of growth of the plankton-herbivore. Dynamical systems which describe the dynamics of nutrient, phytoplankton and zooplankton species are often termed *NPZ* models. All of the above authors have assumed that the consumption rate of a resource is a function of resource availability with the yield of the organism constantly proportional to the amount they consume, and are referred to as *constant yield* models (Monod [34]).

However, there is abundant evidence that the internal concentration of limiting nutrients varies significantly in organisms of many species, which implies that internal nutrient levels must be considered as variables, if nutrient uptake and growth by organisms are to be properly described. Droop [9] remarks:

> A case in point in the algal field was the luxury uptake of phosphorus, first observed by Ketchum [26] and later studied in detail with the marine diatom pheodactylum tricirnutum by Kuenzler and Ketchum [29]. When cells of this algal were placed in fresh medium, virtually all the phosphorus was observed to be taken up by the cells from the new medium before even the first cell division had taken place. Thereafter it was apportioned among the progeny of the

> subsequent cell divisions, which continued until cell phosphorus had dropped sufficiently to arrest cell division. It is apparent that the cell division during the life of the culture must have occurred without direct reference to the external concentration of the substrate.

Many other researchers have considered this aspect, and attempted to model internal nutrient storage of organisms. They include Caperon and Meyer [4, 5], Collins [6], Droop [9], Fuhs [18], Lehman et al. [31] and Rhee [39] among others. Chemostat studies of phytoplankton have indicated that the specific growth rate depends on internal rather than external nutrient levels by Collins [6].

DeAngelis [6] considered the inclusion of internal nutrient concentration as a variable, which was shown to not alter the fundamental nature of the equilibrium. The Monod growth function, involving the limiting nutrient and a single species of organism, was adopted. Variable-yield models are a suitable and reasonable approach to realistically describe the situation.

In the following section, various classical and variable-yield plankton models previously used are discussed, and dynamical differences are summarised.

1.4.1 The classical *NPZ* model

An example of an *NPZ* model, in which the nutrient component has been incorporated together with plankton interaction was adopted by Wroblewski et al. [50]. A two trophic-level food chain model for the plankton densities in different ocean layers was

considered. The stability of this model was subsequently analysed by Busenberg et al. [2], who assumed perfect mixing of the nutrient.

The three interacting components are the phytoplankton (P), the herbivorous zooplankton (Z) and the dissolved nutrient (N). The parameters involved are:

a maximal nutrient uptake rate of the phytoplankton;

k Michelis Menten half saturation constant;

r phytoplankton mortality rate;

b maximal zooplankton ingestion rate;

c per capita saturation exponent;

δ zooplankton nutrient conversion rate;

ε zooplankton death rate; and

δ_1 zooplankton nutrient loss rate.

The following assumptions were made.

i) Nitrogen is assumed to be the primary nutrient responsible for the limiting phytoplankton reproduction.

ii) The total nitrogen level of this trophic is assumed to be constant for the duration of the study, with perfect mixing (i.e. no exchange of nutrient with adjacent layers): thus

$$P + Z + N = N_T = \text{constant},$$

where N_T is some parameter.

iii) There is no net nutrient loss due to death or nutrient conversion. In other words, the phytoplankton is removed through zooplankton predation eventually either adds to the zooplankton biomass or to the available nitrate: i.e.

$$b = \delta + \delta_1$$

(This assumption is only valid during periods when phytoplankton loss due to cell sinking is negligible).

iv) The growth function is chosen to be the Michelis-Menten i.e. $a\left(\frac{N}{k+N}\right)$ and the death functions is chosen to be $b\left(1-e^{-cP}\right)$. These functions are chosen based on data fitting and supported by physiological evidence.

Thus the classical NPZ model represented by the system of ordinary differential equations

$$\begin{aligned}
\frac{dP}{dt} &= aP\left(\frac{N}{k+N}\right) - b\left(1-e^{-cP}\right)Z - rP \\
\frac{dZ}{dt} &= Z\left(\delta\left(1-e^{-cP}\right)-\varepsilon\right) \\
\frac{dN}{dt} &= -aP\left(\frac{N}{k+N}\right) + \delta_1\left(1-e^{-cP}\right)Z + rP + \varepsilon Z
\end{aligned} \tag{1.3}$$

There are three thresholds found-viz. $R_0 = \frac{aN_T}{r(k+N_T)}$, $R_1 = \frac{\delta(1-e^{-c\bar{P}})}{\varepsilon}$ and $\frac{1}{R_2} = bcZ^*(1-\frac{\varepsilon}{\delta}) + \frac{ak(k+N_T-Z^*)}{(k+N_T-Z^*-P^*)^2} \Big/ (a-r)$. The following table summarises the stability of the *NPZ* model:

Thresholds R_0, R_1, R_2	$(0,0,N_T)$	Steady states $(\bar{P},0,N_T-\bar{P})$	(P^*,Z^*,N^*)	Periodic attractors
$R_0<1$	Stable and global attaractors	Not feasible	Not feasible	Not feasible
$R_0>1$, $R_1<1$	Unstable	Stable and global attaractor	Not feasible	Not feasible
$R_0>1$, $R_1>1$, $R_2<1$	Unstable	Unstable	Stable	-
$R_0>1$, $R_1>1$, $R_2>1$	Unstable	Unstable	Unstable	Attracts solutions

Table 1.1: Threshold and stability of steady states in the Wroblewski et al. [49] model, as discussed by Busenberg et al [2].

If $R_0<1$, on average there would be, less than one offspring during the lifetime of each phytoplankton, and the nutrient level would be insufficient to support a stable phytoplankton population. On the other hand, if $R_0>1$ the average reproduction of each phytoplankton is more than one and a stable population can be established. A zooplankton population can therefore coexist with a phytoplankton population if and only if $R_1>1$ i.e. when the expected lifetime productivity of each zooplankton is greater than one. The parameter R_2 reflects certain aspects of the "enrichment paradox" [27]. When

$R_2<1$, the phytoplankton population settles to a coexisting steady state level P^* if any zooplankton is present, and to the level $\bar{P}$ if not. Since $P^* < \bar{P}$, the phytoplankton population level decreases to P^* when N_T increases, to the point where $R_1>1$, from their level at $\bar{P}$ when $R_1<1$. Thus enriching the environment decreases the steady state phytoplankton population level. A further enrichment of the environment, which drives R_2 beyond its threshold level 1, destabilizes the coexistence steady state (P^*,Z^*,N^*). Thus enrichment in this case has a destabilizing effect, leading to a periodic oscillatory coexistence state. Busenberg et al. [2] have shown that the coexisting equilibrium is locally asymptotically stable (and hence attracts all nearby states), but have not proven it is a global attractor. However, there are no periodic solutions, and there is no Hopf bifurcation from $R_2=1$ extending into $R_2<1$. Another gap in **Table 1.1** is $R_0>1$, $R_1>1$, $R_2>1$, where it has not been demonstrated that there can be no more than one periodic solution. However, it has been shown that every state which starts off with some zooplankton and phytoplankton present must tend to a periodic oscillatory coexisting state.

1.4.2 Droop model

The Droop [9] model, also called the *variable-yield* model, effectively decouples the specific growth rate of the organism from external nutrient concentration by introducing an intercellular store of nutrient, providing a good fit for algal growth. Droop relates specific growth rate in steady state systems to nutrient status with more than one nutrient, based on 3 postulates: viz. 1) the uptake depends on the external substrate; 2) growth

depends on the internal substrate concentration, and 3) in a steady state system, the specific rate of uptake (in the absence of significance excretion) is necessarily the product of the specific growth rate and the internal substrate concentration.

Let N be the concentration of limiting nutrient, x the total biomass concentration of the organism, and Q the cell quota i.e. the concentration of the limiting nutrient in the internal pool. Thus, the system of differential equations in the Droop model is:

$$\begin{aligned}
\frac{dN}{dt} &= D[N^0 - N] - \rho x \frac{N}{N+k} \\
\frac{dx}{dt} &= \mu x\left(1 - \frac{Q_{\min}}{Q}\right) - Dx \qquad (1.4) \\
\frac{dQ}{dt} &= \rho \frac{N}{N+k} - \mu[Q - Q_{\min}].
\end{aligned}$$

Here, N^0 is the concentration of influent nutrient, D is dilution rate, ρ the maximum uptake rate, $Q_{\min}$ the minimum cell quota, μ the maximum growth rate, and k the associated half saturation constant.

The biological significance of the terms in (**1.4**) may be understood as follows:

i) $D[N^0 - N]$ is the difference between the rate of ambient nutrient concentration entering the chemostat chamber and the rate of ambient nutrient concentration leaving the chamber;

ii) $\rho P \frac{N}{N+k}$ is the rate of loss of S due to uptake by the organism; and

iii) $\mu P\left(1 - \frac{Q_{\min}}{Q}\right)$ is the growth rate of the total biomass concentration.

Note that when Q drops below Q_{min}, there is insufficient internal nutrient to sustain the organism.

Some of the limitations of the Droop model are:

i) the growth and cell division are not distinguished in the model;

ii) the variable Q must describe the typically many complex biochemical pathways for the nutrient in the cell;

iii) the model makes no provision for excretion or sequestration of the limiting nutrient by the cell; and

iv) the growth and uptake functions are somewhat arbitrary.

According to Lange and Oryarzun [30], who explore the global stability using a comparison theorem (De Bruijn [8]), the Droop model tends to a single global equilibrium. Depending on the particular combination of underlying parameters, this global equilibrium represents either extinction for the chemostat organism or long term survival at a definite fixed level. There is no limit cycle or chaotic behaviour, and the approach to global equilibrium involves no systematic oscillations, since the eigenvalues of the variational matrix at the equilibrium are all negative and real.

1.4.3 Other variable-yield plankton models

Several nutrient-phytoplankton-zooplankton models with internal nutrient storage by phytoplankton were derived and analysed by Jang [24], who showed there is a threshold beyond which the system is uniformly persistent. The so-called self-shading effect of the

phytoplankton in the variable-yield models is also considered. In this thesis, the effect of self shading is not considered.

The variables in the basic model considered by Jang [24] are the phytoplankton (P) and the dissolved nutrient (N); if $u(Q)$ denotes the per-capita growth rate and δ the death rate of the phytoplankton (it is assumed that phytoplankton can be removed through death, but there is no nutrient loss to the system due to death), then $P(t)Q(t)$ is the total amount of stored nitrogen at time t and $\rho(N,Q)$ the per-capita uptake rate of the phytoplankton. The following hypothesis were adopted:

(H1) there exists $Q_0 > 0$ such that $u(Q_0) = 0$, $u'(Q) > 0$ and u' is continuous for $Q \geq Q_0$; and

(H2) $\rho \in C^1(N,Q)$ for $N \geq 0$, $Q \geq Q_0$; $\rho(0,Q) = 0$ for $Q \geq Q_0$ and $\frac{\partial \rho}{\partial N} > 0$, $\frac{\partial \rho}{\partial Q} \leq 0$ for $N \geq 0$, $Q \geq Q_0$.

Thus the basic system of differential equations in the Jang [23] model is:

$$\frac{dN}{dt} = -P\rho(N,Q) + \delta PQ$$

$$\frac{dP}{dt} = P[u(Q) - \delta] \qquad \textbf{(1.5)}$$

Now suppose $\sum(t)$ is the amount of free and stored nitrogen at time t i.e. $\sum(t) = N(t) + P(t)Q(t)$. Assuming the system is closed, the total nitrogen is constant i.e.

$\sum'(t) = 0$ for $t \geq 0$, implying that $P\dfrac{dQ}{dt} = P[\rho(N,Q) - u(Q)Q]$ and consequently $\dfrac{dQ}{dt} = \rho(N,Q) - u(Q)Q$ if $P(t) \neq 0$ for all $t \geq 0$. Therefore the variable-yield version of the Jang [23] model is:

$$\frac{dP}{dt} = P[u(Q) - \delta]$$

$$\frac{dQ}{dt} = \rho(N,Q) - u(Q)Q; \qquad (1.6)$$

and since the total nitrogen is constant (i.e. $\sum(t) = N_T$, for all $t \geq 0$) the system becomes

$$\frac{dP}{dt} = P[u(Q) - \delta]$$

$$\frac{dQ}{dt} = \rho(N_T - PQ, Q) - u(Q)Q \qquad (1.7)$$

Two equilibrium points of this system are $E_0 = (0, \hat{Q})$ and $E_1 = (P_1, Q_1)$. The equilibrium point E_0 always exists with $\hat{Q}$ defined as above, and the point E_1 exists if and only if $u(Q) = \delta$ has a solution $Q_1 > Q_0$ such that $\rho(N_T, Q_1) > \delta Q_1$. The dynamics can be summarized as follows:

i) if $u(Q) < \delta$ (i.e., if E_0 is a local attractor), then E_1 does not exist and every solution of **(1.7)** satisfies; and

ii) if $u(\hat{Q}) > \delta$, then E_1 exists and any solution of **(1.7)** with $P(0) > 0$ satisfies $\lim_{t\to\infty}(P(t), Q(t)) = (P_1, Q_1)$.

A zooplankton species can be added to generalized the system **(1.7)**. If the grazing rate is modelled by a Lotka-Volterra functional response, then the modified system can be

$$\dot{P} = P[u(Q) - \delta - bZ]$$

$$\dot{Q} = \rho\left(N_T - PQ - Z, Q\right) - u(Q)Q$$

$$\dot{Z} = Z[dPQ - \varepsilon]. \qquad \textbf{(1.8)}$$

Here d is the zooplankton net nutrient conversion rate, ε the death rate of zooplankton, and b the zooplankton grazing coefficient (note that $b \geq d$). There are three equilibrium points-viz. $E_0 = (0, \hat{Q}, 0)$, which always exists with $\hat{Q}$ defined above; $E_1 = (P_1, Q_1, 0)$, which exists if and only if $u(Q) = \delta$ has a solution $Q_1 > Q_0$ and $\rho(N_T, Q_1) > \delta Q_1$ (for the existence of a positive equilibrium it is necessary that $N_T > \frac{\varepsilon}{d}$); and $E_2 = (\bar{P}, \bar{Q}, \bar{Z})$, which exists if and only if $u(\bar{Q}) > \delta$, where $\bar{Q}$ satisfies $\rho(N_T - \frac{\varepsilon}{d} - (u(Q) - \delta)/b, Q) = u(Q)Q$, and also $\bar{P} = \frac{\varepsilon}{d\bar{Q}}$ and $\bar{Z} = \frac{u(\bar{Q}) - \delta}{b}$. The dynamics of the dynamical system described by (**1.8**) is similar to classical epidemic models by Hethcote [23] and the stability of E_0 precludes the existence of another equilibrium (E_0 is itself a global attractor). When E_0 is unstable, E_1 exists, and if it is a local attractor, then it is a global attractor. When E_1 is unstable, there exists a positive equilibrium point E_2, which is locally asymptotically stable and the system is uniformly persistent.

Adopting Michelis-Menten to the zooplankton grazing rate, the system **(1.8)** becomes:

$$\frac{dP}{dt} = P\left[u(Q) - \delta - \frac{bZ}{a+P}\right]$$

$$\frac{dQ}{dt} = \rho\left(N_T - PQ - Z, Q\right) - u(Q)Q$$

$$\frac{dZ}{dt} = Z\left[\frac{dPQ}{a+P} - \varepsilon\right] \qquad \textbf{(1.9)}$$

where a is the half saturation constant and d is the maximal growth rate of zooplankton. The dynamics can be summarized as follows. The equilibrium point E_0 is itself a global attractor if E_0 is a local attractor. The local stability of E_1 alone does not eliminate the possible of existence of a positive equilibrium, as was previously the case. However, the instability of both E_0 and E_1 also does not ensure the existence of E_2, so the dynamics of **(1.8)** and **(1.9)** is different. Nevertheless, if E_1 is unstable, the system is uniformly persistent.

The general form of Droop's predator prey model can also be written in the form of **(1.8)** and **(1.9)**-viz.

$$\frac{dN}{dt} = D[N^0 - N] - \rho x(N, Q)$$

$$\frac{dx}{dt} = x\left(u(Q) - D\right) - \hat{f}(x)y$$

$$\frac{dy}{dt} = y[\hat{f}(x)Q - D] \qquad \textbf{(1.10)}$$

where N is the free nutrient in the chemostat, x and y are the concentrations of prey and predator, $\hat{f}$ the general monotone functional response and u, ρ are defined as in (H1)

and (H2). Assuming $\sum(t) = N + xQ + y$ and applying conservation yields $\frac{dQ}{dt} = \rho(N,Q) - u(Q)Q$ if $x(t) \neq 0$ for all $t \geq 0$. Thus the system becomes:

$$\frac{dN}{dt} = D[N^0 - N] - \rho x(N,Q)$$

$$\frac{dx}{dt} = x\left(u(Q) - D\right) - \hat{f}(x)y$$

$$\frac{dQ}{dt} = \rho(N,Q) - u(Q)Q$$

$$\frac{dy}{dt} = y[\hat{f}(x)Q - D] \qquad (1.11)$$

With the limiting system given by

$$\frac{dx}{dt} = x\left(u(Q) - D\right) - \hat{f}(x)y$$

$$\frac{dQ}{dt} = \rho(N^0 - xQ - y, Q) - u(Q)Q$$

$$\frac{dy}{dt} = y[\hat{f}(x)Q - D] \qquad (1.12)$$

The system **(1.11)** and **(1.12)** need not have the same dynamical behaviour since the original system **(1.10)** exhibits asymptotic behaviour while **(1.12)** is the limiting system for where the system is not closed. However, **(1.5)-(1.9)** can be viewed as the limiting system of a chemostat model which is a closed system.

In summary, if the zooplankton is a linear function of the phytoplankton population, the dynamics of the variable-yield models is similar to the dynamics of classical models. However, the zooplankton grazing rate is modeled by Michelis-Menten kinetics, local asymptotic stability of the boundary equilibrium for a positive phytoplankton population does not ensure the nonexistence of a positive equilibrium, unlike the classical epidemic models, possibly due to the combination of nonlinearity of the zooplankton's grazing rate with the internal nutrient storage of phytoplankton. The global dynamics of the Lotka-Volterra zooplankton grazing rate resembles the constant-yield model. Jang [24] found that though the variable-yield nutrient plankton model is more complicated than the classical Monod model, the global dynamics are identical for both models. In other words, there is the same biological prediction of uniform persistence. This is consistent to the literature of variable-yield models of single species by Lange, K. and Orayzun, F.J. [30] and two competing species by Smith and Waltmann [43].

1.5 The development of our model

The model adopted in this thesis follows Ross et al. [41, 42] and is also a variable-yield type (c.f. Droop [9]). The carbon and nitrogen of the phytoplankton are treated separately (this makes the model different from the other variable-yield model described earlier), while the growth of the zooplankton is limited only by carbon content. Ross et al. [41, 42] considered the carnivore species and micro-organisms at different layers mixed by fluxes and turbulences which we have ignored. Only the internal nutrient (carbon) is immediately available for cell growth and metabolism. In other words, the biomass (size) of the phytoplankton is represented by carbon (C) and the physiological status is represented by the ratio of nitrogen to carbon i.e. the internal nitrogen quota. It is this later variable that determines the physiological growth rate. However, the population growth rate is depended on carbon (C).

The limiting nutrient for marine phytoplankton growth is chosen to be nitrogen, for which there is considerable evidence Dugdale [13] (Other nutrients such as phosphorus and silicon are neglected, although in certain circumstances there may also be growth limiting). Dissolved inorganic nitrogen is found in three basic forms in the marine environment –nitrate, nitrite and ammonium. For simplicity, internal differentiation of the inorganic nitrogen pool is neglected. It is assumed that nitrogen is taken up by the phytoplankton in dissolved form and is excreted and lost (due to bacterial activity) by the phytoplankton in organic form, and that the system is closed.

1.5.1 The state variables and definitions of intermediate quantities for our model

The model adopted to describe the dynamics of phytoplankton and zooplankton is intended to be acceptably realistic but still simple enough to obtain an intuitive understanding of the mechanisms involved. It is assumed that the phytoplankton nutrient has an external and internal cellular pool for both nitrogen and carbon. However, only the internal pool is immediately available for cell growth and metabolisms. Carbon is considered to be the limiting factor in the growth of higher trophic levels such as zooplankton. Thus the essential variables in the dynamical phytoplankton –zooplankton population model are the phytoplankton carbon x_1, the phytoplankton nitrogen x_2, zooplankton carbon x_3, and the total free nitrogen x_4.

In summary, the model reflects the following assumptions.

Assumption 1

Carbon is representative of the biomass of the phytoplankton and the zooplankton. There is no limitation at any stage- i.e. there is always an oversupply of carbon for the phytoplankton. This is almost always true in nature. Hence the carbon cycle exercises no control on the dynamics of phytoplankton, and it is unnecessary to conserve carbon in the model system.

Assumption 2

The rate of carbon fixation by the phytoplankton is assumed to be governed by either their current N: C ratio (i.e. Q_p) or by irradiance (i.e. L), whichever is most restrictive (c.f. Tett et al. [49]). Nutrient limitation is defined as in the quota model of Droop [9] i.e. so there is a minimum nutrient quota Q below which carbon fixation cannot take place. Light limitation L is defined by a Michaelis Menten relation of the form used by Andersen et al. [1], such that $\frac{L}{L+L_H}$. Thus the growth of phytoplankton ($\mu^{'}$) is represented by the function:

$$\mu^{'} = \mu_{\max} * \left(1 - \frac{Q}{Q_p}\right)^{+} * \left(\frac{L}{L+L_H}\right), \text{ where } Q_p = \frac{x_2}{x_1},$$

where

$$z^{+} = \begin{cases} z, & z > 0 \\ 0, & \text{otherwise} \end{cases}.$$

It is assumed that the light limitation is on a day and night basis i.e. we assume that $\frac{L}{L+L_H}$ is a constant i.e. 0.5. Thus the total uptake of carbon by the phytoplankton is given by $U_c = \mu^{'} x_1 = \mu(1 - \frac{Q}{Q_p})^{+} x_1$.

Assumption 3

A function which saturates with increasing nitrogen quota, up to the maximum obtainable quota R as shown in **Figure 1.4** is needed to represent the total uptake of inorganic nitrogen by phytoplankton (U_N),. A suitable function is of the form

$$\overline{U} = \frac{U}{\left(1+\exp\left(\frac{Q_p - R}{Q_0}\right)\right)} \text{ where } Q_p = \frac{x_2}{x_1}.$$

A saturating function of the total free nitrogen concentration x_4 satisfies of the form of the Michaelis-Menten relation, such as $\frac{x_4}{x_4 + h}$. Thus a suitable form of the **TYPE II** functional response (c.f. Caperon and Meyer [4, 5])

$$U_N = \frac{\overline{U} x_1 x_4}{(x_4 + h)} = \frac{U x_1 x_4}{(x_4 + h)\left(1+\exp\left(\frac{Q_p - R}{Q_0}\right)\right)}$$

Assumption 4

The carbon of the phytoplankton is taken up by the zooplankton at a rate given by

$$\Gamma_c = \Gamma x_3 \frac{x_1}{x_1 + \hat{C}}$$

Assumption 5

The nitrogen of the phytoplankton is taken up by the zooplankton at a rate given by

$$\Gamma_N = \Gamma x_3 \frac{x_2}{x_1 + \hat{C}}$$

Assumption 6

The grazing rate of the zooplankton Γ_z is assumed to be a **TYPE II FUNCTION** i.e. $\Gamma_z = \Gamma x_3 \frac{x_1}{x_1 + \hat{C}}$. The total uptake of the prey (phytoplankton) by the predator (zooplankton) U_z is then given by

$$U_z = Q_p \Gamma_z / \gamma_2 = \frac{\Gamma x_2 x_3}{\gamma_2 (x_1 + \hat{C})},$$

where γ_2 is the nitrogen quota of the zooplankton (assumed constant).

Assumption 7

Phytoplankton loss other than from grazing is assumed to be mainly through respiration r_p, death d_p and sinking factors δ_p. The total rate loss of the phytoplankton is denoted by γ. (Phytoplankton corpses eventually sink into the bottom layer, where they decompose and are remineralised into nitrogen, which is assumed to return back into the system i.e. the nitrogen is a closed system).

Assumption 8

The loss rate of zooplankton γ_1 is through respiration r_z and death d_z.

Suitable related intermediate quantities are summarized in the following Table 1.1:

Intermediate quantities	Description	Definition
Q_p	Phytoplankton N quota	$\frac{x_1}{x_2}$
U_c	Total uptake rate of C by phytoplankton	$\mu(1-\frac{Q}{Q_p})^+ x_1$
U_N	Total uptake rate of N by phytoplankton	$\frac{Ux_1x_4}{\left(1+\exp\left(\frac{Q_p-R}{Q_0}\right)\right)(x_4+h)}$
Γ_c	Total uptake rate of carbon phytoplankton by zooplankton	$\Gamma x_3 \frac{x_1}{x_1+\hat{C}}$
Γ_N	Total uptake of nitrogen phytoplankton by zooplankton	$\frac{\Gamma x_2 x_3}{(x_1+\hat{C})}$
U_z	Total uptake rate of phytoplankton by zooplankton	$\frac{\Gamma x_2 x_3}{\gamma_2(x_1+\hat{C})}$

Table 1.2: The intermediate quantities

Based on the above assumptions, the mathematical model adopted is represented by the following:

Total production of C of phytoplankton	=	Total uptake of C by phytoplankton	-	Total uptake rate of C phytoplankton by zooplankton	- Total loss rate of C of phytoplankton

i.e. $$\frac{dx_1}{dt} = \mu(1-\frac{Qx_1}{x_2})^+ x_1 - \frac{\Gamma x_1 x_3}{x_1 + \hat{C}} - \gamma x_1$$

Total production of N of phytoplankton = Total uptake of N by phytoplankton - Total uptake rate of N phytoplankton by zooplankton - Total loss rate of N of phytoplankton

i.e. $$\frac{dx_2}{dt} = \frac{Ux_1 x_4}{\left(1+\exp\left(\frac{Q_p - R}{Q_0}\right)\right)(x_4 + h)} - \frac{\Gamma x_2 x_3}{x_1 + \hat{C}} - \gamma x_2$$

Total production of carbon of zooplankton = Total uptake of phytoplankton by zooplankton - Total loss rate of zooplankton

i.e. $$\frac{dx_3}{dt} = \frac{\Gamma x_2 x_3}{\gamma_2 (x_1 + \hat{C})} - \gamma_1 x_3$$

Total production of free N = Total input rate of free N due to lost of phytoplankton + Total input rate of free N due to zooplankton - Total loss rate of free N taken by phytoplankton

i.e. $$\frac{dx_4}{dt} = \gamma x_2 + \gamma_1 \gamma_2 x_3 - \frac{Ux_1 x_4}{\left(1+\exp\left(\frac{Q_p - R}{Q_0}\right)\right)(x_4 + h)}.$$

The parameters to be chosen are based on some ecological literatures and guidance from from ecologist Ross [41, 42] and are summarized in **APPENDIX C: TABLES: T1**.

As suggested earlier, for simplicity most ecological models are assumed to be closed (what leaves the system returns into the system) – c.f. for example, Busenberg et al. [2], Kearns and Folsome [25], May [33], Nisbet et al. [35], Wroblewski [50]. Here, our model is closed, since we have $\dot{x}_2+\gamma_2\dot{x}_3+\dot{x}_4=0$ or $x_4=\lambda-x_2-\gamma_2 x_3$ where λ is a constant determined by the initial conditions. Thus the above system of four differential equations reduces to three in the three variables x_1 (the phytoplankton carbon), x_2 (the phytoplankton nitrogen) and x_3 (the zooplankton carbon) i.e.

$$\frac{dx_1}{dt}=\mu(1-\frac{Qx_1}{x_2})^{+}x_1-\frac{\Gamma x_1 x_3}{x_1+\hat{C}}-\gamma x_1 \tag{1.13}$$

$$\frac{dx_2}{dt}=\frac{Ux_1\left(\lambda-x_2-\gamma_2 x_3\right)}{\left(\lambda+h-x_2-\gamma_2 x_3\right)\left(1+\exp\left(\frac{Q_p-R}{Q_0}\right)\right)}-\frac{\Gamma x_2 x_3}{x_1+\hat{C}}-\gamma x_2 \tag{1.14}$$

$$\frac{dx_3}{dt}=\frac{\Gamma x_2 x_3}{\gamma_2(x_1+\hat{C})}-\gamma_1 x_3 \tag{1.15}$$

This system of ordinary differential equations is to be solved on the domain $\Omega=\{(x_1,\ x_2,\ x_3): x_1\geq 0,\ x_2\geq 0,\ x_3\geq 0\}$.

1.5.2 Slight modification of our model

The analysis is simplified if a slight modification is made to the model, by replacing the exponential terms in the equations i.e. the exponential terms introduced under **Assumption 3** and equation **(1.14)** are replaced by Heaviside terms, according as:

Modified Assumption 3

The total uptake rate of nitrogen by the phytoplankton is

$$U_N = \frac{\overline{U}x_1x_4}{(x_4+h)} = \frac{U\left(1-H\left(\frac{x_2}{x_1}-R\right)\right)x_1x_4}{(x_4+h)},$$

such that $1-H\left(\frac{x_2}{x_1}-R\right) = \begin{cases} 0, \frac{x_2}{x_1} > R \\ 1, \frac{x_2}{x_1} < R \end{cases}$.

The difference between the two terms is illustrated in **Figure 1.5**.

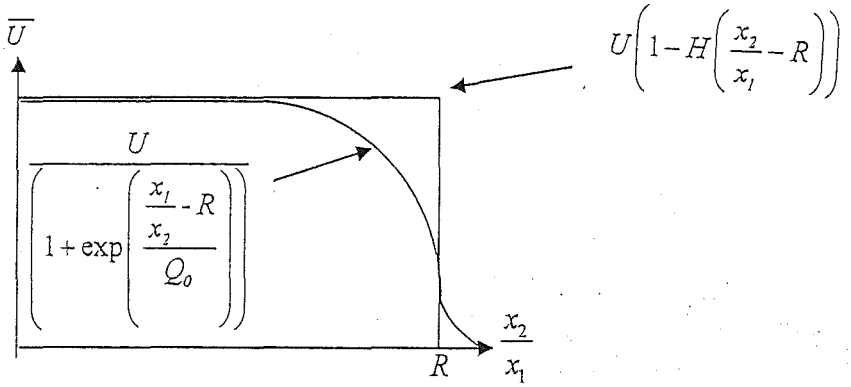

Figure 1.5: The dependence of phytoplankton uptake of nitrogen on the nitrogen quota showing the difference between the exponential term and the Heaviside term.

Thus equation (1.14) becomes

$$\dot{x}_2 = \frac{Ux_1(\lambda - x_2 - \gamma_2 x_3)\left(1-H\left(\frac{x_2}{x_1}-R\right)\right)}{(\lambda+h-x_2-\gamma_2x_3)} - \frac{\Gamma x_2x_3}{x_1+\hat{C}} - \gamma x_2. \qquad (1.16)$$

Note: There can be a slight difference in the numerical results when the exponential terms in (1.14) are replaced by the Heaviside terms in (1.16). The Heaviside term also

present some difficulty in convergence to the steady states, so in the numerical work (1.14) is retained.

1.6 Methodology- Analytical

In this section, the simple analytical tools used to investigate stability of the solutions or steady states are discussed briefly beginning with linear stability analysis and then preceding to bifurcation analysis.

1.6.1 Local stability analysis of non-linear system [14]

The first step in analyzing a system of dynamical equations is to find the steady state i.e. a time-dependent state of the dynamical system. At steady state there is a balance between output and input such that all the dependent variables remain constant, although in reality, there are always small random disturbances. Thus it is important to know if *deviations* from the steady state lead to drastic changes to the overall system, or are damped out (this is the essence of stability).

Note: Local stability analysis considers the consequence of some small deviation from the steady state. For larger disturbances, *global stability analysis* necessary and relevant in deciding the long term survival of each species considered in the system. Global stability analysis is more difficult but there are approaches such as Comparison theory (De Brujin [8]) that may be exploited. Grover [19, 20] attempted the global stability of avariable-yield model, Lange and Oyarzun [30] did so for a single species microorganism, Smith and Waltman [43] for a two species system, and Jang [24] for variable-yield nutrient-plankton-zooplankton models with nutrient recycling and self

shading. Global stability analysis as such shall not be pursued here very much, although in the later chapters there is some global analysis using the comparison theory. More reliance is placed on the use of numerical software, shall be discussed in **Section 1.7**.

For simplicity, let us first consider a *two* ordinary differential equations i.e.

$$\frac{dx_1}{dt} = f_1(x_1, x_2),$$

$$\frac{dx_2}{dt} = f_2(x_1, x_2), \tag{1.17}$$

where f_i are nonlinear functions. Let us assume that $\bar{x} = (\bar{x_1},\ \bar{x_2})$ is the steady state of **(1.17)**, so that

$$f_1(\bar{x_1},\ \bar{x_2}) = f_2(\bar{x_1},\ \bar{x_2}) = 0,$$

And then consider $x_i = \bar{x_i} + u_i$ where the u_i are small ***perturbations***. Substitution into **(1.17)**, yield

$$\frac{d(u_1)}{dt} = f_1(\bar{x_1} + u_1, \bar{x_2} + u_2)$$

$$\frac{d(u_2)}{dt} = f_2(\bar{x_1} + u_1, \bar{x_2} + u_2),$$

Since $\frac{d\bar{x_1}}{dt} = 0$ and $\frac{d\bar{x_2}}{dt} = 0$, and introducing a truncated Taylor expansion produces

$$\frac{dx_1}{dt} = \frac{\partial f_1}{\partial x_1}(\bar{x_1},\ \bar{x_2})u_1 + \frac{\partial f_1}{\partial x_2}(\bar{x_1},\ \bar{x_2})u_2 + g_1(u_1,\ u_2)$$

$$\frac{dx_2}{dt} = \frac{\partial f_2}{\partial x_1}(\bar{x_1},\ \bar{x_2})u_1 + \frac{\partial f_2}{\partial x_2}(\bar{x_1},\ \bar{x_2})u_2 + g_2(u_1,\ u_2) \tag{1.18}$$

where g_i are higher order derivatives such as $\frac{1}{2}\frac{\partial^2 x}{\partial t^2}(x-\bar{x})^2$ that go to zero faster than u_1 and u_2. Specifically, if $\|u\|=\sqrt{u_1^2+u_2^2}$ is the length of the vector u, then

$$\frac{g_i(u_1,u_2)}{\|u\|}\to 0 \text{ as } \|u\|\to 0. \tag{1.19}$$

Thus, in the neighborhood of the fixed point the perturbation equations are

$$\frac{du}{dt}=Au+g(u) \tag{1.20}$$

where

$$u=\begin{pmatrix}u_1\\u_2\end{pmatrix}, \qquad g(u)=\begin{pmatrix}g_1(u_1,u_2)\\g_2(u_1,u_2)\end{pmatrix},$$

$$\text{and } A=\begin{pmatrix}\frac{\partial f_1}{\partial x_1}(\bar{x}_1,\bar{x}_2) & \frac{\partial f_1}{\partial x_2}(\bar{x}_1,\bar{x}_2)\\ \frac{\partial f_2}{\partial x_1}(\bar{x}_1,\bar{x}_2) & \frac{\partial f_2}{\partial x_2}(\bar{x}_1,\bar{x}_2)\end{pmatrix}=\begin{pmatrix}\frac{\partial f_1}{\partial x_1} & \frac{\partial f_1}{\partial x_2}\\ \frac{\partial f_2}{\partial x_1} & \frac{\partial f_2}{\partial x_2}\end{pmatrix}\Bigg|_{(\bar{x}_1,\bar{x}_2)} \tag{1.21}$$

can be approximated by the linear form

$$\frac{du}{dt}=Au. \tag{1.22}$$

The matrix A is the ***Jacobian matrix*** of f at $\bar{x}$ which is often written as $J=\frac{\partial f}{\partial x_i}(\bar{x}_i)$ and the above approximation of the nonlinear system by a linear one are called ***linearization***.

The analysis extend readily to higher dimensional systems, thus the *n*-dimensional nonlinear equation of the form

$$\frac{dx_i}{dt} = f_i(x_1, x_2, ..., x_n) \qquad \text{such that } i = 1, 2, ..., n$$

or $$\frac{dx}{dt} = Ax + g(x) \tag{1.23}$$

is linearised as $\frac{dx}{dt} = Ax$, where the ***Jacobian matrix*** at the steady state $\bar{x}$ is given by

$$J = \frac{\partial f}{\partial x_i}(\bar{x_i}) \text{ or } A = \begin{bmatrix} \frac{\partial f_1}{\partial x_1} & \frac{\partial f_1}{\partial x_2} & . & . & \frac{\partial f_1}{\partial x_n} \\ . & . & . & & \\ . & . & & . & \\ . & . & & & . \\ \frac{\partial f_n}{\partial x_1} & \frac{\partial f_n}{\partial x_2} & . & . & \frac{\partial f_n}{\partial x_n} \end{bmatrix}_{(\bar{x_n})} \tag{1.24}.$$

Suppose the solution of **(1.24)** is of the form $x(t) = ve^{\lambda t}$, where v is a vector independent of time. Substituting into the linearised form of **(1.23)**, yields

$$Av - \lambda Iv = (A - \lambda I)v = 0$$

where $\boldsymbol{I}$ is the identity matrix (a matrix with 1's at the diagonal and 0's elsewhere).

Thus we can solve for the eigenvalues λ by finding the determinant of the matrix, denoted and defined by

$$\det(A-\lambda I)=|A-\lambda I|=\begin{vmatrix} \frac{\partial f_1}{\partial x_1}-\lambda & \frac{\partial f_1}{\partial x_2} & \cdots & \frac{\partial f_1}{\partial x_n} \\ \frac{\partial f_2}{\partial x_1} & \frac{\partial f_2}{\partial x_2}-\lambda & \cdots & \frac{\partial f_2}{\partial x_n} \\ \cdot & \cdot & \cdots & \cdot \\ \cdot & \cdot & \cdots & \cdot \\ \cdot & \cdot & \cdots & \cdot \\ \frac{\partial f_n}{\partial x_1} & \frac{\partial f_n}{\partial x_2} & \cdots & \frac{\partial f_n}{\partial x_n}-\lambda \end{vmatrix}_{(\bar{x}_i)}.$$

The evaluation of the determinant and eigenvalues is straightforward, but requires some linear algebra and usually the use of ***elementary row operations***, especially when dealing with a higher order determinant and to reduce $\det A$ to ***echelon form*** **(see APPENDIX A: LINEAR ALGEBRA: A1, A2 and A3).**

The linear stability of the steady states of n-dimensional non linear differential equations can be represented as in ***Theorem 1.1*** below. The proof of the theorem is available in many textbooks e.g. Hale and Kocak [22] on pages 266-273.

Theorem 1.1: The stability of the n-dimensional nonlinear differential equations

Consider the nonlinear autonomous differential equation of the form $\frac{dx}{dt}=Ax+g(x)$ such that

$$g(x)/\|x\| \equiv g(x)/\max\{|x_1|,.....|x_n|\}$$

is a continuous function of $x_1,.....,x_n$ which vanishes for $\|x\| \to 0$. Then,

a) If all the eigenvalues of the Jacobian matrix A of the linearised equation $\frac{dx}{dt} = Ax$ have *negative real parts*, then its steady state $x(t) \equiv 0$ is *asymptotically stable*. Thus equivalently the steady state $\bar{x}$ of the nonlinear differential equation is also *asymptotically stable*.

b) If at least one of the eigenvalues of A has *positive real part*, the nonlinear differential equation is *unstable* at the steady state $\bar{x}$.

For less complicated matrices we can alternatively use Routh-Hurwitz criteria to establish stability (see Edelstein [14] on pages 231- 235).

1.6.2 Bifurcation Theory

Many books such as Hale and Kocak [22] also discuss generalised bifurcation theory of an ordinary differential equation. A knowledge of elementary bifurcation theory and its processes allows us to have some idea of what to search for and what to expect from the numerical program AUTO; to be discussed in the next section. This program mainly serves to investigate the bifurcation points and steady states as well as periodic branches. ***Bifurcation theory*** is the study of the solution set of dynamical systems as the parameter changes. As the parameters are varied, it might undergo structural changes (the structure of the graph or curve might change) and the stability might change. It is also possible for the equilibrium solutions to be unstable on both sides of a bifurcation points.

Let us consider the system of n-dimensional nonlinear differential equation of the form

$$\frac{dx_i}{dt} = f_i(x_i, \lambda) \qquad (i = 1, 2, ..., n) \tag{1.25}$$

and its steady state solution such that

$$f_i(x_i, \lambda) = 0 \qquad (i = 1, 2, ..., n), \tag{1.26}$$

where $\lambda \in R$ is the parameter and $f, x \in R^n$. It is assumed that f is sufficiently continuously differentiable.

Let $x(\lambda)$ be a critical point or the steady state of **(1.25)** i.e.

$$f_i(x(\lambda), \lambda) = 0. \tag{1.27}$$

As previously indicated, the stability of the steady state $x(\lambda)$ of equation **(1.25)**, depends on the eigenvalues of the linearised equation of **(1.25)** of the form $\frac{dx_i}{dt} = A(\lambda)x_i$ say $\zeta_1(\lambda), \zeta_2(\lambda)....,\zeta_n(\lambda)$ Recall that $A(\lambda) = J(\lambda) = \frac{\partial f_i(x(\lambda))}{\partial x_j(\lambda)}$ is the *Jacobian matrix*. There is the following theorem as a result of ***Theorem 1.1***.

Theorem 1.2: Stability of the n-dimensional system of nonlinear differential equations **[22]**

Recall the n-dimensional system of nonlinear differential equations of the form

$$\dot{x}_i = f_i(x_i, \lambda) \qquad \text{such that } i = 1, 2, ..., n \tag{1.25}$$

where

$$x_i = (x_1(\lambda), x_2(\lambda), ..., x_n(\lambda))$$

$$f_i = (f_1(x_i; \lambda), f_2(x_i; \lambda), ..., f_n(x_i; \lambda)).$$

Let the steady state and the eigenvalues of the linearised equation of **(1.25)** of the form $\dot{x}_i = \frac{dx_i}{dt} = A(\lambda)x_i$ be $x(\lambda)$ and $\zeta_1(\lambda), \zeta_2(\lambda)....,\zeta_n(\lambda)$ respectively, then we have the following:

a) If all the eigenvalues have *negative real part* then the steady state is uniformly and *asymptotically stable.*

b) On the other hand, if one or more of the eigenvalues have a *positive real part* then the steady state is *unstable.*

Note: The function f, Jacobian matrix $A(\lambda)$ and the eigenvalues $\zeta_1(\lambda), \zeta_2(\lambda)....,\zeta_n(\lambda)$ all depends upon the parameter λ.

Let us now consider some important definitions in bifurcations theory.

Definition 1.1: ***Bifurcation analysis***

Bifurcation analysis is the process of finding critical values of the parameter λ at which the solution changes its structure.

Definition 1.2: ***Bifurcation diagram*** [3]

A diagram $[x]$ versus λ, where the pair (x,λ) defines the solution of equation (1.25) and (1.26) is called a ***bifurcation diagram.***

The notation $[x]$ denotes a scalar measure of x, and can be one of the following forms:

- $[x] = x_k$ for any of the n indices, $1 \le k \le n$
- $[x] = \left(x_1^{\,2} + x_2^{\,2} + ... + x_n^{\,2}\right) = \|x\|$ Euclidean norm
- $[x] = \max\left(|u_1|, |u_2|, ..., |u_n|\right)$

Each of these might produce a slightly different bifurcations diagrams. (The Euclidean norm is usually adopted).

In bifurcation diagrams there can be two types of branches. There are the **steady state branches** and the **periodic branches**.

At a **steady state branch**, there can be the following bifurcation points:

- A **branch point** - at a branch point, two branches of steady state with distinct tangents intersect.
- A **limit point** (fold point or turning point) - at a limit point, two solutions or steady states arise or two steady states coexist (at a critical bifurcation point $\lambda = \lambda_0$). Thus there are no solutions on one side of a limit point and at least two solutions on the other side.

At a **periodic branch**, there can be

- Hopf bifurcation point - at a Hopf bifurcation point, a periodic branch or limit cycle appears from a **steady state branch**.

Note: Stable and unstable branches in bifurcation diagrams are usually distinguished from each other by dark bold lines for the stable branch and dashed lines for unstable branch. Similarly, a stable periodic branch is usually made dark and bold (darker than ordinary branch) i.e. consists of dark bold closed circles. Unstable periodic branches are denoted by light circles.

The following theorem is useful to locate the trivial branches and associated bifurcating branches.

Theorem 1.3: The Implicit Function Theorem (existence of a bifurcation point) [3]

Reconsider a one dimensional differential equation of **(1.25)**

$$\frac{dx}{dt} = f(x,\lambda)$$

such that λ is a real parameter ($\lambda \in \Re$) and f is continuously differentiable and depends smoothly on x and λ ($f, x \in \Re^n$).

Suppose

- $f(x_0,\lambda_0) = 0$ i.e. (x_0,λ_0) is the solution of $f(x,\lambda) = 0$;
- f is continuously differentiable in some open region containing the point (x_0,λ_0) in the (x,λ) plane; and
- $f_x(x_0,\lambda_0)$ is non singular.

Then for all intervals $\lambda_1 < \lambda_0 < \lambda_2$ about λ_0 in which a function $x = F(\lambda)$ is defined by $f(x,\lambda) = 0$, there are the following properties:

- $f(F(\lambda),\lambda) = 0$;

- $F(\lambda)$ is unique with $x_0 = F(\lambda_0)$;
- $F(\lambda)$ is continuously differentiable; and
- $\frac{\partial f(x_0,\lambda_0)}{\partial x}\frac{dx}{d\lambda} + \frac{\partial f(x_0,\lambda_0)}{\partial \lambda} = 0$, where $\frac{\partial f(x,\lambda)}{\partial x} \equiv f_x(x,\lambda)$ is the Jacobian matrix and $\frac{\partial f(x,\lambda)}{\partial \lambda} \equiv f_\lambda(x,\lambda)$ is the vector of partial derivatives with respect to the parameter λ.

Note:

(1) ***Theorem (1.3)*** implies that if $f_x(x,\lambda)$ is not singular, there is no bifurcation point i.e. a necessary condition for a bifurcation is that the matrix $f_x(x,\lambda)$ is singular at that point.

(2) If ***Theorem (1.3)*** holds, the branch may be defined to be:

$$S = \{(x(\lambda),\lambda) \big| \lambda_1 < \lambda < \lambda_2, f(x(\lambda),\lambda) = 0\}$$

The solution $(0,\lambda)$ of **(1.25)** is called the *trivial branch* i.e. it corresponds to $f(0,\lambda) = 0$ for all values of λ.

Theorem 1.4: Sufficient condition (existence of a branching point)

If the trivial branch exists and $\lambda_0 = 0$ is an eigenvalue of the Jacobian matrix $f_x(x,\lambda)$, then if λ_0 is an eigenvalue of odd multiplicity, it is a branching point (from the trivial branch).

Note: If the trivial branch does not exist or the bifurcation points from other branches are wanted then ***Theorem 1.4*** cannot be applied. Hence this theorem only locates

bifurcation points which are on the trivial branch. To find bifurcation points from other branches, the system has to be linearised.

Once the bifurcation points are located it has to be categorized as either limit points or branch points. Thus below is the definition of limit points and branch points.

Definition 1.3: ***Limit point*** [3]

A solution (x_l, λ_l) of **(1.25)** is called a **limit point** (or fold point or turning point) if the following conditions hold:

i) $f(x_l, \lambda_l) = 0$

ii) $f_x(x_l, \lambda_l)$ has a simple eigenvalue 0 or equivalently, rank $f_x(x_l, \lambda_l) = n-1$

iii) $f_x(x_l, \lambda_l) \notin range\, f_x(x_l, \lambda_l)$, that is, $rank\ (f_x(x_l, \lambda_l) | f_\lambda(x_l, \lambda_l)) = n$

iv) There is a parameterization $x(\sigma)$, $\lambda(\sigma)$ with $x(\sigma_l) = x_l$, $\lambda(\sigma_l) = \lambda_l$ and $\frac{d^2\lambda(\sigma_l)}{d\sigma^2} \neq 0$.

The difference between a limit point and a branching point can also be looked at from a different angle. If we consider the bifurcation parameter λ to be the $(n+1)st$ component of x, that is

$$x_{n+1} = \lambda,$$

then equation **(1.25)** can be considered as a system of n equations in (n+1) unknowns

$$f_i(x_1, x_2, ..., x_n, x_{n+1}) = 0,\ i = 1, 2, ..., n.$$

The rectangular matrix of the partial derivatives consists of (n+1) columns

$$(f_x | f_\lambda) = (x^1, x^2, ..., x^k, ...x^n, x^{n+1}). \tag{1.28}$$

Now let the *k*th component be the bifurcation parameter. That is

$$\gamma = x_k .$$

The dependence of the remaining *n* components

$$x_1, x_2, ..., x_{k-1}, x_{k+1}, ..., x_n, x_{n+1}$$

on γ is characterized by the new Jacobian which results from equation **(1.28)** by removing the kth column. For a limit point, it is possible to find an index *k* such that the new Jacobian is nonsingular (full *rank* = *n*) whereas for a branching point no such *k* exists (*rank* < *n* for all choices of γ).

Definition 1.4: ***Branching point*** [3]

A solution (x_b, λ_b) of **(1.25)** is called a **simple branching point** if the following conditions hold:

i) $f(x_b, \lambda_b) = 0$

ii) $f_x(x_b, \lambda_b)$ has a simple eigenvalue 0 or equivalently, rank $f_x(x_b, \lambda_b) = n-1$

iii) $f_x(x_b, \lambda_b) \notin range\, f_x(x_b, \lambda_b)$, that is, $rank\ (f_x(x_b, \lambda_b) | f_\lambda(x_b, \lambda_b)) \neq n$

iv) Exactly two branches intersect with two distinct tangents.

In passing that a solution branch or a part of a solution branch is stable (*unstable*) if all of its solutions are stable (*unstable*). A branch is called periodic or symmetric if its solutions are periodic or symmetric.

Note: It is possible λ_0 to be a bifurcation point without there being a change in stability see Perko [35], Sotomayor's Theorem pg 330.

Example 1: (Single bifurcation)

Consider the system

$$f_1(x_1, x_2, \lambda) = x_1^2 - \lambda x_1 = 0$$

$$f_2(x_1, x_2, \lambda) = x_2^2 - \lambda x_2 = 0$$

The system has the trivial solution branch. The Jacobian $\mathbf{f}_u$ is

$$\mathbf{f}_x = \begin{bmatrix} 2x_1 - \lambda & 0 \\ 0 & 2x_2 - \lambda \end{bmatrix}.$$

The trivial branch $(\mathbf{0}, \zeta)$ has a possible bifurcation point at $\lambda = \zeta = 0$. The Jacobian $\mathbf{f}_u(\mathbf{0})$ has a zero eigenvalue of multiplicity 2. However, clearly, $\lambda = x_1$ and $\lambda = x_2$ are nontrivial equilibrium points. Thus solution branches $(\zeta, 0, \zeta)$, $(0, \zeta, \zeta)$ and (ζ, ζ, ζ) exist for all $\zeta \in \mathbf{R}$. Hence $(\mathbf{0}, \mathbf{0})$ is a bifurcation point. Further, the matrix $\left[f_x(0,0) \middle| f_\lambda(0,0) \right]$ is rank deficient. Thus $(\mathbf{0}, \mathbf{0})$ is a branching point. Thus the **Theorem 1.4** does not show whether it is a bifurcation point or not [3].

The following theorem predicts the appearance of a limit cycle about any steady state that undergoes a transition from a stable to an unstable focus, as some parameter is varied. The result is local in the sense that:

- the theorem only holds for parameter values close to the bifurcation value (the value at which the transition between stability and instability occurs).

- the predicted limit cycle is close to the steady state (i.e. it has a small diameter).

Note: an Hopf bifurcation does not specify what happens as the bifurcation parameter is further varied beyond the immediate vicinity of its critical bifurcation point $\lambda = \lambda_0$.

Theorem 1.5: The Hopf Bifurcation Theorem (limit cycle trajectories) (Edelstein [14] pg 342-343)

Consider the system of n-dimensional nonlinear differential equation of the form

$$\dot{x}_i = f_i(x_i, \lambda) \qquad \text{such that } i = 1, 2, ..., n \tag{1.25}$$

where

$$x_i = (x_1(\lambda), x_2(\lambda), ..., x_n(\lambda))$$

$$f_i = (f_1(x_i; \lambda), f_2(x_i; \lambda), ..., f_n(x_i; \lambda))$$

Let the steady state and the eigenvalues of the linearisation equation of **(1.25)** of the form $\dot{x}_i = \frac{dx_i}{dt} = A(\lambda)x_i$ be $\bar{x}(\lambda)$ and $\zeta_1(\lambda), \zeta_2(\lambda)...., \zeta_{n-2}(\lambda), a(\lambda) + b(\lambda)i, a(\lambda) - b(\lambda)i$ respectively. Then if the eigenvalues $\zeta_1(\lambda), \zeta_2(\lambda)...., \zeta_{n-2}(\lambda)$ have *negative real parts* and $\zeta_{n-1}(\lambda), \zeta_n(\lambda)$ (precisely these two) are complex conjugates $a(\lambda) + b(\lambda)i, a(\lambda) - b(\lambda)i$ that cross the imaginary axis when the parameter λ varies through some bifurcation point, the theorem predicts closed (limit cycle) trajectories.

Suppose that there is a bifurcation point $\lambda = \lambda_0$ such that $a(\lambda_0) = 0$ and $b(\lambda_0) \neq 0$, and as λ varies through λ_0 the real parts of the eigenvalues change sign ($da/d\lambda \neq 0$ at $\lambda = \lambda_0$). The following possibilities arise:

- at $\lambda = \lambda_0$, a ***center*** occurs in the steady state, and infinitely many neutrally stable concentric closed orbits surround the steady state point $\bar{x}(\lambda)$.
- when $\lambda_0 < \lambda < c$, a single limit cycle surrounds the steady state $\bar{x}(\lambda)$, then λ is varied, the diameter of the limit cycle changes in proportion to $|\lambda - \lambda_0|^{1/2}$ and there is no other limit cycle near the steady state. (The phenomenon in which the limit cycle exists for λ greater than the critical value λ_0, is called ***supercritical bifurcation***).
- when $d < \lambda < \lambda_0$, a limit cycle exists for λ less than the critical value λ_0 (this phenomenon is called ***subcritical bifurcation***). (Note: The diameter of the limit cycle changes in proportion to $|\lambda_0 - \lambda|^{1/2}$).

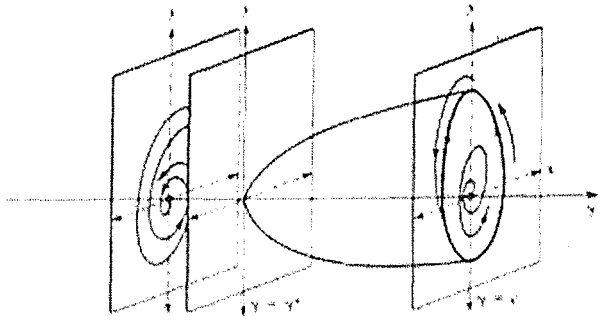

(a)

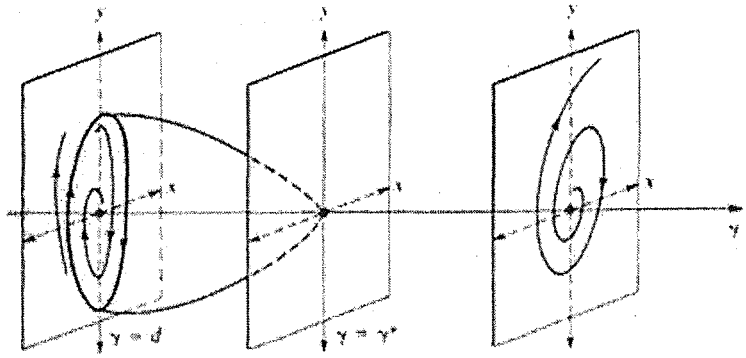

(b)

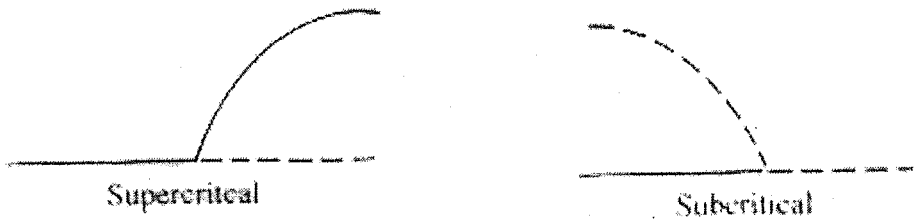

(c) (d)

Figure 1.6: Limit cycle phenomena for the critical value of the parameter λ when a transition from stable to unstable centre occurs at a steady state. Assuming that the steady state is stable when $\lambda < \lambda_0$ and unstable when $\lambda > \lambda_0$. Diagram (a) shows a supercritical bifurcation occurring at $\lambda > \lambda_0$; (b) shows a subcritical bifurcation occurring at $\lambda < \lambda_0$; while (c) and (d) shows the bifurcation diagrams that summarized the parameter dependence of (a) and (b) respectively [14].

The Hopf bifurcation theorem above does not determine whether or not the limit cycle is stable or not. So another test is needed and often involves complicated calculations (c.f. Edelstein [14] pages 344-345), discussing the procedure for the case n=2, Marsden and Mc Cracken [32], Odell [36], Guckenheimer and Holmes [21], Rand, et al. [38].

The Dulac criterion used to predict the presence of limit cycles Edelstein [14] on pages 329-330.

1.7 Methodology- Numerical (XPP)

In this section, a manual and procedure to run the program XPP is discussed. XPP (XPPAUT) is a tool for solving differential equations, difference equations, delay equations, functional equations, boundary value problems and stocastic equations. XPP is now available as a program running under X11 and UNIX, and are more recently MICROSOFT WINDOWS [52].

The basic unit for XPP is a single ASCII file (hereafter called an ODE file) that has the equations, parameters, variables, boundary conditions, and functions for the model. Numerical factors such as time-step size and method of integration may be specified, although these can also be automatically changed within the program. Graphics and post-processing are all done within the program using the mouse and various menus and buttons. However, in the window version, some keys turn out to have different functions, as discussed later. The impatient user should look at some sample *.ode files instead of actually reading the documentation. In addition, XPP uses a file called ***default.opt*** that

describes initializations and memory options for the program. This is not necessary as all of the information contained in this file can now be included in an ODE file.

1.7.1 XPP : How to write the ODE file for our model

To demonstrate the procedure of writing the ODE file for our model, the simplest "one-compartment model" serves an example (named as: **NPZ-new.ode**). It is notable that XPP looks at the extension of a file, and any differential equation model needs to have *name.ode* (if it is *name.dif* XPP assumes the model to be difference equation and treats it as a map). Any additional functions that need to be declared in the program can be referred to "XPPAUT 3.0- the differential equation tool by Ermentrout [15]". Here, only the important functions which are normally used to run the program are discussed.

ODE files are ASCII readable files that the XPP parser reads to create machine usable code. Lines can be continued with the standard backslash character, but the total length of any line cannot exceed 256 characters.

One starts with the program ***title***, to distinguish between similar programs.

NPZ-new.ode

 # Simple nutrient-phytoplankton-zooplankton (the one compartment model)

 # 8 march 2000

Initial data could be added to the file by adding

```
init C_p=1 N_p=0.2 C_z=1
```

Parameters are named quantities that represent constants in the ODE and which can be changed within the program. There can be many declarations on each line. It is very important that there be no spaces between the = sign, and the value of the parameter. Without an = sign and a value, the parameter is set to zero by default.

```
par lamda=5,g_p=0.25,U_nmax=1,F_nh=5,Q_pmax=0.25,Q_off=0.01,
par g_zmax=1,C_hp=100,mu_max=2,Q_pmin=0.05,L_h=50,g_z=0.05,
Q_z=0.25, a_L=50, b_L=0
```

Defined functions and variables The differential equations can be split up, by defining some of the intermediate quantities before introducing the equations for our models. The advantage of this is that any problem which might arise may be identified during the program run.

```
L= max(0,a_L-b_L*sin(2*pi*t))
Q_p=N_p/C_p
F_n=lamda-N_p-(Q_z*C_z)
U_n=U_nmax*C_p*(F_n/(F_n+F_nh))*(1/(1+exp((Q_p-Q_pmax)/Q_off)))
gamma_z=g_zmax*C_z*C_p/(C_p+C_hp)
mu=mu_max*C_p*max(0,(1-Q_pmin/Q_p))*L/(L+L_h)
```

```
dN_p/dt=U_n - g_p*N_p -gamma_z*Q_p
dC_p/dt=mu - g_p*C_p -gamma_z
dC_z/dt=(Q_p/Q_z)*gamma_z-g_z*C_z
aux Ratio=C_p/N_p
```

Setting internal options XPP has many internal parameters that can be set from within the program and four parameters that can only be set before it is run. The four options that can be set outside the program are:

- **MAXSTOR=integer** sets the total number of time steps that will be kept in memory. The default is 5000. To perform very long integration, this default may be changed to some larger number.
- **BACK={black, white}** sets the background to black or white.
- **SMALL=font name** where font name is some font available to the X-server. This sets the "small" font which is used in the Data Browser and in some other windows.
- **BIG=font name** sets the font for all the menus and pop ups.

The remaining options can be set from within the program. Some of them are:

- **XP=name** sets the name of the variable to plot on the x-axis. The default is t, the time variable.
- **YP=name** sets the name of the variable to plot on the y-axis

- **BOUND=value** sets the maximum bound any plotted variable can reach. If any plottable quantity exceeds this, the integrator will halt with a warning, although the program will not stop (default is 100)
- **NJUMP=integer** tells XPP how frequently to output the solution to the ODE. The default is 1, which means at each integration step.
- **TOTAL=value** sets the total amount of time to integrate the equations (default is 20)

```
@ BOUND=1e+12
@ NJMP=1
@ TOTAL=1000
@ XP=T,YP=C_p
@ BELL=off
@ MAXSTOR=1500000
done
```

1.7.2 XPP : How to use XPP to run the program

After writing the program in the notepad, it can be saved it as ODE files, for example NPZ-new.ode. We are then able to execute the program from the bash-shell window.

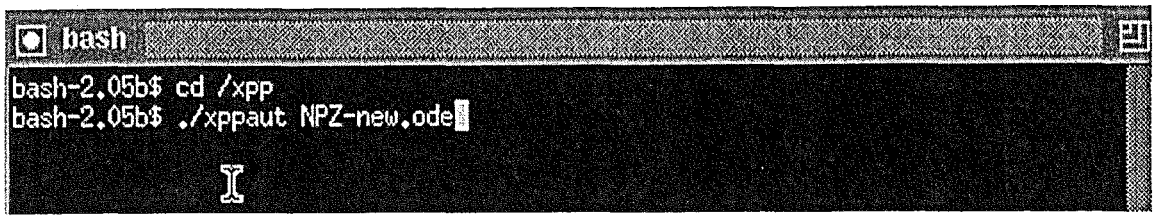

Figure 1.7: The bash-shell, the initial window use to run the XPP program

The command "cd/xpp" is to run the XPP program and then select the ODE files, written and saved by typing ./xppaut FILEname.ode. As soon as ENTER is pressed, the XPP MAIN window is activated (see **Figure 1.8**). In addition to the main window, other windows are available such as the INITIAL DATA window containing the names of the variables and the current initial data; the PARAMATER window, containing the list of all parameters and their current values; the BOUNDARY CONDS window, containing the list of boundary conditions; the EQUATIONS window, containing list of the equations of our model and the DATA VIEWER window, containing the detail of a steady state. These windows constitute the main user with the list of boundary conditions given. These windows constitute the main user editable windows. All of the quantities and formulae contained can be edited within the program (Clicking on any item in these windows will cause the cursor to appear there, for editing).

Some of the keyboard keys do not follow the normal functions. For example:

- The ENTER key can be used to go to the next item in that particular window, and indicates that the edited item is accepted.
- The ESC key can be used to exits the particular window, without changing any value.
- The DELETE buttons is used as backspace.

The buttons in the INITIAL DATA, PARAMETERS and the BOUNDARY CONDS windows have the following functions:

- The OK button can be used to accept the item, but the pointer will be redirected to the main window.
- DEFAULT key will reset any values we changed back to the default value, when the program boots up.
- The CANCEL buttons doesn't have any function.
- The GO key can be used to run the program, and draw the trajectories on the variable against time for a two dimensional plot.

All commands in the main XPP window can be invoked by clicking on the menu with the mouse. Usually most commands can be aborted by pressing the ESC key. Once one of these is chosen by pressing OK, the program begins to calculate and draw the trajectories. To stop the integration prematurely, one may press the ESC key.

Let us next consider some of the important menus available in XPP main window, useful in running the program. Others can be found in the XPP manual.

MENU'X' 1 **Initial conds**. This invokes a list of options for integrating the differential equations. One is:

(G)o which uses the initial data in the IC window and the current numerics parameters to solve the equation. The output is drawn in the current selected graphics window and the data saved for later use. The solution continues until the user aborts by pressing ESC, or the integration is complete, or storage runs out.

To extend the solutions one needs to select **Initial conds.** once again, and then select

(L)ast, which uses the end result of the most recent integration as the starting point of the current integration.

Then to activate the program **AUTO** interface, one may select the following:

MENU'X' 2 **(F)ile** to bring up a menu with several options. (Type ESC to abort, or **(A)uto** to bring up the AUTO window.

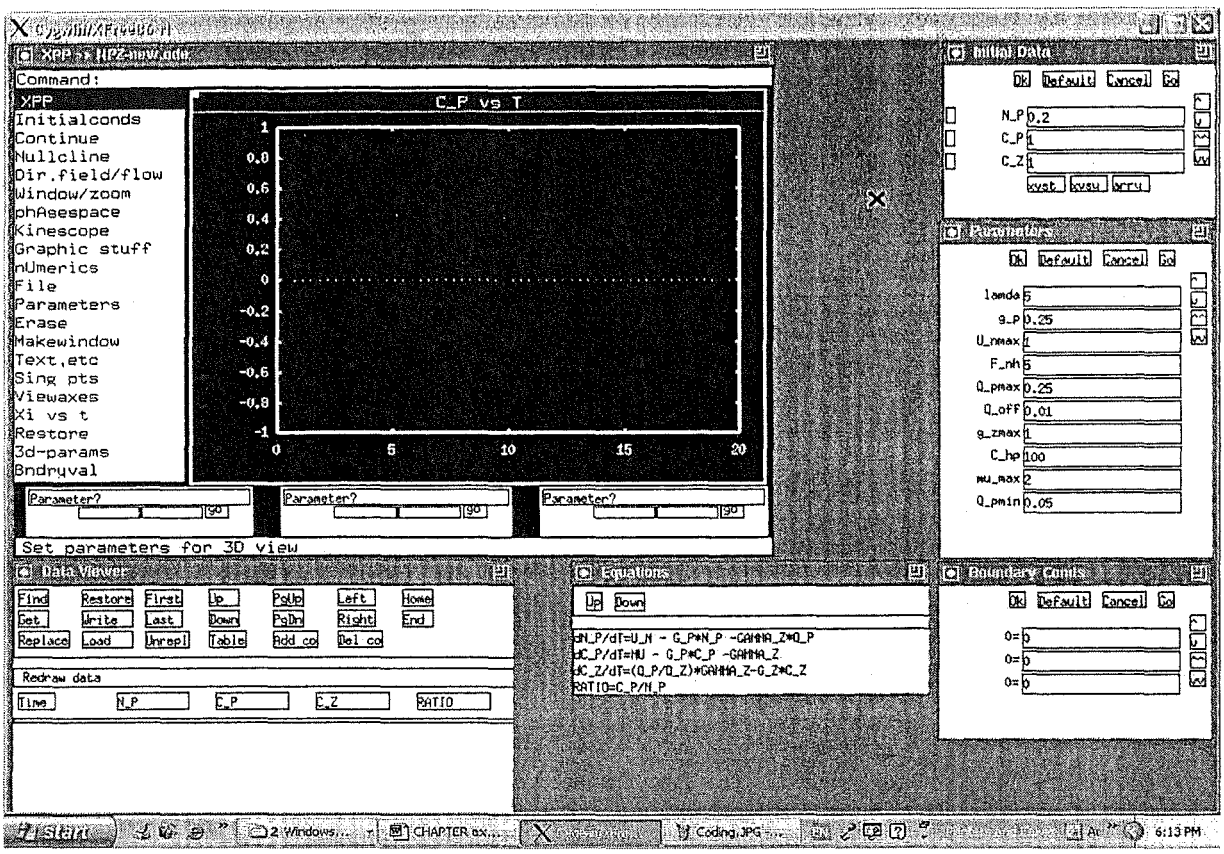

Figure 1.8: The XPP windows- consisting of the Main Window; the Initial Data, the Parameter, the Boundary Conditions, Equations and the Data Viewer windows.

1.8 Methodology- Numerical (AUTO INTERFACE: How to execute bifurcation diagrams and establish important branches)

AUTO is a program written several years ago by Eusebius Doedel [11, 12], which has the ability to track bifurcation curves for steady state and periodic systems. The program is very powerful, particularly for following periodic orbits. The version supported in XPP is

a subset of AUTO, but allows most of the outcomes normally wanted for autonomous ODEs and BVPS. In particular, one can track fixed points, find turning points and Hopf bifurcation points, compute two-parameter curves of turning points and Hopf bifurcation points, compute branches of periodic solutions emanating from a Hopf point, tract period-doubling bifurcations, torus bifurcations and two-parameter curves of fixed period orbits. Points can be imported into XPP as well as complete orbits. The bifurcation diagrams are dynamically produced, and can be moved around using arrow keys. Curves can be saved and reloaded for later use. Diagrams can be saved and imported into the main XPP window.

Given some function $f(x_1, x_2, ...x_n, \lambda)$ and a number of control parameters, AUTO is capable of internally executing the Jacobian of the function , the derivative f_λ and then the following (see Doedel [10]):

i) trace out branches of steady state solutions;

ii) accurately locate steady state bifurcation points;

iii) switch automatically onto bifurcating branches of steady states;

iv) accurately locate Hopf bifurcation points;

v) switch automatically onto branches of periodic solutions and trace out such branches;

vi) compute past turning points without added difficulty, both on branches of steady state solutions and on branches of periodic solutions;

vii) compute stable as well as unstable branches- for periodic solutions this is made possible by reformulating the problem as a boundary value problem on $[0, 2\pi]$;

viii) adapt the mesh to the solution- the discretization used is the method of orthogonal collocation with ii, iii, iv, v, vi and vii collocation points per mesh interval;

ix) adaptive stepsize along branches of periodic solutions;

x) automatic restarting at certain points; and

xi) store plotting information in files- these files can be investigated by an interactive graphics program.

1.8.1 AUTO INTERFACE - Menus

Upon clicking on FILE from the XPP window and choosing AUTO, the AUTO window with several regions or menus appears. Some of the important menus often used are as follows (see **Figure 1.9** on **page 63** for better understanding):

MENU'A' 1 **PARAMETERS** Up to 5 parameters are allowed. In the calculations of this thesis, the settings are PAR 1: lamda and PAR 2: g_p, to produce a two-parameter diagrams are discussed later.

MENU'A' 2 **AXES** There are 6 choices shall appear and some of which are:

(H)i which plots the maximum of the chosen variable

(N)orm which plots the L_2 norm of the solution.

h(I)-lo which plots both the maximum and minimum of the chosen variable (convenient for periodic orbits). An example is:

y axis	C_z
main par	lamda (automatic but can be altered)
2nd par	g_p
Xmin	0
Ymin	0
Xmax	100
Ymax	100

(P)eriod Plot the period versus a parameter

(T)wo par Plot the second parameter versus the primary parameter for two-parameter continuations

(Z)oom Use the mouse to zoom in on a region

last (1) par Use the plot parameters from the last 1-parameter plot

last (2) par Use the plot parameters from the last 2-parameter plot

(F)requency Plot Frequency versus parameter

(A)verage Plot the average of a variable versus the parameter.

The two main menu often used are the **h(I)-lo** menu for the bifurcation plot, and the **(T)wo par** for a two parameter plot which serves the purpose of extending the limit point and Hopf bifurcation only.

Before beginning to run the program, the numerical parameters needs to be set as follows:

MENU'A' 3 **NUMERICAL PARAMETERS** involves the following items:

Ntst This is the number of mesh intervals for discretization of periodic orbits. If apparently non convergent results are produced, this may be increased. For following period doubling bifurcations, it is automatically doubled, but can be reset it later. It was set it to 200 for the model considered.

Nmax The maximum number of steps taken along any branch. If more points are needed, this may be increased. 2000 was chosen.

Npr Give complete info every Npr step.

Ds This is the initial step size for the bifurcation calculation. The sign of Ds tells AUTO the direction to change the parameter Since stepsize is adaptive, Ds is just a "suggestion" (it was set it to be 0.02 to direct the branch to the right and changed to -0.02 to direct the branch to the left).

Dsmin The minimum stepsize (positive)

Dsmax The maximum step size. If this is too big, AUTO sometimes misses important points (it was chosen to be 0.3). The smaller it is the closer will be the "special points".

Par Min This is the left-hand limit of the diagram for the principle parameter- i.e. the calculation stops if the parameter is less.

Par Max This is the right-hand limit of the diagram for the principle parameter i.e. the calculation stops for parameter greater that the set value (it was chosen to be 200).

Norm min The lower bound for the L_2 norm of the solution- less than this, the calculation stops.

Norm max The upper bound for the L_2 norm of the solution- greater than this, the calculation stops.

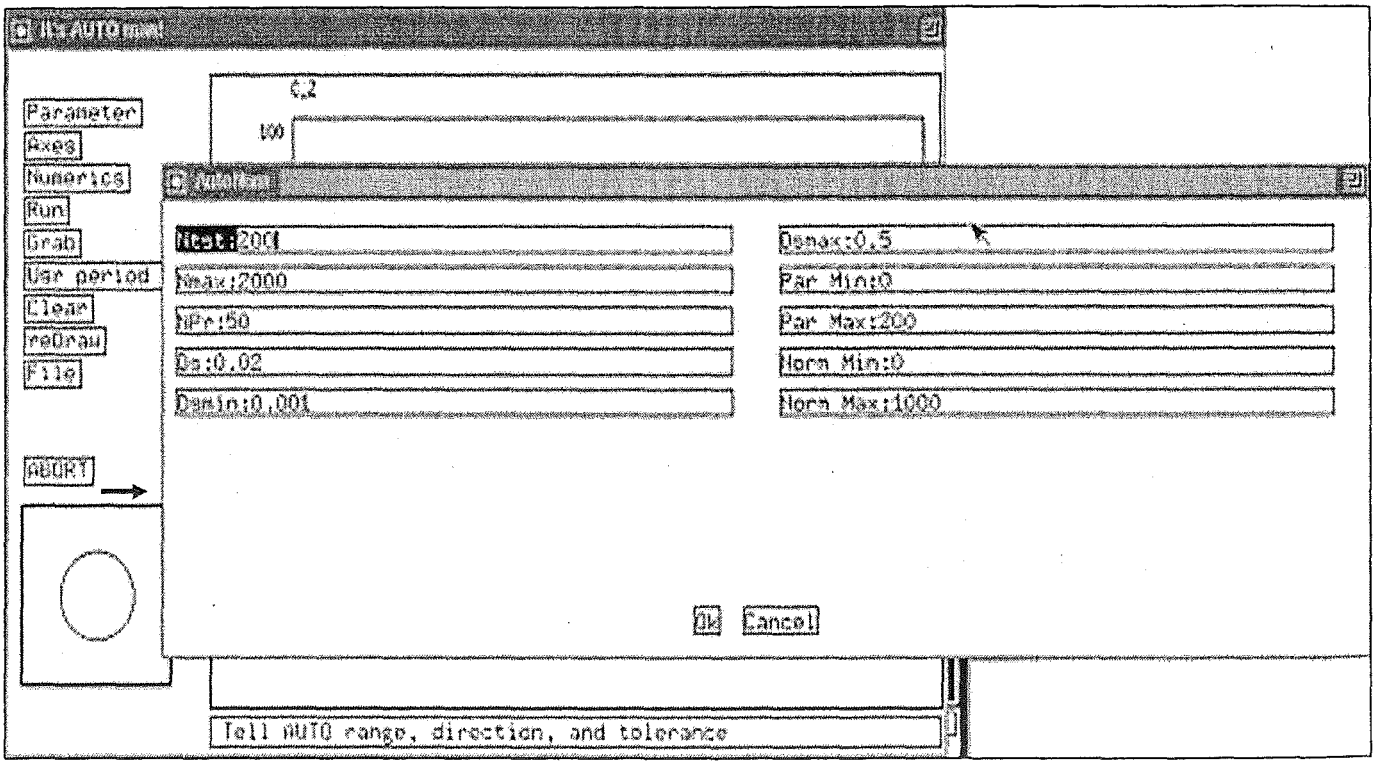

Figure 1.9: The AUTO interface showing the active Numerics window

MENU'A' 4 **RUN STEADY STATES** executes the desired bifurcation plot- many crosses occasionally dispersed with numbers appear. The spaces between the numbers are determined by the **Numerical**

Parameter (i.e. the **Dsmax**). The diagram produced has two different lines and two different circles. Stable fixed points are thick lines, stable periodics are solid circles, unstable fixed points are thin lines and unstable periodics are open circles. The crosses are also called "special" points that AUTO wants to keep, and correspond to the AUTO POINTS in the little window at the bottom of the AUTO window. Special points can be of the following types:

EP Endpoint of a branch

LP Limit point or turning point of a branch

HB Hopf bifurcation point

TR Torus bifurcation from a periodic branch

PD Period doubling bifurcation

UZ User defined function

MX Failure to converge

BP Bifurcation or branch point

MENU'A' 5 **GRAB** The grab item allows the diagram to be observed at a leisurely pace, and to grab special points or regular points for importing into XPP, or to continue a bifurcation calculation. Click on "grab" and information about the points appeared in the info window and a cross appears on the diagram. Use the left and right arrow keys to cruise through the diagram slowly and use TAB to

go from point to point. The right key goes forward and the left backward.

At the bottom of the AUTO main window, information about the particular "special point" under **GRAB** appears – thus the branch (**Br**), the point number (**Pt**), the type of point (**Ty**), the AUTO label (**Lab**), the parameters (**lamda**), value of the norms (**norm**), the y-axis values (**C_z**) and the period (**period**) are given. As the diagram is traversed, stability is shown in the circle. The diagram can be traversed very quickly to the special point, by pressing TAB key. ESC is to exit GRAB, and ENTER to grab the point. If a special point is grabbed, this can be used as a restart point for more AUTO calculations e.g. fixed period, two-parameter studies, and continuations. The AUTO can be re-run, with additional cumulative bifurcation diagrams appended to the old.

The eigenvalues of the specific points can be checked to confirm the stability of a particular point, by grabbing a point and then returning to the XPP window and using the **SING PTS** menu. Besides the eigenvalues, the **Equilibria window** also gives the value of each of the variables, enabling the branch of the steady state to be distinguished (see **Figure 1.10**). A branch of stable equilibrium points appears as a solid line, a branch of unstable equilibrium points appears as light lines, a branch of stable periodic solutions appears as filled in circles, a branch of unstable periodic solutions appears as open circles.

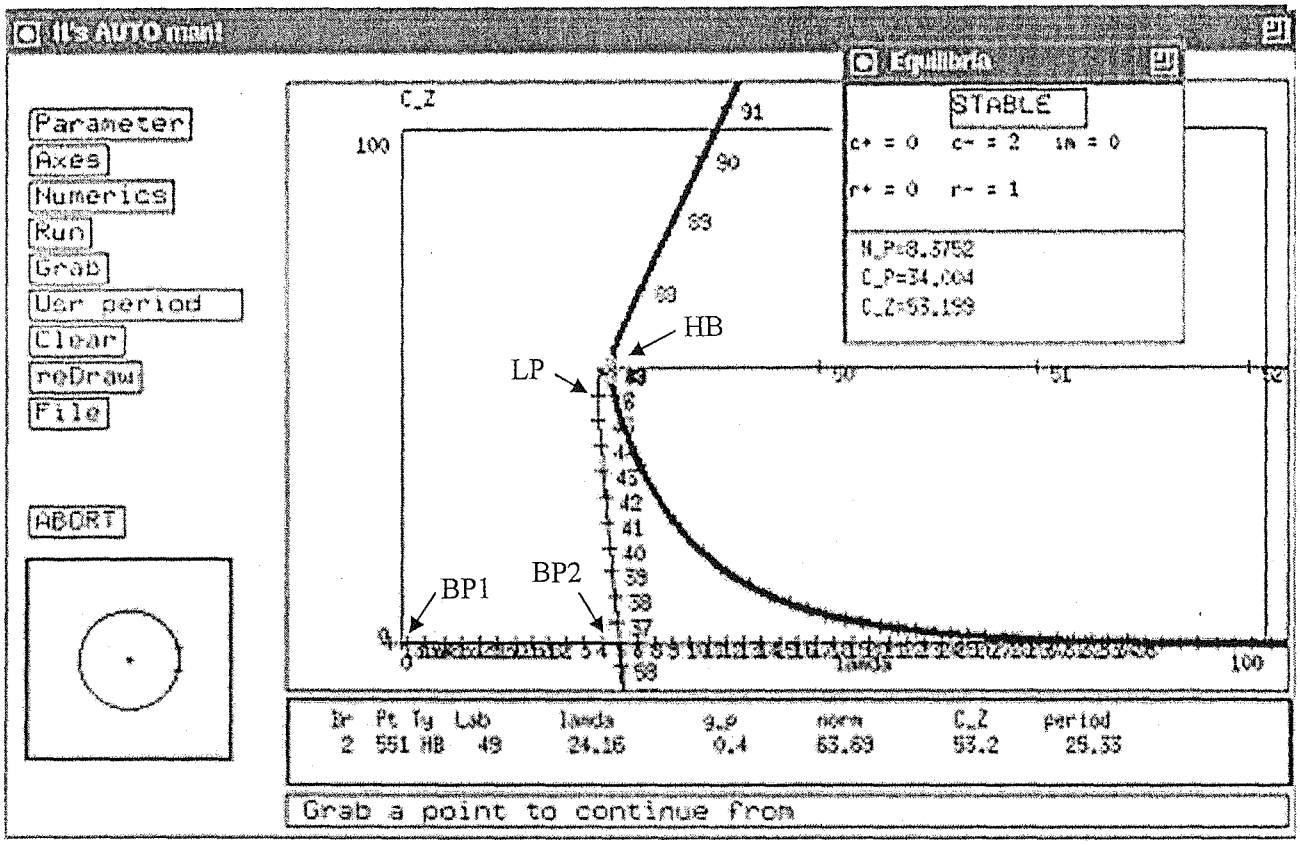

Figure 1.10: The Auto interface showing bifurcation plot of NPZ-new.ode for the one compartment model (featuring BP1 and BP2 which are the bifurcation points, LP the limit points and HB the Hopf Bifurcation or limit cycles)

Finally, in order to save our information in a hardcopy one needs to select:

MENU'A' 6 **FILE**, which allows many actions. However, the two important ones are:

postscript, which enables us to save the bifurcation diagram in hardcopy- e.g. c:\gamma045.ps; and

Reset diagram, which enable us to start another run.

1.8.2 AUTO INTERFACE: Two parameter plot

In order to run a two-parameter plot, first select the **AXES** menu and then set it to the **(T)WO PAR** menu. The special point previously run in the AUTO window (i.e. the bifurcation diagram), can still receive the **GRAB** instruction, and the limit point (LP) and the Hopf bifurcation point (HB) can be extended. As soon as GRAB is selected, a cross appears on a blank 2 parameter axis and TAB allows one to cruise on which point is preferred, simultaneously looking at the bottom most window as an indicator to the type of point been GRAB. Then ENTER and RUN are pressed for a limit point and ENTER, RUN and 2 PARA for a Hopf bifurcation point. To extend the lines to the right, the value of the NUMERICAL PARAMETER must be changed i.e. **DS** positive, and to extend to the left **DS** is changed to a negative value.

1.9 CONCLUSION

Linearization analysis is important, although it is not used extensively in this thesis. The dimension of the system of equations consider, makes them difficult to solve analytically, even to using software MATHEMATICA. Linearization has the advantage of simplifying the nonlinear system of differential equation however, so that an initial stability analysis may be made, although it is of limited assistance especially when there are pure imaginary or zero eigenvalues. Although MATHEMATICA may be used to solve eigenvalues automatically, for a larger dimensions it the matrices need to be reduced to echelon form using elementary operations beforehand.

Bifurcation theory provides a basic understanding of what the package AUTO actually does. Thus while AUTO can do many things, the processes are understood only in terms of bifurcation theory. In particular, AUTO distinguishes steady state or periodic branches.

Chapter 2

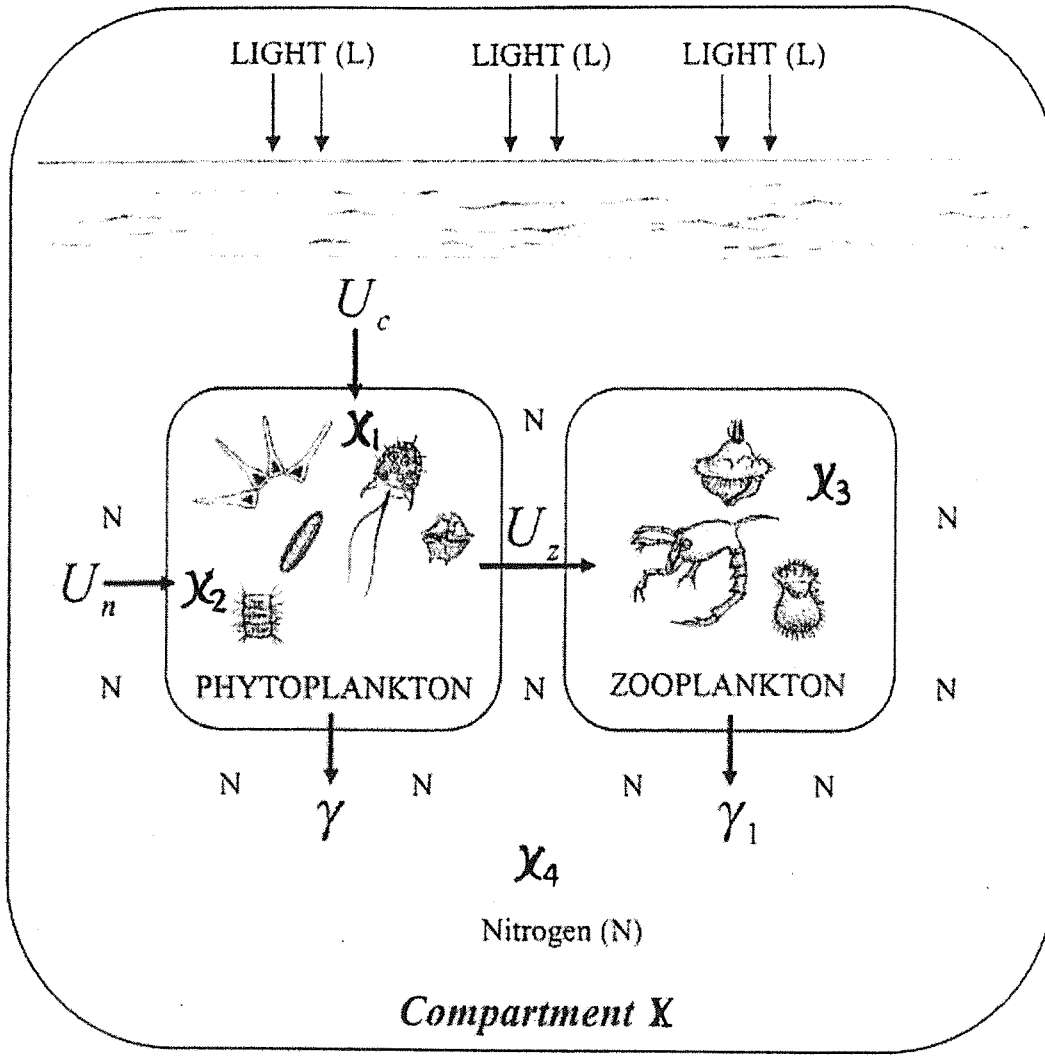

The one compartment phytoplankton-zooplankton-nutrient model

Chapter 2: The one compartment phytoplankton - zooplankton-nutrient model

2.0 Introduction

In this chapter, the mathematical model discussed in Chapter 1 is considered and analyzed. It consists of equation (1.13), (1.14) and (1.15), where the "*exponential term*" in equation (1.14) is replaced by a "*Heaviside term*" of equation (1.16) (see **Section** 1.5.2). Thus, the essential variables in the dynamical population model remain the phytoplankton carbon (x_1) and nitrogen (x_2), the zooplankton carbon (x_3) and the free nitrogen (x_4). The existence of various steady states is investigated in detail with the help of the symbolic software **MATHEMATICA**, and the long term behaviour and the stability of the steady states is further supported by various bifurcation diagrams produced using another sophisticated computer software called **XPP** and **AUTO**.

2.1 The model

Based on the assumptions discussed in Chapter 1 and the assumption that the nutrient (nitrogen) is a closed system such that $\dot{x}_2+\gamma_2\dot{x}_3+\dot{x}_4=0$, recall the mathematical model of a system of three coupled ordinary differential equations in three dependent variables (the phytoplankton carbon x_1 and nitrogen x_2 and the zooplankton carbon x_3)-viz.

$$\dot{x}_1=\mu\left(1-\frac{Qx_1}{x_2}\right)^{+}x_1-\frac{\Gamma x_1x_3}{(x_1+\hat{C})}-\gamma x_1, \tag{2.1}$$

$$\dot{x}_2 = \frac{Ux_1(\lambda - x_2 - \gamma_2 x_3)H\left(R - \frac{x_2}{x_1}\right)}{(\lambda + h - x_2 - \gamma_2 x_3)} - \frac{\Gamma x_2 x_3}{x_1 + \hat{C}} - \gamma x_2, \tag{2.2}$$

$$\dot{x}_3 = \frac{\Gamma x_2 x_3}{\gamma_2(x_1 + \hat{C})} - \gamma_1 x_3. \tag{2.3}$$

This system of ordinary differential equations are to be solved on the domain $\Omega = \{(x, x_2, x_3) : x_1 \geq 0, x_2 \geq 0, x_3 \geq 0\}$.

Note: We have renamed the equations **(1.13)**, **(1.16)** and **(1.15)** as **(2.1)**, **(2.2)** and **(2.3)** respectively for organization purposes.

2.2 Steady states

The steady states of the system **(2.1 – 2.3)** of course correspond to setting the time derivatives to zero. Hence from equation **(2.3)**, either $x_3 = 0$ or $x_2 = \gamma_1\gamma_2(x_1 + \hat{C})/\Gamma$. When $x_3 = 0$, from equation **(2.1)** either $x_1 = 0$ or $x_2 = \frac{Q\mu}{\mu - \gamma}x_1$. Then in the case where $x_3 = 0$ and $x_1 = 0$, equation **(2.2)** implies $x_2 = 0$ so that one of the steady states is the null state $E_0 = (0, 0, 0)$. However, when $x_3 = 0$ and $x_2 = \frac{Q\mu}{\mu - \gamma}x_1$, equation **(2.2)** implies

$$x_2 = \alpha\left(\frac{\gamma(\lambda + h) - \frac{U\lambda(\mu - \gamma)}{Q\mu}}{\frac{\gamma Q\mu}{\mu - \gamma} - U}\right) \text{ where } \alpha = \frac{Q\mu}{\mu - \gamma},$$

or more simply $x_2 = \lambda - \dfrac{Q\mu\gamma h}{\mu U - \gamma(Q\mu + U)}$, provided $\dfrac{x_2}{x_1} < R$ so that $H\left(R - \dfrac{x_2}{x_1}\right) = 1$.

Thus $E_1 = \left(\lambda - \dfrac{Q\mu\gamma h}{\mu U - \gamma(Q\mu + U)},\ \dfrac{Q\mu}{(\mu - \gamma)}\left(\lambda - \dfrac{Q\mu\gamma h}{\mu U + \gamma(Q\mu + U)}\right),\ 0\right)$ is a second steady state. (Note that when $\dfrac{x_2}{x_1} > R$ such that $H\left(R - \dfrac{x_2}{x_1}\right) = 0$, when $x_3 = 0$ there is only the null steady state). On the other hand, for the alternative $x_2 = \gamma_1\gamma_2(x_1 + \hat{C})/\Gamma$ from equation (2.3), either $x_1 = 0$ or $x_3 = \left(-\dfrac{\mu Q}{\gamma_1\gamma_2} + \dfrac{(\mu - \gamma)}{\Gamma}\right)x_1 + \dfrac{\hat{C}(\mu - \gamma)}{\Gamma}$ from (2.1).

The case $x_1 = 0$ would imply $H\left(R - \dfrac{x_2}{x_1}\right) = 0$, so let us proceed to consider $x_3 = \left(-\dfrac{\mu Q}{\gamma_1\gamma_2} + \dfrac{(\mu - \gamma)}{\Gamma}\right)x_1 + \dfrac{\hat{C}(\mu - \gamma)}{\Gamma}$. Thus when $\dfrac{x_2}{x_1} < R$ so that $H\left(R - \dfrac{x_2}{x_1}\right) = 1$, it follows that $\dfrac{Ux_1(\lambda - \dfrac{\gamma_1\gamma_2(x_1 + \hat{C})}{\Gamma} - \gamma x_3)}{(\lambda + h - \dfrac{\gamma_1\gamma_2(x_1 + \hat{C})}{\Gamma} - \gamma x_3)} - \gamma_1\gamma_2 x_3 - \dfrac{\gamma\gamma_1\gamma_2(x_1 + \hat{C})}{\Gamma} = 0$ on substituting $x_2 = \gamma_1\gamma_2(x_1 + \hat{C})/\Gamma$ in (2.2); and substituting $x_3 = \left(-\dfrac{\mu Q}{\gamma_1\gamma_2} + \dfrac{(\mu - \gamma)}{\Gamma}\right)x_1 + \dfrac{\hat{C}(\mu - \gamma)}{\Gamma}$ then yields a quadratic equation of the form $a\left(x_1^*\right)^2 + b\left(x_1^*\right) + c = 0$ in x_1, where

$$a = \left(\frac{\mu Q}{\gamma_1} - \frac{(\mu - \gamma)\gamma_2}{\Gamma} - \frac{\gamma_1\gamma_2}{\Gamma}\right)\left(\left(\frac{(\mu - \gamma)\gamma_1\gamma_2}{\Gamma} - \mu Q + \frac{\gamma\gamma_1\gamma_2}{\Gamma}\right) - U\right)$$

$$b = \left(\frac{\mu Q}{\gamma_1} - \frac{(\mu - \gamma)\gamma_2}{\Gamma} - \frac{\gamma_1\gamma_2}{\Gamma}\right)\left(\frac{(\mu - \gamma)\gamma_1\gamma_2}{\Gamma} - \mu Q + \frac{\gamma\gamma_1\gamma_2}{\Gamma}\right)\hat{C} +$$

$$\left(\frac{(\mu-\gamma)\gamma_1\gamma_2}{\Gamma}-\mu Q+\frac{\gamma\gamma_1\gamma_2}{\Gamma}\right)\left(\lambda+h-\frac{(\mu-\gamma)\hat{C}\gamma_2}{\Gamma}-\frac{\gamma_1\gamma_2\hat{C}}{\Gamma}\right)-U\left(\lambda-\frac{(\mu-\gamma)\hat{C}\gamma_2}{\Gamma}-\frac{\gamma_1\gamma_2\hat{C}}{\Gamma}\right)$$

$c=\left(\frac{(\mu-\gamma)\hat{C}\gamma_1\gamma_2}{\Gamma}+\frac{\gamma\gamma_1\gamma_2\hat{C}}{\Gamma}\right)\left(\lambda+h-\frac{(\mu-\gamma)\hat{C}\gamma_2}{\Gamma}-\frac{\gamma_1\gamma_2\hat{C}}{\Gamma}\right)$. The relevant parameter values are (see **APPENDIX C: TABLES: T1**):

$U=1,\ h=5,\ R=0.25,\ \Gamma=1,\ \hat{C}=100,\ \mu=1,\ Q=0.05,\ \gamma_1=0.25,\ \gamma_2=0.25,$

$\lambda=0.25.$

For these parameter values the roots of the quadratic equation are:

$$x_1^*=\frac{-(20(-4835+3700\gamma+158\lambda\pm2\sqrt{6310900+4410000\gamma^2-399740\lambda+6241\lambda^2+200\gamma(-52130+1659\lambda)}}{79(-9+20\gamma)}$$

(see **APPENDIX B: MATHEMATICA: B1**).

The steady states identified above can be summarized as follows:

a) the null state $E_0=(0,\ 0,\ 0)$;

b) $E_1=\left(\lambda-\frac{Q\mu\gamma h}{\mu U-\gamma(Q\mu+U)},\ \frac{Q\mu}{(\mu-\gamma)}\left(\lambda-\frac{Q\mu\gamma h}{\mu U+\gamma(Q\mu+U)}\right),\ 0\right)$; and

c) $E_2=\left(x_1^*,\ \gamma_1\gamma_2(x_1^*+\hat{C})/\Gamma,\left(-\frac{\mu Q}{\gamma_1\gamma_2}+\frac{(\mu-\gamma)}{\Gamma}\right)x_1^*+\frac{\hat{C}(\mu-\gamma)}{\Gamma}\right)$, where

$$x_1^*=\frac{-(20(-4835+3700\gamma+158\lambda\pm2\sqrt{6310900+4410000\gamma^2-399740\lambda+6241\lambda^2+200\gamma(-52130+1659\lambda)}}{79(-9+20\gamma)}$$

such that λ is the integration constant coming from nutrient conservation and γ is the total rate loss of phytoplankton.

Notes:

i) For $E_1 = \left(x_1,\ \frac{Q\mu}{(\mu-\gamma)} x_1,\ 0 \right)$, the quantity $1 - \frac{Qx_1}{x_2}$ is given by $\frac{\gamma}{\mu}$ which is positive provided $\gamma > 0$.

ii) It is convenient to distinguish the third steady state E_2 as either E_2^+ or E_2^-, depending upon whether $x_3 = \left(-\frac{\mu Q}{\gamma_1 \gamma_2} + \frac{(\mu-\gamma)}{\Gamma} \right) x_1 + \frac{\hat{C}(\mu-\gamma)}{\Gamma}$ is positive or negative (see later).

iii) The singular value $\gamma = \frac{9}{20} = 0.45$ is precluded (because the denominator in the expression for the roots is zero at this point).

2.3 Feasibility regions of the steady states

Before discussing the nature of the steady states, let us consider their regions of feasibility. A priori, all the steady states must satisfy the necessary domain condition $\Omega = \{(x_1, x_2, x_3) : x_1 \geq 0, x_2 \geq 0, x_3 \geq 0\}$ and $Q < \frac{x_2}{x_1} < R$ i.e. $0.05 < \frac{x_2}{x_1} < 0.25$ for the parameters stated in **APPENDIX C: TABLES: T1.**

2.3.1 Feasibility region of the null state E_0

For the null steady state $E_0 = (0,\ 0,\ 0)$, the domain condition is obviously satisfied.

Since $\frac{d}{dt}\left(\frac{x_2}{x_1}\right) = \frac{\dot{x}_2}{x_1} - \frac{x_2}{x_1}\frac{\dot{x}_1}{x_1}$; from the linearized forms of equations (**2.1 to 2.3**) we have $\frac{\dot{x}_1}{x_1} = \mu\left(1 - Q\frac{x_1}{x_2}\right)^+ - \gamma$ and $\frac{\dot{x}_2}{x_1} = \frac{U\lambda}{\lambda + h} H\left(R - \frac{x_2}{x_1}\right) - \gamma\frac{x_2}{x_1}$, it follows that

$$\frac{d}{dt}\left(\frac{x_2}{x_1}\right)+\mu\frac{x_2}{x_1}=\begin{cases}\dfrac{U\lambda}{\lambda+h}+Q\mu, & \dfrac{x_2}{x_1}<R \text{ and } \dfrac{x_2}{x_1}>Q\\ Q\mu, & \dfrac{x_2}{x_1}>R \text{ and } \dfrac{x_2}{x_1}>Q\end{cases}$$

This implies that $\frac{x_2}{x_1}=Ce^{-\mu t}+\frac{U\lambda}{\lambda+h}H\left(R-\frac{x_2}{x_1}\right)+Q\mu$ where C is a constant. Thus as $t\to\infty$, $\frac{x_2}{x_1}=\frac{U\lambda}{\lambda+h}H\left(R-\frac{x_2}{x_1}\right)+Q\mu$. Hence provided $Q<\frac{x_2}{x_1}<R$, $Q<\frac{U\lambda}{\lambda+h}+Q\mu<R$. Thus $0<\frac{U\lambda}{(\lambda+h)}+Q(\mu-1)<R-Q$ so that $0<U\lambda+(\lambda+h)Q(\mu-1)<R-Q(\lambda+h)$, whereas $0<\lambda<\frac{(R-Q)\mu h}{U-(R-Q)\mu}$. Therefore E_0 is only feasible for $0<\lambda<1.25$, using parameter stated in **APPENDIX C: TABLES: T1**.

2.3.2 Feasibility region of the steady state E_1

For the steady state $E_1=\left(\lambda-\frac{Q\mu\gamma h}{\mu U-\gamma(Q\mu+U)}, \frac{Q\mu}{(\mu-\gamma)}\left(\lambda-\frac{Q\mu\gamma h}{\mu U+\gamma(Q\mu+U)}\right), 0\right)$, the domain condition is satisfied when $x_1\geq 0$ (we are not interested in negative values), thus we have $\lambda-\frac{\gamma Q\mu h}{\mu U-\gamma(Q\mu+U)}\geq 0$. The inequality $\lambda\geq\frac{\gamma Q\mu h}{\mu U-\gamma(Q\mu+U)}$ then yields $\lambda\geq\frac{20\gamma}{4(20-21\gamma)}$ or $\gamma\leq\frac{20\lambda}{5+21\lambda}$ for the parameters in **APPENDIX C: TABLES: T1**. For E_1 to satisfy the condition $Q<\frac{x_2}{x_1}<R$, note that $0<\gamma<\mu(1-\frac{Q}{R})$, or $0<\gamma<0.8$ for the parameters stated in **APPENDIX C: TABLES: T1**.

2.3.3 Feasibility region of the steady state E_2

For the steady state $E_2 = \left(x_1^*,\ \gamma_1\gamma_2(x_1^* + \hat{C})/\Gamma, \left(-\frac{\mu Q}{\gamma_1\gamma_2} + \frac{(\mu-\gamma)}{\Gamma} \right) x_1^* + \frac{\hat{C}(\mu-\gamma)}{\Gamma} \right)$ such that

$$x_1^* = \frac{-(20(-4835 + 3700\gamma + 158\lambda \pm 2\sqrt{6310900 + 4410000\gamma^2 - 399740\lambda + 6241\lambda^2 + 200\gamma(-52130 + 1659\lambda)}}{79(-9 + 20\gamma)}$$

the domain condition requires $\gamma_1\gamma_2(x_1^* + \hat{C})/\Gamma > 0$ and $\left(-\frac{\mu Q}{\gamma_1\gamma_2} + \frac{\mu-\gamma}{\Gamma} \right) x_1 * + \hat{C}\frac{\mu-\gamma}{\Gamma} > 0$

for all $x_1^* > 0$. Thus it has to be in the region $x_1^* < \hat{C}$ (or $x_1^* < 100$) and $x_1^* > \frac{500(\gamma-1)}{1-5\gamma}$

respectively for the parameters stated in **APPENDIX C: TABLES: T1**. The additional requirement $Q < \frac{x_2}{x_1} < R$ is satisfied provided $\frac{100}{3} < x_1^*$ and $x_1^* > -500$ using parameter stated in **APPENDIX C: TABLES: T1**.

2.4 Stability of the steady states

In this section, the stability of the three steady states is analyzed in detail. In linearised theory, stability corresponds to three negative eigenvalues, for model involving three dependent variables. It is convenient to use the software **MATHEMATICA**. The analytical calculation is most complicated in the case of the steady state E_2 so the stability is further investigated using diagrams produced by the program **XPP** and **AUTO**.

2.4.1 Stability of the null state E_0

Let us first of all consider the stability of the null state $E_0 = (0,\ 0,\ 0)$. In addition to determining the *local (linear)* stability of the null state, the *global* stability is also investigated.

Theorem 2.1

The null state E_0 is locally asymptotically stable if and only if it falls in the feasible region $0 < \lambda < 1.25$ (see **section 2.3.1**) and $\lambda < \dfrac{\gamma Q\mu h}{U\mu - \gamma(Q\mu + U)}$ (i.e. $\lambda < \dfrac{5\gamma}{20 - 21\gamma}$) or $\gamma < \dfrac{U\lambda\mu}{Q\mu(\lambda + h) + U\lambda}$ (i.e. $\gamma < \dfrac{20\lambda}{5 + 21\lambda}$).

Proof:

The linearized form of equation **(2.3)** is $\dot{x}_3 = -\gamma_1 x_3$. Thus $x_3 = x_3(0)e^{-\gamma_1 t}$, corresponding to the negative eigenvalue $-\gamma_1$. The priori assumption that $x_1 = ae^{\alpha t}$ and $x_2 = be^{\alpha t}$ as $x_1,\ x_2 \to 0$ is consistent with $\dfrac{x_2}{x_1} = \text{constant}$ as shown in **section 2.3.1**.

Substituting $x_1 = ae^{\alpha t}$ into the linearized form of equation of **(2.1)** yields $a\alpha e^{\alpha t} = \mu(1 - \dfrac{Qx_1}{x_2})^{+} ae^{\alpha t} - \gamma ae^{\alpha t}$ and therefore for $a \neq 0$ one has $\alpha = \mu(1 - \dfrac{Qa}{b}) - \gamma$.

Substituting $x_1 = ae^{\alpha t}$ and $x_2 = be^{\alpha t}$ into the linearized form of equation **(2.2)** yields $\alpha be^{\alpha t} = \dfrac{U\lambda ae^{\alpha t}}{(\lambda + h)} - \gamma be^{\alpha t}$ so that $\alpha = \dfrac{U\lambda a}{(\lambda + h)b} - \gamma$, and combining with $\alpha = \mu(1 - \dfrac{Qa}{b}) - \gamma$ the result $\dfrac{a}{b} = \dfrac{\mu\left(1 - \dfrac{Qa}{b}\right)(\lambda + h)}{U\lambda}$ or $\dfrac{a}{b} = \dfrac{\mu}{Q\mu + \dfrac{U\lambda}{(\lambda + h)}}$ follows.

Thus the corresponding eigenvalue is $\alpha = \left(\frac{U\lambda\mu}{Q\mu(\lambda+h)+U\lambda}\right) - \gamma$, so the null state E_0 is stable if and only if $\left(\frac{U\lambda\mu}{Q\mu(\lambda+h)+U\lambda}\right) - \gamma < 0$. Thus we have $\lambda < \left(\frac{\gamma Q\mu h}{U\mu - \gamma(Q\mu+U)}\right)$ (i.e. $\lambda < \frac{5\gamma}{20-21\gamma}$) or $\gamma < \frac{U\lambda\mu}{Q\mu(\lambda+h)+U\lambda}$ (i.e. $\gamma < \frac{20\lambda}{5+21\lambda}$).

(cf. **Figure 2.1**). ■

Note: For $a = 0$, substituting $x_2 = be^{\alpha t}$ into the linearized form of equation of (**2.2**) yields $b\alpha e^{\alpha t} = -\gamma b e^{\alpha t}$ so that $\alpha = -\gamma$ (i.e. another strictly negative eigenvalue).

Theorem 2.2

The null state E_0 is globally asymptotically stable (*g. a. s*) if $\gamma > \mu\left(1 - \frac{Q}{R}\right)$, or $\gamma > 0.8$ for the parameters stated in **APPENDIX C: TABLES: T1**.

Proof:

Firstly if $x_1(t) \to 0$ as $t \to \infty$, then $x_2(t), x_3(t) \to 0$ as $t \to \infty$. In order to prove that the null state E_0 is globally asymptotically stable (g. a. s), appropriate lower (i.e. $y_1(t)$) and upper (i.e. $z_1(t)$) bounds for equation (**2.1**) such that $z_1(t) \geq x_1(t) \geq y_1(t)$ must be found. Obviously, a lower bound is $y_1(t) \equiv 0$. Now from equation (**2.1**) $\dot{x_1}(t) \leq \left(\mu\left(1 - \frac{Q}{R}\right) - \gamma\right)x_1$, hence $x_1(t) \leq x_1(0)\exp\left((\mu\left(1 - \frac{Q}{R}\right) - \gamma)t\right)$ $t \to 0$ as $t \to \infty$ if $\mu\left(1 - \frac{Q}{R}\right) - \gamma < 0$ (i.e. $\gamma > 0.8$ for the parameters of **APPENDIX C: TABLES: T1**).

Thus the null state E_0 is globally asymptotically stable (*g.a.s*) provided $\gamma > \mu\left(1-\frac{Q}{R}\right)$

or $\gamma > 0.8$ for the parameters stated in **APPENDIX C: TABLES: T1.**

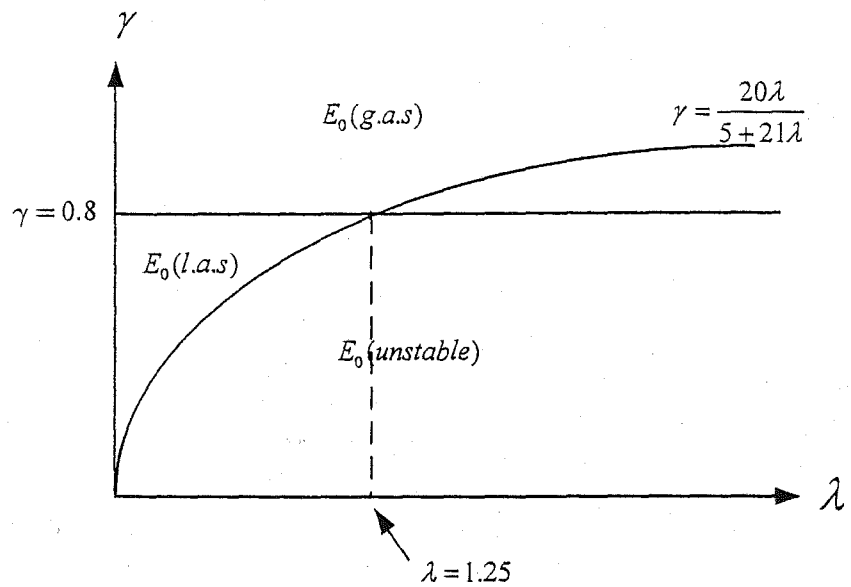

Figure 2.1: The feasibility and stability boundary of the null states E_0 (Recall that the feasible region is given by $0 < \lambda < 1.25$, locally asymptotically table (*l.a.s*) at $\lambda < \frac{5\gamma}{20-21\gamma}$ or $\gamma < \frac{20\lambda}{5+21\lambda}$ and globally asymptotically stable (*g.a.s*) at $\gamma > 0.8$)

2.4.2 Stability of the steady state E_1

In order to prove that the steady state $E_1 = \left(\lambda - \frac{Q\mu\gamma h}{\mu U - \gamma(Q\mu+U)}, \frac{Q\mu}{(\mu-\gamma)}\left(\lambda - \frac{Q\mu\gamma h}{\mu U+\gamma(Q\mu+U)}\right), 0\right)$ is locally stable, equations (2.1 – 2.3) are linearized about the steady state E_1 and the determinant of the

associated Jacobian matrix is considered (local stability corresponds to all three of its eigenvalues being negative - see **APPENDIX B: MATHEMATICA: B2**). Recall that from (2.2) it is only necessary to consider the case $\frac{x_2}{x_1}\langle R$ when $H\left(R-\frac{x_2}{x_1}\right)=1$. The Jacobian matrix J is: $J(\bar{x_1},\bar{x_2},\bar{x_3})=\begin{vmatrix} J_{11} & J_{12} & J_{13} \\ J_{21} & J_{22} & J_{23} \\ J_{31} & j_{32} & J_{33} \end{vmatrix}_{(\bar{x_1},\bar{x_2},\bar{x_3})}$, where

$$J_{11}=(\mu-\gamma)-\left(\frac{2\mu Q\bar{x_1}}{\bar{x_2}}\right)^{+}-\frac{\Gamma\bar{x_3}}{\bar{x_1}+\hat{C}}-\frac{\Gamma\bar{x_1}\bar{x_3}}{\left(\bar{x_1}+\hat{C}\right)^2},\qquad J_{12}=\frac{\mu Q\bar{x_1}^2}{\bar{x_2}^2},\qquad J_{13}=-\frac{\Gamma\bar{x_1}}{\bar{x_1}+\hat{C}},$$

$$J_{21}=\frac{U(\lambda-\bar{x_2}-\gamma_2\bar{x_3})}{(\lambda+h-\bar{x_2}-\gamma_2\bar{x_3})}+\frac{\Gamma\bar{x_2}\bar{x_3}}{\left(\bar{x_1}+\hat{C}\right)^2},$$

$$J_{22}=-\frac{U\bar{x_1}}{(\lambda+h-\bar{x_2}-\gamma_2\bar{x_3})}+\frac{U\bar{x_1}(\lambda-\bar{x_2}-\gamma_2\bar{x_3})}{(\lambda+h-\bar{x_2}-\gamma_2\bar{x_3})^2}-\frac{\Gamma\bar{x_3}}{\bar{x_1}+\hat{C}}-\gamma,$$

$$J_{23}=-\frac{U\bar{x_1}\gamma_2}{(\lambda+h-\bar{x_2}-\gamma_2\bar{x_3})}+\frac{U\bar{x_1}\gamma_2(\lambda-\bar{x_2}-\gamma_2\bar{x_3})}{(\lambda+h-\bar{x_2}-\gamma_2\bar{x_3})^2}\frac{\Gamma\bar{x_2}}{\bar{x_1}+\hat{C}},$$

$$J_{31}=-\frac{\Gamma\bar{x_2}\bar{x_3}}{\gamma_2\left(\bar{x_1}+\hat{C}\right)^2},\ J_{32}=\frac{\Gamma\bar{x_3}}{\gamma_2\left(\bar{x_1}+\hat{C}\right)},\ J_{33}=\frac{\Gamma\bar{x_2}}{\gamma_2\left(\bar{x_1}+\hat{C}\right)}-\gamma_1.$$

Substituting $\bar{x_1}=\frac{(\mu-\gamma)}{Q\mu}\left(\lambda+\frac{Q\mu\gamma h}{Q\mu\gamma-U(\mu-\gamma)}\right)$, $\bar{x_2}=\lambda+\frac{Q\mu\gamma h}{Q\mu\gamma-U(\mu-\gamma)}$, $\bar{x_3}=0$,

and again using parameter stated in **APPENDIX C: TABLES: T1**, after elementary row operations the Jacobian matrix can be rewritten as

$$J(\bar{x_1},\bar{x_2},0)=\begin{bmatrix} J_{33} & 0 & 0 \\ J_{23} & J_{22} & J_{21} \\ J_{13} & J_{12} & J_{11} \end{bmatrix},$$

where $J_{11}=\gamma-1,$ $J_{12}=20(1-\gamma)^2,$ $J_{21}=\dfrac{\gamma}{20(1-\gamma)},$

$$J_{22}=-\frac{\gamma^2}{20(1-\gamma)}-\frac{\lambda(21\gamma-20)^2}{100(1-\gamma)} \text{ and } J_{33}=-\frac{1}{4}+\frac{4\bar{x_2}}{(\bar{x_1}+100)}.$$

Note that J_{13} and J_{23} are irrelevant in determining the eigenvalues. However, obviously one of the eigenvalues is J_{33}. With this the bifurcation value is found to be $\lambda<\dfrac{25}{5\gamma-1}+\dfrac{5\gamma}{20-21\gamma}$ and the other two eigenvalues follow from simple algebra. The quadratic equation is $a\alpha^2+b\alpha+c=0$ where

$$a=1$$

$$b=\left(\frac{21\gamma-20}{20(1-\gamma)}\right)\left[\gamma-\frac{(20-21\gamma)\lambda}{5}\right]+1$$

$$c=\left(\frac{20-21\gamma}{20}\right)\left[-\gamma+\frac{(20-21\gamma)\lambda}{5}\right].$$

Now $b>0$ and $c>0$, given the previous inequalities $\lambda>\dfrac{5\gamma}{20-21\gamma}$ and $\gamma<1$. Thus the other two eigenvalues are of the form $\alpha_1,\alpha_2=\dfrac{-b\pm\sqrt{b^2-4c}}{2}$ where $\sqrt{b^2-4c}<|b|$ since $c>0$, and hence negative if they are real since $b>0$. Moreover, if these eigenvalues are complex, their real part $-b$ is negative. Thus the steady state E_1 is locally asymptotically stable (*l.a.s*) provided $\lambda<\dfrac{25}{5\gamma-1}+\dfrac{5\gamma}{20-21\gamma}$ and $\lambda>\dfrac{5\gamma}{20-21\gamma}$. Recall that E_1 is only feasible when $0<\gamma<0.8$ (its feasibility and asymptotically

stable regions are shown in **Figure 2.2**, together with the boundary for the null state E_0).

Note: E_0 is only stable if $\lambda < \frac{5\gamma}{20-21\gamma}$ while E_1 is only stable if $\lambda > \frac{5\gamma}{20-21\gamma}$. Thus it is impossible for both E_0 and E_1 to be stable together.

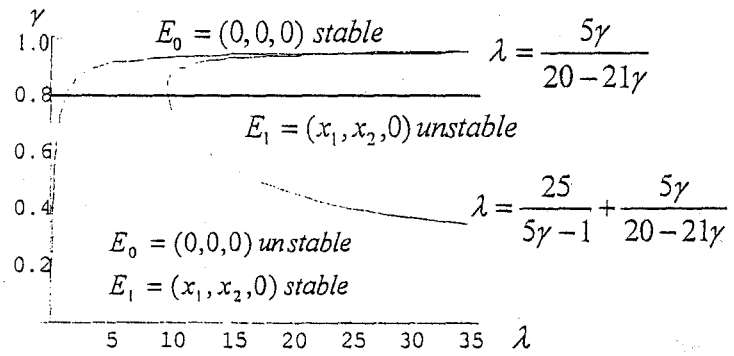

Figure 2.2: The feasibility region and the asymptotically stable region for the steady state E_1. (Recall that the feasible region is given by $\lambda > \frac{5\gamma}{20-21\gamma}$ and $0 < \gamma < 0.8$, locally asymptotically table (*l.a.s*) at $\lambda < \frac{25}{5\gamma-1} + \frac{5\gamma}{20-21\gamma}$ and $\lambda > \frac{5\gamma}{20-21\gamma}$)

2.4.3 Stability of the steady state E_2

Let us now analyze the stability of the third steady state

$$E_2 = \left(x_1^*,\ \gamma_1\gamma_2(x_1^* + \hat{C})/\Gamma, \left(-\frac{\mu Q}{\gamma_1\gamma_2} + \frac{(\mu-\gamma)}{\Gamma} \right) x_1^* + \frac{\hat{C}(\mu-\gamma)}{\Gamma} \right),$$

where

$$x_1^* = \frac{-(20(-4835+3700\gamma+158\lambda \pm 2\sqrt{6310900+4410000\gamma^2-399740\lambda+6241\lambda^2+200\gamma(-52130+1659\lambda)}}{79(-9+20\gamma)}$$

for the parameters of **APPENDIX C: TABLES: T1**. In order to prove that the steady state is locally stable, the equations (**2.1 - 2.3**) are now of course linearized about the steady state E_2. Again let us consider the case when $\frac{x_2}{x_1} < R$ such that $H\left(R-\frac{x_2}{x_1}\right)=1$.

For the parameters of **APPENDIX C: TABLES: T1**, the Jacobian matrix J is:

$$J(\bar{x}_1,\bar{x}_2,\bar{x}_3)=\begin{vmatrix} J_{11} & J_{12} & J_{13} \\ J_{21} & J_{22} & J_{23} \\ J_{31} & j_{32} & J_{33} \end{vmatrix}_{(\bar{x}_1,\bar{x}_2,\bar{x}_3)}, \text{ where}$$

$$J_{11}=(1-\gamma)-\left(\frac{\bar{x}_1}{10\bar{x}_2}\right)^{+}-\frac{\bar{x}_3}{\bar{x}_1+100}-\frac{\bar{x}_1\bar{x}_3}{\left(\bar{x}_1+100\right)^2},\ J_{12}=\frac{\bar{x}_1^{\,2}}{20\bar{x}_2^{\,2}},$$

$$J_{13}=-\frac{\bar{x}_1}{\bar{x}_1+100},\ J_{21}=\frac{(\lambda-\bar{x}_2-\frac{\bar{x}_3}{4})}{(\lambda+5-\bar{x}_2-\frac{\bar{x}_3}{4})}+\frac{\bar{x}_2\bar{x}_3}{\left(\bar{x}_1+100\right)^2},$$

$$J_{22}=-\frac{\bar{x}_1}{(\lambda+5-\bar{x}_2-\frac{\bar{x}_3}{4})}+\frac{\bar{x}_1(\lambda-\bar{x}_2-\frac{\bar{x}_3}{4})}{(\lambda+5-\bar{x}_2-\frac{\bar{x}_3}{4})^2}-\frac{\bar{x}_3}{\bar{x}_1+100}-\gamma,$$

$$J_{23}=-\frac{\bar{x}_1}{4(\lambda+5-\bar{x}_2-\frac{\bar{x}_3}{4})}+\frac{\bar{x}_1\gamma_2(\lambda-\bar{x}_2-\frac{\bar{x}_3}{4})}{4(\lambda+5-\bar{x}_2-\frac{\bar{x}_3}{4})^2}-\frac{\bar{x}_2}{\bar{x}_1+100},$$

$$J_{31}=-\frac{4\bar{x}_2\bar{x}_3}{\left(\bar{x}_1+100\right)^2},\ J_{32}=\frac{4\bar{x}_3}{\left(\bar{x}_1+100\right)},\ J_{33}=\frac{4\bar{x}_2}{\left(\bar{x}_1+100\right)}-\frac{1}{4}.$$

Multiplying the third column by 4 and subtracting the second and then substituting $\bar{x}_2 = \frac{\bar{x}_1 + \hat{C}}{16}$ and $\bar{x}_3 = -\frac{4\bar{x}_1}{5} + (1-\gamma)(\bar{x}_1 + \hat{C})$, yields:

$$J_{11} = \frac{\bar{x}_1}{(\bar{x}_1+100)}\left(\frac{1}{5}-\gamma\right) - \frac{4\bar{x}_1^{\,2}}{5\left(\bar{x}_1+100\right)^2},\ J_{12} = -\frac{64\,\bar{x}_1^{\,2}}{5(\bar{x}_1+100)^2} - \frac{4\,\bar{x}_1}{(\bar{x}_1+100)},$$

$$J_{13} = -\frac{\bar{x}_1}{\bar{x}_1+100},\ J_{21} = -\frac{5}{5+\left(\lambda+\left(-\frac{5}{16}+\frac{\gamma}{4}\right)\left(\bar{x}_1+100\right)+\frac{\bar{x}_1}{5}\right)} - \frac{\bar{x}_1}{20\left(\bar{x}_1+100\right)} + \frac{17}{16} - \frac{\gamma}{16},$$

$$J_{22} = \frac{3}{4} - \frac{4\,\bar{x}_1}{5(\bar{x}_1+100)},$$

$$J_{23} = -\frac{5\,\bar{x}_1}{4\left(\lambda+5+\left(-\frac{5}{16}+\frac{\gamma}{4}\right)\left(\bar{x}_1+100\right)+\frac{\bar{x}_1}{5}\right)^2} - \frac{1}{16},$$

$$J_{31} = -\frac{(1-\gamma)}{4} + \frac{\bar{x}_1}{5\left(\bar{x}_1+100\right)},\ J_{32} = -4(1-\gamma) + \frac{16\,\bar{x}_1}{5\left(\bar{x}_1+100\right)},\ J_{33} = 0.$$

Now dividing the second row by 16 and interchanging the second and third columns renders the matrix $|J-\alpha I|$ such that $J_{11} = \frac{\bar{x}_1}{(\bar{x}_1+100)}\left(-\frac{9}{20}+\gamma\right)$, $J_{12} = -\frac{\bar{x}_1}{(\bar{x}_1+100)}$,

$$J_{13} = -\frac{64\,\bar{x}_1^{\,2}}{5(\bar{x}_1+100)^2} - \frac{4\,\bar{x}_1}{(\bar{x}_1+100)},$$

$$J_{21}=\frac{5}{5+\left(\lambda+\left(-\frac{5}{16}+\frac{\gamma}{4}\right)\left(\bar{x}_1+100\right)+\frac{\bar{x}_1}{5}\right)}-\frac{65}{64}+\frac{\gamma}{16}$$

$$J_{22}=-\frac{5\bar{x}_1}{4\left(\lambda+5+\left(-\frac{5}{16}+\frac{\gamma}{4}\right)\left(\bar{x}_1+100\right)+\frac{\bar{x}_1}{5}\right)^2}-\frac{1}{16},$$

$$J_{23}=\frac{3}{4}-\frac{4\bar{x}_1}{5(\bar{x}_1+100)}$$

$J_{31}=0,\ J_{32}=0,\ J_{33}=-4(1-\gamma)+\frac{16\bar{x}_1}{5(\bar{x}_1+100)}$. The eigenvalues α of the Jacobian matrix therefore satisfy $(J_{33}-\alpha)\left[(J_{11}-\alpha)(J_{22}-\alpha)-J_{12}J_{21}\right]=0$, so one of the eigenvalues is $J_{33}=-4(1-\gamma)+\frac{16\bar{x}_1}{5(\bar{x}_1+100)}$. Using MATHEMATICA, one obtains

$\lambda=\frac{500-530\gamma+25\gamma^2}{-20+121\gamma-105\gamma^2}=\frac{25}{5\gamma-1}+\frac{5\gamma}{20-21\gamma}$. This expression found is the stability curve which represents the boundary of the steady state E_1 and E_2 and it is consistent with the stability analysis about the steady state E_1 in **section 2.4.2** (see **APPENDIX B: MATHEMATICA: B3**). The solution of the equation $(J_{11}-\alpha)(J_{22}-\alpha)-J_{12}J_{21}=0$ from the square bracket has not been found, because the expression is too complicated (the steady state itself involves a quadratic equation). Rather, the stability of the steady state E_2 has been explored via bifurcation diagrams produced by the computer software **XPP** and **AUTO** by Doedel [10,11] as discussed in the next section.

2.5 Bifurcation analysis of the one compartment model

This section describes the bifurcation diagrams for the one compartment model via the software package **XPP** and **AUTO**. While the nature of the steady states E_0 and E_1 are fairly well understood, this is not the case for the our steady state E_2, and in any case the computation also can confirm their behaviour. The objectives are:

i) to identify the points where states change from one state to another (**Bifurcation Points** or **BP**), the coexistence of steady states (**Limit Points** or **LP**) and the presence of any periodic solutions (**Hopf Bifurcation Points** or **HB**), and

ii) to confirm the *stability* of the steady states (since **AUTO** can give the eigenvalues at each point).

All the parameters are kept fixed except γ and λ. Various values of γ between 0 to 0.8 were selected, since we know (c.f. **Theorem 2.2**) E_0 is globally asymptotically stable (*g. a. s*) when $\gamma > 0.8$. Each computation provides a one-dimensional cross-section of parameter space, where a dependent variable x_2 is plotted against the parameter λ (see **Figure 2.3** to **Figure 2.15**). However, by grabbing a limit point (**LP**) or a Hopf bifurcation point (**HB**) from the one-dimensional diagram, we can automatically produce a two-parameter diagram such as parameter γ against λ. However, **AUTO** cannot provide to a two-parameter diagram in the case of bifurcation point **BP**.

Let us now proceed to discuss details of the bifurcation diagrams for the one-compartment model shown in **Figure 2.3** to **Figure 2.15** for the value $0.4 < \gamma < 0.9$,

and in particular observe how the steady states change from one form into another (see **APPENDIX C: TABLES: T2a** for the bifurcation points).

i) **Figure 2.3** and **Figure 2.4** show the respective bifurcation diagrams for x_2 and x_3 against the parameter λ at $\gamma = 0.4$. Viewed from the left to the right, the first obvious feature is **BP1** at the point $\lambda = 0.1724$ (Before that there is a narrow region where the steady state E_0 is stable. The diagram is magnified to show this. It can also be detected by grabbing the point when using **AUTO** program). At $\lambda = 0.1724$, the null state E_0 becomes unstable, and the system moves to the steady state E_1 which is stable for larger λ (c.f. **Theorem 2.1** and **APPENDIX C: TABLES: T2b**). An **LP** then occurs at $\lambda = 22.66$, when E_2^+ is noticeably stable at the *tip* just before **HB** - indeed, E_2^+ is simultaneously stable with E_1 until the Hopf bifurcation or the periodic branch (**HB**) is reached at $\lambda = 24.16$. There is another bifurcation point (**BP2**) at $\lambda = 25.17$ (c.f. **APPENDIX C: TABLES: T2c**), so that E_2^+ coexists with E_1 from $\lambda = 22.66$ to $\lambda = 25.17$, from $\lambda = 24.16$ to $\lambda = 25.17$ with the **HB** coexisting with E_1. The steady state E_2^- is also stable, but it is ignored because x_3 is negative i.e. unfeasible (c.f. the bifurcation diagram of x_3 against λ in **Figure 2.4**).

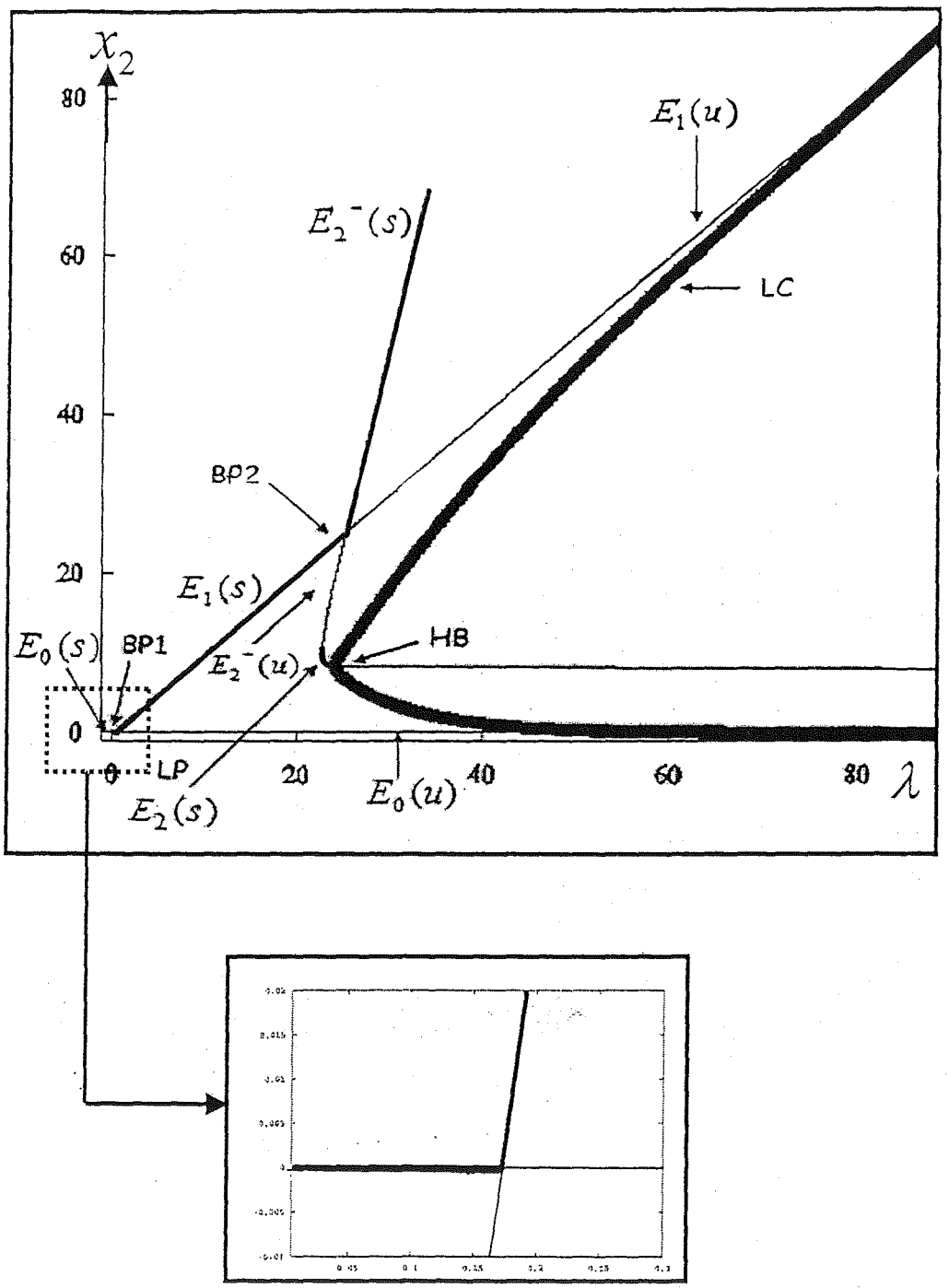

Figure 2.3: The bifurcation diagram x_2 against λ for one compartment model at $\gamma = 0.4$ showing the bifurcation point BP1 (λ = 0.1724), BP2 (λ = 25.17); limit point LP (λ = 22.66) and the Hopf bifurcation point HB (λ = 24.16).

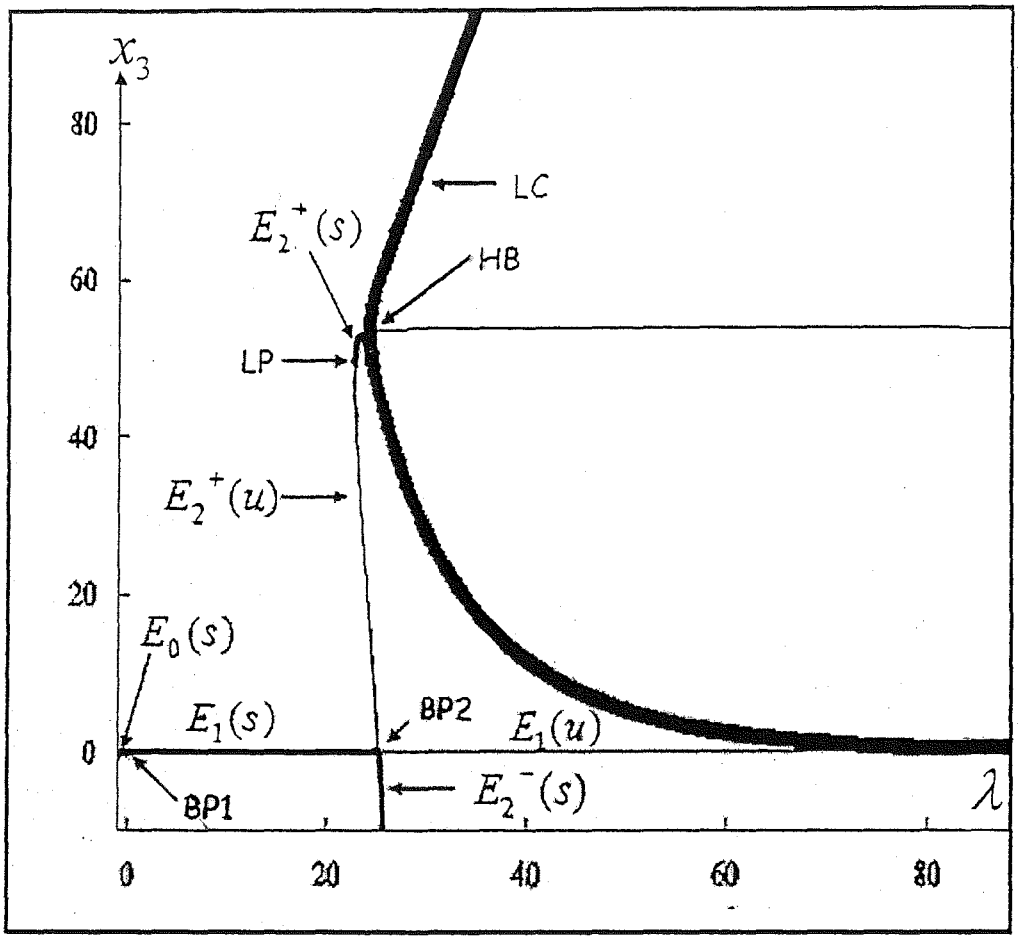

Figure 2.4: The bifurcation diagram x_3 against λ for one compartment model at $\gamma = 0.4$ showing the bifurcation point BP1(λ= 0.1724), BP2 (λ= 25.17); limit point LP (λ= 22.66) and the Hopf bifurcation point HB (λ= 24.16) (Note: It is mentioned that the steady state E_2^- is stable and yet unfeasible. The transition of a steady state solution from a feasible region to an unfeasible region is sometimes known as a *boundary bifurcation*).

ii) **Figure 2.5** and **Figure 2.6** show the respective bifurcation diagrams for x_2 and x_3 against the parameter λ when $\gamma = 0.45$. There is a bifurcation point (**BP1**) at the point $\lambda = 0.2132$, where the null state E_0 changes from stable to unstable and the

steady state E_1 occurs (c.f. **Theorem 2.1** and **APPENDIX C: TABLES: T2b**). The next bifurcation point (**BP2**) occurs at $\lambda = 20.21$, where E_1 becomes unstable and the stable E_2^+ branch occurs (c.f. **APPENDIX C: TABLES: T2c**). Periodicity then follows at the Hopf bifurcation point (**HB**) at $\lambda = 22.55$. The Limit point is not featured here which is found in **Figure 2.3** and **Figure 2.4**.

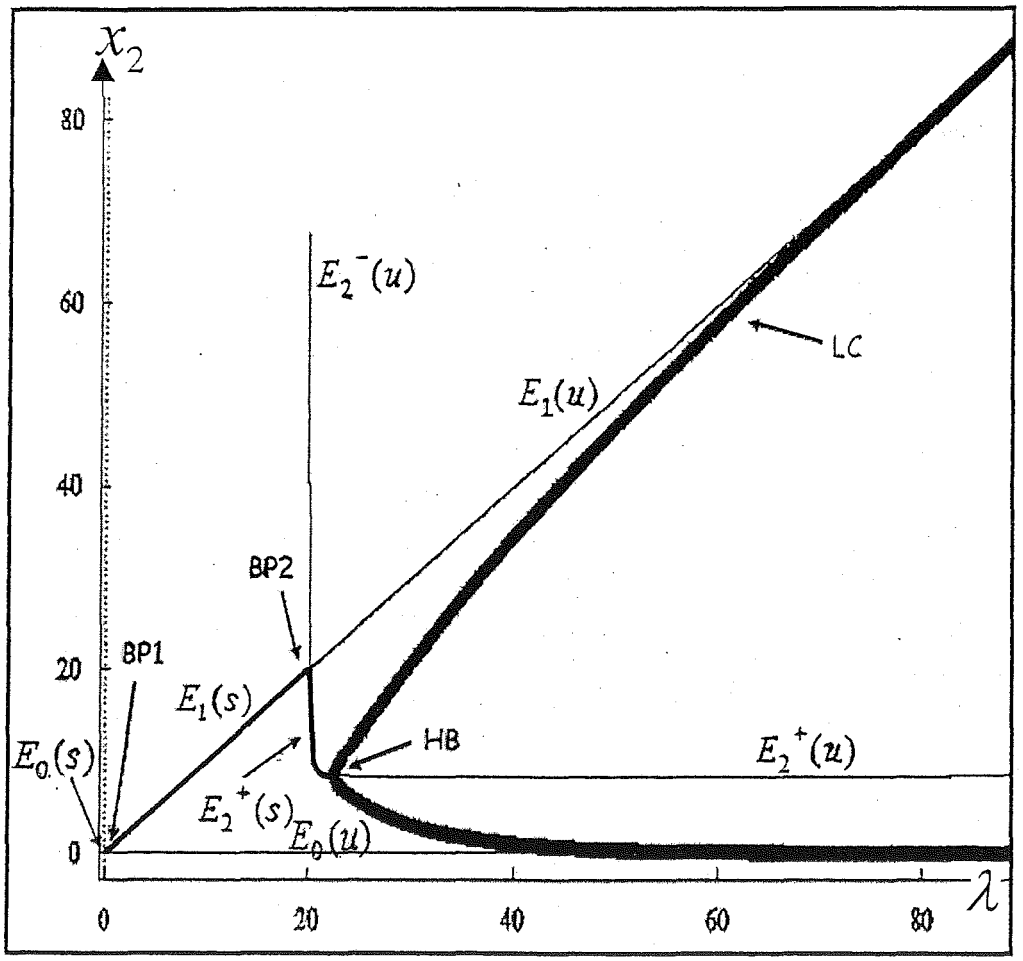

Figure 2.5: The bifurcation diagram x_2 against λ for one compartment model at $\gamma = 0.45$ showing the bifurcation point BP1 ($\lambda = 0.2132$), BP2 ($\lambda = 20.21$) and the Hopf bifurcation point HB ($\lambda = 22.55$) (Note: Here the unfeasible steady state E_2^- is now unstable).

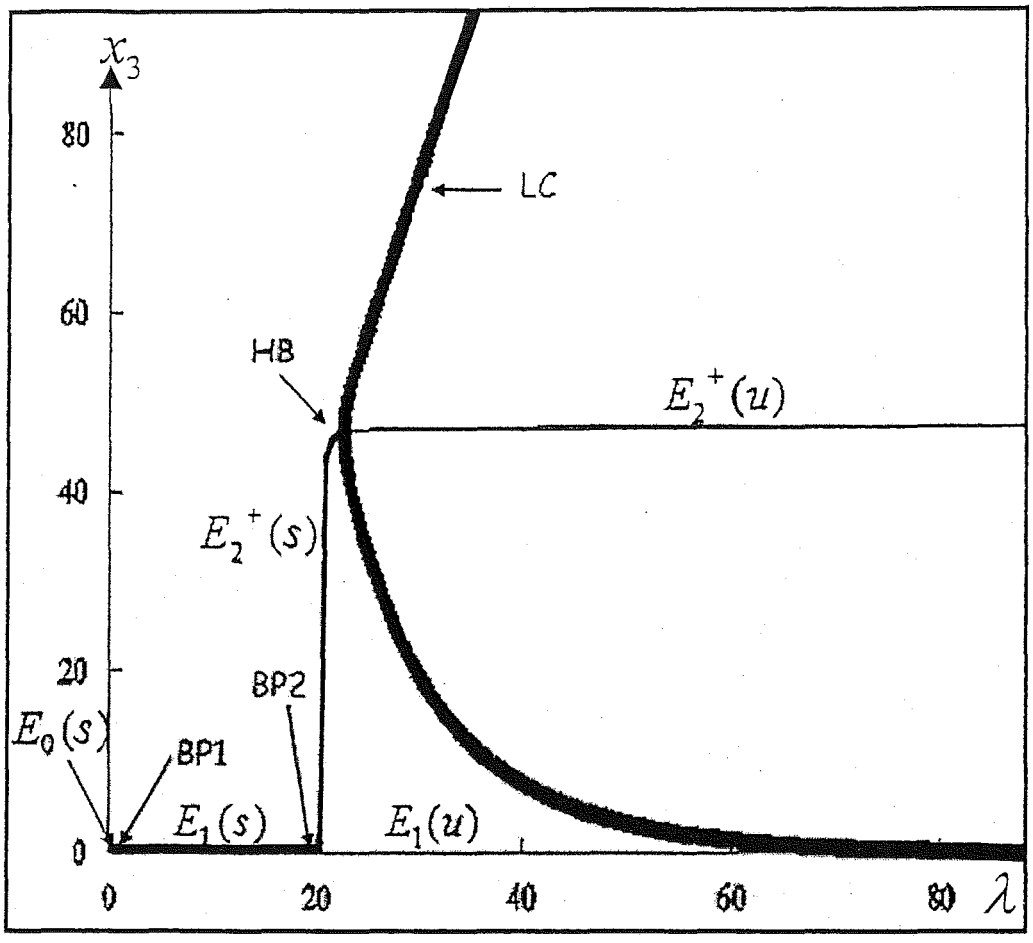

Figure 2.6: The bifurcation diagram x_3 against λ for one compartment model at $\gamma = 0.45$ showing the bifurcation point BP1 ($\lambda = 0.2132$), BP2 ($\lambda = 20.21$) and the Hopf bifurcation point HB ($\lambda = 22.55$).

iii) **Figure 2.7** and **Figure 2.8** are the respective bifurcation diagrams for x_2 and x_3 against the parameter λ, when $\gamma = 0.5$. The first bifurcation point (**BP1**) occurs at the point $\lambda = 0.2631$, where the null state E_0 changes from stable to unstable and the steady state E_1 occurs (c.f. **Theorem 2.1** and **APPENDIX C: TABLES: T2b**). The next bifurcation point (BP2) is at $\lambda = 16.93$, where the steady state E_1 becomes

unstable and the stable E_2^+ branch occurs (c.f. APPENDIX C: TABLES: T2c). Periodicity then follows at the Hopf bifurcation point (HB) at $\lambda = 20.96$. The bifurcation diagram thus resembles $\gamma = 0.45$, whereby limit point (LP) is not featured here.

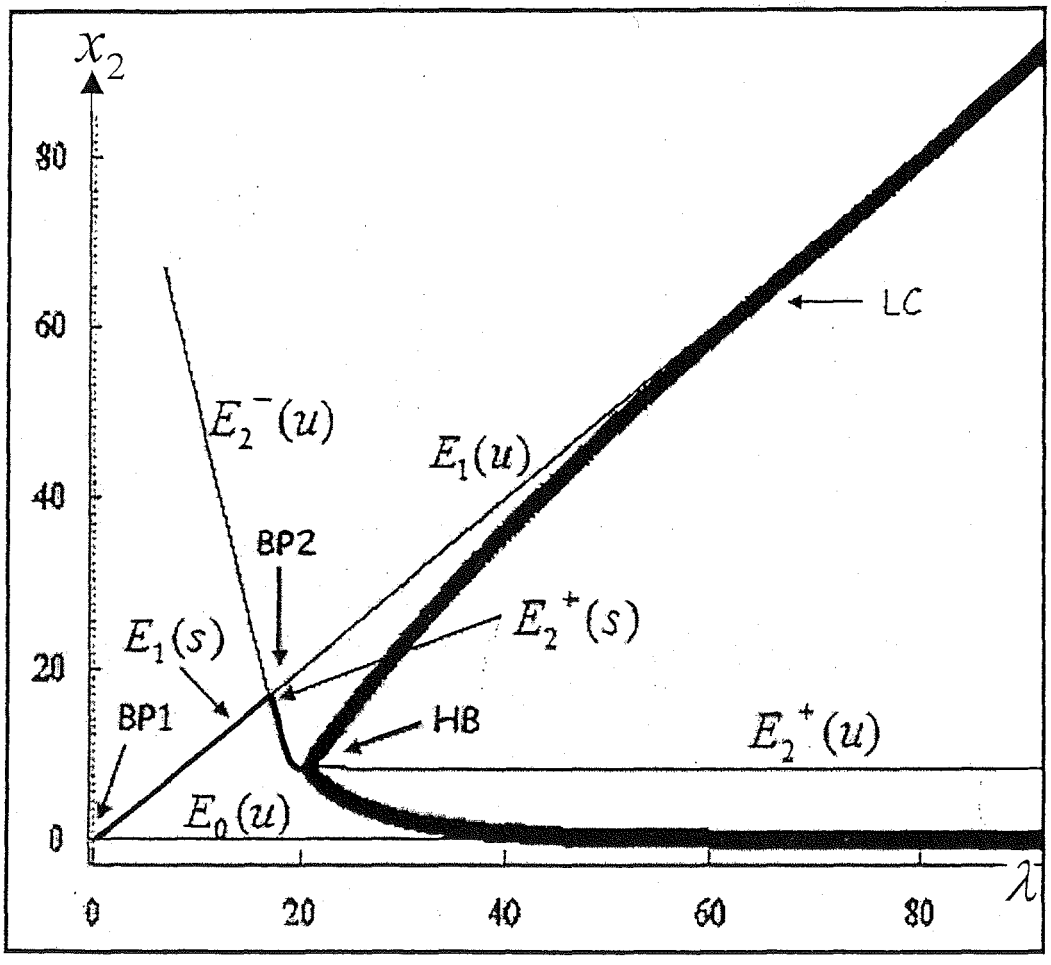

Figure 2.7: The bifurcation diagram x_2 against λ for one compartment model at $\gamma = 0.5$ showing the bifurcation point BP1 ($\lambda = 0.2631$), BP2 ($\lambda = 16.93$) and the Hopf bifurcation point HB ($\lambda = 20.96$) (Note: Here the unfeasible steady state E_2^- is now unstable).

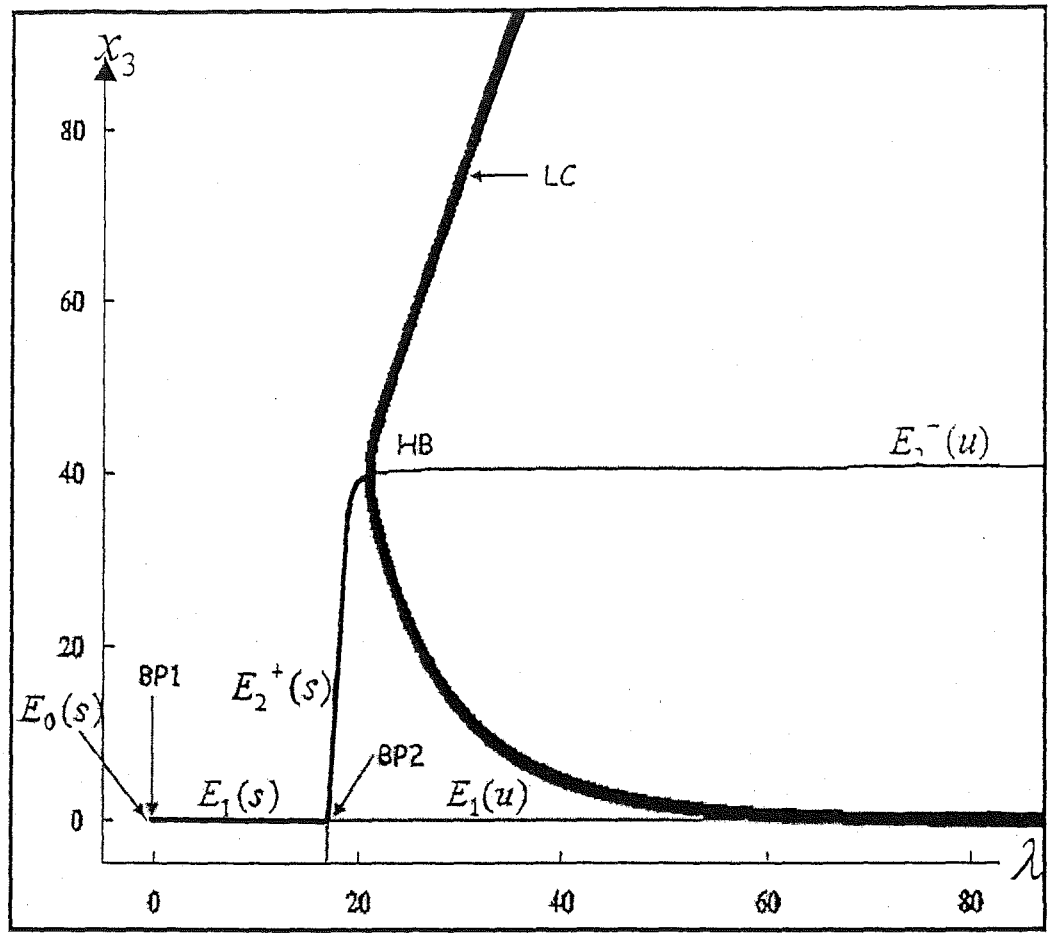

Figure 2.8: The bifurcation diagram x_3 against λ for one compartment model at $\gamma = 0.5$ showing the bifurcation point BP1 ($\lambda = 0.2631$), BP2 ($\lambda = 16.93$) and the Hopf bifurcation point HB ($\lambda = 20.96$).

ii) **Figure 2.9** and **Figure 2.10** are the respective bifurcation diagram for x_2 and x_3 against the parameter λ when $\gamma = 0.6$. The first bifurcation point (**BP1**) occurs at the point $\lambda = 0.4053$, where the null state E_0 changes from stable to unstable and the steady state E_1 occurs (c.f. **Theorem 2.1** and **APPENDIX C: TABLES: T2b**). The next bifurcation point (**BP2**) is at $\lambda = 12.91$, where the

steady state E_1 becomes unstable and the stable E_2^+ branch occurs (c.f. APPENDIX C: TABLES: T2c). Periodicity then follows at the Hopf bifurcation point (HB) at $\lambda = 17.91$. The bifurcation diagrams resemble $\gamma = 0.45$ and $\gamma = 0.5$, whereby no limit point is featured.

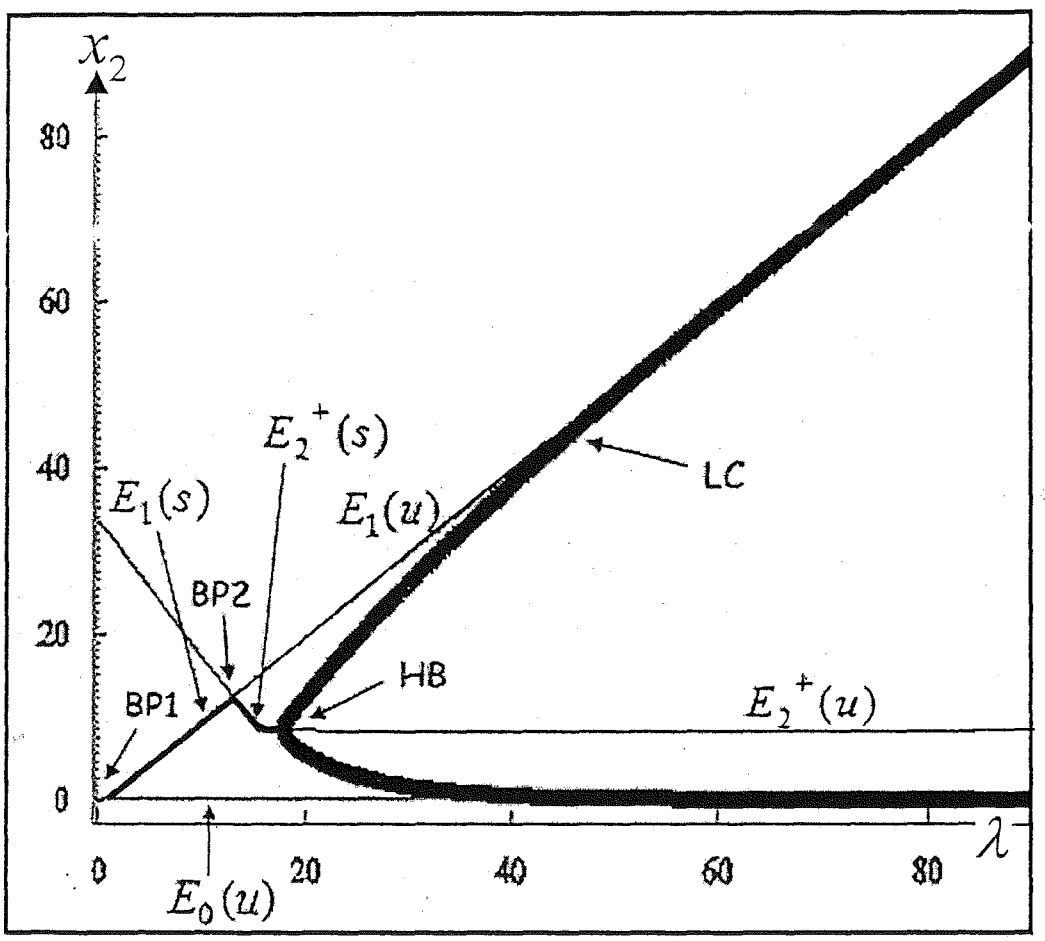

Figure 2.9: The bifurcation diagram x_2 against λ for one compartment model at $\gamma = 0.6$ showing the bifurcation point BP1 ($\lambda = 0.4053$), BP2 ($\lambda = 12.91$) and the Hopf bifurcation point HB ($\lambda = 17.91$).

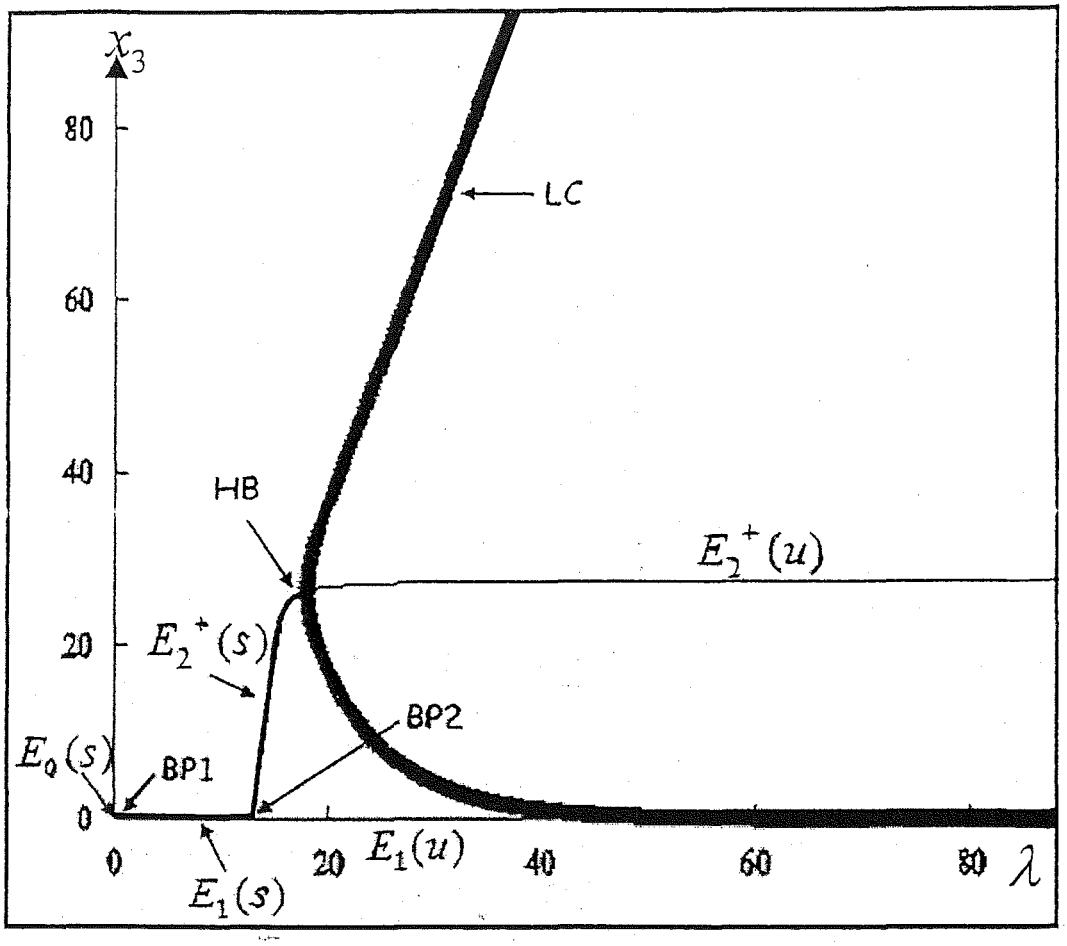

Figure 2.10: The bifurcation diagram x_3 against λ for one compartment model at $\gamma = 0.6$ showing the bifurcation point BP1 (λ= 0.4053), BP2 (λ= 12.91) and the Hopf bifurcation point HB ($\lambda = 17.91$).

v) **Figure 2.11** and **Figure 2.12** shows the respective bifurcation diagrams x_2 and x_3 against the parameter λ when $\gamma = 0.7$. The first bifurcation point (**BP1**) is at the point $\lambda = 0.6604$, where the null state E_0 changes form stable to unstable and the steady state E_1 occurs (c.f. **Theorem 2.1** and **APPENDIX C: TABLES: T2b**). The next bifurcation point (**BP2**) is at $\lambda = 10.66$, where the steady state E_1 becomes

unstable and the stable E_2^+ branch occurs (c.f. APPENDIX C: TABLES: T2c). Periodicity then follows at the Hopf bifurcation point (HB) at $\lambda = 15.34$. The bifurcation diagrams resemble $\gamma = 0.45$, $\gamma = 0.5$ and $\gamma = 0.6$, whereby no limit point is featured.

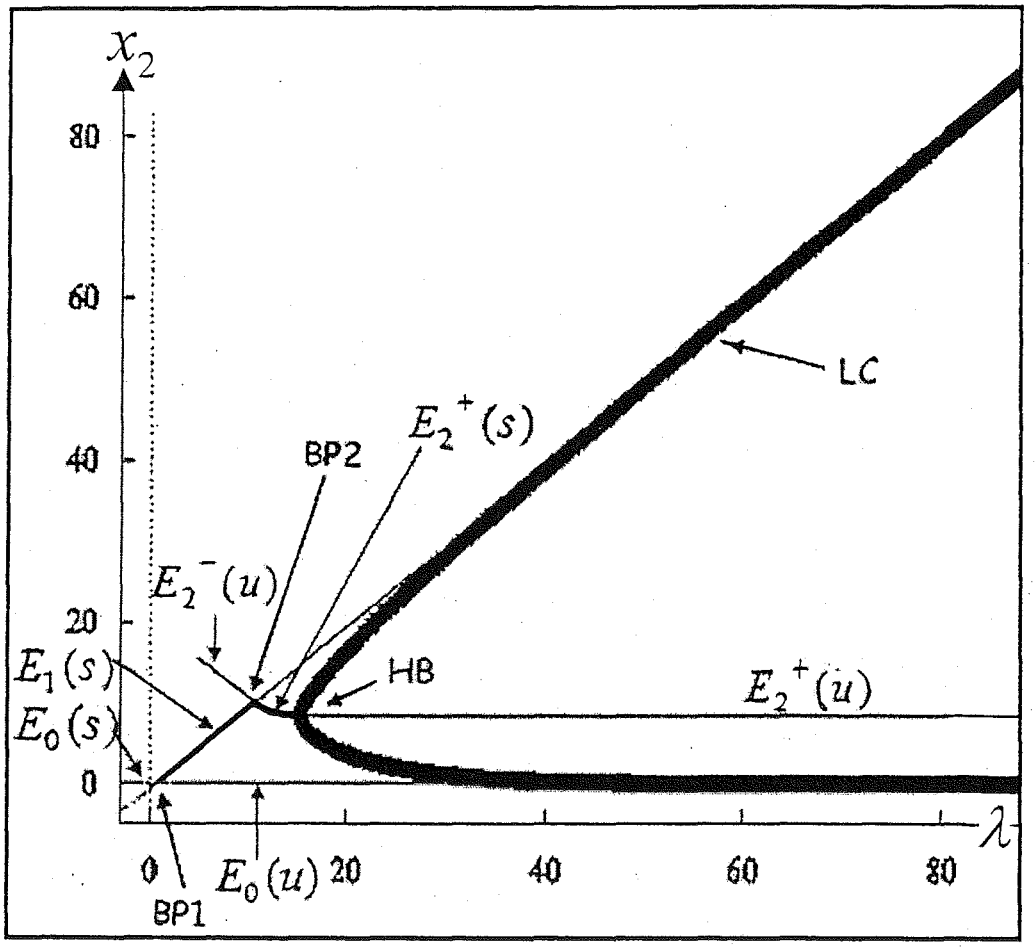

Figure 2.11: The bifurcation diagram x_2 against λ for one compartment model at $\gamma = 0.7$ showing the bifurcation point BP1 ($\lambda = 0.6604$), BP2 ($\lambda = 10.66$) and the Hopf bifurcation point HB ($\lambda = 15.34$).

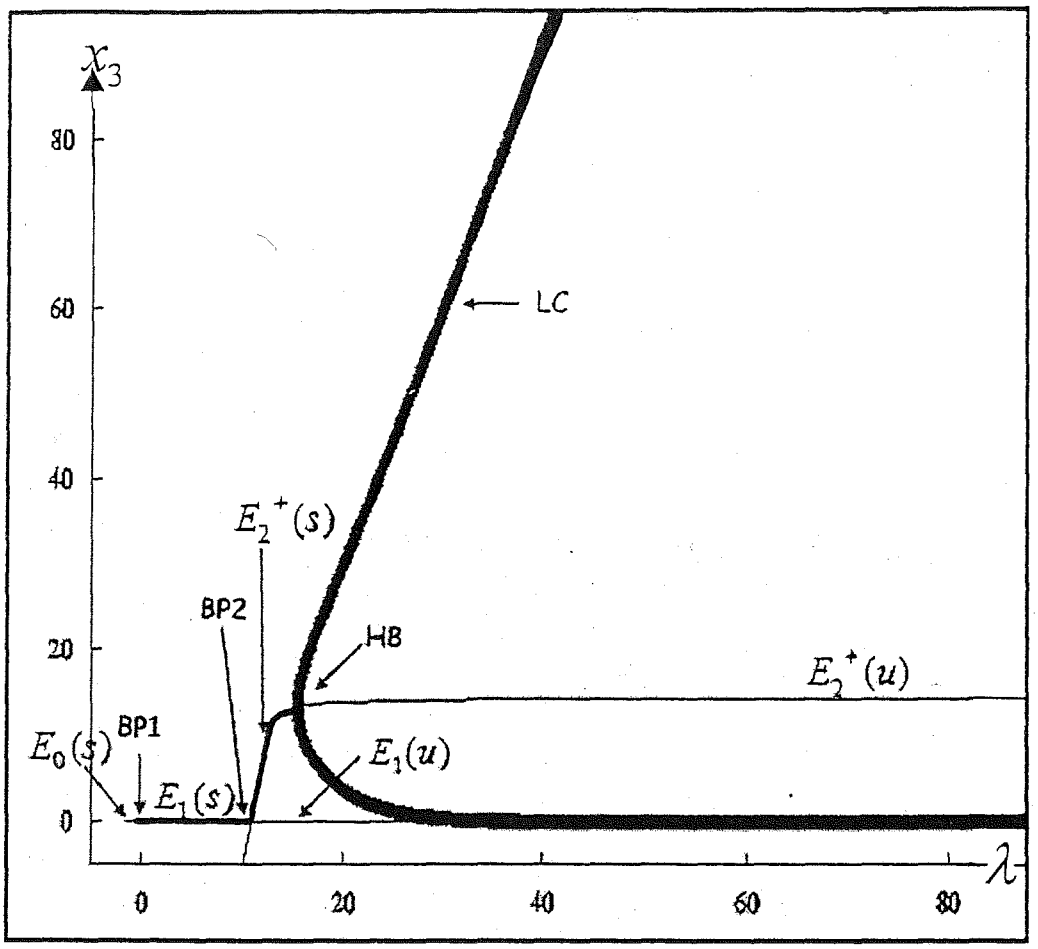

Figure 2.12: The bifurcation diagram x_3 against λ for one compartment model at $\gamma = 0.7$ showing the bifurcation point BP1 ($\lambda = 0.6604$), BP2 ($\lambda = 10.66$) and the Hopf bifurcation point HB ($\lambda = 15.34$).

vi) **Figure 2.13** and **Figure 2.14** are the respective bifurcation diagram for x_2 and x_3 against the parameter λ, when $\gamma = 0.8$. The first bifurcation point (**BP1**) is at the point $\lambda = 3.333$, where the null state E_0 changes from stable to unstable and the steady state E_1 occurs (c.f. **Theorem 2.1** and **APPENDIX C: TABLES: T2b**). The next

bifurcation point (BP2) is at $\lambda = 11.67$, where the steady state E_1 becomes unstable and the stable E_2^+ branch occurs (c.f. **APPENDIX C: TABLES: T2c**). Periodicity then follows at the Hopf bifurcation point (HB) at $\lambda = 21.82$. The bifurcation diagrams resemble $\gamma = 0.45$, $\gamma = 0.5$, $\gamma = 0.6$ and $\gamma = 0.7$, whereby no limit point is featured.

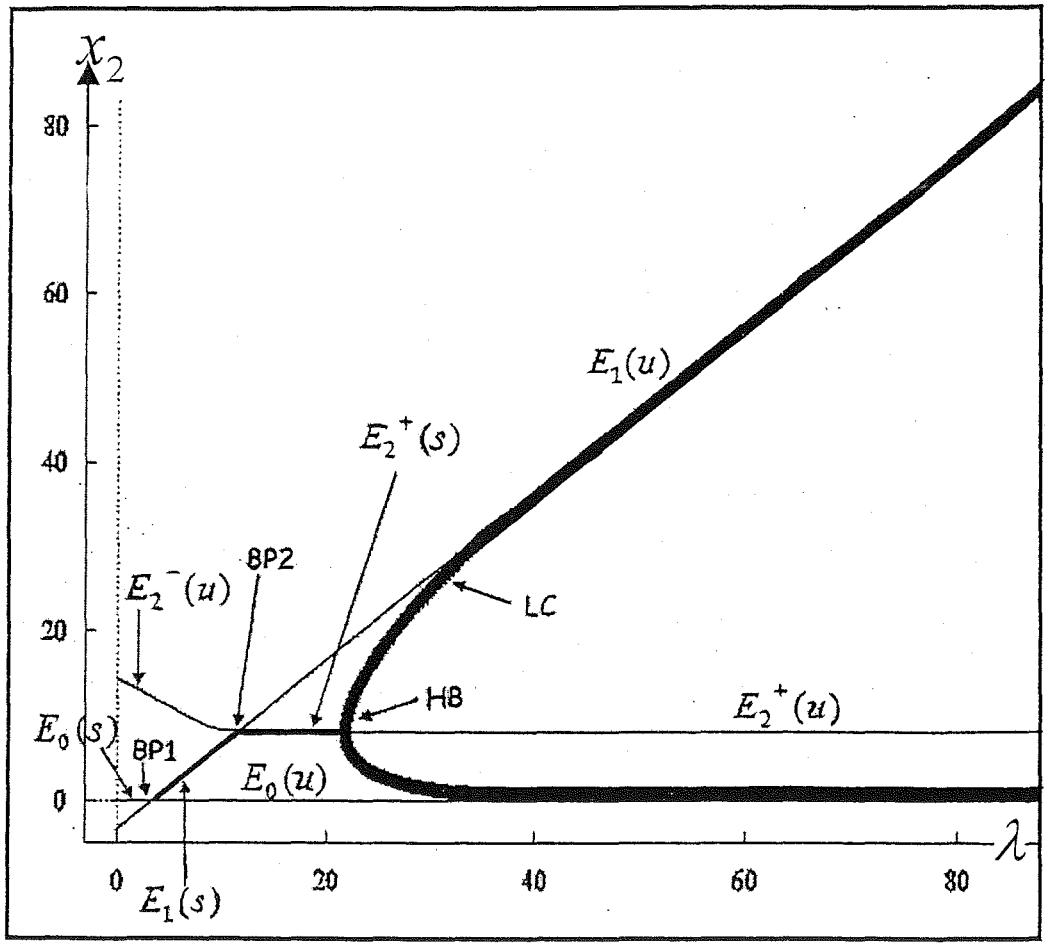

Figure 2.13: The bifurcation diagram x_2 against λ for one compartment model at $\gamma = 0.8$ showing the bifurcation point BP1 ($\lambda = 3.333$), BP2 ($\lambda = 11.67$) and the Hopf bifurcation point HB ($\lambda = 21.82$). (Note: Here the unfeasible steady state E_2^- is again featured and it is unstable).

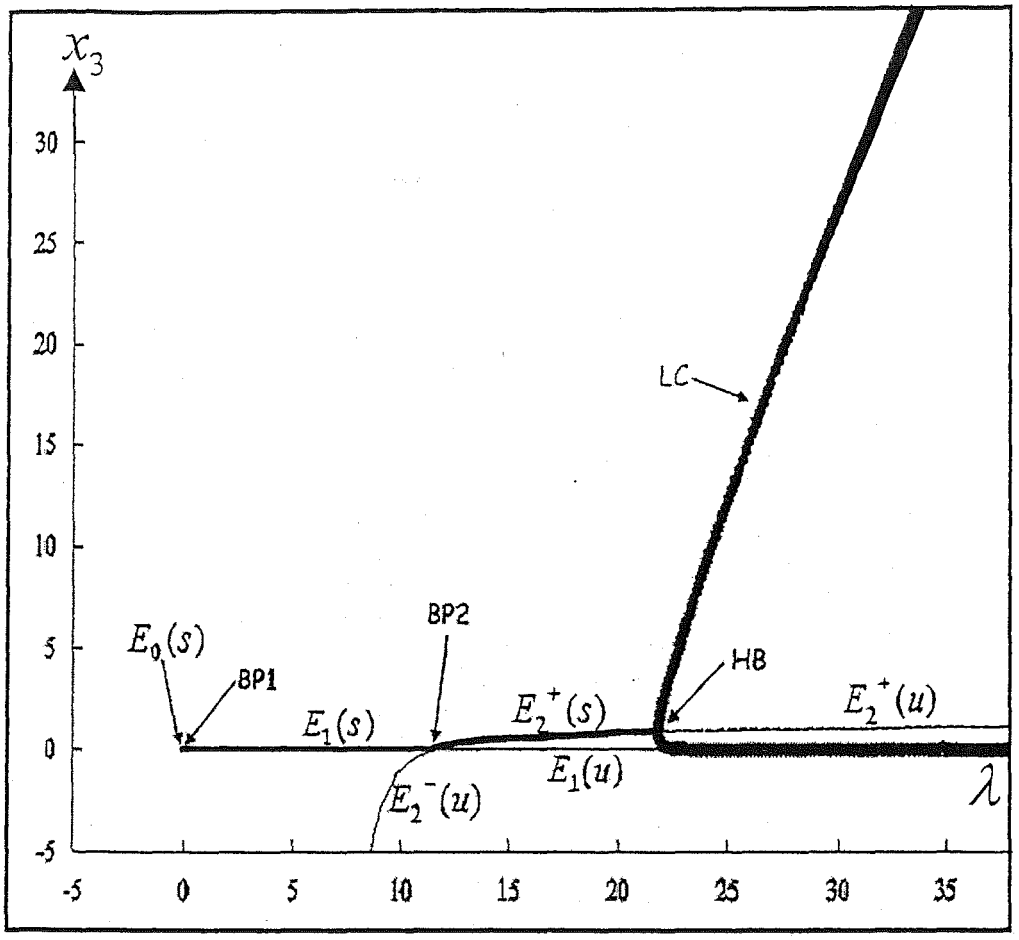

Figure 2.14: The bifurcation diagram x_3 against λ for one compartment model at $\gamma = 0.8$ showing the bifurcation point BP1 ($\lambda = 3.333$), BP2 ($\lambda = 11.67$) and the Hopf bifurcation point HB ($\lambda = 21.82$). (Note: Here the unfeasible steady state E_2^- is again featured and it is unstable).

vii) **Figure 2.15** is the bifurcation diagram for x_2 against the parameter λ for $\gamma = 0.9$. The graph only shows a bold horizontal line. This indicates that the only steady state which is stable is E_0. (**Note**: This is consistent with the result found analytically in **Section 2.3.1** and **2.3.2** and **Theorem 2.2**).

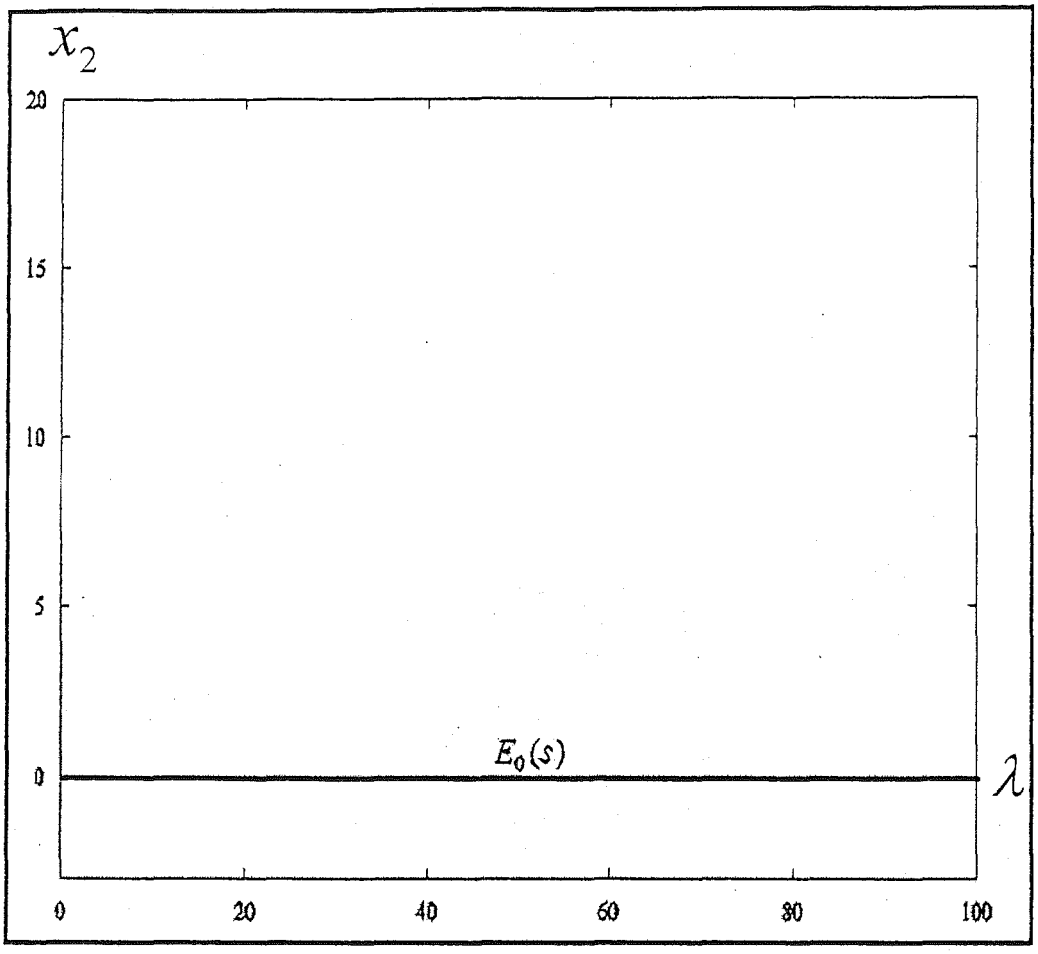

Figure 2.16: The bifurcation diagram x_2 against λ for one compartment model at $\gamma = 0.9$.

viii) **Figure 2.16** is a two parameter diagram of γ against λ, showing the extension of the limit point (**LP**) and the Hopf Bifurcation point (**HB**) only. The extension of **BP1** and **BP2** loci is not shown here. Since this diagram is executed by AUTO and AUTO is not capable of doing the extension for bifurcation points. However, later in **Figure 2.17**, these results are combined with the results produced by MATHEMATICA, the software which shall be used to execute the analytic results found earlier.

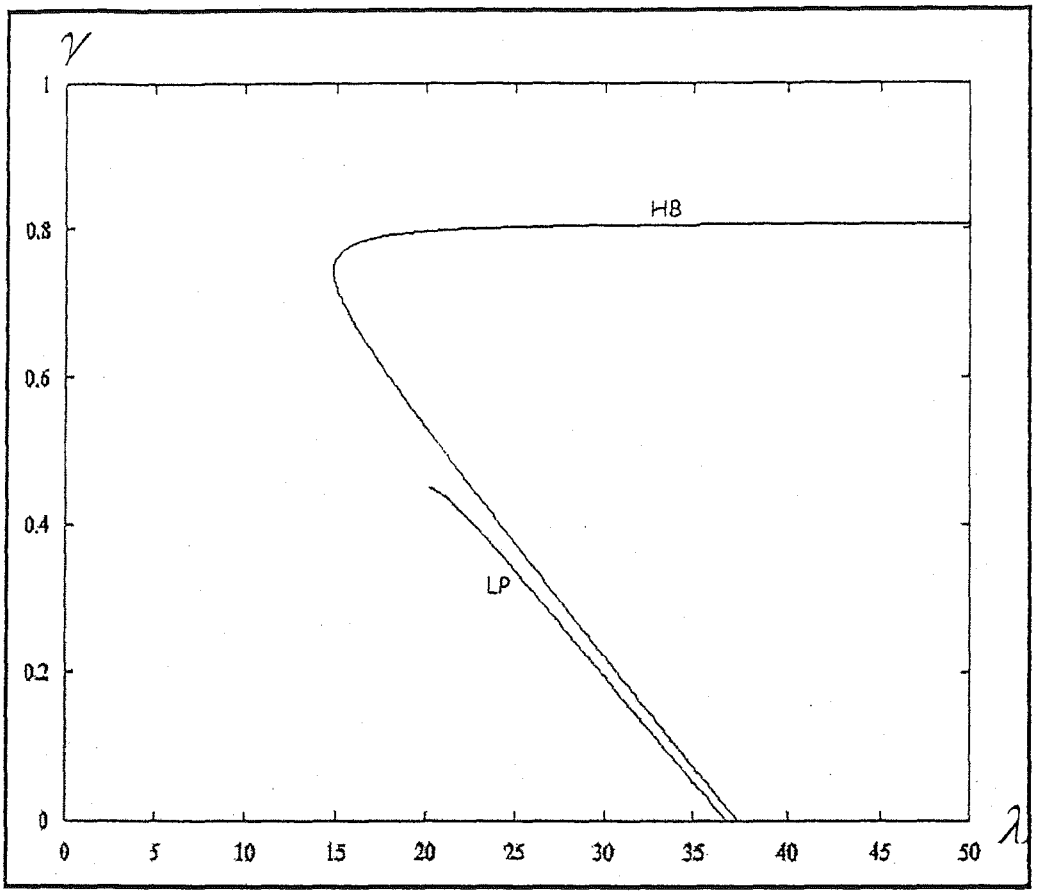

Figure 2.17: The two parameter diagram γ against λ for one compartment model produced by AUTO showing the Limit point locus (LP) and the Hopf bifurcation point locus (HB).

Note: From i) to vii), it appears that for values $\gamma \geq 0.45$, the bifurcation diagrams have similar behaviour i.e. there is no indication of the presence of the limit point (LP). For $\gamma < 0.45$, for example, at $\gamma = 0.4$, there exist a LP which indicate the coexistence of two steady states; and/or a steady state and a Hopf bifurcation (HB).

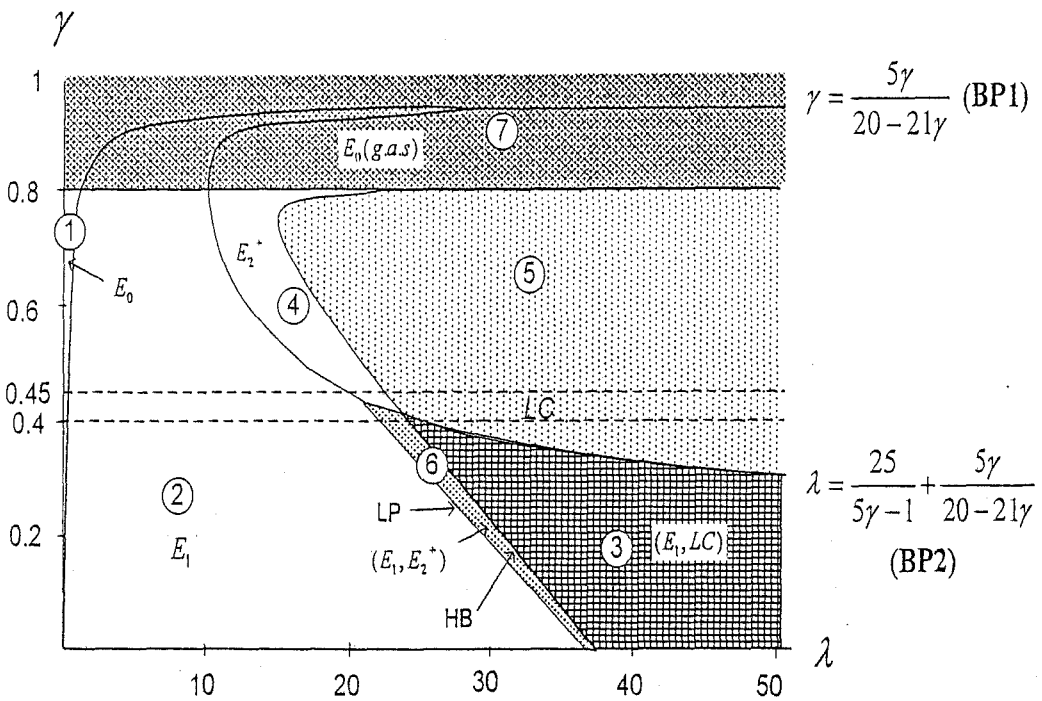

Figure 2.17: The overall 2-parameter plot for a one-compartment model showing the stability of the three steady states (E_0, E_1 and E_2), the location of the coexistence between steady states or periodic solutions and the presence of limit cycles or periodic solutions.

Figure 2.17 combines all of the information obtained from AUTO (for the Limit Point (**LP**) and Hopf bifurcation (**HB**) curves only) with that of **Theorem 2.1** to **2.2** and **section 2.3.2** (c.f. **Figure 2.1** and **2.2**) using MATHEMATICA (see **APPENDIX B: MATHEMATICA: B4**). The overall two-parameter diagram clearly shows the stability of the three steady states, the location of the coexistence between steady states or periodic solutions, and the existence of limit cycles or periodic solutions. In summary:

i) the null state E_0 is only stable in the small region ①, and when $\gamma > 0.8$ (i.e. in the region ⑦) where it is globally asymptotically stable;

ii) E_1 is stable in region ②, coexists with E_2 in region ⑥, and coexists with the limit cycle or the periodic solution in region ③;

iii) E_2 is stable in region ④ and coexists with E_1 in region ⑥; and

iv) the limit cycle or periodic solution appears in region ⑤ and ③.

2.6 Conclusion

Let us first recall that:

i) E_0 is the steady state in which none of the species (neither the phytoplankton nor the zooplankton) survive;

ii) E_1 is the steady state in which the only surviving species is the phytoplankton;

iii) E_2 is the most important steady state, where both the phytoplankton and zooplankton species survive; and

iv) the periodic or limit cycle is when the phytoplankton and zooplankton alternately dominate. As the grazing rate of the zooplankton species increases, the phytoplankton population decreases. As the population of phytoplankton decreases, the grazing rate of the zooplankton decreases and thus the population of zooplankton decreases due to food limitation. Since the grazing rate consequently decreases, the phytoplankton species then begins to increase, and the cycle continues.

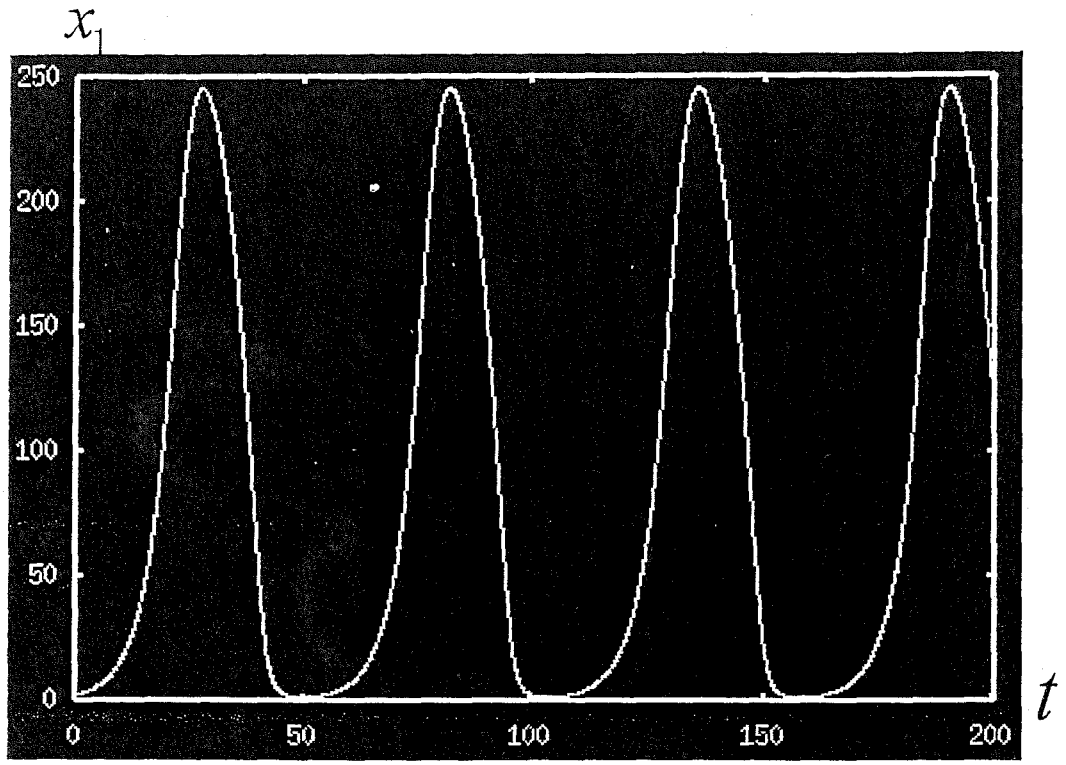

Figure 2.18: The phytoplankton carbon x_1 against time t.

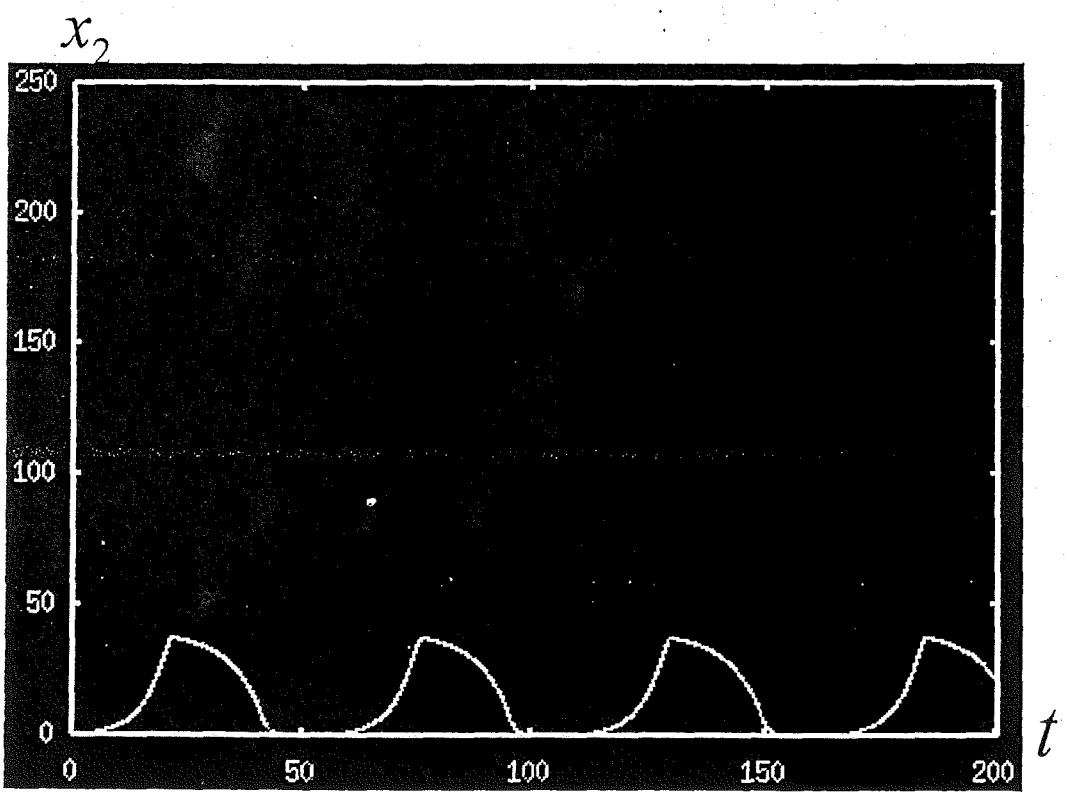

Figure 2.19: The phytoplankton nitrogen x_2 against time t.

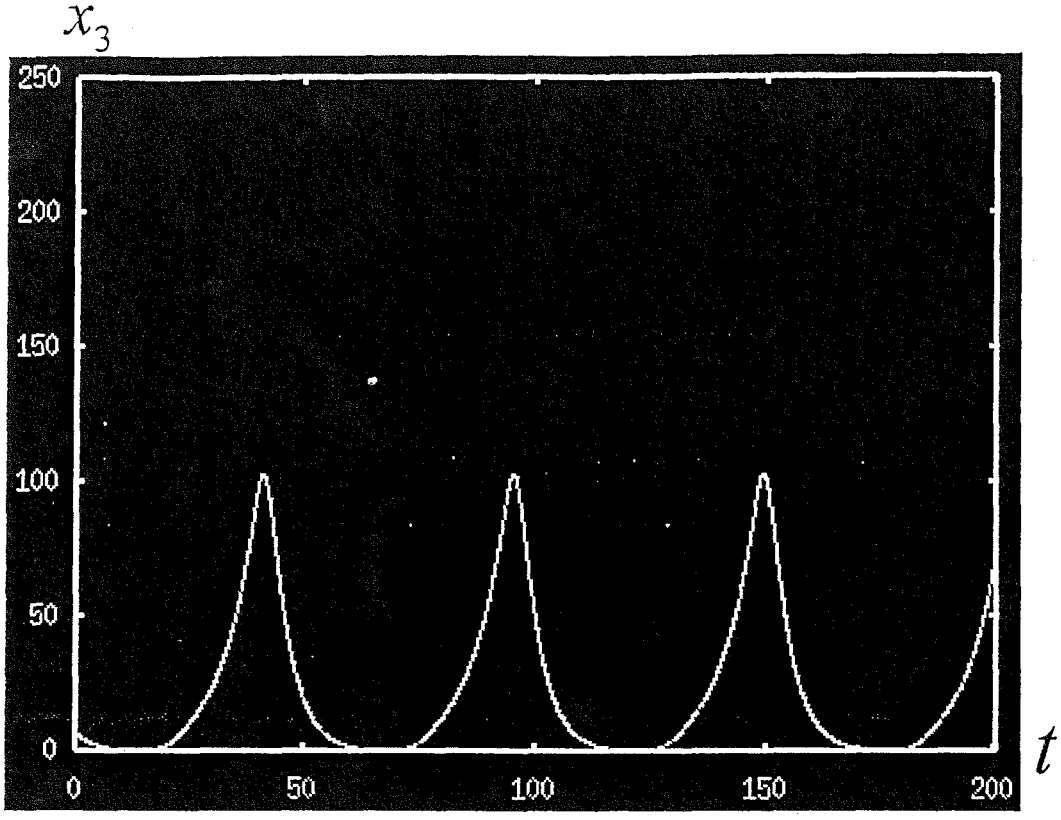

Figure 2.20: The zooplankton carbon x_3 against time t.

In summary, nothing survives at region ①, especially in region ⑦. In region ②, only the phytoplankton will survive. Region ④ is considered the most important where both the species survived. Coexistence between steady states is only evident when $\gamma < 0.45$ i.e. in the regions ③ and ⑥. Region ⑥ show a small region for coexistence between the phenomena of only the phytoplankton survived E_1 and when both the phytoplankton and zooplankton existed E_2. There is a smaller "window of opportunity" for populations to coexist. The edges of these regions are points where gross changes in outcomes are likely to occur. Region ⑥ can be expanded by increasing the value of R. It shows that increasing R would shift the Hopf bifurcation boundary to the right while the limit point boundary remains. Changing Q will tells a different story since the rest

of the boundaries is dependent on Q. For example considering at $\gamma = 0.4$, changing Q = 0.06 (previous was 0.05) and R remains unchanged at 0.25, will give a different bifurcation points, the limit points disappeared and the Hopf bifurcation points is shifted to the left at $\lambda = 22.88$ instead of at $\lambda = 24.16$. Feasibility regions will also be affected by changing Q and R since one of the necessary conditions applies to the steady state is $Q < \frac{x_2}{x_1} < R$. The limit cycle or the periodic solutions in reality is a natural phenomenon as long as the populations remain feasible (positive biomass) for survival however, many population cannot sustain oscillations of large amplitude.

Chapter 3

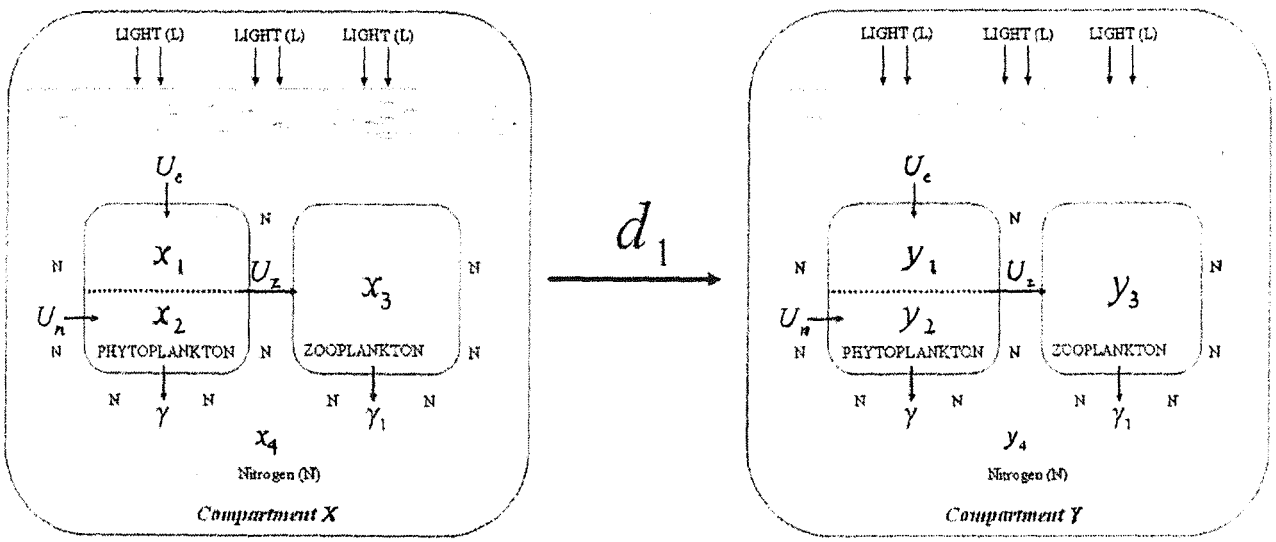

The two compartment phytoplankton-zooplankton-nutrient model

Chapter 3: The two compartment phytoplankton-zooplankton-nutrient model

3.0 Introduction

In this chapter, the one compartment model in Chapter 2 is developed into two compartment model. Two one-compartment models are linked to each other at a constant diffusion rate $d_1\ s^{-1}$. Assuming that the compartment is equally mixed, in other words, we assumed that two ponds are connected to each other with a membrane having a membrane diffusion coefficient d_1 (s^{-1} unit) and that the species from each pond are free to move from one compartment to another. This is serves as first part of discretization process. We let one of the compartments corresponds to $X's$ components while the other corresponds to $Y's$ components. Thus the essential variables for the respective compartments becomes the phytoplankton carbon (x_1 and y_1) and phytoplankton nitrogen (x_2 and y_2), the zooplankton carbon (x_3 and y_3) and the free nitrogen (x_4 and y_4). Thus, we have seven coupled ordinary differential equations in seven dependent variables (i.e. by conserving the free nitrogen x_4). The growth of phytoplankton (carbon) represented by the parameter μ's first of all taken to be the same in both compartments i.e. $\mu_1 = \mu_2$ as a control experiment or analysis to see whether it is behaving like the one compartment model or otherwise. Then the consequences of a different growth rate of the phytoplankton for each compartment are considered or $\mu_1 \neq \mu_2$. The existence of various steady states is investigated another sophisticated computer software called **XPP** and in detail with the help of the symbolic software **MATHEMATICA**, and the long term behaviour and the stability of the

steady states is further supported by various bifurcation diagrams produced using **AUTO**, which gives the eigenvalues defining the stability automatically.

3.1 The model

Based on the assumptions in Chapter 1 and Chapter 2 and that the nutrient (nitrogen) is a closed system such that $\dot{x}_4+\dot{x}_2+\gamma_2\dot{x}_3+\dot{y}_2+\dot{y}_4+\gamma_2\dot{y}_3=0$ (i.e. we conserved the free nitrogen x_4), the mathematical model is now a system of seven coupled ordinary differential equations in seven dependent variables; the phytoplankton carbon x_1, the phytoplankton nitrogen x_2, the zooplankton carbon x_3 in one compartment; and the phytoplankton carbon y_1, the phytoplankton nitrogen y_2, the zooplankton carbon y_3, the free nitrogen y_4 in the other compartment-viz.

$$\dot{x}_1=\mu_1\left(1-\frac{Qx_1}{x_2}\right)^{+}x_1-\frac{\Gamma x_1x_3}{\hat{(x_1+C)}}-\gamma x_1-d_1(x_1-y_1) \tag{3.1}$$

$$\dot{x}_2=\frac{Ux_1(2\lambda-x_2-\gamma_2x_3-y_2-y_4-\gamma_2y_3)H\left(R-\frac{x_2}{x_1}\right)}{(2\lambda+h-x_2-\gamma_2x_3-y_2-y_4-\gamma_2y_3)}-\frac{\Gamma x_2x_3}{\hat{x_1+C}}-d_1(x_2-y_2)-\gamma x_2 \tag{3.2}$$

$$\dot{x}_3=\frac{\Gamma x_2x_3}{\gamma_2\hat{(x_1+C)}}-d_1(x_3-y_3)-\gamma_1x_3 \tag{3.3}$$

$$\dot{y}_1=\mu_2\left(1-\frac{Qy_1}{y_2}\right)^{+}y_1-\frac{\Gamma y_1y_3}{\hat{(y_1+C)}}-\gamma y_1-d_1(y_1-x_1) \tag{3.4}$$

$$\dot{y}_2=\frac{Uy_1y_4H\left(R-\frac{y_2}{y_1}\right)}{(y_4+h)}-\frac{\Gamma y_2y_3}{\hat{y_1+C}}-d_1(y_2-x_2)-\gamma y_2 \tag{3.5}$$

$$\dot{y}_3 = \frac{\Gamma y_2 y_3}{\gamma_2 (y_1 + \hat{C})} - d_1 (y_3 - x_3) - \gamma_1 y_3 \tag{3.6}$$

$$\dot{y}_4 = \gamma y_2 - \gamma_1 \gamma_2 y_3 - \frac{U y_1 y_4 H\left(R - \frac{y_2}{y_1}\right)}{(y_4 + h)} - d_1 (y_4 - 2\lambda + x_2 + \gamma_2 x_3 + y_2 + y_4 + \gamma_2 y_3) \tag{3.7}$$

This system of ordinary differential equations are to be solved on the domain

$\Omega = \{(x_1, x_2, x_3, y_1, y_2, y_3, y_4) : x_1 \geq 0, x_2 \geq 0, x_3 \geq 0, y_1 \geq 0, y_2 \geq 0, y_3 \geq 0, y_4 \geq 0\}$.

3.2 Steady states assuming an equal growth parameter for the phytoplankton ($\mu_1 = \mu_2 = 1$)

The steady states of the system (**3.1-3.7**) assuming that the growth parameter for the phytoplankton in both the compartments is equal to one another, may be obtained analytically. However, numerically, **AUTO** has identified the steady state branch (0, 0, 0, 0, 0, 0, λ) and another is of the form (x_1, x_2, 0, x_1, x_2, 0, y_4). The steady states of the system (**3.1 - 3.7**) of course correspond to setting the time derivatives to zero. When $x_3 = y_3 = 0$, $x_1 = y_1$ and $x_2 = y_2$, from equation (**3.1**) and (**3.4**), either $x_1 = y_1 = 0$ or $\alpha = \frac{x_2}{x_1} = \frac{Q\mu}{\mu - \gamma} = \frac{y_2}{y_1}$. Then in the case where $x_3 = y_3 = 0$ and $x_1 = y_1 = 0$, equation (**3.2**) and (**3.5**) implies $y_4 = \lambda$ so that one of the steady states is $E_0 = (0, 0, 0, 0, 0, 0, \lambda)$. However, when $x_3 = y_3 = 0$ and $x_2 = \frac{Q\mu_1}{\mu_1 - \gamma} x_1$ or $y_2 = \frac{Q\mu_1}{\mu_1 - \gamma} y_1$, equation (**3.2**) and (**3.5**), equation (**3.2**) implies

$$x_2 = y_2 = \alpha\left(\frac{\gamma(\lambda+h)-\dfrac{U\lambda(\mu_1-\gamma)}{Q\mu}}{\dfrac{\gamma Q\mu_1}{(\mu_1-\gamma)}-U}\right) \text{ where } \alpha = \frac{Q\mu_1}{\mu_1-\gamma},$$

or more simply $x_2 = y_2 = \lambda - \dfrac{Q\mu_1\gamma h}{\mu_1 U - \gamma(Q\mu_1+U)}$, provided $\dfrac{x_2}{x_1} < R$ and $\dfrac{y_2}{y_1} < R$ so that $H\left(R-\dfrac{x_2}{x_1}\right)=1$ and $H\left(R-\dfrac{y_2}{y_1}\right)=1$. Thus

$$E_1 = \left(\lambda - \frac{Q\mu_1\gamma h}{\mu_1 U-\gamma(Q\mu_1+U)},\ \frac{Q\mu}{(\mu_1-\gamma)}\left(\lambda-\frac{Q\mu_1\gamma h}{\mu_1 U-\gamma(Q\mu_1+U)}\right),\ 0,\ \lambda-\frac{Q\mu_1\gamma h}{\mu_1 U-\gamma(Q\mu_1+U)},\right.$$

$$\left.\frac{Q\mu}{(\mu_1-\gamma)}\left(\lambda-\frac{Q\mu_1\gamma h}{\mu_1 U-\gamma(Q\mu_1+U)}\right), 0, \lambda-\left(\lambda-\frac{Q\mu_1\gamma h}{\mu_1 U-\gamma(Q\mu_1+U)}\right)\right) \text{ is a second}$$

steady state which is identified to be of the same form as the steady state E_1 found for the one compartment model. (**Note**: when $\dfrac{x_2}{x_1} < R$ and $\dfrac{y_2}{y_1} < R$ such that $H\left(R-\dfrac{x_2}{x_1}\right)=0$ and $H\left(R-\dfrac{y_2}{y_1}\right)=0$ respectively, when $x_3 = y_3 = 0$ there is only $E_0 = (0,\ 0,\ 0, 0, 0, 0, \lambda)$).

Another steady state identified by **AUTO** is of the form $(x_1,\ x_2,\ x_3,\ x_1,\ x_2,\ x_3,\ y_4)$. Thus, the third steady state solution may be derived analytically. Hence, equation (**3.1**) and (**3.4**), (**3.2**) and (**3.5**) and (**3.3**) and (**3.6**) is of the similar form and it assembles the one compartment model in Chapter 2. In other words, we can solve equation (**3.1**)–(**3.3**) the same way as the one compartment model in **section 2.2** of Chapter 2. Thus the third steady state is given by $E_2 = (x_1^*,\ x_2^*,\ x_3^*,\ x_1^*,\ x_2^*,\ x_3^*,\ y_4^*)$ such that

$$x_1^* = -\left(20\left(-4835+3700\gamma+158\lambda \pm 2\sqrt{6310900+4410000\gamma^2-399740\lambda+6241\lambda^2}\right.\right.$$

$$\sqrt{+200\gamma(-52130+1659\lambda)}\Big)\Big)/79(-9+20\gamma)$$

$$x_2^*= \gamma_1\gamma_2(x_1^* + \hat{C})/\Gamma$$

$$x_3^* = \left(-\frac{\mu_1 Q}{\gamma_1\gamma_2} + \frac{(\mu_1-\gamma)}{\Gamma}\right)x_1^* + \frac{\hat{C}(\mu_1-\gamma)}{\Gamma}$$

$$y_4^* = (-6.18568\times10^{31} + 1.84391\times10^{31}d_1 + 5.13436\times10^{31}\gamma - 5.26743\times10^{31}d_1\gamma + 2.59967\times10^{31}d_1\gamma^2$$
$$+1.9315\times10^{30}\lambda - 4.40088\times10^{29}d_1\lambda + 9.77973\times10^{29}d_1\gamma\lambda - 2.44493\times10^{28}\sqrt{4.41\times10^6\gamma^2}$$
$$\sqrt{+6241(-35.8228+\lambda)(-28.2278+\lambda)+\gamma(-1.0426\times10^7+331800\lambda)}$$

$$-5.57073\times10^{27}d_1\sqrt{4.41\times10^6\gamma^2+6241(-35.8228+\lambda)(-28.2278+\lambda)+\gamma(-1.0426\times10^7+331800\lambda)}$$
$$+1.23794\times10^{28}d_1\gamma\sqrt{4.41\times10^6\gamma^2+6241(-35.8228+\lambda)(-28.2278+\lambda)+\gamma(-1.0426\times10^7+331800\lambda)}$$
$$\pm0.5\sqrt{\Big(-4d_1(-1.76035\times10^{30}+3.91189\times10^{30}\gamma)\Big(2.00237\times10^{31}-5.53978\times10^{31}\gamma+2.44493\times10^{29}\lambda$$
$$\sqrt{-3.09485\times10^{27}\sqrt{4.41\times10^6\gamma^2+6241(-35.8228+\lambda)(-28.2278+\lambda)+\gamma(-1.0426\times10^7+331800\lambda)}}$$
$$\sqrt{d_1\Big(-1.40382\times10^{32}-2.59967\times10^{32}\gamma^2+4.40088\times10^{38}\lambda+5.57073\times10^{28}\sqrt{4.41\times10^6\gamma^2+6241}}$$
$$\sqrt{\sqrt{(-35.8228+\lambda)(-28.2278+\lambda)+\gamma(-1.0426\times10^7+331800\lambda)}+\gamma\Big(4.28946\times10^{32}}$$

$$\sqrt{-9.77973\times10^{30}\lambda-1.23794\times10^{29}\sqrt{4.41\times10^6\gamma^2+6241(-35.8228+\lambda)(-28.2278+\lambda)}}$$

$$\sqrt{\sqrt{+\gamma(-1.0426\times10^7+331800\lambda)}\Big)\Big)}+\Big(1.23714\times10^{32}-1.02687\times10^{32}\gamma-3.86299\times10^{30}\lambda$$

$$\sqrt{+4.88986\times10^{28}\sqrt{4.41\times10^6\gamma^2+6241(-35.8228+\lambda)(-28.2278+\lambda)+\gamma(-1.0426\times10^7+331800\lambda)}}$$
$$\sqrt{+d_1\Big(-3.68782\times10^{31}-5.19935\times10^{31}\gamma^2+8.80175\times10^{29}\lambda+1.11415\times10^{28}\sqrt{4.41\times10^6\gamma^2}}$$
$$\sqrt{\sqrt{+6241(-35.8228+\lambda)(-28.2278+\lambda)+\gamma(-1.0426\times10^7+331800\lambda)}}$$

$$\sqrt{+\gamma\Big(1.05349\times10^{32}-1.95595\times10^{30}\lambda-2.47588\times10^{28}\sqrt{4.41\times10^6\gamma^2+6241(-35.8228+\lambda)}}$$
$$\sqrt{\sqrt{(-28.2278+\lambda)+\gamma(-1.0426\times10^7+331800\lambda)}\Big)\Big)}^2\Big)\Big)/(d_1(-1.76035\times10^{30}+3.91189\times10^{30}\gamma)$$

(Refer to: **APPENDIX B: MATHEMATICA: B5**)

Numerically, **AUTO** has also identified the following *unfeasible* steady states:

$ufss1 = (x_1, x_2, -x_3, x_1, x_2, -x_3, y_4)$, $ufss2 = (x_1, x_2, -x_3, y_1, y_2, y_3, y_4)$

$ufss3 = (x_1, x_2, x_3, y_1, y_2, -y_3, y_4)$ $ufss4 = (x_1, x_2, -x_3, y_1, y_2, -y_3, y_4)$

$ufss5 = (-x_1, -x_2, 0, -x_1, -x_2, 0, y_4)$.

Note: In summary, the three steady states of interest are as follows:

a) $E_0 = (0,\ 0,\ 0,\ 0,\ 0,\ 0,\ \lambda)$,

b)

$$E_1 = \left(\frac{(\mu_1-\gamma)}{Q\mu}\left(\lambda - \frac{Q\mu_1\gamma h}{\mu_1 U - \gamma(Q\mu_1+U)}\right),\ \lambda - \frac{Q\mu_1\gamma h}{\mu_1 U - \gamma(Q\mu_1+U)},\ 0,\ \frac{(\mu_1-\gamma)}{Q\mu_1}\left(\lambda - \frac{Q\mu_1\gamma h}{\mu_1 U - \gamma(Q\mu_1+U)}\right),\right.$$
$$\left.\lambda - \frac{Q\mu_1\gamma h}{\mu_1 U - \gamma(Q\mu_1+U)},\ 0, \lambda - \left(\lambda - \frac{Q\mu_1\gamma h}{\mu_1 U - \gamma(Q\mu_1+U)}\right)\right)$$

c) $E_2 = (x_1^*,\ x_2^*,\ x_3^*,\ x_1^*,\ x_2^*,\ x_3^*,\ y_4^*)$ such that

$$x_1^* = -\left(20\left(-4835 + 3700\gamma + 158\lambda \pm 2\sqrt{6310900 + 4410000\gamma^2 - 399740\lambda + 6241\lambda^2}\right.\right.$$

$$\left.\left.\sqrt{+200\gamma(-52130 + 1659\lambda)}\right)\right) / 79(-9 + 20\gamma)$$

$$x_2^* = \gamma_1\gamma_2(x_1^* + \hat{C})/\Gamma$$

$$x_3^* = \left(-\frac{\mu_1 Q}{\gamma_1\gamma_2} + \frac{(\mu_1-\gamma)}{\Gamma}\right)x_1^* + \frac{\hat{C}(\mu_1-\gamma)}{\Gamma}$$

$$y_4^* = (-6.18568\times10^{31} + 1.84391\times10^{31}d_1 + 5.13436\times10^{31}\gamma - 5.26743\times10^{31}d_1\gamma + 2.59967\times10^{31}d_1\gamma^2$$
$$+1.9315\times10^{30}\lambda - 4.40088\times10^{29}d_1\lambda + 9.77973\times10^{29}d_1\gamma\lambda - 2.44493\times10^{28}\sqrt{4.41\times10^6\gamma^2}$$
$$\sqrt{+6241(-35.8228+\lambda)(-28.2278+\lambda) + \gamma(-1.0426\times10^7 + 331800\lambda)}$$

$$-5.57073\times10^{27}d_1\sqrt{4.41\times10^6\gamma^2 + 6241(-35.8228+\lambda)(-28.2278+\lambda) + \gamma(-1.0426\times10^7 + 331800\lambda)}$$
$$+1.23794\times10^{28}d_1\gamma\sqrt{4.41\times10^6\gamma^2 + 6241(-35.8228+\lambda)(-28.2278+\lambda) + \gamma(-1.0426\times10^7 + 331800\lambda)}$$
$$\pm0.5\sqrt{\left(-4d_1(-1.76035\times10^{30} + 3.91189\times10^{30}\gamma)\left(2.00237\times10^{31} - 5.53978\times10^{31}\gamma + 2.44493\times10^{29}\lambda\right.\right.}$$

$$\sqrt{-3.09485\times10^{27}\sqrt{4.41\times10^{6}\gamma^{2}+6241(-35.8228+\lambda)(-28.2278+\lambda)+\gamma(-1.0426\times10^{7}+331800\lambda)}}$$
$$\sqrt{d_1\left(-1.40382\times10^{32}-2.59967\times10^{32}\gamma^{2}+4.40088\times10^{38}\lambda+5.57073\times10^{28}\sqrt{4.41\times10^{6}\gamma^{2}+6241}\right.}$$
$$\sqrt{\sqrt{(-35.8228+\lambda)(-28.2278+\lambda)+\gamma(-1.0426\times10^{7}+331800\lambda)}+\gamma\left(4.28946\times10^{32}\right.}$$

$$\sqrt{-9.77973\times10^{30}\lambda-1.23794\times10^{29}\sqrt{4.41\times10^{6}\gamma^{2}+6241(-35.8228+\lambda)(-28.2278+\lambda)}}$$

$$\left.\left.\sqrt{\sqrt{+\gamma(-1.0426\times10^{7}+331800\lambda)}}\right)\right)+\left(1.23714\times10^{32}-1.02687\times10^{32}\gamma-3.86299\times10^{30}\lambda\right.$$

$$\sqrt{+4.88986\times10^{28}\sqrt{4.41\times10^{6}\gamma^{2}+6241(-35.8228+\lambda)(-28.2278+\lambda)+\gamma(-1.0426\times10^{7}+331800\lambda)}}$$
$$\sqrt{+d\left(-3.68782\times10^{31}-5.19935\times10^{31}\gamma^{2}+8.80175\times10^{29}\lambda+1.11415\times10^{28}\sqrt{4.41\times10^{6}\gamma^{2}}\right.}$$
$$\sqrt{\sqrt{+6241(-35.8228+\lambda)(-28.2278+\lambda)+\gamma(-1.0426\times10^{7}+331800\lambda)}}$$

$$\sqrt{+\gamma\left(1.05349\times10^{32}-1.95595\times10^{30}\lambda-2.47588\times10^{28}\sqrt{4.41\times10^{6}\gamma^{2}+6241(-35.8228+\lambda)}\right.}$$
$$\left.\left.\left.\sqrt{\sqrt{(-28.2278+\lambda)+\gamma(-1.0426\times10^{7}+331800\lambda)}}\right)\right)^{2}\right)\Big/(d_1(-1.76035\times10^{30}+3.91189\times10^{30}\gamma)$$

Note:

i) The expression $x_3^{*}=\left(-\frac{\mu_1 Q}{\gamma_1\gamma_2}+\frac{(\mu_1-\gamma)}{\Gamma}\right)x_1^{*}+\frac{\hat{C}(\mu_1-\gamma)}{\Gamma}$ for our third steady state E_2 can be positive or negative. Thus we distinguish our third steady state as E_2 and *ufss*1 respectively.

ii) The singular value $\gamma=\frac{9}{20}=0.45$ is precluded (because the denominator in the expression for the roots is zero at this point).

iii) All the three steady states resemble those of one compartment model.

It follows that the feasibility regions are the same as the one compartment model.

3.3 Stability of the steady states assuming an equal growth parameter for the phytoplankton $\mu_1 = \mu_2 = 1$

In this section, the stability of the *feasible* steady state is investigated in detail using local stability analysis. Stability corresponds to seven negative eigenvalues, for model involving seven dependent variables. It is convenient to use the software **MATHEMATICA**. Local stability analysis is developed whenever possible to obtain the ***transcritical*** bifurcation points or curves where an exchange of stability occurs. The analytical calculation is most complicated in the case of the steady state E_2 so the stability is further investigated from the bifurcation diagrams produced by **AUTO**.

3.3.1 Stability of the steady state E_0

Let us first of all consider the stability of the steady state $E_0 = (0,\ 0,\ 0,\ 0,\ 0,\ 0,\ \lambda)$. In addition to the local stability, the *global* stability is also investigated.

Theorem 3.1

The steady state E_0 is locally asymptotically stable if and only if it falls in the feasible region $0 < \lambda < \frac{5}{4}$ (see **section 2.4.1**) and $\lambda < \left(\frac{(\gamma + d_1) Q \mu_1 h}{U\mu_1 - (\gamma + d_1)(Q\mu_1 + U)} \right)$.

Proof:

The linearized form of equation (3.3) is $\dot{x}_3 = (-\gamma_1 - d_1)x_3$, hence $x_3 = x_3(0)e^{(-\gamma_1 - d_1)t}$ corresponding to one negative eigenvalue $-\gamma_1 - d_1$. The priori assumption that $x_1 = ae^{\alpha t}$ and $x_2 = be^{\alpha t}$ as $x_1,\ x_2 \to 0$ is consistent with $\frac{x_2}{x_1} = \text{constant}$ as shown in

section 2.4.1. Substituting $x_1 = ae^{\alpha t}$ into the linearized equation of **(3.1)** or **(3.4)** yields $a\alpha e^{\alpha t} = \mu_1\left(1-\frac{Qx_1}{x_2}\right)^+ ae^{\alpha t} - (\gamma + d_1)ae^{\alpha t}$ and therefore for $\alpha \neq 0$ one has $\alpha = \mu_1\left(1-\frac{Qa}{b}\right)^+ - (\gamma + d_1)$. Substituting $x_1 = ae^{\alpha t}$ and $x_2 = be^{\alpha t}$ into the linearized form of equation of **(3.2)** or **(3.5)** yields $\alpha be^{\alpha t} = \frac{U\lambda ae^{\alpha t}}{(\lambda + h)} - (\gamma + d_1)be^{\alpha t}$, so that $\alpha = \frac{U\lambda a}{(\lambda + h)b} - (\gamma + d_1)$ and hence $\frac{a}{b} = \frac{\mu_1\left(1-\frac{Qa}{b}\right)^+(\lambda + h)}{U\lambda}$ or $\frac{a}{b} = \frac{\mu_1}{Q\mu_1 + \frac{U\lambda}{\lambda + h}}$, since $\alpha = \mu_1\left(1-\frac{Qa}{b}\right)^+ - (\gamma + d_1)$. Therefore another eigenvalue is $\alpha = \frac{U\lambda\mu_1}{Q\mu_1(\lambda + h) + U\lambda} - (\gamma + d_1)$, so that the steady state E_0 is stable if and only if $\frac{U\lambda\mu}{Q\mu_1(\lambda + h) + U\lambda} - (\gamma + d_1) < 0$ or $\lambda < \left(\frac{(\gamma + d_1)Q\mu_1 h}{U\mu_1 - (\gamma + d_1)(Q\mu_1 + U)}\right)$ (c.f **Figure 3.1**). ■

Note: $a = 0$, substituting $x_2 = be^{\alpha t}$ into the linearized form of equation **(3.2)** yields $b\alpha e^{\alpha t} = -(\gamma + d_1)be^{\alpha t}$ so that $\alpha = -(\gamma + d_1)$ (i.e another strictly negative eigenvalue). The linearized form of equation of **(3.7)** is given by $\dot{y}_4 = -2d_1 y_4$ so that $y_4 = y_4(0)e^{-(2d_1)t}$. In summary, the seven negative eigenvalues are $-\gamma_1 - d_1$ (twice), $-\gamma - d_1$ (twice) and another two provided $\lambda < \left(\frac{(\gamma + d_1)Q\mu_1 h}{U\mu_1 - (\gamma + d_1)(Q\mu_1 + U)}\right)$ and $-2d_1$ ■

3.3.2 The stability of the steady state E_1

In order to prove that the steady state

$$E_1=\left(\frac{(\mu_1-\gamma)}{Q\mu}\left(\lambda-\frac{Q\mu_1\gamma h}{\mu_1U-\gamma(Q\mu_1+U)}\right),\ \lambda-\frac{Q\mu_1\gamma h}{\mu_1U-\gamma(Q\mu_1+U)},\ 0,\ \frac{(\mu_1-\gamma)}{Q\mu_1}\left(\lambda-\frac{Q\mu_1\gamma h}{\mu_1U-\gamma(Q\mu_1+U)}\right),\right.$$
$$\left.\lambda-\frac{Q\mu_1\gamma h}{\mu_1U-\gamma(Q\mu_1+U)},\ 0,\lambda-\left(\lambda-\frac{Q\mu_1\gamma h}{\mu_1U-\gamma(Q\mu_1+U)}\right)\right)$$

is locally stable, equations **(3.1 – 3.7)** are linearized about the steady state E_1 and the determinant of the associated Jacobian matrix is considered (local stability corresponds to all seven eigenvalues being negative (see **APPENDIX B: MATHEMATICA: B6**). However, for the time being we shall identify the stability boundary such that the eigenvalues are equal zero. The stability shall be investigated by **AUTO** in the next section when the complete bifurcation diagrams are analyzed. For equation **(3.2)** and **(3.5)**, it is only necessary to consider the case $\frac{x_2}{x_1}<R$ when $1-H\left((\frac{x_2}{x_1}-R)\right)=1$ and the other parameters are taken to be as in **APPENDIX C: TABLES: T1** keeping λ and γ unknowns. The Jacobian matrix J is:

$$J(\bar{x_1},\bar{x_2},\bar{x_3}\,\bar{y_1},\bar{y_2},\bar{y_3},\bar{y_4})=\begin{bmatrix} J_{11} & J_{12} & J_{13} & J_{14} & 0 & 0 & 0 \\ J_{21} & J_{22} & J_{23} & 0 & J_{25} & J_{26} & J_{27} \\ 0 & 0 & J_{33} & 0 & 0 & J_{36} & 0 \\ J_{41} & 0 & 0 & J_{44} & J_{45} & J_{46} & 0 \\ 0 & J_{52} & 0 & J_{54} & J_{55} & J_{56} & J_{57} \\ 0 & 0 & J_{63} & 0 & 0 & J_{66} & 0 \\ 0 & J_{72} & J_{73} & J_{74} & J_{75} & J_{76} & J_{77} \end{bmatrix}_{(\bar{x_1},\bar{x_2},\bar{x_3},\bar{y_1},\bar{y_2},\bar{y_3},\bar{y_4})}, \text{ where}$$

$$J_{11}=1-d_1-2(1-\gamma)-\gamma,\ J_{12}=20(1-\gamma)^2,\ J_{13}=-\frac{20(1-\gamma)\left(\frac{5\gamma}{-20+21\gamma}+\lambda\right)}{100+20(1-\gamma)\left(\frac{5\gamma}{-20+21\gamma}+\lambda\right)},$$

$$J_{14}=d_1,\qquad J_{15}=0,\qquad J_{16}=0,\qquad J_{17}=0,$$

$$J_{21}=-\frac{\left(-\frac{5\gamma}{20-21\gamma}-\frac{10\gamma}{-20+21\gamma}\right)}{5-\left(\frac{5\gamma}{20-21\gamma}-\frac{10\gamma}{-20+21\gamma}\right)},$$

$$J_{22}=-d_1-\gamma+-\frac{20(1-\gamma)\left(-\frac{5\gamma}{20-21\gamma}-\frac{10\gamma}{-20+21\gamma}\right)\left(\frac{5\gamma}{-20+21\gamma}+\lambda\right)}{\left(5-\frac{5\gamma}{20-21\gamma}-\frac{10\gamma}{-20+21\gamma}\right)^2}-\frac{20(1-\gamma)\left(\frac{5\gamma}{-20+21\gamma}+\lambda\right)}{5-\frac{5\gamma}{20-21\gamma}-\frac{10\gamma}{-20+21\gamma}}$$

$$J_{23}=-\frac{5(1-\gamma)\left(-\frac{5\gamma}{20-21\gamma}-\frac{10\gamma}{-20+21\gamma}\right)\left(\frac{5\gamma}{-20+21\gamma}+\lambda\right)}{\left(5-\frac{5\gamma}{20-21\gamma}-\frac{10\gamma}{-20+21\gamma}\right)^2}-\frac{5(1-\gamma)\left(\frac{5\gamma}{-20+21\gamma}+\lambda\right)}{5-\frac{5\gamma}{20-21\gamma}-\frac{10\gamma}{-20+21\gamma}}-$$

$$\frac{5(1-\gamma)\left(\frac{5\gamma}{-20+21\gamma}+\lambda\right)}{5-\frac{5\gamma}{20-21\gamma}-\frac{10\gamma}{-20+21\gamma}}-\frac{\left(\frac{5\gamma}{-20+21\gamma}+\lambda\right)}{100+20(1-\gamma)\left(\frac{5\gamma}{-20+21\gamma}+\lambda\right)},\qquad J_{24}=0,$$

$$J_{25}=d_1+\frac{20(1-\gamma)\left(-\frac{5\gamma}{20-21\gamma}-\frac{10\gamma}{-20+21\gamma}\right)\left(\frac{5\gamma}{-20+21\gamma}+\lambda\right)}{\left(5-\frac{5\gamma}{20-21\gamma}-\frac{10\gamma}{-20+21\gamma}\right)^2}-\frac{20(1-\gamma)\left(\frac{5\gamma}{-20+21\gamma}+\lambda\right)}{5-\frac{5\gamma}{20-21\gamma}-\frac{10\gamma}{-20+21\gamma}}$$

$$J_{26}=\frac{5(1-\gamma)\left(-\frac{5\gamma}{20-21\gamma}-\frac{10\gamma}{-20+21\gamma}\right)\left(\frac{5\gamma}{-20+21\gamma}+\lambda\right)}{\left(5-\frac{5\gamma}{20-21\gamma}-\frac{10\gamma}{-20+21\gamma}\right)^2}-\frac{5(1-\gamma)\left(\frac{5\gamma}{-20+21\gamma}+\lambda\right)}{5-\frac{5\gamma}{20-21\gamma}-\frac{10\gamma}{-20+21\gamma}}$$

$$J_{27}=\frac{20(1-\gamma)\left(-\frac{5\gamma}{20-21\gamma}-\frac{10\gamma}{-20+21\gamma}\right)\left(\frac{5\gamma}{-20+21\gamma}+\lambda\right)}{\left(5-\frac{5\gamma}{20-21\gamma}-\frac{10\gamma}{-20+21\gamma}\right)^2}-\frac{20(1-\gamma)\left(\frac{5\gamma}{-20+21\gamma}+\lambda\right)}{5-\frac{5\gamma}{20-21\gamma}-\frac{10\gamma}{-20+21\gamma}}$$

$$J_{31}=0,\ J_{32}=0,\ J_{33}=-\frac{1}{4}-d_1+\frac{4\left(\frac{5\gamma}{-20+21\gamma}+\lambda\right)}{100+20(1-\gamma)\left(\frac{5\gamma}{-20+21\gamma}+\lambda\right)},\ J_{34}=0,\ J_{35}=0,$$

$$J_{36}=d_1,\ J_{37}=0,\ J_{41}=d_1,\ J_{42}=0,\ J_{43}=0,\ J_{44}=1-d_1-2(1-\gamma)-\gamma,$$

$$J_{45}=20(1-\gamma)^2,\ J_{46}=-\frac{20(1-\gamma)\left(\frac{5\gamma}{-20+21\gamma}+\lambda\right)}{100+20(1-\gamma)\left(\frac{5\gamma}{-20+21\gamma}+\lambda\right)},\ J_{47}=0,$$

$$J_{51}=0, J_{52}=d_1, J_{53}=0,\ J_{54}=\frac{5\gamma}{(20-21\gamma)\left(5+\frac{5\gamma}{20-21\gamma}\right)},\ J_{55}=-d_1-\gamma,$$

$$J_{56}=-\frac{\left(\frac{5\gamma}{-20+21\gamma}+\lambda\right)}{100+20(1-\gamma)\left(\frac{5\gamma}{-20+21\gamma}+\lambda\right)},$$

$$J_{57}=-\frac{100(1-\gamma)\gamma\left(\frac{5\gamma}{-20+21\gamma}+\lambda\right)}{(20-21\gamma)\left(5+\frac{5\gamma}{20-21\gamma}\right)^2}+\frac{20(1-\gamma)\left(\frac{5\gamma}{-20+21\gamma}+\lambda\right)}{5+\frac{5\gamma}{20-21\gamma}},\ J_{61}=0,\ J_{62}=0,$$

$$J_{63}=d_1,\ J_{64}=0,\ J_{65}=0,\ J_{66}=-\frac{1}{4}-d_1+\frac{4\left(\frac{5\gamma}{-20+21\gamma}+\lambda\right)}{100+20(1-\gamma)\left(\frac{5\gamma}{-20+21\gamma}+\lambda\right)},$$

$$J_{67}=0,\ J_{71}=0,\ J_{72}=-d_1,\ J_{73}=-\frac{d_1}{4},\ J_{74}=\frac{5\gamma}{(20-21\gamma)\left(5+\frac{5\gamma}{20-21\gamma}\right)},$$

$$J_{75}=-d_1+\gamma,\ J_{76}=\frac{1}{16}-\frac{d_1}{4},$$

$$J_{77}=-2d_1+\frac{100(1-\gamma)\gamma\left(\frac{5\gamma}{-20+21\gamma}+\lambda\right)}{(20-21\gamma)\left(5+\frac{5\gamma}{20-21\gamma}\right)^2}-\frac{20(1-\gamma)\left(\frac{5\gamma}{-20+21\gamma}+\lambda\right)}{5+\frac{5\gamma}{20-21\gamma}}.$$

The results for the eigenvalues are evaluated using **MATHEMATICA** (see **APPENDIX B: MATHEMATICA: B6**), which is given by:

$V_1=-2d_1,$

$$V_2 = \frac{-500+530\gamma-25\gamma^2-20\lambda+121\gamma\lambda-105\gamma^2\lambda}{2000-2200\gamma+100\gamma^2+400\lambda-820\gamma\lambda+420\gamma^2\lambda},$$

$$V_3 = \left(-500-4000d_1+530\gamma+4400d_1\gamma-25\gamma^2-200d_1\gamma^2-20\lambda-800d_1\lambda+121\gamma\lambda+1640d_1\gamma\lambda \right.$$
$$\left. -105\gamma^2\lambda-840d_1\gamma^2\lambda\right)/\left(2000-2200\gamma+100\gamma^2+400\lambda-820\gamma\lambda+420\gamma^2\lambda\right),$$

$$V_4 = \left(100-400d_1-200\gamma-400d_1\gamma+105\gamma^2+400\lambda-840\gamma\lambda+441\gamma^2\lambda+\sqrt{10000-61000\gamma^2}\right.$$
$$\sqrt{+82000\gamma^3-30975\gamma^4-80000\lambda+328000\gamma\lambda-500200\gamma^2\lambda+336000\gamma^3\lambda-83790\gamma^4\lambda}$$
$$\left.\sqrt{+160000\lambda^2-672000\gamma\lambda^2+1058400\gamma^2\lambda^2-740880\gamma^3\lambda^2+194481\gamma^4\lambda^2}\right)/(2(-100+100\gamma))$$

$$V_5 = \left(100-400d_1-200\gamma-400d_1\gamma+105\gamma^2+400\lambda-840\gamma\lambda+441\gamma^2\lambda-\sqrt{10000-61000\gamma^2}\right.$$
$$\sqrt{+82000\gamma^3-30975\gamma^4-80000\lambda+328000\gamma\lambda-500200\gamma^2\lambda+336000\gamma^3\lambda-83790\gamma^4\lambda}$$
$$\left.\sqrt{+160000\lambda^2-672000\gamma\lambda^2+1058400\gamma^2\lambda^2-740880\gamma^3\lambda^2+194481\gamma^4\lambda^2}\right)/(2(-100+100\gamma))$$

$$V_6 = \left(100-200\gamma+105\gamma^2+400\lambda-840\gamma\lambda+441\gamma^2\lambda-\sqrt{\left(-100+200\gamma-105\gamma^2-400\lambda+840\gamma\lambda-441\gamma^2\lambda\right)^2}\right.$$
$$\left.\sqrt{-4(-100+100\gamma)\left(100\gamma-205\gamma^2+105\gamma^3-400\lambda+1240\gamma\lambda-1281\gamma^2\lambda+441\gamma^3\lambda\right)}\right)/(2(-100+100\gamma))$$

$$V_7 = \left(100-200\gamma+105\gamma^2+400\lambda-840\gamma\lambda+441\gamma^2\lambda+\sqrt{\left(-100+200\gamma-105\gamma^2-400\lambda+840\gamma\lambda-441\gamma^2\lambda\right)^2}\right.$$
$$\left.\sqrt{-4(-100+100\gamma)\left(100\gamma-205\gamma^2+105\gamma^3-400\lambda+1240\gamma\lambda-1281\gamma^2\lambda+441\gamma^3\lambda\right)}\right)/(2(-100+100\gamma))$$

Note: V_3, V_4 and V_5 are dependent upon the rate of diffusion d_1. Thus the stability boundary when the eigenvalues V_1, V_2, V_3, V_4, V_5, V_6 and V_7 are equal zero, we have:

i) From V_1, the transcritical bifurcation point is $d_1 = 0$;

ii) From V_2, it is given by $\gamma = \dfrac{530+121\lambda \pm \sqrt{230900-83740\lambda+6241\lambda^2}}{50+210\lambda}$ or

$$\lambda = \frac{5(100-106\gamma+5\gamma^2)}{20-121\gamma+105\gamma^2};$$

iii) From V_3, when we substitute $d_1 = 0.02$, we have

$$\gamma = \frac{1545 \pm 195.5\sqrt{-11.2197+\lambda}\sqrt{-4.58588+\lambda} + 384.5\lambda}{145+609\lambda};$$

iv) From V_4 and V_5 gives a same result, when we substitute $d_1 = 0.02$, we have

2 complex and one real result i.e.

$$\gamma = \Big(1743.33+10822\lambda+\Big((0.209987-0.363708i)\big(-6.0589\times10^6+580440\lambda$$
$$-933156\lambda^2\big)\Big)/\big(-2.86427\times10^{10}+1.43179\times10^{10}\lambda+1.45709\times10^{10}\lambda^2+1.80286$$
$$\times10^9\lambda^3+7.65532\times10^9\sqrt{-1.64109+\lambda}\,(0.238095+\lambda)\sqrt{12.7097+4.52397+\lambda^2}\Big)^{\frac{1}{3}}$$
$$-(0.132283+0.229122i)\big(-2.86427\times10^{10}+1.43179\times10^{10}\lambda+1.43179\times10^{10}\lambda^2$$
$$+1.80286\times10^9\lambda^3+7.65532\times10^9\sqrt{-1.64109+\lambda}\,(0.238095+\lambda)\sqrt{12.7097+}$$
$$\sqrt{4.52397\lambda+\lambda^2}\Big)^{\frac{1}{3}}\Big)/(2625+11025\lambda)$$

$$\gamma = \Big(1743.33+10822\lambda+\Big((0.209987+0.363708i)\big(-6.0589\times10^6+580440\lambda$$
$$-933156\lambda^2\big)\Big)/\big(-2.86427\times10^{10}+1.43179\times10^{10}\lambda+1.45709\times10^{10}\lambda^2+1.80286$$
$$\times10^9\lambda^3+7.65532\times10^9\sqrt{-1.64109+\lambda}\,(0.238095+\lambda)\sqrt{12.7097+4.52397+\lambda^2}\Big)^{\frac{1}{3}}$$
$$-(0.132283-0.229122i)\big(-2.86427\times10^{10}+1.43179\times10^{10}\lambda+1.43179\times10^{10}\lambda^2$$
$$+1.80286\times10^9\lambda^3+7.65532\times10^9\sqrt{-1.64109+\lambda}\,(0.238095+\lambda)\sqrt{12.7097+}$$
$$\sqrt{4.52397\lambda+\lambda^2}\Big)^{\frac{1}{3}}\Big)/(2625+11025\lambda)$$

$$\gamma = \Big(1743.33+10822\lambda+\big(2.54458\times10^6-243770\lambda+391901\lambda^2\big)/\big(-2.86427\times10^{10}$$
$$1.43179\times10^{10}\lambda+1.43179\times10^{10}\lambda^2+1.80286\times10^9\lambda^3+7.65532\times10^9\sqrt{-1.64109+\lambda}$$
$$(0.238095+\lambda)\sqrt{12.7097+4.52397+\lambda^2}\Big)^{\frac{1}{3}}+0.264567\big(-2.86427\times10^{10}+1.43179\times10^{10}\lambda$$
$$1.43179\times10^{10}\lambda^2+1.80286\times10^9\lambda^3+7.65532\times10^9\sqrt{-1.64109+\lambda}\,(0.238095+\lambda)$$
$$\sqrt{12.7097+4.52397\lambda+\lambda^2}\Big)^{\frac{1}{3}}\Big)/(2625+11025\lambda);$$

v) V_6 and V_7 gives a same result, when we substitute $d_1 = 0.02$, we have $\gamma = \frac{20}{21}$ and $\gamma = \frac{20\lambda}{5+21\lambda}$.

Note: The choice of d_1=0.02, is not found in literatures. The value is chosen based on a couple of bifurcation runs that we have done on the later sections, whereby all the rich behaviour are observed at this value.

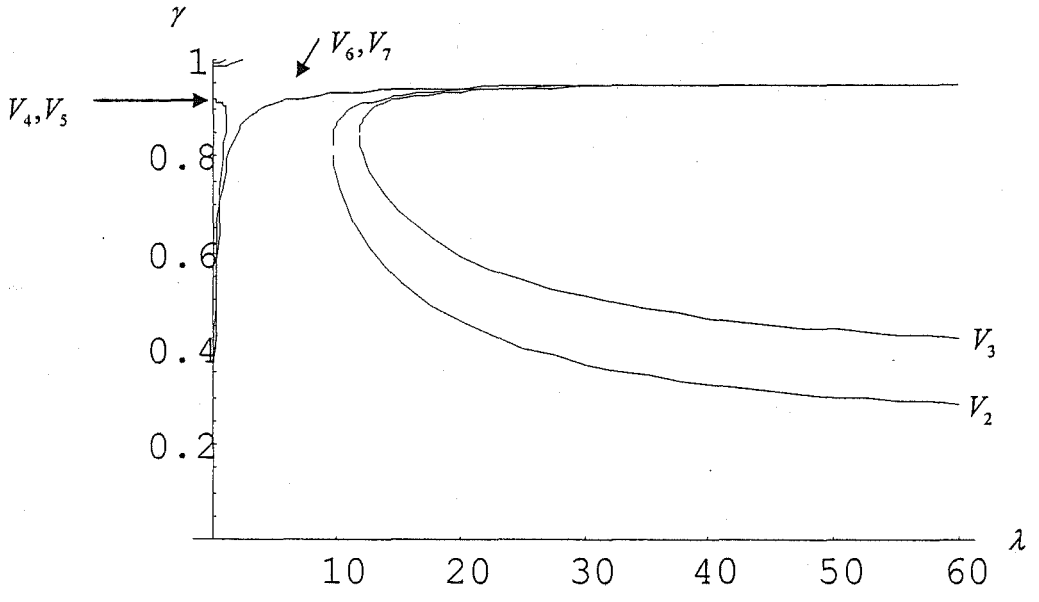

Figure 3.1: The stability boundary such that the eigenvalues $\lambda's$ obtained from $\det(A-\lambda I)=0$ about the steady state E_1 is set to zero (computed by the computer software MATHEMATICA).

3.3.3 The stability of the third steady state E_2

In order to prove that the steady state E_2 is locally stable, equation **(3.1 – 3.7)** are linearized about the steady state E_2 and the determinant of the associated Jacobian matrix is considered. **MATHEMATICA** is again used for this purpose (see **APPENDIX B: MATHEMATICA: B7**). However, it is proved difficult to handle a tedious and complicated quadratic E_2.

To this point only the stability lines or curves have been identified but not the regions of stability of the seven steady states, nor the regions of Hopf bifurcation **(HB)** and limit points **(LP)**. In order to do so, the bifurcation diagrams are explored which is executed by the computer software **AUTO**.

3.4 Bifurcation analysis assuming an equal growth parameter for the phytoplankton ($\mu_1 = \mu_2 = 1$)

So far features of the stability lines or curves have been found which defines the boundary of the three steady state E_0, E_1 and E_2. However, there are possibilities of other regions of stability such as the periodic branch (Hopf bifurcation point) or limit point. This section will describes the bifurcation diagrams for the two compartment model via the software package **XPP** and **AUTO** in **section 2.5**. Auto has the following advantages:

i) identifying the position where one steady states changes to another but not necessarily changes in the stability (**Bifurcation Point** or **BP**), the

coexistence of steady states (**Limit Points** or **LP**) and the presence of any periodic solutions (**Hopf Bifurcation Point** or **HB**); and

ii) confirming the *stability* of the steady state and the periodic branches by grabbing the particular point of interest. It gives the eigenvalues at each point.

(**Note:** it is possible for the equilibrium solutions to be unstable on both sides of a bifurcation points)

For each execution of the bifurcation diagrams we have set all the parameters fixed except for γ and λ. Then we produce bifurcation diagrams for each value of γ between 0.4 and 0.9. Note that, changing the diffusion parameter d_1 produced the same bifurcation diagram at a particular value of γ. For a start, the diffusion parameter is chosen to be $d_1 = 0.02$. Each computation at a particular value of γ provides a one-dimensional cross-section of parameter space, for example the dependent variable x_2 and x_3 against the parameter λ (see **Figure 3.2** to **Figure 3.14**). However, by grabbing a limit point (**LP**) or a Hopf bifurcation point (**HB**) from the bifurcation diagram we can automatically produce a two-parameter diagram such as for the parameter γ against λ (see **Figure 3.15** to Figure **3.26**). However, AUTO cannot extend the bifurcation point **BP** to a two parameter diagram. The procedure for doing a two parameter plot can be found in **section 1.4.2**. The overall diagram shown in **Figure 3.28** combines the results from **MATHEMATICA** and **AUTO**.

In the following paragraphs, let now interpret each of the bifurcation diagrams obtained for our two compartment model ($\mu_1 = \mu_2$) for the value $0.4 < \gamma < 0.9$, starting from the

left-hand side of the diagram and moving towards the right concentrating on the feasible branch. The complete information about the bifurcation points executed by AUTO is summarized in **APPENDIX C: TABLES: T3a**.

i) **Figure 3.2 and Figure 3.3** show the respective bifurcation diagram x_2 and x_3 against the parameter λ, when $\gamma = 0.4$. Viewed from the left to right, the first obvious feature is ufBP1 at the point $\lambda = 0.1434$ (This is the stability curves V_4 or V_5). This is the *unfeasible* steady state *ufss*5 which is unstable everywhere (This cannot be seen from our bifurcation diagram since it is a narrow region which is too short to be obvious). At $\lambda = 0.1724$, the steady state E_0 becomes unstable, and the system moves to the steady state which is stable for larger λ (This is denoted as **BP1** - c.f. **APPENDIX C: TABLES: T3b**; and this correspond to the stability curves V_6 or V_7). An **LP** then occurs at $\lambda = 22.66$, when E_2 is noticeably stable at the *tip* just before the **HB** – indeed, E_2 is simultaneously stable with E_1 until the Hopf bifurcation or the periodic branch (**HB1**) is reached at $\lambda = 24.16$. There is another bifurcation point (**BP2**) at $\lambda = 25.17$ (this is the stability curve V_2 - c.f. **APPENDIX C: TABLES: T3a** and **T3c**), so that E_2 coexists with E_1 from $\lambda = 22.66$ to $\lambda = 25.17$, from $\lambda = 24.16$ to $\lambda = 25.17$ with the **HB** coexisting with E_1. The second unstable periodic orbits **HB2** occurred at $\lambda = 31.4$. Other unstable unfeasible steady states occur at $\lambda = 55.94$ are *ufss*2 and *ufss*3 (This is the stability curve V_3 from **Figure 3.1**) and *ufss*1 is stable, but is ignored because x_3 is negative (c.f. the bifurcation diagram of x_3 against λ in **Figure 3.3**) it is not seen in the diagram.

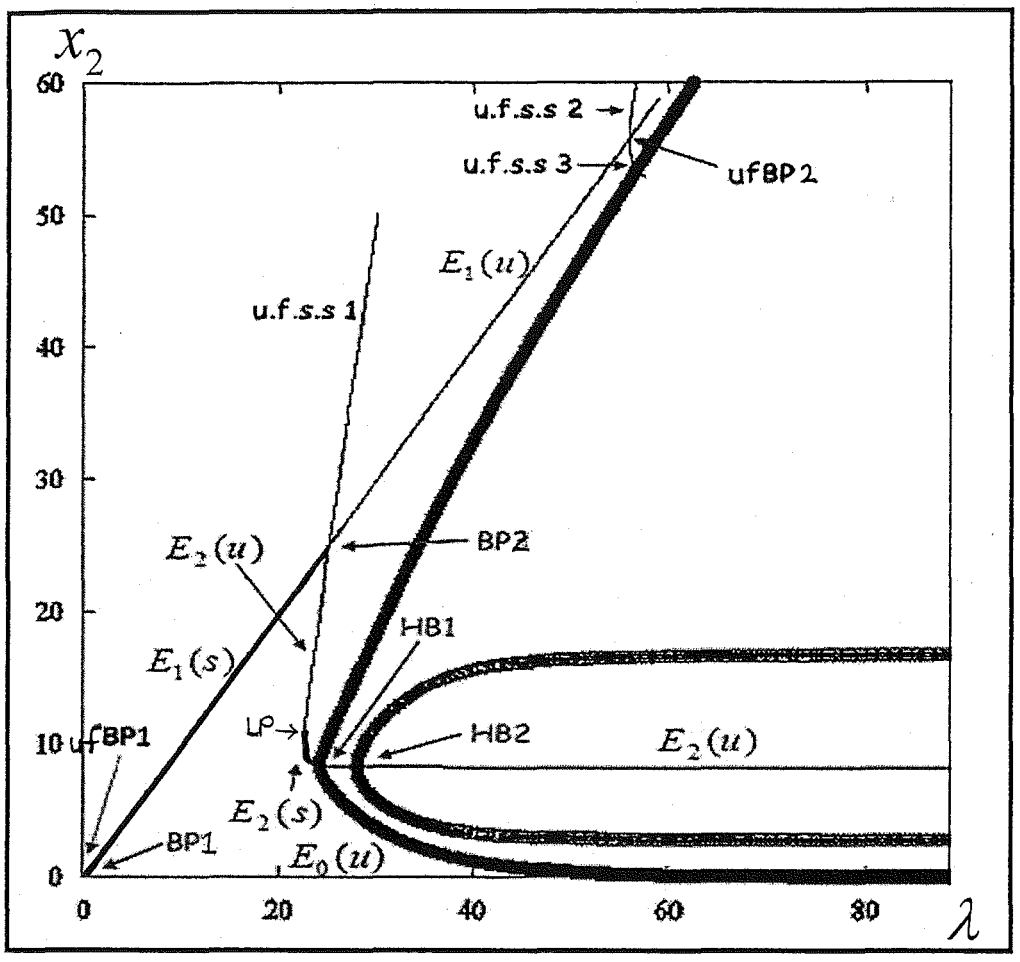

Figure 3.2: The bifurcation diagram x_2 against λ for two compartment model ($\mu_1 = \mu_2$) when $\gamma = 0.4$ and $d_1 = 0.02$ showing the bifurcation points BP1 (λ=0.1724), BP2 (λ=25.17); Limit point LP (λ=22.66) and the Hopf bifurcation points HB1 (λ=24.16) and unstable HB2 (λ=28.07). Other unfeasible steady state found are of the form u.f.s.s1 = $(x_1, x_2, -x_3, x_1, x_2, -x_3, y_4)$, u.f.s.s2 = $(x_1, x_2, -x_3, y_1, y_2, y_3, y_4)$ and u.f.s.s3 = $(x_1, x_2, x_3, y_1, y_2, -y_3, y_4)$; thus the unfeasible bifurcation points are ufBP1 (λ=0.1434) and ufBP2 (λ= 55.94).

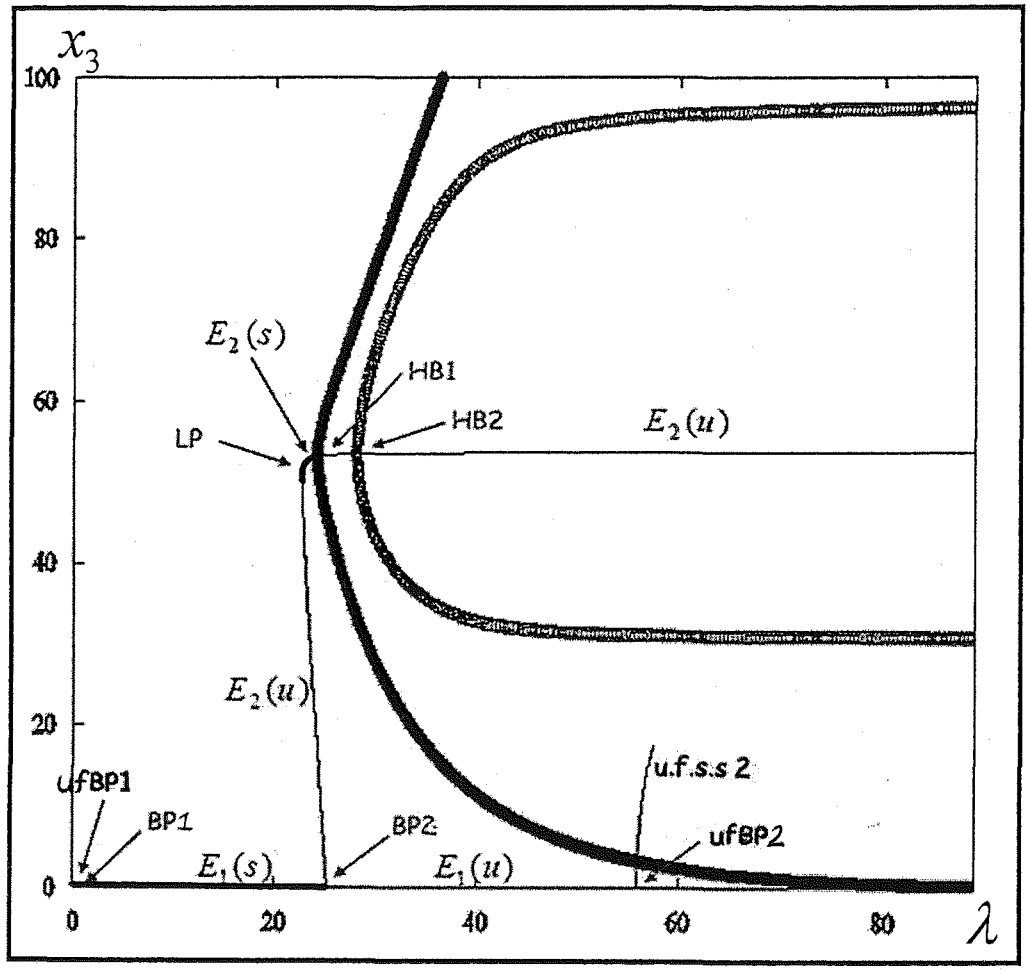

Figure 3.3: The bifurcation diagram x_3 against λ for two compartment model ($\mu_1 = \mu_2$) when $\gamma = 0.4$ and $d_1 = 0.02$ showing the bifurcation points BP1 (λ=0.1724), BP2 (λ=25.17); Limit point LP (λ=22.66) and the Hopf bifurcation points HB1 (λ=24.16) HB2 (λ=28.07). Other unfeasible steady state found is of the form u.f.s.s2 = $(x_1, x_2, -x_3, y_1, y_2, y_3, y_4)$ and thus the unfeasible bifurcation points are ufBP1 (λ=0.1434) and ufBP2 (λ= 55.94).

ii) **Figure 3.4 and Figure 3.5** show the respective bifurcation diagram x_2 and x_3 against the parameter λ, when $\gamma = 0.45$. Viewed from the left to right,

the first obvious feature is ufBP1 at the point $\lambda = 0.1784$ (This is the stability curves V_4 or V_5). This is the *unfeasible* steady state *ufss*5 which is unstable everywhere (This cannot be seen from our bifurcation diagram since it is a narrow region which is too short to be obvious). At $\lambda = 0.2132$, the steady state E_0 changes from stable to unstable and the steady state E_1 occurs (This is denoted as **BP1** and this correspond to the stability curves V_6 or V_7 - c.f. **APPENDIX C: TABLES: T3b**). The next bifurcation point (**BP2**) at $\lambda = 20.21$, where E_1 becomes unstable and the stable E_2 branch occurs (this is the stability curves V_2 - c.f. **APPENDIX C: TABLES: T3a** and **T3c**). Periodicity then follows at the Hopf bifurcation point (**HB1**) at $\lambda = 22.55$ and the second Hopf bifurcation point (**HB2**) is at $\lambda = 31.4$, which produces unstable periodic orbits. Other unstable unfeasible steady states at occur $\lambda = 36.02$ are *ufss*2 and *ufss*3 (This is the stability curve V_3 from **Figure 3.1**) and *ufss*1 is seen unstable. Thus, the difference between the bifurcation diagram when $\gamma = 0.40$ and $\gamma = 0.45$ is that the former has a limit point **LP** whilst the latter does not. However, both have two Hopf bifurcation points **HB**; one giving a stable periodic orbits and the other produce an unstable periodic orbits.

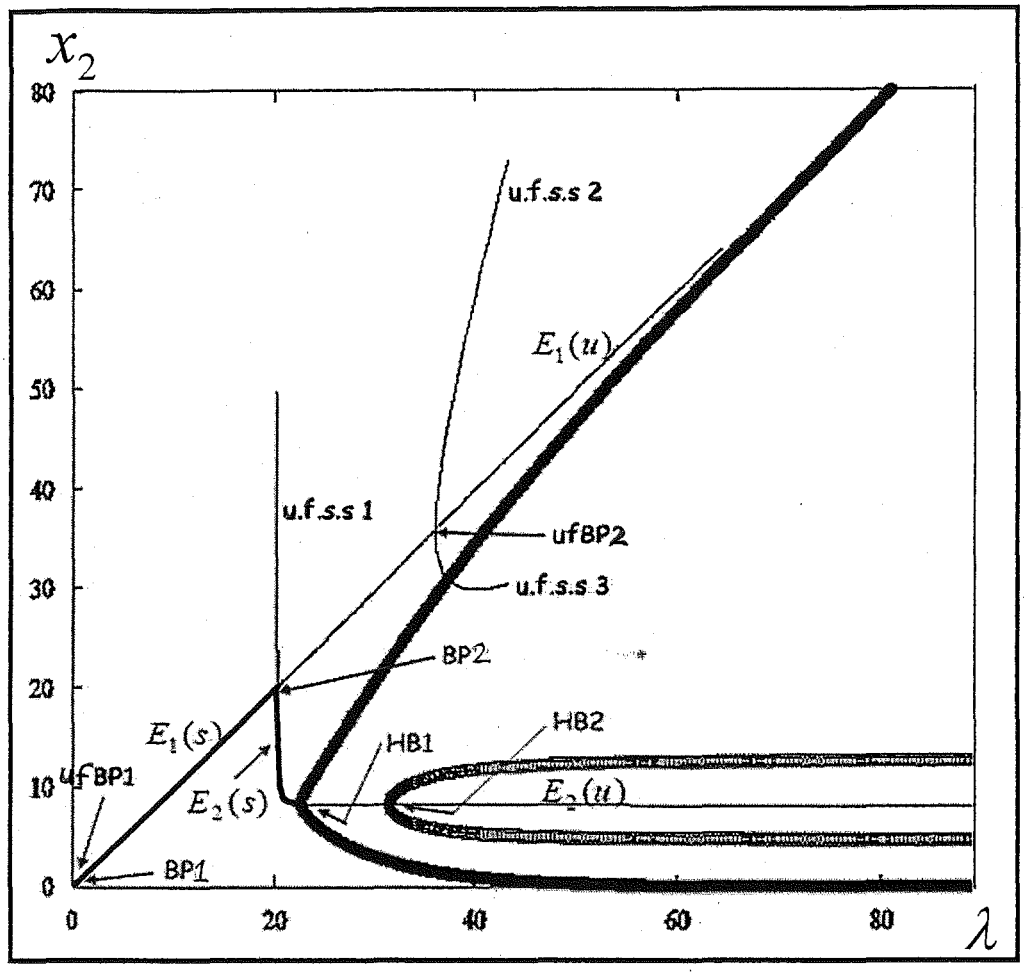

Figure 3.4: The bifurcation diagram x_2 against λ for two compartment model ($\mu_1 = \mu_2$) when $\gamma = 0.45$ and $d_1 = 0.02$ showing the bifurcation points BP1 (λ=0.2132), BP2 (λ=20.21) and the Hopf bifurcation points HB1 (λ=22.55) and unstable HB2 (λ=31.4). Other unfeasible steady state found are of the form u.f.s.s1 = $(x_1, x_2, -x_3, x_1, x_2, -x_3, y_4)$, u.f.s.s2 = $(x_1, x_2, -x_3, y_1, y_2, y_3, y_4)$ and u.f.s.s3 = $(x_1, x_2, x_3, y_1, y_2, -y_3, y_4)$; thus the unfeasible bifurcation points are ufBP1 (λ=0.1784) and ufBP2 (λ= 36.02).

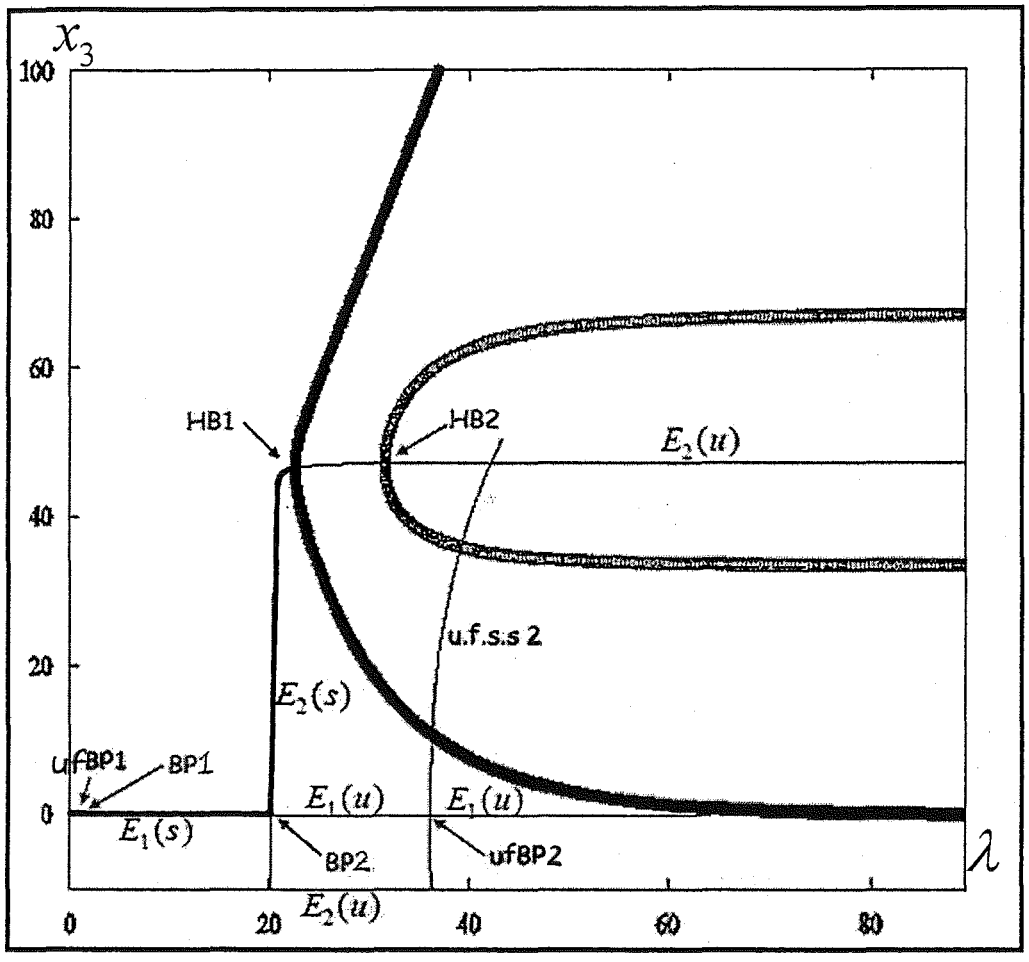

Figure 3.5: The bifurcation diagram x_3 against λ for two compartment model ($\mu_1 = \mu_2$) when $\gamma = 0.45$ and $d_1 = 0.02$ showing the bifurcation points BP1 (λ=0.2132), BP2 (λ=20.21) and the Hopf bifurcation points HB1 (λ=22.55) and unstable HB2 (λ=31.4). Other unfeasible steady state found is of the form u.f.s.s2 = $(x_1, x_2, -x_3, y_1, y_2, y_3, y_4)$ and thus the unfeasible bifurcation points are ufBP1 (λ=0.1784) and ufBP2 (λ= 36.02).

iii) **Figure 3.6** and **Figure 3.7** show the respective bifurcation diagram x_2 and x_3 against the parameter λ, when $\gamma = 0.5$. Viewed from the left to right, the first obvious feature is ufBP1 at the point $\lambda = 0.2205$ (This is the stability curves V_4 or V_5). This is the *unfeasible* steady state *ufss*5 which is unstable everywhere (This cannot be seen from our bifurcation diagram since it is a narrow region which is too short to be obvious). At $\lambda = 0.2631$, the steady state E_0 changes from stable to unstable and the steady state E_1 occurs (This is denoted as **BP1** and this is the stability curves V_6 or V_7 - c.f. **APPENDIX C: TABLES: TABLE3b**). The next bifurcation point (**BP2**) at $\lambda = 16.93$, where E_1 becomes unstable and the stable E_2 branch occurs (this is the stability curve V_2 - c.f. **APPENDIX C: TABLES: T3a** and **T3c**). Periodicity then follows at the Hopf bifurcation point (**HB1**) at $\lambda = 20.96$. Other unstable unfeasible steady states at occur $\lambda = 26.63$ are *ufss*2 and *ufss*3 (This is the stability curve V_3 from **Figure 3.1**) and *ufss*1 is seen unstable. The bifurcation diagram when $\gamma = 0.45$ and $\gamma = 0.5$ has a similar structure; both has no limit point which is found when $\gamma = 0.4$. However, when $\gamma = 0.45$, there are two Hopf bifurcation points (**HB**) such that one produced the stable and the other unstable periodic orbits in which when $\gamma = 0.5$, only the Hopf bifurcation point (**HB**) which produce the stable periodic orbits is visible.

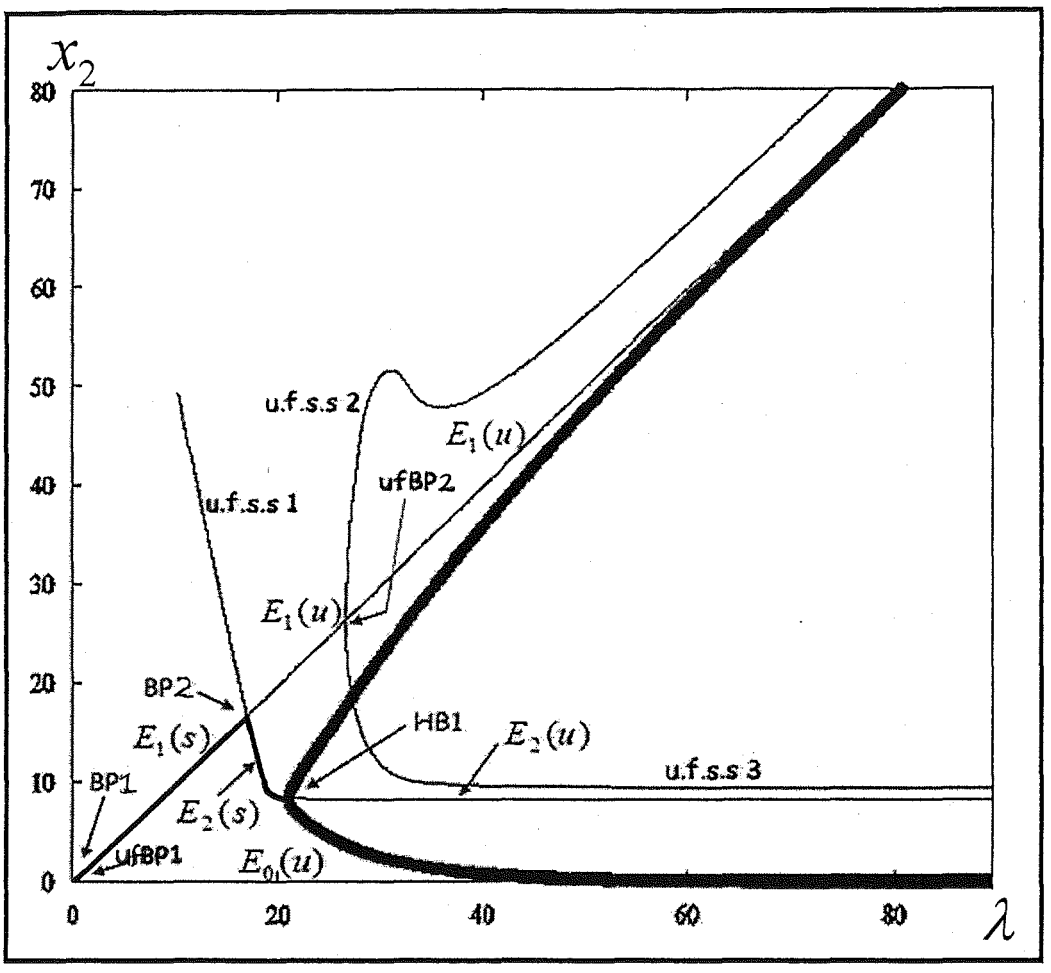

Figure 3.6: The bifurcation diagram x_2 against λ for two compartment model ($\mu_1 = \mu_2$) when $\gamma = 0.5$ and $d_1 = 0.02$ showing the bifurcation points BP1 (λ=0.2631), BP2 (λ=16.93) and the Hopf bifurcation points HB1 (λ=20.96). Other unfeasible steady state found are of the form u.f.s.s1 = $(x_1, x_2, -x_3, x_1, x_2, -x_3, y_4)$, u.f.s.s2 = $(x_1, x_2, -x_3, y_1, y_2, y_3, y_4)$ and u.f.s.s3 = $(x_1, x_2, x_3, y_1, y_2, -y_3, y_4)$; thus the unfeasible bifurcation points are ufBP1 (λ=0.2205) and ufBP2 (λ= 26.63).

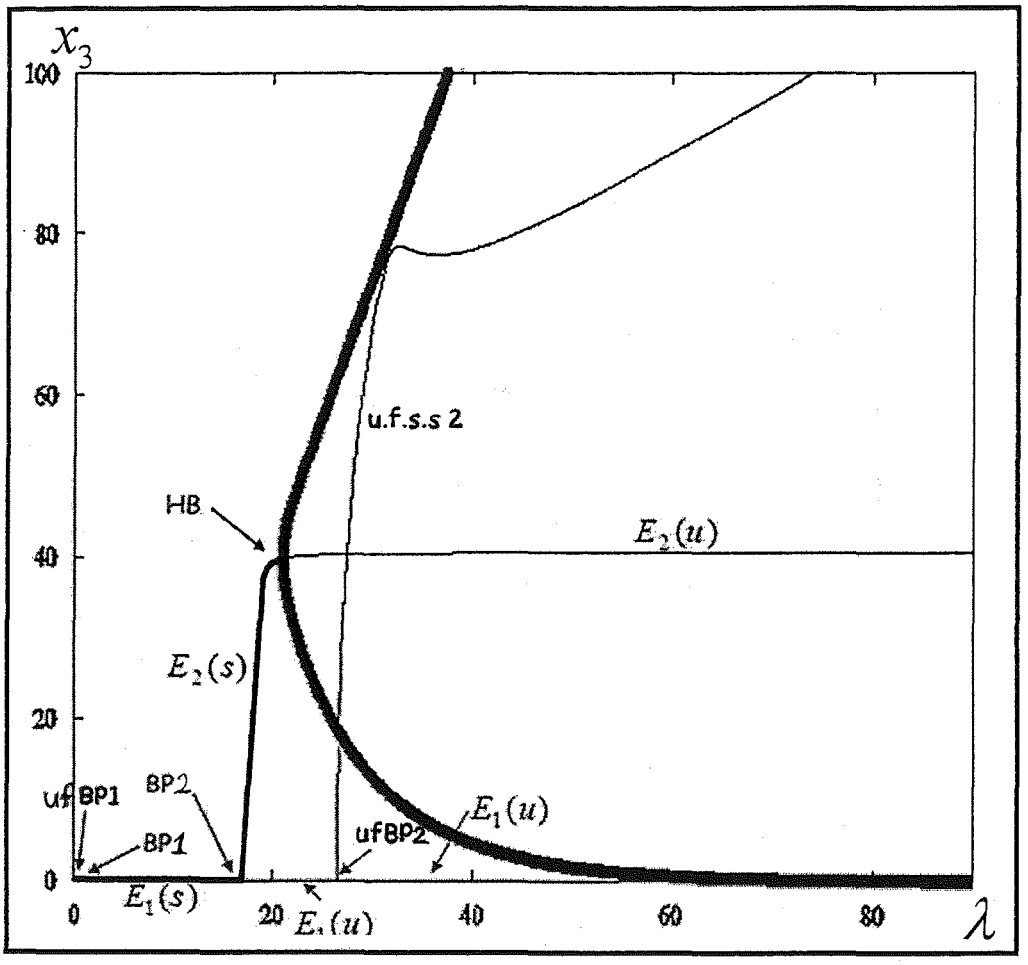

Figure 3.7: The bifurcation diagram x_3 against λ for two compartment model ($\mu_1 = \mu_2$) when $\gamma = 0.5$ and $d_1 = 0.02$ showing the bifurcation points BP1 (λ=0.2631), BP2 (λ=16.93) and the Hopf bifurcation points HB1 (λ=20.96). Other unfeasible steady state found is of the form u.f.s.s2 = $(x_1, x_2, -x_3, y_1, y_2, y_3, y_4)$ and thus the unfeasible bifurcation points are ufBP1 (λ=0.2205) and ufBP2 (λ= 26.63).

iv) **Figure 3.8** and **Figure 3.9** show the respective bifurcation diagram x_2 and x_3 against the parameter λ, when $\gamma = 0.6$. Viewed from the left to right, the first obvious feature is ufBP1 at the point $\lambda = 0.3363$ (This is the stability curves V_4 or V_5). This is the *unfeasible* steady state *ufss*5 which is unstable everywhere (This cannot be seen from our bifurcation diagram since it is a narrow region which is too short to be obvious). At $\lambda = 0.4054$, the steady state E_0 changes from stable to unstable and the steady state E_1 occurs (This is denoted as **BP1** and this is the stability curves V_6 or V_7 - c.f. **APPENDIX C: TABLES: T3b**). The next bifurcation point (**BP2**) occurs at $\lambda = 12.91$ (this is the stability curve V_2 c.f. **APPENDIX C: TABLES: T3a** and **T3c**), where E_1 becomes unstable and the stable E_2 branch occurs. Periodicity then follows at the Hopf bifurcation point (**HB1**) at $\lambda = 17.91$. Other unfeasible steady states at occur $\lambda = 4.444$ (ufBP2) is the unfeasible steady state *ufss*4 and at $\lambda = 17.67$ (ufBP3) are *ufss*2 and *ufss*3 (This is the stability curve V_3 from **Figure 3.1**) and *ufss*1 is seen unstable. The bifurcation diagram when $\gamma = 0.5$ and $\gamma = 0.6$ both have the same structure.

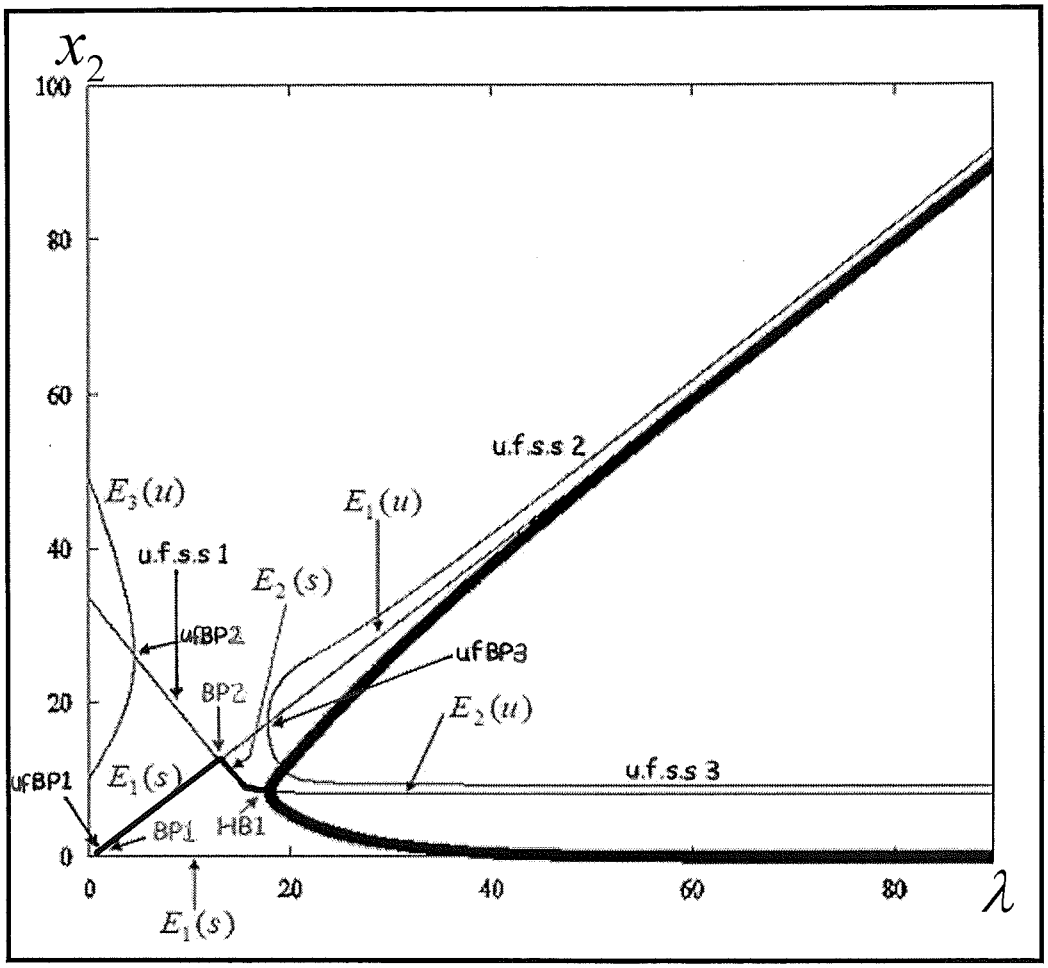

Figure 3.8: The bifurcation diagram x_2 against λ for two compartment model ($\mu_1 = \mu_2$) when $\gamma = 0.6$ and $d_1 = 0.02$ showing the bifurcation points BP1 (λ=0.4054), BP2 (λ=12.91) and the Hopf bifurcation points HB1 (λ=17.91). Other unfeasible steady state found are of the form u.f.s.s1 = $(x_1, x_2, -x_3, x_1, x_2, -x_3, y_4)$, u.f.s.s2 = $(x_1, x_2, -x_3, y_1, y_2, y_3, y_4)$ and u.f.s.s3 = $(x_1, x_2, x_3, y_1, y_2, -y_3, y_4)$; thus the unfeasible bifurcation points are ufBP1 (λ=0.3363), ufBP2 (λ= 4.444) and ufBP3 (λ= 17.67).

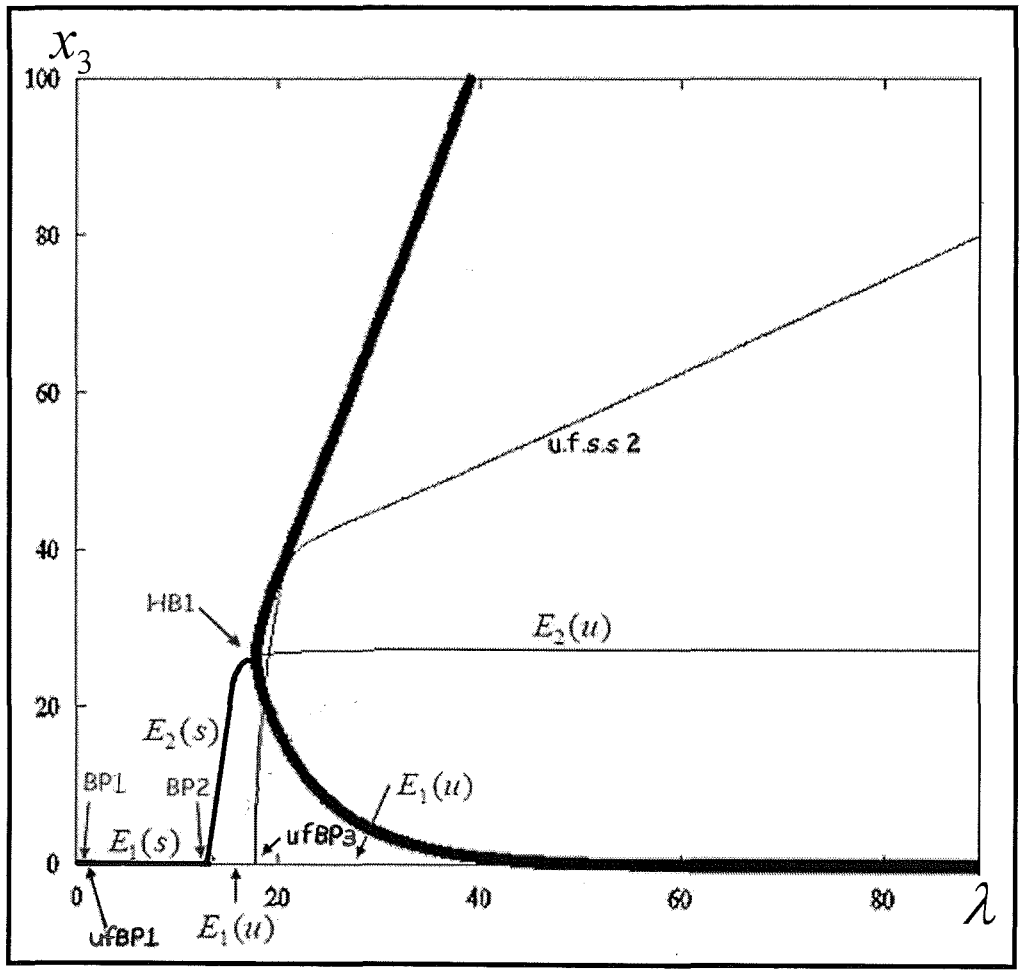

Figure 3.9: The bifurcation diagram x_3 against λ for two compartment model ($\mu_1 = \mu_2$) when $\gamma = 0.6$ and $d_1 = 0.02$ showing the bifurcation points BP1 (λ=0.4054), BP2 (λ=12.91) and the Hopf bifurcation points HB1 (λ=17.91). Other unfeasible steady state found is of the form u.f.s.s2 = $(x_1, x_2, -x_3, y_1, y_2, y_3, y_4)$ and thus the unfeasible bifurcation points are ufBP1 (λ=0.3363), ufBP2 (λ= 4.444) and ufBP3 (λ= 17.67).

v) **Figure 3.10** and **Figure 3.11** show the respective bifurcation diagram x_2 and x_3 against the parameter λ, when $\gamma = 0.7$. Viewed from the left to

right, the first obvious feature is ufBP1 at the point $\lambda = 0.5295$ (This is the stability curves V_4 or V_5). This is the *unfeasible* steady state *ufss*5 which is unstable everywhere (This cannot be seen from our bifurcation diagram since it is a narrow region which is too short to be obvious). At $\lambda = 0.6606$, the steady state E_0 changes from stable to unstable and the steady state E_1 occurs (This is denoted as **BP1** - see **APPENDIX C: TABLES: T3b** and this is the stability curves V_6 or V_7). The next bifurcation point (**BP2**) occurs at $\lambda = 10.66$, where E_1 becomes unstable and the stable E_2 branch occurs (this is the stability curve V_2 - c.f. **APPENDIX C: TABLES: T3a** and **T3c**). Periodicity then follows at the Hopf bifurcation point (**HB1**) at $\lambda = 15.34$. Other unfeasible steady states at occur $\lambda = 7.259$ (ufBP2) is the unfeasible steady state *ufss*4 and at $\lambda = 13.49$ (ufBP3) are *ufss*2 and *ufss*3 (This is the stability curve V_3 from **Figure 3.1**) and *ufss*1 is seen unstable. Thus the bifurcation diagram when $\gamma = 0.7$ has a similar structure as those when $\gamma = 0.5$ and $\gamma = 0.6$.

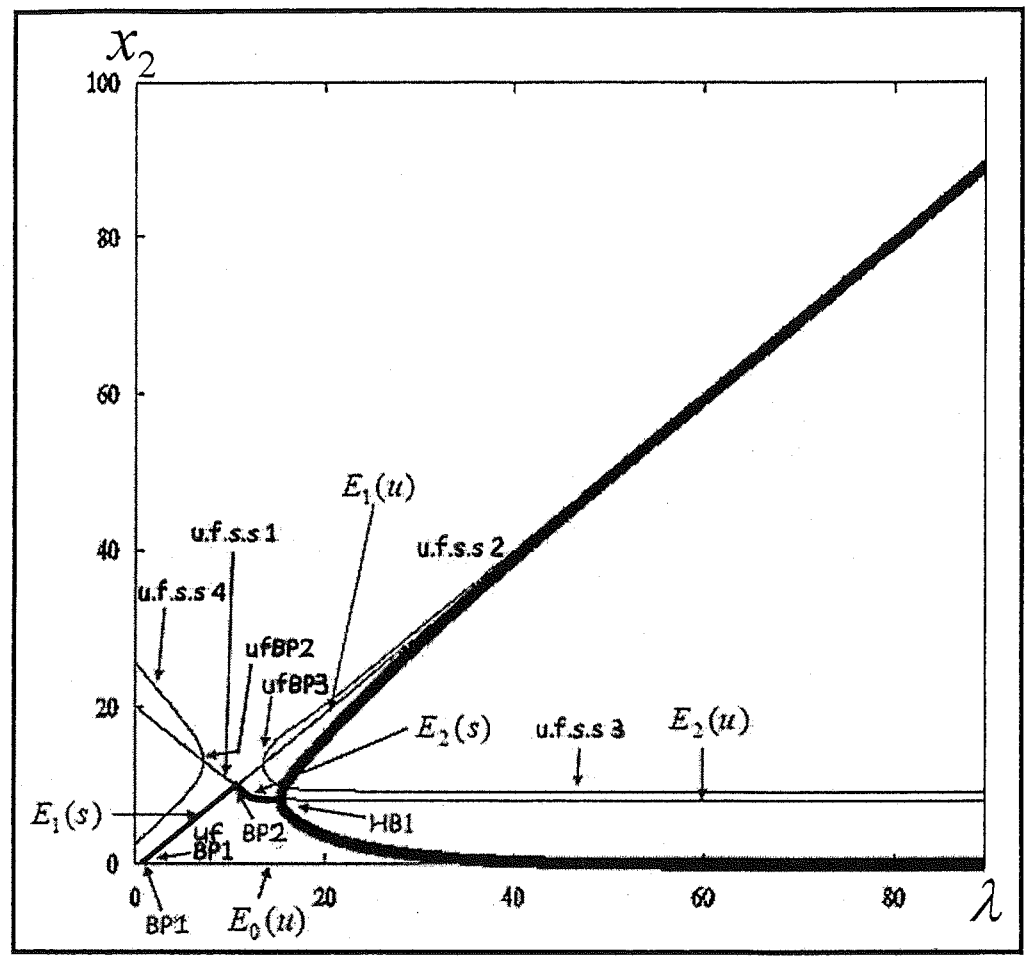

Figure 3.10: The bifurcation diagram x_2 against λ for two compartment model ($\mu_1 = \mu_2$) when $\gamma = 0.7$ and $d_1 = 0.02$ showing the bifurcation points BP1 (λ=0.6606), BP2 (λ=10.66) and the Hopf bifurcation points HB1 (λ=15.34). Other unfeasible steady state found are of the form u.f.s.s1 = $(x_1, x_2, -x_3, x_1, x_2, -x_3, y_4)$, u.f.s.s2 = $(x_1, x_2, -x_3, y_1, y_2, y_3, y_4)$, u.f.s.s3 = $(x_1, x_2, x_3, y_1, y_2, -y_3, y_4)$ and u.f.s.s4 = $(x_1, x_2, -x_3, y_1, y_2, -y_3, y_4)$; thus the unfeasible bifurcation points are ufBP1 (λ=0.5295), ufBP2 (λ= 7.259) and ufBP3 (λ= 13.47).

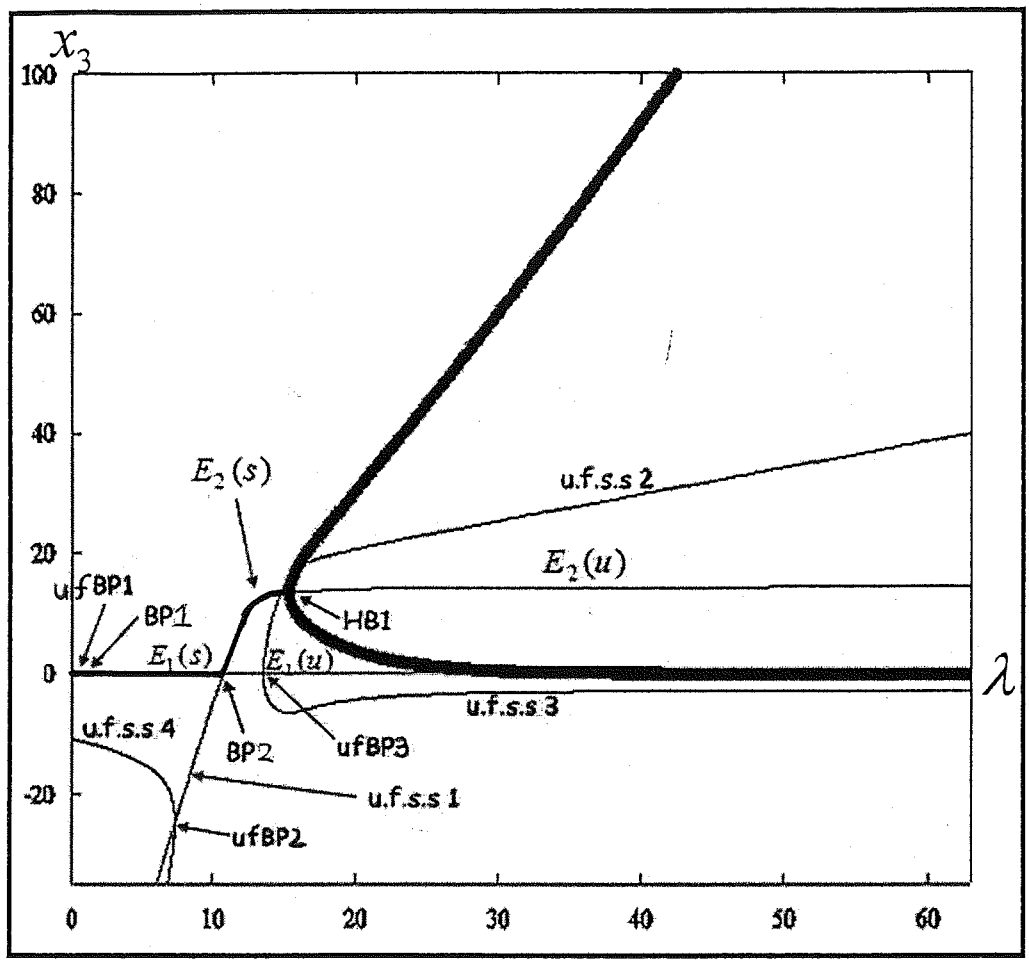

Figure 3.11: The bifurcation diagram x_3 against λ for two compartment model ($\mu_1 = \mu_2$) when $\gamma = 0.7$ and $d_1 = 0.02$ showing the bifurcation points BP1 (λ=0.6606), BP2 (λ=10.66) and the Hopf bifurcation points HB1 (λ=15.34). Other unfeasible steady state found are of the form u.f.s.s1 = $(x_1, x_2, -x_3, x_1, x_2, -x_3, y_4)$, u.f.s.s2 = $(x_1, x_2, -x_3, y_1, y_2, y_3, y_4)$, u.f.s.s3 = $(x_1, x_2, x_3, y_1, y_2, -y_3, y_4)$ and u.f.s.s4 = $(x_1, x_2, -x_3, y_1, y_2, -y_3, y_4)$; thus the unfeasible bifurcation points are ufBP1 (λ=0.5295), ufBP2 (λ= 7.259) and ufBP3 (λ= 13.47).

Figure 3.12 and **Figure 3.13** show the respective bifurcation diagram x_2 and x_3 against the parameter λ, when $\gamma = 0.8$. Viewed from the left

to right, the first obvious feature is ufBP1 at the point $\lambda = 0.1784$ (This is the stability curves V_4 or V_5). This is the *unfeasible* steady state *ufss*5 which is unstable everywhere (This cannot be seen from our bifurcation diagram since it is a narrow region which is too short to be obvious). At $\lambda = 3.336$, the steady state E_0 changes from stable to unstable and the steady state E_1 occurs (This is denoted as **BP1** – c.f. **APPENDIX C: TABLES: T3b** and this is the stability curves V_6 or V_7). The next bifurcation point (**BP2**) occurs at $\lambda = 11.67$, where E_1 becomes unstable and the stable E_2 branch occurs (this is the stability V_2 - c.f. **APPENDIX C: TABLES: T3a** and **T3c**). Periodicity then follows at the Hopf bifurcation point (HB1) at $\lambda = 21.82$. Other unfeasible steady states occur at $\lambda = 7.361$ (ufBP2) is the unfeasible steady state *ufss*4 and at $\lambda = 13.54$ (ufBP3) are *ufss*2 and *ufss*3 (This is the stability V_3 from **Figure 3.1**) and *ufss*1 is seen unstable. Thus the bifurcation diagram when $\gamma = 0.8$ has a similar structure as those when $\gamma = 0.5$, $\gamma = 0.6$ and $\gamma = 0.7$.

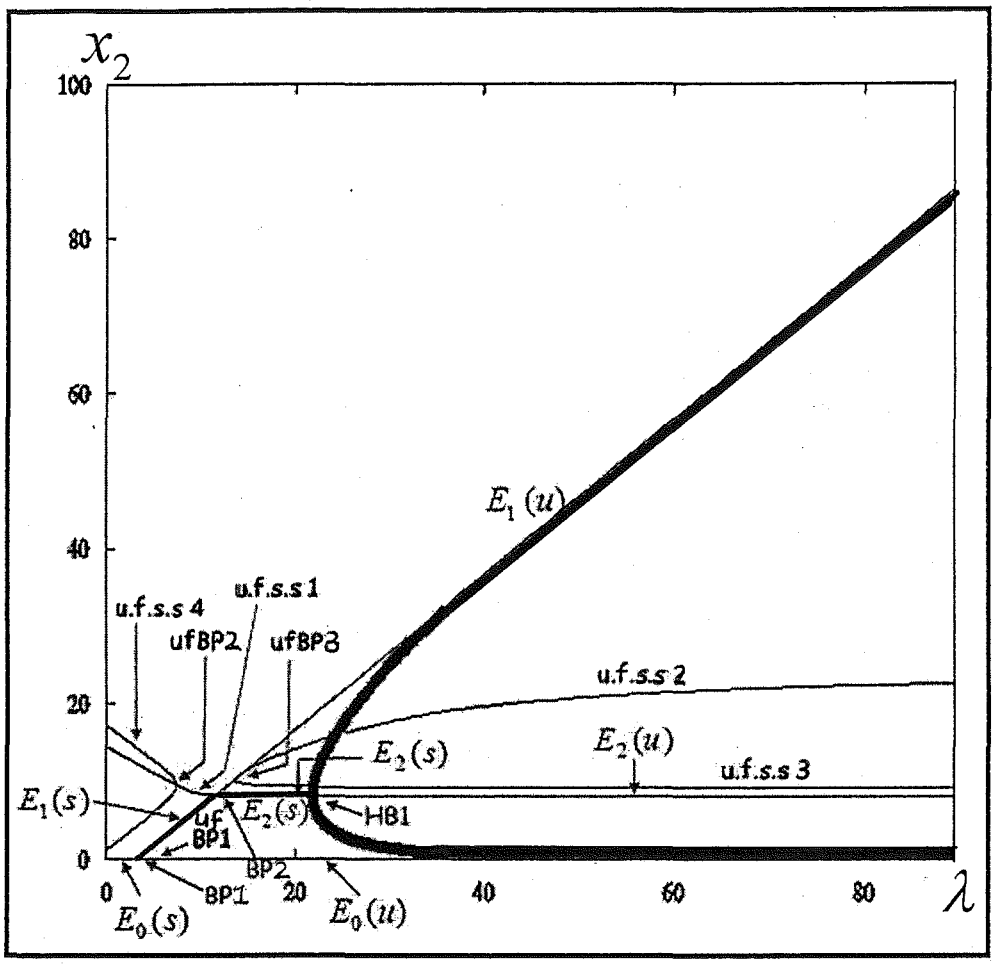

Figure 3.12: The bifurcation diagram x_2 against λ for two compartment model ($\mu_1 = \mu_2$) when $\gamma = 0.8$ and $d_1 = 0.02$ showing the bifurcation points BP1 (λ=3.336), BP2 (λ=11.67) and the Hopf bifurcation points HB1 (λ=21.82). Other unfeasible steady state found are of the form u.f.s.s1 = $(x_1, x_2, -x_3, x_1, x_2, -x_3, y_4)$, u.f.s.s2 = $(x_1, x_2, -x_3, y_1, y_2, y_3, y_4)$, u.f.s.s3 = $(x_1, x_2, x_3, y_1, y_2, -y_3, y_4)$ and u.f.s.s4 = $(x_1, x_2, -x_3, y_1, y_2, -y_3, y_4)$; thus the unfeasible bifurcation points are ufBP1 (λ=0.1784), ufBP2 (λ= 7.361) and ufBP3 (λ= 13.54).

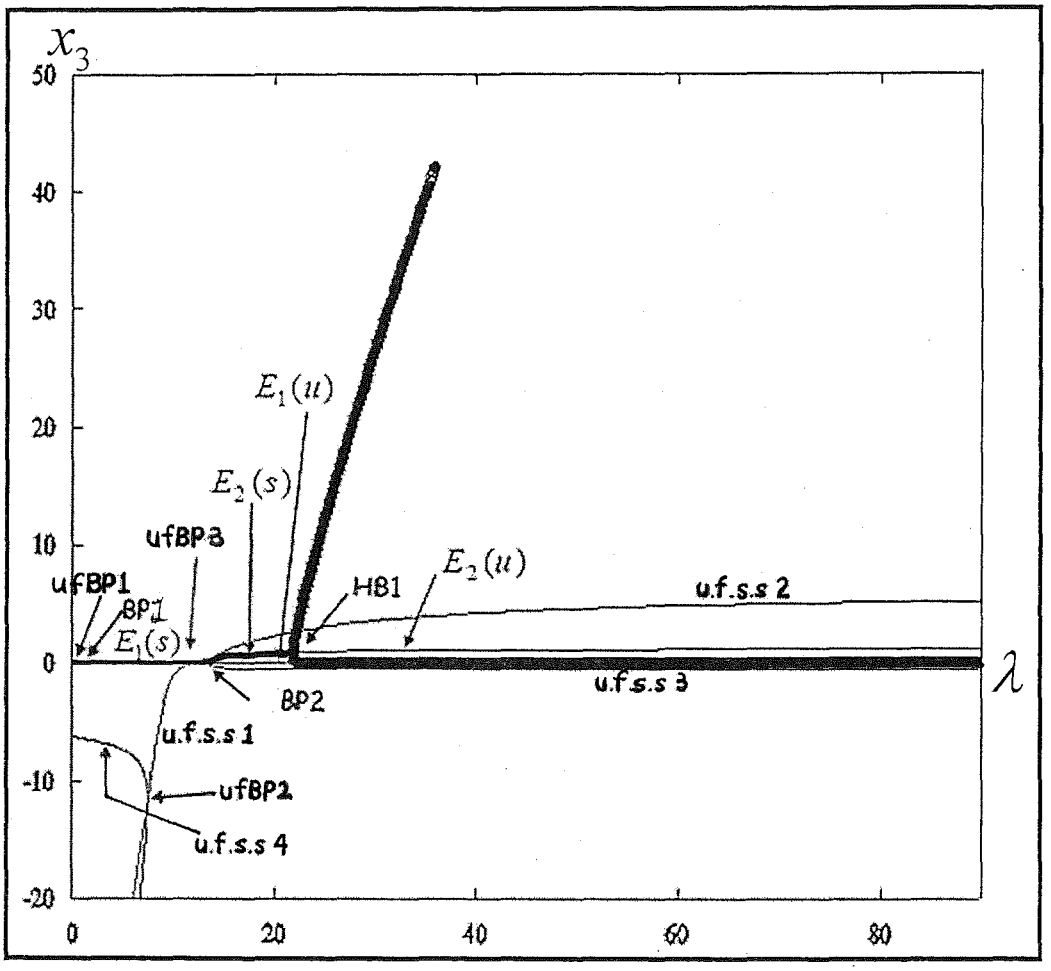

Figure 3.13: The bifurcation diagram x_3 against λ for two compartment model ($\mu_1 = \mu_2$) when $\gamma = 0.8$ and $d_1 = 0.02$ showing the bifurcation points BP1 (λ=3.336), BP2 (λ=11.67) and the Hopf bifurcation points HB1 (λ=21.82). Other unfeasible steady state found are of the form u.f.s.s1 = $(x_1, x_2, -x_3, x_1, x_2, -x_3, y_4)$, u.f.s.s2 = $(x_1, x_2, -x_3, y_1, y_2, y_3, y_4)$, u.f.s.s3 = $(x_1, x_2, x_3, y_1, y_2, -y_3, y_4)$ and u.f.s.s4 = $(x_1, x_2, -x_3, y_1, y_2, -y_3, y_4)$; thus the unfeasible bifurcation points are ufBP1 (λ=0.1784), ufBP2 (λ= 7.361) and ufBP3 (λ= 13.54).

vi) **Figure 3.14** shows the bifurcation diagram x_2 against the parameter λ when $\gamma = 0.9$. It is seen the steady state E_0 is the only steady state is stable at this point.

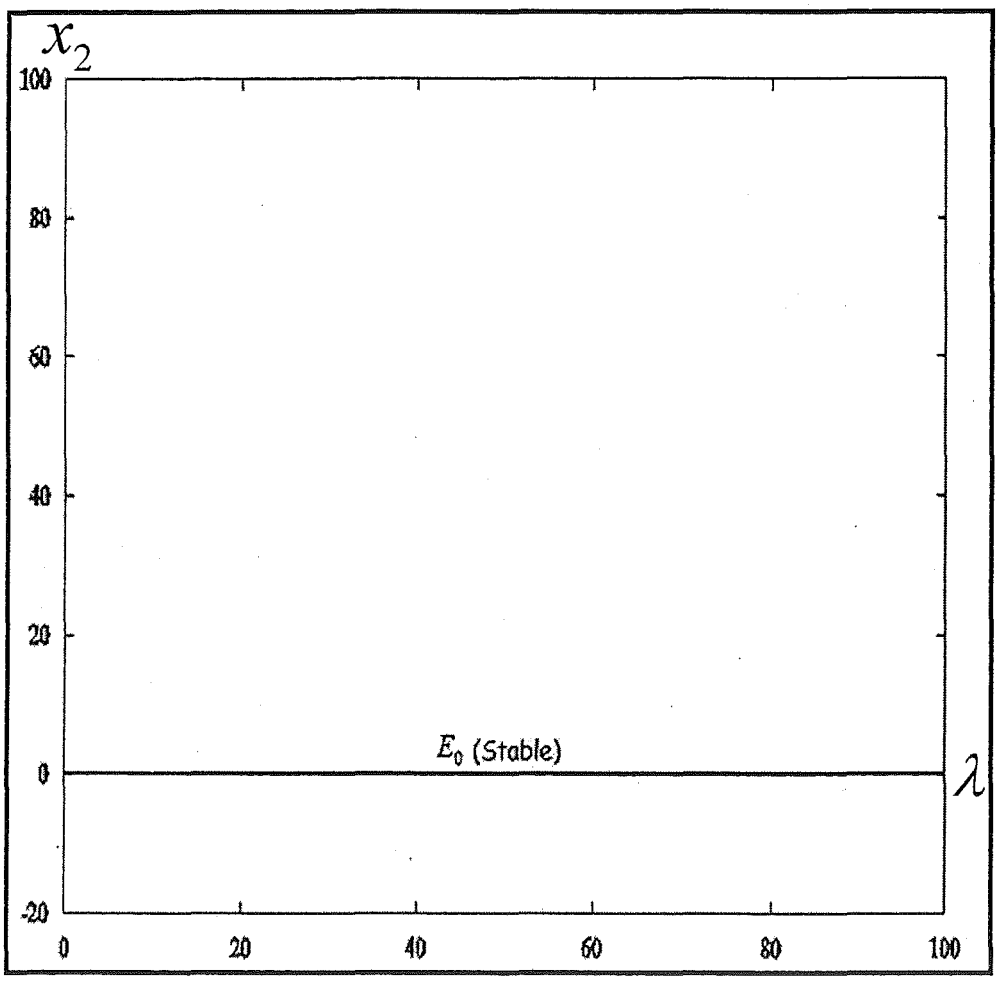

Figure 3.14: The bifurcation diagram x_3 against λ for two compartment model ($\mu_1 = \mu_2$) when $\gamma = 0.9$ and $d_1 = 0.02$ showing that only the steady state E_0 is stable.

vii) **Figure 3.15 to Figure 3.26** show the two parameter diagram γ and λ with varying d_1 between 0.1 and 0.005. It shows the extension of the **LP** and **HB** points (one which produces a stable periodic orbit and the other unstable periodic orbits). It shows that as d_1 is getting large the Hopf point which produces the unstable periodic orbits (**HB2**) is getting to the right of the diagram and vanishes, that is why it is not seen in **Figure 3.15** when $d_1 = 0.1$. It is first seen at $d_1 = 0.024$ and lower values. However, as we observed from **Figure 3.18** to **Figure 3.26** as d_1 gets smaller, the unstable Hopf point (**HB2**) is getting to the left and overlap with the stable Hopf point (**HB1**). Thus we see that for a one compartment model when $d_1 = 0$, the unstable Hopf point (**HB2**) is not present.

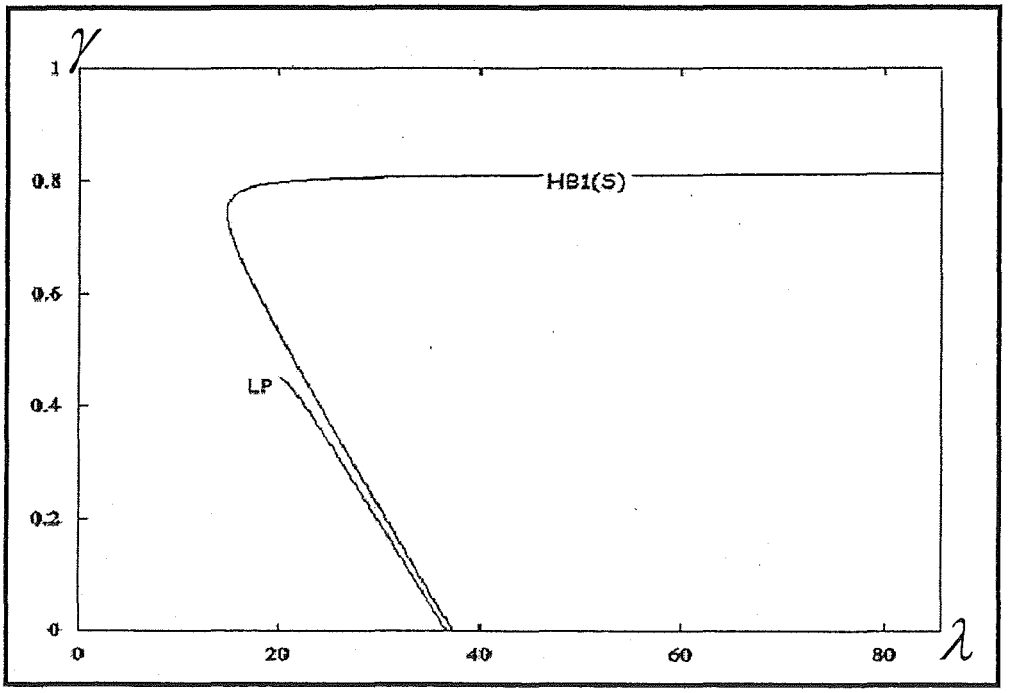

Figure 3.15: The two parameter plot γ against λ for two compartment model ($\mu_1 = \mu_2$) at $d_1 = 0.1$.

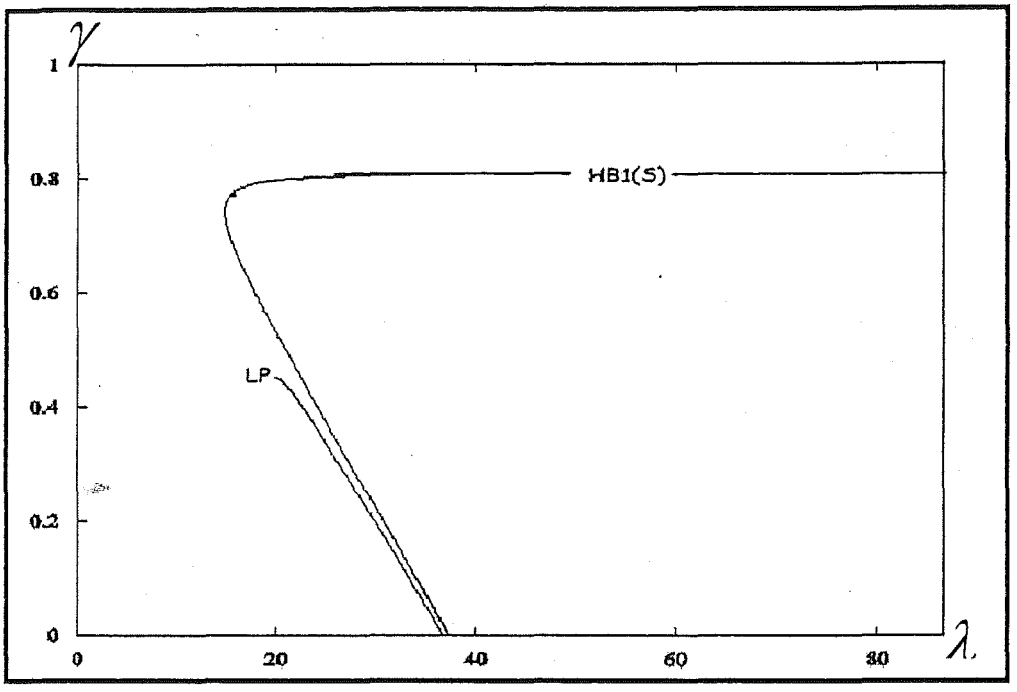

Figure 3.16: The two parameter plot γ against λ for two compartment model $(\mu_1 = \mu_2)$ at $d_1 = 0.03$.

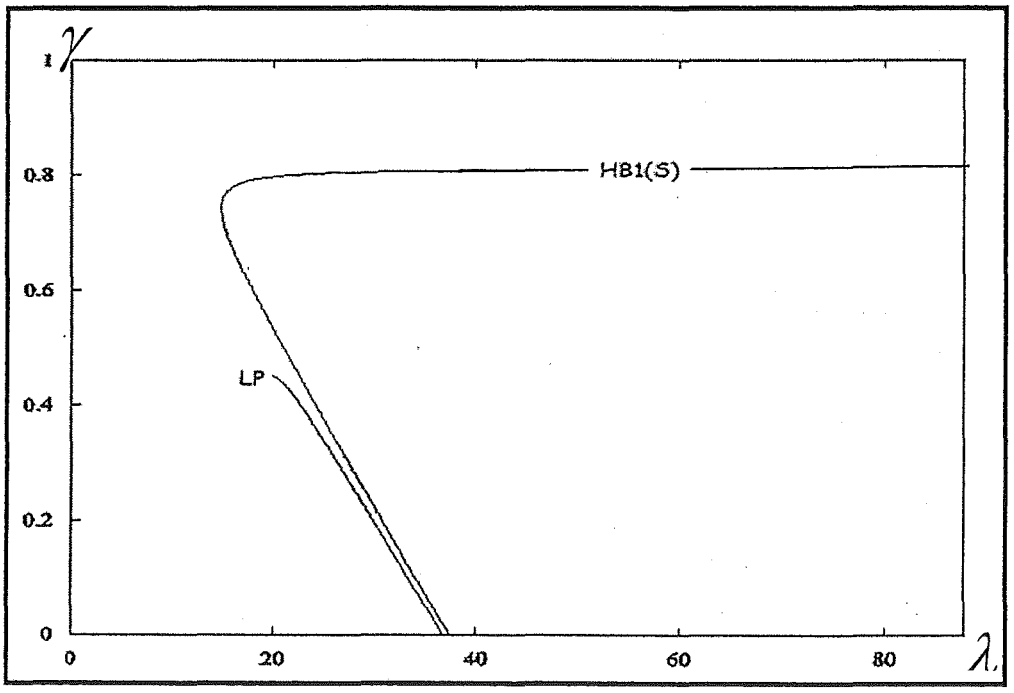

Figure 3.17: The two parameter plot γ against λ for two compartment model $(\mu_1 = \mu_2)$ at $d_1 = 0.026$.

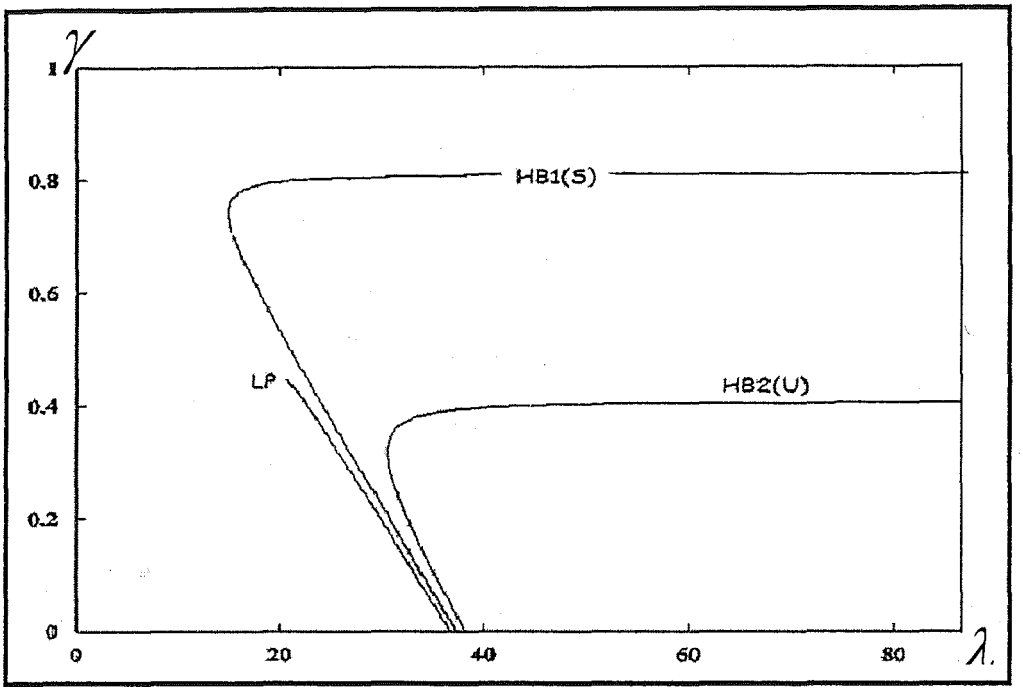

Figure 3.18: The two parameter plot γ against λ for two compartment model $(\mu_1 = \mu_2)$ at $d_1 = 0.024$.

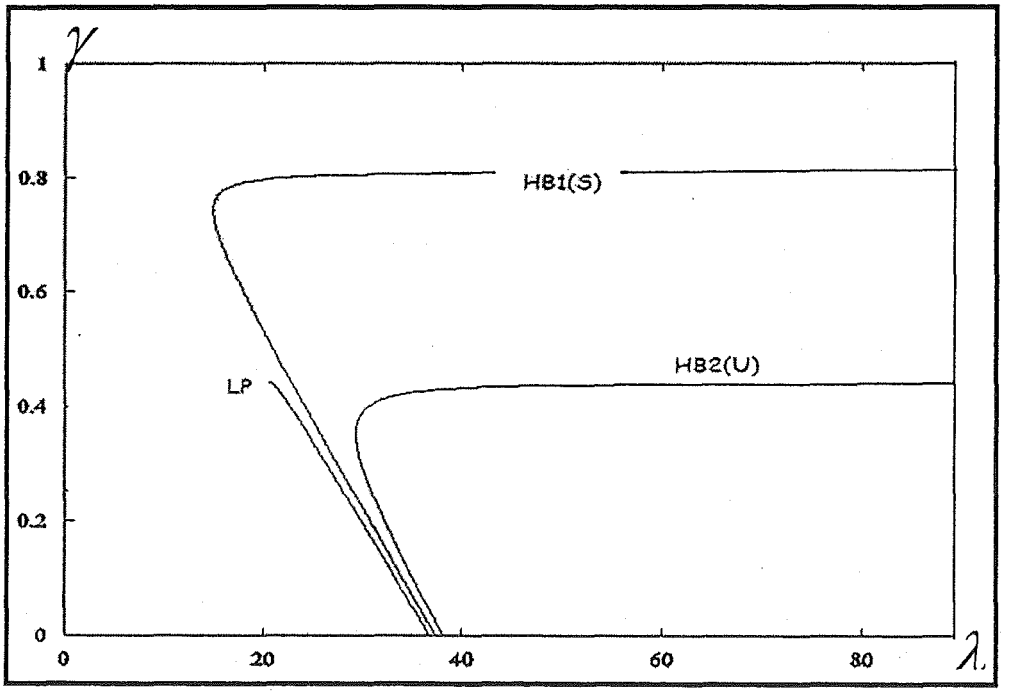

Figure 3.19: The two parameter plot γ against λ for two compartment model $(\mu_1 = \mu_2)$ at $d_1 = 0.022$.

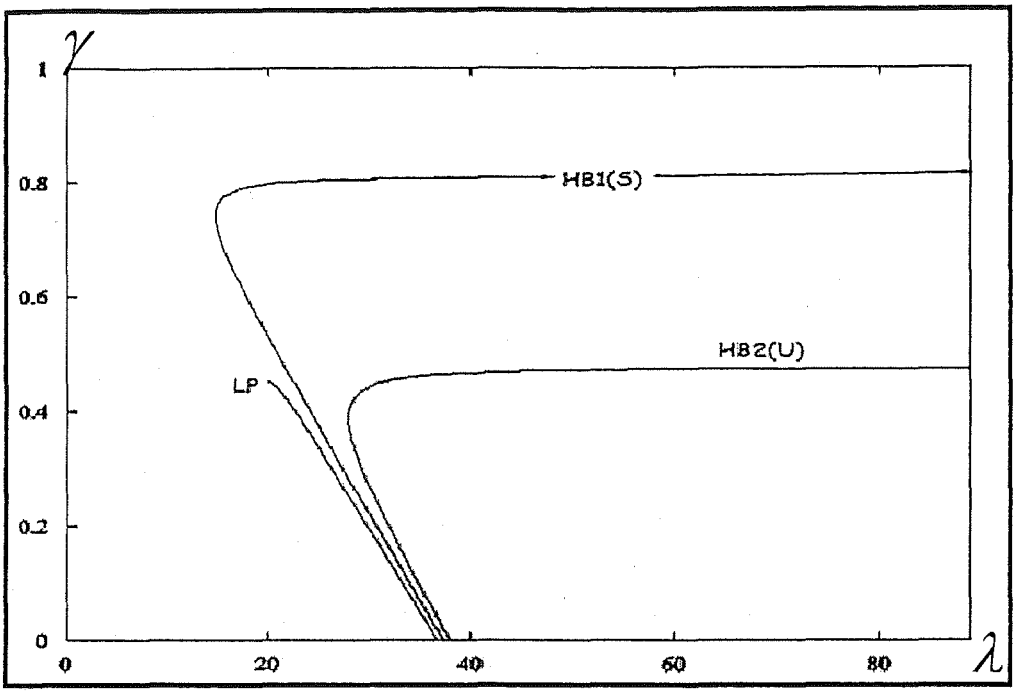

Figure 3.20: The two parameter plot γ against λ for two compartment model $(\mu_1 = \mu_2)$ at $d_1 = 0.02$.

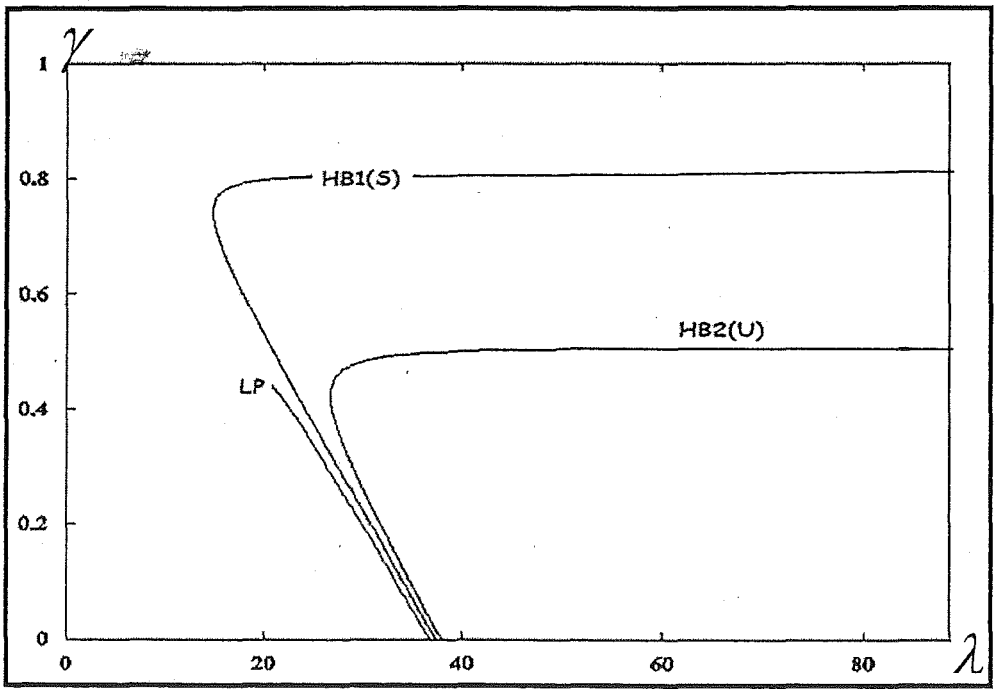

Figure 3.21: The two parameter plot γ against λ for two compartment model $(\mu_1 = \mu_2)$ at $d_1 = 0.018$.

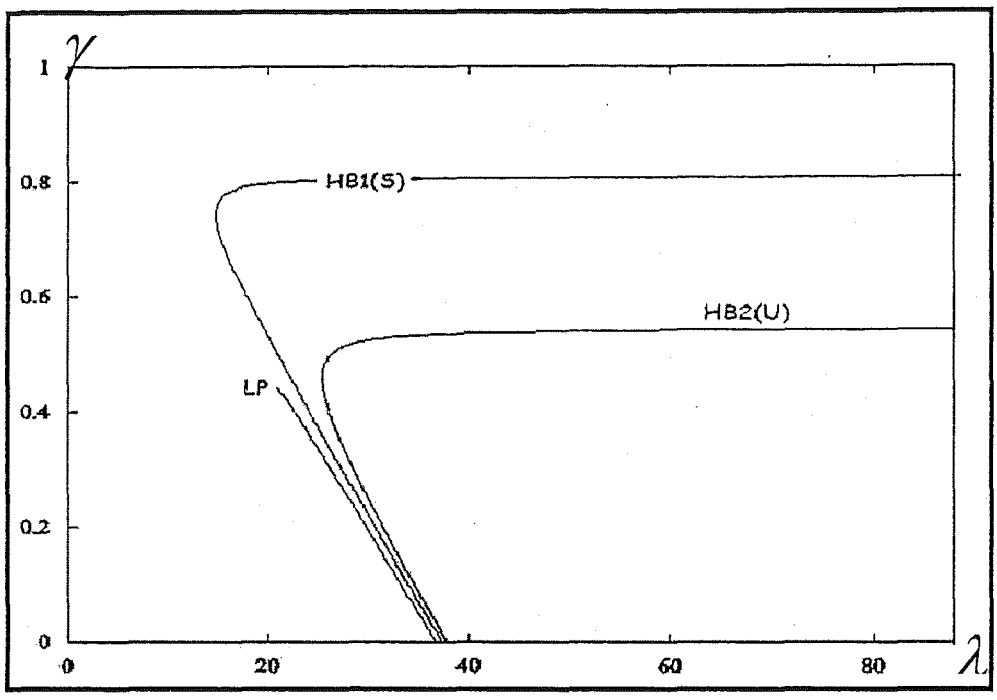

Figure 3.22: The two parameter plot γ against λ for two compartment model $(\mu_1 = \mu_2)$ at $d_1 = 0.016$.

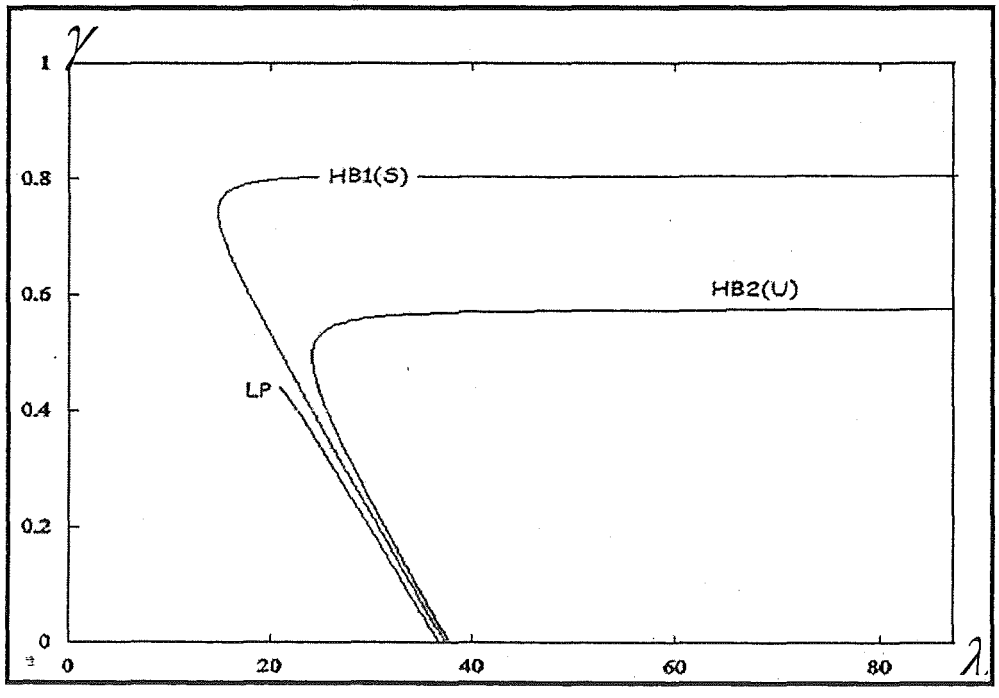

Figure 3.23: The two parameter plot γ against λ for two compartment model $(\mu_1 = \mu_2)$ at $d_1 = 0.014$.

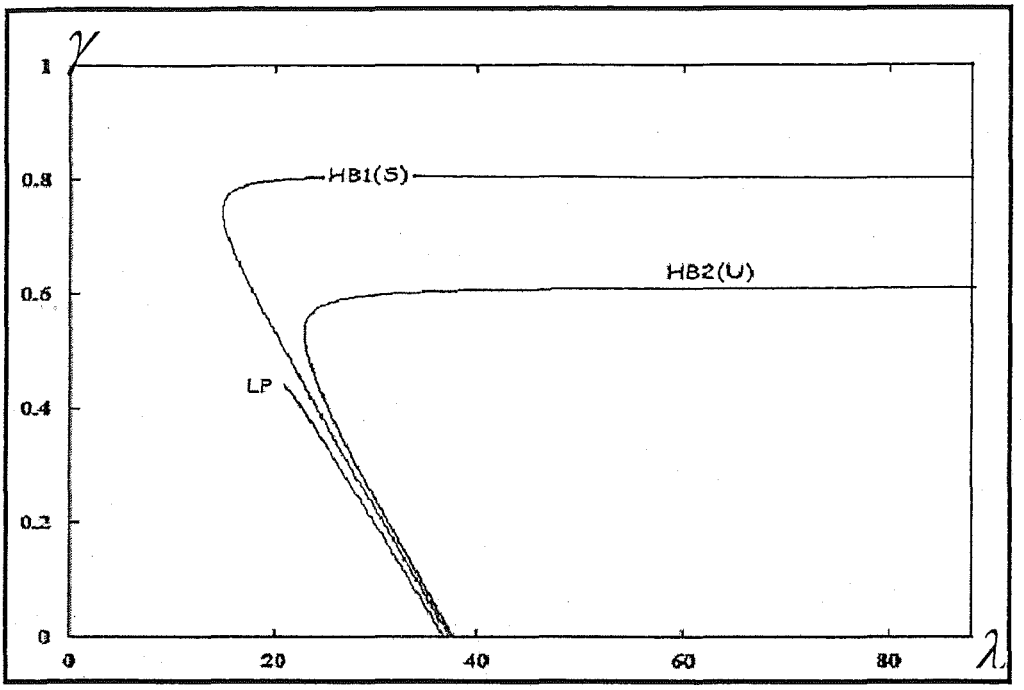

Figure 3.24: The two parameter plot γ against λ for two compartment model $(\mu_1 = \mu_2)$ at $d_1 = 0.012$.

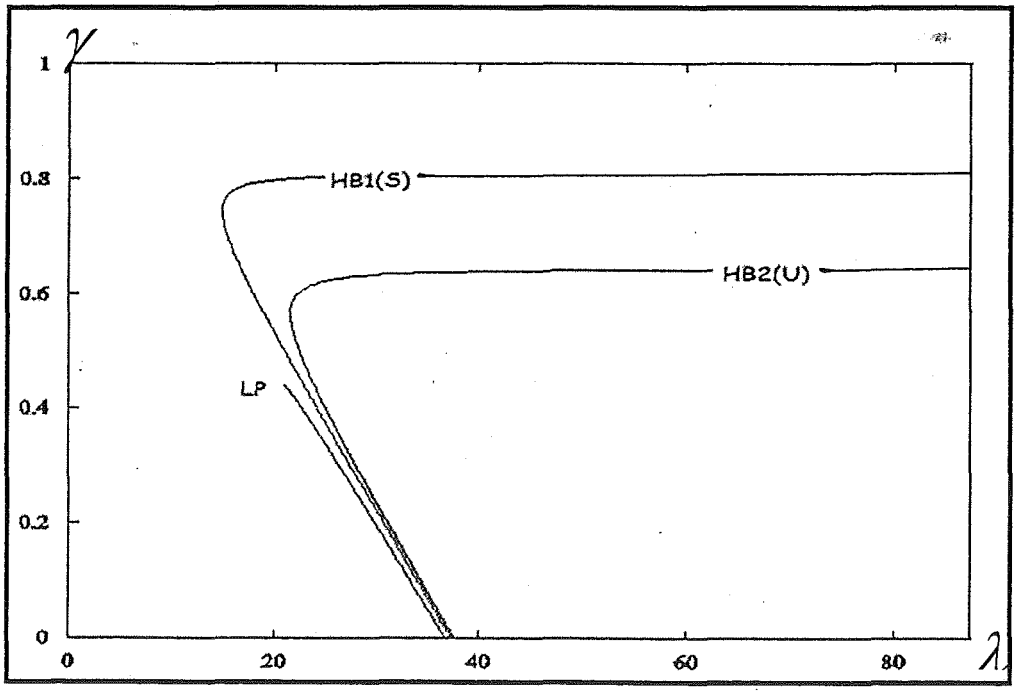

Figure 3.25: The two parameter plot γ against λ for two compartment model $(\mu_1 = \mu_2)$ at $d_1 = 0.01$.

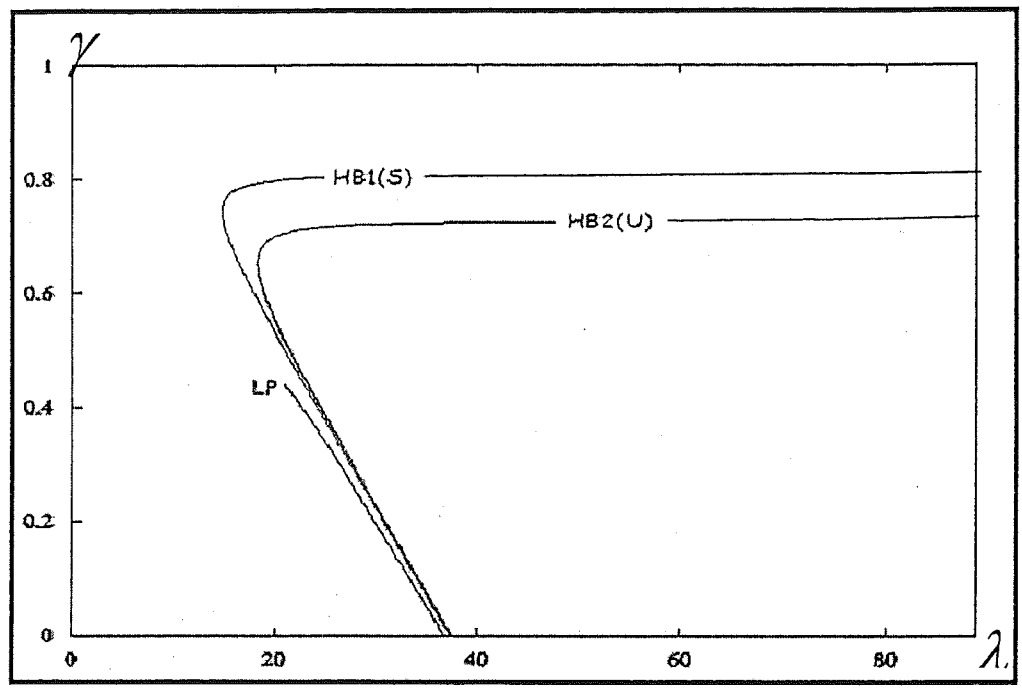

Figure 3.26: The two parameter plot γ against λ for two compartment model ($\mu_1 = \mu_2$) at $d_1 = 0.005$.

Note: There is a remarkable difference compare to the calculated value, for example at $\gamma = 0.7$, we obtained the calculated value to be at $\lambda = 0.660377$ for the curve V_5V_6 while the simulations result is given by $\lambda = 0.6606$; while at $\gamma = 0.8$, we obtained the calculated value to be at $\lambda = 1.25$ for the curve V_5V_6 while the simulations result is given by $\lambda = 3.336$ (see **APPENDIX T: TABLES: T3a** and **Table 3b**; **Figure 3.10** and **Figure 3.12** respectively). The reason for this is, for our simulations we have run an exponential model instead of using the Heaviside while for the calculated we have used the exponential function. This is because for the simulation, it encounters problem of converging if we to use the Heaviside model in our program.

We observed the dependency on d_1 (see **section 3.3.2**) is seen for curves V_2, V_3 and V_4 as the μ's is equal for each of the compartment. However, from our simulation results, we observed that i) V_2 is simply the branch that result where the unfeasible steady states $ufss2 = (x_1, x_2, -x_3, y_1, y_2, y_3, y_4)$ and $ufss3 = (x_1, x_2, x_3, y_1, y_2, -y_3, y_4)$ met and it is unstable (see **Figure 3.10**) and ii) we observed that there exist the unfeasible steady state $ufss5 = (-x_1, -x_2, 0, -x_1, -x_2, 0, y_4)$, which is unstable on the curve V_3 and V_4. Therefore, our system does not dependent on the diffusion parameter d_1 and we shall ignore the curves V_2, V_3 and V_4. Only the unstable Hopf Bifurcation (**HB2**) changes as d_1 changes (see **Figure 3.15** to **Figure 3.26**). It does not have any effect on the limit point and stable Hopf bifurcation branches. For d_1 large **HB2** is not seen. It is first observed at $d = 0.024$ (see **Figure 3.18**). As d_1's become smaller the **HB2** curve gets closer to the **HB1** (stable) and emerges with it as $d_1 = 0$. It is thus consistent with the one compartment model.

Figure 3.27 combines the points obtained from simulations using the software AUTO (for the Limit Point and Hopf bifurcation curves); with the automatic plots from the linear stability analysis of **section 3.3.1** and **3.3.2** by using **MATHEMATICA** (**c.f. APPENDIX M: MATHEMATICA: M7**). All unfeasible and unstable steady states, and possible different results for different d_1 are ignored. Thus **Figure 3.27** gives an overall two parameter diagram which clearly shows the stability of the three *feasible* steady states, the location of the coexistence between steady states or periodic solutions, and the existence of limit cycles or periodic solutions.

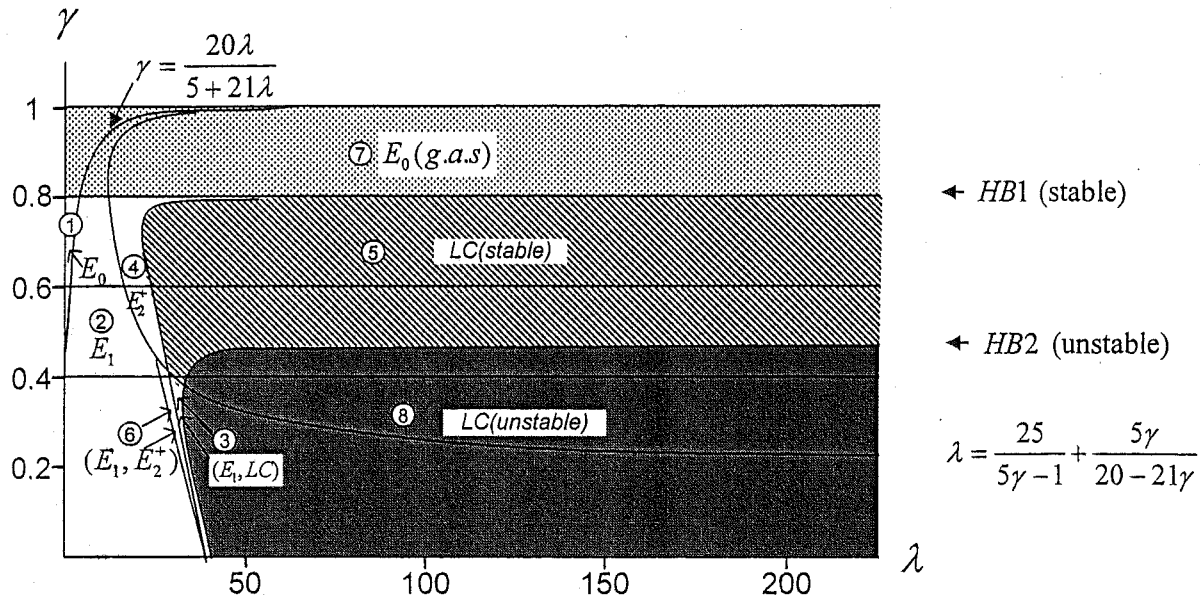

Figure 3.27: The overall 2-parameter plot for a two-compartments model with growth parameter $\mu_1 = \mu_2 = 1$; showing the stability of the three steady states (E_0, E_1 and E_2) i.e. the feasible steady state only, the location of the coexistence between feasible steady states or periodic solutions and the presence of limit cycles or periodic solution at $d_1 = 0.02$.

From the above diagram, it clearly shows the stability of the three *feasible* steady states, the location of the coexistence between steady states or periodic solutions, and the existence of limit cycles or periodic solutions for the two compartments model with the growth parameter $\mu_1 = \mu_2$ and diffusion rate $d_1 = 0.02$;. In summary:

i) the steady state E_0 is only stable in the small region ①, and when $\gamma > 0.8$ (i.e. in the region ⑦) where it is globally asymptotically stable;.

ii) E_1 is stable in region ②, coexist with E_2^+ in region ⑥ and coexist with the limit cycle or the periodic solution in region ③;

iii) E_2 is stable in region ④ and coexist with E_1 in region ⑥;

iv) the stable limit cycle or the periodic solution occurs in region ⑤ and coexists with E_1 in region ③; and

v) the unstable limit cycle occurs at region ⑧.

3.5 Bifurcation analysis assuming a different growth parameter for the phytoplankton ($\mu_1 \neq \mu_2$)

This section describes the bifurcation digrams for the two compartment model via the software package **AUTO**. As has been seen, the bifurcation diagrams becomes more complicated as the compartment grew in size with many unnecessary *unfeasible* steady state branches. Thus, one may ignore all *unfeasible* steady state branches and corresponding Limit points and stable Hopf bifurcation point that branch from it, and other unstable Hopf bifurcation branches. Recall that *unfeasible* steady state is when one of its variables component is negative, for example, $ufss3 = (x_1, x_2, x_3, y_1, y_2, -y_3, y_4)$. **MATHEMATICA** has failed to execute any result due to the obvious complexity. Thus, the behavior of our model with growth parameter $\mu_1 \neq \mu_2$ is analyzed numerically using the software **AUTO**. In the various subsections, the diagrams are presented in the following fashion: bifurcation diagrams with varying μ_1 and μ_2 kept fixed; a two-parameter plot of μ_1 against μ_2 with varying d_1; a two-parameter plot of γ against d_1, and a two parameter plot of μ_1 against d_1.

3.5.1 Varying μ_1 and fixing μ_2.

For simplicity, let us adopt $\mu_2 = 1$, $\gamma = 0.4$ and $d_1 = 0.02$, but varying the parameter μ_1 within the range 0.3 to 0.9.

Recall that the *feasible* steady states are of the form $E_0 = (0, 0, 0, 0, 0, 0, \lambda)$, $E_1 = (x_1, x_2, 0, y_1, y_2, 0, y_4)$ and $E_2 = (x_1, x_2, x_3, y_1, y_2, y_3, y_4)$, while the rest are *unfeasible* steady states and so ignored.

Let us now proceed to discuss details of the bifurcation diagrams for the two-compartments model with growth parameter $\mu_1 \neq \mu_2$ shown in **Figure 3.28** to **Figure 3.33** for the value $0.3 < \mu_1 < 0.9$ and $\mu_2 = 1$, and in particular observe how the steady states changes from one into another. We shall compute the dependent variable x_3 against the parameter λ only since it shows the presence of *unfeasible* steady states clearly so as we don't get it mixed up with the *feasible* ones.

i) **Figure 3.28** shows the bifurcation diagram x_3 against the parameter λ, when $d = 0.02$, $\gamma = 0.4$, $\mu_2 = 1$ and $\mu_1 = 0.3$. Viewed from left to the right, the first obvious feature is **BP1** at the point $\lambda = 0.186$ (Before that there is actually a narrow region where the steady state E_0 is stable, but it is too short to be obvious- Although it can be detected by grabbing the point when using AUTO). At $\lambda = 0.186$, the steady state E_0 becomes unstable, and the system moves to the steady state E_1 which is stable for larger λ. There is

another bifurcation point (**BP2**) occurs at $\lambda = 23.06$ and a limit point (**LP2**) started at $\lambda = 23.45$ which shows that E_2 is stable after the LP1 just before it hits the Hopf bifurcation point (**HB1**) at $\lambda = 24.77$. Thus from $\lambda = 23.06$ to $\lambda = 23.45$ the steady state E_2 is stable. Another limit point (**LP1**) occurs at $\lambda = 26.82$ where it is seen that the steady state E_2 is stable from $\lambda = 23.06$ to $\lambda = 26.82$. The Hopf bifurcation point (**HB 1**) occurs at $\lambda = 24.77$; thus from $\lambda = 24.77$ to $\lambda = 26.82$ the steady state E_2 coexisting with the limit cycle.

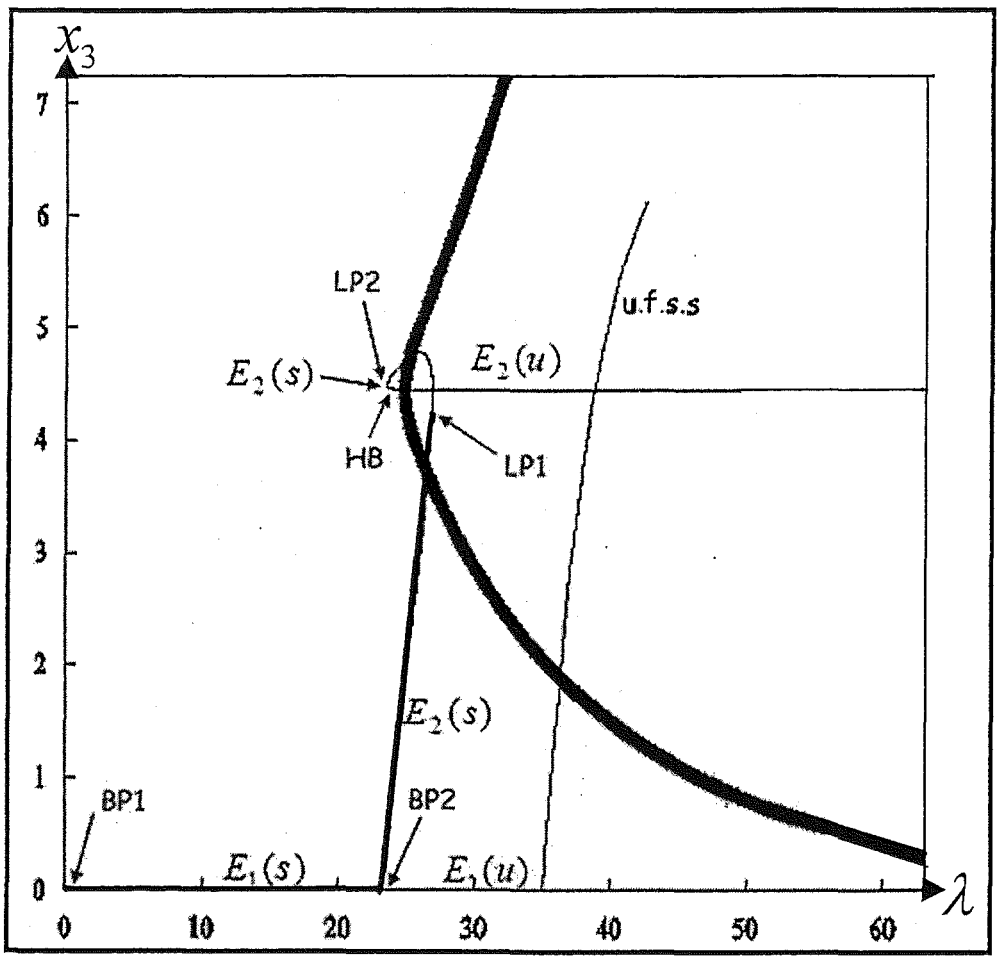

Figure 3.28: The bifurcation diagram x_3 against λ for two compartment model ($\mu_1 \neq \mu_2$) when $\gamma = 0.4$, $d_1 = 0.02$, $\mu_1 = 0.3$ and $\mu_2 = 1$ showing the bifurcation points BP1 (λ=0.186), BP2 (λ=23.06); the Limit points LP1 (λ=26.82) and LP2 (λ=23.45) and the Hopf bifurcation points HB1 (λ=21.82). Other unfeasible steady state found are of the form $(x_1, x_2, x_3, y_1, y_2, -y_3, y_4)$.

ii) **Figure 3.29** shows the bifurcation diagram x_3 against the parameter λ, when $d_1 = 0.02$, $\gamma = 0.4$, $\mu_2 = 1$ and $\mu_1 = 0.5$. There is a bifurcation point (**BP1**) at the point $\lambda = 0.1851$, where the steady state E_0 changes from stable to unstable and the steady state E_1 becomes unstable. The steady state E_2 branch occurs at the next bifurcation point (**BP2**) occurs at $\lambda = 10.44$, when the steady state E_1 is unstable and E_2 is stable. The limit points **LP1** and **LP2** started at $\lambda = 24.51$ and $\lambda = 23.5$ respectively. Thus the steady state E_2 is seen stable from $\lambda = 10.44$ to $\lambda = 24.51$. The limit point indicates the *folding point* or the continuation of the stability of the steady states. Periodicity follows at the Hopf bifurcation (**HB1**) at $\lambda = 24.92$.

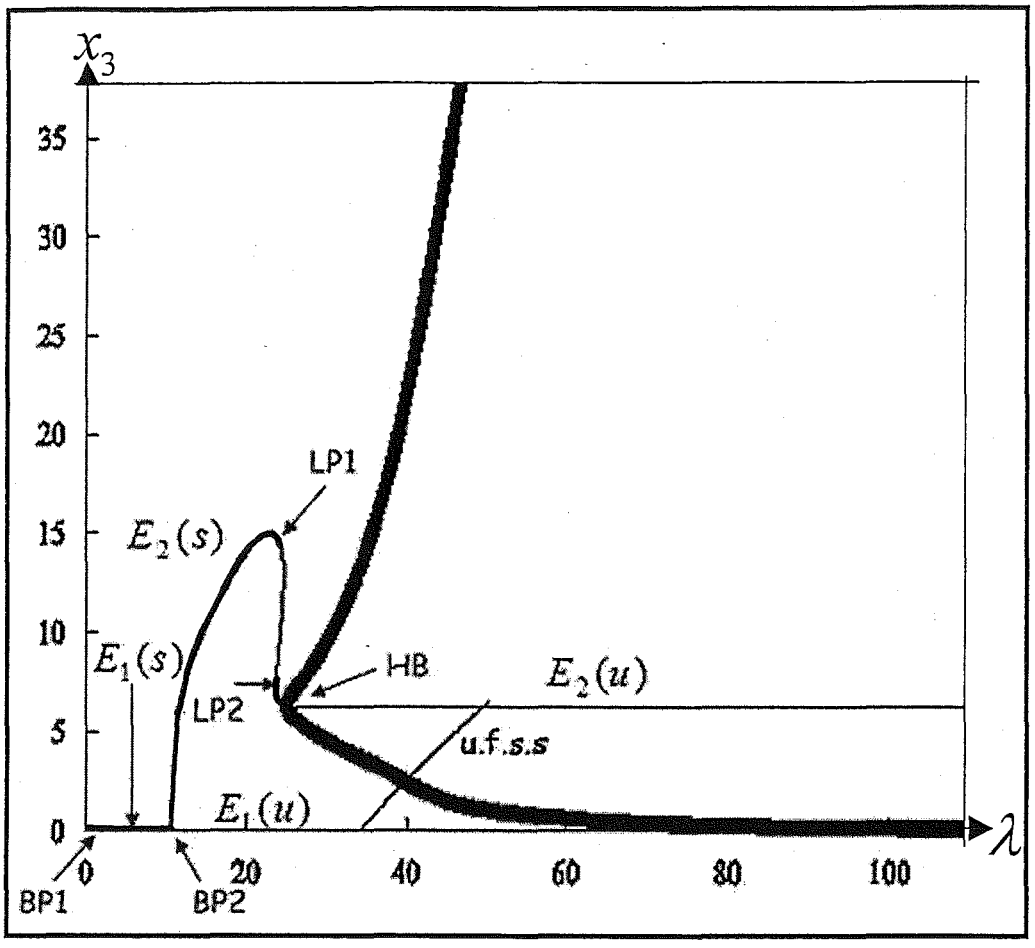

Figure 3.29: The bifurcation diagram x_3 against λ for two compartment model $(\mu_1 \neq \mu_2)$ when $\gamma = 0.4$, $d_1 = 0.02$, $\mu_1 = 0.5$ and $\mu_2 = 1$ showing the bifurcation points BP1 (λ=0.1851), BP2 (λ=10.44); the Limit points LP1 (λ=24.51) and LP2 (λ=23.5) and the Hopf bifurcation points HB1 (λ=24.92). Other unfeasible steady state found are of the form $(x_1, x_2, x_3, y_1, y_2, -y_3, y_4)$.

iii) **Figure 3.30** shows the bifurcation diagram x_3 against the parameter λ, when $d_1 = 0.02$, $\gamma = 0.4$, $\mu_2 = 1$ and $\mu_1 = 0.6$. There is a bifurcation point (**BP1**) at the point $\lambda = 0.1844$, where the steady state E_0 changes from stable to unstable and the steady state E_1 becomes unstable. The steady state E_2 branch occurs at the next bifurcation point (**BP2**) occurs at $\lambda = 12.76$, when the steady state E_1 is unstable and E_2 is stable. The limit points **LP1** and **LP2** started at $\lambda = 23.65$ and $\lambda = 23.43$ respectively. Thus the steady state E_2 is seen stable from $\lambda = 12.76$ to $\lambda = 23.65$. The limit point indicates the *folding point* or the continuation of the stability of the steady states. Periodicity follows at the Hopf bifurcation (HB1) at $\lambda = 25.08$.

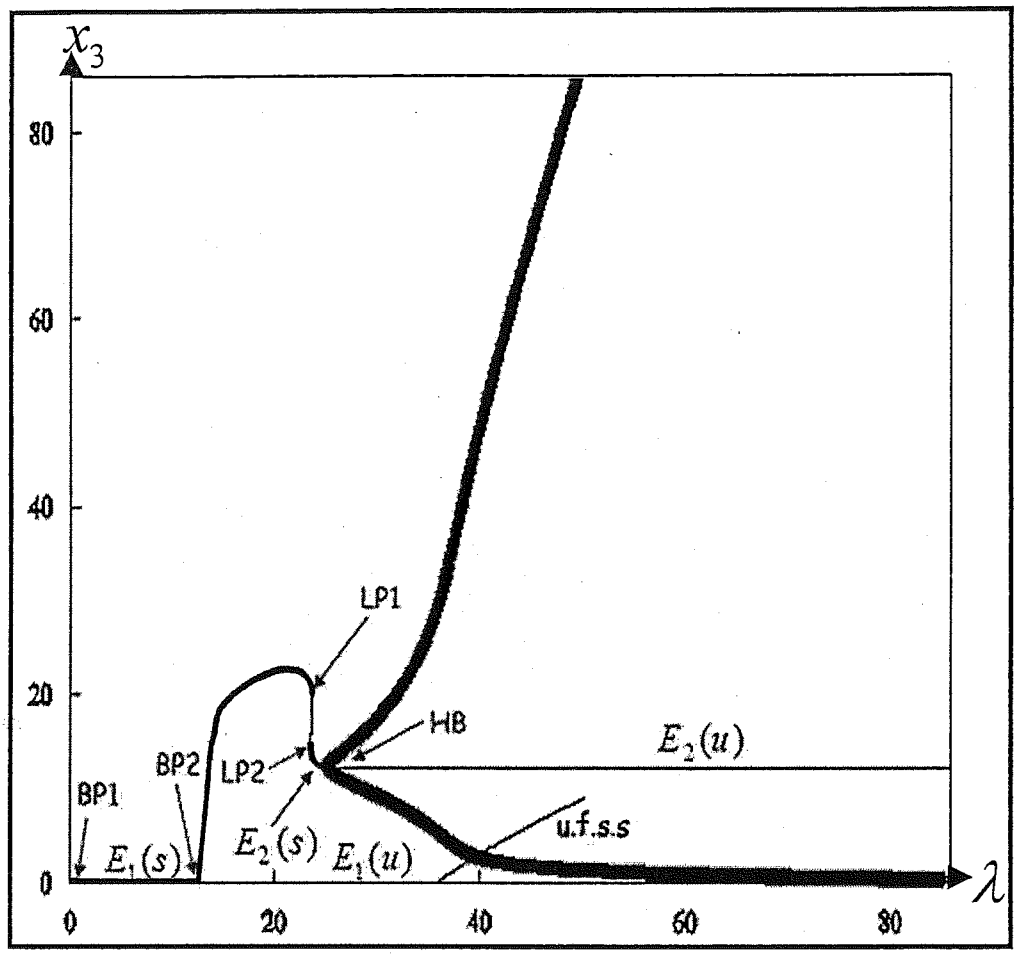

Figure 3.30: The bifurcation diagram x_3 against λ for two compartment model ($\mu_1 \neq \mu_2$) when $\gamma = 0.4$, $d_1 = 0.02$, $\mu_1 = 0.6$ and $\mu_2 = 1$ showing the bifurcation points BP1 (λ=0.1844), BP2 (λ=12.76); the Limit points LP1 (λ=23.65) and LP2 (λ=23.43) and the Hopf bifurcation points HB1 (λ=25.08). Other unfeasible steady state found are of the form $(x_1, x_2, x_3, y_1, y_2, -y_3, y_4)$.

iv) **Figure 3.31** shows the bifurcation diagram x_3 against the parameter λ, when $d_1 = 0.02$, $\gamma = 0.4$, $\mu_2 = 1$ and $\mu_1 = 0.7$. There is a bifurcation point (**BP1**) at the point $\lambda = 0.1832$, where the steady state E_0 changes from stable to unstable and the steady state E_1 becomes unstable. The steady state E_2 branch occurs at the next bifurcation point (BP2) occurs at $\lambda = 15.69$, when the steady state E_1 is unstable and E_2 is stable. The limit points **LP1** and **LP2** started at $\lambda = 23.65$ and $\lambda = 23.43$ respectively. Thus the steady state E_2 is seen stable from $\lambda = 12.76$ to $\lambda = 23.65$. The limit point indicates the *folding point* or the continuation of the stability of the steady states. Periodicity follows at the Hopf bifurcation (**HB1**) at $\lambda = 25.07$.

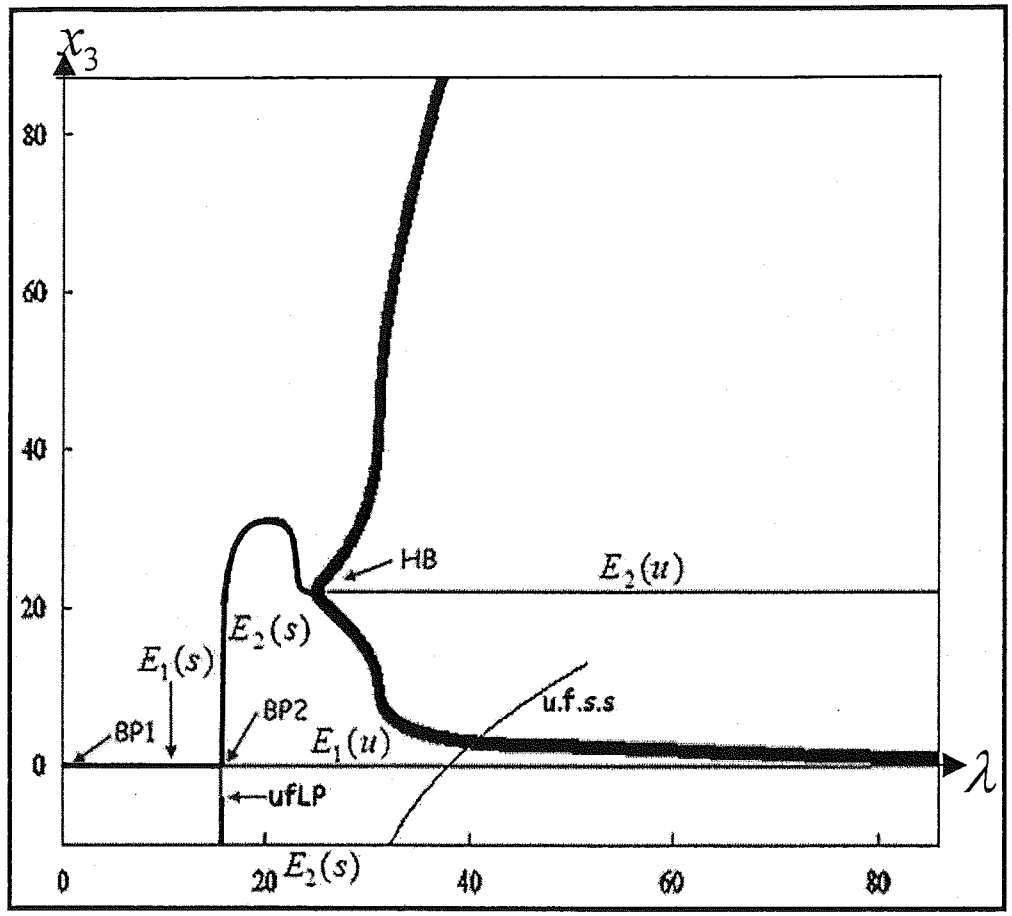

Figure 3.31: The bifurcation diagram x_3 against λ for two compartment model ($\mu_1 \neq \mu_2$) when $\gamma = 0.4$, $d_1 = 0.02$, $\mu_1 = 0.7$ and $\mu_2 = 1$ showing the bifurcation points BP1 (λ=0.1832), BP2 (λ=15.69) and the Hopf bifurcation points HB1 (λ=25.07). Other unfeasible steady state found are of the form $(x_1, x_2, x_3, y_1, y_2, -y_3, y_4)$ and thus the unfeasible bifurcation points are ufLP (λ=15.68).

v) **Figure 3.32** shows the bifurcation diagram x_3 against the parameter λ, when $d_1 = 0.02$, $\gamma = 0.4$, $\mu_2 = 1$ and $\mu_1 = 0.8$. There is a bifurcation point (**BP1**) at the point $\lambda = 0.1811$, where the steady state E_0 changes from stable to unstable and the steady state E_1 becomes unstable. A Limit point (**LP**) occur first at $\lambda = 18.7$ and is follows by the next bifurcation point (**BP2**) occurs at $\lambda = 19$, when the steady state E_1 is unstable and E_2 is stable. Thus from $\lambda = 18.7$ to $\lambda = 19$, E_1 coexisting with E_2. Then E_2 is continues to be stable from $\lambda = 19$ until it reaches stable periodicity at the Hopf point (**HB1**) $\lambda = 23.54$. This is follows by the unstable Hopf point (**HB2**) occurs at $\lambda = 25.02$.

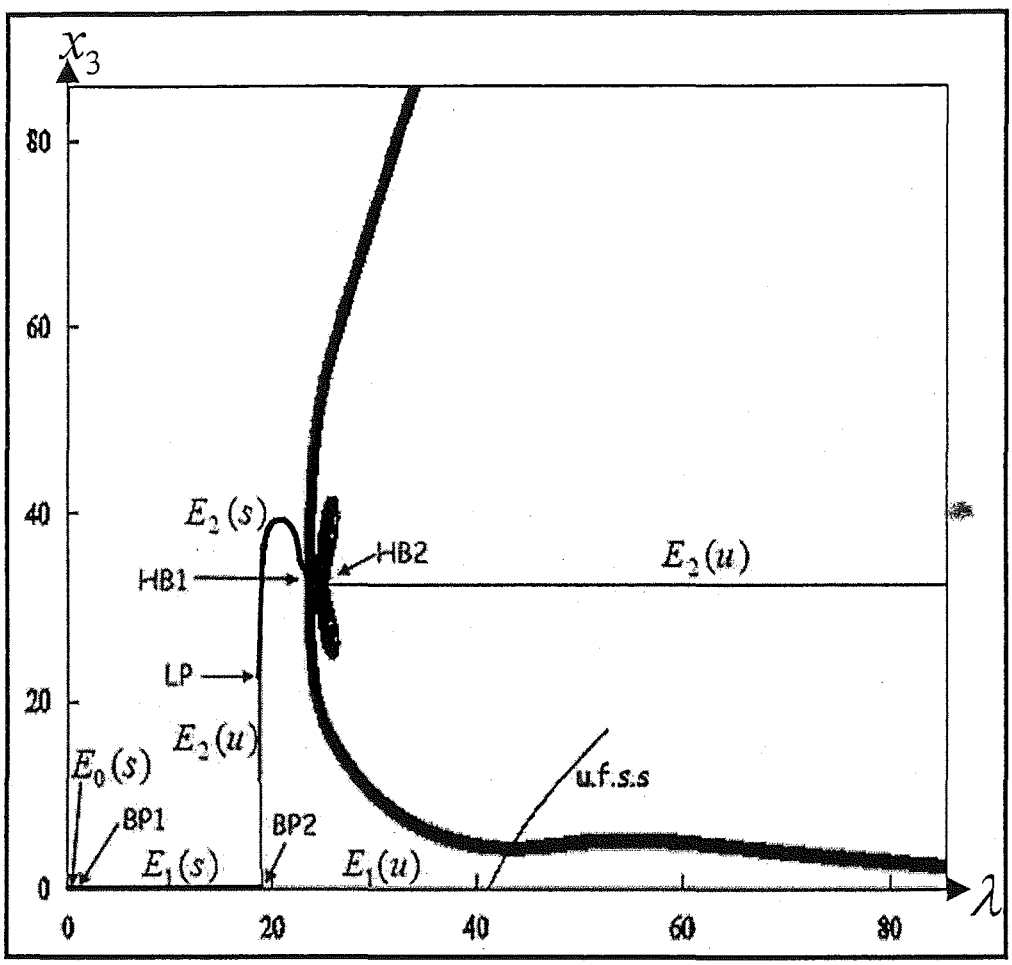

Figure 3.32: The bifurcation diagram x_3 against λ for two compartment model ($\mu_1 \neq \mu_2$) when $\gamma = 0.4$, $d_1 = 0.02$, $\mu_1 = 0.8$ and $\mu_2 = 1$ showing the bifurcation points BP1 (λ=0.1811), BP2 (λ=19); the limit point LP1 (λ=18.7) and the Hopf bifurcation points HB1 (λ=23.54) and HB2 (λ=25.02). Other unfeasible steady state found are of the form $(x_1, x_2, x_3, y_1, y_2, -y_3, y_4)$.

vi) **Figure 3.33** shows the bifurcation diagram x_3 against the parameter λ, when $d_1 = 0.02$, $\gamma = 0.4$, $\mu_2 = 1$ and $\mu_1 = 0.9$. There is a bifurcation point (**BP1**) at the point $\lambda = 0.1775$, where the null state E_0 changes from stable to unstable and the steady state E_1 becomes unstable. A Limit point (**LP**) occur first at $\lambda = 21.15$ and is follows by the next bifurcation point (**BP2**) occurs at $\lambda = 22.32$, when the steady state E_1 is unstable and E_2 is stable. Thus from $\lambda = 21.15$ to $\lambda = 22.32$, E_1 coexisting with E_2. Then E_2 is continues to be stable from $\lambda = 22.32$ until it reaches stable periodicity at the Hopf point (**HB1**) $\lambda = 22.93$. This is follows by the unstable Hopf point (**HB2**) occurrs at $\lambda = 27.65$.

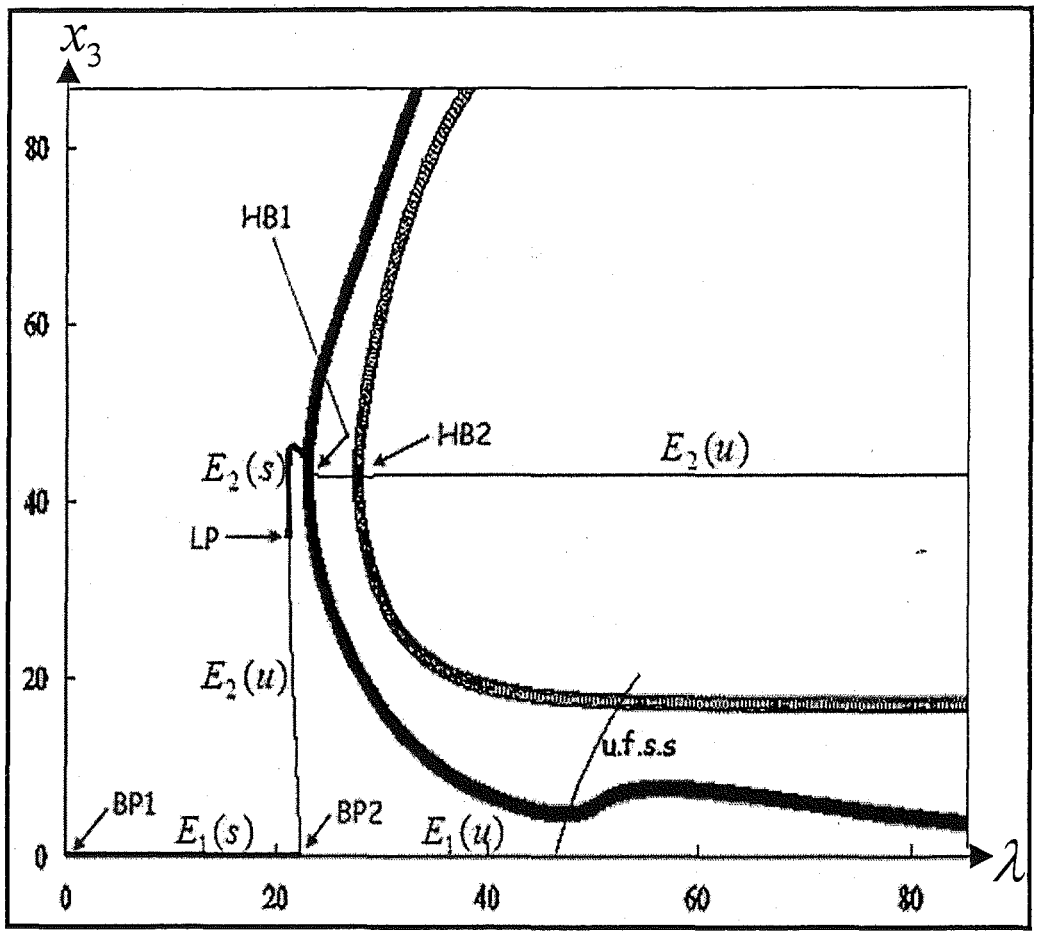

Figure 3.33: The bifurcation diagram x_3 against λ for two compartment model ($\mu_1 \neq \mu_2$) when $\gamma = 0.4$, $d_1 = 0.02$, $\mu_1 = 0.9$ and $\mu_2 = 1$ showing the bifurcation points BP1 (λ=0.1775), BP2 (λ=22.32); the limit point LP1 (λ=21.15) and the Hopf bifurcation points HB1 (λ=22.93) and HB2 (λ=27.65). Other unfeasible steady state found are of the form $(x_1, x_2, x_3, y_1, y_2, -y_3, y_4)$.

vii) **Figure 3.34** to **Figure 3.39** show the two parameter diagram γ against λ for our bifurcation diagrams in **Figure 3.28** to **Figure 3.33** for $0.3 < \mu < 0.9$. There are showing the extended lines for the Limit points (LP) and the Hopf points (**HB**) automatically produced by **AUTO**. We have fixed the parameters: $\mu_2 = 1$, $\gamma = 0.4$ and $d_1 = 0.02$. Not a particularly useful diagram since we cannot obtain the extension of the other bifurcation points as we have done mathematically with the one compartment and two compartment model with the growth parameter $\mu_1 = \mu_2$.

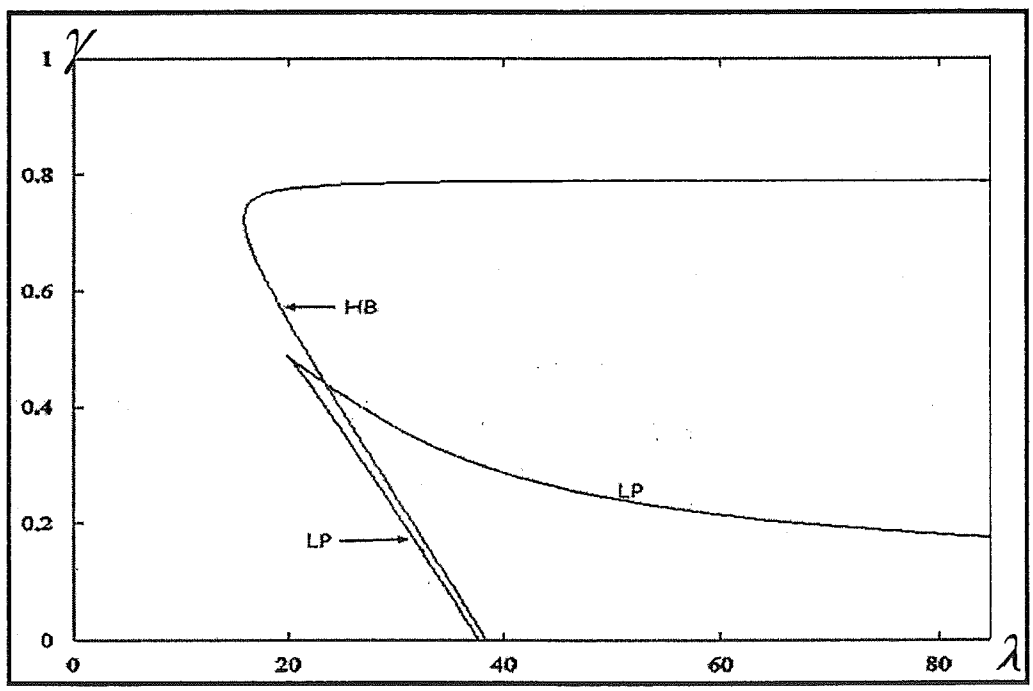

Figure 3.34: The two parameter plot γ against λ for two compartment model ($\mu_1 \neq \mu_2$) at $\gamma = 0.4$, $d_1 = 0.02$, $\mu_1 = 0.3$ and $\mu_2 = 1$.

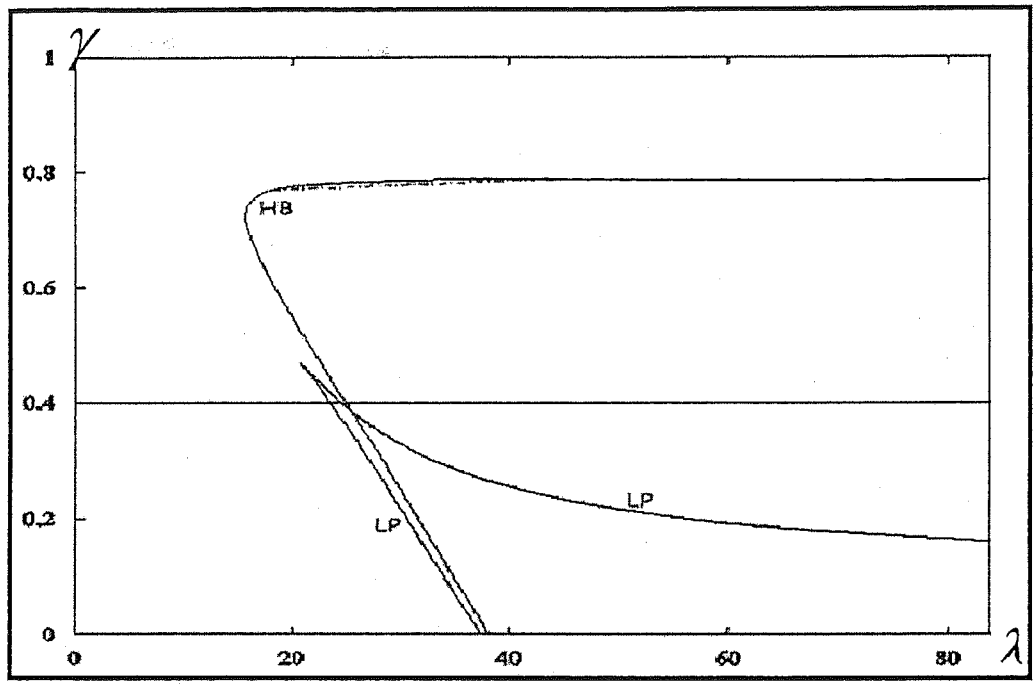

Figure 3.35: The two parameter plot γ against λ for two compartment model $(\mu_1 \neq \mu_2)$ at $\gamma = 0.4$, $d_1 = 0.02$, $\mu_1 = 0.5$ and $\mu_2 = 1$.

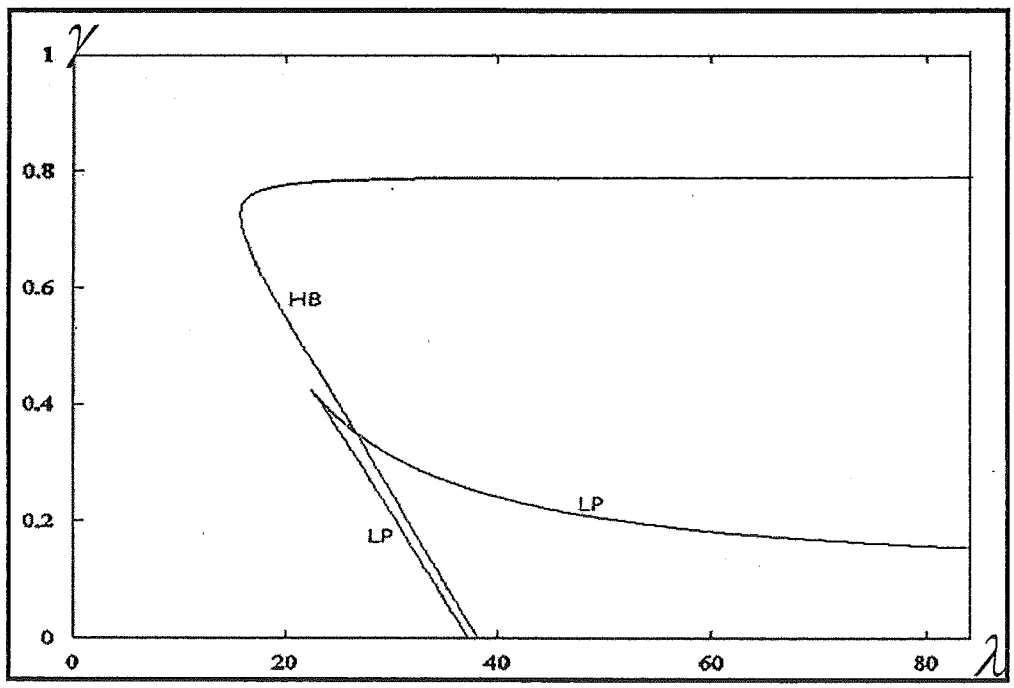

Figure 3.36: The two parameter plot γ against λ for two compartment model $(\mu_1 \neq \mu_2)$ at $\gamma = 0.4$, $d_1 = 0.02$, $\mu_1 = 0.6$ and $\mu_2 = 1$.

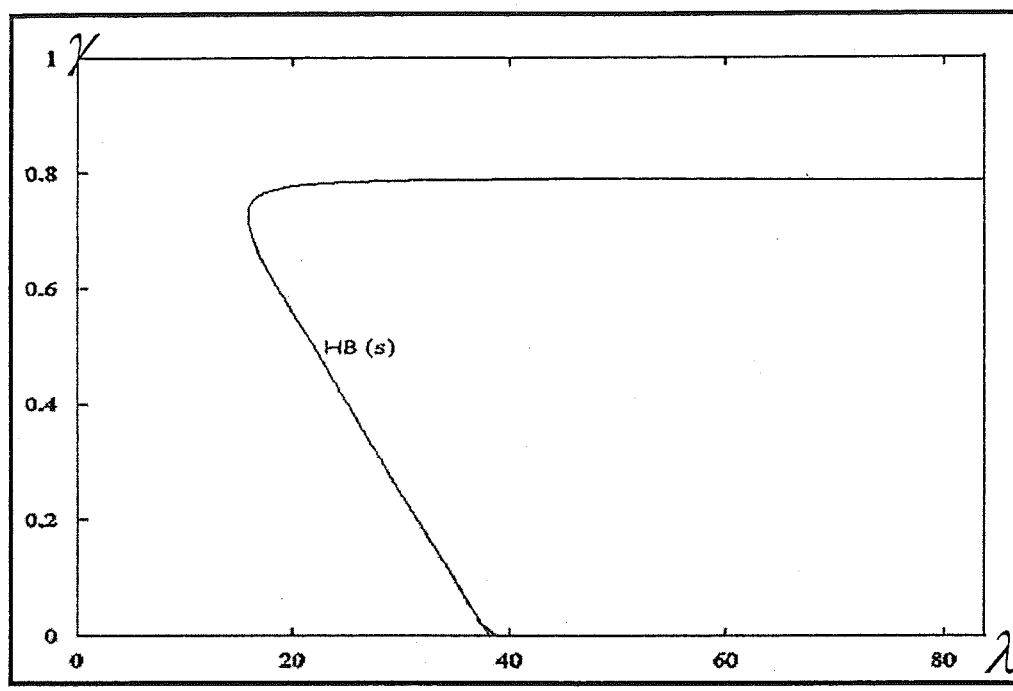

Figure 3.37: The two parameter plot γ against λ for two compartment model $(\mu_1 \neq \mu_2)$ at $\gamma = 0.4$, $d_1 = 0.02$, $\mu_1 = 0.7$ and $\mu_2 = 1$.

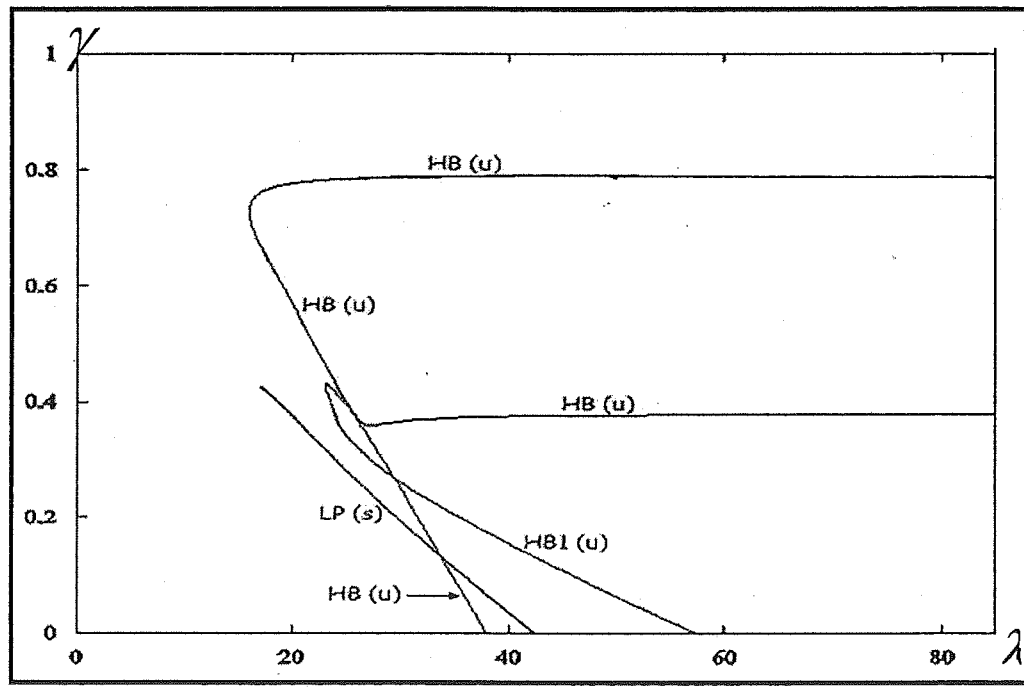

Figure 3.38: The two parameter plot γ against λ for two compartment model $(\mu_1 \neq \mu_2)$ at $\gamma = 0.4$, $d_1 = 0.02$, $\mu_1 = 0.8$ and $\mu_2 = 1$.

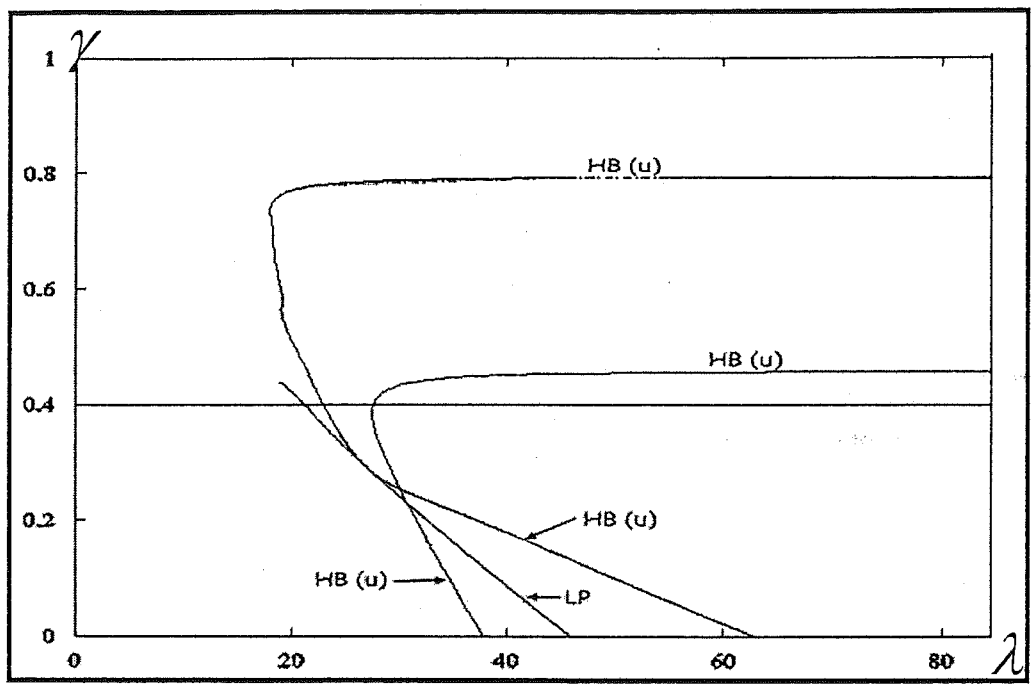

Figure 3.39: The two parameter plot γ against λ for two compartment model ($\mu_1 \neq \mu_2$) at $\gamma = 0.4$, $d_1 = 0.02$, $\mu_1 = 0.8$ and $\mu_2 = 1$.

3.5.2 Two parameter plot of μ_2 against μ_1 with varying d_1

Two-parameter diagrams of μ_2 against μ_1 are shown in **Figures 3.40** to **Figure 3.45**, to demonstrate the conjecture that the diagram has to be symmetrical and at the same time examine the quality of the plots. Thus we shall investigate the range of μ's in which we can observed all the rich behaviour (i.e. the limit points and the Hopf bifurcation branches) can be seen together is considered. The unstable Hopf bifurcation is ignored.

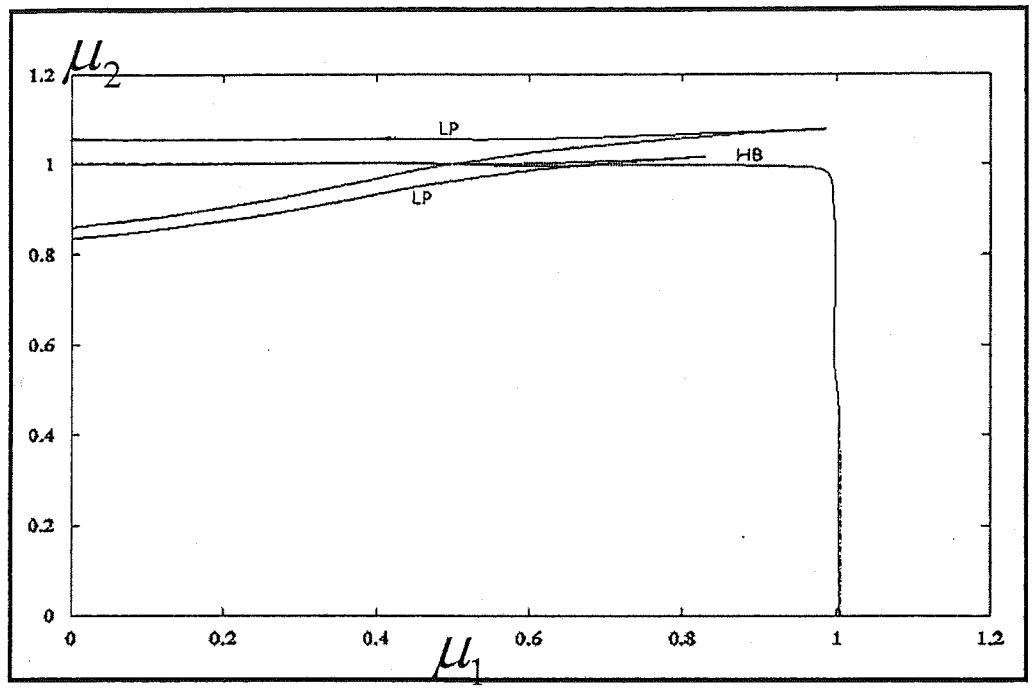

Figure 3.40: The two parameter plot γ against λ for two compartment model $(\mu_1 \neq \mu_2)$ when $\gamma = 0.4$ and $d_1 = 0.01$; with starting point $\mu_1 = 0.5$ and $\mu_2 = 1$.

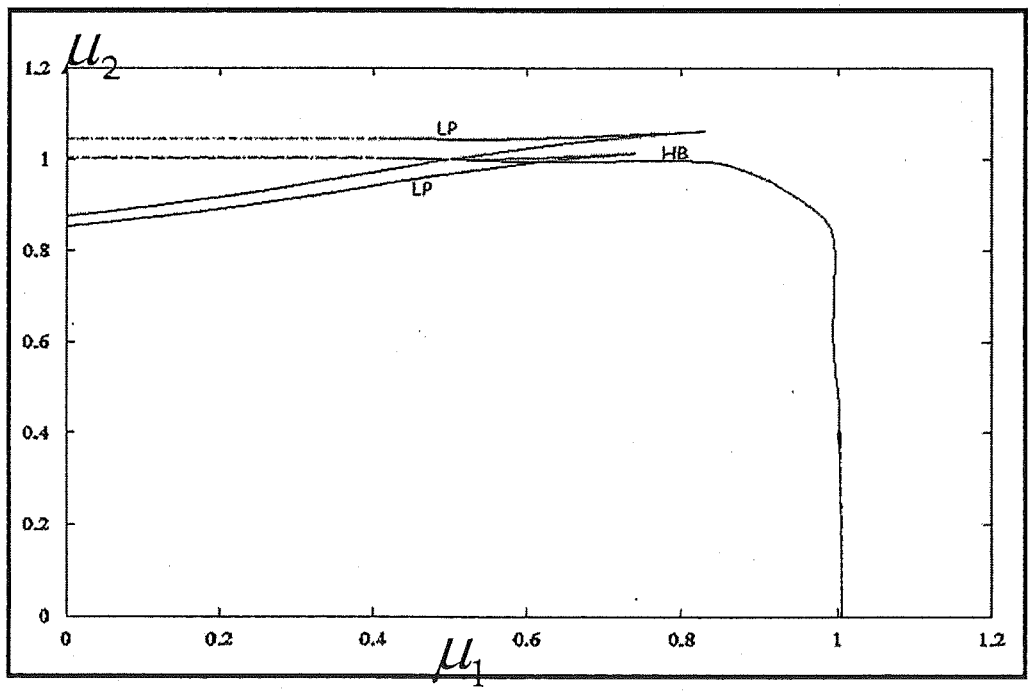

Figure 3.41: The two parameter plot γ against λ for two compartment model $(\mu_1 \neq \mu_2)$ when $\gamma = 0.4$ and $d_1 = 0.015$; with starting point $\mu_1 = 0.5$ and $\mu_2 = 1$.

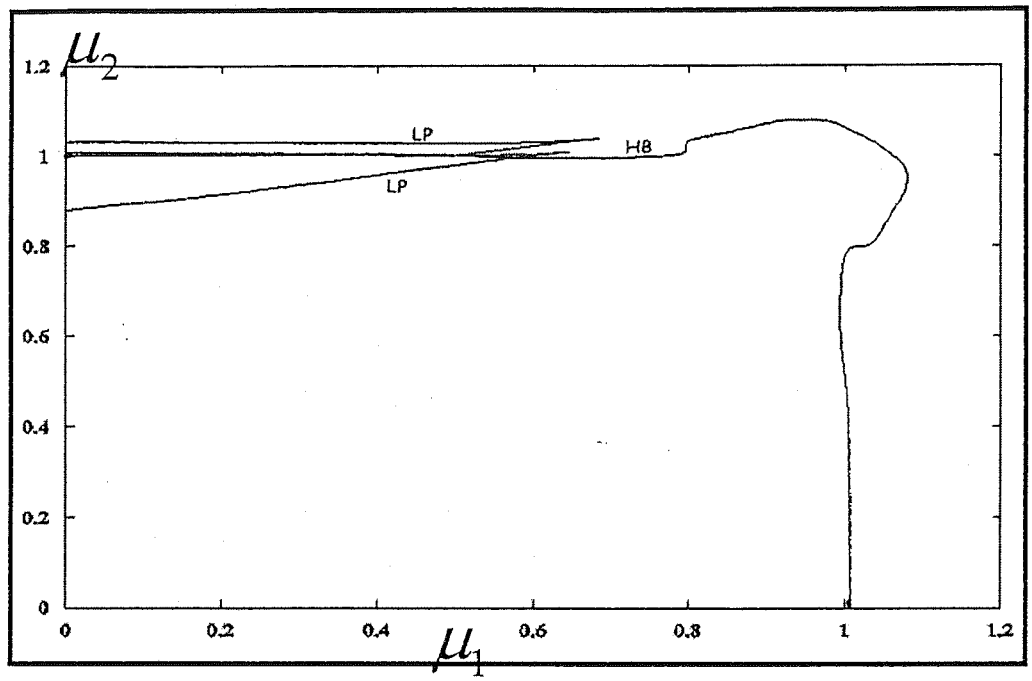

Figure 3.42: The two parameter plot γ against λ for two compartment model $(\mu_1 \neq \mu_2)$ when $\gamma = 0.4$ and $d_1 = 0.02$; with starting point $\mu_1 = 0.5$ and $\mu_2 = 1$.

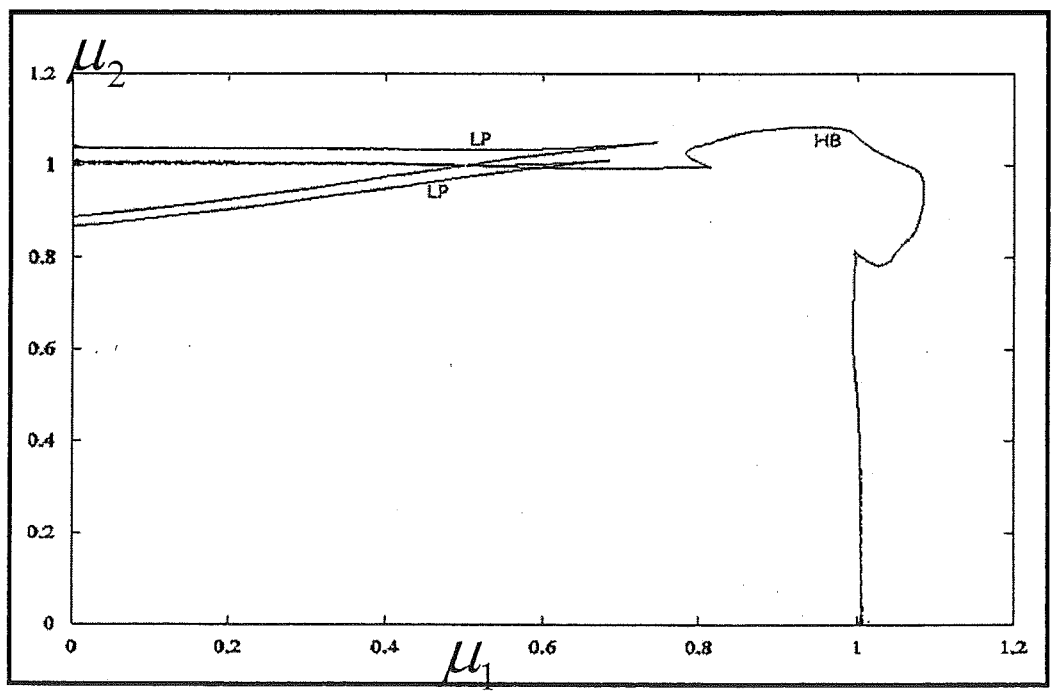

Figure 3.43: The two parameter plot γ against λ for two compartment model $(\mu_1 \neq \mu_2)$ when $\gamma = 0.4$ and $d_1 = 0.025$; with starting point $\mu_1 = 0.5$ and $\mu_2 = 1$.

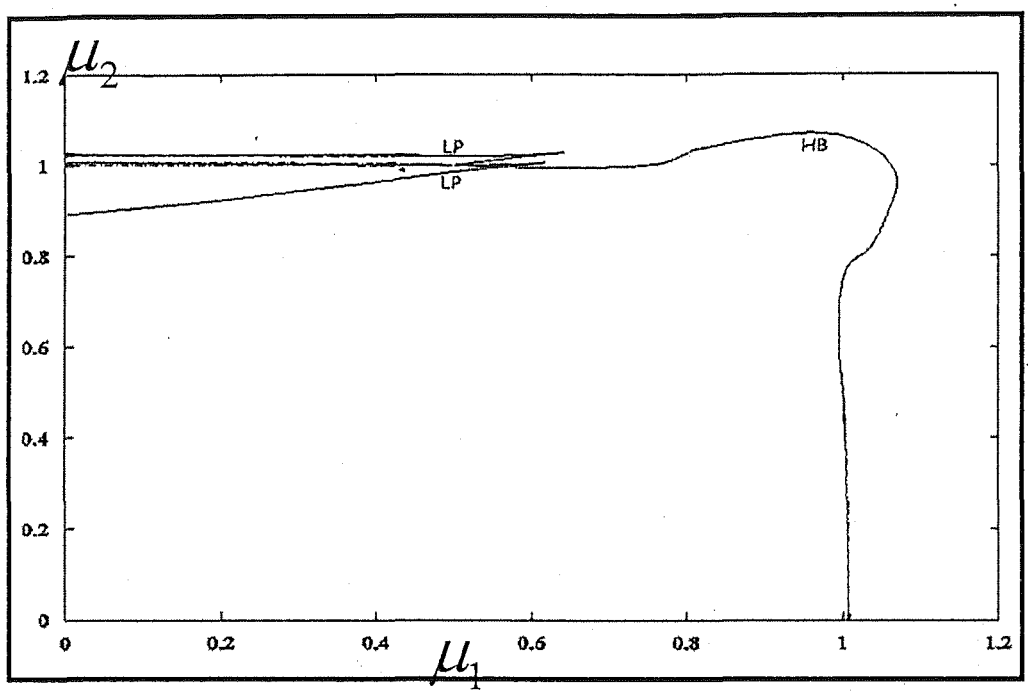

Figure 3.44: The two parameter plot γ against λ for two compartment model $(\mu_1 \neq \mu_2)$ when $\gamma = 0.4$ and $d_1 = 0.03$; with starting point $\mu_1 = 0.5$ and $\mu_2 = 1$.

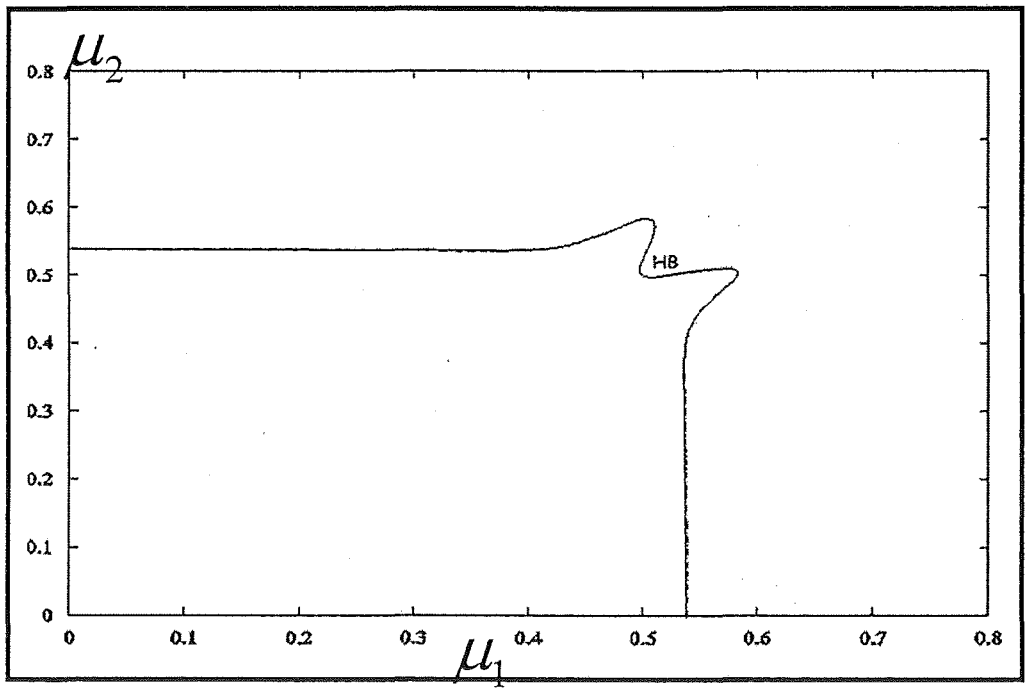

Figure 3.45: The two parameter plot γ against λ for two compartment model $(\mu_1 \neq \mu_2)$ when $\gamma = 0.4$ and $d_1 = 0.03$; with starting point $\mu_1 = 0.5$ and $\mu_2 = 0.5$.

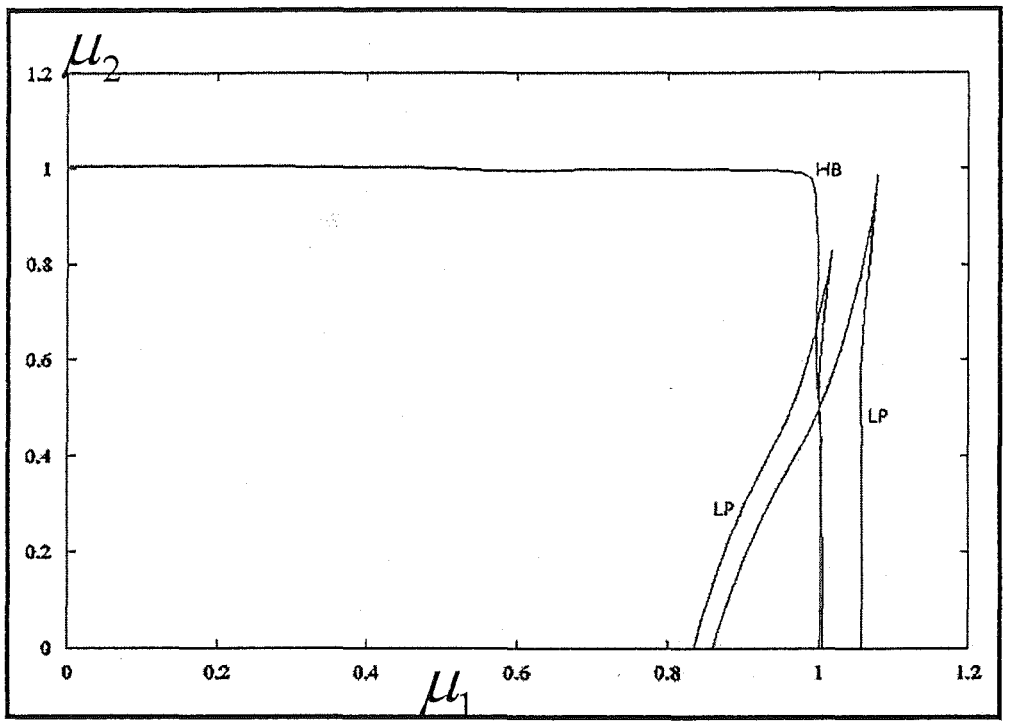

Figure 3.46: The two parameter plot μ_2 against μ_1 for two compartment model ($\mu_1 \neq \mu_2$) when $\gamma = 0.4$ and $d_1 = 0.01$; with starting point $\mu_1 = 1$ and $\mu_2 = 0.5$.

The following are some observations of some interest:

i) In **Figures 3.40** to **3.44**, the quality of the Hopf bifurcation curve at the corner changes as d_1 varies. It is straightened as $d_1 < 0.015$ at the starting point $\mu_1 = 0.5$ and $\mu_2 = 1$, but curvy as $d_1 > 0.015$. This is the basis for choosing $\gamma = 0.4$ and d_1 ranging from 0.01 to 0.03, and the starting point $\mu_1 = 0.5$ and $\mu_2 = 1$.

ii) The "*rich*" behavior can be seen all at once when $0.8 < \mu_2 < 1.1$ and μ_1 is any value less than 1.

iii) **Figure 3.45** is obtained with the parameters $\gamma = 0.4$ and $d = 0.03$, and the starting point of $\mu_1 = 0.5$ and $\mu_2 = 0.5$, a choice which eliminates the rich behavior. The graph is symmetrical at the diagonal, for the plot of μ_2 against μ_1 (Note that the axes are slightly of different scale).

iv) The question whether μ_2 is symmetrical to μ_1 was tested by executing **Figure 3.46**, where the parameters are $\gamma = 0.4$ and $d_1 = 0.01$ and the starting point is the reverse of **Figure 3.40**, viz $\mu_1 = 1$ and $\mu_2 = 0.5$.

3.5.3 Two parameter plot of γ against d_1 with fixed μ_1 and μ_2

From **section 3.5.2**, it appears that "*rich*" behaviour is sensitive to values of μ_1 and μ_2 so the choice made are $\mu_1 = 0.5$ and $\mu_2 = 1$ and the starting value $d_1 = 0.02$ and $\gamma = 0.4$. Thus in **Figure 3.47**, it is observed that value of γ that attracts the *rich* behavior is $\gamma = 0.4$, and to get both limit points one may choose $d_1 < 0.055$.

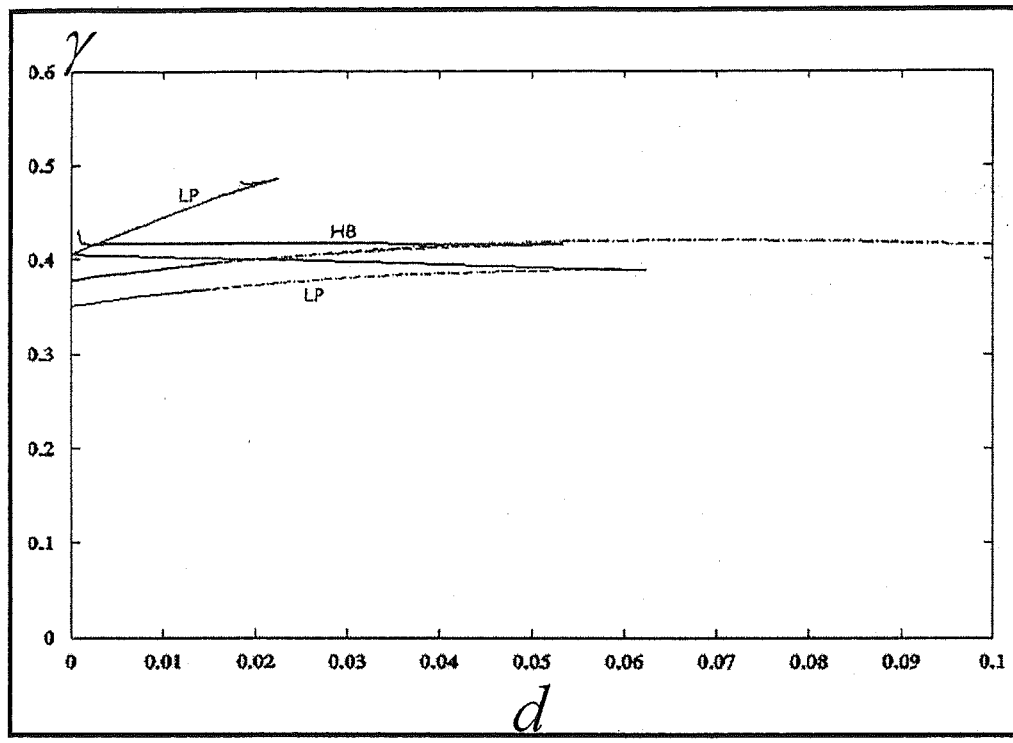

Figure 3.47: The two parameter plot γ against d_1 for two compartment model ($\mu_1 \neq \mu_2$) when $\mu_1 = 0.5$ and $\mu_2 = 1$; with starting point $\gamma = 0.4$ and $d_1 = 0.02$.

3.5.4 The two parameter plot μ_2 against d_1 with fixed μ_1 and γ

The purpose of **Figure 3.48** defines the sensitive values of μ_2 and d_1. It is consistent with the earlier finding sensitivity when either μ_1 or μ_2 lies between 0.9 and 1.1 (i.e. when we choose either one of μ_1 to be anything between 0.9 and 1.1 and μ_1 can be any value below 1 or vice versa) and d_1 is less than 0.5.

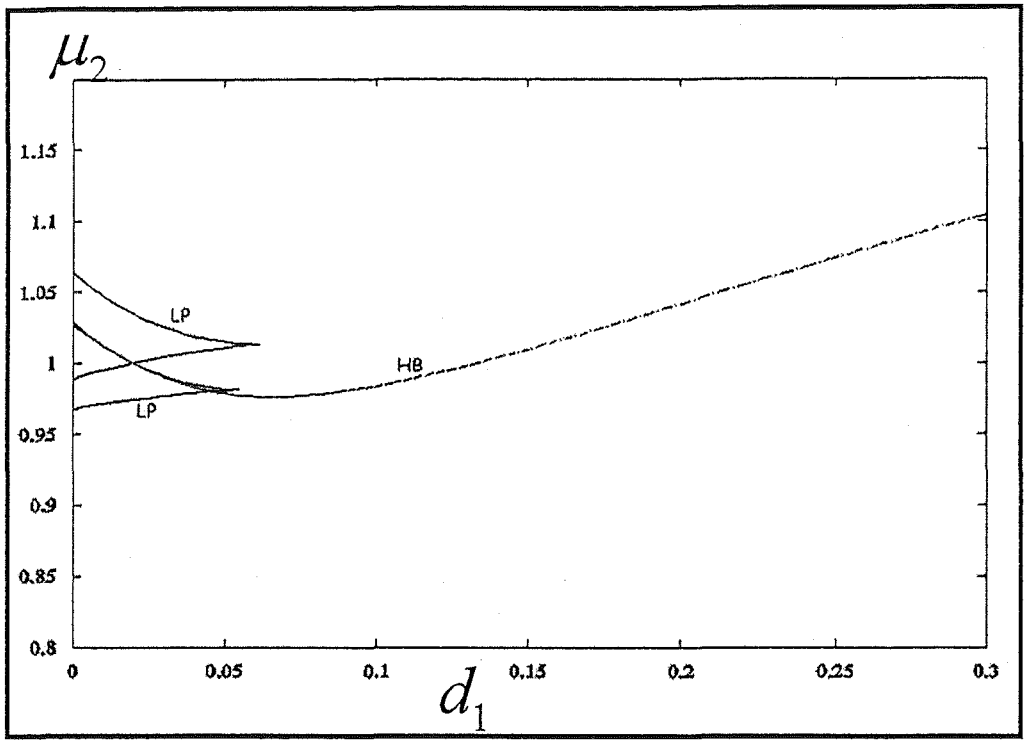

Figure 3.48: The two parameter plot μ_2 against d_1 for two compartment model ($\mu_1 \neq \mu_2$) when $\mu_1 = 0.5$, $\gamma = 0.4$ and $d_1 = 0.02$ with starting point $\mu_2 = 1$.

Figure 3.49 and **Figure 3.50** demonstrate the conjecture that the plot of μ_1 against d_1 and μ_2 against d_1 is the same. Thus **Figure 3.49** (μ_1 against d_1 when $\mu_2 = 0.5$ and starting point $\mu_1 = 1$) produces the same plot when μ_2 is plotted against d_1 when $\mu_1 = 0.5$ and starting point $\mu_2 = 1$; and **Figure 3.50** (μ_2 against d_1 with $\mu_1 = 1$ and starting point $\mu_2 = 0.5$) produces the same plot when μ_1 is plotted against d_1 with $\mu_2 = 1$ and starting point $\mu_1 = 0.5$. Thus μ_1 is symmetrical to μ_2.

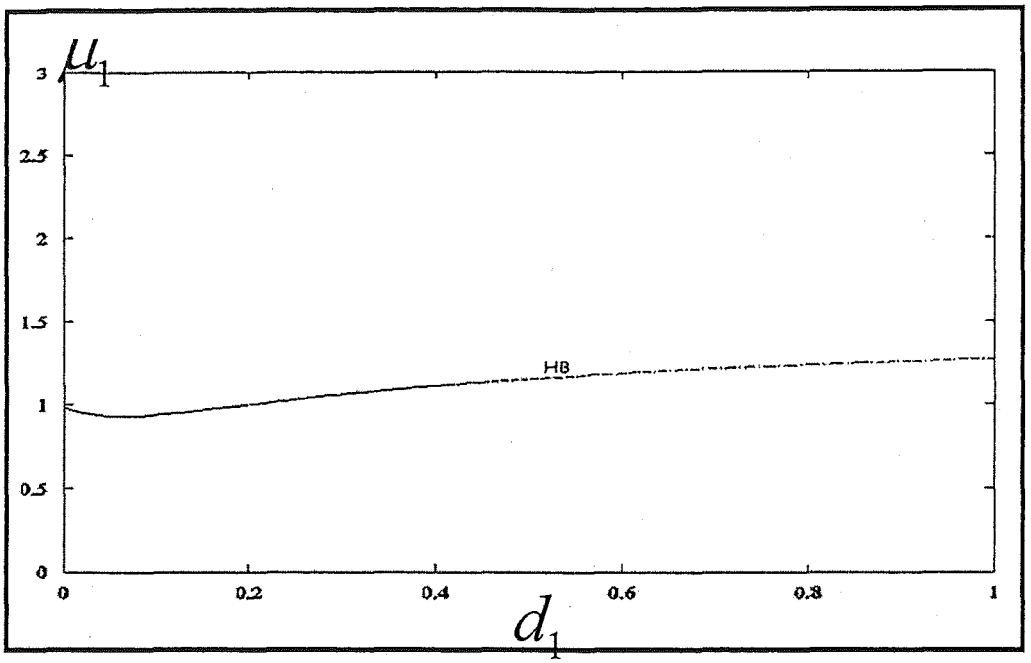

Figure 3.49: The two parameter plot μ_1 against d_1 for two compartment model ($\mu_1 \neq \mu_2$) when $\mu_1 = 0.5$, $\gamma = 0.4$ and $d_1 = 0.2$ with starting point $\mu_1 = 1$.

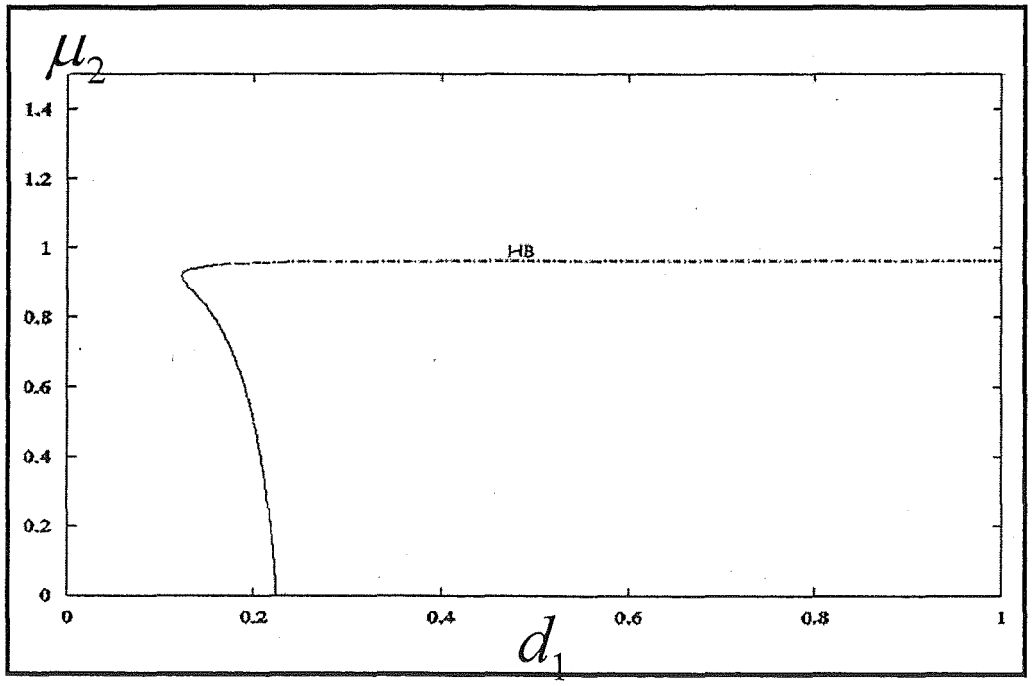

Figure 3.50: The two parameter plot μ_2 against d_1 for two compartment model ($\mu_1 \neq \mu_2$) when $\mu_1 = 1$, $\gamma = 0.4$ and $d_1 = 0.2$ with starting point $\mu_2 = 0.5$.

3.6 Conclusions

The behaviour of the two compartment model with equal growth parameter in both compartments i.e. $\mu_1 = \mu_2$ resembles the one compartment model, thus:

i) E_0 is the steady state in which none of the species (neither the phytoplankton nor the zooplankton survive;

ii) E_1 is the steady state in which phytoplankton is the only species that survives;

iii) E_2 is the most important steady state, where both the phytoplankton and zooplankton species survive;

iv) the periodic or limit cycle defines the phytoplankton and zooplankton alternately dominate. As the grazing rate of the zooplankton species increases, the phytoplankton population decreases. However, when the population of the phytoplankton decreases, the grazing rate of the zooplankton will also decreases. Thus the population of zooplankton decreases due to limitation of food. Since the grazing rate now decreases, the phytoplankton species will begin to increase and thus the periodic cycle continues.

v) the unstable periodic is unattainable solutions which did not give any edge for a basin of stability.

In summary, nothing survives at region ①, especially in region ⑦. In region ②, only the phytoplankton will survive. Region ④, both the phytoplankton and zooplankton survive which is the most important region. While in region ⑤, periodic cycle exist whereby phytoplankton and zooplankton alternately surviving. Coexistence between steady states only visible at $\gamma < 0.45$ i.e. in region ⑥; while the coexistence between the steady state E_1 and limit cycle is found in region ③. Region ⑥ show a small region

for coexistence between the phenomena of only the phytoplankton survived (E_1) and when both the phytoplankton and zooplankton existed (E_2). Region ④ and ⑥ are considered to be the most important regions since those are the region when both the species phytoplankton and zooplankton survive. The two compartment model with equal growth parameter ($\mu_1 = \mu_2$) resembles as our one compartment model with the exceptional that the region ③ is smaller and is dominated by the presence of the unstable limit cycle.

Further, the two compartment model ($\mu_1 \neq \mu_2$), has three *feasible* steady states similar to that of two compartment ($\mu_1 = \mu_2$). There are $E_0 = (0,0,0,0,0,0,\lambda)$, $E_1 = (x_1, x_2, 0, y_1, y_2, 0, y_4)$ and $E_2 = (x_1, x_2, x_3, y_1, y_2, y_3, y_4)$. Furthermore, it does not have any unstable Hopf bifurcation point. The unstable Hopf bifurcation point is only present when the value of μ between the two compartments is closed to one another (see **Figure 3.32** and **Figure 3.33**). It is first visible when $\mu_1 = 0.8$ and $\mu_2 = 1$. Obviously, the bifurcation diagrams give totally a different outcome for a different choice of μ**'s.** Another additional feature is that there are fold points or 2 limit points is observed at $\mu_1 < 0.7$ and $\mu_2 = 1$ (see **Figure 3.34** to **Figure 3.39**). It proved impossible to extend the bifurcation points lines, and to achieve the complete result via linearization using **MATHEMATICA** such as was done for the one and two compartment model ($\mu_1 = \mu_2$). Nevertheless, the following conclusion may be made:

i) sensitive values (where all limit points and Hopf bifurcation points are found) are $d_1 < 0.055$, $\gamma = 0.4$ and either μ_1 or μ_2 has to be between 0.9 and 1.1, with the other be less than 1.1.

ii) the two μ's are self-symmetrical c.f. the two parameter plot of μ_1 against μ_2 in **Figure 3.45**, and comparison of **Figure 3.42** with **Figure 3.46**; and **Figure 3.49** with **Figure 3.50** (though we have to take caution with the starting points).

In addition, the case $\mu_1 = 1$ and $\mu_2 = 0.9999$ obviously resembles the two compartment model ($\mu_1 = \mu_2$).

Chapter 4

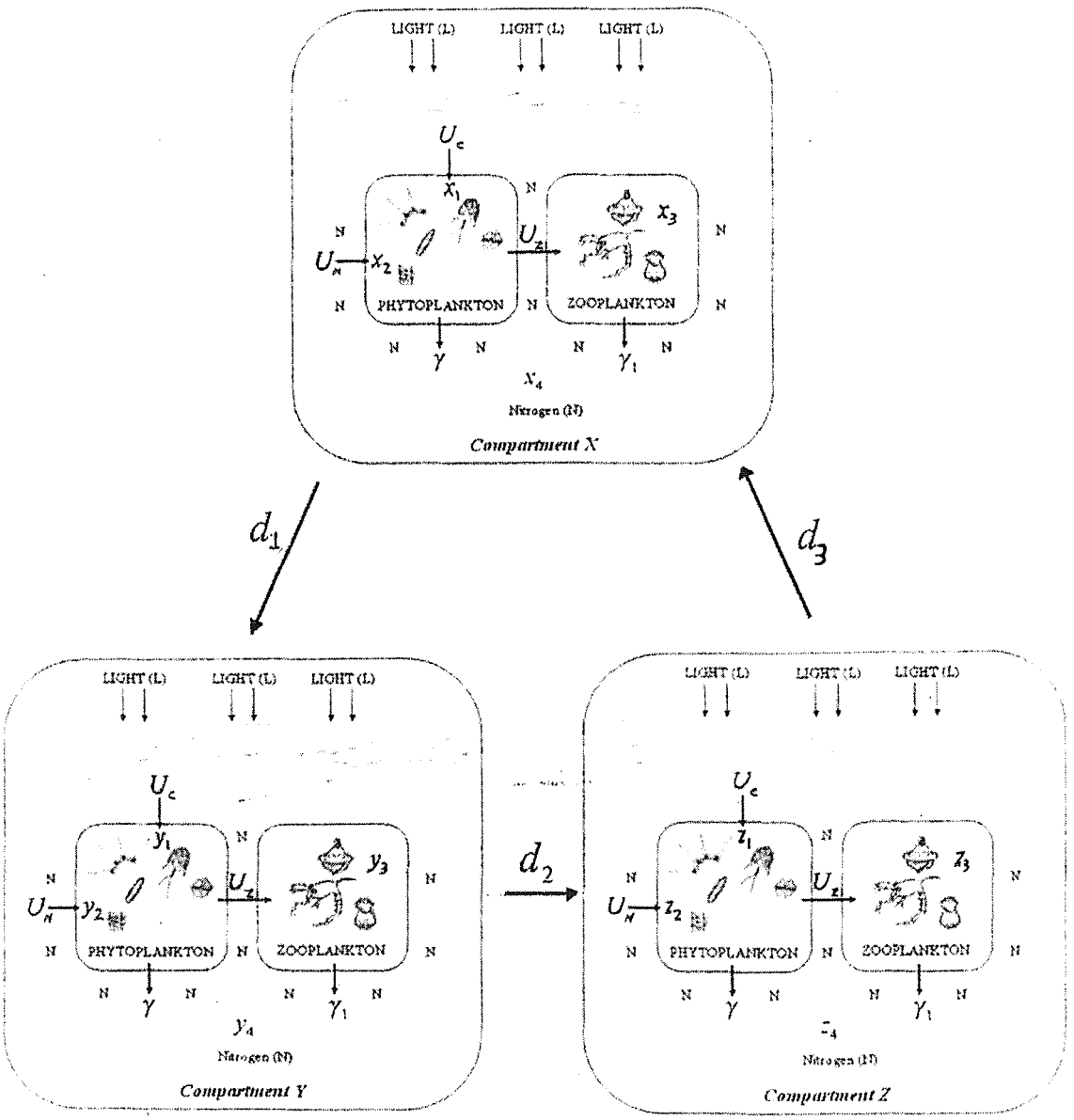

The three compartment phytoplankton-zooplankton-nutrient model

Chapter 4: The three compartment phytoplankton-zooplankton-nutrient model

4.0 Introduction

In this chapter, the one and two compartment models presented in Chapters 2 and 3 are extended to a three compartment model. The three one-compartments are connected to each other with a constant diffusion rates of d_1, d_2 and d_3. The compartments are denoted by X, Y and Z respectively. Thus the essential variables for the respective compartments are now the phytoplankton carbon (x_1, y_1 and z_1) and phytoplankton nitrogen (x_2, y_2 and z_2), the zooplankton carbon (x_3, y_3 and z_3) and the free nitrogen (x_4, y_4 and z_4). It is assumed that the three compartments are connected in a cycle so that each compartment has two neighbours. It is possible to have a linear network in which compartments X and Z are connected to only one compartment whilst Y is connected to two compartments which is left for future study. In reality, lakes and ponds are somehow related or connected to one another in a cyclic manner. The growth parameter of the phytoplankton (carbon) i.e. μ is first assumed to be the same in all the compartments as a control analysis to observe any resemblance in behaviour with the one and two-compartments models, before introducing different growth rates of phytoplankton. The question is whether introducing three compartments makes a difference to the quality of the bifurcation diagrams it produces and to observe any differences that might occur in the general behaviour of our model. It is too complicated to solve the equations analytically, but bifurcation analysis using the computer software AUTO is again used.

4.1 The model

Based on the same assumptions discussed in Chapter 1 and that the nutrient (nitrogen) is a closed system such that $\dot{y}_4+\dot{y}_2+\gamma_2\dot{y}_3+\dot{x}_4+\dot{x}_2+\gamma_2\dot{x}_3+\dot{z}_2+\dot{z}_4+\gamma_2\dot{z}_3=0$, we have $y_4=3\lambda-y_2-\gamma_2y_3-x_4-x_2-\gamma_2x_3-z_4-z_2-\gamma_2z_3$. The mathematical model is now reduced to a system of eleven coupled ordinary differential equation in eleven dependent variables-viz the phytoplankton carbon (x_1, y_1 and z_1) and phytoplankton nitrogen (x_2, y_2 and z_2), the zooplankton carbon (x_3, y_3 and z_3) and the free nitrogen (x_4 and z_4). Thus the system of ordinary differential equations to be solved on the domain

$\Omega=\{(x_1, x_2, x_3, x_4, y_1, y_2, y_3, y_4, z_1, z_2, z_3): x_1\geq 0,\ x_2\geq 0,\ x_3\geq 0,\ y_1\geq 0,\ y_2\geq 0,$
$y_3\geq 0, y_4\geq 0,\ z_1\geq 0,\ z_2\geq 0,\ z_3\geq 0,\ z_4\geq 0\}$ is

$$\dot{x}_1=\mu_1\left(1-\frac{Qx_1}{x_2}\right)^{+}x_1-\frac{\Gamma x_1x_3}{(x_1+\hat{C})}-\gamma x_1-d_1(x_1-y_1)-d_3(x_1-z_1) \tag{4.1}$$

$$\dot{x}_2=\frac{Ux_1x_4H\left(R-\frac{x_2}{x_1}\right)}{(x_4+h)}-\frac{\Gamma x_2x_3}{x_1+\hat{C}}-\gamma x_2-d_1(x_2-y_2)-d_3(x_2-z_2) \tag{4.2}$$

$$\dot{x}_3=\frac{\Gamma x_2x_3}{\gamma_2(x_1+\hat{C})}-\gamma_1x_3-d_1(x_3-y_3)-d_3(x_3-z_3) \tag{4.3}$$

$$\dot{x}_4=\gamma x_2+\gamma_1\gamma_2x_3-\frac{Ux_1x_4H\left(R-\frac{x_2}{x_1}\right)}{(x_4+h)}-d_1(x_4-3\lambda+y_2+\gamma_2y_3+x_4+x_2+\gamma_2x_3+z_4+z_2+\gamma_2z_3)$$
$$-d_3(x_4-z_4) \tag{4.4}$$

$$\dot{y}_1 = \mu_2\left(1-\frac{Qy_1}{y_2}\right)^{+} y_1 - \frac{\Gamma y_1 y_3}{(y_1+\hat{C})} - \gamma y_1 - d_1(y_1-x_1) - d_2(y_1-z_1) \tag{4.5}$$

$$\dot{y}_2 = \frac{Uy_1\left(3\lambda - y_2 - \gamma_2 y_3 - x_4 - x_2 - \gamma_2 x_3 - z_4 - z_2 - \gamma_2 z_3\right) H\left(R-\frac{y_2}{y_1}\right)}{(3\lambda - y_2 - \gamma_2 y_3 - x_4 - x_2 - \gamma_2 x_3 - z_4 - z_2 - \gamma_2 z_3 + h)} \tag{4.6}$$
$$-\frac{\Gamma y_2 y_3}{y_1+\hat{C}} - \gamma y_2 - d_1(y_2-x_2) - d_2(y_2-z_2)$$

$$\dot{y}_3 = \frac{\Gamma y_2 y_3}{\gamma_2(y_1+\hat{C})} - \gamma_1 y_3 - d_1(y_3-x_3) - d_2(y_3-z_3) \tag{4.7}$$

$$\dot{z}_1 = \mu_3\left(1-\frac{Qz_1}{z_2}\right)^{+} z_1 - \frac{\Gamma z_1 z_3}{(z_1+\hat{C})} - \gamma z_1 - d_3(z_1-x_1) - d_2(z_1-y_1) \tag{4.8}$$

$$\dot{z}_2 = \frac{Uz_1 z_4 H\left(R-\frac{z_2}{z_1}\right)}{(z_4+h)} - \frac{\Gamma z_2 z_3}{z_1+\hat{C}} - \gamma z_2 - d_3(z_2-x_2) - d_2(z_2-y_2) \tag{4.9}$$

$$\dot{z}_3 = \frac{\Gamma z_2 z_3}{\gamma_2(z_1+\hat{C})} - \gamma_1 z_3 - d_3(z_3-x_3) - d_2(z_3-y_3) \tag{4.10}$$

$$\dot{z}_4 = \gamma z_2 + \gamma_1\gamma_2 z_3 - \frac{Uz_1 z_4 H\left(R-\frac{z_2}{z_1}\right)}{(z_4+h)} - d_3(z_4-x_4) \tag{4.11}$$
$$-d_2(z_4-3\lambda+y_2+\gamma_2 y_3+x_4+x_2+\gamma_2 x_3+z_4+z_2+\gamma_2 z_3)$$

4.2 Steady states assuming an equal growth parameter for the phytoplankton ($\mu_1 = \mu_2 = \mu_3$)

Solving the system of eleven-ordinary differential equation is complicated and **MATHEMATICA** failed to give a result but the behaviour of the steady states may be analyzed using the computer software **AUTO**. Let us first define the steady states. One

of the steady states is evidently $(0,\ 0,\ 0,\ \lambda,\ 0,\ 0,\ 0,\ 0,\ 0,\ 0,\ \lambda)$, and another is of the form $(x_1,\ x_2,\ 0,\ x_4,\ x_1,\ x_2,\ 0,\ x_1,\ x_2,\ 0, x_4)$. From (4.1), $x_1\left[\mu\left(1-\frac{Qx_1}{x_2}\right)^{+}-\gamma\right]=0$ which implies that $x_1=0$ or $\alpha=\frac{x_2}{x_1}=\frac{Q\mu}{\mu-\gamma}=\frac{y_2}{y_1}=\frac{z_2}{z_1}$. From (4.2), $\frac{Ux_1x_4}{(x_4+h)}-\gamma x_2=0$ which implies that $x_4=\frac{\gamma\alpha h}{(U-\gamma\alpha)}$ and from (4.9), implies $z_4=\frac{\gamma\alpha h}{(U-\gamma\alpha)}$. From (4.6) $\frac{Uy_1(3\lambda-3x_2-2x_4)}{\gamma y_2(3\lambda-3x_2-2x_4+h)}=1$ or $3\lambda-3x_2-2x_4=\frac{\alpha\gamma h}{U-\alpha\gamma}$. Substituting $x_4=\frac{\gamma\alpha h}{(U-\gamma\alpha)}$ and simplifying yields $x_2=\lambda-\frac{\gamma\alpha h}{U-\gamma\alpha}$ and thus $x_1=\frac{1}{\alpha}\left[\lambda-\frac{\gamma\alpha h}{U-\gamma\alpha}\right]$. Therefore the second steady state

$$\left(\frac{1}{\alpha}\left[\lambda-\frac{\gamma\alpha h}{U-\gamma\alpha}\right],\ \lambda-\frac{\gamma\alpha h}{U-\gamma\alpha},\ 0,\ \frac{\gamma\alpha h}{U-\gamma\alpha},\ \frac{1}{\alpha}\left[\lambda-\frac{\gamma\alpha h}{U-\gamma\alpha}\right],\ \lambda-\frac{\gamma\alpha h}{U-\gamma\alpha},\ 0,\frac{1}{\alpha}\left[\lambda-\frac{\gamma\alpha h}{U-\gamma\alpha}\right]\right.$$
$$\left.\lambda-\frac{\gamma\alpha h}{U-\gamma\alpha},0,\frac{\gamma\alpha h}{U-\gamma\alpha}\right)$$ or

$$\left(\frac{(\mu-\gamma)}{Q\mu}\beta,\ \beta,\ 0,\ \lambda\text{-}\beta,\frac{(\mu-\gamma)}{Q\mu}\beta,\ \beta,\ 0,\frac{(\mu-\gamma)}{Q\mu}\beta,\ \beta,0,\ \lambda-\beta\right)$$ such that

$\beta=\lambda+\frac{Q\mu\gamma h}{Q\mu\gamma-U(\mu-\gamma)}$. Another steady state emerging from the bifurcation diagram is of the form $(x_1,\ x_2,\ x_3,\ x_4,\ x_1,\ x_2,\ x_3,\ x_1,\ x_2,\ x_3,\ x_4)$. Thus, from (4.1) one has $\mu\left(1-\frac{Qx_1}{x_2}\right)^{+}x_1-\frac{\Gamma x_1x_3}{(x_1+\hat{C})}-\gamma x_1=0$, and the same result follows from equations (4.5) and (4.8). Equation (4.2) also becomes similar to equation (4.6) and (4.9); and equation (4.3) with equation (4.7) and (4.10). Consider this steady state as if it were that of a one compartment model. From the bifurcation diagrams in **Figures 4.1** to **4.11**, the relevant

feasible steady state resembles the one compartment model. In summary, the steady states are

$$E_0 = (0,\ 0,\ 0,\ \lambda,\ 0,\ 0,\ 0,\ 0,\ 0,\ 0,\ \lambda),$$

$$E_1 = \left(\frac{(\mu-\gamma)}{Q\mu}\beta,\ \beta,\ 0,\ \lambda\text{-}\beta, \frac{(\mu-\gamma)}{Q\mu}\beta,\ \beta,\ 0, \frac{(\mu-\gamma)}{Q\mu}\beta,\ \beta, 0,\ \lambda-\beta\right) \quad \text{such that}$$

$$\beta = \lambda + \frac{Q\mu\gamma h}{Q\mu\gamma - U(\mu-\gamma)} \text{ and } E_2 = (x_1,\ x_2,\ x_3,\ x_4,\ x_1,\ x_2,\ x_3,\ x_1,\ x_2,\ x_3,\ x_4) \text{ such that}$$

$$x_1 = \frac{-(20(-4835+3700\gamma+158\lambda \pm 2\sqrt{6310900+4410000\gamma^2-399740\lambda+6241\lambda^2+200\gamma(-52130+1659\lambda)}}{79(-9+20\gamma)}$$

$$x_2 = \gamma_1\gamma_2(x_1^* + \hat{C})/\Gamma$$

$$x_3 = \left(-\frac{\mu Q}{\gamma_1\gamma_2} + \frac{(\mu-\gamma)}{\Gamma}\right)x_1^* + \frac{\hat{C}(\mu-\gamma)}{\Gamma}$$

$$x_4 = (-6.18568\times10^{31} + 1.84391\times10^{31}d_1 + 5.13436\times10^{31}\gamma - 5.26743\times10^{31}d_1\gamma + 2.59967\times10^{31}d_1\gamma^2$$
$$+1.9315\times10^{30}\lambda - 4.40088\times10^{29}d_1\lambda + 9.77973\times10^{29}d_1\gamma\lambda - 2.44493\times10^{28}\sqrt{4.41\times10^6\gamma^2}$$
$$\sqrt{+6241(-35.8228+\lambda)(-28.2278+\lambda)+\gamma(-1.0426\times10^7+331800\lambda)}$$

$$-5.57073\times10^{27}d_1\sqrt{4.41\times10^6\gamma^2+6241(-35.8228+\lambda)(-28.2278+\lambda)+\gamma(-1.0426\times10^7+331800\lambda)}$$
$$+1.23794\times10^{28}d_1\gamma\sqrt{4.41\times10^6\gamma^2+6241(-35.8228+\lambda)(-28.2278+\lambda)+\gamma(-1.0426\times10^7+331800\lambda)}$$
$$\pm0.5\sqrt{\left(-4d_1(-1.76035\times10^{30}+3.91189\times10^{30}\gamma)\left(2.00237\times10^{31}-5.53978\times10^{31}\gamma+2.44493\times10^{29}\lambda\right.\right.}$$
$$\sqrt{-3.09485\times10^{27}\sqrt{4.41\times10^6\gamma^2+6241(-35.8228+\lambda)(-28.2278+\lambda)+\gamma(-1.0426\times10^7+331800\lambda)}}$$
$$\sqrt{d_1\left(-1.40382\times10^{32}-2.59967\times10^{32}\gamma^2+4.40088\times10^{38}\lambda+5.57073\times10^{28}\sqrt{4.41\times10^6\gamma^2+6241}\right.}$$
$$\sqrt{\sqrt{(-35.8228+\lambda)(-28.2278+\lambda)+\gamma(-1.0426\times10^7+331800\lambda)}+\gamma\left(4.28946\times10^{32}\right.}$$
$$\sqrt{-9.77973\times10^{30}\lambda-1.23794\times10^{29}\sqrt{4.41\times10^6\gamma^2+6241(-35.8228+\lambda)(-28.2278+\lambda)}}$$

$$\sqrt{\sqrt{+\gamma(-1.0426\times10^{7}+331800\lambda)}}\Big)\Big)+\Big(1.23714\times10^{32}-1.02687\times10^{32}\gamma-3.86299\times10^{30}\lambda$$

$$\sqrt{+4.88986\times10^{28}\sqrt{4.41\times10^{6}\gamma^{2}+6241(-35.8228+\lambda)(-28.2278+\lambda)+\gamma(-1.0426\times10^{7}+331800\lambda)}}$$
$$\sqrt{+d\Big(-3.68782\times10^{31}-5.19935\times10^{31}\gamma^{2}+8.80175\times10^{29}\lambda+1.11415\times10^{28}\sqrt{4.41\times10^{6}\gamma^{2}}}$$
$$\sqrt{\sqrt{+6241(-35.8228+\lambda)(-28.2278+\lambda)+\gamma(-1.0426\times10^{7}+331800\lambda)}}$$

$$\sqrt{+\gamma\Big(1.05349\times10^{32}-1.95595\times10^{30}\lambda-2.47588\times10^{28}\sqrt{4.41\times10^{6}\gamma^{2}+6241(-35.8228+\lambda)}}$$
$$\sqrt{\sqrt{(-28.2278+\lambda)+\gamma(-1.0426\times10^{7}+331800\lambda)}}\Big)\Big)^{2}\Big)\Big)/(d_{1}(-1.76035\times10^{30}+3.91189\times10^{30}\gamma)$$

The other *unfeasible* steady states observed from the bifurcation plots x_3 against λ are as follows:

$ufss1 = (-x_1,\ -x_2,\ 0,\ x_4,\ y_1,\ y_2,\ 0,\ -x_1,\ -x_2,\ 0,\ x_4)$

$ufss2 = (x_1,\ x_2,\ 0,\ x_4,\ -y_1,\ -y_2,\ 0,\ x_1,\ x_2,\ 0,\ x_4)$

$ufss3 = (x_1,\ x_2,\ x_3,\ x_4,\ -y_1,\ -y_2,\ y_3,\ x_1,\ x_2,\ x_3,\ x_4)$

$ufss4 = (-x_1,\ -x_2,\ x_3,\ x_4,\ y_1,\ y_2,\ y_3,\ -x_1,\ -x_2,\ x_3,\ x_4)$

$ufss5 = (x_1,\ x_2,\ -x_3,\ x_4,\ x_1,\ x_2,\ -x_3,\ x_1,\ x_2,\ -x_3,\ x_4)$.

Thus for simplicity let us focus on the feasible steady states only i.e. those where all the relevant variables are positive. Numerically, using **AUTO**, the *feasible* steady states are confirmed to be E_0, E_1 and E_2 only. The unfeasible steady state such as $ufss1$, $ufss2$, $ufss3$, $ufss4$ and $ufss5$ and other *unfeasible* steady state which is not featured in the bifurcations diagrams that follows in the next section shall be ignored.

4.3 Bifurcation analysis assuming an equal growth parameter for the phytoplankton ($\mu_1 = \mu_2 = \mu_3$)

Recall the three *feasible* steady state are E_0, E_1 and E_2. This section describes the bifurcation diagrams for the three compartment model via the software package *AUTO*. The various regions of stability of the steady states, the limit point (i.e. the coexistence between steady states) and the presence of limit cycles are identified. Our bifurcation diagrams are capable of:

i) identifying the position where one steady states changes to another (**Bifurcation Point** or **BP**), the coexistence of steady states (**Limit Points** or **LP**) and the presence of any periodic solutions (**Hopf Bifurcation Point** or **HB**).

ii) To confirming the *stability* of the steady states by grabbing a particular point and **AUTO** will also gives the eigenvalues of each point.

The parameters in (**APPENDIX C: TABLES: C1**) are again adopted, except for λ. λ=15 is assumed to be the starting point for producing plots of x_3 against λ. Initially, the diffusion parameter from each of the three compartments is assumed to have the same value-viz $d_1 = d_2 = d_3 = 0.02$. Recall from Chapter 3 that $d_1 = 0.02$ is a sensitive value for our model).

Let us proceed to discuss details of the bifurcation diagrams for the three-compartment model with the growth parameter $\mu_1 = \mu_2 = \mu_3 = 1$ for $\gamma = 0.4$, focusing on how the steady states change from one form to another ignoring any *unfeasible* branch (see **APPENDIX C: TABLES: C4**).

i) **Figure 4.1** shows the bifurcation diagram of the parameter x_3 against λ, when $\gamma = 0.4$, $d_1 = 0.02$, $d_2 = 0.02$ and $d_3 = 0.02$. Viewed from left to the right, the first obvious feature is **BP1** at the point $\lambda = 0.1724$ (before that there is actually a narrow region where the null state E_0 is stable, but it is too short to be obvious, although it can be detected by grabbing the point when using **AUTO**). At $\lambda = 0.1724$, the null state E_0 becomes unstable, and the system moves to the steady state E_1 which is stable for larger λ. A limit point (**LP**) then occurs at $\lambda = 22.66$, when E_2 is notably stable just before the Hopf bifurcation point or the periodic branch (**HB**) occurs. Indeed E_2 is simultaneously stable with E_1 until the HB is reached at $\lambda = 24.16$. Another bifurcation point (**BP2**) occurs at $\lambda = 25.17$, so that E_2 coexists with E_1 from $\lambda = 22.66$ to $\lambda = 25.17$; from $\lambda = 24.16$ to $\lambda = 25.17$, **HB** coexists with E_1. Another Hopf bifurcation point occurs at $\lambda = 28.07$, which produces unstable periodic orbits. The other bifurcation points, limit points or Hopf Bifurcation points that occur on an unfeasible branch (*ufss*) are ignored.

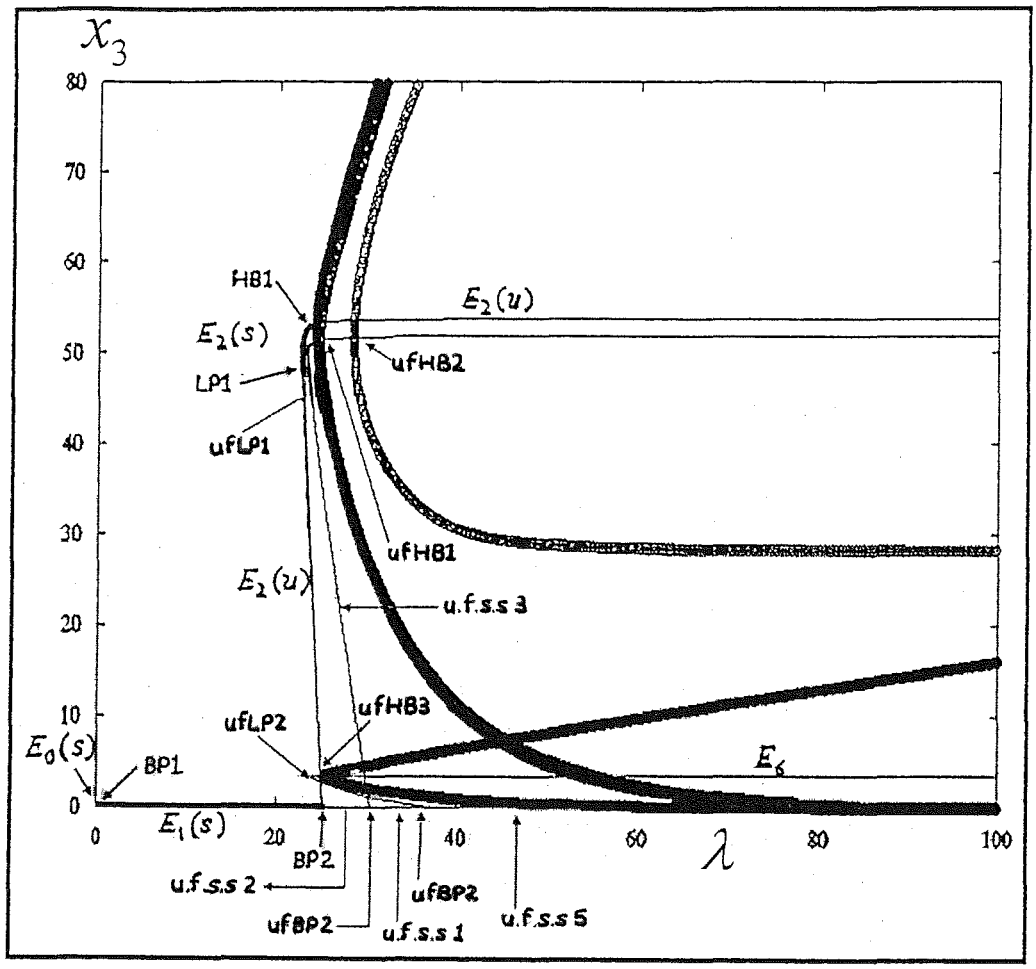

Figure 4.1: The bifurcation diagram x_3 against λ for three compartment model ($\mu_1 = \mu_2 = \mu_3 = 1$) when $\gamma = 0.4$ and $d_1 = d_2 = d_3 = 0.02$ showing the bifurcation points BP1 (λ=0.1724), BP2 (λ=25.17); Limit point LP1 (λ=22.66) and the Hopf bifurcation point HB1 (λ=24.16(stable)). Other unfeasible steady state found is of the form u.f.s.s1 = $(-x_1, -x_2, 0, x_4, y_1, y_2, 0, -x_1, -x_2, 0, x_4)$, u.f.s.s2 = $(x_1, x_2, 0, x_4, -y_1, -y_2, 0, x_1, x_2, 0, x_4)$, u.f.s.s3 = $(x_1, x_2, x_3, x_4, -y_1, -y_2, y_3, x_1, x_2, x_3, x_4)$, u.f.s.s5 = $(-x_1, -x_2, -x_3, x_4, y_1, y_2, -y_3, -x_1, -x_2, -x_3, x_4)$ and thus the unfeasible bifurcation points are ufBP1 (λ=0.3045), ufBP2 (λ= 37.21), ufLP1 (λ=23.25), ufLP2 (λ= 24.02), ufHB1 (λ=24.56 (unstable)), ufHB2 (λ= 28.34(unstable)) and ufHB3 (λ= 25.23).

ii) **Figure 4.2** shows the bifurcation diagram of the parameter x_3 against λ, when $d_1 = 0.01$, $d_2 = 0.02$ and $d_3 = 0.02$ or $d_1 = 0.02$, $d_2 = 0.01$ and $d_3 = 0.02$ or $d_1 = 0.02$, $d_2 = 0.02$ and $d_3 = 0.01$ labeled as **3m1m1m1d001d002d002**, **3m1m1m1d002d001d002** and **3m1m1m1d002d002d001** respectively. All produce the same bifurcation diagram. There is a bifurcation point (**BP1**) at the point $\lambda = 0.1724$, where the null state E_0 changes from stable to unstable and the steady state E_1 occurs. A limit point (**LP**) then occurs at $\lambda = 22.66$, when E_2 is noticeably stable just before the Hopf bifurcation point or the periodic branch (**HB1**) occurs. Indeed E_2 is simultaneously stable with E_1 until the **HB1** is reached at $\lambda = 24.16$. There is another bifurcation point (**BP2**) at $\lambda = 25.17$, so that E_2 coexists with E_1 from $\lambda = 22.66$ to $\lambda = 25.17$; from $\lambda = 24.16$ to $\lambda = 25.17$, **HB1** coexists with E_1. Another Hopf bifurcation point (**HB2**) occurs at $\lambda = 28.07$ which produces an unstable periodic orbits. Thus, the feasible bifurcation points resembles **Figure 4.1** when $d_1 = d_2 = d_3 = 0.02$ except that here an extra unstable Hopf bifurcation point (**HB2**) which produces unstable periodic orbits are featured and the unfeasible solution is not found in this case.

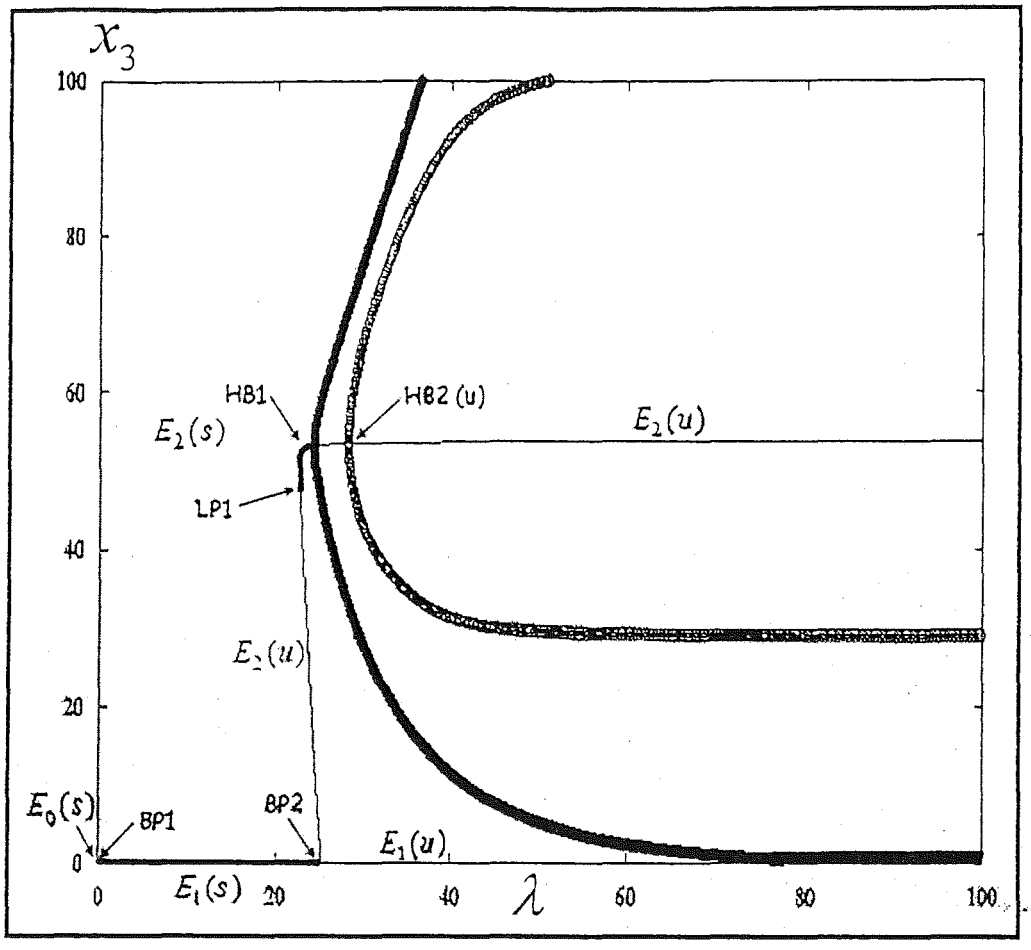

Figure 4.2: The bifurcation diagram x_3 against λ for three compartment model ($\mu_1 = \mu_2 = \mu_3 = 1$) when $\gamma = 0.4$ and $d_1 = d_2 = d_3 = 0.02$ showing the bifurcation points BP1 (λ=0.1724), BP2 (λ=25.17); Limit point LP1 (λ=22.66) and the Hopf bifurcation points HB1 (λ=24.16 (stable)) HB2 (λ=28.07 (unstable)).

iii) **Figure 4.3** shows the bifurcation diagram of the parameter x_3 against λ, when $d_1 = 0.03$, $d_2 = 0.02$ and $d_3 = 0.02$ or $d_1 = 0.02$, $d_2 = 0.03$ and $d_3 = 0.02$ or $d_1 = 0.02$, $d_2 = 0.02$ and $d_3 = 0.03$ or $d_1 = 0.04$, $d_2 = 0.02$ and $d_3 = 0.02$ or $d_1 = 0.02$, $d_2 = 0.04$ and $d_3 = 0.02$ or $d_1 = 0.02$, $d_2 = 0.02$ and $d_3 = 0.04$. These are labeled as **3m1m1m1d003d002d002,**

3m1m1m1d002d003d002, **3m1m1m1d002d002d003**, **3m1m1m1d004d002d002**, **3m1m1m1d002d004d002** and **3m1m1m1d002d002d004** respectively. All produce the same bifurcation diagram. There is a bifurcation point (**BP1**) at the point $\lambda = 0.1724$, where the null state E_0 changes from stable to unstable and the steady state E_1 occurs. A limit point (**LP**) then occurs at $\lambda = 22.66$, when E_2 is noticeably stable just before the Hopf bifurcation point or the periodic branch (**HB**) occurs. Indeed E_2 is simultaneously stable with E_1 until the **HB** is reached at $\lambda = 24.16$. Another bifurcation point (**BP2**) occurs at $\lambda = 25.17$, so that E_2 coexists with E_1 from $\lambda = 22.66$ to $\lambda = 25.17$; from $\lambda = 24.16$ to $\lambda = 25.17$, **HB** coexists with E_1. Thus, it resembles the feasible solutions of **Figure 4.1** and that of **Figure 4.2** when $d_1 = d_2 = d_3 = 0.02$ and $d_1 = 0.01$, $d_2 = d_3 = 0.02$ respectively. However, the unfeasible solutions are not found here and the unstable Hopf bifurcation point (**HB2**) which produces unstable periodic orbits is also not featured.

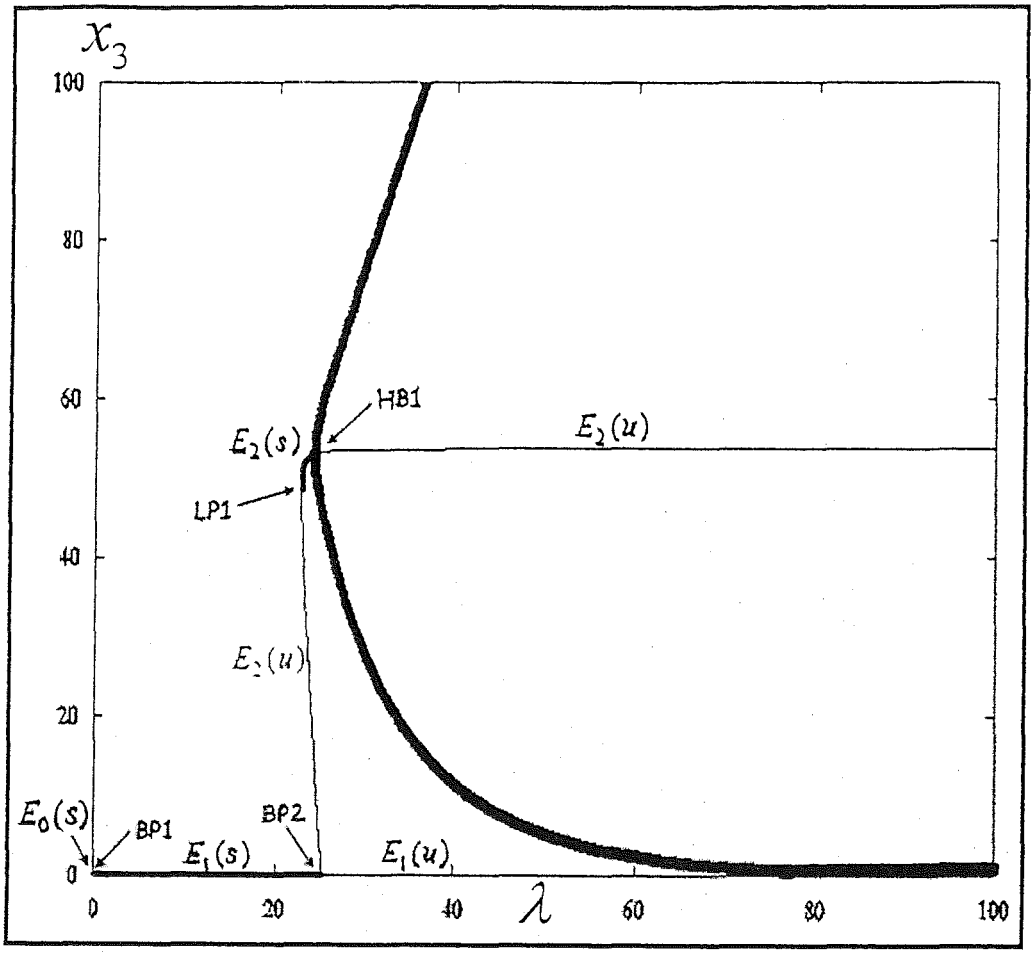

Figure 4.3: The bifurcation diagram x_3 against λ for three compartment model ($\mu_1 = \mu_2 = \mu_3 = 1$) when $\gamma = 0.4$ and $d_1 = 0.03$, $d_2 = 0.02$ and $d_3 = 0.02$ or $d_1 = 0.02$, $d_2 = 0.03$ and $d_3 = 0.02$ or $d_1 = 0.02$, $d_2 = 0.02$ and $d_3 = 0.03$ or $d_1 = 0.04$, $d_2 = 0.02$ and $d_3 = 0.02$ or $d_1 = 0.02$, $d_2 = 0.04$ and $d_3 = 0.02$ or $d_1 = 0.02$, $d_2 = 0.02$ and $d_3 = 0.04$, showing the bifurcation points BP1 (λ=0.1724), BP2 (λ=25.17); Limit point LP1 (λ=22.66) and the Hopf bifurcation point HB1 (λ=24.16 (stable)).

Let us now investigate the two-parameter plots of μ_1 against μ_2, μ_2 against μ_3 and μ_1 against μ_3. Note: The axes are not labeled since diagrams with same features are represented as one diagram.

iv) **Figure 4.4** shows the two-parameter plot of μ_1 against μ_2, when $d_1 = 0.01$, $d_2 = 0.02$ and $d_3 = 0.02$ (**3Pm1m2-m1m1m1d001d002d002**). This is the same as the two-parameter plot of μ_2 against μ_3 when $d_1 = 0.02$, $d_2 = 0.01$ and $d_3 = 0.02$ (**3Pm2m3-m1m1m1d002d001d002**) and the two-parameter plot of μ_1 against μ_3 when $d_1 = 0.02$, $d_2 = 0.02$ and $d_3 = 0.01$ (**3Pm2m3-m1m1m1d002d002d001**).

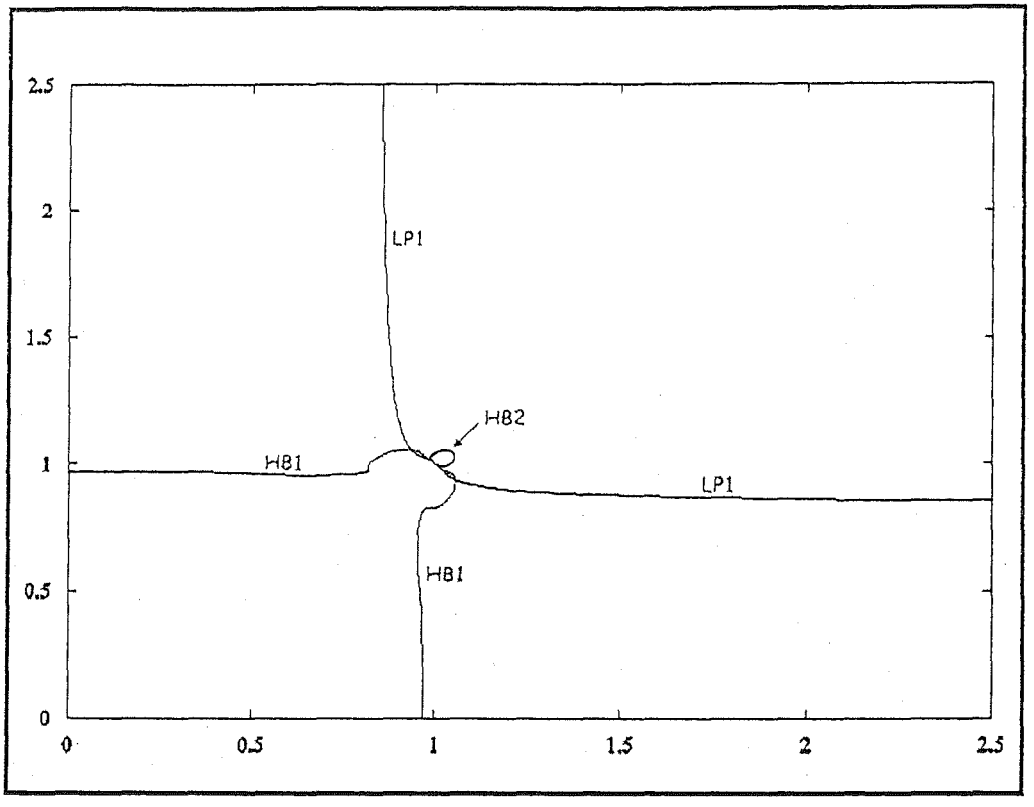

Figure 4.4: The two parameter plot : a) μ_1 against μ_2 when $d_1 = 0.01$, $d_2 = 0.02$ and $d_3 = 0.02$; b) μ_2 against μ_3 when $d_1 = 0.02$, $d_2 = 0.01$ and $d_3 = 0.02$; and c) μ_1 against μ_3 when $d_1 = 0.02$, $d_2 = 0.02$ and $d_3 = 0.01$ for the three compartment model ($\mu_1 = \mu_2 = \mu_3 = 1$) at $\gamma = 0.4$; showing the extended lines of Limit point LP1 and Hopf bifurcation points HB1 and HB2.

v) **Figure 4.5** shows the two-parameter plot of μ_1 against μ_2, when $d_1 = 0.02$, $d_2 = 0.02$ and $d_3 = 0.01$ (**3Pm1m2-m1m1m1d002d002d001**). This is the same as the two parameter plot of μ_2 against μ_3 when $d_1 = 0.01$, $d_2 = 0.02$ and $d_3 = 0.02$ (**3Pm2m3-m1m1m1d001d002d002**) and the two-

parameter plot of μ_1 against μ_3 when $d_1 = 0.01$, $d_2 = 0.02$ and $d_3 = 0.02$ (**3Pm1m3-m1m1m1d001d002d002**).

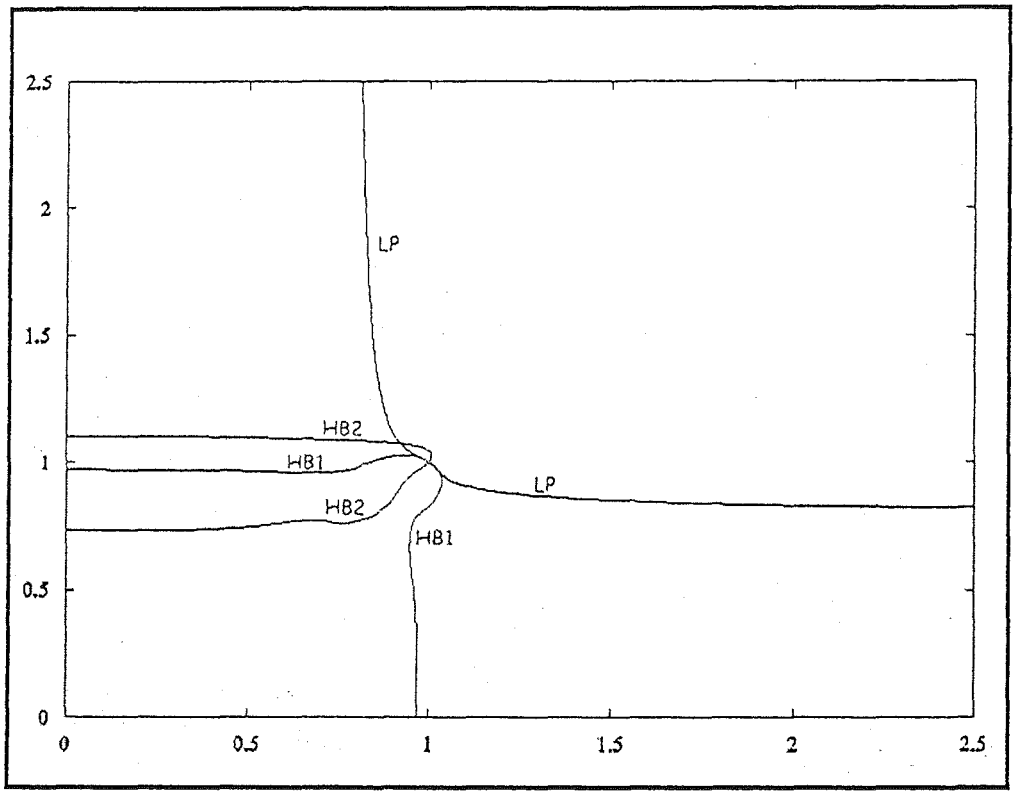

Figure 4.5: The two parameter plot : a) μ_1 against μ_2 when $d_1 = 0.02$, $d_2 = 0.02$ and $d_3 = 0.01$; b) μ_2 against μ_3 when $d_1 = 0.01$, $d_2 = 0.02$ and $d_3 = 0.02$; and c) μ_1 against μ_3 when $d_1 = 0.01$, $d_2 = 0.02$ and $d_3 = 0.02$ for the three compartment model ($\mu_1 = \mu_2 = \mu_3 = 1$) at $\gamma = 0.4$; showing the extended lines of Limit point LP1 and Hopf bifurcation points HB1 and HB2.

vi) **Figure 4.6** shows the two-parameter plot of μ_1 against μ_2 when $d_1 = 0.02$, $d_2 = 0.01$ and $d_3 = 0.02$ (**3Pm1m2-m1m1m1d002d001002**). This is the same as the two-parameter plot of μ_2 against μ_3 when $d_1 = 0.02$,

$d_2 = 0.02$ and $d_3 = 0.01$ (**3Pm2m3-m1m1m1d002d002d001**) and the two-parameter plot of μ_1 against μ_3 when $d_1 = 0.02$, $d_2 = 0.01$ and $d_3 = 0.02$ (**3Pm1m3-m1m1m1d002d001d002**).

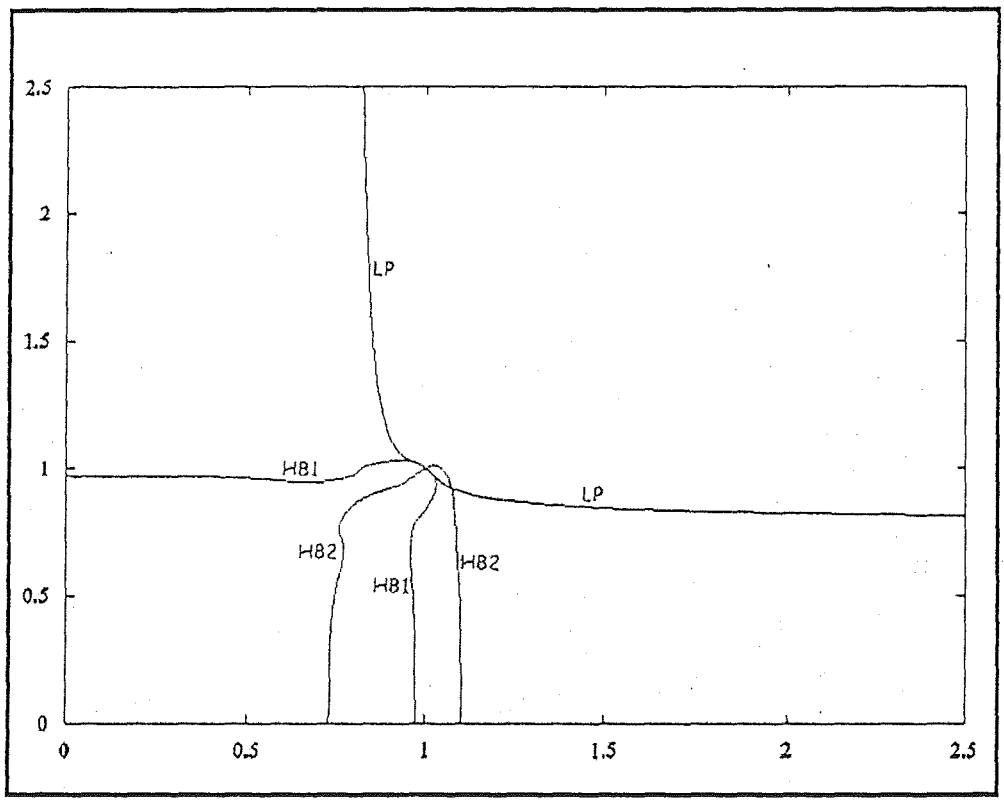

Figure 4.6: The two parameter plot : a) μ_1 against μ_2 when $d_1 = 0.02$, $d_2 = 0.01$ and $d_3 = 0.02$; b) μ_2 against μ_3 when $d_1 = 0.02$, $d_2 = 0.02$ and $d_3 = 0.01$; and c) μ_1 against μ_3 when $d_1 = 0.02$, $d_2 = 0.01$ and $d_3 = 0.02$ for the three compartment model ($\mu_1 = \mu_2 = \mu_3 = 1$) at $\gamma = 0.4$; showing the extended lines of Limit point LP1 and Hopf bifurcation points HB1 and HB2.

vii) **Figure 4.7** shows the two-parameter plot of μ_1 against μ_2, when $d_1 = 0.03$, $d_2 = 0.02$ and $d_3 = 0.02$ (**3Pm1m2-m1m1m1d003d002d002**). This is the same as the two parameter plot of μ_2 against μ_3 when $d_1 = 0.02$, $d_2 = 0.03$ and $d_3 = 0.02$ (**3Pm2m3-m1m1m1d002d003d002**); the-two parameter plot of μ_1 against μ_3 when $d_1 = 0.02$, $d_2 = 0.02$ and $d_3 = 0.03$ (**3Pm2m3-m1m1m1d002d002d003**); the two-parameter plot of μ_2 against μ_1 when $d_1 = 0.04$, $d_2 = 0.02$ and $d_3 = 0.02$ (**3Pm1m2-m1m1m1d004d002d002**). This is the same as the two-parameter plot of μ_3 against μ_2 when $d_1 = 0.02$, $d_2 = 0.04$ and $d_3 = 0.02$ (**3Pm2m3-m1m1m1d002d004d002**) and the two-parameter plot of μ_1 against μ_3 when $d_1 = 0.02$, $d_2 = 0.02$ and $d_3 = 0.04$ (**3Pm2m3-m1m1m1d002d002d004**).

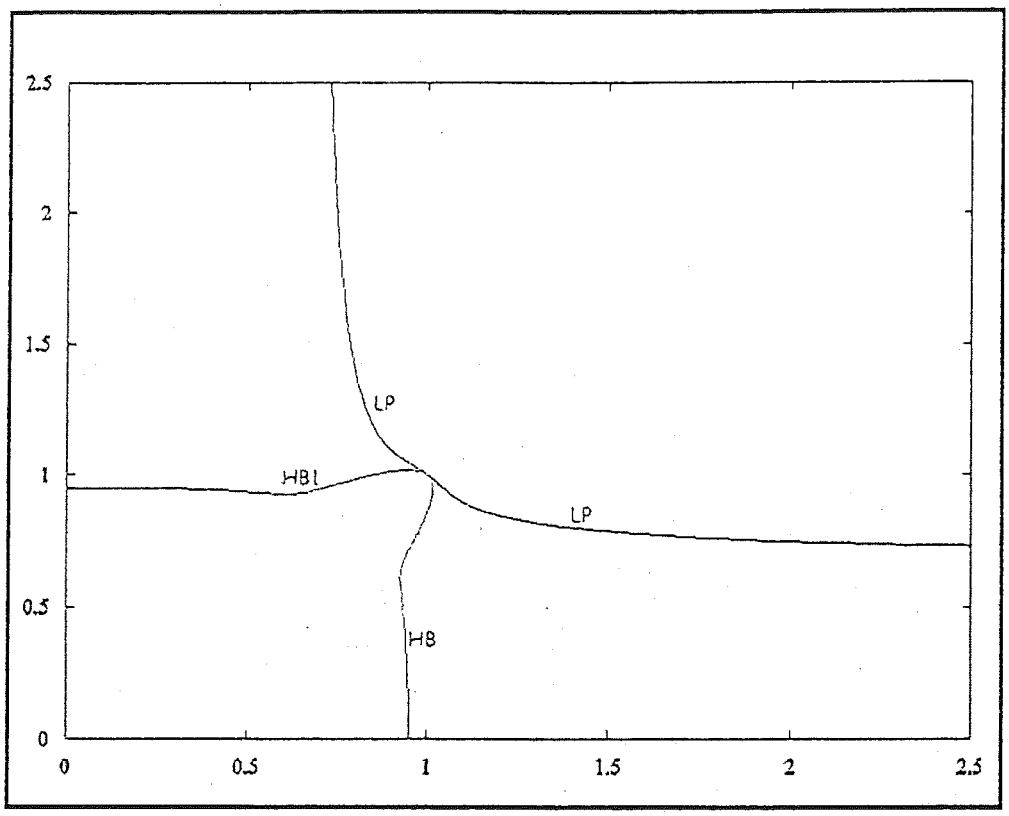

Figure 4.7: The two parameter plot : a) μ_1 against μ_2 when $d_1 = 0.03$, $d_2 = 0.02$ and $d_3 = 0.02$; b) μ_2 against μ_3 when $d_1 = 0.02$, $d_2 = 0.03$ and $d_3 = 0.02$; c) μ_1 against μ_3 when $d_1 = 0.02$, $d_2 = 0.02$ and $d_3 = 0.03$; d) μ_1 against μ_2 when $d_1 = 0.04$, $d_2 = 0.02$ and $d_3 = 0.02$; e) μ_2 against μ_3 when $d_1 = 0.02$, $d_2 = 0.04$ and $d_3 = 0.02$; and f) μ_1 against μ_3 when $d_1 = 0.02$, $d_2 = 0.02$ and $d_3 = 0.04$ for the three compartment model ($\mu_1 = \mu_2 = \mu_3 = 1$) at $\gamma = 0.4$; showing the extended lines of Limit point LP1 and Hopf bifurcation points HB1.

viii) **Figure 4.8** shows the two-parameter plot of μ_1 against μ_2, when $d_1 = 0.02$, $d_2 = 0.02$ and $d_3 = 0.03$ (**3Pm1m2-m1m1m1d002d002d003**). This is the same as the two-parameter plot of μ_2 against μ_3, when $d_1 = 0.03$,

$d_2 = 0.02$ and $d_3 = 0.02$ (**3Pm2m3-m1m1m1d003d002d002**) and the two-parameter plot of μ_1 against μ_3, when $d_1 = 0.03$, $d_2 = 0.02$ and $d_3 = 0.02$ (**3Pm1m3-m1m1m1d003d002d002**).

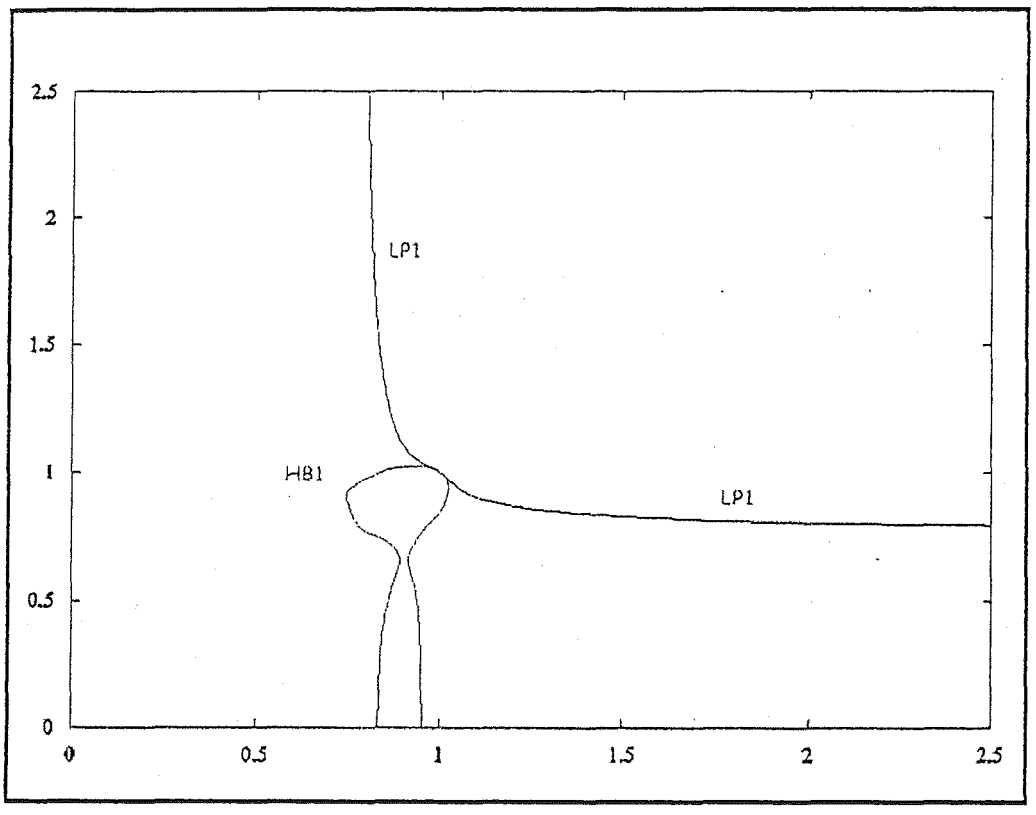

Figure 4.8: The two parameter plot : a) μ_1 against μ_2 when $d_1 = 0.02$, $d_2 = 0.02$ and $d_3 = 0.03$; b) μ_2 against μ_3 when $d_1 = 0.03$, $d_2 = 0.02$ and $d_3 = 0.02$; and c) μ_1 against μ_3 when $d_1 = 0.03$, $d_2 = 0.02$ and $d_3 = 0.02$ for the three compartment model ($\mu_1 = \mu_2 = \mu_3 = 1$) at $\gamma = 0.4$; showing the extended lines of Limit point LP1 and Hopf bifurcation points HB1.

ix) **Figure 4.9** shows the two-parameter plot of μ_1 against μ_2, when $d_1 = 0.02$, $d_2 = 0.03$ and $d_3 = 0.02$ (**3Pm1m2-m1m1m1d002d003002**). This is the same as the two-parameter plot of μ_2 against μ_3 when $d_1 = 0.02$, $d_2 = 0.02$ and $d_3 = 0.03$ (**3Pm2m3-m1m1m1d002d002d003**) and the two-parameter plot of μ_3 against μ_1 when $d_1 = 0.02$, $d_2 = 0.03$ and $d_3 = 0.02$ (**3Pm1m3-m1m1m1d002d003d002**).

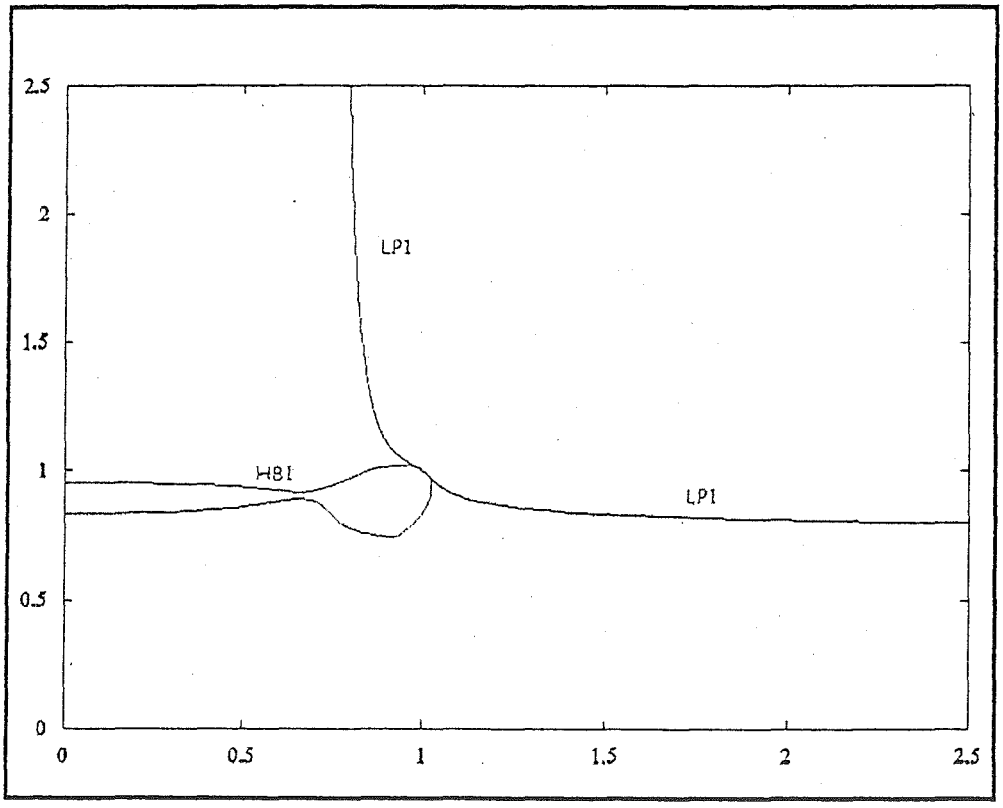

Figure 4.9: The two parameter plot : a) μ_1 against μ_2 when $d_1 = 0.02$, $d_2 = 0.03$ and $d_3 = 0.02$; b) μ_2 against μ_3 when $d_1 = 0.02$, $d_2 = 0.02$ and $d_3 = 0.03$; and c) μ_1 against μ_3 when $d_1 = 0.02$, $d_2 = 0.03$ and $d_3 = 0.02$ for the three compartment model ($\mu_1 = \mu_2 = \mu_3 = 1$) at $\gamma = 0.4$; showing the extended lines of Limit point LP1 and Hopf bifurcation points HB1.

x) **Figure 4.10** shows the two-parameter plot of μ_1 against μ_2, when $d_1 = 0.02$, $d_2 = 0.02$ and $d_3 = 0.04$ (**3Pm1m2-m1m1m1d002d002d004**). This is the same as the two-parameter plot of μ_2 against μ_3 when $d_1 = 0.04$, $d_2 = 0.02$ and $d_3 = 0.02$ (**3Pm2m3-m1m1m1d004d002d002**) and the two-parameter plot of μ_1 against μ_3, when $d_1 = 0.04$, $d_2 = 0.02$ and $d_3 = 0.02$ (**3Pm1m3-m1m1m1d004d002d002**).

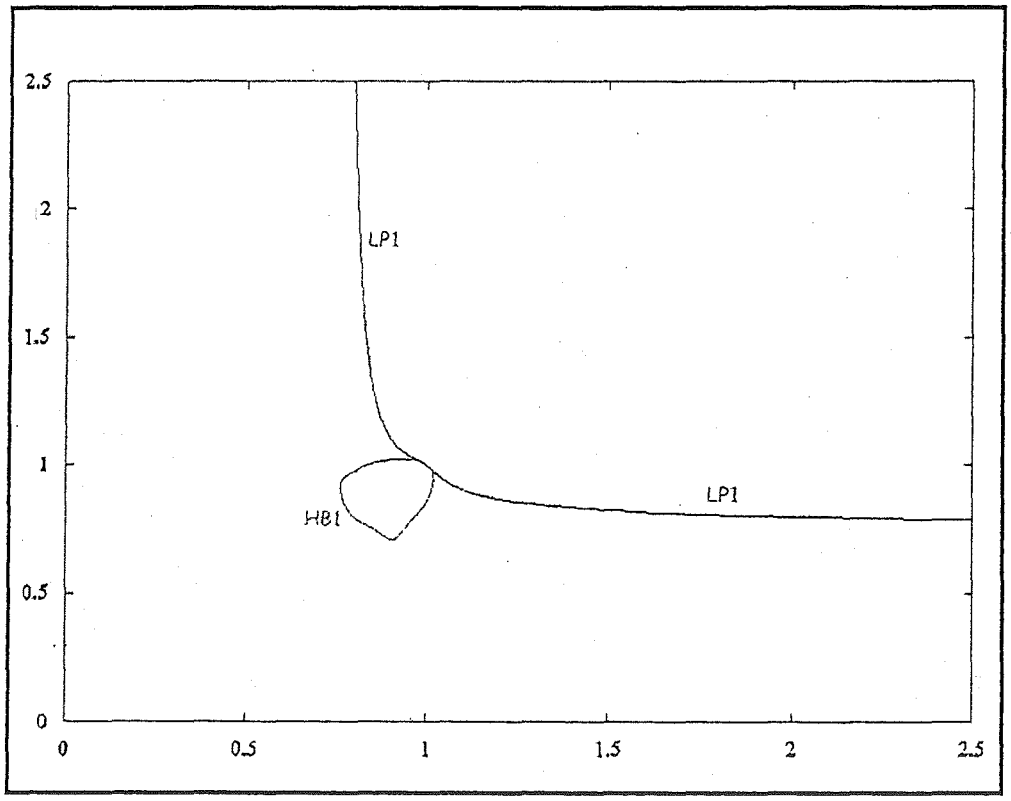

Figure 4.10: The two parameter plot : a) μ_1 against μ_2 when $d_1 = 0.02$, $d_2 = 0.02$ and $d_3 = 0.04$; b) μ_2 against μ_3 when $d_1 = 0.04$, $d_2 = 0.02$ and $d_3 = 0.02$; and c) μ_1 against μ_3 when $d_1 = 0.04$, $d_2 = 0.02$ and $d_3 = 0.02$ for the three compartment model ($\mu_1 = \mu_2 = \mu_3 = 1$) at $\gamma = 0.4$; showing the extended lines of Limit point LP1 and Hopf bifurcation points HB1.

xi) **Figure 4.11** shows the two-parameter plot of μ_1 against μ_2, when $d_1 = 0.02$, $d_2 = 0.04$ and $d_3 = 0.02$ (**3Pm1m2-m1m1m1d002d004002**). This is the same as the two-parameter plot of μ_2 against μ_3 when $d_1 = 0.02$, $d_2 = 0.02$ and $d_3 = 0.04$ (**3Pm2m3-m1m1m1d002d002d004**) and the two-parameter plot of μ_1 against μ_3, when $d_1 = 0.02$, $d_2 = 0.04$ and $d_3 = 0.02$ (**3Pm1m3-m1m1m1d002d004d002**).

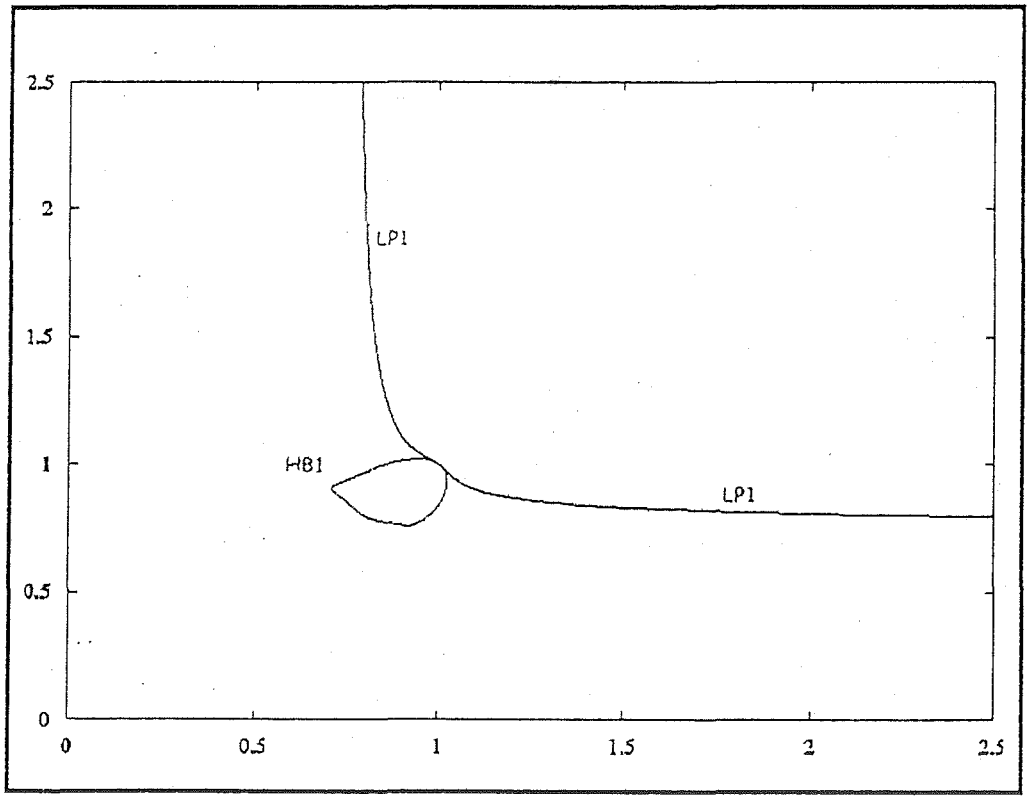

Figure 4.11: The two parameter plot : a) μ_1 against μ_2 when $d_1 = 0.02$, $d_2 = 0.04$ and $d_3 = 0.02$; b) μ_2 against μ_3 when $d_1 = 0.02$, $d_2 = 0.02$ and $d_3 = 0.04$; and c) μ_1 against μ_3 when $d_1 = 0.02$, $d_2 = 0.04$ and $d_3 = 0.02$ for the three compartment model ($\mu_1 = \mu_2 = \mu_3 = 1$) at $\gamma = 0.4$; showing the extended lines of Limit point LP1 and Hopf bifurcation points HB1.

In summary, the two-parameter plot of γ against λ for the three-compartment model, with equal growth parameter i.e. $\mu_1 = \mu_2 = \mu_3 = 1$ and one of the diffusion parameter is $d \geq 0.02$ (others fixed as 0.02), resembles the one-compartment model (c.f. APPENDIX C: TABLES: C2a, C3a and C4a), thus:

i) the steady state E_0 is only stable in the small region ①, and when $\gamma > 0.8$ (i.e. in the region ⑦, where it is globally stable;

ii) E_1 is stable in region ②, coexists with E_2^+ in region ⑥ and coexist with the limit cycle or the periodic solution in region ③;

iii) E_2^+ is stable in region ④ and coexists with E_1 in region ⑥; and

iv) the stable limit cycle or the periodic solution appears to be in region ⑤ and coexists with E_1 in region ③.

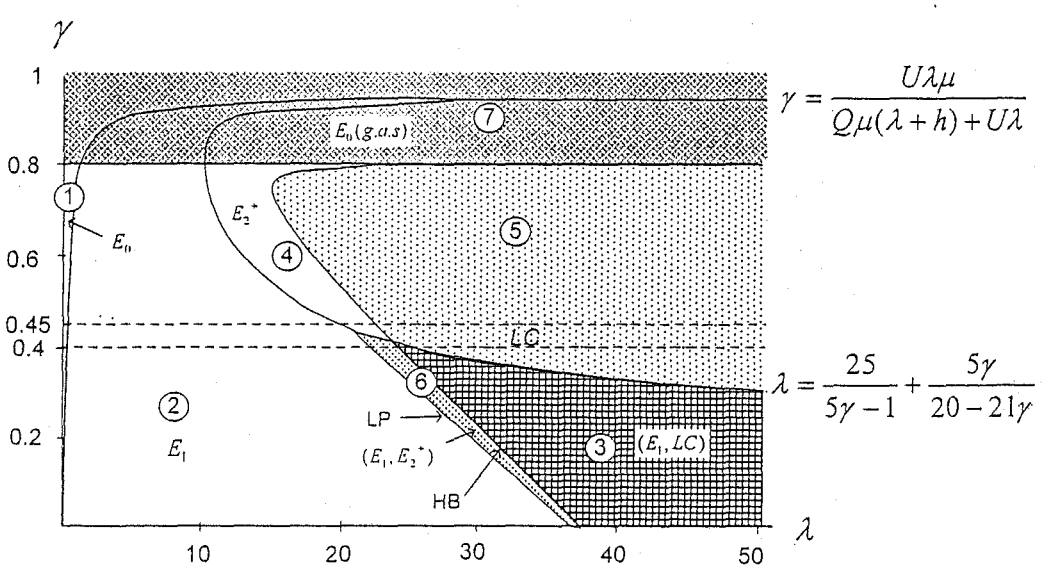

Figure 4.12: The overall 2-parameter plot for the three-compartment model showing the stability of the three feasible steady states (E_0, E_1 and E_2), the location of the coexistence between feasible steady states or periodic solutions and

the presence of limit cycles or periodic solution, when the growth parameter $\mu_1 = \mu_2 = \mu_3 = 1$ and one of the diffusion parameter is $d \geq 0.02$ (others fixed as 0.02).

The three-compartment model with the growth parameter $\mu_1 = \mu_2 = \mu_3 = 1$ and the diffusion parameter $d < 0.02$, it resembles the two-compartment model with the growth parameters $\mu_1 = \mu_2 = 1$, thus

i) the steady state E_0 is only stable in the small region ①, and when $\gamma > 0.8$ (i.e. in the region ⑦ where it is globally stable;

ii) E_1 is stable in region ②, coexists with E_2^+ in region ⑥ and coexists with the limit cycle or the periodic solution in region ③;

iii) E_2^+ is stable in region ④ and coexists with E_1 in region ⑥;

iv) the stable limit cycle or the periodic solution appears to be in region ⑤ and coexists with E_1 in region ③; and

v) there is an unstable limit cycle in region ⑧.

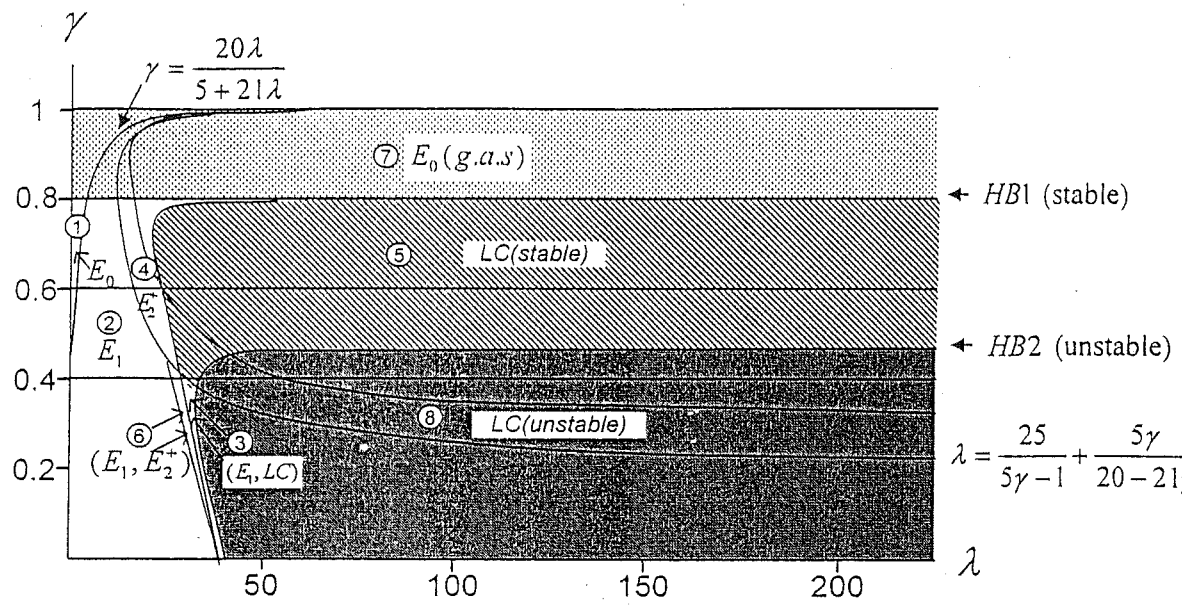

Figure 4.13: The overall 2-parameter plot for the three-compartment model showing the stability of the three feasible steady states (E_0, E_1 and E_2), the location of the coexistence between feasible steady states or periodic solutions and the presence of limit cycles or periodic solution when the growth parameter $\mu_1 = \mu_2 = \mu_3 = 1$ and one of the diffusion parameter is $d < 0.02$ (others fixed as 0.02).

There are several other interesting features as follows:

i) changing d do not change the position of the stable bifurcation points, limits points or the periodic branch. However, when the diffusion parameter d's are identical for all the three compartments (i.e. $d_1 = d_2 = d_3 = 0.02$), a few additional but unfeasible bifurcation points, limit points and Hopf bifurcation points are featured (see **Figure 4.1**).

Thus the three compartment model gives results consistent with the one and two compartment models.

ii) The two parameter plots of μ's diagrams produce the same quality diagram when the specific positions of the d's is altered and thus it produces a pattern for the positions of d's with respect to the choice of μ chosen for the axes. This is only true when one of the d's is altered while the other two remain the same. The pattern of the positions of d's can be classified as three categories, and thus is summarized as:

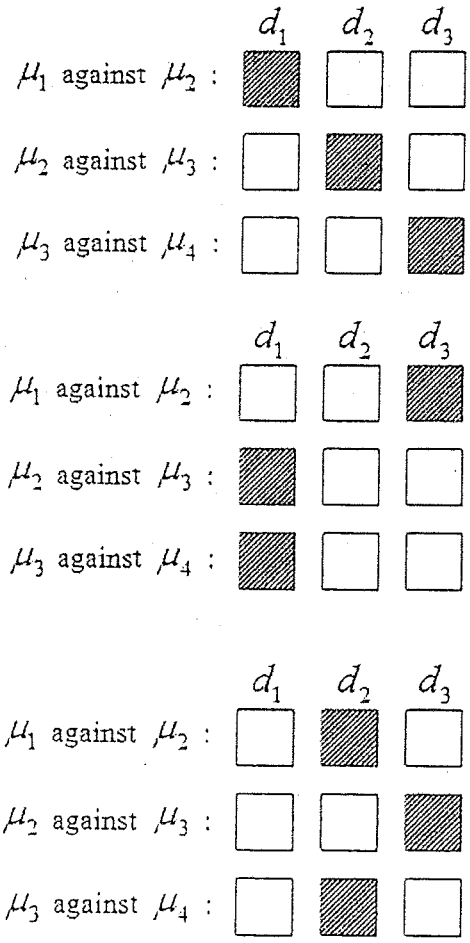

Thus for the plots of μ_1 against μ_2, μ_2 against μ_3 and μ_1 against μ_3; $d_1 = 0.01$, $d_2 = 0.02$, $d_3 = 0.02$ is equivalent to $d_1 = 0.02$, $d_2 = 0.01$, $d_3 = 0.02$; and this is equivalent to $d_1 = 0.02$, $d_2 = 0.02$, $d_3 = 0.01$ respectively. And $d_1 = 0.02$, $d_2 = 0.02$, $d_3 = 0.01$ is equivalent to $d_1 = 0.01$, $d_2 = 0.02$, $d_3 = 0.02$ and equivalent to $d_1 = 0.01$, $d_2 = 0.02$, $d_3 = 0.02$ for the plots of μ_1 against μ_2, μ_2 against μ_3 and μ_1 against μ_3 respectively. Also $d_1 = 0.02$, $d_2 = 0.01$, $d_3 = 0.02$ is equivalent to $d_1 = 0.02$, $d_2 = 0.02$, $d_3 = 0.01$ and is equivalent to $d_1 = 0.02$, $d_2 = 0.01$, $d_3 = 0.02$ for the plots of μ_1 against μ_2, μ_2 against μ_3 and μ_1 against μ_3 respectively. The same pattern is observed when one of the d values is set at 0.03 or 0.04.

4.4 Bifurcation analysis assuming a different growth parameter for the phytoplankton and equal diffusion parameter ($d_1 = d_2 = d_3 = 0.02$)

This section describes the bifurcation diagrams for the three-compartment with at least one of the growth parameters μ different but the diffusion parameter d is the same viz- $d_1 = d_2 = d_3 = 0.02$), via the software package **AUTO**. As such, it is assumed that at least one of the three compartments now does not have the same conditions and thus the growth rate is different. For example: the radiance rate L $\mu Einstm^{-2}s^{-1}$ (see Chapter 1, **Assumption 2** on pg 27) is different in one of the compartments thus this resulted in a different growth rate.

Only the *feasible* steady states are considered here. The unfeasible steady state are categorized as "seen" and "unseen" unfeasible steady states (*u.f.s.s*) or the Limit Points and Hopf Bifurcation that branch out from the unfeasible branch (labeled *u.f.l.p* and *u.f.h.b* respectively) through our bifurcation diagrams. In addition, the various regions of stability of all the feasible steady states, the limit point (i.e. the coexistence between steady states) and the presence of limit cycles are identified from the bifurcation diagram analysis.

Note: A "seen" *unfeasible* steady state is the one which can be observed in plotting x_3 against λ i.e. when x_3 is feasible but the other variable is unfeasible (negative)

whereas an "unseen" *unfeasible* steady state is one where the variable x_3 is unfeasible (negative).

From the bifurcation diagrams, we have identified some of the *feasible* steady state to be of the following:

$E_0 = (0,\ 0,\ 0,\ 3\lambda, 0,\ 0,\ 0,\ 0,\ 0,\ 0,\ 3\lambda)$

$E_1 = (x_1,\ x_2,\ 0,\ x_4, y_1,\ y_2,\ 0, y_1,\ y_2,\ 0,\ z_4)$

$E_2 = (x_1,\ x_2,\ x_3,\ x_4, y_1,\ y_2,\ y_3, y_1,\ y_2,\ y_3,\ z_4)$

$E_3 = (x_1,\ x_2,\ 0,\ x_4, y_1,\ y_2,\ 0, x_1,\ x_2,\ 0,\ x_4)$

$E_4 = (x_1,\ x_2,\ x_3,\ x_4, y_1,\ y_2,\ y_3, x_1,\ x_2,\ x_3,\ x_4)$

$E_5 = (x_1,\ x_2,\ 0,\ x_4, x_1,\ x_2,\ 0, z_1,\ z_2,\ 0,\ z_4)$

$E_6 = (x_1,\ x_2,\ x_3,\ x_4, x_1,\ x_2,\ x_3, z_1,\ z_2,\ z_3,\ z_4)$;

and some of the "seen" *unfeasible* steady state are identified to be of the following:

$(x_1,\ x_2,\ x_3,\ x_4, y_1,\ y_2,\ -y_3, y_1,\ y_2,\ -y_3,\ z_4)$

$(x_1,\ x_2,\ x_3,\ x_4, y_1,\ y_2,\ -y_3, x_1,\ x_2,\ x_3,\ x_4)$

$(x_1,\ x_2,\ x_3,\ x_4, x_1,\ x_2,\ x_3, z_1,\ z_2,\ -z_3,\ z_4)$.

Noticed that the feasible steady states identified above are symmetric solutions in which the steady states values in two compartments are the same. It is not possible to have an non-symmetric solutions because it is not identified in any of the bifurcation diagrams produced. If, there is any non-symmetric solutions it shall be unfeasible anyway.

At first, the parameters chosen are again as in **APPENDIX C: TABLES: C1** except for λ (set at the starting point of 15), to produce plots of x_3 against λ. Initially, it is

assumed that the diffusion d from each of the three compartment is equal-viz $d_1 = d_2 = d_3 = 0.02$. The growth parameter in the X compartment is chosen to be $\mu_1 = 0.5$, in the Y compartment to be $\mu_2 = 1$ and in the Z compartment to be $\mu_3 = 1$ (labeled as **3m05m1m1d002d002d002**). The growth parameter in the Y compartment is then chosen to be $\mu_2 = 0.5$, but the other growth parameters (in the X and Z compartments) set at $\mu_1 = 1$ and $\mu_3 = 1$ respectively (labeled as **3m1m05m1d002d002d002**). Then the growth parameter of the Z compartment is changed (**3m1m1m05d002d002d002**). The purpose is to see whether swapping the growth parameter around changes the quality of the bifurcation diagram (another symmetry check).

Let us now proceed to discuss details of the bifurcation diagrams for the three-compartment model with the growth parameter μ different and the diffusion parameter $d_1 = d_2 = d_3 = 0.02$ for the value of $\gamma = 0.4$, and in particular observe how the steady states change from one form to another (see **APPENDIX C: TABLES: C4b**).

xii) **Figure 4.14** shows the bifurcation diagram of the parameter x_3 against λ with diffusion parameters $d_1 = d_2 = d_3 = 0.02$ and the growth parameters $\mu_1 = 0.5$, $\mu_2 = 1$ and $\mu_3 = 1$ (labeled as **3m05m1m1d002d002d002**). There is a bifurcation point (**BP1**) at the point $\lambda = 0.1494$, where the null state E_0 changes from stable to unstable and the steady state E_1 occurs until the next bifurcation point (**BP2**) is reached at $\lambda = 12.01$. At this point, E_2 becomes stable until the Hopf bifurcation point (**HB1**) is reached at $\lambda = 24.78$.

Another Hopf bifurcation point occurs at $\lambda = 31.19$ which produces an unstable periodic orbits.

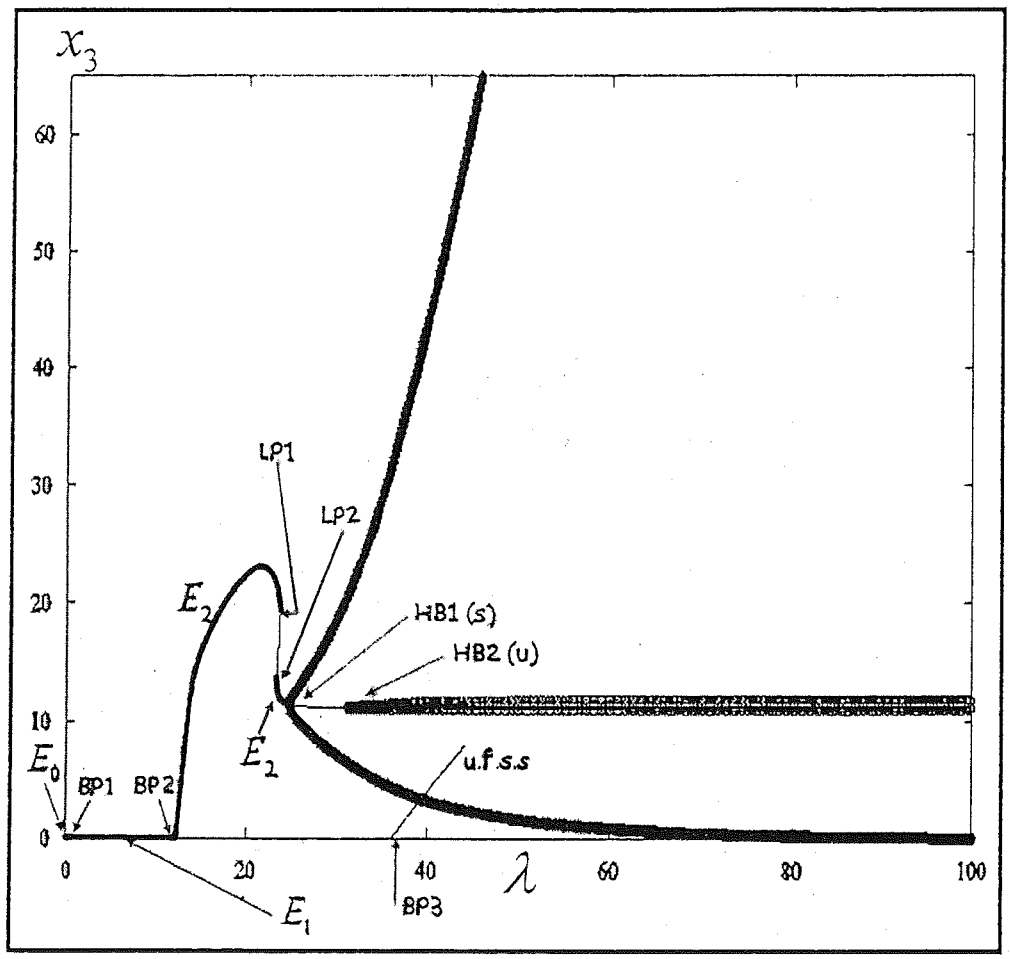

Figure 4.14: The bifurcation diagram x_3 against λ for three compartment model at $\gamma = 0.4$ when $\mu_1 = 0.5$, $\mu_2 = 1$ and $\mu_3 = 1$; and $d_1 = d_2 = d_3 = 0.02$; showing the bifurcation points BP1 (λ=0.1494), BP2 (λ=12.01); Limit point LP1 (λ=23.34) and the Hopf bifurcation points HB1 (λ=24.78 (stable)) and HB2 (λ=31.19 (unstable)). Other unfeasible steady state found is of the form u.f.s.s. = $(x_1, x_2, x_3, x_4, y_1, y_2, -y_3, y_1, y_2, -y_2, z_4)$.

xiii) **Figure 4.15** shows the bifurcation diagram of the parameter x_3 against λ with diffusion parameters $d_1 = d_2 = d_3 = 0.02$ and growth parameters $\mu_1 = 1$, $\mu_2 = 0.5$ and $\mu_3 = 1$ (labeled **3m1m05m1d002d002d002**). There is a bifurcation point (**BP1**) at the point $\lambda = 0.1494$, where the null state E_0 changes from stable to unstable and the steady state E_1 occurs until the next bifurcation point (**BP2**) is reached at $\lambda = 12.01$. At this point, E_2 becomes stable until it reached the Hopf bifurcation point (**HB1**) is reached at $\lambda = 24.78$. Another Hopf bifurcation point occur at $\lambda = 31.19$ which produces an unstable periodic orbits.

xiv) **Figure 4.16** shows the bifurcation diagram of the parameter x_3 against λ with diffusion parameters $d_1 = d_2 = d_3 = 0.02$ and growth parameters $\mu_1 = 1$, $\mu_2 = 1$ and $\mu_3 = 0.5$ (labeled as **3m1m1m05d002d002d002**). There is a bifurcation point (**BP1**) at the point $\lambda = 0.1494$, where the null state E_0 changes from stable to unstable and the steady state E_1 occurs until the next bifurcation point (**BP2**) is reached at $\lambda = 12.01$. At this point, E_2 becomes stable until it reached the Hopf bifurcation point (**HB1**) is reached at $\lambda = 24.78$. Another Hopf bifurcation point occur at $\lambda = 31.19$ which produces an unstable periodic orbits.

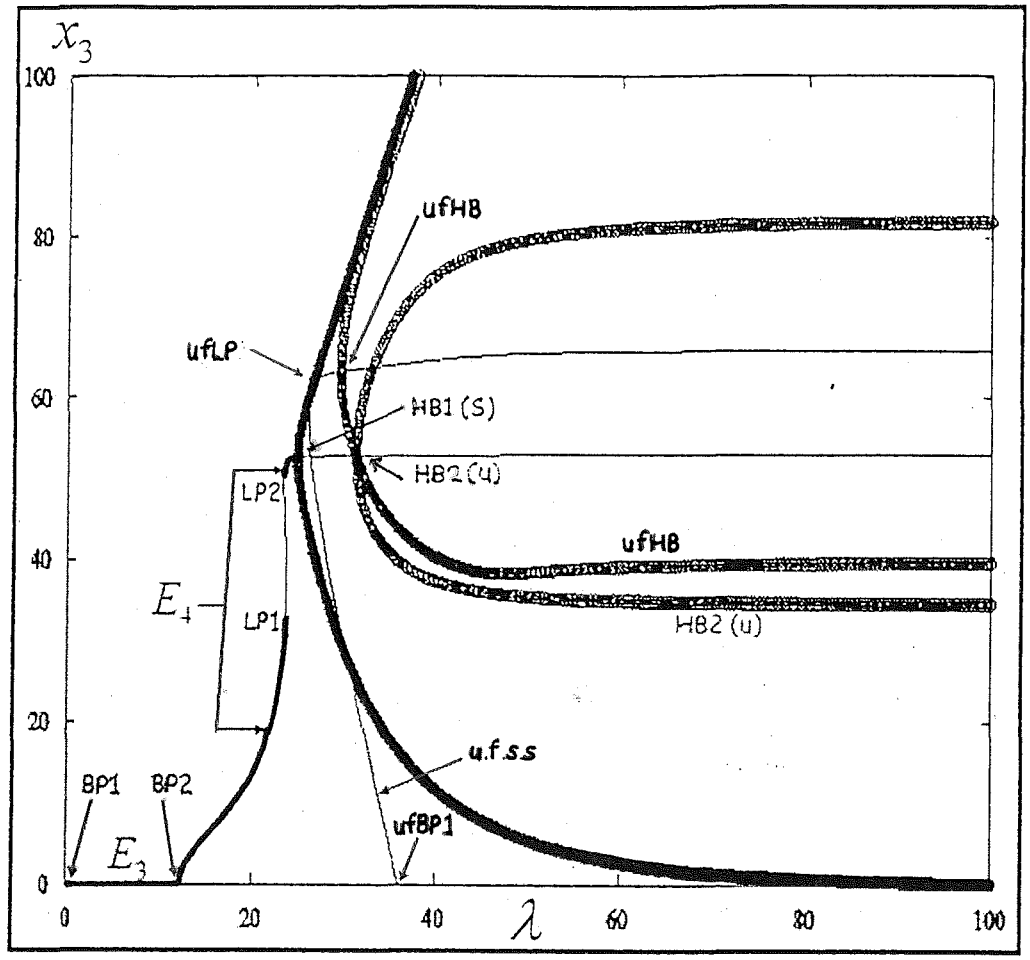

Figure 4.15: The bifurcation diagram x_3 against λ for three compartment model at $\gamma = 0.4$ when $\mu_1 = 1$, $\mu_2 = 0.5$ and $\mu_3 = 1$; and $d_1 = d_2 = d_3 = 0.02$; showing the bifurcation points BP1 (λ=0.1494), BP2 (λ=12.01); Limit point LP1 (λ=23.34) and the Hopf bifurcation points HB1 (λ=24.78 (stable)) and HB2 (λ=31.19 (unstable)). Other unfeasible steady state found is of the form u.f.s.s. = $(x_1, x_2, x_3, x_4, y_1, y_2, -y_3, x_1, x_2, x_3, x_4)$ and thus the unfeasible bifurcation points are ufBP1 (λ=36.13), ufLP (λ=26) and ufHB (λ= 24.49).

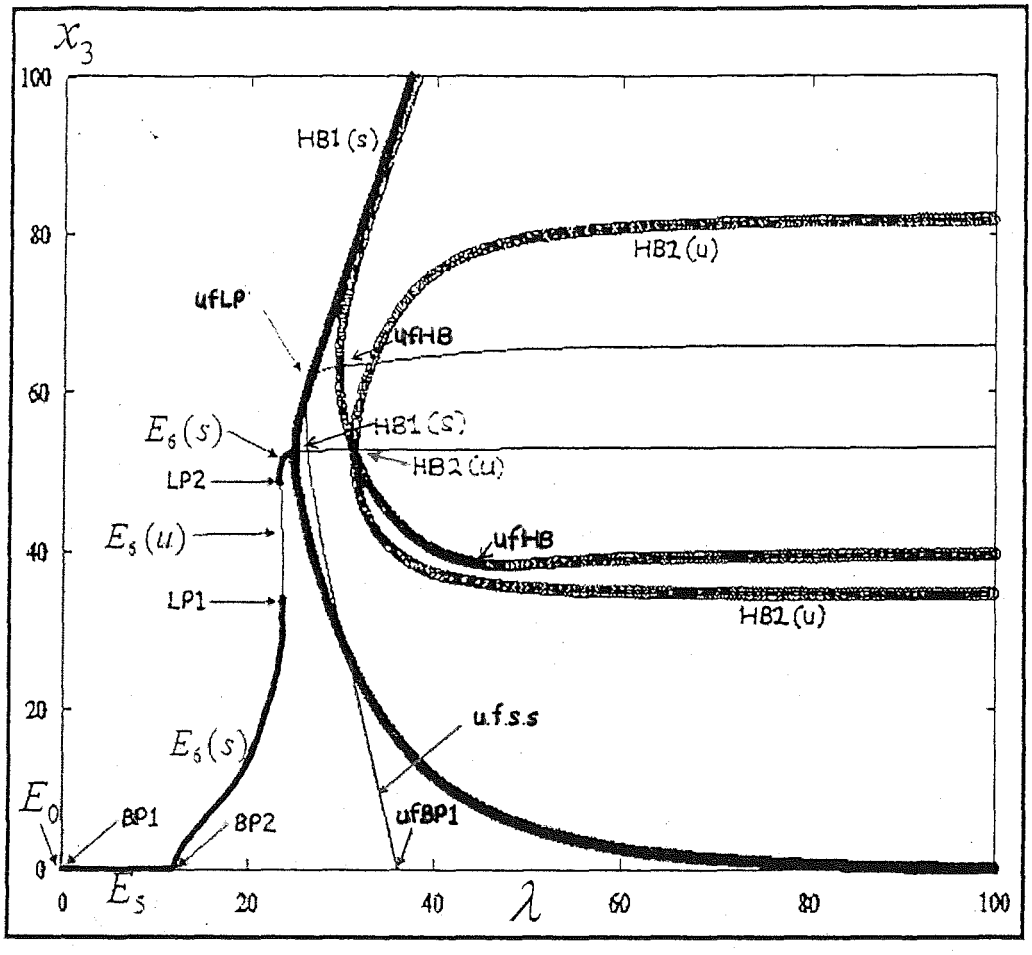

Figure 4.16: The bifurcation diagram x_3 against λ for three compartment model at $\gamma = 0.4$ when $\mu_1 = 1$, $\mu_2 = 1$ and $\mu_3 = 0.5$; and $d_1 = d_2 = d_3 = 0.02$; showing the bifurcation points BP1 (λ=0.1494), BP2 (λ=12.01); Limit point LP1 (λ=23.34) and the Hopf bifurcation points HB1 (λ=24.78 (stable)) and HB2 (λ=31.19 (unstable)). Other unfeasible steady state found is of the form u.f.s.s. = $(x_1, x_2, x_3, x_4, x_1, x_2, x_3, z_1, z_2, -z_3, z_4)$ and thus the unfeasible bifurcation points are ufBP1 (λ=36.13), ufLP (λ=26) and ufHB (λ= 24.49).

Therefore, changing the position of the μ does not affect the position of the bifurcation points, limit points and Hopf bifurcation points involved. In terms of the quality of the bifurcation diagrams **Figures 4.14** is slightly different from that of **Figure 4.15** and **Figure 4.16**. The only difference between **3m05m1m1d002d002d002**, **3m1m05m1d002d002d002**, **3m1m1m05d002d002d002** is that the steady states involved are (E_1 and E_2), (E_3 and E_4) and (E_5 and E_6) respectively.

4.5 Bifurcation analysis assuming a different growth parameter for the phytoplankton μ and a different diffusion parameter d

This section describes the bifurcation diagrams for the three-compartment model with different growth parameters μ and the diffusion parameter d different via the software package **AUTO**. Only one of the growth parameter and one diffusion parameter shall be altered.

Firstly; let us again adopt all the parameters as in **APPENDIX C : TABLES: C1** except for λ (set at a starting point 15) to produce plots of x_3 against λ. For simplicity, one of the values of the growth parameter μ is chosen to be 0.5 and the others two to be 1; and then swap as before for the diffusion parameters, one of the d's is chosen to be 0.04 and the other two to be 0.02; and swap as before.

From the bifurcation diagrams which follow, some of the *feasible* steady state are found to be the following:

$E_0 = (0,\ 0,\ 0,\ \lambda, 0,\ 0,\ 0,\ 0,\ 0,\ 0,\ \lambda)$,

$E_1 = (x_1,\ x_2,\ 0,\ x_4,\ y_1,\ y_2,\ 0,\ y_1,\ y_2,\ 0,\ z_4)$,

$E_2 = (x_1,\ x_2,\ x_3,\ x_4,\ y_1,\ y_2,\ y_3,\ y_1,\ y_2,\ y_3,\ z_4)$,

$E_5 = (x_1,\ x_2,\ 0,\ x_4,\ x_1,\ x_2,\ 0,\ z_1,\ z_2,\ 0,\ z_4)$,

$E_6 = (x_1,\ x_2,\ x_3,\ x_4, x_1,\ x_2,\ x_3,\ z_1,\ z_2,\ z_3,\ z_4)$,

$E_7 = (x_1,\ x_2,\ 0,\ x_4,\ y_1,\ y_2,\ 0,\ z_1,\ z_2,\ 0,\ z_4)$, and

$E_8 = (x_1,\ x_2,\ x_3,\ x_4,\ y_1,\ y_2,\ y_3,\ z_1,\ z_2,\ z_3,\ z_4)$,

and some of the *unfeasible* steady state to be of the following:

$(x_1,\ x_2,\ x_3,\ x_4,\ y_1,\ y_2,\ -y_3,\ z_1,\ z_2,\ -z_3,\ z_4)$,

$(x_1,\ x_2,\ x_3,\ x_4,\ y_1,\ y_2,\ -y_3,\ y_1,\ y_2,\ -y_3,\ z_4)$,

$(x_1,\ x_2,\ x_3,\ x_4,\ y_1,\ y_2,\ -y_3,\ x_1,\ x_2,\ x_3,\ x_4)$,

$(x_1,\ x_2,\ x_3,\ x_4,\ y_1,\ y_2,\ -y_3,\ z_1,\ z_2,\ z_3,\ z_4)$,

$(x_1,\ x_2,\ x_3,\ x_4,\ y_1,\ y_2,\ -y_3,\ z_1,\ z_2,\ z_3,\ z_4)$,

$(x_1,\ x_2,\ x_3,\ x_4,\ x_1,\ x_2,\ x_3,\ z_1,\ z_2,\ -z_3,\ z_4)$, and

$(x_1,\ x_2,\ x_3,\ x_4,\ y_1,\ y_2,\ y_3,\ z_1,\ z_2,\ -z_3,\ z_4)$,

Let us now proceed to discuss details of the bifurcation diagrams for the three-compartment model with the growth parameter μ and the diffusion parameter d different for the value of $\gamma = 0.4$, and in particular observe how the steady state change from one form to another (see **APPENDIX C: TABLES: Table C4c**).

xv) **Figure 4.17** shows the bifurcation diagram of the parameter x_3 against λ with diffusion parameters $d_1 = 0.02$, $d_2 = 0.04$ and $d_3 = 0.02$ and growth parameters $\mu_1 = 0.5$, $\mu_2 = 1$ and $\mu_3 = 1$ (labeled as **3m05m1m1d002d004d002**). There is a bifurcation point (**BP1**) at the point $\lambda = 0.1831$, where the steady state E_0 changes from stable to unstable and the steady state E_1 until the next bifurcation point (**BP2**) is reached at $\lambda = 12.01$. At this point, E_2 becomes stable until it reached the Limit points (**LP1** and **LP2**) at $\lambda = 23.63$ and $\lambda = 23.34$ respectively. The Hopf bifurcation point (**HB1**) occurs at $\lambda = 24.78$.

xvi) **Figure 4.18** shows the bifurcation diagram of the parameter x_3 against λ with diffusion parameters $d_1 = 0.02$, $d_2 = 0.02$ and $d_3 = 0.04$ and growth parameters $\mu_1 = 1$, $\mu_2 = 0.5$ and $\mu_3 = 1$ (denoted as **3m1m05m1d002d002d004**). The bifurcation points featured here is similar to that of **Figure 4.18**, however the steady states involved is different. There is a bifurcation point (**BP1**) at the point $\lambda = 0.1832$, where the steady state E_0 changes from stable to unstable and the steady state E_3 occurs until the next bifurcation point (**BP2**) is reached at $\lambda = 12.01$. At this point, E_4 becomes stable until the limit points (**LP1** and **LP2**) is reached at $\lambda = 23.63$ and $\lambda = 23.34$ respectively. The Hopf bifurcation point (**HB1**) occurs at $\lambda = 24.78$.

xvii) **Figure 4.19** shows the bifurcation diagram of the parameter x_3 against λ with diffusion parameters $d_1 = 0.04$, $d_2 = 0.02$ and $d_3 = 0.02$ and growth parameters $\mu_1 = 1$, $\mu_2 = 1$ and $\mu_3 = 0.5$ (denoted as **3m1m1m05d004d002d002**). There is a bifurcation point (**BP1**) at the point $\lambda = 0.1832$, where the steady state E_0 changes from stable to unstable and the steady state E_5 occurs until the next bifurcation point (**BP2**) is reached at $\lambda = 12.01$. At this point, E_6 becomes stable until the limit points (**LP1** and **LP2**) is reached at $\lambda = 23.63$ and $\lambda = 23.34$ respectively. The Hopf bifurcation point (**HB1**) is reached at $\lambda = 24.78$.

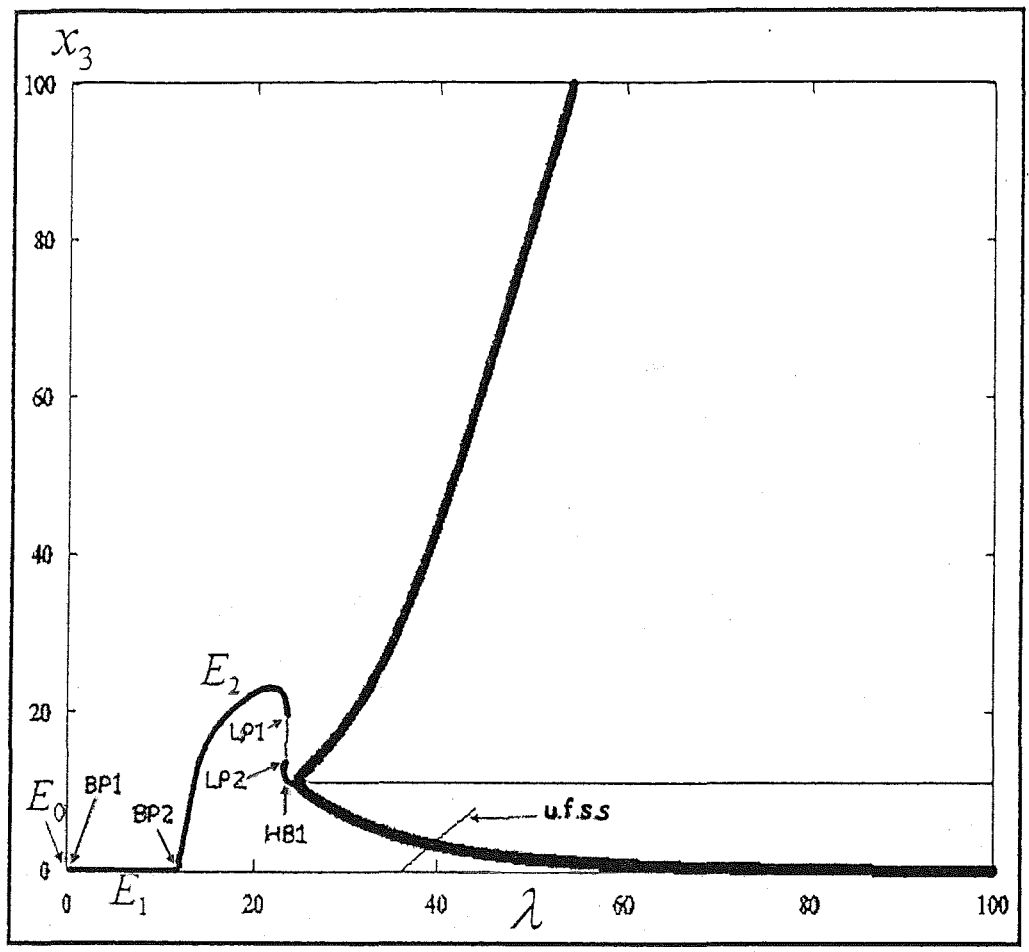

Figure 4.17: The bifurcation diagram x_3 against λ for three compartment model at $\gamma = 0.4$ when $\mu_1 = 0.5$, $\mu_2 = 1$ and $\mu_3 = 1$; $d_1 = 0.02$, $d_2 = 0.04$ and $d_3 = 0.02$; showing the bifurcation points BP1 (λ=0.1831), BP2 (λ=12.01); Limit point LP1 (λ=23.63), LP2 (λ= 23.34) and the Hopf bifurcation points HB1 (λ=24.78 (stable)). Other unfeasible steady state found is of the form u.f.s.s. = $(x_1, x_2, x_3, x_4, y_1, y_2, -y_3, y_1, -y_2, -y_3, z_4)$.

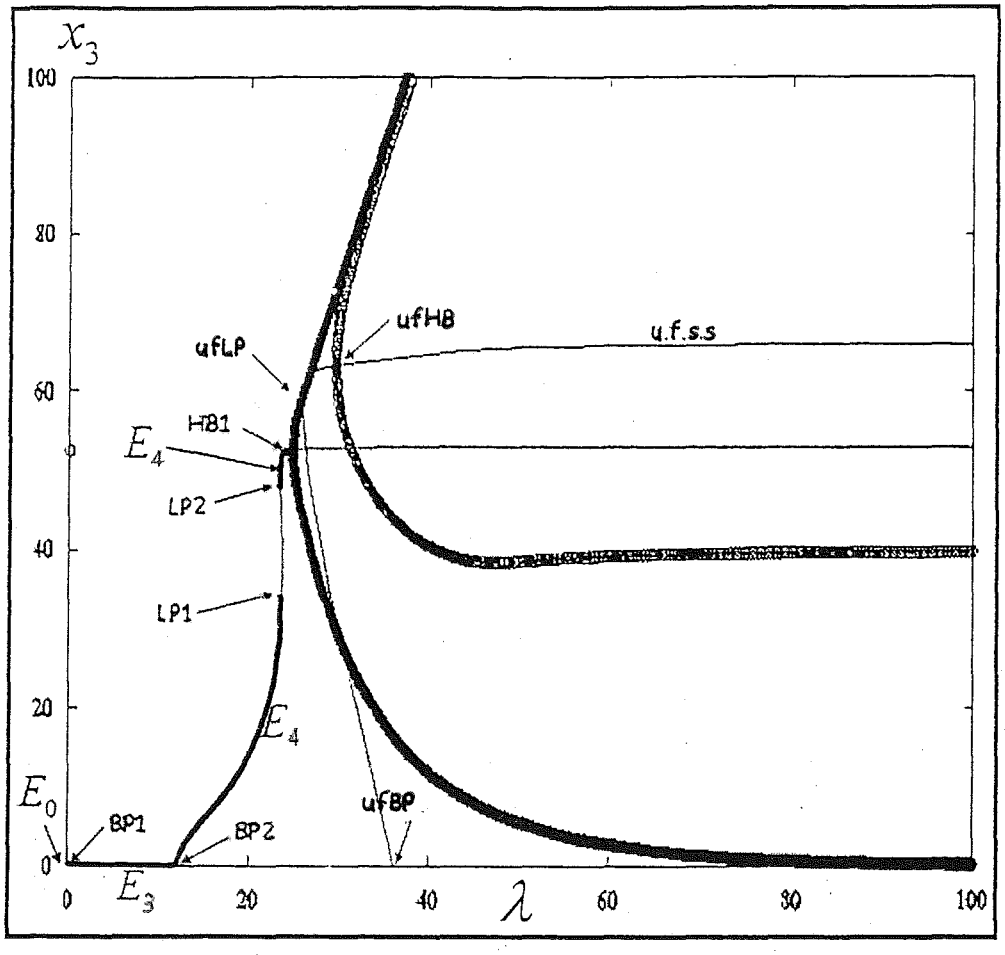

Figure 4.18: The bifurcation diagram x_3 against λ for three compartment model at $\gamma = 0.4$ when $\mu_1 = 1$, $\mu_2 = 0.5$ and $\mu_3 = 1$; $d_1 = 0.02$, $d_2 = 0.02$ and $d_3 = 0.04$; showing the bifurcation points BP1 (λ=0.1831), BP2 (λ=12.01); Limit point LP1 (λ=23.63), LP2 (λ= 23.34) and the Hopf bifurcation points HB1 (λ=24.78 (stable)). Other unfeasible steady state found is of the form u.f.s.s. = $(x_1, x_2, x_3, x_4, y_1, y_2, -y_3, x_1, x_2, x_3, x_4)$ and thus the unfeasible bifurcation points are ufBP (λ=36.13), ufLP (λ=26) and ufHB (λ= 24.49).

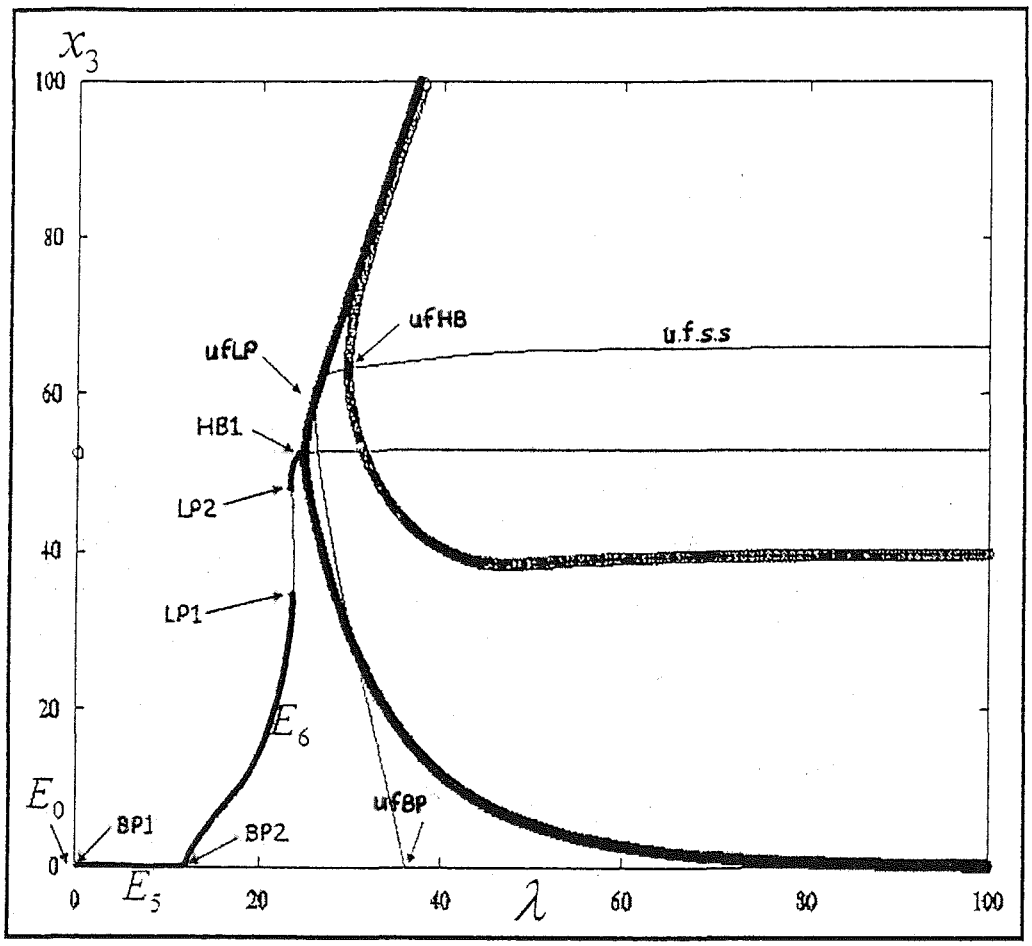

Figure 4.19: The bifurcation diagram x_3 against λ for three compartment model at $\gamma = 0.4$ when $\mu_1 = 1$, $\mu_2 = 1$ and $\mu_3 = 0.5$; $d_1 = 0.04$, $d_2 = 0.02$ and $d_3 = 0.02$; showing the bifurcation points BP1 (λ=0.1831), BP2 (λ=12.01); Limit point LP1 (λ=23.63), LP2 (λ= 23.34) and the Hopf bifurcation points HB1 (λ=24.78 (stable)). Other unfeasible steady state found is of the form u.f.s.s. = $(x_1, x_2, x_3, x_4, x_1, x_2, x_3, z_1, z_2, -z_3, z_4)$ and thus the unfeasible bifurcation points are ufBP (λ=36.13), ufLP (λ=26) and ufHB (λ= 24.49).

Note: In terms of bifurcation points, 3m05m1m1d002d004d002 (Figure 4.17), 3m1m05m1d002d002d004 (Figure 4.18) and 3m1m1m05d004d002d002) (Figure

4.19), there are all found to be identical. The only difference is that the steady states involved for the respective diagrams are E_1 and E_2, E_3 and E_4 and E_5 and E_6.

xviii) **Figure 4.20** shows the bifurcation diagram of the parameter x_3 against λ with diffusion parameters $d_1 = 0.04$, $d_2 = 0.02$ and $d_3 = 0.02$ and growth parameters $\mu_1 = 0.5$, $\mu_2 = 1$ and $\mu_3 = 1$ (denoted as **3m05m1m1d004d002d002**) and diffusion parameters $d_1 = 0.02$, $d_2 = 0.02$ and $d_3 = 0.04$ and growth parameters $\mu_1 = 0.5$, $\mu_2 = 1$ and $\mu_3 = 1$ (denoted as **3m05m1m1d002d002d004**); **Figure 4.21** shows the bifurcation diagram of the parameter x_3 against λ with diffusion parameters $d_1 = 0.02$, $d_2 = 0.04$ and $d_3 = 0.02$ and growth parameters $\mu_1 = 1$, $\mu_2 = 0.5$ and $\mu_3 = 1$ (denoted as **3m1m05m1d002d004d002**); **Figure 4.22** shows the bifurcation diagram of the parameter x_3 against λ with diffusion parameters $d_1 = 0.04$, $d_2 = 0.02$ and $d_3 = 0.02$ and growth parameters $\mu_1 = 1$, $\mu_2 = 0.5$ and $\mu_3 = 1$ (denoted as **3m1m05m1d004d002d002**); **Figure 4.23** shows the bifurcation diagram of the parameter x_3 against λ with diffusion parameters $d_1 = 0.02$, $d_2 = 0.04$ and $d_3 = 0.02$ and growth parameters $\mu_1 = 1$, $\mu_2 = 1$ and $\mu_3 = 0.5$ (denoted as **3m1m1m05d002d004d002**) and **Figure 4.24** shows the bifurcation diagram of the parameter x_3 against λ with diffusion parameters $d_1 = 0.02$, $d_2 = 0.02$ and $d_3 = 0.04$ and growth parameters $\mu_1 = 1$, $\mu_2 = 1$ and $\mu_3 = 0.5$ (denoted as **3m1m1m05d002d002d004**). All those figures

mentioned shared a common bifurcation points i.e. there is a bifurcation point (**BP1**) at $\lambda = 0.186$, where the steady state E_0 changes from stable to unstable and the steady state E_7 occurs until the next bifurcation point (**BP2**) is reached at $\lambda = 13.1$. At this point, E_8 becomes stable until the Hopf bifurcation point (**HB1**) is reached at $\lambda = 24.93$. Limit points (**LP1** and **LP2**) are also featured, both at $\lambda = 23.43$. Another Hopf bifurcation point occur at $\lambda = 37.76$ which produces an unstable periodic orbits.

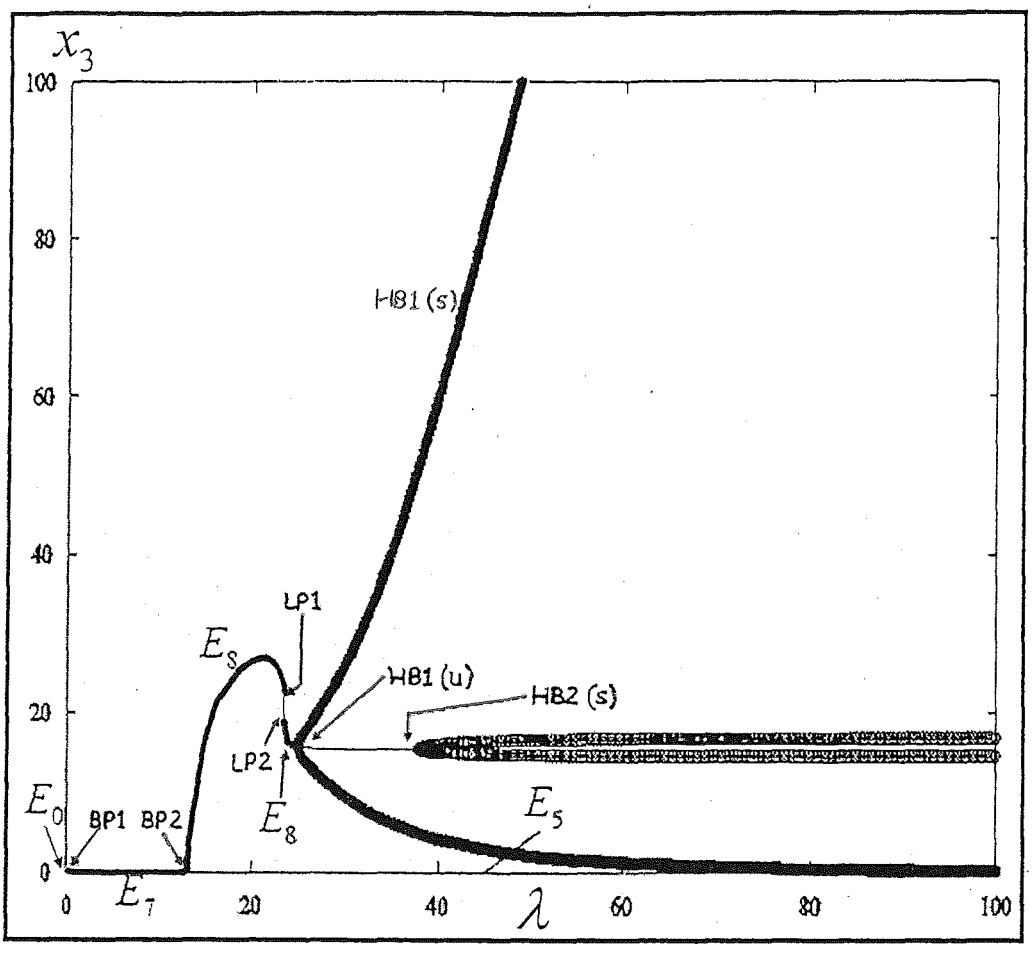

Figure 4.20: The bifurcation diagram x_3 against λ for three compartment model at $\gamma = 0.4$ when $\mu_1 = 0.5$, $\mu_2 = 1$ and $\mu_3 = 1$; $d_1 = 0.04$, $d_2 = 0.02$ and $d_3 = 0.02$ (denoted as 3m05m1m1d004d002d002) and $\mu_1 = 0.5$, $\mu_2 = 1$ and $\mu_3 = 1$; $d_1 = 0.02$, $d_2 = 0.02$ and $d_3 = 0.04$ (denoted as 3m05m1m1d002d002d004); showing the bifurcation points BP1 (λ=0.186), BP2 (λ=13.1); Limit point LP1 (λ=23.43) and LP 2 (λ=23.43) and the Hopf bifurcation points HB1 (λ=24.93 (stable)) and HB2 (λ=37.76 (unstable)). Other unfeasible steady state found is of the form u.f.s.s. = $(x_1, x_2, x_3, x_4, y_1, y_2, -y_3, z_1, z_2, -z_3, z_4)$ and thus the unfeasible bifurcation points are ufBP1 (λ=44.97).

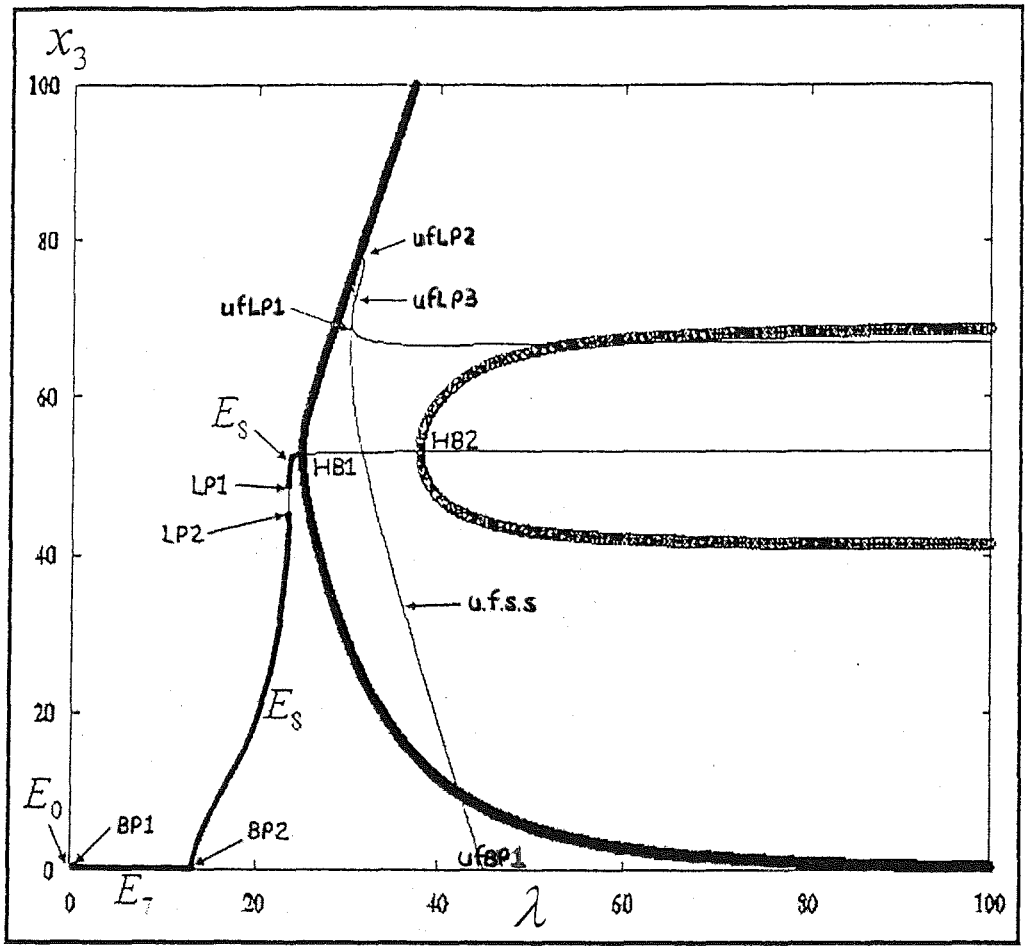

Figure 4.21: The bifurcation diagram x_3 against λ for three compartment model at $\gamma = 0.4$ when $\mu_1 = 1$, $\mu_2 = 0.5$ and $\mu_3 = 1$; $d_1 = 0.02$, $d_2 = 0.04$ and $d_3 = 0.02$ (denoted as 3m1m05m1d002d004d002); showing the bifurcation points BP1 (λ=0.186), BP2 (λ=13.1); Limit point LP1 (λ=23.43) and LP 2 (λ=23.43) and the Hopf bifurcation points HB1 (λ=24.93 (stable)) and HB2 (λ=37.76 (unstable)). Other unfeasible steady state found is of the form u.f.s.s. = $(x_1, x_2, x_3, x_4, y_1, y_2, -y_3, z_1, z_2, -z_3, z_4)$ and thus the unfeasible bifurcation points are ufBP1 (λ=44.97), ufLP1 (λ=30.17), ufLP2 (λ=31.55) and ufLP3 (λ=30.25).

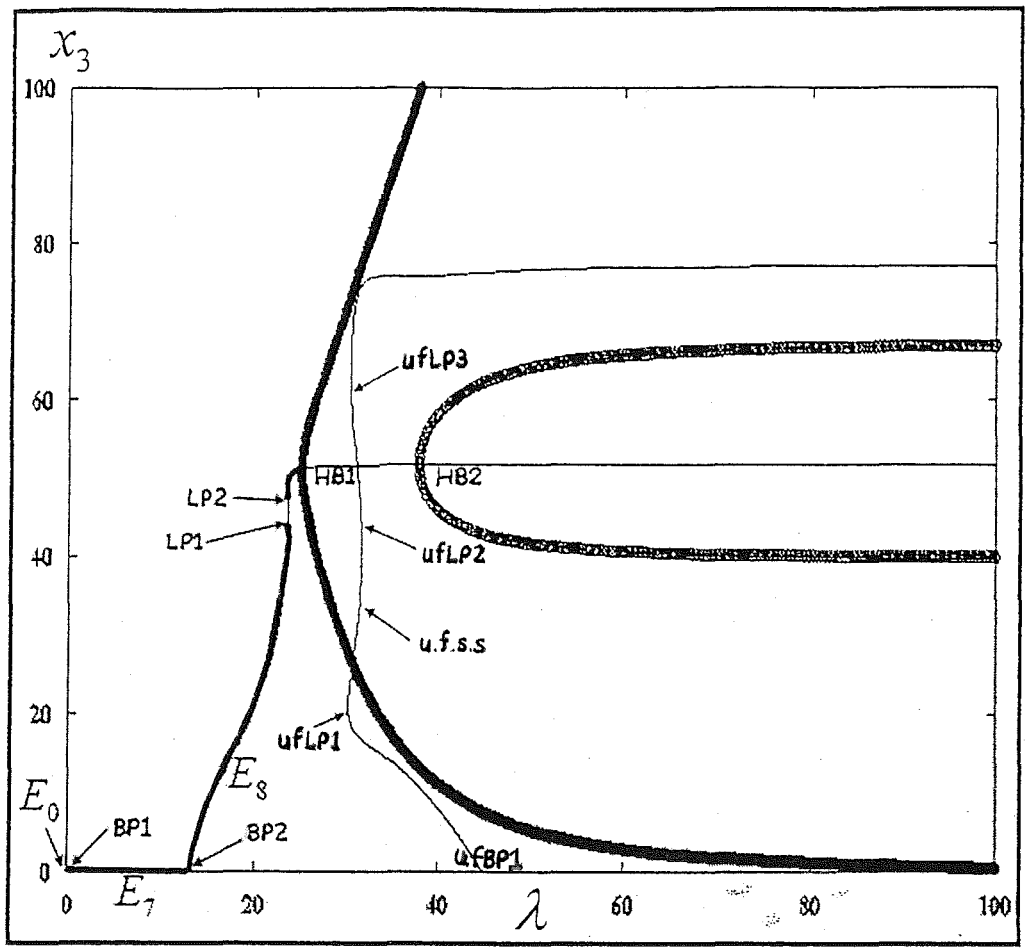

Figure 4.22: The bifurcation diagram x_3 against λ for three compartment model at $\gamma = 0.4$ when $\mu_1 = 1$, $\mu_2 = 0.5$ and $\mu_3 = 1$; $d_1 = 0.04$, $d_2 = 0.02$ and $d_3 = 0.02$ (denoted as 3m1m05m1d004d002d002); showing the bifurcation points BP1 (λ=0.186), BP2 (λ=13.1); Limit point LP1 (λ=23.43) and LP 2 (λ=23.43) and the Hopf bifurcation points HB1 (λ=24.93 (stable)) and HB2 (λ=37.76 (unstable)). Other unfeasible steady state found is of the form u.f.s.s. = $(x_1, x_2, x_3, x_4, y_1, y_2, -y_3, z_1, z_2, -z_3, z_4)$ and thus the unfeasible bifurcation points are ufBP1 (λ=44.97), ufLP1 (λ=30.17), ufLP2 (λ=31.55) and ufLP3 (λ=30.25).

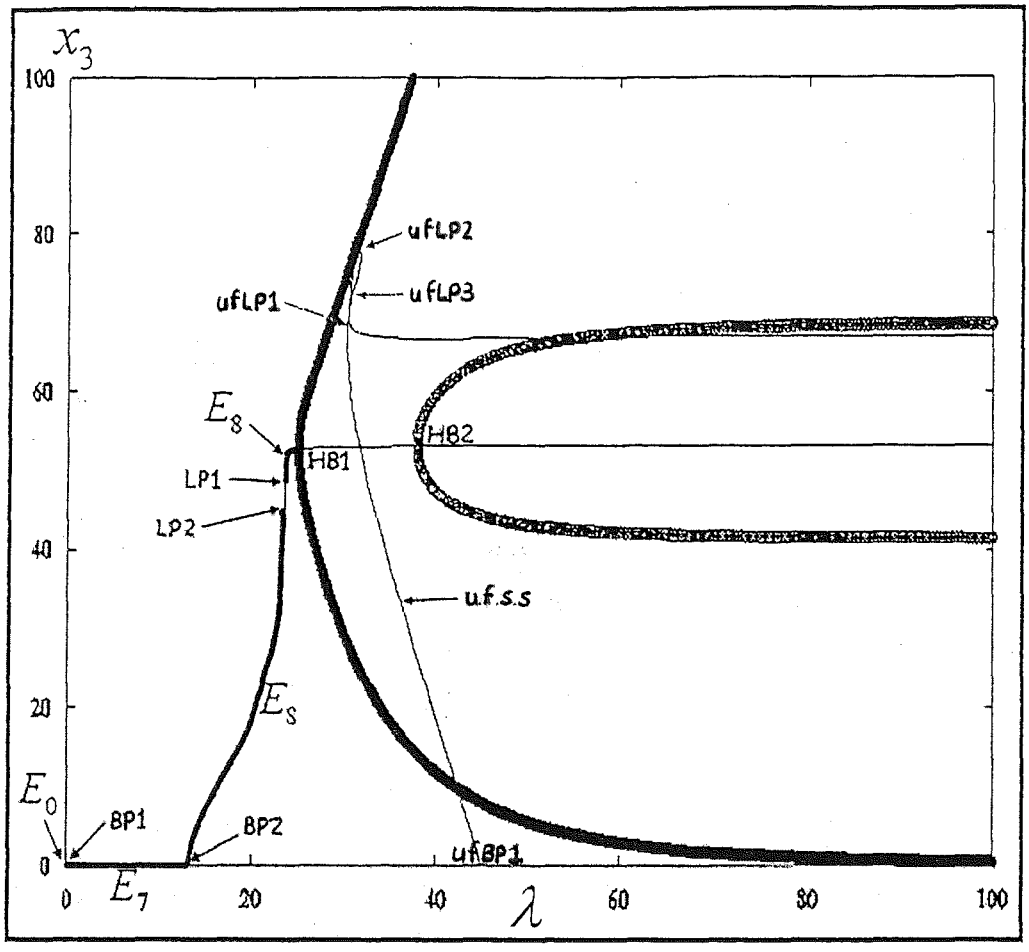

Figure 4.23: The bifurcation diagram x_3 against λ for three compartment model at $\gamma = 0.4$ when $\mu_1 = 1$, $\mu_2 = 1$ and $\mu_3 = 0.5$; $d_1 = 0.02$, $d_2 = 0.04$ and $d_3 = 0.02$ (denoted as 3m1m1m05d002d004d002); showing the bifurcation points BP1 (λ=0.186), BP2 (λ=13.1); Limit point LP1 (λ=23.43) and LP 2 (λ=23.43) and the Hopf bifurcation points HB1 (λ=24.93 (stable)) and HB2 (λ=37.76 (unstable)). Other unfeasible steady state found is of the form u.f.s.s. = $(x_1, x_2, x_3, x_4, y_1, y_2, -y_3, z_1, z_2, -z_3, z_4)$ and thus the unfeasible bifurcation points are ufBP1 (λ=44.97), ufLP1 (λ=30.17), ufLP2 (λ=31.55) and ufLP3 (λ=30.25).

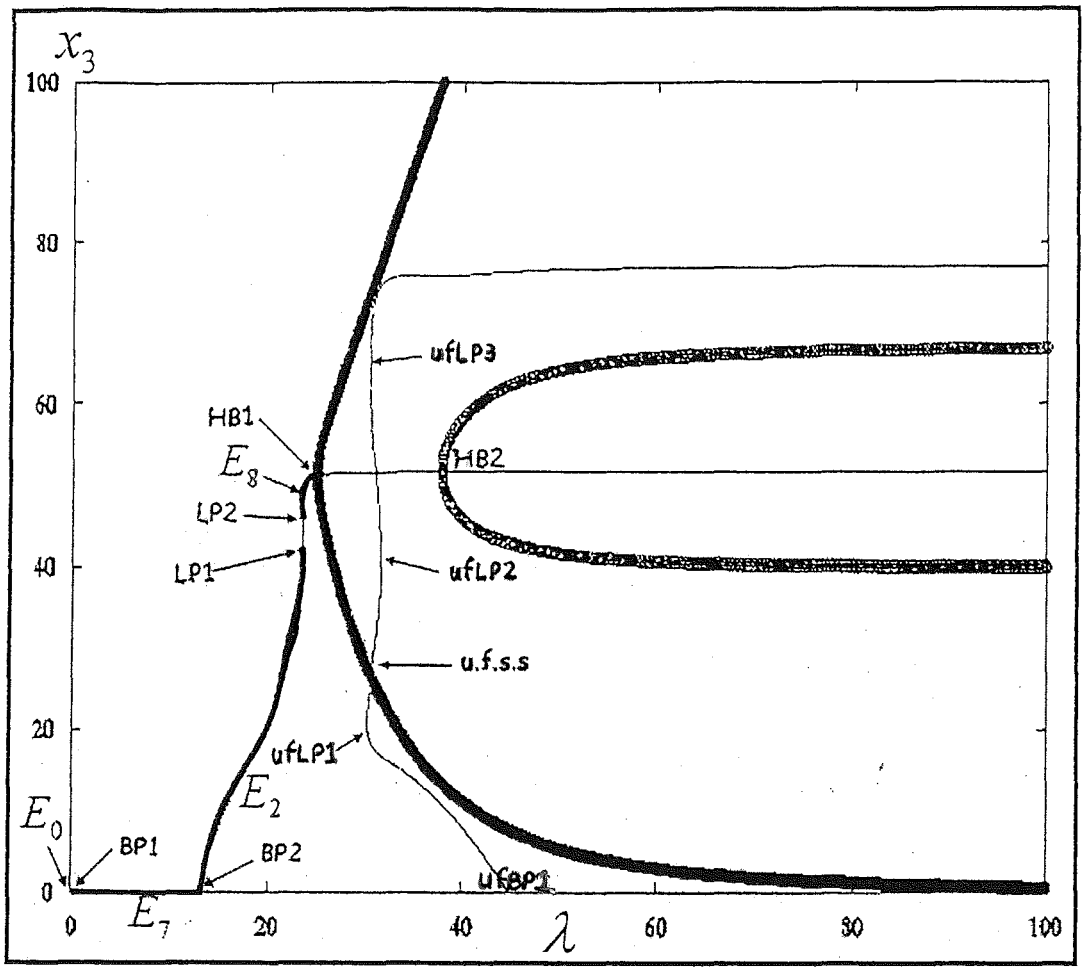

Figure 4.24: The bifurcation diagram x_3 against λ for three compartment model at $\gamma = 0.4$ when $\mu_1 = 1$, $\mu_2 = 1$ and $\mu_3 = 0.5$; $d_1 = 0.02$, $d_2 = 0.02$ and $d_3 = 0.04$ (denoted as 3m1m1m05d002d002d004); showing the bifurcation points BP1 (λ=0.186), BP2 (λ=13.1); Limit point LP1 (λ=23.43) and LP 2 (λ=23.43) and the Hopf bifurcation points HB1 (λ=24.93 (stable)) and HB2 (λ=37.76 (unstable)). Other unfeasible steady state found is of the form u.f.s.s. = $(x_1, x_2, x_3, x_4, y_1, y_2, -y_3, z_1, z_2, -z_3, z_4)$ and thus the unfeasible bifurcation points are ufBP1 (λ=44.97), ufLP1 (λ=30.17), ufLP2 (λ=31.55) and ufLP3 (λ=30.25).

For the three-compartment model when the growth parameter μ's and the diffusion parameter d's are different, the bifurcation diagrams produced a pattern with one μ is 0.5 and the other two 1; and one of the d's 0.04 and the other 0.02; as follow in the pattern below:

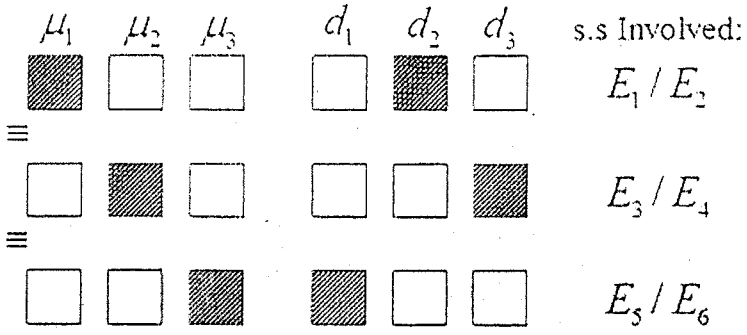

i.e. $\mu_1 = 0.5$, $\mu_2 = 1$, $\mu_3 = 1$, $d_1 = 0.02$, $d_2 = 0.04$ and $d_3 = 0.02$ (**m05m1m1d002d004d002**) is equivalent to $\mu_1 = 1$, $\mu_2 = 0.5$ and $\mu_3 = 1$; $d_1 = 0.02$, $d_2 = 0.02$ and $d_3 = 0.04$ (**m1m05m1d002d002d004**) and is equivalent to $\mu_1 = 1$, $\mu_2 = 1$ and $\mu_3 = 0.5$; $d_1 = 0.04$, $d_2 = 0.02$ and $d_3 = 0.02$ (**m1m1m05d004d002d002**). These have equivalent in terms of bifurcation diagrams it produces and Bifurcation points, limit points and periodic points (see **APPENDIX C: TABLES: C4c**). However, it involves the steady states E_1 and E_2; E_3 and E_4 and E_5 and E_6 respectively.

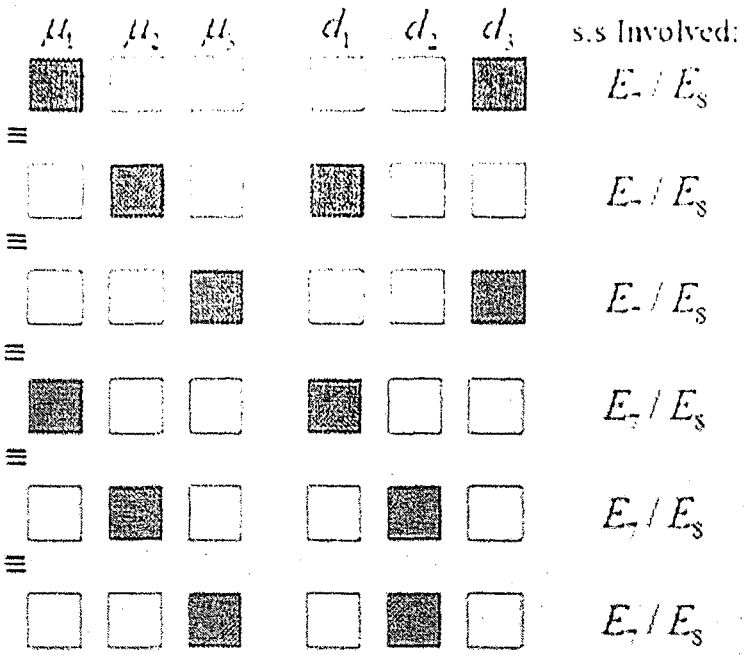

And that $\mu_1 = 0.5$, $\mu_2 = 1$, $\mu_3 = 1$, $d_1 = 0.02$, $d_2 = 0.02$ and $d_3 = 0.04$ (**m05m1m1d002d002d004**) is equivalent to $\mu_1 = 1$, $\mu_2 = 0.5$ and $\mu_3 = 1$; $d_1 = 0.04$, $d_2 = 0.02$ and $d_3 = 0.02$ (**m1m05m1d004d002d002**) is equivalent to $\mu_1 = 1$, $\mu_2 = 1$ and $\mu_3 = 0.5$; $d_1 = 0.02$, $d_2 = 0.02$ and $d_3 = 0.04$ (**m1m1m05d002d002d004**) is equivalent to $\mu_1 = 0.5$, $\mu_2 = 1$, $\mu_3 = 1$, $d_1 = 0.04$, $d_2 = 0.02$ and $d_3 = 0.02$ (**m05m1m1d004d002d002**) is equivalent to $\mu_1 = 1$, $\mu_2 = 0.5$ and $\mu_3 = 1$; $d_1 = 0.02$, $d_2 = 0.04$ and $d_3 = 0.02$ (**m1m05m1d002d004d002**) and is equivalent to $\mu_1 = 1$, $\mu_2 = 1$ and $\mu_3 = 0.5$; $d_1 = 0.02$, $d_2 = 0.04$ and $d_3 = 0.02$ (**m1m1m05d002d004d002**). These have equivalent in terms of bifurcation diagrams it produces and Bifurcation points, limit points and periodic points (see **APPENDIX C: TABLES: C4c**). However, it involves the steady states E_1 and E_2; E_3 and E_4 and E_5 and E_6 respectively. These have equivalent in terms of bifurcation diagrams it

produces and Bifurcation points, limit points and periodic points (see **APPENDIX C: TABLES: C4c**). There all involve the steady states E_7 and E_8.

4.6 Conclusions

In conclusion, the three compartments model has the following properties:

i) With the growth parameters $\mu_1 = \mu_2 = \mu_3 = 1$, and one of the diffusion parameter $d \geq 0.02$ and the other two to be $d = 0.02$, it resembles the one-compartment model;

ii) With the growth parameters $\mu_1 = \mu_2 = \mu_3 = 1$ and one of the diffusion parameter $d < 0.02$ and the other two to be $d = 0.02$, it resembles the two compartment with the growth parameters equal growth parameter ($\mu = 1$).

(**Note**: Swapping the $d's$ between compartments does not affects the quality of the bifurcation diagrams)

iii) With different growth parameters μ and equal diffusion parameters ($d_1 = d_2 = d_3 = 0.02$), there is slightly different result-viz the value of the bifurcation point, limit points and the Hopf bifurcation points are different from the one- and two-compartment model, and there are additional limit points and Hopf bifurcation points. However, swapping the growth parameters around does not change the results (c.f. **APPENDIX C: TABLES: C4b**).

iv) With both the growth parameters μ and the diffusion parameters $d's$ different, there are two sets of results with similar bifurcation points, limit points and the Hopf points i.e. **m05m1m1d002d004d002** ≡ **m1m05m1d002d002d004** ≡ **m1m1m05d004d002d002** have equivalent patterns and feature the steady states E_1 and

E_2; E_3 and E_4 and E_5 and E_6 respectively; whereas **m05m1m1d002d002d004** ≡ **m1m05m1d004d002d002** ≡ **m1m1m05d002d002d004** ≡ **m05m1m1d004d002d002** ≡ **m1m05m1d002d004d002** ≡ **m1m1m05d002d004d002** have equivalent pattern and all feature the steady states E_7 and E_8.

Chapter 5

Conclusions

Chapter 5: Conclusions

In this chapter, various conclusions concerning the multi-compartment phytoplankton-zooplankton-nutrient model can be drawn. Thus, whether adding more compartments or adding complexity to the model changes the behaviour of the solutions or produces additional interesting phenomena can be answered.

For the **one-compartment model**, there are three steady states-viz. $E_0 = (0, 0, 0)$, the steady state where neither the phytoplankton nor the zooplankton survive; $E_1 = (x_1, x_2, 0)$, the steady state in where the only surviving species is the phytoplankton; and $E_2 = (x_1, x_2, x_3)$, the most important steady state where both the phytoplankton and zooplankton species survive. In addition, a periodic branch (or limit cycle) is also present, for which the phytoplankton and zooplankton alternately dominate. The most important steady state is E_2, noticeable at the range of $10 < \lambda < 40$ and $\gamma < 0.8$ (λ being the integration constant coming from the conservation of nutrient $mgNday^{-1}$ and that the realistic values for that is $\lambda > 0\ mgNday^{-1}$ and since the realistic growth rate of phytoplankton is taken to be $1\ day^{-1}$, thus the death parameter of phytoplankton is reasonably estimated to be $\gamma < 1\ day^{-1}$) for any happenings to be observed). The coexistence between the two steady states E_1 and E_2 is only evident when the death rate of the phytoplankton is fairly low ($\gamma < 0.45$) and covers a small region, so there is only a small "window of opportunity" for the populations to coexist. Coexistence of the steady state E_1 and periodic solutions or limit cycles then occurs

following the coexistence between the two steady states just mentioned, and covers a larger region ($\gamma < 0.45$). The edges of these regions are points where gross changes in outcomes are likely to occur. Limit cycles or the periodic solutions in reality are natural as long as populations remain feasible (positive biomass) for survival in practice. However, many populations cannot sustain oscillations of large amplitude.

The **two-compartment model with equal growth parameter** in both compartments (i.e. $\mu_1 = \mu_2$) resembles the one-compartment model. There are again three steady states –viz. $E_0 = (0,\ 0,\ 0, 0, 0, 0, \lambda)$, the steady state where neither the phytoplankton nor the zooplankton survive; $E_1 = (x_1,\ x_2,\ 0,\ x_1,\ x_2,\ 0,\ \lambda - x_2)$, the steady state in where phytoplankton is the only species that survives; and $E_2 = (x_1,\ x_2,\ x_3,\ x_1,\ x_2,\ x_3,\ y_4)$, the most important steady state where both the phytoplankton and zooplankton species survive. Similarly, these are periodic or limit cycle which define the phytoplankton and zooplankton alternately dominant. In addition, there is unstable periodic solution (unattainable solution) which did not give any edge for a basin of stability. Otherwise, in comparison with the one-compartment model there is no additional feature found, although the region in which the steady state E_1 and the stable limit cycle coexists now covers a smaller region, dominated by the presence of the unstable limit cycle. Changing the diffusion parameter d_1 does not alter any existence behaviour but merely shifts the position of the unstable periodic solutions to the right when it is large, and towards the stable periodic solution, until eventually merges with it and disappears, when it is small (i.e. approaching the one-compartment model).

The **two-compartment model with different growth parameters in each compartment** ($\mu_1 \neq \mu_2$) also has three *feasible* steady states- viz. $E_0 = (0, 0, 0, 0, 0, 0, \lambda)$, $E_1 = (x_1, x_2, 0, y_1, y_2, 0, y_4)$, $E_2 = (x_1, x_2, x_3, y_1, y_2, y_3, y_4)$ and a lot of unfeasible steady state solutions to be ignored. The three steady states resemble the one- and two-compartment (equal growth parameter) models but there are different features for various choices of μ_1 and μ_2. An unstable Hopf bifurcation point appears when the difference between μ_1 and μ_2 is small, and there are 2-fold or limit points observed when $\mu_1 < 0.7$ and $\mu_2 = 1$ (c.f. **Figure 3.35** to **Figure 3.40**).

The **three compartment model with equal growth parameter** ($\mu_1 = \mu_2 = \mu_3 = 1$) also has three *feasible* steady states- viz. $E_0 = (0, 0, 0, \lambda, 0, 0, 0, 0, 0, 0, \lambda)$, $E_1 = (x_1, x_2, 0, \lambda - x_2, x_1, x_2, 0, x_1, x_2, \lambda - x_2)$ and $E_2 = (x_1, x_2, x_3, x_4, x_1, x_2, x_3, x_1, x_2, x_3, x_4)$. When one of the diffusion parameter is $d \geq 0.02$ and the others are kept fixed at 0.02, this model resembles the one-compartment model (c.f. **APPENDIX C: TABLES: C2a, C3a** and **C4a**), and when one of the diffusion parameter is $d < 0.02$ and the others are kept fixed at 0.02 it resembles the two-compartment model with equal growth parameters. (**Note**: Swapping the values of the diffusion parameter between compartments does not affect the quality of the bifurcation diagrams).

The **three-compartment model with different growth parameter** produces the following results:

i) The model with different growth parameters μ (with only one altered) and equal diffusion parameters $(d_1 = d_2 = d_3 = 0.02)$ has the steady states $E_0 = (0,\ 0,\ 0,\ 3\lambda,\ 0,\ 0,\ 0,\ 0,\ 0,\ 0,\ 3\lambda)$, $E_1 = (x_1,\ x_2,\ 0,\ x_4,\ y_1,\ y_2,\ 0,\ y_1,\ y_2,\ 0,\ z_4)$, $E_2 = (x_1,\ x_2,\ x_3,\ x_4,\ y_1,\ y_2,\ y_3,\ y_1,\ y_2,\ y_3,\ z_4)$, $E_3 = (x_1,\ x_2,\ 0,\ x_4,\ y_1,\ y_2,\ 0,\ x_1,\ x_2,\ 0,\ x_4)$ $E_4 = (x_1,\ x_2,\ x_3,\ x_4, y_1,\ y_2,\ y_3,\ x_1,\ x_2,\ x_3,\ x_4)$, $E_5 = (x_1,\ x_2,\ 0,\ x_4,\ x_1,\ x_2,\ 0,\ z_1,\ z_2,\ 0,\ z_4)$ $E_6 = (x_1,\ x_2,\ x_3,\ x_4, x_1,\ x_2,\ x_3,\ z_1,\ z_2,\ z_3,\ z_4)$. The value of the bifurcation point, limit points and the Hopf bifurcation points differ from those in one- and two-compartment models, and there is one additional limit point and also unstable Hopf bifurcation points. Swapping the growth parameter values between the compartments does not change the results (c.f. **APPENDIX C: TABLES: C4b**).

ii) The model where the growth parameters μ and the diffusion parameters $d's$ are all different produces two sets of results with similar bifurcation points, limit points and Hopf points i.e. **m05m1m1d002d004d002** ≡ **m1m05m1d002d002d004** ≡ **m1m1m05d004d002d002** have equivalent patterns and feature the steady states E_1 and E_2; E_3 and E_4 and E_5 and E_6 respectively; whereas **m05m1m1d002d002d004** ≡ **m1m05m1d004d002d002** ≡ **m1m1m05d002d002d004** ≡ **m05m1m1d004d002d002** ≡ **m1m05m1d002d004d002** ≡ **m1m1m05d002d004d002** have equivalent patterns and all exhibit additional steady states E_7 and E_8 i.e. the steady states then are $E_0 = (0,\ 0,\ 0,\ \lambda,\ 0,\ 0,\ 0,\ 0,\ 0,\ 0,\ \lambda)$, $E_1 = (x_1,\ x_2,\ 0,\ x_4,\ y_1,\ y_2,\ 0,\ y_1,\ y_2,\ 0,\ z_4)$, $E_2 = (x_1,\ x_2,\ x_3,\ x_4,\ y_1,\ y_2,\ y_3,\ y_1,\ y_2,\ y_3,\ z_4)$, $E_5 = (x_1,\ x_2,\ 0,\ x_4,\ x_1,\ x_2,\ 0,\ z_1,\ z_2,\ 0,\ z_4)$,

$E_6 = (x_1, x_2, x_3, x_4, x_1, x_2, x_3, z_1, z_2, z_3, z_4)$, $E_7 = (x_1, x_2, 0, x_4, y_1, y_2, 0, z_1, z_2, 0, z_4)$, and $E_8 = (x_1, x_2, x_3, x_4, y_1, y_2, y_3, z_1, z_2, z_3, z_4)$.

In conclusion, as the numbers of compartments increases, for identical growth parameter there are no significant changes in the stability of the solutions. The quality of the bifurcation diagrams does not have much difference to the trial model (one-compartment), besides the additional unfeasible steady state branches present. Varying the diffusion parameters seems important, for that only serves to shift the position of the unstable Hopf bifurcation branch. Models with different growth and diffusion parameters do show some changes of behaviour- viz. there is another limit point and unstable Hopf bifurcation branch, and additional but unimportant unfeasible steady states and Hopf bifurcation branches.

APPENDIX A

LINEAR ALGEBRA

A1 Higher Order Determinants

Definition: Minors and Cofactors

Let $A=\left[a_{ij}\right]$ be an n x n matrix. The ijth **minor** of A (also called the **minor** of a_{ij}) is the determinant M_{ij} of the $(n\text{-}1)$ x $(n\text{-}1)$ submatrix that remains after deleting the ith row and the jth column of A. The ijth **cofactor** A_{ij} of A (or the **cofactor** of a_{ij}) is defined to be

$$A_{ij}=(-1)^{i+j}M_{ij} \tag{1}$$

Example [1]: The **minor** of a_{12} in a 3 x 3 matrix

$$M_{12}=\begin{vmatrix} a_{11} & a_{12} & a_{13} \\ a_{21} & a_{22} & a_{23} \\ a_{31} & a_{32} & a_{33} \end{vmatrix}=\begin{vmatrix} a_{21} & a_{23} \\ a_{31} & a_{33} \end{vmatrix}$$

and the **minor** of a_{32} in a 4 x 4 matrix is

$$M_{32}=\begin{vmatrix} a_{11} & a_{12} & a_{13} & a_{14} \\ a_{21} & a_{22} & a_{23} & a_{24} \\ a_{31} & a_{32} & a_{33} & a_{34} \\ a_{41} & a_{42} & a_{43} & a_{44} \end{vmatrix}=\begin{vmatrix} a_{11} & a_{13} & a_{14} \\ a_{21} & a_{23} & a_{24} \\ a_{41} & a_{43} & a_{44} \end{vmatrix}$$

According to equation (1), the cofactor A_{ij} is obtained by attaching the sign $(-1)^{i+j}$ to the **minor** M_{ij}. This sign is most remember as is represented in the following checkerboard arrays:

$$\begin{vmatrix} + & - & + \\ - & + & - \\ + & - & + \end{vmatrix} \quad \text{and} \quad \begin{vmatrix} + & - & + & - \\ - & + & - & + \\ + & - & + & - \\ - & + & - & + \end{vmatrix}$$

A2 Properties of an n x n matrix

PROPERTY 1: If the n x n matrix B is obtained from A by multiplying a single row (or column) of A by the constant k, then det B= k det A.

PROPERTY 2: If the n x n matrix B is obtained from A by interchanging two rows (or two columns), then det B= - det A.

PROPERTY 3: If two rows (or two columns) of the n x n matrix A are identical, then det A=0.

PROPERTY 4: Suppose that the n x n matrices A_1, A_2 and B are identical except for their ith rows- that is, the other n-1 rows of the three matrices are identical- and the ith row of B is the sum of the ith row of B is the sum of the ith rows of A_1 and A_2. Then

$$\det B = \det A_1 + \det A_2 .$$

This holds if columns are involved instead of rows.

PROPERTY 5: If the n x n matrix B is obtained by adding a constant multiple of one row (or column) of A to another row (or column) of A, then det B = det A.

A3 Elementary row operations

The following are the types of **elementary row operations** on the matrix A:

1. Multiply any (single) row of A by a nonzero constant

2. Interchange two rows of A

3. Add a constant multiple of one row of A to another row.

Notation for elementary row operations can be summarized in the following table:

Type	Row Operation	Notation
1	Multiply row p by c	cR_p
2	Interchange row p to row q	SWAP(R_p R_q)
3	Add c times row p to row q	$(c)R_p + R_q$

A4 Echelon Matrix

The matrix E is called an echelon matrix provided it has the following two properties:

1. Every row of E that consists entirely of zeros (if any) lies *beneath* every row that contains a nonzero element.

2. In each row of E that contains a nonzero element, the first nonzero element lies strictly to the *right* of the first nonzero element in the preceding row (if there is a preceding row).

Note: 1) The first (from the left) *nonzero* element in each of the other rows is called its **leading entry**.

2) **Leading variables**: Those variables that correspond to columns containing leading entries are called leading variables.

3) **Free variables**: All the other variables.

Example 1: Example of Echelon matrix

$$E = \begin{bmatrix} 2 & -1 & 0 & 4 & 7 \\ 0 & 1 & 2 & 0 & -5 \\ 0 & 0 & 0 & 3 & 0 \\ 0 & 0 & 0 & 0 & 0 \end{bmatrix}$$

is an example of an echelon matrix.

But $A = \begin{bmatrix} 1 & 3 & -2 \\ 0 & 0 & 0 \\ 0 & 1 & 5 \end{bmatrix}$ and $B = \begin{bmatrix} 0 & 1 & 5 \\ 1 & 3 & -2 \\ 0 & 0 & 0 \end{bmatrix}$

are not echelon matrix because A does not have Property 1 and B does not have property.

Example 2: The computation of $\det A$ **by using row operations reducing it to Echelon matrix**

$$\begin{vmatrix} 2 & 2 & -2 & 0 \\ -4 & 2 & 3 & 1 \\ 0 & 4 & -1 & -4 \\ 3 & 1 & 3 & -1 \end{vmatrix} = 2 \begin{vmatrix} 1 & 1 & -1 & 0 \\ -4 & 2 & 3 & 1 \\ 0 & 4 & -1 & -4 \\ 3 & 1 & 3 & -1 \end{vmatrix}$$

We have divided row 1 by 2

$$= 2 \begin{vmatrix} 1 & 1 & -1 & 0 \\ 0 & 6 & -1 & 1 \\ 0 & 4 & -1 & -4 \\ 0 & -2 & 6 & -1 \end{vmatrix}$$

We added 4 times row 1 to row 2, and -3 times row 1 to row 4.

$$= 2 \begin{vmatrix} 1 & 1 & -1 & 0 \\ 0 & 0 & 17 & -2 \\ 0 & 0 & 11 & -6 \\ 0 & -2 & 6 & -1 \end{vmatrix}$$

We added 3 times row 4 to row 2, and 2 times row 4 to row 3.

$$= -2 \begin{vmatrix} 1 & 1 & -1 & 0 \\ 0 & -2 & 6 & -1 \\ 0 & 0 & 11 & -6 \\ 0 & 0 & 17 & -2 \end{vmatrix}$$

We have interchanged row 2 and 4.

$$= -22\begin{vmatrix} 1 & 1 & -1 & 0 \\ 0 & -2 & 6 & -1 \\ 0 & 0 & 1 & -6/11 \\ 0 & 0 & 17 & -2 \end{vmatrix}$$

We have divided row 3 by 11.

$$= -22\begin{vmatrix} 1 & 1 & -1 & 0 \\ 0 & -2 & 6 & -1 \\ 0 & 0 & 1 & -6/11 \\ 0 & 0 & 0 & 80/11 \end{vmatrix}$$

We have added -17 times row 3to row 4.

$$= (-22)(1)(-2)(1)(80/11) = 320$$

APPENDIX B

MATHEMATICA

B1 Solving the steady state E2 of one-compartment model

```
EQ =
 U * x1 * (L - x2 - (gamma2 * x3)) / (L + h - x2 - (gamma2 * x3)) - (G * x2 * x3 / (x1 + C)) - gamma * x2 == 0
```

$$-\text{gamma}\ x2 - \frac{G\ x2\ x3}{C + x1} + \frac{U\ x1\ (L - x2 - \text{gamma2}\ x3)}{h + L - x2 - \text{gamma2}\ x3} == 0$$

```
x3 -> (-(mu * Q / (gamma1 * gamma2)) + ((mu - gamma) / G)) * x1 + (C * (mu - gamma) / G)
```

$$x3 \to \frac{C\ (-\text{gamma} + \text{mu})}{G} + \left(\frac{-\text{gamma} + \text{mu}}{G} - \frac{\text{mu}\ Q}{\text{gamma1}\ \text{gamma2}}\right) x1$$

```
x2 -> gamma1 * gamma2 (x1 + C) / G
```

$$x2 \to \frac{\text{gamma1}\ \text{gamma2}\ (C + x1)}{G}$$

```
SolveEQ = EQ /. {x2 -> gamma1 * gamma2 (x1 + C) / G, x3 ->
      (-(mu * Q / (gamma1 * gamma2)) + ((mu - gamma) / G)) * x1 + (C * (mu - gamma) / G)} // Simplify
```

$$\frac{C\ \text{gamma1}\ \text{gamma2}\ (\text{gamma} - \text{mu}) + (\text{gamma}\ \text{gamma1}\ \text{gamma2} - \text{gamma1}\ \text{gamma2}\ \text{mu} + G\ \text{mu}\ Q)\ x1}{G} +$$
$$(U\ x1\ (C\ \text{gamma1}\ \text{gamma2}\ (-\text{gamma} + \text{gamma1} + \text{mu}) + \text{gamma1}\ \text{gamma2}\ (-\text{gamma} + \text{gamma1} + \text{mu})\ x1 - G\ (\text{gamma1}\ L + \text{mu}\ Q\ x1))) /$$
$$(C\ \text{gamma1}\ \text{gamma2}\ (-\text{gamma} + \text{gamma1} + \text{mu}) + \text{gamma1}\ \text{gamma2}\ (-\text{gamma} + \text{gamma1} + \text{mu})\ x1 - G\ (\text{gamma1}\ (h + L) + \text{mu}\ Q\ x1)) == \frac{\text{gamma}\ \text{gamma1}\ \text{gamma2}\ (C + x1)}{G}$$

```
SubSolveEQ = SolveEQ /. {U -> 1, h -> 5, R -> 1 / 4, Q -> 1 / 20,
    C -> 100, mu -> 1, gamma1 -> 1 / 4, gamma2 -> 1 / 4, G -> 1} // Simplify
```

$$\frac{1050000 - 193400\ x1 - 711\ x1^2 + 80\ L\ (-500 + 79\ x1) + 20\ \text{gamma}\ (-50000 + 7400\ x1 + 79\ x1^2)}{80\ (-2100 + 80\ L - 9\ x1 + 20\ \text{gamma}\ (100 + x1))} == 0$$

```
SolSubSolveEQ = Solve[SubSolveEQ, x1] // Simplify
```

$$\left\{\left\{x1 \to -\frac{1}{79\ (-9 + 20\ \text{gamma})}\left(20\left(-4835 + 3700\ \text{gamma} + 158\ L + 2\sqrt{6310900 + 4410000\ \text{gamma}^2 - 399740\ L + 6241\ L^2 + 200\ \text{gamma}\ (-52130 + 1659\ L)}\right)\right)\right\},\right.$$
$$\left.\left\{x1 \to \frac{1}{79\ (-9 + 20\ \text{gamma})}\left(20\left(4835 - 3700\ \text{gamma} - 158\ L + 2\sqrt{6310900 + 4410000\ \text{gamma}^2 - 399740\ L + 6241\ L^2 + 200\ \text{gamma}\ (-52130 + 1659\ L)}\right)\right)\right\}\right\}$$

B2 Solving the eigenvalues about E1 of one-compartment model

g is gamma and L is lamda

```
c11 = g - 1
```

$$-1+g$$

```
c12 = 20 * (1 - g) ^ 2
```

$$20\,(1-g)^2$$

```
c21 = g / (20 * (1 - g))
```

$$\frac{g}{20\,(1-g)}$$

```
c22 = -g ^ 2 / (20 * (1 - g)) - (L * (21 * g - 20) ^ 2 / (100 * (1 - g)))
```

$$-\frac{g^2}{20\,(1-g)}-\frac{(-20+21\,g)^2\,L}{100\,(1-g)}$$

```
c33 = -1 / 4 + 4 * x2 / (x1 + 100)
```

$$-\frac{1}{4}+\frac{4\,x2}{100+x1}$$

```
x1 = 20 (1 - g) * A
```

$$20\,A\,(1-g)$$

```
x2 = A
```

$$A$$

```
A = L + g / (4 * ((g / 20) - (1 - g)))
```

$$\frac{g}{4\left(-1+\frac{21\,g}{20}\right)}+L$$

```
ma = {{c11, c12, c13}, {c21, c22, c23}, {0, 0, c33}}
```

$$\left\{\{-1+g,\ 20\,(1-g)^2,\ c13\},\ \left\{\frac{g}{20\,(1-g)},\ -\frac{g^2}{20\,(1-g)}-\frac{(-20+21\,g)^2\,L}{100\,(1-g)},\ c23\right\},\right.$$
$$\left.\left\{0,\ 0,\ -\frac{1}{4}+\frac{4\left(\frac{g}{4\left(-1+\frac{21\,g}{20}\right)}+L\right)}{100+20\,(1-g)\left(\frac{g}{4\left(-1+\frac{21\,g}{20}\right)}+L\right)}\right\}\right\}$$

```
eigen = Eigenvalues[ma]
```

$$\left\{-\frac{1}{4}+\frac{4\left(\frac{g}{4\left(-1+\frac{11g}{10}\right)}+L\right)}{100+20\,(1-g)\left(\frac{g}{4\left(-1+\frac{11g}{10}\right)}+L\right)},\right.$$

$$\frac{1}{2\,(-100+100\,g)}\left(100-200\,g+105\,g^2+400\,L-840\,g\,L+441\,g^2\,L-\right.$$
$$\sqrt{\left((-100+200\,g-105\,g^2-400\,L+840\,g\,L-441\,g^2\,L)^2-\right.}$$
$$\left.\left.4\,(-100+100\,g)\,(100\,g-205\,g^2+105\,g^3-400\,L+1240\,g\,L-1281\,g^2\,L+441\,g^3\,L)\right)\right),$$

$$\frac{1}{2\,(-100+100\,g)}\left(100-200\,g+105\,g^2+400\,L-840\,g\,L+441\,g^2\,L+\right.$$
$$\sqrt{\left((-100+200\,g-105\,g^2-400\,L+840\,g\,L-441\,g^2\,L)^2-\right.}$$
$$\left.\left.\left.4\,(-100+100\,g)\,(100\,g-205\,g^2+105\,g^3-400\,L+1240\,g\,L-1281\,g^2\,L+441\,g^3\,L)\right)\right)\right\}$$

$$E1 = -\frac{1}{4}+\frac{4\left(\frac{g}{4\left(-1+\frac{11g}{10}\right)}+L\right)}{100+20\,(1-g)\left(\frac{g}{4\left(-1+\frac{11g}{10}\right)}+L\right)}$$

$$-\frac{1}{4}+\frac{4\left(\frac{g}{4\left(-1+\frac{11g}{10}\right)}+L\right)}{100+20\,(1-g)\left(\frac{g}{4\left(-1+\frac{11g}{10}\right)}+L\right)}$$

$$E2 = \frac{1}{2\,(-100+100\,g)}\left(100-200\,g+105\,g^2+400\,L-\right.$$
$$840\,g\,L+441\,g^2\,L-\sqrt{\left((-100+200\,g-105\,g^2-400\,L+840\,g\,L-441\,g^2\,L)^2-\right.}$$
$$\left.\left.4\,(-100+100\,g)\,(100\,g-205\,g^2+105\,g^3-400\,L+1240\,g\,L-1281\,g^2\,L+441\,g^3\,L)\right)\right)$$

$$\frac{1}{2\,(-100+100\,g)}\left(100-200\,g+105\,g^2+400\,L-\right.$$
$$840\,g\,L+441\,g^2\,L-\sqrt{\left((-100+200\,g-105\,g^2-400\,L+840\,g\,L-441\,g^2\,L)^2-\right.}$$
$$\left.\left.4\,(-100+100\,g)\,(100\,g-205\,g^2+105\,g^3-400\,L+1240\,g\,L-1281\,g^2\,L+441\,g^3\,L)\right)\right)$$

$$E3 = \frac{1}{2\,(-100+100\,g)}\left(100-200\,g+105\,g^2+400\,L-\right.$$
$$840\,g\,L+441\,g^2\,L+\sqrt{\left((-100+200\,g-105\,g^2-400\,L+840\,g\,L-441\,g^2\,L)^2-\right.}$$
$$\left.\left.4\,(-100+100\,g)\,(100\,g-205\,g^2+105\,g^3-400\,L+1240\,g\,L-1281\,g^2\,L+441\,g^3\,L)\right)\right)$$

$$\frac{1}{2\,(-100+100\,g)}\left(100-200\,g+105\,g^2+400\,L-\right.$$
$$840\,g\,L+441\,g^2\,L+\sqrt{\left((-100+200\,g-105\,g^2-400\,L+840\,g\,L-441\,g^2\,L)^2-\right.}$$
$$\left.\left.4\,(-100+100\,g)\,(100\,g-205\,g^2+105\,g^3-400\,L+1240\,g\,L-1281\,g^2\,L+441\,g^3\,L)\right)\right)$$

```
V1 = Solve[E1 == 0] // Simplify
```

```
Solve::svars : Equations may not give solutions for all "solve" variables.
```

$$\left\{\left\{L\to\frac{500-530\,g+25\,g^2}{-20+121\,g-105\,g^2}\right\}\right\}$$

```
V1 ' = Solve[E1 == 0, g] // Simplify
```

$$\left\{\left\{g \to \frac{530 + 121\,L + \sqrt{230900 - 83740\,L + 6241\,L^2}}{50 + 210\,L}\right\}, \left\{g \to \frac{530 + 121\,L - \sqrt{230900 - 83740\,L + 6241\,L^2}}{50 + 210\,L}\right\}\right\}$$

```
V2 = Solve[E2 == 0] // Simplify
```

```
Solve::svars : Equations may not give solutions for all "solve" variables.
```

$$\left\{\left\{L \to \frac{5\,g}{20 - 21\,g}\right\}, \left\{g \to \frac{20}{21}\right\}\right\}$$

```
V2 ' = Solve[E2 == 0, g] // Simplify
```

$$\left\{\left\{g \to \frac{20}{21}\right\}, \left\{g \to \frac{20\,L}{5 + 21\,L}\right\}\right\}$$

```
V3 = Solve[E3 == 0] // Simplify
```

```
Solve::svars : Equations may not give solutions for all "solve" variables.
```

$$\left\{\left\{L \to \frac{5\,g}{20 - 21\,g}\right\}\right\}$$

```
V3 ' = Solve[E3 == 0, g] // Simplify
```

$$\left\{\left\{g \to \frac{20\,L}{5 + 21\,L}\right\}\right\}$$

```
Show[Plot[(530 + 121 L + Sqrt[230900 - 83740 L + 6241 L^2])/(50 + 210 L),
  {L, 0, 35}, AxesStyle -> Thickness[0.005], PlotRange -> {0, 1},
  GridLines -> Automatic, AxesLabel -> {"gamma", "Lamda"}],
 Plot[(530 + 121 L - Sqrt[230900 - 83740 L + 6241 L^2])/(50 + 210 L), {L, 0, 35}, AxesStyle -> Thickness[0.005],
  PlotRange -> {0, 1}, GridLines -> Automatic, AxesLabel -> {"gamma", "Lamda"}],
 Plot[20 L/(5 + 21 L), {L, 0, 35}, AxesStyle -> Thickness[0.005], PlotRange -> {0, 1},
  GridLines -> Automatic, AxesLabel -> {"gamma", "Lamda"}],
 Plot[20/21, {L, 0, 35}, AxesStyle -> Thickness[0.005], PlotRange -> {0, 1},
  GridLines -> Automatic, AxesLabel -> {"gamma", "Lamda"}]]
```

```
Plot::plnr : (530 + 121 L + Sqrt[230900 - 83740 L + 6241 L^2])/(50 + 210 L) is not a machine-size real number at L = 4.406323795598606`.

Plot::plnr : (530 + 121 L + Sqrt[230900 - 83740 L + 6241 L^2])/(50 + 210 L) is not a machine-size real number at L = 4.074614160960829`.

Plot::plnr :
 (530 + 121 L + Sqrt[230900 - 83740 L + 6241 L^2])/(50 + 210 L) is not a machine-size real number at L = 3.8916454600965187`.

General::stop : Further output of Plot::plnr will be suppressed during this calculation.
```

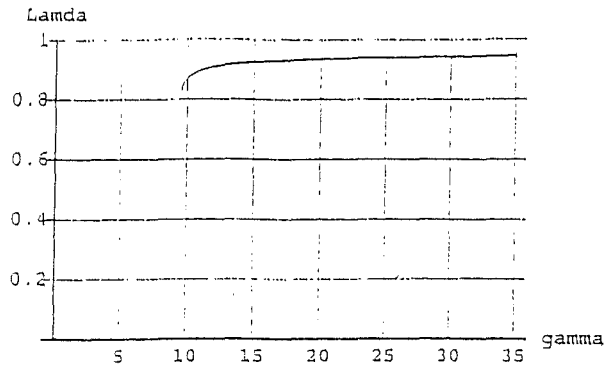
Lamda
1
0.8
0.6
0.4
0.2
5
10
15
20
25
30
35
gamma

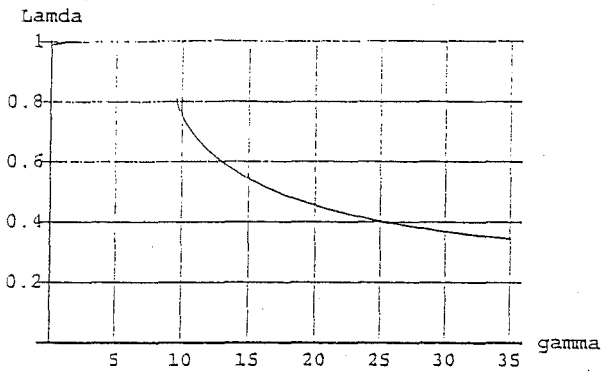
Lamda
1
0.8
0.6
0.4
0.2
5
10
15
20
25
30
35
gamma

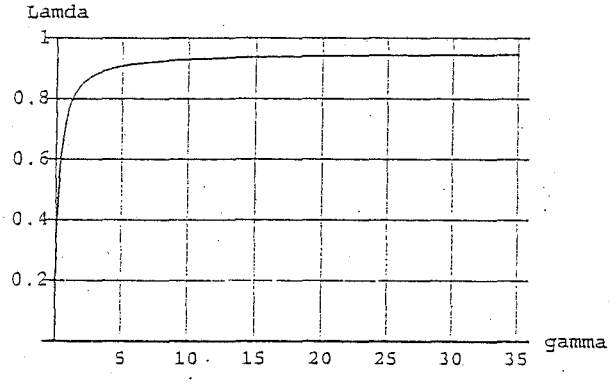
Lamda
1
0.8
0.6
0.4
0.2
5
10
15
20
25
30
35
gamma

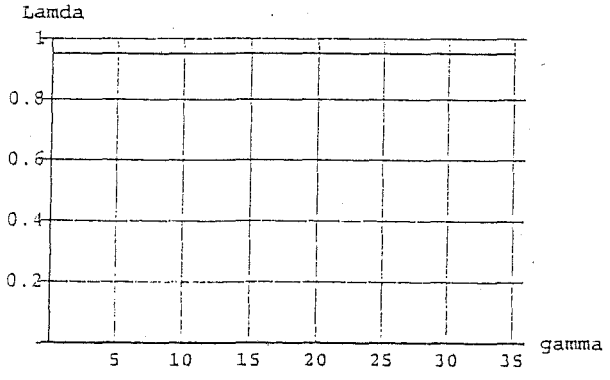
Lamda
1
0.8
0.6
0.4
0.2
5
10
15
20
25
30
35
gamma

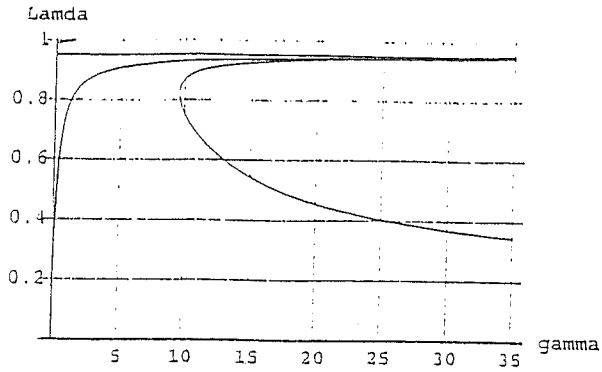

- Graphics -

B3 Solving the eigenvalues about E2 of one-compartment model

m is mu, g is gamma and L is lamda

```
c11 = x1 / (x1 + 100) ((-9 / 20) + g)
```

$$\frac{\left(-\frac{9}{20}+g\right)\,x1}{100+x1}$$

```
c12 = -x1 / (x1 + 100)
```

$$-\frac{x1}{100+x1}$$

```
c13 = -((64 * x1^2) / (5 * (x1 + 100)^2)) - (4 * x1 / (x1 + 100))
```

$$-\frac{64\,x1^2}{5\,(100+x1)^2}-\frac{4\,x1}{100+x1}$$

```
c21 = (5 / (5 + (L + ((-5 / 16) + (g / 4)) * (x1 + 100) + (x1 / 5)))) - (65 / 64) + (g / 16)
```

$$-\frac{65}{64}+\frac{g}{16}+\frac{5}{5+L+\frac{x1}{5}+\left(-\frac{5}{16}+\frac{g}{4}\right)\,(100+x1)}$$

```
c22 = -(5 * x1 / (4 * (5 + (L + ((-5 / 16) + (g / 4)) * (x1 + 100) + (x1 / 5)))^2)) - 1 / 16
```

$$-\frac{1}{16}-\frac{5\,x1}{4\,\left(5+L+\frac{x1}{5}+\left(-\frac{5}{16}+\frac{g}{4}\right)\,(100+x1)\right)^2}$$

```
c23 = 3 / 4 - 4 * x1 / (5 * (x1 + 100))
```

$$\frac{3}{4}-\frac{4\,x1}{5\,(100+x1)}$$

```
c31 = 0
```

0

```
c32 = 0
```

0

```
c33 = 16 * x1 / (5 * (x1 + 100)) - 4 * (1 - g)
```

$$-4\,(1-g)+\frac{16\,x1}{5\,(100+x1)}$$

```
x1 = 20 (4835 - 3700 * g - 158 * L + 2 * Sqrt[6310900 + 4410000 * g^2 -
        399740 * L + 6241 * L^2 + 200 * g (-52130 + 1659 * L)]) / (79 * (-9 + 20 * g))
```

$$\frac{20\left(4835-3700\,g-158\,L+2\sqrt{6310900+4410000\,g^2-399740\,L+6241\,L^2+200\,g\,(-52130+1659\,L)}\right)}{79\,(-9+20\,g)}$$

```
ma = {{c11, c12, c13}, {c21, c22, c23}, {c31, c32, c33}}
```

$$\left\{\left\{\left(20\left(-\frac{9}{20}+g\right)\left(4835-3700\,g-158\,L+2\sqrt{6310900+4410000\,g^2-399740\,L+6241\,L^2+200\,g\,(-52130+1659\,L)}\right)\right)\Big/\left(79\,(-9+20\,g)\left(100+\frac{1}{79\,(-9+20\,g)}\left(20\left(4835-3700\,g-158\,L+2\sqrt{6310900+4410000\,g^2-399740\,L+6241\,L^2+200\,g\,(-52130+1659\,L)}\right)\right)\right)\right)\right),\right.$$

$$-\left(20\left(4835-3700\,g-158\,L+2\sqrt{6310900+4410000\,g^2-399740\,L+6241\,L^2+200\,g\,(-52130+1659\,L)}\right)\right)\Big/\left(79\,(-9+20\,g)\left(100+\frac{1}{79\,(-9+20\,g)}\left(20\left(4835-3700\,g-158\,L+2\sqrt{6310900+4410000\,g^2-399740\,L+6241\,L^2+200\,g\,(-52130+1659\,L)}\right)\right)\right)\right),$$

$$-\left(5120\left(4835-3700\,g-158\,L+2\sqrt{6310900+4410000\,g^2-399740\,L+6241\,L^2+200\,g\,(-52130+1659\,L)}\right)^2\right)\Big/\left(6241\,(-9+20\,g)^2\left(100+\frac{1}{79\,(-9+20\,g)}\left(20\left(4835-3700\,g-158\,L+2\sqrt{6310900+4410000\,g^2-399740\,L+6241\,L^2+200\,g\,(-52130+1659\,L)}\right)\right)\right)^2\right)-$$

$$\left(80\left(4835-3700\,g-158\,L+2\sqrt{6310900+4410000\,g^2-399740\,L+6241\,L^2+200\,g\,(-52130+1659\,L)}\right)\right)\Big/\left(79\,(-9+20\,g)\left(100+\frac{1}{79\,(-9+20\,g)}\left(20\left(4835-3700\,g-158\,L+2\sqrt{6310900+4410000\,g^2-399740\,L+6241\,L^2+200\,g\,(-52130+1659\,L)}\right)\right)\right)\right)\Big\}\Big\},$$

$$\left\{-\frac{65}{64}+\frac{g}{16}+5\Big/\left(5+L+\frac{1}{79\,(-9+20\,g)}\left(4\left(4835-3700\,g-158\,L+2\sqrt{6310900+4410000\,g^2-399740\,L+6241\,L^2+200\,g\,(-52130+1659\,L)}\right)\right)+\left(-\frac{5}{16}+\frac{g}{4}\right)\left(100+\frac{1}{79\,(-9+20\,g)}\left(20\left(4835-3700\,g-158\,L+2\sqrt{6310900+4410000\,g^2-399740\,L+6241\,L^2+200\,g\,(-52130+1659\,L)}\right)\right)\right)\right)\right),$$

$$-\frac{1}{16}-\left(25\left(4835-3700\,g-158\,L+2\sqrt{6310900+4410000\,g^2-399740\,L+6241\,L^2+200\,g\,(-52130+1659\,L)}\right)\right)\Big/\left(79\,(-9+20\,g)\left(5+L+\frac{1}{79\,(-9+20\,g)}\left(4\left(4835-3700\,g-158\,L+2\sqrt{6310900+4410000\,g^2-399740\,L+6241\,L^2+200\,g\,(-52130+1659\,L)}\right)\right)+\left(-\frac{5}{16}+\frac{g}{4}\right)\left(100+\frac{1}{79\,(-9+20\,g)}\left(20\left(4835-3700\,g-158\,L+2\sqrt{6310900+4410000\,g^2-399740\,L+6241\,L^2+200\,g\,(-52130+1659\,L)}\right)\right)\right)^2\right)\right),$$

$$\frac{3}{4}-\left(16\left(4835-3700\,g-158\,L+2\sqrt{6310900+4410000\,g^2-399740\,L+6241\,L^2+200\,g\,(-52130+1659\,L)}\right)\right)\Big/\left(79\,(-9+20\,g)\left(100+\frac{1}{79\,(-9+20\,g)}\left(20\left(4835-3700\,g-158\,L+2\sqrt{6310900+4410000\,g^2-399740\,L+6241\,L^2+200\,g\,(-52130+1659\,L)}\right)\right)\right)\right)\Big\}\Big\},$$

$$\left\{0,\ 0,\ -4\,(1-g)+\left(64\left(4835-3700\,g-158\,L+\right.\right.\right.$$

$$2\sqrt{6310900 + 4410000\,g^2 - 399740\,L + 6241\,L^2 + 200\,g\,(-52130 + 1659\,L)}\,)\,)\,/$$
$$\Big(79\,(-9+20\,g)\,\Big(100 + \frac{1}{79\,(-9+20\,g)}\,\Big(20\,\Big(4835 - 3700\,g - 158\,L +$$
$$2\sqrt{6310900 + 4410000\,g^2 - 399740\,L + 6241\,L^2 + 200\,g\,(-52130 + 1659\,L)}\,\Big)\Big)\Big)\Big)\Big\}$$

```
eigen = Eigenvalues[ma]
```

$$\Big\{-4\,(1-g) + \Big(64\,\Big(4835 - 3700\,g - 158\,L +$$
$$2\sqrt{6310900 + 4410000\,g^2 - 399740\,L + 6241\,L^2 + 200\,g\,(-52130 + 1659\,L)}\,\Big)\Big)\,/$$
$$\Big(79\,(-9+20\,g)\,\Big(100 + \frac{1}{79\,(-9+20\,g)}\,\Big(20\,\Big(4835 - 3700\,g - 158\,L +$$
$$2\sqrt{6310900 + 4410000\,g^2 - 399740\,L + 6241\,L^2 + 200\,g\,(-52130 + 1659\,L)}\,\Big)\Big)\Big)\Big)\Big),$$
$$\Big(10434680000000 - 12928488800000\,g + 16126730000000\,g^2 - 22785860000000\,g^3 +$$
$$14872000000000\,g^4 - 3528000000000\,g^5 - 871080070000\,L + 798399280000\,g\,L -$$
$$941648400000\,g^2\,L + 881008000000\,g^3\,L - 265440000000\,g^4\,L +$$
$$17293811000\,L^2 - 7751322000\,g\,L^2 + 11982720000\,g^2\,L^2 - 4992800000\,g^3\,L^2 +$$
$$5570062100\sqrt{6310900 + 4410000\,g^2 - 399740\,L + 6241\,L^2 + 200\,g\,(-52130 + 1659\,L)} -$$
$$9817820000\,g\sqrt{6310900 + 4410000\,g^2 - 399740\,L + 6241\,L^2 + 200\,g\,(-52130 + 1659\,L)} +$$
$$21278970000\,g^2\sqrt{6310900 + 4410000\,g^2 - 399740\,L + 6241\,L^2 + 200\,g\,(-52130 + 1659\,L)} -$$
$$18377000000\,g^3\sqrt{6310900 + 4410000\,g^2 - 399740\,L + 6241\,L^2 + 200\,g\,(-52130 + 1659\,L)} +$$
$$5376000000\,g^4\sqrt{6310900 + 4410000\,g^2 - 399740\,L + 6241\,L^2 + 200\,g\,(-52130 + 1659\,L)} -$$
$$328019060\,L\sqrt{6310900 + 4410000\,g^2 - 399740\,L + 6241\,L^2 + 200\,g\,(-52130 + 1659\,L)} +$$
$$639915800\,g\,L\sqrt{6310900 + 4410000\,g^2 - 399740\,L + 6241\,L^2 + 200\,g\,(-52130 + 1659\,L)} -$$
$$998876000\,g^2\,L\sqrt{6310900 + 4410000\,g^2 - 399740\,L + 6241\,L^2 + 200\,g\,(-52130 + 1659\,L)} +$$
$$467680000\,g^3\,L\sqrt{6310900 + 4410000\,g^2 - 399740\,L + 6241\,L^2 + 200\,g\,(-52130 + 1659\,L)} +$$
$$2302929\,L^2\sqrt{6310900 + 4410000\,g^2 - 399740\,L + 6241\,L^2 + 200\,g\,(-52130 + 1659\,L)} -$$
$$9611140\,g\,L^2\sqrt{6310900 + 4410000\,g^2 - 399740\,L + 6241\,L^2 + 200\,g\,(-52130 + 1659\,L)} +$$
$$9985600\,g^2\,L^2\sqrt{6310900 + 4410000\,g^2 - 399740\,L + 6241\,L^2 + 200\,g\,(-52130 + 1659\,L)} -$$
$$369\,(6310900 + 4410000\,g^2 - 399740\,L + 6241\,L^2 + 200\,g\,(-52130 + 1659\,L))^{3/2} +$$
$$1540\,g\,(6310900 + 4410000\,g^2 - 399740\,L + 6241\,L^2 + 200\,g\,(-52130 + 1659\,L))^{3/2} -$$
$$1600\,g^2\,(6310900 + 4410000\,g^2 - 399740\,L + 6241\,L^2 + 200\,g\,(-52130 + 1659\,L))^{3/2} -$$
$$\sqrt{\Big(-4\,\Big(-11434523040000 + 76382336000000\,g - 178472208000000\,g^2 + 171561600000000\,g^3 -$$
$$59270400000000\,g^4 + 874404864000\,L - 4870166720000\,g\,L + 8511270400000\,g^2\,L -$$
$$4459392000000\,g^3\,L - 16985505600\,L^2 + 75491136000\,g\,L^2 - 83879040000\,g^2\,L^2 +$$
$$560520000\sqrt{6310900 + 4410000\,g^2 - 399740\,L + 6241\,L^2 + 200\,g\,(-52130 + 1659\,L)} -$$
$$9773280000\,g\sqrt{6310900 + 4410000\,g^2 - 399740\,L + 6241\,L^2 + 200\,g\,(-52130 + 1659\,L)} +$$
$$28476000000\,g^2\sqrt{6310900 + 4410000\,g^2 - 399740\,L + 6241\,L^2 + 200\,g\,(-52130 + 1659\,L)} -$$
$$21168000000\,g^3\sqrt{6310900 + 4410000\,g^2 - 399740\,L + 6241\,L^2 + 200\,g\,(-52130 + 1659\,L)} +$$
$$72806400\,L\sqrt{6310900 + 4410000\,g^2 - 399740\,L + 6241\,L^2 + 200\,g\,(-52130 + 1659\,L)} +$$
$$77104000\,g\,L\sqrt{6310900 + 4410000\,g^2 - 399740\,L + 6241\,L^2 + 200\,g\,(-52130 + 1659\,L)} -$$
$$530880000\,g^2\,L\sqrt{6310900 + 4410000\,g^2 - 399740\,L + 6241\,L^2 + 200\,g\,(-52130 + 1659\,L)} -$$
$$4493520\,L^2\sqrt{6310900 + 4410000\,g^2 - 399740\,L + 6241\,L^2 + 200\,g\,(-52130 + 1659\,L)} +$$
$$9985600\,g\,L^2\sqrt{6310900 + 4410000\,g^2 - 399740\,L + 6241\,L^2 + 200\,g\,(-52130 + 1659\,L)} +$$
$$720\,(6310900 + 4410000\,g^2 - 399740\,L + 6241\,L^2 + 200\,g\,(-52130 + 1659\,L))^{3/2} -$$
$$1600\,g\,(6310900 + 4410000\,g^2 - 399740\,L + 6241\,L^2 + 200\,g\,(-52130 + 1659\,L))^{3/2}\Big)$$

$$\Big(-6169693612500 + 21659623550000\,g - 18269757250000\,g^2 - 2235700000000\,g^3 + 3483900000000\,g^4 + 390795817500\,L - 1050703555000\,g\,L + 287086000000\,g^2\,L + 262122000000\,g^3\,L - 61013576255\,L^2 + 11339897000\,g\,L^2 + 4930390000\,g^2\,L^2 + 1460145150\sqrt{6310900 + 4410000\,g^2 - 399740\,L + 6241\,L^2 + 200\,g\,(-52130 + 1659\,L)} - 7602130500\,g\sqrt{6310900 + 4410000\,g^2 - 399740\,L + 6241\,L^2 + 200\,g\,(-52130 + 1659\,L)} + 12071990000\,g^2\sqrt{6310900 + 4410000\,g^2 - 399740\,L + 6241\,L^2 + 200\,g\,(-52130 + 1659\,L)} - 5308800000\,g^3\sqrt{6310900 + 4410000\,g^2 - 399740\,L + 6241\,L^2 + 200\,g\,(-52130 + 1659\,L)} - 181706715\,L\sqrt{6310900 + 4410000\,g^2 - 399740\,L + 6241\,L^2 + 200\,g\,(-52130 + 1659\,L)} + 611618000\,g\,L\sqrt{6310900 + 4410000\,g^2 - 399740\,L + 6241\,L^2 + 200\,g\,(-52130 + 1659\,L)} - 461834000\,g^2\,L\sqrt{6310900 + 4410000\,g^2 - 399740\,L + 6241\,L^2 + 200\,g\,(-52130 + 1659\,L)} + 4437351\,L^2\sqrt{6310900 + 4410000\,g^2 - 399740\,L + 6241\,L^2 + 200\,g\,(-52130 + 1659\,L)} - 9860780\,g\,L^2\sqrt{6310900 + 4410000\,g^2 - 399740\,L + 6241\,L^2 + 200\,g\,(-52130 + 1659\,L)} - 711\,(6310900 + 4410000\,g^2 - 399740\,L + 6241\,L^2 + 200\,g\,(-52130 + 1659\,L))^{3/2} + 1580\,g\,(6310900 + 4410000\,g^2 - 399740\,L + 6241\,L^2 + 200\,g\,(-52130 + 1659\,L))^{3/2}\Big) + \Big(-10434680000000 + 12928488800000\,g - 16126730000000\,g^2 + 22785860000000\,g^3 - 14872000000000\,g^4 + 3528000000000\,g^5 + 871080070000\,L - 798399280000\,g\,L + 941648400000\,g^2\,L - 881008000000\,g^3\,L + 265440000000\,g^4\,L - 17293811000\,L^2 + 7751322000\,g\,L^2 - 11982720000\,g^2\,L^2 + 4992800000\,g^3\,L^2 - 5570062100\sqrt{6310900 + 4410000\,g^2 - 399740\,L + 6241\,L^2 + 200\,g\,(-52130 + 1659\,L)} + 9817820000\,g\sqrt{6310900 + 4410000\,g^2 - 399740\,L + 6241\,L^2 + 200\,g\,(-52130 + 1659\,L)} - 21278970000\,g^2\sqrt{6310900 + 4410000\,g^2 - 399740\,L + 6241\,L^2 + 200\,g\,(-52130 + 1659\,L)} + 18377000000\,g^3\sqrt{6310900 + 4410000\,g^2 - 399740\,L + 6241\,L^2 + 200\,g\,(-52130 + 1659\,L)} - 5376000000\,g^4\sqrt{6310900 + 4410000\,g^2 - 399740\,L + 6241\,L^2 + 200\,g\,(-52130 + 1659\,L)} + 328019060\,L\sqrt{6310900 + 4410000\,g^2 - 399740\,L + 6241\,L^2 + 200\,g\,(-52130 + 1659\,L)} - 639915800\,g\,L\sqrt{6310900 + 4410000\,g^2 - 399740\,L + 6241\,L^2 + 200\,g\,(-52130 + 1659\,L)} + 998876000\,g^2\,L\sqrt{6310900 + 4410000\,g^2 - 399740\,L + 6241\,L^2 + 200\,g\,(-52130 + 1659\,L)} - 467680000\,g^3\,L\sqrt{6310900 + 4410000\,g^2 - 399740\,L + 6241\,L^2 + 200\,g\,(-52130 + 1659\,L)} - 2302929\,L^2\sqrt{6310900 + 4410000\,g^2 - 399740\,L + 6241\,L^2 + 200\,g\,(-52130 + 1659\,L)} + 9611140\,g\,L^2\sqrt{6310900 + 4410000\,g^2 - 399740\,L + 6241\,L^2 + 200\,g\,(-52130 + 1659\,L)} - 9985600\,g^2\,L^2\sqrt{6310900 + 4410000\,g^2 - 399740\,L + 6241\,L^2 + 200\,g\,(-52130 + 1659\,L)} + 369\,(6310900 + 4410000\,g^2 - 399740\,L + 6241\,L^2 + 200\,g\,(-52130 + 1659\,L))^{3/2} - 1540\,g\,(6310900 + 4410000\,g^2 - 399740\,L + 6241\,L^2 + 200\,g\,(-52130 + 1659\,L))^{3/2} + 1600\,g^2\,(6310900 + 4410000\,g^2 - 399740\,L + 6241\,L^2 + 200\,g\,(-52130 + 1659\,L))^{3/2}\Big)^2\Big)\Big) \Big/$$

$$\Big(2\,\Big(-11434523040000 + 76382336000000\,g - 178472208000000\,g^2 + 171561600000000\,g^3 - 59270400000000\,g^4 + 874404864000\,L - 4870166720000\,g\,L + 8511270400000\,g^2\,L - 4459392000000\,g^3\,L - 16985505600\,L^2 + 75491136000\,g\,L^2 - 83879040000\,g^2\,L^2 + 560520000\sqrt{6310900 + 4410000\,g^2 - 399740\,L + 6241\,L^2 + 200\,g\,(-52130 + 1659\,L)} - 9773280000\,g\sqrt{6310900 + 4410000\,g^2 - 399740\,L + 6241\,L^2 + 200\,g\,(-52130 + 1659\,L)} + 28476000000\,g^2\sqrt{6310900 + 4410000\,g^2 - 399740\,L + 6241\,L^2 + 200\,g\,(-52130 + 1659\,L)} - 21168000000\,g^3\sqrt{6310900 + 4410000\,g^2 - 399740\,L + 6241\,L^2 + 200\,g\,(-52130 + 1659\,L)} + 72806400\,L\sqrt{6310900 + 4410000\,g^2 - 399740\,L + 6241\,L^2 + 200\,g\,(-52130 + 1659\,L)} + 77104000\,g\,L\sqrt{6310900 + 4410000\,g^2 - 399740\,L + 6241\,L^2 + 200\,g\,(-52130 + 1659\,L)} - 530880000\,g^2\,L\sqrt{6310900 + 4410000\,g^2 - 399740\,L + 6241\,L^2 + 200\,g\,(-52130 + 1659\,L)} - 4493520\,L^2\sqrt{6310900 + 4410000\,g^2 - 399740\,L + 6241\,L^2 + 200\,g\,(-52130 + 1659\,L)} + 9985600\,g\,L^2\sqrt{6310900 + 4410000\,g^2 - 399740\,L + 6241\,L^2 + 200\,g\,(-52130 + 1659\,L)} +$$

$$
\begin{aligned}
&720\,(6310900+4410000\,g^2-399740\,L+6241\,L^2+200\,g\,(-52130+1659\,L))^{3/2}-\\
&1600\,g\,(6310900+4410000\,g^2-399740\,L+6241\,L^2+200\,g\,(-52130+1659\,L))^{3/2})),\\
&(10434680000000-12928488800000\,g+16126730000000\,g^2-\\
&22785860000000\,g^3+\\
&14872000000000\,g^4-\\
&3528000000000\,g^5-\\
&871080070000\,L+\\
&798399280000\,g\,L-\\
&941648400000\,g^2\,L+\\
&881008000000\,g^3\,L-\\
&265440000000\,g^4\,L+\\
&17293811000\,L^2-\\
&7751322000\,g\,L^2+\\
&11982720000\,g^2\,L^2-\\
&4992800000\,g^3\,L^2+\\
&5570062100\\
&\sqrt{6310900+4410000\,g^2-399740\,L+6241\,L^2+200\,g\,(-52130+1659\,L)}-\\
&9817820000\,g\,\sqrt{6310900+4410000\,g^2-399740\,L+6241\,L^2+200\,g\,(-52130+1659\,L)}+\\
&21278970000\,g^2\\
&\sqrt{6310900+4410000\,g^2-399740\,L+6241\,L^2+200\,g\,(-52130+1659\,L)}-\\
&18377000000\,g^3\,\sqrt{6310900+4410000\,g^2-399740\,L+6241\,L^2+200\,g\,(-52130+1659\,L)}+\\
&5376000000\,g^4\\
&\sqrt{6310900+4410000\,g^2-399740\,L+6241\,L^2+200\,g\,(-52130+1659\,L)}-\\
&328019060\,L\,\sqrt{6310900+4410000\,g^2-399740\,L+6241\,L^2+200\,g\,(-52130+1659\,L)}+\\
&639915800\,g\,L\\
&\sqrt{6310900+4410000\,g^2-399740\,L+6241\,L^2+200\,g\,(-52130+1659\,L)}-\\
&998876000\,g^2\,L\,\sqrt{6310900+4410000\,g^2-399740\,L+6241\,L^2+200\,g\,(-52130+1659\,L)}+\\
&467680000\,g^3\,L\\
&\sqrt{6310900+4410000\,g^2-399740\,L+6241\,L^2+200\,g\,(-52130+1659\,L)}+\\
&2302929\,L^2\,\sqrt{6310900+4410000\,g^2-399740\,L+6241\,L^2+200\,g\,(-52130+1659\,L)}-\\
&9611140\,g\,L^2\,\sqrt{6310900+4410000\,g^2-399740\,L+6241\,L^2+200\,g\,(-52130+1659\,L)}+\\
&9985600\,g^2\,L^2\,\sqrt{6310900+4410000\,g^2-399740\,L+6241\,L^2+200\,g\,(-52130+1659\,L)}-\\
&369\,(6310900+4410000\,g^2-399740\,L+6241\,L^2+200\,g\,(-52130+1659\,L))^{3/2}+\\
&1540\,g\,(6310900+4410000\,g^2-399740\,L+6241\,L^2+200\,g\,(-52130+1659\,L))^{3/2}-\\
&1600\,g^2\,(6310900+4410000\,g^2-399740\,L+6241\,L^2+200\,g\,(-52130+1659\,L))^{3/2}+\\
&\sqrt{(-4\,(-11434523040000+76382336000000\,g-178472208000000\,g^2+171561600000000\,g^3-\\
&\quad 59270400000000\,g^4+874404864000\,L-4870166720000\,g\,L+8511270400000\,g^2\,L-\\
&\quad 4459392000000\,g^3\,L-16985505600\,L^2+75491136000\,g\,L^2-83879040000\,g^2\,L^2+\\
&\quad 560520000\,\sqrt{6310900+4410000\,g^2-399740\,L+6241\,L^2+200\,g\,(-52130+1659\,L)}-\\
&\quad 9773280000\,g\,\sqrt{6310900+4410000\,g^2-399740\,L+6241\,L^2+200\,g\,(-52130+1659\,L)}+\\
&\quad 28476000000\,g^2\,\sqrt{6310900+4410000\,g^2-399740\,L+6241\,L^2+200\,g\,(-52130+1659\,L)}-\\
&\quad 21168000000\,g^3\,\sqrt{6310900+4410000\,g^2-399740\,L+6241\,L^2+200\,g\,(-52130+1659\,L)}+\\
&\quad 72806400\,L\,\sqrt{6310900+4410000\,g^2-399740\,L+6241\,L^2+200\,g\,(-52130+1659\,L)}+\\
&\quad 77104000\,g\,L\,\sqrt{6310900+4410000\,g^2-399740\,L+6241\,L^2+200\,g\,(-52130+1659\,L)}-\\
&\quad 530880000\,g^2\,L\,\sqrt{6310900+4410000\,g^2-399740\,L+6241\,L^2+200\,g\,(-52130+1659\,L)}-\\
&\quad 4493520\,L^2\,\sqrt{6310900+4410000\,g^2-399740\,L+6241\,L^2+200\,g\,(-52130+1659\,L)}+\\
&\quad 9985600\,g\,L^2\,\sqrt{6310900+4410000\,g^2-399740\,L+6241\,L^2+200\,g\,(-52130+1659\,L)}+
\end{aligned}
$$

$$
\begin{aligned}
&720\,(6310900+4410000\,g^2-399740\,L+6241\,L^2+200\,g\,(-52130+1659\,L))^{3/2}-\\
&1600\,g\,(6310900+4410000\,g^2-399740\,L+6241\,L^2+200\,g\,(-52130+1659\,L))^{3/2}\Big)\\
&\Big(-6169693612500+21659623550000\,g-18269757250000\,g^2-223570000000\,g^3+\\
&3483900000000\,g^4+390795817500\,L-1050703555000\,g\,L+287086000000\,g^2\,L+\\
&262122000000\,g^3\,L-6101357625\,L^2+11339897000\,g\,L^2+4930390000\,g^2\,L^2+\\
&1460145150\sqrt{6310900+4410000\,g^2-399740\,L+6241\,L^2+200\,g\,(-52130+1659\,L)}-\\
&7602130500\,g\sqrt{6310900+4410000\,g^2-399740\,L+6241\,L^2+200\,g\,(-52130+1659\,L)}+\\
&12071990000\,g^2\sqrt{6310900+4410000\,g^2-399740\,L+6241\,L^2+200\,g\,(-52130+1659\,L)}-\\
&5308800000\,g^3\sqrt{6310900+4410000\,g^2-399740\,L+6241\,L^2+200\,g\,(-52130+1659\,L)}-\\
&181706715\,L\sqrt{6310900+4410000\,g^2-399740\,L+6241\,L^2+200\,g\,(-52130+1659\,L)}+\\
&611618000\,g\,L\sqrt{6310900+4410000\,g^2-399740\,L+6241\,L^2+200\,g\,(-52130+1659\,L)}-\\
&461834000\,g^2\,L\sqrt{6310900+4410000\,g^2-399740\,L+6241\,L^2+200\,g\,(-52130+1659\,L)}+\\
&4437351\,L^2\sqrt{6310900+4410000\,g^2-399740\,L+6241\,L^2+200\,g\,(-52130+1659\,L)}-\\
&9860780\,g\,L^2\sqrt{6310900+4410000\,g^2-399740\,L+6241\,L^2+200\,g\,(-52130+1659\,L)}-\\
&711\,(6310900+4410000\,g^2-399740\,L+6241\,L^2+200\,g\,(-52130+1659\,L))^{3/2}+\\
&1580\,g\,(6310900+4410000\,g^2-399740\,L+6241\,L^2+200\,g\,(-52130+1659\,L))^{3/2}\Big)+\\
&\Big(-10434680000000+12928488800000\,g-16126730000000\,g^2+22785860000000\,g^3-\\
&14872000000000\,g^4+3528000000000\,g^5+871080070000\,L-798399280000\,g\,L+\\
&941648400000\,g^2\,L-881008000000\,g^3\,L+265440000000\,g^4\,L-\\
&17293811000\,L^2+7751322000\,g\,L^2-11982720000\,g^2\,L^2+4992800000\,g^3\,L^2-\\
&5570062100\sqrt{6310900+4410000\,g^2-399740\,L+6241\,L^2+200\,g\,(-52130+1659\,L)}+\\
&9817820000\,g\sqrt{6310900+4410000\,g^2-399740\,L+6241\,L^2+200\,g\,(-52130+1659\,L)}-\\
&21278970000\,g^2\sqrt{6310900+4410000\,g^2-399740\,L+6241\,L^2+200\,g\,(-52130+1659\,L)}+\\
&18377000000\,g^3\sqrt{6310900+4410000\,g^2-399740\,L+6241\,L^2+200\,g\,(-52130+1659\,L)}-\\
&5376000000\,g^4\sqrt{6310900+4410000\,g^2-399740\,L+6241\,L^2+200\,g\,(-52130+1659\,L)}+\\
&328019060\,L\sqrt{6310900+4410000\,g^2-399740\,L+6241\,L^2+200\,g\,(-52130+1659\,L)}-\\
&639915800\,g\,L\sqrt{6310900+4410000\,g^2-399740\,L+6241\,L^2+200\,g\,(-52130+1659\,L)}+\\
&998876000\,g^2\,L\sqrt{6310900+4410000\,g^2-399740\,L+6241\,L^2+200\,g\,(-52130+1659\,L)}-\\
&467680000\,g^3\,L\sqrt{6310900+4410000\,g^2-399740\,L+6241\,L^2+200\,g\,(-52130+1659\,L)}-\\
&2302929\,L^2\sqrt{6310900+4410000\,g^2-399740\,L+6241\,L^2+200\,g\,(-52130+1659\,L)}+\\
&9611140\,g\,L^2\sqrt{6310900+4410000\,g^2-399740\,L+6241\,L^2+200\,g\,(-52130+1659\,L)}-\\
&9985600\,g^2\,L^2\sqrt{6310900+4410000\,g^2-399740\,L+6241\,L^2+200\,g\,(-52130+1659\,L)}+\\
&369\,(6310900+4410000\,g^2-399740\,L+6241\,L^2+200\,g\,(-52130+1659\,L))^{3/2}-\\
&1540\,g\,(6310900+4410000\,g^2-399740\,L+6241\,L^2+200\,g\,(-52130+1659\,L))^{3/2}+\\
&1600\,g^2\,(6310900+4410000\,g^2-399740\,L+6241\,L^2+200\,g\,(-52130+1659\,L))^{3/2}\Big)^2\Big)\Big)\Big/\\
&\Big(2\,\Big(-11434523040000+76382336000000\,g-178472208000000\,g^2+171561600000000\,g^3-\\
&59270400000000\,g^4+874404864000\,L-4870166720000\,g\,L+\\
&8511270400000\,g^2\,L-4459392000000\,g^3\,L-\\
&16985505600\,L^2+75491136000\,g\,L^2-83879040000\,g^2\,L^2+\\
&560520000\sqrt{6310900+4410000\,g^2-399740\,L+6241\,L^2+200\,g\,(-52130+1659\,L)}-\\
&9773280000\,g\sqrt{6310900+4410000\,g^2-399740\,L+6241\,L^2+200\,g\,(-52130+1659\,L)}+\\
&28476000000\,g^2\sqrt{6310900+4410000\,g^2-399740\,L+6241\,L^2+200\,g\,(-52130+1659\,L)}-\\
&21168000000\,g^3\sqrt{6310900+4410000\,g^2-399740\,L+6241\,L^2+200\,g\,(-52130+1659\,L)}+\\
&72806400\,L\sqrt{6310900+4410000\,g^2-399740\,L+6241\,L^2+200\,g\,(-52130+1659\,L)}+\\
&77104000\,g\,L\sqrt{6310900+4410000\,g^2-399740\,L+6241\,L^2+200\,g\,(-52130+1659\,L)}-\\
&530880000\,g^2\,L\sqrt{6310900+4410000\,g^2-399740\,L+6241\,L^2+200\,g\,(-52130+1659\,L)}-
\end{aligned}
$$

$$4493520\,L^2\sqrt{6310900+4410000\,g^2-399740\,L+6241\,L^2+200\,g\,(-52130+1659\,L)}+$$
$$9985600\,g\,L^2\sqrt{6310900+4410000\,g^2-399740\,L+6241\,L^2+200\,g\,(-52130+1659\,L)}+$$
$$720\,(6310900+4410000\,g^2-399740\,L+6241\,L^2+200\,g\,(-52130+1659\,L))^{3/2}-$$
$$1600\,g\,(6310900+4410000\,g^2-399740\,L+6241\,L^2+200\,g\,(-52130+1659\,L))^{3/2})))\}$$

$$E1=-4\,(1-g)+\left(64\left(4835-3700\,g-158\,L+2\sqrt{6310900+4410000\,g^2-399740\,L+6241\,L^2+200\,g\,(-52130+1659\,L)}\right)\right)\Big/$$
$$\left(79\,(-9+20\,g)\left(100+\frac{1}{79\,(-9+20\,g)}\left(20\left(4835-3700\,g-158\,L+2\sqrt{6310900+4410000\,g^2-399740\,L+6241\,L^2+200\,g\,(-52130+1659\,L)}\right)\right)\right)\right)$$

$$-4\,(1-g)+\frac{64\left(4835-3700\,g-158\,L+2\sqrt{6310900+4410000\,g^2-399740\,L+6241\,L^2+200\,g\,(-52130+1659\,L)}\right)}{79\,(-9+20\,g)\left(100+\frac{20\left(4835-3700\,g-158\,L+2\sqrt{6310900+4410000\,g^2-399740\,L+6241\,L^2+200\,g\,(-52130+1659\,L)}\right)}{79\,(-9+20\,g)}\right)}$$

$$E2=\Big(10434680000000-12928488800000\,g+16126730000000\,g^2-$$
$$22785860000000\,g^3+14872000000000\,g^4-3528000000000\,g^5-871080070000\,L+$$
$$798399280000\,g\,L-941648400000\,g^2\,L+881008000000\,g^3\,L-265440000000\,g^4\,L+$$
$$17293811000\,L^2-7751322000\,g\,L^2+11982720000\,g^2\,L^2-4992800000\,g^3\,L^2+$$
$$5570062100\sqrt{6310900+4410000\,g^2-399740\,L+6241\,L^2+200\,g\,(-52130+1659\,L)}-$$
$$9817820000\,g\sqrt{6310900+4410000\,g^2-399740\,L+6241\,L^2+200\,g\,(-52130+1659\,L)}+$$
$$21278970000\,g^2\sqrt{6310900+4410000\,g^2-399740\,L+6241\,L^2+200\,g\,(-52130+1659\,L)}-$$
$$18377000000\,g^3\sqrt{6310900+4410000\,g^2-399740\,L+6241\,L^2+200\,g\,(-52130+1659\,L)}+$$
$$5376000000\,g^4\sqrt{6310900+4410000\,g^2-399740\,L+6241\,L^2+200\,g\,(-52130+1659\,L)}-$$
$$328019060\,L\sqrt{6310900+4410000\,g^2-399740\,L+6241\,L^2+200\,g\,(-52130+1659\,L)}+$$
$$639915800\,g\,L\sqrt{6310900+4410000\,g^2-399740\,L+6241\,L^2+200\,g\,(-52130+1659\,L)}-$$
$$998876000\,g^2\,L\sqrt{6310900+4410000\,g^2-399740\,L+6241\,L^2+200\,g\,(-52130+1659\,L)}+$$
$$467680000\,g^3\,L\sqrt{6310900+4410000\,g^2-399740\,L+6241\,L^2+200\,g\,(-52130+1659\,L)}+$$
$$2302929\,L^2\sqrt{6310900+4410000\,g^2-399740\,L+6241\,L^2+200\,g\,(-52130+1659\,L)}-$$
$$9611140\,g\,L^2\sqrt{6310900+4410000\,g^2-399740\,L+6241\,L^2+200\,g\,(-52130+1659\,L)}+$$
$$9985600\,g^2\,L^2\sqrt{6310900+4410000\,g^2-399740\,L+6241\,L^2+200\,g\,(-52130+1659\,L)}-$$
$$369\,(6310900+4410000\,g^2-399740\,L+6241\,L^2+200\,g\,(-52130+1659\,L))^{3/2}+$$
$$1540\,g\,(6310900+4410000\,g^2-399740\,L+6241\,L^2+200\,g\,(-52130+1659\,L))^{3/2}-$$
$$1600\,g^2\,(6310900+4410000\,g^2-399740\,L+6241\,L^2+200\,g\,(-52130+1659\,L))^{3/2}-$$
$$\sqrt{\Big(-4\,\big(-11434523040000+76382336000000\,g-178472208000000\,g^2+171561600000000\,g^3-$$
$$59270400000000\,g^4+874404864000\,L-4870166720000\,g\,L+8511270400000\,g^2\,L-$$
$$4459392000000\,g^3\,L-16985505600\,L^2+75491136000\,g\,L^2-83879040000\,g^2\,L^2+$$
$$560520000\sqrt{6310900+4410000\,g^2-399740\,L+6241\,L^2+200\,g\,(-52130+1659\,L)}-$$
$$9773280000\,g\sqrt{6310900+4410000\,g^2-399740\,L+6241\,L^2+200\,g\,(-52130+1659\,L)}+$$
$$28476000000\,g^2\sqrt{6310900+4410000\,g^2-399740\,L+6241\,L^2+200\,g\,(-52130+1659\,L)}-$$
$$21168000000\,g^3\sqrt{6310900+4410000\,g^2-399740\,L+6241\,L^2+200\,g\,(-52130+1659\,L)}+$$
$$72806400\,L\sqrt{6310900+4410000\,g^2-399740\,L+6241\,L^2+200\,g\,(-52130+1659\,L)}+$$

$$
\begin{aligned}
&77104000\,g\,L\sqrt{6310900+4410000\,g^2-399740\,L+6241\,L^2+200\,g\,(-52130+1659\,L)}-\\
&530880000\,g^2\,L\sqrt{6310900+4410000\,g^2-399740\,L+6241\,L^2+200\,g\,(-52130+1659\,L)}-\\
&4493520\,L^2\sqrt{6310900+4410000\,g^2-399740\,L+6241\,L^2+200\,g\,(-52130+1659\,L)}+\\
&9985600\,g\,L^2\sqrt{6310900+4410000\,g^2-399740\,L+6241\,L^2+200\,g\,(-52130+1659\,L)}+\\
&720\,(6310900+4410000\,g^2-399740\,L+6241\,L^2+200\,g\,(-52130+1659\,L))^{3/2}-\\
&1600\,g\,(6310900+4410000\,g^2-399740\,L+6241\,L^2+200\,g\,(-52130+1659\,L))^{3/2}\Big)\\
&\Big(-6169693612500+21659623550000\,g-13269757250000\,g^2-223570000000\,g^3+\\
&3483900000000\,g^4+390795817500\,L-1050703555000\,g\,L+287086000000\,g^2\,L+\\
&262122000000\,g^3\,L-61013576251^2+11339897000\,g\,L^2+4930390000\,g^2\,L^2+\\
&1460145150\sqrt{6310900+4410000\,g^2-399740\,L+6241\,L^2+200\,g\,(-52130+1659\,L)}-\\
&7602130500\,g\sqrt{6310900+4410000\,g^2-399740\,L+6241\,L^2+200\,g\,(-52130+1659\,L)}+\\
&12071990000\,g^2\sqrt{6310900+4410000\,g^2-399740\,L+6241\,L^2+200\,g\,(-52130+1659\,L)}-\\
&5308800000\,g^3\sqrt{6310900+4410000\,g^2-399740\,L+6241\,L^2+200\,g\,(-52130+1659\,L)}-\\
&181706715\,L\sqrt{6310900+4410000\,g^2-399740\,L+6241\,L^2+200\,g\,(-52130+1659\,L)}+\\
&611618000\,g\,L\sqrt{6310900+4410000\,g^2-399740\,L+6241\,L^2+200\,g\,(-52130+1659\,L)}-\\
&461834000\,g^2\,L\sqrt{6310900+4410000\,g^2-399740\,L+6241\,L^2+200\,g\,(-52130+1659\,L)}+\\
&4437351\,L^2\sqrt{6310900+4410000\,g^2-399740\,L+6241\,L^2+200\,g\,(-52130+1659\,L)}-\\
&9860780\,g\,L^2\sqrt{6310900+4410000\,g^2-399740\,L+6241\,L^2+200\,g\,(-52130+1659\,L)}-\\
&711\,(6310900+4410000\,g^2-399740\,L+6241\,L^2+200\,g\,(-52130+1659\,L))^{3/2}+\\
&1580\,g\,(6310900+4410000\,g^2-399740\,L+6241\,L^2+200\,g\,(-52130+1659\,L))^{3/2}\Big)+\\
&\Big(-10434680000000+12928488800000\,g-16126730000000\,g^2+22785860000000\,g^3-\\
&14872000000000\,g^4+3528000000000\,g^5+871080070000\,L-798399280000\,g\,L+\\
&941648400000\,g^2\,L-881008000000\,g^3\,L+265440000000\,g^4\,L-\\
&17293811000\,L^2+7751322000\,g\,L^2-11982720000\,g^2\,L^2+4992800000\,g^3\,L^2-\\
&5570062100\sqrt{6310900+4410000\,g^2-399740\,L+6241\,L^2+200\,g\,(-52130+1659\,L)}+\\
&9817820000\,g\sqrt{6310900+4410000\,g^2-399740\,L+6241\,L^2+200\,g\,(-52130+1659\,L)}-\\
&21278970000\,g^2\sqrt{6310900+4410000\,g^2-399740\,L+6241\,L^2+200\,g\,(-52130+1659\,L)}+\\
&18377000000\,g^3\sqrt{6310900+4410000\,g^2-399740\,L+6241\,L^2+200\,g\,(-52130+1659\,L)}-\\
&5376000000\,g^4\sqrt{6310900+4410000\,g^2-399740\,L+6241\,L^2+200\,g\,(-52130+1659\,L)}+\\
&328019060\,L\sqrt{6310900+4410000\,g^2-399740\,L+6241\,L^2+200\,g\,(-52130+1659\,L)}-\\
&639915800\,g\,L\sqrt{6310900+4410000\,g^2-399740\,L+6241\,L^2+200\,g\,(-52130+1659\,L)}+\\
&998876000\,g^2\,L\sqrt{6310900+4410000\,g^2-399740\,L+6241\,L^2+200\,g\,(-52130+1659\,L)}-\\
&467680000\,g^3\,L\sqrt{6310900+4410000\,g^2-399740\,L+6241\,L^2+200\,g\,(-52130+1659\,L)}-\\
&2302929\,L^2\sqrt{6310900+4410000\,g^2-399740\,L+6241\,L^2+200\,g\,(-52130+1659\,L)}+\\
&9611140\,g\,L^2\sqrt{6310900+4410000\,g^2-399740\,L+6241\,L^2+200\,g\,(-52130+1659\,L)}-\\
&9985600\,g^2\,L^2\sqrt{6310900+4410000\,g^2-399740\,L+6241\,L^2+200\,g\,(-52130+1659\,L)}+\\
&369\,(6310900+4410000\,g^2-399740\,L+6241\,L^2+200\,g\,(-52130+1659\,L))^{3/2}-\\
&1540\,g\,(6310900+4410000\,g^2-399740\,L+6241\,L^2+200\,g\,(-52130+1659\,L))^{3/2}+\\
&1600\,g^2\,(6310900+4410000\,g^2-399740\,L+6241\,L^2+200\,g\,(-52130+1659\,L))^{3/2}\Big)^2\Big)\Big)\Big/\\
&\Big(2\,\Big(-11434523040000+76382336000000\,g-178472208000000\,g^2+171561600000000\,g^3-\\
&59270400000000\,g^4+874404864000\,L-4870166720000\,g\,L+\\
&8511270400000\,g^2\,L-4459392000000\,g^3\,L-
\end{aligned}
$$

$$16985505600\,L^1 + 75491136000\,g\,L^1 - 83879040000\,g^2\,L^1 +$$
$$560520000\sqrt{6310900 + 4410000\,g^1 - 399740\,L + 6241\,L^1 + 200\,g\,(-52130 + 1659\,L)} -$$
$$9773280000\,g\sqrt{6310900 + 4410000\,g^1 - 399740\,L + 6241\,L^2 + 200\,g\,(-52130 + 1659\,L)} +$$
$$28476000000\,g^2\sqrt{6310900 + 4410000\,g^1 - 399740\,L + 6241\,L^2 + 200\,g\,(-52130 + 1659\,L)} -$$
$$21168000000\,g^3\sqrt{6310900 + 4410000\,g^1 - 399740\,L + 6241\,L^2 + 200\,g\,(-52130 + 1659\,L)} +$$
$$72806400\,L\sqrt{6310900 + 4410000\,g^2 - 399740\,L + 6241\,L^2 + 200\,g\,(-52130 + 1659\,L)} +$$
$$77104000\,g\,L\sqrt{6310900 + 4410000\,g^2 - 399740\,L + 6241\,L^2 + 200\,g\,(-52130 + 1659\,L)} -$$
$$530880000\,g^1\,L\sqrt{6310900 + 4410000\,g^2 - 399740\,L + 6241\,L^2 + 200\,g\,(-52130 + 1659\,L)} -$$
$$4493520\,L^2\sqrt{6310900 + 4410000\,g^2 - 399740\,L + 6241\,L^2 + 200\,g\,(-52130 + 1659\,L)} +$$
$$9985600\,g\,L^2\sqrt{6310900 + 4410000\,g^2 - 399740\,L + 6241\,L^2 + 200\,g\,(-52130 + 1659\,L)} +$$
$$720\,(6310900 + 4410000\,g^2 - 399740\,L + 6241\,L^2 + 200\,g\,(-52130 + 1659\,L))^{3/2} -$$
$$1600\,g\,(6310900 + 4410000\,g^2 - 399740\,L + 6241\,L^2 + 200\,g\,(-52130 + 1659\,L))^{3/2})\Big)$$

$$\Big(10434680000000 - 12928488800000\,g + 16126730000000\,g^2 -$$
$$22785860000000\,g^3 + 14872000000000\,g^4 - 3528000000000\,g^5 - 871080070000\,L +$$
$$798399280000\,g\,L - 941648400000\,g^2\,L + 881008000000\,g^3\,L - 265440000000\,g^4\,L +$$
$$17293811000\,L^2 - 7751322000\,g\,L^2 + 11982720000\,g^2\,L^2 - 4992800000\,g^3\,L^2 +$$
$$5570062100\sqrt{6310900 + 4410000\,g^2 - 399740\,L + 6241\,L^2 + 200\,g\,(-52130 + 1659\,L)} -$$
$$9817820000\,g\sqrt{6310900 + 4410000\,g^2 - 399740\,L + 6241\,L^2 + 200\,g\,(-52130 + 1659\,L)} +$$
$$21278970000\,g^2\sqrt{6310900 + 4410000\,g^2 - 399740\,L + 6241\,L^2 + 200\,g\,(-52130 + 1659\,L)} -$$
$$18377000000\,g^3\sqrt{6310900 + 4410000\,g^2 - 399740\,L + 6241\,L^2 + 200\,g\,(-52130 + 1659\,L)} +$$
$$5376000000\,g^4\sqrt{6310900 + 4410000\,g^2 - 399740\,L + 6241\,L^2 + 200\,g\,(-52130 + 1659\,L)} -$$
$$328019060\,L\sqrt{6310900 + 4410000\,g^2 - 399740\,L + 6241\,L^2 + 200\,g\,(-52130 + 1659\,L)} +$$
$$639915800\,g\,L\sqrt{6310900 + 4410000\,g^2 - 399740\,L + 6241\,L^2 + 200\,g\,(-52130 + 1659\,L)} -$$
$$998876000\,g^2\,L\sqrt{6310900 + 4410000\,g^2 - 399740\,L + 6241\,L^2 + 200\,g\,(-52130 + 1659\,L)} +$$
$$467680000\,g^3\,L\sqrt{6310900 + 4410000\,g^2 - 399740\,L + 6241\,L^2 + 200\,g\,(-52130 + 1659\,L)} +$$
$$2302929\,L^2\sqrt{6310900 + 4410000\,g^2 - 399740\,L + 6241\,L^2 + 200\,g\,(-52130 + 1659\,L)} -$$
$$9611140\,g\,L^2\sqrt{6310900 + 4410000\,g^2 - 399740\,L + 6241\,L^2 + 200\,g\,(-52130 + 1659\,L)} +$$
$$9985600\,g^2\,L^2\sqrt{6310900 + 4410000\,g^2 - 399740\,L + 6241\,L^2 + 200\,g\,(-52130 + 1659\,L)} -$$
$$369\,(6310900 + 4410000\,g^2 - 399740\,L + 6241\,L^2 + 200\,g\,(-52130 + 1659\,L))^{3/2} +$$
$$1540\,g\,(6310900 + 4410000\,g^2 - 399740\,L + 6241\,L^2 + 200\,g\,(-52130 + 1659\,L))^{3/2} -$$
$$1600\,g^2\,(6310900 + 4410000\,g^2 - 399740\,L + 6241\,L^2 + 200\,g\,(-52130 + 1659\,L))^{3/2} -$$
$$\sqrt{\Big(-4\,\big(-11434523040000 + 76382336000000\,g - 178472208000000\,g^2 + 171561600000000\,g^3 -$$
$$59270400000000\,g^4 + 874404864000\,L - 4870166720000\,g\,L + 8511270400000\,g^2\,L -$$
$$4459392000000\,g^3\,L - 16985505600\,L^2 + 75491136000\,g\,L^2 - 83879040000\,g^2\,L^2 +$$
$$560520000\sqrt{6310900 + 4410000\,g^2 - 399740\,L + 6241\,L^2 + 200\,g\,(-52130 + 1659\,L)} -$$
$$9773280000\,g\sqrt{6310900 + 4410000\,g^2 - 399740\,L + 6241\,L^2 + 200\,g\,(-52130 + 1659\,L)} +$$
$$28476000000\,g^2\sqrt{6310900 + 4410000\,g^2 - 399740\,L + 6241\,L^2 + 200\,g\,(-52130 + 1659\,L)} -$$
$$21168000000\,g^3\sqrt{6310900 + 4410000\,g^2 - 399740\,L + 6241\,L^2 + 200\,g\,(-52130 + 1659\,L)} +$$
$$72806400\,L\sqrt{6310900 + 4410000\,g^2 - 399740\,L + 6241\,L^2 + 200\,g\,(-52130 + 1659\,L)} +$$
$$77104000\,g\,L\sqrt{6310900 + 4410000\,g^2 - 399740\,L + 6241\,L^2 + 200\,g\,(-52130 + 1659\,L)} -$$
$$530880000\,g^2\,L\sqrt{6310900 + 4410000\,g^2 - 399740\,L + 6241\,L^2 + 200\,g\,(-52130 + 1659\,L)} -$$
$$4493520\,L^2\sqrt{6310900 + 4410000\,g^2 - 399740\,L + 6241\,L^2 + 200\,g\,(-52130 + 1659\,L)} +$$
$$9985600\,g\,L^2\sqrt{6310900 + 4410000\,g^2 - 399740\,L + 6241\,L^2 + 200\,g\,(-52130 + 1659\,L)} +$$
$$720\,(6310900 + 4410000\,g^2 - 399740\,L + 6241\,L^2 + 200\,g\,(-52130 + 1659\,L))^{3/2} -$$

$$1600\,g\,(6310900+4410000\,g^2-399740\,L+6241\,L^2+200\,g\,(-52130+1659\,L))^{3/2})$$
$$(-6169693612500+21659623550000\,g-18269757250000\,g^2-223570000000\,g^3+$$
$$3483900000000\,g^4+390795817500\,L-1050703555000\,g\,L+287086000000\,g^2\,L+$$
$$262122000000\,g^3\,L-6101357625\,L^2+11339897000\,g\,L^2+4930390000\,g^2\,L^2+$$
$$1460145150\sqrt{6310900+4410000\,g^2-399740\,L+6241\,L^2+200\,g\,(-52130+1659\,L)}-$$
$$7602130500\,g\sqrt{6310900+4410000\,g^2-399740\,L+6241\,L^2+200\,g\,(-52130+1659\,L)}+$$
$$12071990000\,g^2\sqrt{6310900+4410000\,g^2-399740\,L+6241\,L^2+200\,g\,(-52130+1659\,L)}-$$
$$5308800000\,g^3\sqrt{6310900+4410000\,g^2-399740\,L+6241\,L^2+200\,g\,(-52130+1659\,L)}-$$
$$181706715\,L\sqrt{6310900+4410000\,g^2-399740\,L+6241\,L^2+200\,g\,(-52130+1659\,L)}+$$
$$611618000\,g\,L\sqrt{6310900+4410000\,g^2-399740\,L+6241\,L^2+200\,g\,(-52130+1659\,L)}-$$
$$461834000\,g^2\,L\sqrt{6310900+4410000\,g^2-399740\,L+6241\,L^2+200\,g\,(-52130+1659\,L)}+$$
$$4437351\,L^2\sqrt{6310900+4410000\,g^2-399740\,L+6241\,L^2+200\,g\,(-52130+1659\,L)}-$$
$$9860780\,g\,L^2\sqrt{6310900+4410000\,g^2-399740\,L+6241\,L^2+200\,g\,(-52130+1659\,L)}-$$
$$711\,(6310900+4410000\,g^2-399740\,L+6241\,L^2+200\,g\,(-52130+1659\,L))^{3/2}+$$
$$1580\,g\,(6310900+4410000\,g^2-399740\,L+6241\,L^2+200\,g\,(-52130+1659\,L))^{3/2})+$$
$$(-10434680000000+12928488800000\,g-16126730000000\,g^2+22785860000000\,g^3-$$
$$14872000000000\,g^4+3528000000000\,g^5+871080070000\,L-798399280000\,g\,L+$$
$$941648400000\,g^2\,L-881008000000\,g^3\,L+265440000000\,g^4\,L-$$
$$17293811000\,L^2+7751322000\,g\,L^2-11982720000\,g^2\,L^2+4992800000\,g^3\,L^2-$$
$$5570062100\sqrt{6310900+4410000\,g^2-399740\,L+6241\,L^2+200\,g\,(-52130+1659\,L)}+$$
$$9817820000\,g\sqrt{6310900+4410000\,g^2-399740\,L+6241\,L^2+200\,g\,(-52130+1659\,L)}-$$
$$21278970000\,g^2\sqrt{6310900+4410000\,g^2-399740\,L+6241\,L^2+200\,g\,(-52130+1659\,L)}+$$
$$18377000000\,g^3\sqrt{6310900+4410000\,g^2-399740\,L+6241\,L^2+200\,g\,(-52130+1659\,L)}-$$
$$5376000000\,g^4\sqrt{6310900+4410000\,g^2-399740\,L+6241\,L^2+200\,g\,(-52130+1659\,L)}+$$
$$328019060\,L\sqrt{6310900+4410000\,g^2-399740\,L+6241\,L^2+200\,g\,(-52130+1659\,L)}-$$
$$639915800\,g\,L\sqrt{6310900+4410000\,g^2-399740\,L+6241\,L^2+200\,g\,(-52130+1659\,L)}+$$
$$998876000\,g^2\,L\sqrt{6310900+4410000\,g^2-399740\,L+6241\,L^2+200\,g\,(-52130+1659\,L)}-$$
$$467680000\,g^3\,L\sqrt{6310900+4410000\,g^2-399740\,L+6241\,L^2+200\,g\,(-52130+1659\,L)}-$$
$$2302929\,L^2\sqrt{6310900+4410000\,g^2-399740\,L+6241\,L^2+200\,g\,(-52130+1659\,L)}+$$
$$9611140\,g\,L^2\sqrt{6310900+4410000\,g^2-399740\,L+6241\,L^2+200\,g\,(-52130+1659\,L)}-$$
$$9985600\,g^2\,L^2\sqrt{6310900+4410000\,g^2-399740\,L+6241\,L^2+200\,g\,(-52130+1659\,L)}+$$
$$369\,(6310900+4410000\,g^2-399740\,L+6241\,L^2+200\,g\,(-52130+1659\,L))^{3/2}-$$
$$1540\,g\,(6310900+4410000\,g^2-399740\,L+6241\,L^2+200\,g\,(-52130+1659\,L))^{3/2}+$$
$$1600\,g^2\,(6310900+4410000\,g^2-399740\,L+6241\,L^2+200\,g\,(-52130+1659\,L))^{3/2})^2))/$$
$$(2\,(-11434523040000+76382336000000\,g-178472208000000\,g^2+171561600000000\,g^3-$$
$$59270400000000\,g^4+874404864000\,L-$$
$$4870166720000\,g\,L+8511270400000\,g^2\,L-$$
$$4459392000000\,g^3\,L-16985505600\,L^2+$$
$$75491136000\,g\,L^2-83879040000\,g^2\,L^2+$$
$$560520000\sqrt{6310900+4410000\,g^2-399740\,L+6241\,L^2+200\,g\,(-52130+1659\,L)}-$$
$$9773280000\,g\sqrt{6310900+4410000\,g^2-399740\,L+6241\,L^2+200\,g\,(-52130+1659\,L)}+$$
$$28476000000\,g^2\sqrt{6310900+4410000\,g^2-399740\,L+6241\,L^2+200\,g\,(-52130+1659\,L)}-$$
$$21168000000\,g^3\sqrt{6310900+4410000\,g^2-399740\,L+6241\,L^2+200\,g\,(-52130+1659\,L)}+$$
$$72806400\,L\sqrt{6310900+4410000\,g^2-399740\,L+6241\,L^2+200\,g\,(-52130+1659\,L)}+$$
$$77104000\,g\,L\sqrt{6310900+4410000\,g^2-399740\,L+6241\,L^2+200\,g\,(-52130+1659\,L)}-$$
$$530880000\,g^2\,L\sqrt{6310900+4410000\,g^2-399740\,L+6241\,L^2+200\,g\,(-52130+1659\,L)}-$$

$$4493520\,L^2\sqrt{6310900+4410000\,g^2-399740\,L+6241\,L^2+200\,g\,(-52130+1659\,L)}+$$
$$9985600\,g\,L^2\sqrt{6310900+4410000\,g^2-399740\,L+6241\,L^2+200\,g\,(-52130+1659\,L)}+$$
$$720\,(6310900+4410000\,g^2-399740\,L+6241\,L^2+200\,g\,(-52130+1659\,L))^{3/2}-$$
$$1600\,g\,(6310900+4410000\,g^2-399740\,L+6241\,L^2+200\,g\,(-52130+1659\,L))^{3/2}\Big)\Big)$$

$$E3=\Big(10434680000000-12928488800000\,g+16126730000000\,g^2-$$
$$22785860000000\,g^3+14872000000000\,g^4-3528000000000\,g^5-871080070000\,L+$$
$$798399280000\,g\,L-941648400000\,g^2\,L+881008000000\,g^3\,L-265440000000\,g^4\,L+$$
$$17293811000\,L^2-7751322000\,g\,L^2+11982720000\,g^2\,L^2-4992800000\,g^3\,L^2+$$
$$5570062100\sqrt{6310900+4410000\,g^2-399740\,L+6241\,L^2+200\,g\,(-52130+1659\,L)}-$$
$$9817820000\,g\sqrt{6310900+4410000\,g^2-399740\,L+6241\,L^2+200\,g\,(-52130+1659\,L)}+$$
$$21278970000\,g^2\sqrt{6310900+4410000\,g^2-399740\,L+6241\,L^2+200\,g\,(-52130+1659\,L)}-$$
$$18377000000\,g^3\sqrt{6310900+4410000\,g^2-399740\,L+6241\,L^2+200\,g\,(-52130+1659\,L)}+$$
$$5376000000\,g^4\sqrt{6310900+4410000\,g^2-399740\,L+6241\,L^2+200\,g\,(-52130+1659\,L)}-$$
$$328019060\,L\sqrt{6310900+4410000\,g^2-399740\,L+6241\,L^2+200\,g\,(-52130+1659\,L)}+$$
$$639915800\,g\,L\sqrt{6310900+4410000\,g^2-399740\,L+6241\,L^2+200\,g\,(-52130+1659\,L)}-$$
$$998876000\,g^2\,L\sqrt{6310900+4410000\,g^2-399740\,L+6241\,L^2+200\,g\,(-52130+1659\,L)}+$$
$$467680000\,g^3\,L\sqrt{6310900+4410000\,g^2-399740\,L+6241\,L^2+200\,g\,(-52130+1659\,L)}+$$
$$2302929\,L^2\sqrt{6310900+4410000\,g^2-399740\,L+6241\,L^2+200\,g\,(-52130+1659\,L)}-$$
$$9611140\,g\,L^2\sqrt{6310900+4410000\,g^2-399740\,L+6241\,L^2+200\,g\,(-52130+1659\,L)}+$$
$$9985600\,g^2\,L^2\sqrt{6310900+4410000\,g^2-399740\,L+6241\,L^2+200\,g\,(-52130+1659\,L)}-$$
$$369\,(6310900+4410000\,g^2-399740\,L+6241\,L^2+200\,g\,(-52130+1659\,L))^{3/2}+$$
$$1540\,g\,(6310900+4410000\,g^2-399740\,L+6241\,L^2+200\,g\,(-52130+1659\,L))^{3/2}-$$
$$1600\,g^2\,(6310900+4410000\,g^2-399740\,L+6241\,L^2+200\,g\,(-52130+1659\,L))^{3/2}+$$
$$\sqrt{\Big(-4\,\big(-11434523040000+76382336000000\,g-178472208000000\,g^2+171561600000000\,g^3-$$
$$59270400000000\,g^4+874404864000\,L-4870166720000\,g\,L+8511270400000\,g^2\,L-$$
$$4459392000000\,g^3\,L-16985505600\,L^2+75491136000\,g\,L^2-83879040000\,g^2\,L^2+$$
$$560520000\sqrt{6310900+4410000\,g^2-399740\,L+6241\,L^2+200\,g\,(-52130+1659\,L)}-$$
$$9773280000\,g\sqrt{6310900+4410000\,g^2-399740\,L+6241\,L^2+200\,g\,(-52130+1659\,L)}+$$
$$28476000000\,g^2\sqrt{6310900+4410000\,g^2-399740\,L+6241\,L^2+200\,g\,(-52130+1659\,L)}-$$
$$21168000000\,g^3\sqrt{6310900+4410000\,g^2-399740\,L+6241\,L^2+200\,g\,(-52130+1659\,L)}+$$
$$72806400\,L\sqrt{6310900+4410000\,g^2-399740\,L+6241\,L^2+200\,g\,(-52130+1659\,L)}+$$
$$77104000\,g\,L\sqrt{6310900+4410000\,g^2-399740\,L+6241\,L^2+200\,g\,(-52130+1659\,L)}-$$
$$530880000\,g^2\,L\sqrt{6310900+4410000\,g^2-399740\,L+6241\,L^2+200\,g\,(-52130+1659\,L)}-$$
$$4493520\,L^2\sqrt{6310900+4410000\,g^2-399740\,L+6241\,L^2+200\,g\,(-52130+1659\,L)}+$$
$$9985600\,g\,L^2\sqrt{6310900+4410000\,g^2-399740\,L+6241\,L^2+200\,g\,(-52130+1659\,L)}+$$
$$720\,(6310900+4410000\,g^2-399740\,L+6241\,L^2+200\,g\,(-52130+1659\,L))^{3/2}-$$
$$1600\,g\,(6310900+4410000\,g^2-399740\,L+6241\,L^2+200\,g\,(-52130+1659\,L))^{3/2}\big)$$
$$\big(-6169693612500+21659623550000\,g-18269757250000\,g^2-223570000000\,g^3+$$
$$3483900000000\,g^4+390795817500\,L-1050703555000\,g\,L+287086000000\,g^2\,L+$$
$$262122000000\,g^3\,L-6101357625\,L^2+11339897000\,g\,L^2+4930390000\,g^2\,L^2+$$
$$1460145150\sqrt{6310900+4410000\,g^2-399740\,L+6241\,L^2+200\,g\,(-52130+1659\,L)}-$$

$$
\begin{aligned}
&7602130500\,g\,\sqrt{6310900+4410000\,g^2-399740\,L+6241\,L^2+200\,g\,(-52130+1659\,L)}+\\
&12071990000\,g^2\,\sqrt{6310900+4410000\,g^2-399740\,L+6241\,L^2+200\,g\,(-52130+1659\,L)}-\\
&5308800000\,g^3\,\sqrt{6310900+4410000\,g^2-399740\,L+6241\,L^2+200\,g\,(-52130+1659\,L)}-\\
&181706715\,L\,\sqrt{6310900+4410000\,g^2-399740\,L+6241\,L^2+200\,g\,(-52130+1659\,L)}+\\
&611618000\,g\,L\,\sqrt{6310900+4410000\,g^2-399740\,L+6241\,L^2+200\,g\,(-52130+1659\,L)}-\\
&461834000\,g^2\,L\,\sqrt{6310900+4410000\,g^2-399740\,L+6241\,L^2+200\,g\,(-52130+1659\,L)}+\\
&4437351\,L^2\,\sqrt{6310900+4410000\,g^2-399740\,L+6241\,L^2+200\,g\,(-52130+1659\,L)}-\\
&9860780\,g\,L^2\,\sqrt{6310900+4410000\,g^2-399740\,L+6241\,L^2+200\,g\,(-52130+1659\,L)}-\\
&711\,(6310900+4410000\,g^2-399740\,L+6241\,L^2+200\,g\,(-52130+1659\,L))^{3/2}+\\
&1580\,g\,(6310900+4410000\,g^2-399740\,L+6241\,L^2+200\,g\,(-52130+1659\,L))^{3/2}\Big)+\\
&\Big(-10434680000000+12928488800000\,g-16126730000000\,g^2+22785860000000\,g^3-\\
&14872000000000\,g^4+3528000000000\,g^5+871080070000\,L-798399280000\,g\,L+\\
&941648400000\,g^2\,L-881008000000\,g^3\,L+265440000000\,g^4\,L-\\
&17293811000\,L^2+7751322000\,g\,L^2-11982720000\,g^2\,L^2+4992800000\,g^3\,L^2-\\
&5570062100\,\sqrt{6310900+4410000\,g^2-399740\,L+6241\,L^2+200\,g\,(-52130+1659\,L)}+\\
&9817820000\,g\,\sqrt{6310900+4410000\,g^2-399740\,L+6241\,L^2+200\,g\,(-52130+1659\,L)}-\\
&21278970000\,g^2\,\sqrt{6310900+4410000\,g^2-399740\,L+6241\,L^2+200\,g\,(-52130+1659\,L)}+\\
&18377000000\,g^3\,\sqrt{6310900+4410000\,g^2-399740\,L+6241\,L^2+200\,g\,(-52130+1659\,L)}-\\
&5376000000\,g^4\,\sqrt{6310900+4410000\,g^2-399740\,L+6241\,L^2+200\,g\,(-52130+1659\,L)}+\\
&328019060\,L\,\sqrt{6310900+4410000\,g^2-399740\,L+6241\,L^2+200\,g\,(-52130+1659\,L)}-\\
&639915800\,g\,L\,\sqrt{6310900+4410000\,g^2-399740\,L+6241\,L^2+200\,g\,(-52130+1659\,L)}+\\
&998876000\,g^2\,L\,\sqrt{6310900+4410000\,g^2-399740\,L+6241\,L^2+200\,g\,(-52130+1659\,L)}-\\
&467680000\,g^3\,L\,\sqrt{6310900+4410000\,g^2-399740\,L+6241\,L^2+200\,g\,(-52130+1659\,L)}-\\
&2302929\,L^2\,\sqrt{6310900+4410000\,g^2-399740\,L+6241\,L^2+200\,g\,(-52130+1659\,L)}+\\
&9611140\,g\,L^2\,\sqrt{6310900+4410000\,g^2-399740\,L+6241\,L^2+200\,g\,(-52130+1659\,L)}-\\
&9985600\,g^2\,L^2\,\sqrt{6310900+4410000\,g^2-399740\,L+6241\,L^2+200\,g\,(-52130+1659\,L)}+\\
&369\,(6310900+4410000\,g^2-399740\,L+6241\,L^2+200\,g\,(-52130+1659\,L))^{3/2}-\\
&1540\,g\,(6310900+4410000\,g^2-399740\,L+6241\,L^2+200\,g\,(-52130+1659\,L))^{3/2}+\\
&1600\,g^2\,(6310900+4410000\,g^2-399740\,L+6241\,L^2+200\,g\,(-52130+1659\,L))^{3/2}\Big)^2\Big)\Big)\Big/\\
&\Big(2\,\Big(-11434523040000+76382336000000\,g-178472208000000\,g^2+171561600000000\,g^3-\\
&59270400000000\,g^4+874404864000\,L-4870166720000\,g\,L+\\
&8511270400000\,g^2\,L-4459392000000\,g^3\,L-\\
&16985505600\,L^2+75491136000\,g\,L^2-83879040000\,g^2\,L^2+\\
&560520000\,\sqrt{6310900+4410000\,g^2-399740\,L+6241\,L^2+200\,g\,(-52130+1659\,L)}-\\
&9773280000\,g\,\sqrt{6310900+4410000\,g^2-399740\,L+6241\,L^2+200\,g\,(-52130+1659\,L)}+\\
&28476000000\,g^2\,\sqrt{6310900+4410000\,g^2-399740\,L+6241\,L^2+200\,g\,(-52130+1659\,L)}-\\
&21168000000\,g^3\,\sqrt{6310900+4410000\,g^2-399740\,L+6241\,L^2+200\,g\,(-52130+1659\,L)}+\\
&72806400\,L\,\sqrt{6310900+4410000\,g^2-399740\,L+6241\,L^2+200\,g\,(-52130+1659\,L)}+\\
&77104000\,g\,L\,\sqrt{6310900+4410000\,g^2-399740\,L+6241\,L^2+200\,g\,(-52130+1659\,L)}-\\
&530880000\,g^2\,L\,\sqrt{6310900+4410000\,g^2-399740\,L+6241\,L^2+200\,g\,(-52130+1659\,L)}-\\
&4493520\,L^2\,\sqrt{6310900+4410000\,g^2-399740\,L+6241\,L^2+200\,g\,(-52130+1659\,L)}+
\end{aligned}
$$

$$9985600\,g\,L^2\sqrt{6310900+4410000\,g^2-399740\,L+6241\,L^2+200\,g\,(-52130+1659\,L)}+$$
$$720\,(6310900+4410000\,g^2-399740\,L+6241\,L^2+200\,g\,(-52130+1659\,L))^{3/2}-$$
$$1600\,g\,(6310900+4410000\,g^2-399740\,L+6241\,L^2+200\,g\,(-52130+1659\,L))^{3/2}\Big)\Big)$$

$$\Big(10434680000000-12928488800000\,g+16126730000000\,g^2-$$
$$22785860000000\,g^3+14872000000000\,g^4-3528000000000\,g^5-871080070000\,L+$$
$$798399280000\,g\,L-941648400000\,g^2\,L+881008000000\,g^3\,L-265440000000\,g^4\,L+$$
$$17293811000\,L^2-7751322000\,g\,L^2+11982720000\,g^2\,L^2-4992800000\,g^3\,L^2+$$
$$5570062100\sqrt{6310900+4410000\,g^2-399740\,L+6241\,L^2+200\,g\,(-52130+1659\,L)}-$$
$$9817820000\,g\sqrt{6310900+4410000\,g^2-399740\,L+6241\,L^2+200\,g\,(-52130+1659\,L)}+$$
$$21278970000\,g^2\sqrt{6310900+4410000\,g^2-399740\,L+6241\,L^2+200\,g\,(-52130+1659\,L)}-$$
$$18377000000\,g^3\sqrt{6310900+4410000\,g^2-399740\,L+6241\,L^2+200\,g\,(-52130+1659\,L)}+$$
$$5376000000\,g^4\sqrt{6310900+4410000\,g^2-399740\,L+6241\,L^2+200\,g\,(-52130+1659\,L)}-$$
$$328019060\,L\sqrt{6310900+4410000\,g^2-399740\,L+6241\,L^2+200\,g\,(-52130+1659\,L)}+$$
$$639915800\,g\,L\sqrt{6310900+4410000\,g^2-399740\,L+6241\,L^2+200\,g\,(-52130+1659\,L)}-$$
$$998876000\,g^2\,L\sqrt{6310900+4410000\,g^2-399740\,L+6241\,L^2+200\,g\,(-52130+1659\,L)}+$$
$$467680000\,g^3\,L\sqrt{6310900+4410000\,g^2-399740\,L+6241\,L^2+200\,g\,(-52130+1659\,L)}+$$
$$2302929\,L^2\sqrt{6310900+4410000\,g^2-399740\,L+6241\,L^2+200\,g\,(-52130+1659\,L)}-$$
$$9611140\,g\,L^2\sqrt{6310900+4410000\,g^2-399740\,L+6241\,L^2+200\,g\,(-52130+1659\,L)}+$$
$$9985600\,g^2\,L^2\sqrt{6310900+4410000\,g^2-399740\,L+6241\,L^2+200\,g\,(-52130+1659\,L)}-$$
$$369\,(6310900+4410000\,g^2-399740\,L+6241\,L^2+200\,g\,(-52130+1659\,L))^{3/2}+$$
$$1540\,g\,(6310900+4410000\,g^2-399740\,L+6241\,L^2+200\,g\,(-52130+1659\,L))^{3/2}-$$
$$1600\,g^2\,(6310900+4410000\,g^2-399740\,L+6241\,L^2+200\,g\,(-52130+1659\,L))^{3/2}+$$
$$\sqrt{\Big(-4\,\big(-11434523040000+76382336000000\,g-178472208000000\,g^2+171561600000000\,g^3-$$
$$59270400000000\,g^4+874404864000\,L-4870166720000\,g\,L+8511270400000\,g^2\,L-$$
$$4459392000000\,g^3\,L-16985505600\,L^2+75491136000\,g\,L^2-83879040000\,g^2\,L^2+$$
$$560520000\sqrt{6310900+4410000\,g^2-399740\,L+6241\,L^2+200\,g\,(-52130+1659\,L)}-$$
$$9773280000\,g\sqrt{6310900+4410000\,g^2-399740\,L+6241\,L^2+200\,g\,(-52130+1659\,L)}+$$
$$28476000000\,g^2\sqrt{6310900+4410000\,g^2-399740\,L+6241\,L^2+200\,g\,(-52130+1659\,L)}-$$
$$21168000000\,g^3\sqrt{6310900+4410000\,g^2-399740\,L+6241\,L^2+200\,g\,(-52130+1659\,L)}+$$
$$72806400\,L\sqrt{6310900+4410000\,g^2-399740\,L+6241\,L^2+200\,g\,(-52130+1659\,L)}+$$
$$77104000\,g\,L\sqrt{6310900+4410000\,g^2-399740\,L+6241\,L^2+200\,g\,(-52130+1659\,L)}-$$
$$530880000\,g^2\,L\sqrt{6310900+4410000\,g^2-399740\,L+6241\,L^2+200\,g\,(-52130+1659\,L)}-$$
$$4493520\,L^2\sqrt{6310900+4410000\,g^2-399740\,L+6241\,L^2+200\,g\,(-52130+1659\,L)}+$$
$$9985600\,g\,L^2\sqrt{6310900+4410000\,g^2-399740\,L+6241\,L^2+200\,g\,(-52130+1659\,L)}+$$
$$720\,(6310900+4410000\,g^2-399740\,L+6241\,L^2+200\,g\,(-52130+1659\,L))^{3/2}-$$
$$1600\,g\,(6310900+4410000\,g^2-399740\,L+6241\,L^2+200\,g\,(-52130+1659\,L))^{3/2}\big)$$
$$\big(-6169693612500+21659623550000\,g-18269757250000\,g^2-223570000000\,g^3+$$
$$3483900000000\,g^4+390795817500\,L-1050703555000\,g\,L+287086000000\,g^2\,L+$$
$$262122000000\,g^3\,L-6101357625\,L^2+11339897000\,g\,L^2+4930390000\,g^2\,L^2+$$
$$1460145150\sqrt{6310900+4410000\,g^2-399740\,L+6241\,L^2+200\,g\,(-52130+1659\,L)}-$$
$$7602130500\,g\sqrt{6310900+4410000\,g^2-399740\,L+6241\,L^2+200\,g\,(-52130+1659\,L)}+$$
$$12071990000\,g^2\sqrt{6310900+4410000\,g^2-399740\,L+6241\,L^2+200\,g\,(-52130+1659\,L)}-$$
$$5308800000\,g^3\sqrt{6310900+4410000\,g^2-399740\,L+6241\,L^2+200\,g\,(-52130+1659\,L)}-$$
$$181706715\,L\sqrt{6310900+4410000\,g^2-399740\,L+6241\,L^2+200\,g\,(-52130+1659\,L)}+$$
$$611618000\,g\,L\sqrt{6310900+4410000\,g^2-399740\,L+6241\,L^2+200\,g\,(-52130+1659\,L)}-$$

$$461834000\,g^2\,L\sqrt{6310900+4410000\,g^2-399740\,L+6241\,L^2+200\,g\,(-52130+1659\,L)}+4437351\,L^2\sqrt{6310900+4410000\,g^2-399740\,L+6241\,L^2+200\,g\,(-52130+1659\,L)}-9860780\,g\,L^2\sqrt{6310900+4410000\,g^2-399740\,L+6241\,L^2+200\,g\,(-52130+1659\,L)}-711\,(6310900+4410000\,g^2-399740\,L+6241\,L^2+200\,g\,(-52130+1659\,L))^{3/2}+1580\,g\,(6310900+4410000\,g^2-399740\,L+6241\,L^2+200\,g\,(-52130+1659\,L))^{3/2}\Big)+\Big(-10434680000000+12928488800000\,g-16126730000000\,g^2+22785860000000\,g^3-14872000000000\,g^4+3528000000000\,g^5+871080070000\,L-798399280000\,g\,L+941648400000\,g^2\,L-881008000000\,g^3\,L+265440000000\,g^4\,L-17293811000\,L^2+7751322000\,g\,L^2-11982720000\,g^2\,L^2+4992800000\,g^3\,L^2-5570062100\sqrt{6310900+4410000\,g^2-399740\,L+6241\,L^2+200\,g\,(-52130+1659\,L)}+9817820000\,g\sqrt{6310900+4410000\,g^2-399740\,L+6241\,L^2+200\,g\,(-52130+1659\,L)}-21278970000\,g^2\sqrt{6310900+4410000\,g^2-399740\,L+6241\,L^2+200\,g\,(-52130+1659\,L)}+18377000000\,g^3\sqrt{6310900+4410000\,g^2-399740\,L+6241\,L^2+200\,g\,(-52130+1659\,L)}-5376000000\,g^4\sqrt{6310900+4410000\,g^2-399740\,L+6241\,L^2+200\,g\,(-52130+1659\,L)}+328019060\,L\sqrt{6310900+4410000\,g^2-399740\,L+6241\,L^2+200\,g\,(-52130+1659\,L)}-639915800\,g\,L\sqrt{6310900+4410000\,g^2-399740\,L+6241\,L^2+200\,g\,(-52130+1659\,L)}+998876000\,g^2\,L\sqrt{6310900+4410000\,g^2-399740\,L+6241\,L^2+200\,g\,(-52130+1659\,L)}-467680000\,g^3\,L\sqrt{6310900+4410000\,g^2-399740\,L+6241\,L^2+200\,g\,(-52130+1659\,L)}-2302929\,L^2\sqrt{6310900+4410000\,g^2-399740\,L+6241\,L^2+200\,g\,(-52130+1659\,L)}+9611140\,g\,L^2\sqrt{6310900+4410000\,g^2-399740\,L+6241\,L^2+200\,g\,(-52130+1659\,L)}-9985600\,g^2\,L^2\sqrt{6310900+4410000\,g^2-399740\,L+6241\,L^2+200\,g\,(-52130+1659\,L)}+369\,(6310900+4410000\,g^2-399740\,L+6241\,L^2+200\,g\,(-52130+1659\,L))^{3/2}-1540\,g\,(6310900+4410000\,g^2-399740\,L+6241\,L^2+200\,g\,(-52130+1659\,L))^{3/2}+1600\,g^2\,(6310900+4410000\,g^2-399740\,L+6241\,L^2+200\,g\,(-52130+1659\,L))^{3/2}\Big)^2\Big)\Big/\Big(2\,\Big(-11434523040000+76382336000000\,g-178472208000000\,g^2+171561600000000\,g^3-59270400000000\,g^4+874404864000\,L-4870166720000\,g\,L+8511270400000\,g^2\,L-4459392000000\,g^3\,L-16985505600\,L^2+75491136000\,g\,L^2-83879040000\,g^2\,L^2+560520000\sqrt{6310900+4410000\,g^2-399740\,L+6241\,L^2+200\,g\,(-52130+1659\,L)}-9773280000\,g\sqrt{6310900+4410000\,g^2-399740\,L+6241\,L^2+200\,g\,(-52130+1659\,L)}+28476000000\,g^2\sqrt{6310900+4410000\,g^2-399740\,L+6241\,L^2+200\,g\,(-52130+1659\,L)}-21168000000\,g^3\sqrt{6310900+4410000\,g^2-399740\,L+6241\,L^2+200\,g\,(-52130+1659\,L)}+72806400\,L\sqrt{6310900+4410000\,g^2-399740\,L+6241\,L^2+200\,g\,(-52130+1659\,L)}+77104000\,g\,L\sqrt{6310900+4410000\,g^2-399740\,L+6241\,L^2+200\,g\,(-52130+1659\,L)}-530880000\,g^2\,L\sqrt{6310900+4410000\,g^2-399740\,L+6241\,L^2+200\,g\,(-52130+1659\,L)}-4493520\,L^2\sqrt{6310900+4410000\,g^2-399740\,L+6241\,L^2+200\,g\,(-52130+1659\,L)}+9985600\,g\,L^2\sqrt{6310900+4410000\,g^2-399740\,L+6241\,L^2+200\,g\,(-52130+1659\,L)}+720\,(6310900+4410000\,g^2-399740\,L+6241\,L^2+200\,g\,(-52130+1659\,L))^{3/2}-1600\,g\,(6310900+4410000\,g^2-399740\,L+6241\,L^2+200\,g\,(-52130+1659\,L))^{3/2}\Big)\Big)$$

```
V1 = Solve[E1 == 0] // Simplify
```

```
Solve::svars : Equations may not give solutions for all "solve" variables.
```

$$\left\{\left\{L \to \frac{500-530\,g+25\,g^2}{-20+121\,g-105\,g^2}\right\}\right\}$$

```
V1 ' = Solve[E1 == 0, g] // Simplify
```

$$\left\{\left\{g \to \frac{530 + 121\,L - \sqrt{230900 - 83740\,L + 6241\,L^2}}{50 + 210\,L}\right\}, \left\{g \to \frac{530 + 121\,L + \sqrt{230900 - 83740\,L + 6241\,L^2}}{50 + 210\,L}\right\}\right\}$$

```
V2 = Solve[E2 == 0] // Simplify
```

```
No more memory available.
Mathematica kernel has shut down.
Try quitting other applications and then retry.
```

```
Show[Plot[(530 + 121 L + Sqrt[230900 - 83740 L + 6241 L^2])/(50 + 210 L),
  {L, 0, 35}, AxesStyle -> Thickness[0.005], PlotRange -> {0, 1},
  GridLines -> Automatic, AxesLabel -> {"gamma", "Lamda"}],
 Plot[(530 + 121 L - Sqrt[230900 - 83740 L + 6241 L^2])/(50 + 210 L), {L, 0, 35}, AxesStyle -> Thickness[0.005],
  PlotRange -> {0, 1}, GridLines -> Automatic, AxesLabel -> {"gamma", "Lamda"}]]
```

Plot::plnr : $\frac{530 + 121\,L + \sqrt{230900 - 83740\,L + 6241\,L^2}}{50 + 210\,L}$ is not a machine-size real number at L = 4.406323795598606`.

Plot::plnr : $\frac{530 + 121\,L + \sqrt{230900 - 83740\,L + 6241\,L^2}}{50 + 210\,L}$ is not a machine-size real number at L = 4.074614160960829`.

Plot::plnr : $\frac{530 + 121\,L + \sqrt{230900 - 83740\,L + 6241\,L^2}}{50 + 210\,L}$ is not a machine-size real number at L = 3.39164546009651873`.

General::stop : Further output of Plot::plnr will be suppressed during this calculation.

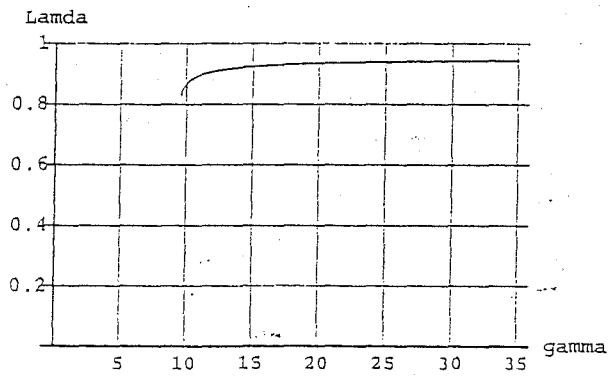

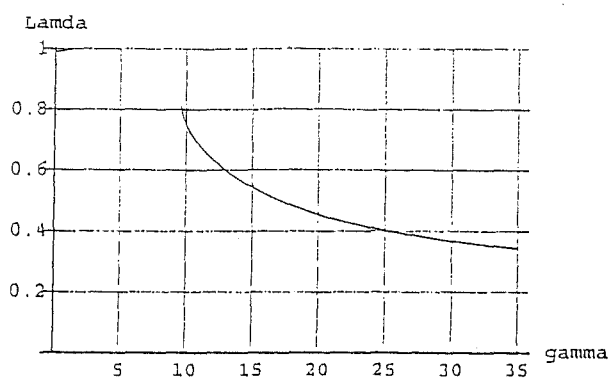

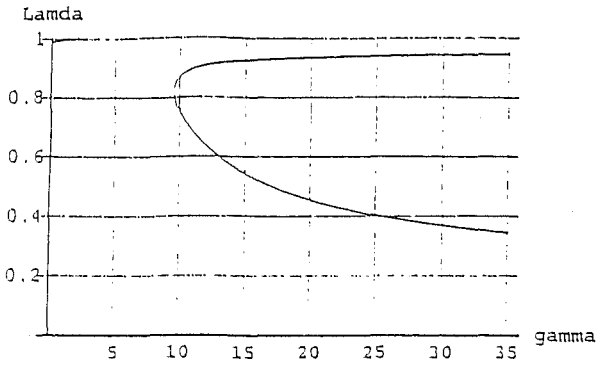

- Graphics -

B4 Overall plots from AUTO and analytical results of one-compartment model

```
data3 = {{40.22, -0.0857}, {36.89, 0.0141}, {35.92, 0.0432}, {34.2, 0.09488},
  {32.32, 0.1516}, {28.73, 0.2601}, {28.22, 0.2757}, {28.08, 0.28}, {27.75, 0.29},
  {27.42, 0.3}, {25.78, 0.35}, {25.17, 0.3689}, {23.84, 0.41}, {23.51, 0.42},
  {24.16, 0.4}, {22.87, 0.44}, {22.55, 0.45}, {21.66, 0.4779}, {20.96, 0.5},
  {18.28, 0.5875}, {17.91, 0.6}, {17.75, 0.6054}, {15.34, 0.7}, {14.85, 0.75},
  {15.67, 0.7759}, {21.82, 0.8}, {26.16, 0.8036}, {37.75, 0.807}, {49.45, 0.8081},
  {61.19, 0.8086}, {72.94, 0.8089}, {84.69, 0.8091}, {96.45, 0.8093},
  {108.2, 0.8094}, {120, 0.8094}, {162.5, 0.8096}, {43.23, 0.8076}}
```

```
{{40.22, -0.0857}, {36.89, 0.0141}, {35.92, 0.0432}, {34.2, 0.09488},
 {32.32, 0.1516}, {28.73, 0.2601}, {28.22, 0.2757}, {28.08, 0.28}, {27.75, 0.29},
 {27.42, 0.3}, {25.78, 0.35}, {25.17, 0.3689}, {23.84, 0.41}, {23.51, 0.42},
 {24.16, 0.4}, {22.87, 0.44}, {22.55, 0.45}, {21.66, 0.4779}, {20.96, 0.5},
 {18.28, 0.5875}, {17.91, 0.6}, {17.75, 0.6054}, {15.34, 0.7}, {14.85, 0.75},
 {15.67, 0.7759}, {21.82, 0.8}, {26.16, 0.8036}, {37.75, 0.807}, {49.45, 0.8081},
 {61.19, 0.8086}, {72.94, 0.8089}, {84.69, 0.8091}, {96.45, 0.8093},
 {108.2, 0.8094}, {120, 0.8094}, {162.5, 0.8096}, {43.23, 0.8076}}
```

```
graph3 = ListPlot[data3, PlotRange → {0, 1}, PlotJoined → True]
```

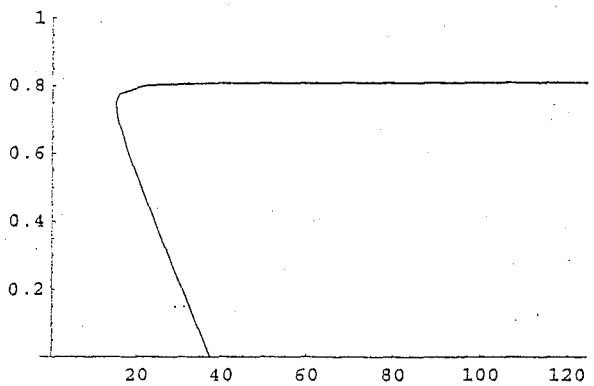

- Graphics -

```
LP = {{20.9, 0.44}, {21.84, 0.42}, {22.26, 0.41}, {22.66, 0.4},
  {23.31, 0.383}, {24.52, 0.35}, {25.88, 0.3123}, {26.31, 0.3}, {26.66, 0.29},
  {27.02, 0.28}, {29.41, 0.2116}, {33.05, 0.1068}, {36.7, 0.0007455}}
```

```
{{20.9, 0.44}, {21.84, 0.42}, {22.26, 0.41}, {22.66, 0.4},
 {23.31, 0.383}, {24.52, 0.35}, {25.88, 0.3123}, {26.31, 0.3}, {26.66, 0.29},
 {27.02, 0.28}, {29.41, 0.2116}, {33.05, 0.1068}, {36.7, 0.0007455}}
```

```
graphLP = ListPlot[LP, PlotRange → {0, 1}, PlotJoined → True]
```

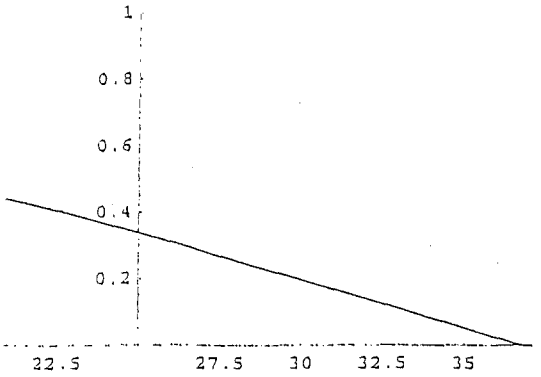

- Graphics -

- Graphics -

```
Show[Plot[(530 + 121 L + √(230900 - 83740 L + 6241 L²))/(50 + 210 L),
  {L, 0, 70}, AxesStyle → Thickness[0.005], PlotRange → {0, 1},
  GridLines → Automatic, AxesLabel → {"gamma", "Lamda"}],
 Plot[(530 + 121 L - √(230900 - 83740 L + 6241 L²))/(50 + 210 L), {L, 0, 70}, AxesStyle → Thickness[0.005],
  PlotRange → {0, 1}, GridLines → Automatic, AxesLabel → {"gamma", "Lamda"}],
 Plot[(20 L)/(5 + 21 L), {L, 0, 70}, AxesStyle → Thickness[0.005], PlotRange → {0, 1},
  GridLines → Automatic, AxesLabel → {"gamma", "Lamda"}],
 Plot[20 / 21, {L, 0, 70}, AxesStyle → Thickness[0.005], PlotRange → {0, 1},
  GridLines → Automatic, AxesLabel → {"gamma", "Lamda"}], graph3, graphLP]
```

Plot::plnr : $\frac{530 + 121\,L + \sqrt{230900 - 83740\,L + 6241\,L^2}}{50 + 210\,L}$ is not a machine-size real number at L = 5.936615990156159`.

Plot::plnr : $\frac{530 + 121\,L + \sqrt{230900 - 83740\,L + 6241\,L^2}}{50 + 210\,L}$ is not a machine-size real number at L = 4.347283795319742`.

Plot::plnr : $\frac{530 + 121\,L + \sqrt{230900 - 83740\,L + 6241\,L^2}}{50 + 210\,L}$ is not a machine-size real number at L = 3.9377689773115425`.

General::stop : Further output of Plot::plnr will be suppressed during this calculation.

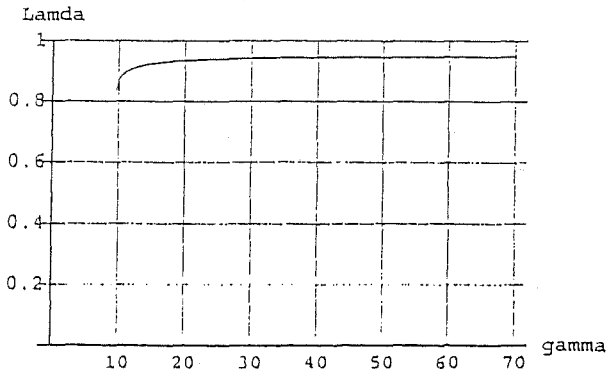

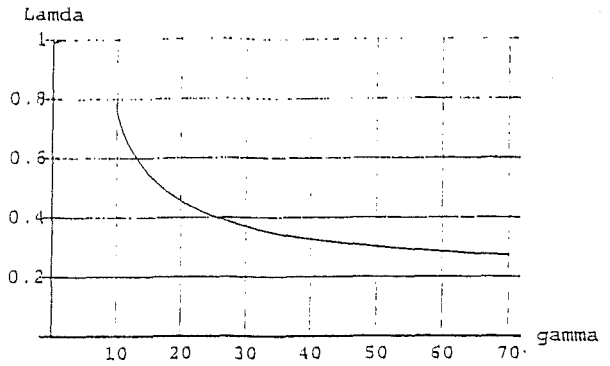
Lamda
1
0.8
0.6
0.4
0.2
10
20
30
40
50
60
70
gamma

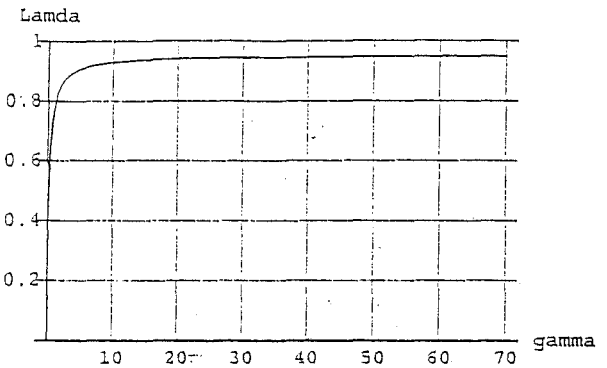
Lamda
1
0.8
0.6
0.4
0.2
10
20
30
40
50
60
70
gamma

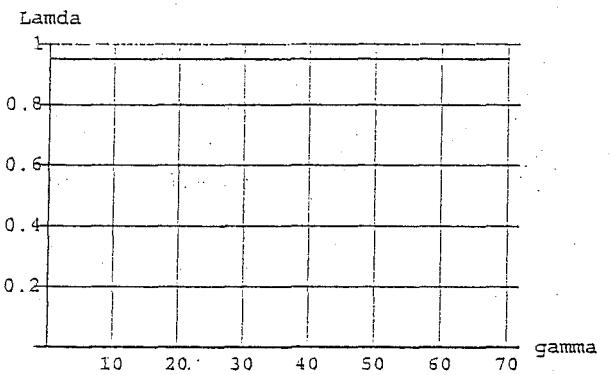
Lamda
1
0.8
0.6
0.4
0.2
10
20
30
40
50
60
70
gamma

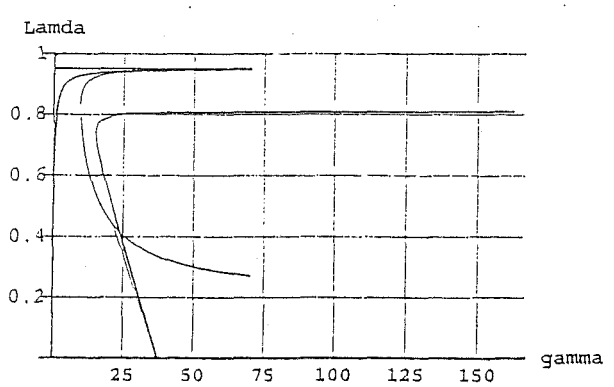
Lamda
1
0.8
0.6
0.4
0.2
25
50
75
100
125
150
gamma

- Graphics -

B5 Solving the steady state E2 for the two-compartment model (equal growth parameter)

PART 1 OF y1

```
equation7 =
 g * y2 + (g1 * g2 * y3) - (U * y1 * y4 / (y4 + h)) - d (y4 - (2 * L - y2 - g2 * y3 - y4 - y2 - g2 * y3))
```

$$g\,y2 + g1\,g2\,y3 - \frac{U\,y1\,y4}{h + y4} - d\,(-2\,L + 2\,y2 + 2\,g2\,y3 + 2\,y4)$$

```
y1 =
 (20 * (4835 - 3700 * g - 158 * L + 2 * Sqrt[6310900 + 4410000 * g^2 - 399740 * L + 6241 * L^2 + 200 *
        g * (-52130 + 1659 * L)])) / (79 * (-9 + 20 * g))
```

$$\frac{20\left(4835 - 3700\,g - 158\,L + 2\sqrt{6310900 + 4410000\,g^2 - 399740\,L + 6241\,L^2 + 200\,g\,(-52130 + 1659\,L)}\right)}{79\,(-9 + 20\,g)}$$

```
y2 = (y1 + 100) / 16
```

$$\frac{1}{16}\left(100 + \frac{1}{79\,(-9 + 20\,g)}\left(20\left(4835 - 3700\,g - 158\,L + 2\sqrt{6310900 + 4410000\,g^2 - 399740\,L + 6241\,L^2 + 200\,g\,(-52130 + 1659\,L)}\right)\right)\right)$$

```
y3 = ((-4 / 5) + (1 - g)) * y1 + (100 * (1 - g))
```

$$100\,(1 - g) + \frac{1}{79\,(-9 + 20\,g)}\left(20\left(\frac{1}{5} - g\right)\left(4835 - 3700\,g - 158\,L + 2\sqrt{6310900 + 4410000\,g^2 - 399740\,L + 6241\,L^2 + 200\,g\,(-52130 + 1659\,L)}\right)\right)$$

```
Sequation7 =
 equation7 /. {g1 → 0.25, g2 → 0.25, h → 5, U → 1, C → 100, m → 1, Q → 1 / 20} // Simplify
```

$$\frac{1}{79\,(-9 + 20\,g)\,(5 + y4)}\left(-16175. - 197.5\,L + 2.5\sqrt{6310900 + 4410000\,g^2 - 399740\,L + 6241\,L^2 + 200\,g\,(-52130 + 1659\,L)} - 99935.\,y4 + 3120.5\,L\,y4 - 39.5\sqrt{6310900 + 4410000\,g^2 - 399740\,L + 6241\,L^2 + 200\,g\,(-52130 + 1659\,L)}\,y4 + g\,(44750. + 82950.\,y4) + d\left(113400. - 3555.\,L - 45.\sqrt{6310900 + 4410000\,g^2 - 399740\,L + 6241\,L^2 + 200\,g\,(-52130 + 1659\,L)} + 29790.\,y4 - 711.\,L\,y4 - 9.\sqrt{6310900 + 4410000\,g^2 - 399740\,L + 6241\,L^2 + 200\,g\,(-52130 + 1659\,L)}\,y4 + 1422.\,y4^2 + g^2\,(210000. + 42000.\,y4) + g\left(-346500. + 7900.\,L + 100.\sqrt{6310900 + 4410000\,g^2 - 399740\,L + 6241\,L^2 + 200\,g\,(-52130 + 1659\,L)} - 85100.\,y4 + 1580.\,L\,y4 + 20.\sqrt{6310900 + 4410000\,g^2 - 399740\,L + 6241\,L^2 + 200\,g\,(-52130 + 1659\,L)}\,y4 - 3160.\,y4^2\right)\right)\right)$$

```
Result = Solve[Sequation7 == 0, y4] // Simplify
```

$$\{\{y4 \to \left(-6.18568\times10^{31} + 1.84391\times10^{31}\,d + 5.13436\times10^{31}\,g - 5.26743\times10^{31}\,d\,g + 2.59967\times10^{31}\,d\,g^2 + 1.9315\times10^{30}\,L - 4.40088\times10^{29}\,d\,L + 9.77973\times10^{29}\,d\,g\,L - 2.44493\times10^{28}\sqrt{4.41\times10^6\,g^2 + 6241.\,(-35.8228+L)\,(-28.2278+L) + g\,(-1.0426\times10^7 + 331800.\,L)} - 5.57073\times10^{27}\,d\sqrt{4.41\times10^6\,g^2 + 6241.\,(-35.8228+L)\,(-28.2278+L) + g\,(-1.0426\times10^7 + 331800.\,L)} + 1.23794\times10^{28}\,d\,g\sqrt{4.41\times10^6\,g^2 + 6241.\,(-35.8228+L)\,(-28.2278+L) + g\,(-1.0426\times10^7 + 331800.\,L)} - 0.5\sqrt{\left(-4.\,d\,(-1.76035\times10^{30} + 3.91189\times10^{30}\,g)\left(2.00237\times10^{31} - 5.53978\times10^{31}\,g + 2.44493\times10^{29}\,L - 3.09485\times10^{27}\sqrt{4.41\times10^6\,g^2 + 6241.\,(-35.8228+L)\,(-28.2278+L) + g\,(-1.0426\times10^7 + 331800.\,L)} + d\left(-1.40382\times10^{32} - 2.59967\times10^{32}\,g^2 + 4.40088\times10^{30}\,L + 5.57073\times10^{28}\sqrt{4.41\times10^6\,g^2 + 6241.\,(-35.8228+L)\,(-28.2278+L) + g\,(-1.0426\times10^7 + 331800.\,L)} + g\left(4.28946\times10^{32} - 9.77973\times10^{30}\,L - 1.23794\times10^{29}\sqrt{4.41\times10^6\,g^2 + 6241.\,(-35.8228+L)\,(-28.2278+L) + g\,(-1.0426\times10^7 + 331800.\,L)}\right)\right)\right) + \left(1.23714\times10^{32} - 1.02687\times10^{32}\,g - 3.86299\times10^{30}\,L + 4.88986\times10^{28}\sqrt{4.41\times10^6\,g^2 + 6241.\,(-35.8228+L)\,(-28.2278+L) + g\,(-1.0426\times10^7 + 331800.\,L)} + d\left(-3.68782\times10^{31} - 5.19935\times10^{31}\,g^2 + 8.80175\times10^{29}\,L + 1.11415\times10^{28}\sqrt{4.41\times10^6\,g^2 + 6241.\,(-35.8228+L)\,(-28.2278+L) + g\,(-1.0426\times10^7 + 331800.\,L)} + g\left(1.05349\times10^{32} - 1.95595\times10^{30}\,L - 2.47588\times10^{28}\sqrt{4.41\times10^6\,g^2 + 6241.\,(-35.8228+L)\,(-28.2278+L) + g\,(-1.0426\times10^7 + 331800.\,L)}\right)\right)\right)\text{^}2\right)\Big/ (d\,(-1.76035\times10^{30} + 3.91189\times10^{30}\,g))\},\ \{y4 \to \left(-6.18568\times10^{31} + 1.84391\times10^{31}\,d + 5.13436\times10^{31}\,g - 5.26743\times10^{31}\,d\,g + 2.59967\times10^{31}\,d\,g^2 + 1.9315\times10^{30}\,L - 4.40088\times10^{29}\,d\,L + 9.77973\times10^{29}\,d\,g\,L - 2.44493\times10^{28}\sqrt{4.41\times10^6\,g^2 + 6241.\,(-35.8228+L)\,(-28.2278+L) + g\,(-1.0426\times10^7 + 331800.\,L)} - 5.57073\times10^{27}\,d\sqrt{4.41\times10^6\,g^2 + 6241.\,(-35.8228+L)\,(-28.2278+L) + g\,(-1.0426\times10^7 + 331800.\,L)} + 1.23794\times10^{28}\,d\,g\sqrt{4.41\times10^6\,g^2 + 6241.\,(-35.8228+L)\,(-28.2278+L) + g\,(-1.0426\times10^7 + 331800.\,L)} + 0.5\sqrt{\left(-4.\,d\,(-1.76035\times10^{30} + 3.91189\times10^{30}\,g)\left(2.00237\times10^{31} - 5.53978\times10^{31}\,g + 2.44493\times10^{29}\,L - 3.09485\times10^{27}\sqrt{4.41\times10^6\,g^2 + 6241.\,(-35.8228+L)\,(-28.2278+L) + g\,(-1.0426\times10^7 + 331800.\,L)} + d\left(-1.40382\times10^{32} - 2.59967\times10^{32}\,g^2 + 4.40088\times10^{30}\,L + 5.57073\times10^{28}\sqrt{4.41\times10^6\,g^2 + 6241.\,(-35.8228+L)\,(-28.2278+L) + g\,(-1.0426\times10^7 + 331800.\,L)} + g\left(4.28946\times10^{32} - 9.77973\times10^{30}\,L - 1.23794\times10^{29}\sqrt{4.41\times10^6\,g^2 + 6241.\,(-35.8228+L)\,(-28.2278+L) + g\,(-1.0426\times10^7 + 331800.\,L)}\right)\right)\right) +$$

$$\left(1.23714\times10^{32}-1.02687\times10^{32}\,g-3.86299\times10^{30}\,L+4.88986\times10^{30}\sqrt{(4.41\times10^{6}\,g^2+6241.\,(-35.8228+L)\,(-28.2278+L)+g\,(-1.0426\times10^{7}+331800.\,L))}+d\left(-3.68782\times10^{31}-5.19935\times10^{31}\,g^2+8.80175\times10^{29}\,L+1.11415\times10^{28}\sqrt{(4.41\times10^{6}\,g^2+6241.\,(-35.8228+L)\,(-28.2278+L)+g\,(-1.0426\times10^{7}+331800.\,L))}+g\left(1.05349\times10^{32}-1.95595\times10^{30}\,L-2.47588\times10^{28}\sqrt{(4.41\times10^{6}\,g^2+6241.\,(-35.8228+L)\,(-28.2278+L)+g\,(-1.0426\times10^{7}+331800.\,L))}\right)\right)\right)\text{^}2\right)\Big/\left(d\,(-1.76035\times10^{30}+3.91189\times10^{30}\,g)\right)\Big\}\Big\}$$

```
result1 = Result /. {d → 0.02} // Simplify
```

$$\Big\{\Big\{y4\to\Big(-3.0744\times10^{33}+2.5145\times10^{33}\,g+2.59967\times10^{31}\,g^2+9.61347\times10^{31}\,L+9.77973\times10^{29}\,g\,L-1.22804\times10^{30}\sqrt{4.41\times10^{6}\,g^2+6241.\,(-35.8228+L)\,(-28.2278+L)+g\,(-1.0426\times10^{7}+331800.\,L)}+1.23794\times10^{28}\,g\sqrt{4.41\times10^{6}\,g^2+6241.\,(-35.8228+L)\,(-28.2278+L)+g\,(-1.0426\times10^{7}+331800.\,L)}-25.\sqrt{(-0.08\,(-1.76035\times10^{30}+3.91189\times10^{30}\,g)\left(1.7216\times10^{31}-5.19935\times10^{30}\,g^2+3.32511\times10^{29}\,L-1.9807\times10^{27}\sqrt{(4.41\times10^{6}\,g^2+6241.\,(-35.8228+L)\,(-28.2278+L)+g\,(-1.0426\times10^{7}+331800.\,L))}+g\left(-4.68189\times10^{31}-1.95595\times10^{29}\,L-2.47588\times10^{27}\sqrt{(4.41\times10^{6}\,g^2+6241.\,(-35.8228+L)\,(-28.2278+L)+g\,(-1.0426\times10^{7}+331800.\,L))}\right)\right)+\left(1.22976\times10^{32}-1.03987\times10^{30}\,g^2-3.84539\times10^{30}\,L+4.91215\times10^{28}\sqrt{(4.41\times10^{6}\,g^2+6241.\,(-35.8228+L)\,(-28.2278+L)+g\,(-1.0426\times10^{7}+331800.\,L))}+g\left(-1.0058\times10^{32}-3.91189\times10^{28}\,L-4.95176\times10^{26}\sqrt{(4.41\times10^{6}\,g^2+6241.\,(-35.8228+L)\,(-28.2278+L)+g\,(-1.0426\times10^{7}+331800.\,L))}\right)\right)\text{^}2\right)\Big/(-1.76035\times10^{30}+3.91189\times10^{30}\,g)\Big\},\Big\{y4\to\Big(-3.0744\times10^{33}+2.5145\times10^{33}\,g+2.59967\times10^{31}\,g^2+9.61347\times10^{31}\,L+9.77973\times10^{29}\,g\,L-1.22804\times10^{30}\sqrt{4.41\times10^{6}\,g^2+6241.\,(-35.8228+L)\,(-28.2278+L)+g\,(-1.0426\times10^{7}+331800.\,L)}+1.23794\times10^{28}\,g\sqrt{4.41\times10^{6}\,g^2+6241.\,(-35.8228+L)\,(-28.2278+L)+g\,(-1.0426\times10^{7}+331800.\,L)}+25.\sqrt{(-0.08\,(-1.76035\times10^{30}+3.91189\times10^{30}\,g)\left(1.7216\times10^{31}-5.19935\times10^{30}\,g^2+3.32511\times10^{29}\,L-1.9807\times10^{27}\sqrt{(4.41\times10^{6}\,g^2+6241.\,(-35.8228+L)\,(-28.2278+L)+g\,(-1.0426\times10^{7}+331800.\,L))}+g\left(-4.68189\times10^{31}-1.95595\times10^{29}\,L-2.47588\times10^{27}\sqrt{(4.41\times10^{6}\,g^2+6241.\,(-35.8228+L)\,(-28.2278+L)+g\,(-1.0426\times10^{7}+331800.\,L))}\right)\right)+\left(1.22976\times10^{32}-1.03987\times10^{30}\,g^2-3.84539\times10^{30}\,L+4.91215\times10^{28}\sqrt{(4.41\times10^{6}\,g^2+6241.\,(-35.8228+L)\,(-28.2278+L)+g\,(-1.0426\times10^{7}+331800.\,L))}+g\left(-1.0058\times10^{32}-3.91189\times10^{28}\,L-4.95176\times10^{26}\sqrt{(4.41\times10^{6}\,g^2+6241.\,(-35.8228+L)\,(-28.2278+L)+g\,(-1.0426\times10^{7}+331800.\,L))}\right)\right)\text{^}2\right)\Big/(-1.76035\times10^{30}+3.91189\times10^{30}\,g)\Big\}\Big\}$$

```
y4 = (-3.074399328764478`*^33 + 2.5145038077964823`*^33 g +
     2.599674082499317`*^31 g^2 + 9.613470963078546`*^31 L + 9.779726310354575`*^29 g L -
     1.228036518971106`*^30 √(4.41`*^6 g^2 + 6241.` (-35.82278481012657` + L)
          (-28.227848101265828` + L) + g (-1.0426`*^7 + 331800.` L)) +
     1.237940039285389`*^28 g √(4.41`*^6 g^2 + 6241.` (-35.82278481012657` + L)
          (-28.227848101265828` + L) + g (-1.0426`*^7 + 331800.` L)) -
     25.` √(-0.08` (-1.7603507358638234`*^30 + 3.911890524141829`*^30 g)
          (1.7216032126341905`*^31 - 5.199348164998634`*^30 g^2 + 3.325106945520555`*^29 L -
            1.9807040628566228`*^27 √(4.41`*^6 g^2 + 6241.` (-35.82278481012657` + L)
                 (-28.227848101265828` + L) + g (-1.0426`*^7 + 331800.` L)) +
            g (-4.681889228577342`*^31 - 1.955945262070915`*^29 L -
               2.475880078570778`*^27 √(4.41`*^6 g^2 + 6241.` (-35.82278481012657` + L)
                    (-28.227848101265828` + L) + g (-1.0426`*^7 + 331800.` L)))) +
          (1.2297597315057913`*^32 - 1.0398696329997269`*^30 g^2 - 3.8453883852314183`*^30 L +
            4.912146075884424`*^28 √(4.41`*^6 g^2 + 6241.` (-35.82278481012657` + L)
                 (-28.227848101265828` + L) + g (-1.0426`*^7 + 331800.` L)) +
            g (-1.005801523118593`*^32 - 3.9118905241418296`*^28 L -
               4.9517601571415564`*^26 √(4.41`*^6 g^2 + 6241.` (-35.82278481012657` + L)
                    (-28.227848101265828` + L) + g (-1.0426`*^7 + 331800.` L)))))^2)) /
     (-1.7603507358638234`*^30 + 3.911890524141829`*^30 g)

(-3.0744×10^33 + 2.5145×10^33 g +
   2.59967×10^31 g^2 + 9.61347×10^31 L + 9.77973×10^29 g L - 1.22804×10^30
    √(4.41×10^6 g^2 + 6241. (-35.8228 + L) (-28.2278 + L) + g (-1.0426×10^7 + 331800. L)) +
   1.23794×10^28 g
    √(4.41×10^6 g^2 + 6241. (-35.8228 + L) (-28.2278 + L) + g (-1.0426×10^7 + 331800. L)) -
   25. √(-0.08 (-1.76035×10^30 + 3.91189×10^30 g)
        (1.7216×10^31 - 5.19935×10^30 g^2 + 3.32511×10^29 L - 1.9807×10^27
          √(4.41×10^6 g^2 + 6241. (-35.8228 + L) (-28.2278 + L) + g (-1.0426×10^7 + 331800. L)) +
         g (-4.68189×10^31 - 1.95595×10^29 L - 2.47588×10^27 √(4.41×10^6 g^2 +
              6241. (-35.8228 + L) (-28.2278 + L) + g (-1.0426×10^7 + 331800. L)))) +
       (1.22976×10^32 - 1.03987×10^30 g^2 - 3.84539×10^30 L + 4.91215×10^28
          √(4.41×10^6 g^2 + 6241. (-35.8228 + L) (-28.2278 + L) + g (-1.0426×10^7 + 331800. L)) +
         g (-1.0058×10^32 - 3.91189×10^28 L - 4.95176×10^26
            √(4.41×10^6 g^2 + 6241. (-35.8228 + L) (-28.2278 + L) +
              g (-1.0426×10^7 + 331800. L)))^2)) / (-1.76035×10^30 + 3.91189×10^30 g)
```

B6 Solving the eigenvalues about E1 for the two-compartment model (equal growth parameter)

```
d = 0.02
```

```
0.02
```

```
y1 =
 (20 * (4835 - 3700 * g - 158 * L + 2 * Sqrt[6310900 + 4410000 * g^2 - 399740 * L + 6241 * L^2 + 200 *
          g * (-52130 + 1659 * L)])) / (79 * (-9 + 20 * g))
```

$$\frac{20\left(4835 - 3700\,g - 158\,L + 2\sqrt{6310900 + 4410000\,g^2 - 399740\,L + 6241\,L^2 + 200\,g\,(-52130 + 1659\,L)}\right)}{79\,(-9 + 20\,g)}$$

```
x1 = y1
```

$$\frac{20\left(4835 - 3700\,g - 158\,L + 2\sqrt{6310900 + 4410000\,g^2 - 399740\,L + 6241\,L^2 + 200\,g\,(-52130 + 1659\,L)}\right)}{79\,(-9 + 20\,g)}$$

```
y2 = (y1 + 100) / 16
```

$$\frac{1}{16}\left(100 + \frac{1}{79\,(-9 + 20\,g)}\left(20\left(4835 - 3700\,g - 158\,L + 2\sqrt{6310900 + 4410000\,g^2 - 399740\,L + 6241\,L^2 + 200\,g\,(-52130 + 1659\,L)}\right)\right)\right)$$

```
x2 = y2
```

$$\frac{1}{16}\left(100 + \frac{1}{79\,(-9 + 20\,g)}\left(20\left(4835 - 3700\,g - 158\,L + 2\sqrt{6310900 + 4410000\,g^2 - 399740\,L + 6241\,L^2 + 200\,g\,(-52130 + 1659\,L)}\right)\right)\right)$$

```
y3 = ((-4 / 5) + (1 - g)) * y1 + (100 * (1 - g))
```

$$100\,(1 - g) + \frac{1}{79\,(-9 + 20\,g)}\left(20\left(\frac{1}{5} - g\right)\left(4835 - 3700\,g - 158\,L + 2\sqrt{6310900 + 4410000\,g^2 - 399740\,L + 6241\,L^2 + 200\,g\,(-52130 + 1659\,L)}\right)\right)$$

```
x3 = y3
```

$$100\,(1 - g) + \frac{1}{79\,(-9 + 20\,g)}\left(20\left(\frac{1}{5} - g\right)\left(4835 - 3700\,g - 158\,L + 2\sqrt{6310900 + 4410000\,g^2 - 399740\,L + 6241\,L^2 + 200\,g\,(-52130 + 1659\,L)}\right)\right)$$

```
c11 = 1 - x1 / (10 * x2) - x3 / (x1 + 100) + (x1 * x3 / (x1 + 100) ^ 2) - g - d
```

$$1 - d - g - \frac{32\left(4835 - 3700\,g - 158\,L + 2\sqrt{6310900 + 4410000\,g^2 - 399740\,L + 6241\,L^2 + 200\,g\,(-52130 + 1659\,L)}\right)}{79\,(-9 + 20\,g)\left(100 + \frac{20\left(4835 - 3700\,g - 158\,L + 2\sqrt{6310900 + 4410000\,g^2 - 399740\,L + 6241\,L^2 + 200\,g\,(-52130 + 1659\,L)}\right)}{79\,(-9 + 20\,g)}\right)} +$$

$$\left(20\left(4835 - 3700\,g - 158\,L + 2\sqrt{6310900 + 4410000\,g^2 - 399740\,L + 6241\,L^2 + 200\,g\,(-52130 + 1659\,L)}\right)\left(100\,(1 - g) + \frac{1}{79\,(-9 + 20\,g)}\left(20\left(\frac{1}{5} - g\right)\left(4835 - 3700\,g - 158\,L + 2\sqrt{6310900 + 4410000\,g^2 - 399740\,L + 6241\,L^2 + 200\,g\,(-52130 + 1659\,L)}\right)\right)\right)\right) \Big/ \left(79\,(-9 + 20\,g)\left(100 + \frac{1}{79\,(-9 + 20\,g)}\left(20\left(4835 - 3700\,g - 158\,L + 2\sqrt{6310900 + 4410000\,g^2 - 399740\,L + 6241\,L^2 + 200\,g\,(-52130 + 1659\,L)}\right)\right)\right)^2\right) -$$

$$\frac{100\,(1 - g) + \frac{20\left(\frac{1}{5} - g\right)\left(4835 - 3700\,g - 158\,L + 2\sqrt{6310900 + 4410000\,g^2 - 399740\,L + 6241\,L^2 + 200\,g\,(-52130 + 1659\,L)}\right)}{79\,(-9 + 20\,g)}}{100 + \frac{20\left(4835 - 3700\,g - 158\,L + 2\sqrt{6310900 + 4410000\,g^2 - 399740\,L + 6241\,L^2 + 200\,g\,(-52130 + 1659\,L)}\right)}{79\,(-9 + 20\,g)}}$$

```
c21 = (2 * L - x2 - (x3 / 4) - y4 - y2 - (y3 / 4)) /
    (2 * L - x2 - (x3 / 4) - y4 - y2 - (y3 / 4) + 5) + (x2 * x3 / (x1 + 100) ^ 2)
```

$$\frac{100\,(1 - g) + \frac{20\left(\frac{1}{5} - g\right)\left(4835 - 3700\,g - 158\,L + 2\sqrt{6310900 + 4410000\,g^2 - 399740\,L + 6241\,L^2 + 200\,g\,(-52130 + 1659\,L)}\right)}{79\,(-9 + 20\,g)}}{16\left(100 + \frac{20\left(4835 - 3700\,g - 158\,L + 2\sqrt{6310900 + 4410000\,g^2 - 399740\,L + 6241\,L^2 + 200\,g\,(-52130 + 1659\,L)}\right)}{79\,(-9 + 20\,g)}\right)} +$$

$$\left(2\,L + \frac{1}{8}\left(-100 - \frac{1}{79\,(-9 + 20\,g)}\left(20\left(4835 - 3700\,g - 158\,L + 2\sqrt{6310900 + 4410000\,g^2 - 399740\,L + 6241\,L^2 + 200\,g\,(-52130 + 1659\,L)}\right)\right)\right) + \frac{1}{2}\left(-100\,(1 - g) - \frac{1}{79\,(-9 + 20\,g)}\left(20\left(\frac{1}{5} - g\right)\left(4835 - 3700\,g - 158\,L + 2\sqrt{6310900 + 4410000\,g^2 - 399740\,L + 6241\,L^2 + 200\,g\,(-52130 + 1659\,L)}\right)\right)\right) - y4\right) \Big/ \left(5 + 2\,L + \frac{1}{8}\left(-100 - \frac{1}{79\,(-9 + 20\,g)}\left(20\left(4835 - 3700\,g - 158\,L + 2\sqrt{6310900 + 4410000\,g^2 - 399740\,L + 6241\,L^2 + 200\,g\,(-52130 + 1659\,L)}\right)\right)\right) + \frac{1}{2}\left(-100\,(1 - g) - \frac{1}{79\,(-9 + 20\,g)}\left(20\left(\frac{1}{5} - g\right)\left(4835 - 3700\,g - 158\,L + 2\sqrt{6310900 + 4410000\,g^2 - 399740\,L + 6241\,L^2 + 200\,g\,(-52130 + 1659\,L)}\right)\right)\right) - y4\right)$$

c31 = -x2 * x3 / ((1 / 4) * (x1 + 100) ^ 2)

$$\left(\left(-100 - \frac{1}{79\,(-9+20\,g)}\left(20\left(4835 - 3700\,g - 158\,L + 2\sqrt{6310900 + 4410000\,g^2 - 399740\,L + 6241\,L^2 + 200\,g\,(-52130 + 1659\,L)}\right)\right)\right)\left(100\,(1-g) + \frac{1}{79\,(-9+20\,g)}\left(20\left(\frac{1}{5} - g\right)\left(4835 - 3700\,g - 158\,L + 2\sqrt{6310900 + 4410000\,g^2 - 399740\,L + 6241\,L^2 + 200\,g\,(-52130 + 1659\,L)}\right)\right)\right)\right) \Big/ \left(4\left(100 + \frac{1}{79\,(-9+20\,g)}\left(20\left(4835 - 3700\,g - 158\,L + 2\sqrt{6310900 + 4410000\,g^2 - 399740\,L + 6241\,L^2 + 200\,g\,(-52130 + 1659\,L)}\right)\right)\right)^2\right)$$

c41 = d

d

c51 = 0

0

c61 = 0

0

c71 = 0

0

c12 = x1 ^ 2 / (20 * x2 ^ 2)

$$\left(5120\left(4835 - 3700\,g - 158\,L + 2\sqrt{6310900 + 4410000\,g^2 - 399740\,L + 6241\,L^2 + 200\,g\,(-52130 + 1659\,L)}\right)^2\right) \Big/ \left(6241\,(-9+20\,g)^2\left(100 + \frac{1}{79\,(-9+20\,g)}\left(20\left(4835 - 3700\,g - 158\,L + 2\sqrt{6310900 + 4410000\,g^2 - 399740\,L + 6241\,L^2 + 200\,g\,(-52130 + 1659\,L)}\right)\right)\right)^2\right)$$

```
c22 = -x1 / (2 * L - x2 - (x3 / 4) - y4 - y2 - (y3 / 4) + 5) +
   x1 * (2 * L - x2 - (x3 / 4) - y4 - y2 - (y3 / 4)) / (2 * L - x2 - (x3 / 4) - y4 - y2 - (y3 / 4) + 5) ^ 2 -
   x3 / (x1 + 100) - g - d
```

$$-d-g-\frac{100\,(1-g)+\frac{20\left(\frac{1}{5}-g\right)\left(4835-3700\,g-158\,L+2\sqrt{6310900+4410000\,g^2-399740\,L+6241\,L^2+200\,g\,(-52130+1659\,L)}\right)}{79\,(-9+20\,g)}}{100+\frac{20\left(4835-3700\,g-158\,L+2\sqrt{6310900+4410000\,g^2-399740\,L+6241\,L^2+200\,g\,(-52130+1659\,L)}\right)}{79\,(-9+20\,g)}}+$$

$$\left(20\left(4835-3700\,g-158\,L+2\sqrt{6310900+4410000\,g^2-399740\,L+6241\,L^2+200\,g\,(-52130+1659\,L)}\right)\right.$$
$$\left(2\,L+\frac{1}{8}\left(-100-\frac{1}{79\,(-9+20\,g)}\left(20\left(4835-3700\,g-158\,L+\right.\right.\right.\right.$$
$$\left.\left.\left.\left.2\sqrt{6310900+4410000\,g^2-399740\,L+6241\,L^2+200\,g\,(-52130+1659\,L)}\right)\right)\right)+$$
$$\frac{1}{2}\left(-100\,(1-g)-\frac{1}{79\,(-9+20\,g)}\left(20\left(\frac{1}{5}-g\right)\left(4835-3700\,g-158\,L+\right.\right.\right.$$
$$\left.\left.\left.2\sqrt{6310900+4410000\,g^2-399740\,L+6241\,L^2+200\,g\,(-52130+1659\,L)}\right)\right)\right)-y4\Bigg)\Bigg)\Bigg/$$
$$\left(79\,(-9+20\,g)\left(5+2\,L+\frac{1}{8}\left(-100-\frac{1}{79\,(-9+20\,g)}\left(20\left(4835-3700\,g-158\,L+2\right.\right.\right.\right.\right.$$
$$\left.\left.\left.\left.\sqrt{6310900+4410000\,g^2-399740\,L+6241\,L^2+200\,g\,(-52130+1659\,L)}\right)\right)\right)+$$
$$\frac{1}{2}\left(-100\,(1-g)-\frac{1}{79\,(-9+20\,g)}\left(20\left(\frac{1}{5}-g\right)\left(4835-3700\,g-158\,L+2\right.\right.\right.$$
$$\left.\left.\left.\left.\sqrt{6310900+4410000\,g^2-399740\,L+6241\,L^2+200\,g\,(-52130+1659\,L)}\right)\right)\right)-$$
$$y4\Big)^2\Bigg)-\left(20\left(4835-3700\,g-158\,L+2\right.\right.$$
$$\left.\left.\sqrt{6310900+4410000\,g^2-399740\,L+6241\,L^2+200\,g\,(-52130+1659\,L)}\right)\right)\Bigg/$$
$$\left(79\,(-9+20\,g)\left(5+2\,L+\frac{1}{8}\left(-100-\frac{1}{79\,(-9+20\,g)}\left(20\left(4835-3700\,g-158\,L+\right.\right.\right.\right.\right.$$
$$\left.\left.\left.\left.2\sqrt{6310900+4410000\,g^2-399740\,L+6241\,L^2+200\,g\,(-52130+1659\,L)}\right)\right)\right)+$$
$$\frac{1}{2}\left(-100\,(1-g)-\frac{1}{79\,(-9+20\,g)}\left(20\left(\frac{1}{5}-g\right)\left(4835-3700\,g-158\,L+\right.\right.\right.$$
$$\left.\left.\left.\left.2\sqrt{6310900+4410000\,g^2-399740\,L+6241\,L^2+200\,g\,(-52130+1659\,L)}\right)\right)\right)-y4\Bigg)\Bigg)$$

```
c32 = x3 / ((1 / 4) * (x1 + 100))
```

$$\frac{4\left(100\,(1-g)+\frac{20\left(\frac{1}{5}-g\right)\left(4835-3700\,g-158\,L+2\sqrt{6310900+4410000\,g^2-399740\,L+6241\,L^2+200\,g\,(-52130+1659\,L)}\right)}{79\,(-9+20\,g)}\right)}{100+\frac{20\left(4835-3700\,g-158\,L+2\sqrt{6310900+4410000\,g^2-399740\,L+6241\,L^2+200\,g\,(-52130+1659\,L)}\right)}{79\,(-9+20\,g)}}$$

```
c42 = 0
```

```
0
```

```
c52 = d
```

```
d
```

```
c62 = 0
```

```
0
```

c72 = -d

-d

c13 = -x1 / (x1 + 100)

$$-\frac{20\left(4835-3700\,g-158\,L+2\sqrt{6310900+4410000\,g^2-399740\,L+6241\,L^2+200\,g\,(-52130+1659\,L)}\right)}{79\,(-9+20\,g)\left(100+\frac{20\left(4835-3700\,g-158\,L+2\sqrt{6310900+4410000\,g^2-399740\,L+6241\,L^2+200\,g\,(-52130+1659\,L)}\right)}{79\,(-9+20\,g)}\right)}$$

c23 = -(1 / 4) * x1 / (2 * L + 5 - x2 - (x3 / 4) - y4 - y2 - (y3 / 4)) +
(1 / 4) * x1 (2 * L - x2 - (x3 / 4) - y4 - y2 - (y3 / 4)) /
((2 * L + 5 - x2 - (x3 / 4) - y4 - y2 - (y3 / 4))) ^ 2 - (x2 / (x1 + 100))

$$-\frac{1}{16}+\left(5\left(4835-3700\,g-158\,L+2\sqrt{6310900+4410000\,g^2-399740\,L+6241\,L^2+200\,g\,(-52130+1659\,L)}\right)\left(2\,L+\frac{1}{8}\left(-100-\frac{1}{79\,(-9+20\,g)}\left(20\left(4835-3700\,g-158\,L+2\sqrt{6310900+4410000\,g^2-399740\,L+6241\,L^2+200\,g\,(-52130+1659\,L)}\right)\right)\right)+\frac{1}{2}\left(-100\,(1-g)-\frac{1}{79\,(-9+20\,g)}\left(20\left(\frac{1}{5}-g\right)\left(4835-3700\,g-158\,L+2\sqrt{6310900+4410000\,g^2-399740\,L+6241\,L^2+200\,g\,(-52130+1659\,L)}\right)\right)\right)-y4\right)\right)\Big/\left(79\,(-9+20\,g)\left(5+2\,L+\frac{1}{8}\left(-100-\frac{1}{79\,(-9+20\,g)}\left(20\left(4835-3700\,g-158\,L+2\sqrt{6310900+4410000\,g^2-399740\,L+6241\,L^2+200\,g\,(-52130+1659\,L)}\right)\right)\right)+\frac{1}{2}\left(-100\,(1-g)-\frac{1}{79\,(-9+20\,g)}\left(20\left(\frac{1}{5}-g\right)\left(4835-3700\,g-158\,L+2\sqrt{6310900+4410000\,g^2-399740\,L+6241\,L^2+200\,g\,(-52130+1659\,L)}\right)\right)\right)-y4\right)^2\right)-\left(5\left(4835-3700\,g-158\,L+2\sqrt{6310900+4410000\,g^2-399740\,L+6241\,L^2+200\,g\,(-52130+1659\,L)}\right)\right)\Big/\left(79\,(-9+20\,g)\left(5+2\,L+\frac{1}{8}\left(-100-\frac{1}{79\,(-9+20\,g)}\left(20\left(4835-3700\,g-158\,L+2\sqrt{6310900+4410000\,g^2-399740\,L+6241\,L^2+200\,g\,(-52130+1659\,L)}\right)\right)\right)+\frac{1}{2}\left(-100\,(1-g)-\frac{1}{79\,(-9+20\,g)}\left(20\left(\frac{1}{5}-g\right)\left(4835-3700\,g-158\,L+2\sqrt{6310900+4410000\,g^2-399740\,L+6241\,L^2+200\,g\,(-52130+1659\,L)}\right)\right)\right)-y4\right)\right)$$

c33 = x2 / ((1 / 4) * (x1 + 100)) - (1 / 4) - d

-d

c43 = 0

0

c53 = 0

0

```
c63 = d
```

```
d
```

```
c73 = -d / 4
```

$$-\frac{d}{4}$$

```
c14 = d
```

```
d
```

```
c24 = 0
```

```
0
```

```
c34 = 0
```

```
0
```

```
c44 = 1 - (y1 / (10 * y2)) - ((y3 / (y1 + 100)) - (y1 * y3 / (y1 + 100) ^ 2)) - d - g
```

$$1 - d - g - \frac{32\left(4835 - 3700\,g - 158\,L + 2\sqrt{6310900 + 4410000\,g^2 - 399740\,L + 6241\,L^2 + 200\,g\,(-52130 + 1659\,L)}\right)}{79\,(-9 + 20\,g)\left(100 + \frac{20\left(4835 - 3700\,g - 158\,L + 2\sqrt{6310900 + 4410000\,g^2 - 399740\,L + 6241\,L^2 + 200\,g\,(-52130 + 1659\,L)}\right)}{79\,(-9 + 20\,g)}\right)} + \left(20\left(4835 - 3700\,g - 158\,L + 2\sqrt{6310900 + 4410000\,g^2 - 399740\,L + 6241\,L^2 + 200\,g\,(-52130 + 1659\,L)}\right)\left(100\,(1 - g) + \frac{1}{79\,(-9 + 20\,g)}\left(20\left(\frac{1}{5} - g\right)\left(4835 - 3700\,g - 158\,L + 2\sqrt{6310900 + 4410000\,g^2 - 399740\,L + 6241\,L^2 + 200\,g\,(-52130 + 1659\,L)}\right)\right)\right)\right) \Big/ \left(79\,(-9 + 20\,g)\left(100 + \frac{1}{79\,(-9 + 20\,g)}\left(20\left(4835 - 3700\,g - 158\,L + 2\sqrt{6310900 + 4410000\,g^2 - 399740\,L + 6241\,L^2 + 200\,g\,(-52130 + 1659\,L)}\right)\right)\right)^2\right) - \frac{100\,(1 - g) + \frac{20\left(\frac{1}{5} - g\right)\left(4835 - 3700\,g - 158\,L + 2\sqrt{6310900 + 4410000\,g^2 - 399740\,L + 6241\,L^2 + 200\,g\,(-52130 + 1659\,L)}\right)}{79\,(-9 + 20\,g)}}{100 + \frac{20\left(4835 - 3700\,g - 158\,L + 2\sqrt{6310900 + 4410000\,g^2 - 399740\,L + 6241\,L^2 + 200\,g\,(-52130 + 1659\,L)}\right)}{79\,(-9 + 20\,g)}}$$

```
c54 = (y4 / (y4 + 5)) + (y2 * y3 / (y1 + 100) ^ 2)
```

$$\frac{100\,(1 - g) + \frac{20\left(\frac{1}{5} - g\right)\left(4835 - 3700\,g - 158\,L + 2\sqrt{6310900 + 4410000\,g^2 - 399740\,L + 6241\,L^2 + 200\,g\,(-52130 + 1659\,L)}\right)}{79\,(-9 + 20\,g)}}{16\left(100 + \frac{20\left(4835 - 3700\,g - 158\,L + 2\sqrt{6310900 + 4410000\,g^2 - 399740\,L + 6241\,L^2 + 200\,g\,(-52130 + 1659\,L)}\right)}{79\,(-9 + 20\,g)}\right)} + \frac{y4}{5 + y4}$$

```
c64 = -4 * y2 * y3 / (y1 + 100) ^ 2
```

$$-\frac{100\,(1 - g) + \frac{20\left(\frac{1}{5} - g\right)\left(4835 - 3700\,g - 158\,L + 2\sqrt{6310900 + 4410000\,g^2 - 399740\,L + 6241\,L^2 + 200\,g\,(-52130 + 1659\,L)}\right)}{79\,(-9 + 20\,g)}}{4\left(100 + \frac{20\left(4835 - 3700\,g - 158\,L + 2\sqrt{6310900 + 4410000\,g^2 - 399740\,L + 6241\,L^2 + 200\,g\,(-52130 + 1659\,L)}\right)}{79\,(-9 + 20\,g)}\right)}$$

```
c74 = -y4 / (y4 + 5)
```

$$-\frac{y4}{5+y4}$$

```
c15 = 0
```

$$0$$

```
c25 = -x1 / (2 * L + 5 - x2 - (x3 / 4) - y4 - y2 - (y3 / 4)) +
  x1 * (2 * L - x2 - (x3 / 4) - y4 - y2 - (y3 / 4)) / (2 * L + 5 - x2 - (x3 / 4) - y4 - y2 - (y3 / 4)) ^ 2 + d
```

$$d + \left(20\left(4835 - 3700\,g - 158\,L + 2\sqrt{6310900 + 4410000\,g^2 - 399740\,L + 6241\,L^2 + 200\,g\,(-52130 + 1659\,L)}\right)\right.$$
$$\left(2\,L + \frac{1}{8}\left(-100 - \frac{1}{79\,(-9+20\,g)}\left(20\left(4835 - 3700\,g - 158\,L + \right.\right.\right.\right.$$
$$\left.\left.\left.\left.2\sqrt{6310900 + 4410000\,g^2 - 399740\,L + 6241\,L^2 + 200\,g\,(-52130 + 1659\,L)}\right)\right)\right) +$$
$$\frac{1}{2}\left(-100\,(1-g) - \frac{1}{79\,(-9+20\,g)}\left(20\left(\frac{1}{5} - g\right)\left(4835 - 3700\,g - 158\,L + \right.\right.\right.$$
$$\left.\left.\left.2\sqrt{6310900 + 4410000\,g^2 - 399740\,L + 6241\,L^2 + 200\,g\,(-52130 + 1659\,L)}\right)\right)\right) - y4\Big)\Big) \Big/$$
$$\left(79\,(-9+20\,g)\left(5 + 2\,L + \frac{1}{8}\left(-100 - \frac{1}{79\,(-9+20\,g)}\left(20\left(4835 - 3700\,g - 158\,L + 2\right.\right.\right.\right.\right.$$
$$\left.\left.\left.\left.\left.\sqrt{6310900 + 4410000\,g^2 - 399740\,L + 6241\,L^2 + 200\,g\,(-52130 + 1659\,L)}\right)\right)\right) +\right.$$
$$\frac{1}{2}\left(-100\,(1-g) - \frac{1}{79\,(-9+20\,g)}\left(20\left(\frac{1}{5} - g\right)\left(4835 - 3700\,g - 158\,L + 2\right.\right.\right.$$
$$\left.\left.\left.\left.\sqrt{6310900 + 4410000\,g^2 - 399740\,L + 6241\,L^2 + 200\,g\,(-52130 + 1659\,L)}\right)\right)\right) -$$
$$\left.y4\right)^2\Big) - \Big(20\left(4835 - 3700\,g - 158\,L + 2\right.$$
$$\left.\sqrt{6310900 + 4410000\,g^2 - 399740\,L + 6241\,L^2 + 200\,g\,(-52130 + 1659\,L)}\right)\Big) \Big/$$
$$\left(79\,(-9+20\,g)\left(5 + 2\,L + \frac{1}{8}\left(-100 - \frac{1}{79\,(-9+20\,g)}\left(20\left(4835 - 3700\,g - 158\,L + \right.\right.\right.\right.\right.$$
$$\left.\left.\left.\left.\left.2\sqrt{6310900 + 4410000\,g^2 - 399740\,L + 6241\,L^2 + 200\,g\,(-52130 + 1659\,L)}\right)\right)\right) +\right.$$
$$\frac{1}{2}\left(-100\,(1-g) - \frac{1}{79\,(-9+20\,g)}\left(20\left(\frac{1}{5} - g\right)\left(4835 - 3700\,g - 158\,L + \right.\right.\right.$$
$$\left.\left.\left.\left.2\sqrt{6310900 + 4410000\,g^2 - 399740\,L + 6241\,L^2 + 200\,g\,(-52130 + 1659\,L)}\right)\right)\right) - y4\Big)\Big)$$

```
c35 = 0
```

$$0$$

```
c45 = y1^2 / (20 * y2^2)
```

$$\left(5120\left(4835 - 3700\,g - 158\,L + \right.\right.$$
$$\left.\left.2\sqrt{6310900 + 4410000\,g^2 - 399740\,L + 6241\,L^2 + 200\,g\,(-52130 + 1659\,L)}\right)^2\Big) \Big/$$
$$\left(6241\,(-9+20\,g)^2\left(100 + \frac{1}{79\,(-9+20\,g)}\left(20\left(4835 - 3700\,g - 158\,L + \right.\right.\right.\right.$$
$$\left.\left.\left.\left.2\sqrt{6310900 + 4410000\,g^2 - 399740\,L + 6241\,L^2 + 200\,g\,(-52130 + 1659\,L)}\right)\right)\right)^2\right)$$

```
c55 = -(y3 / (y1 + 100)) - g - d
```

$$-d - g - \frac{100\,(1-g) + \frac{20\left(\frac{1}{5}-g\right)\left(4835-3700\,g-158\,L+2\sqrt{6310900+4410000\,g^2-399740\,L+6241\,L^2+200\,g\,(-52130+1659\,L)}\right)}{79\,(-9+20\,g)}}{100 + \frac{20\,(4835-3700\,g-158\,L-2\sqrt{6310900+4410000\,g^2-399740\,L+6241\,L^2+200\,g\,(-52130+1659\,L)})}{79\,(-9+20\,g)}}$$

```
c65 = 4 * y3 / (y1 + 100)
```

$$\frac{4\left(100\,(1-g) + \frac{20\left(\frac{1}{5}-g\right)\left(4835-3700\,g-158\,L+2\sqrt{6310900+4410000\,g^2-399740\,L+6241\,L^2+200\,g\,(-52130+1659\,L)}\right)}{79\,(-9+20\,g)}\right)}{100 + \frac{20\,(4835-3700\,g-158\,L-2\sqrt{6310900+4410000\,g^2-399740\,L+6241\,L^2+200\,g\,(-52130+1659\,L)})}{79\,(-9+20\,g)}}$$

```
c75 = g - d
```

```
-d + g
```

```
c16 = 0
```

```
0
```

```
c26 = -x1 / (4 * (2 * L + 5 - x2 - (x3 / 4) - y4 - y2 - (y3 / 4))) +
  x1 * (2 * L - x2 - (x3 / 4) - y4 - y2 - (y3 / 4)) / (4 * (2 * L + 5 - x2 - (x3 / 4) - y4 - y2 - (y3 / 4)) ^ 2)
```

$$\Bigg(5\left(4835-3700\,g-158\,L+2\sqrt{6310900+4410000\,g^2-399740\,L+6241\,L^2+200\,g\,(-52130+1659\,L)}\right)\Bigg(2\,L+\frac{1}{8}\Bigg(-100-\frac{1}{79\,(-9+20\,g)}\Bigg(20\Bigg(4835-3700\,g-158\,L+2\sqrt{6310900+4410000\,g^2-399740\,L+6241\,L^2+200\,g\,(-52130+1659\,L)}\Bigg)\Bigg)\Bigg)+\frac{1}{2}\Bigg(-100\,(1-g)-\frac{1}{79\,(-9+20\,g)}\Bigg(20\left(\frac{1}{5}-g\right)\Bigg(4835-3700\,g-158\,L+2\sqrt{6310900+4410000\,g^2-399740\,L+6241\,L^2+200\,g\,(-52130+1659\,L)}\Bigg)\Bigg)-y4\Bigg)\Bigg)\Bigg/$$
$$\Bigg(79\,(-9+20\,g)\Bigg(5+2\,L+\frac{1}{8}\Bigg(-100-\frac{1}{79\,(-9+20\,g)}\Bigg(20\Bigg(4835-3700\,g-158\,L+2\sqrt{6310900+4410000\,g^2-399740\,L+6241\,L^2+200\,g\,(-52130+1659\,L)}\Bigg)\Bigg)\Bigg)+\frac{1}{2}\Bigg(-100\,(1-g)-\frac{1}{79\,(-9+20\,g)}\Bigg(20\left(\frac{1}{5}-g\right)\Bigg(4835-3700\,g-158\,L+2\sqrt{6310900+4410000\,g^2-399740\,L+6241\,L^2+200\,g\,(-52130+1659\,L)}\Bigg)\Bigg)-y4\Bigg)^2\Bigg)-\Bigg(5\Bigg(4835-3700\,g-158\,L+2\sqrt{6310900+4410000\,g^2-399740\,L+6241\,L^2+200\,g\,(-52130+1659\,L)}\Bigg)\Bigg)\Bigg/$$
$$\Bigg(79\,(-9+20\,g)\Bigg(5+2\,L+\frac{1}{8}\Bigg(-100-\frac{1}{79\,(-9+20\,g)}\Bigg(20\Bigg(4835-3700\,g-158\,L+2\sqrt{6310900+4410000\,g^2-399740\,L+6241\,L^2+200\,g\,(-52130+1659\,L)}\Bigg)\Bigg)\Bigg)+\frac{1}{2}\Bigg(-100\,(1-g)-\frac{1}{79\,(-9+20\,g)}\Bigg(20\left(\frac{1}{5}-g\right)\Bigg(4835-3700\,g-158\,L+2\sqrt{6310900+4410000\,g^2-399740\,L+6241\,L^2+200\,g\,(-52130+1659\,L)}\Bigg)\Bigg)-y4\Bigg)\Bigg)$$

```
c36 = d
```

```
d
```

```
c46 = -y1 / (y1 + 100)
```

$$-\frac{20\left(4835-3700\,g-158\,L+2\sqrt{6310900+4410000\,g^2-399740\,L+6241\,L^2+200\,g\,(-52130+1659\,L)}\right)}{79\,(-9+20\,g)\left(100+\frac{20\left(4835-3700\,g-158\,L+2\sqrt{6310900+4410000\,g^2-399740\,L+6241\,L^2+200\,g\,(-52130+1659\,L)}\right)}{79\,(-9+20\,g)}\right)}$$

```
c56 = -y2 / (y1 + 100)
```

$$\frac{-100-\frac{20\left(4835-3700\,g-158\,L+2\sqrt{6310900+4410000\,g^2-399740\,L+6241\,L^2+200\,g\,(-52130+1659\,L)}\right)}{79\,(-9+20\,g)}}{16\left(100-\frac{20\left(4835-3700\,g-158\,L+2\sqrt{6310900+4410000\,g^2-399740\,L+6241\,L^2+200\,g\,(-52130+1659\,L)}\right)}{79\,(-9+20\,g)}\right)}$$

```
c66 = 4 * y2 / (y1 + 100) - (1 / 4) - d
```

$$-d$$

```
c76 = (1 / 16) - (d / 4)
```

$$\frac{1}{16}-\frac{d}{4}$$

```
c17 = 0
```

$$0$$

```
c27 = -x1 / (2 * L + 5 - x2 - (x3 / 4) - y4 - y2 - (y3 / 4)) +
  x1 * (2 * L - x2 - (x3 / 4) - y4 - y2 - (y3 / 4)) / ((2 * L + 5 - x2 - (x3 / 4) - y4 - y2 - (y3 / 4)) ^ 2)
```

$$\left(20\left(4835-3700\,g-158\,L+2\sqrt{6310900+4410000\,g^2-399740\,L+6241\,L^2+200\,g\,(-52130+1659\,L)}\right)\right.$$
$$\left(2\,L+\frac{1}{8}\left(-100-\frac{1}{79\,(-9+20\,g)}\left(20\left(4835-3700\,g-158\,L+\right.\right.\right.\right.$$
$$\left.\left.\left.\left.2\sqrt{6310900+4410000\,g^2-399740\,L+6241\,L^2+200\,g\,(-52130+1659\,L)}\right)\right)\right)+$$
$$\frac{1}{2}\left(-100\,(1-g)-\frac{1}{79\,(-9+20\,g)}\left(20\left(\frac{1}{5}-g\right)\left(4835-3700\,g-158\,L+\right.\right.\right.$$
$$\left.\left.\left.2\sqrt{6310900+4410000\,g^2-399740\,L+6241\,L^2+200\,g\,(-52130+1659\,L)}\right)\right)-y4\right)\Bigg)\Bigg/$$
$$\left(79\,(-9+20\,g)\left(5+2\,L+\frac{1}{8}\left(-100-\frac{1}{79\,(-9+20\,g)}\left(20\left(4835-3700\,g-158\,L+2\right.\right.\right.\right.$$
$$\left.\left.\left.\left.\sqrt{6310900+4410000\,g^2-399740\,L+6241\,L^2+200\,g\,(-52130+1659\,L)}\right)\right)\right)+$$
$$\frac{1}{2}\left(-100\,(1-g)-\frac{1}{79\,(-9+20\,g)}\left(20\left(\frac{1}{5}-g\right)\left(4835-3700\,g-158\,L+2\right.\right.\right.$$
$$\left.\left.\left.\left.\sqrt{6310900+4410000\,g^2-399740\,L+6241\,L^2+200\,g\,(-52130+1659\,L)}\right)\right)\right)-$$
$$y4\Big)^2\Bigg)-\left(20\left(4835-3700\,g-158\,L+2\right.\right.$$
$$\left.\left.\sqrt{6310900+4410000\,g^2-399740\,L+6241\,L^2+200\,g\,(-52130+1659\,L)}\right)\right)\Bigg/$$
$$\left(79\,(-9+20\,g)\left(5+2\,L+\frac{1}{8}\left(-100-\frac{1}{79\,(-9+20\,g)}\left(20\left(4835-3700\,g-158\,L+\right.\right.\right.\right.$$
$$\left.\left.\left.\left.2\sqrt{6310900+4410000\,g^2-399740\,L+6241\,L^2+200\,g\,(-52130+1659\,L)}\right)\right)\right)+$$
$$\frac{1}{2}\left(-100\,(1-g)-\frac{1}{79\,(-9+20\,g)}\left(20\left(\frac{1}{5}-g\right)\left(4835-3700\,g-158\,L+\right.\right.\right.$$
$$\left.\left.\left.\left.2\sqrt{6310900+4410000\,g^2-399740\,L+6241\,L^2+200\,g\,(-52130+1659\,L)}\right)\right)-y4\right)\right)$$

c37 = 0

0

c47 = 0

0

c57 = y1 / (y4 + 5) - y1 * y4 / (y4 + 5) ^ 2

$$-\frac{1}{79\,(-9+20\,g)\,(5+y4)^2}\left(20\left(4835-3700\,g-158\,L+2\sqrt{6310900+4410000\,g^2-399740\,L+6241\,L^2+200\,g\,(-52130+1659\,L)}\right)y4\right)+\frac{20\left(4835-3700\,g-158\,L+2\sqrt{6310900+4410000\,g^2-399740\,L+6241\,L^2+200\,g\,(-52130+1659\,L)}\right)}{79\,(-9+20\,g)\,(5+y4)}$$

c67 = 0

0

c77 = -y1 / (y4 + 5) + y1 * y4 / (y4 + 5) ^ 2 - 2 d

$$-2\,d+\frac{1}{79\,(-9+20\,g)\,(5+y4)^2}\left(20\left(4835-3700\,g-158\,L+2\sqrt{6310900+4410000\,g^2-399740\,L+6241\,L^2+200\,g\,(-52130+1659\,L)}\right)y4\right)-\frac{20\left(4835-3700\,g-158\,L+2\sqrt{6310900+4410000\,g^2-399740\,L+6241\,L^2+200\,g\,(-52130+1659\,L)}\right)}{79\,(-9+20\,g)\,(5+y4)}$$

```
ma = {{c11, c12, c13, c14, c15, c16, c17},
  {c21, c22, c23, c24, c25, c26, c27}, {c31, c32, c33, c34, c35, c36, c37},
  {c41, c42, c43, c44, c45, c46, c47}, {c51, c52, c53, c54, c55, c56, c57},
  {c61, c62, c63, c64, c65, c66, c67}, {c71, c72, c73, c74, c75, c76, c77}}
```

$$\left\{\left\{1-d-g-\left(32\left(4835-3700\,g-158\,L+2\sqrt{6310900+4410000\,g^2-399740\,L+6241\,L^2+200\,g\,(-52130+1659\,L)}\right)\right)\Big/\left(79\,(-9+20\,g)\left(100+\frac{1}{79\,(-9+20\,g)}\left(20\left(4835-3700\,g-158\,L+2\sqrt{6310900+4410000\,g^2-399740\,L+6241\,L^2+200\,g\,(-52130+1659\,L)}\right)\right)\right)\right)+\left(20\left(4835-3700\,g-158\,L+2\sqrt{6310900+4410000\,g^2-399740\,L+6241\,L^2+200\,g\,(-52130+1659\,L)}\right)\left(100\,(1-g)+\frac{1}{79\,(-9+20\,g)}\left(20\left(\frac{1}{5}-g\right)\left(4835-3700\,g-158\,L+2\sqrt{6310900+4410000\,g^2-399740\,L+6241\,L^2+200\,g\,(-52130+1659\,L)}\right)\right)\right)\right)\Big/\left(79\,(-9+20\,g)\left(100+\frac{1}{79\,(-9+20\,g)}\left(20\left(4835-3700\,g-158\,L+2\sqrt{6310900+4410000\,g^2-399740\,L+6241\,L^2+200\,g\,(-52130+1659\,L)}\right)\right)\right)^2\right)-$$

$$\frac{100\,(1-g)+\frac{20\left(\frac{1}{5}-g\right)\left(4835-3700\,g-158\,L+2\sqrt{6310900+4410000\,g^2-399740\,L+6241\,L^2+200\,g\,(-52130+1659\,L)}\right)}{79\,(-9+20\,g)}}{100+\frac{20\left(4835-3700\,g-158\,L+2\sqrt{6310900+4410000\,g^2-399740\,L+6241\,L^2+200\,g\,(-52130+1659\,L)}\right)}{79\,(-9+20\,g)}},$$

$$\left(5120\left(4835-3700\,g-158\,L+2\sqrt{6310900+4410000\,g^2-399740\,L+6241\,L^2+200\,g\,(-52130+1659\,L)}\right)^2\right)\Big/\left(6241\,(-9+20\,g)^2\left(100+\frac{1}{79\,(-9+20\,g)}\left(20\left(4835-3700\,g-158\,L+2\sqrt{6310900+4410000\,g^2-399740\,L+6241\,L^2+200\,g\,(-52130+1659\,L)}\right)\right)\right)^2\right),$$

$$-\left(20\left(4835-3700\,g-158\,L+2\sqrt{6310900+4410000\,g^2-399740\,L+6241\,L^2+200\,g\,(-52130+1659\,L)}\right)\right)\Big/\left(79\,(-9+20\,g)\left(100+\frac{1}{79\,(-9+20\,g)}\left(20\left(4835-3700\,g-158\,L+2\sqrt{6310900+4410000\,g^2-399740\,L+6241\,L^2+200\,g\,(-52130+1659\,L)}\right)\right)\right)\right), d, 0, 0,$$

$$0\Big\}, \Big\{\frac{100\,(1-g)+\frac{20\left(\frac{1}{5}-g\right)\left(4835-3700\,g-158\,L+2\sqrt{6310900+4410000\,g^2-399740\,L+6241\,L^2+200\,g\,(-52130+1659\,L)}\right)}{79\,(-9+20\,g)}}{16\left(100+\frac{20\left(4835-3700\,g-158\,L+2\sqrt{6310900+4410000\,g^2-399740\,L+6241\,L^2+200\,g\,(-52130+1659\,L)}\right)}{79\,(-9+20\,g)}\right)}+$$

$$\left(2\,L+\frac{1}{8}\left(-100-\frac{1}{79\,(-9+20\,g)}\left(20\left(4835-3700\,g-158\,L+2\sqrt{6310900+4410000\,g^2-399740\,L+6241\,L^2+200\,g\,(-52130+1659\,L)}\right)\right)\right)+\frac{1}{2}\left(-100\,(1-g)-\frac{1}{79\,(-9+20\,g)}\left(20\left(\frac{1}{5}-g\right)\left(4835-3700\,g-158\,L+2\sqrt{6310900+4410000\,g^2-399740\,L+6241\,L^2+200\,g\,(-52130+1659\,L)}\right)\right)\right)-y4\right)\Big/$$

$$\left(5+2\,L+\frac{1}{8}\left(-100-\frac{1}{79\,(-9+20\,g)}\left(20\left(4835-3700\,g-158\,L+2\sqrt{6310900+4410000\,g^2-399740\,L+6241\,L^2+200\,g\,(-52130+1659\,L)}\right)\right)\right)+\frac{1}{2}\left(-100\,(1-g)-\frac{1}{79\,(-9+20\,g)}\left(20\left(\frac{1}{5}-g\right)\left(4835-3700\,g-158\,L+2\sqrt{6310900+4410000\,g^2-399740\,L+6241\,L^2+200\,g\,(-52130+1659\,L)}\right)\right)\right)-y4\right),$$

$$-d-g-\frac{100\,(1-g)+\frac{20\left(\frac{1}{5}-g\right)\left(4835-3700\,g-158\,L+2\sqrt{6310900+4410000\,g^2-399740\,L+6241\,L^2+200\,g\,(-52130+1659\,L)}\right)}{79\,(-9+20\,g)}}{100+\frac{20\left(4835-3700\,g-158\,L+2\sqrt{6310900+4410000\,g^2-399740\,L+6241\,L^2+200\,g\,(-52130+1659\,L)}\right)}{79\,(-9+20\,g)}}+$$

$$\left(20\left(4835-3700\,g-158\,L+2\sqrt{6310900+4410000\,g^2-399740\,L+6241\,L^2+200\,g\,(-52130+1659\,L)}\right)\left(2\,L+\frac{1}{8}\left(-100-\frac{1}{79\,(-9+20\,g)}\left(20\left(4835-3700\,g-158\,L+2\sqrt{6310900+4410000\,g^2-399740\,L+6241\,L^2+200\,g\,(-52130+1659\,L)}\right)\right)\right)+\frac{1}{2}\left(-100\,(1-g)-\frac{1}{79\,(-9+20\,g)}\left(20\left(\frac{1}{5}-g\right)\left(4835-3700\,g-158\,L+2\sqrt{6310900+4410000\,g^2-399740\,L+6241\,L^2+200\,g\,(-52130+1659\,L)}\right)\right)\right)-y4\right)\right)\Big/\left(79\,(-9+20\,g)\left(5+2\,L+\frac{1}{8}\left(-100-\frac{1}{79\,(-9+20\,g)}\left(20\left(4835-3700\,g-158\,L+2\sqrt{6310900+4410000\,g^2-399740\,L+6241\,L^2+200\,g\,(-52130+1659\,L)}\right)\right)\right)+$$

$$\frac{1}{2}\left(-100\,(1-g)-\frac{1}{79\,(-9+20\,g)}\left(20\left(\frac{1}{5}-g\right)\left(4835-3700\,g-158\,L+2\sqrt{6310900+4410000\,g^2-399740\,L+6241\,L^2+200\,g\,(-52130+1659\,L)}\right)\right)\right)-y4\Bigg)^2\Bigg)-\left(20\left(4835-3700\,g-158\,L+2\sqrt{6310900+4410000\,g^2-399740\,L+6241\,L^2+200\,g\,(-52130+1659\,L)}\right)\right)\Bigg/$$

$$\Bigg(79\,(-9+20\,g)\left(5+2\,L+\frac{1}{8}\left(-100-\frac{1}{79\,(-9+20\,g)}\left(20\left(4835-3700\,g-158\,L+2\sqrt{6310900+4410000\,g^2-399740\,L+6241\,L^2+200\,g\,(-52130+1659\,L)}\right)\right)\right)+\frac{1}{2}\left(-100\,(1-g)-\frac{1}{79\,(-9+20\,g)}\left(20\left(\frac{1}{5}-g\right)\left(4835-3700\,g-158\,L+2\sqrt{6310900+4410000\,g^2-399740\,L+6241\,L^2+200\,g\,(-52130+1659\,L)}\right)\right)\right)-y4\Bigg),\ -\frac{1}{16}+\Bigg(5\left(4835-3700\,g-158\,L+2\sqrt{6310900+4410000\,g^2-399740\,L+6241\,L^2+200\,g\,(-52130+1659\,L)}\right)$$

$$\left(2\,L+\frac{1}{8}\left(-100-\frac{1}{79\,(-9+20\,g)}\left(20\left(4835-3700\,g-158\,L+2\sqrt{6310900+4410000\,g^2-399740\,L+6241\,L^2+200\,g\,(-52130+1659\,L)}\right)\right)\right)+\frac{1}{2}\left(-100\,(1-g)-\frac{1}{79\,(-9+20\,g)}\left(20\left(\frac{1}{5}-g\right)\left(4835-3700\,g-158\,L+2\sqrt{6310900+4410000\,g^2-399740\,L+6241\,L^2+200\,g\,(-52130+1659\,L)}\right)\right)\right)-y4\Bigg)\Bigg/$$

$$\Bigg(79\,(-9+20\,g)\left(5+2\,L+\frac{1}{8}\left(-100-\frac{1}{79\,(-9+20\,g)}\left(20\left(4835-3700\,g-158\,L+2\sqrt{6310900+4410000\,g^2-399740\,L+6241\,L^2+200\,g\,(-52130+1659\,L)}\right)\right)\right)+\frac{1}{2}\left(-100\,(1-g)-\frac{1}{79\,(-9+20\,g)}\left(20\left(\frac{1}{5}-g\right)\left(4835-3700\,g-158\,L+2\sqrt{6310900+4410000\,g^2-399740\,L+6241\,L^2+200\,g\,(-52130+1659\,L)}\right)\right)\right)-y4\Bigg),\ 0,\ d+\Bigg(20\left(4835-3700\,g-158\,L+2\sqrt{6310900+4410000\,g^2-399740\,L+6241\,L^2+200\,g\,(-52130+1659\,L)}\right)$$

$$\left(2\,L+\frac{1}{8}\left(-100-\frac{1}{79\,(-9+20\,g)}\left(20\left(4835-3700\,g-158\,L+2\sqrt{6310900+4410000\,g^2-399740\,L+6241\,L^2+200\,g\,(-52130+1659\,L)}\right)\right)\right)+\frac{1}{2}\left(-100\,(1-g)-\frac{1}{79\,(-9+20\,g)}\left(20\left(\frac{1}{5}-g\right)\left(4835-3700\,g-158\,L+2\sqrt{6310900+4410000\,g^2-399740\,L+6241\,L^2+200\,g\,(-52130+1659\,L)}\right)\right)\right)-y4\Bigg)\Bigg/$$

$$\left(79\,(-9+20\,g)\,\left(5+2\,L+\frac{1}{8}\,\left(-100-\frac{1}{79\,(-9+20\,g)}\,\left(20\,\left(4835-3700\,g-158\,L+2\,\sqrt{6310900+4410000\,g^2-399740\,L+6241\,L^2+200\,g\,(-52130+1659\,L)}\right)\right)\right)+\frac{1}{2}\,\left(-100\,(1-g)-\frac{1}{79\,(-9+20\,g)}\,\left(20\,\left(\frac{1}{5}-g\right)\,\left(4835-3700\,g-158\,L+2\,\sqrt{6310900+4410000\,g^2-399740\,L+6241\,L^2+200\,g\,(-52130+1659\,L)}\right)\right)\right)-y4\right)^2\right)-\left(20\,\left(4835-3700\,g-158\,L+2\,\sqrt{6310900+4410000\,g^2-399740\,L+6241\,L^2+200\,g\,(-52130+1659\,L)}\right)\right)\Big/\left(79\,(-9+20\,g)\,\left(5+2\,L+\frac{1}{8}\,\left(-100-\frac{1}{79\,(-9+20\,g)}\,\left(20\,\left(4835-3700\,g-158\,L+2\,\sqrt{6310900+4410000\,g^2-399740\,L+6241\,L^2+200\,g\,(-52130+1659\,L)}\right)\right)\right)+\frac{1}{2}\,\left(-100\,(1-g)-\frac{1}{79\,(-9+20\,g)}\,\left(20\,\left(\frac{1}{5}-g\right)\,\left(4835-3700\,g-158\,L+2\,\sqrt{6310900+4410000\,g^2-399740\,L+6241\,L^2+200\,g\,(-52130+1659\,L)}\right)\right)\right)-y4\right)\right),$$

$$\left(5\,\left(4835-3700\,g-158\,L+2\,\sqrt{6310900+4410000\,g^2-399740\,L+6241\,L^2+200\,g\,(-52130+1659\,L)}\right)\left(2\,L+\frac{1}{8}\,\left(-100-\frac{1}{79\,(-9+20\,g)}\,\left(20\,\left(4835-3700\,g-158\,L+2\,\sqrt{6310900+4410000\,g^2-399740\,L+6241\,L^2+200\,g\,(-52130+1659\,L)}\right)\right)\right)+\frac{1}{2}\,\left(-100\,(1-g)-\frac{1}{79\,(-9+20\,g)}\,\left(20\,\left(\frac{1}{5}-g\right)\,\left(4835-3700\,g-158\,L+2\,\sqrt{6310900+4410000\,g^2-399740\,L+6241\,L^2+200\,g\,(-52130+1659\,L)}\right)\right)\right)-y4\right)\right)\Big/\left(79\,(-9+20\,g)\,\left(5+2\,L+\frac{1}{8}\,\left(-100-\frac{1}{79\,(-9+20\,g)}\,\left(20\,\left(4835-3700\,g-158\,L+2\,\sqrt{6310900+4410000\,g^2-399740\,L+6241\,L^2+200\,g\,(-52130+1659\,L)}\right)\right)\right)+\frac{1}{2}\,\left(-100\,(1-g)-\frac{1}{79\,(-9+20\,g)}\,\left(20\,\left(\frac{1}{5}-g\right)\,\left(4835-3700\,g-158\,L+2\,\sqrt{6310900+4410000\,g^2-399740\,L+6241\,L^2+200\,g\,(-52130+1659\,L)}\right)\right)\right)-y4\right)^2\right)-\left(5\,\left(4835-3700\,g-158\,L+2\,\sqrt{6310900+4410000\,g^2-399740\,L+6241\,L^2+200\,g\,(-52130+1659\,L)}\right)\right)\Big/\left(79\,(-9+20\,g)\,\left(5+2\,L+\frac{1}{8}\,\left(-100-\frac{1}{79\,(-9+20\,g)}\,\left(20\,\left(4835-3700\,g-158\,L+2\,\sqrt{6310900+4410000\,g^2-399740\,L+6241\,L^2+200\,g\,(-52130+1659\,L)}\right)\right)\right)+\frac{1}{2}\,\left(-100\,(1-g)-\frac{1}{79\,(-9+20\,g)}\,\left(20\,\left(\frac{1}{5}-g\right)\,\left(4835-3700\,g-158\,L+2\,\sqrt{6310900+4410000\,g^2-399740\,L+6241\,L^2+200\,g\,(-52130+1659\,L)}\right)\right)\right)-y4\right)\right),\left(20\,\left(4835-3700\,g-158\,L+2\,\sqrt{6310900+4410000\,g^2-399740\,L+6241\,L^2+200\,g\,(-52130+1659\,L)}\right)\left(2\,L+\frac{1}{8}\,\left(-100-\frac{1}{79\,(-9+20\,g)}\,\left(20\,\left(4835-3700\,g-158\,L+2\,\sqrt{6310900+4410000\,g^2-399740\,L+6241\,L^2+200\,g\,(-52130+1659\,L)}\right)\right)\right)+\frac{1}{2}\,\left(-100\,(1-g)-\frac{1}{79\,(-9+20\,g)}\,\left(20\,\left(\frac{1}{5}-g\right)\,\left(4835-3700\,g-158\,L+2\right.\right.\right.$$

$$\sqrt{6310900 + 4410000\,g^2 - 399740\,L + 6241\,L^2 + 200\,g\,(-52130 + 1659\,L)}\Big)\Big)\Big) - y4\Big)\Big)\Big/$$

$$\Big(79\,(-9 + 20\,g)\,\Big(5 + 2\,L + \frac{1}{8}\,\Big(-100 - \frac{1}{79\,(-9 + 20\,g)}\,\big(20\,\big(4835 - 3700\,g - 158\,L +$$

$$2\,\sqrt{6310900 + 4410000\,g^2 - 399740\,L + 6241\,L^2 + 200\,g\,(-52130 + 1659\,L)}\big)\Big)\Big) +$$

$$\frac{1}{2}\,\Big(-100\,(1 - g) - \frac{1}{79\,(-9 + 20\,g)}\,\Big(20\,\Big(\frac{1}{5} - g\Big)\,\big(4835 - 3700\,g - 158\,L +$$

$$2\,\sqrt{6310900 + 4410000\,g^2 - 399740\,L + 6241\,L^2 + 200\,g\,(-52130 + 1659\,L)}\big)\Big)\Big) -$$

$$y4\Big)^2\Big) - \big(20\,\big(4835 - 3700\,g - 158\,L + 2$$

$$\sqrt{6310900 + 4410000\,g^2 - 399740\,L + 6241\,L^2 + 200\,g\,(-52130 + 1659\,L)}\big)\big)\Big/$$

$$\Big(79\,(-9 + 20\,g)\,\Big(5 + 2\,L + \frac{1}{8}\,\Big(-100 - \frac{1}{79\,(-9 + 20\,g)}\,\big(20\,\big(4835 - 3700\,g - 158\,L + 2$$

$$\sqrt{6310900 + 4410000\,g^2 - 399740\,L + 6241\,L^2 + 200\,g\,(-52130 + 1659\,L)}\big)\Big)\Big) +$$

$$\frac{1}{2}\,\Big(-100\,(1 - g) - \frac{1}{79\,(-9 + 20\,g)}\,\Big(20\,\Big(\frac{1}{5} - g\Big)\,\big(4835 - 3700\,g - 158\,L + 2$$

$$\sqrt{6310900 + 4410000\,g^2 - 399740\,L + 6241\,L^2 + 200\,g\,(-52130 + 1659\,L)}\big)\Big)\Big) - y4\Big)\Big)\Big\},$$

$$\Big\{\Big(\Big(-100 - \frac{1}{79\,(-9 + 20\,g)}\,\big(20\,\big(4835 - 3700\,g - 158\,L + 2$$

$$\sqrt{6310900 + 4410000\,g^2 - 399740\,L + 6241\,L^2 + 200\,g\,(-52130 + 1659\,L)}\big)\Big)$$

$$\Big(100\,(1 - g) + \frac{1}{79\,(-9 + 20\,g)}\,\Big(20\,\Big(\frac{1}{5} - g\Big)\,\big(4835 - 3700\,g - 158\,L +$$

$$2\,\sqrt{6310900 + 4410000\,g^2 - 399740\,L + 6241\,L^2 + 200\,g\,(-52130 + 1659\,L)}\big)\Big)\Big)\Big)\Big/$$

$$\Big(4\,\Big(100 + \frac{1}{79\,(-9 + 20\,g)}\,\big(20\,\big(4835 - 3700\,g - 158\,L +$$

$$2\,\sqrt{6310900 + 4410000\,g^2 - 399740\,L + 6241\,L^2 + 200\,g\,(-52130 + 1659\,L)}\big)\Big)^2\Big),$$

$$\frac{4\,\Big(100\,(1 - g) + \frac{20\,\left(\frac{1}{5} - g\right)\,\left(4835 - 3700\,g - 158\,L + 2\,\sqrt{6310900 + 4410000\,g^2 - 399740\,L + 6241\,L^2 + 200\,g\,(-52130 + 1659\,L)}\right)}{79\,(-9 + 20\,g)}\Big)}{100 + \frac{20\,\left(4835 - 3700\,g - 158\,L + 2\,\sqrt{6310900 + 4410000\,g^2 - 399740\,L + 6241\,L^2 + 200\,g\,(-52130 + 1659\,L)}\right)}{79\,(-9 + 20\,g)}},$$

$$-d,$$
$$0,$$
$$0,$$
$$d,$$
$$0\},$$
$$\{d,$$
$$0,$$
$$0,$$
$$1 -$$
$$d -$$
$$g -$$
$$\big(32$$
$$\big(4835 - 3700\,g - 158\,L +$$
$$2\,\sqrt{6310900 + 4410000\,g^2 - 399740\,L + 6241\,L^2 + 200\,g\,(-52130 + 1659\,L)}\big)\Big/$$
$$\Big(79\,(-9 + 20\,g)\,\Big(100 + \frac{1}{79\,(-9 + 20\,g)}\,\big(20\,\big(4835 - 3700\,g - 158\,L +$$
$$2\,\sqrt{6310900 + 4410000\,g^2 - 399740\,L + 6241\,L^2 + 200\,g\,(-52130 + 1659\,L)}\big)\Big)\Big) +$$

$$\left(20\left(4835-3700\,g-158\,L+2\sqrt{6310900+4410000\,g^2-399740\,L+6241\,L^2+200\,g\,(-52130+1659\,L)}\right)\left(100\,(1-g)+\frac{1}{79\,(-9+20\,g)}\left(20\left(\frac{1}{5}-g\right)\left(4835-3700\,g-158\,L+2\sqrt{6310900+4410000\,g^2-399740\,L+6241\,L^2+200\,g\,(-52130+1659\,L)}\right)\right)\right)\right)\Big/\left(79\,(-9+20\,g)\left(100+\frac{1}{79\,(-9+20\,g)}\left(20\left(4835-3700\,g-158\,L+2\sqrt{6310900+4410000\,g^2-399740\,L+6241\,L^2+200\,g\,(-52130+1659\,L)}\right)\right)\right)^2\right)-\frac{100\,(1-g)+\frac{20\left(\frac{1}{5}-g\right)\left(4835-3700\,g-158\,L+2\sqrt{6310900+4410000\,g^2-399740\,L+6241\,L^2+200\,g\,(-52130+1659\,L)}\right)}{79\,(-9+20\,g)}}{100+\frac{20\left(4835-3700\,g-158\,L+2\sqrt{6310900+4410000\,g^2-399740\,L+6241\,L^2+200\,g\,(-52130+1659\,L)}\right)}{79\,(-9+20\,g)}},$$

$$\left(5120\left(4835-3700\,g-158\,L+2\sqrt{6310900+4410000\,g^2-399740\,L+6241\,L^2+200\,g\,(-52130+1659\,L)}\right)^2\right)\Big/\left(6241\,(-9+20\,g)^2\left(100+\frac{1}{79\,(-9+20\,g)}\left(20\left(4835-3700\,g-158\,L+2\sqrt{6310900+4410000\,g^2-399740\,L+6241\,L^2+200\,g\,(-52130+1659\,L)}\right)\right)\right)^2\right),$$

$$-\left(20\left(4835-3700\,g-158\,L+2\sqrt{6310900+4410000\,g^2-399740\,L+6241\,L^2+200\,g\,(-52130+1659\,L)}\right)\right)\Big/\left(79\,(-9+20\,g)\left(100+\frac{1}{79\,(-9+20\,g)}\left(20\left(4835-3700\,g-158\,L+2\sqrt{6310900+4410000\,g^2-399740\,L+6241\,L^2+200\,g\,(-52130+1659\,L)}\right)\right)\right)\right),\ 0\Big\},$$

$$\left\{0,\ d,\ 0,\ \frac{100\,(1-g)+\frac{20\left(\frac{1}{5}-g\right)\left(4835-3700\,g-158\,L+2\sqrt{6310900+4410000\,g^2-399740\,L+6241\,L^2+200\,g\,(-52130+1659\,L)}\right)}{79\,(-9+20\,g)}}{16\left(100+\frac{20\left(4835-3700\,g-158\,L+2\sqrt{6310900+4410000\,g^2-399740\,L+6241\,L^2+200\,g\,(-52130+1659\,L)}\right)}{79\,(-9+20\,g)}\right)}+\frac{y4}{5+y4},\right.$$

$$-d-g-\frac{100\,(1-g)+\frac{20\left(\frac{1}{5}-g\right)\left(4835-3700\,g-158\,L+2\sqrt{6310900+4410000\,g^2-399740\,L+6241\,L^2+200\,g\,(-52130+1659\,L)}\right)}{79\,(-9+20\,g)}}{100+\frac{20\left(4835-3700\,g-158\,L+2\sqrt{6310900+4410000\,g^2-399740\,L+6241\,L^2+200\,g\,(-52130+1659\,L)}\right)}{79\,(-9+20\,g)}},$$

$$\frac{-100-\frac{20\left(4835-3700\,g-158\,L+2\sqrt{6310900+4410000\,g^2-399740\,L+6241\,L^2+200\,g\,(-52130+1659\,L)}\right)}{79\,(-9+20\,g)}}{16\left(100+\frac{20\left(4835-3700\,g-158\,L+2\sqrt{6310900+4410000\,g^2-399740\,L+6241\,L^2+200\,g\,(-52130+1659\,L)}\right)}{79\,(-9+20\,g)}\right)},$$

$$-\frac{1}{79\,(-9+20\,g)\,(5+y4)^2}\left(20\left(4835-3700\,g-158\,L+2\sqrt{6310900+4410000\,g^2-399740\,L+6241\,L^2+200\,g\,(-52130+1659\,L)}\right)y4\right)+\frac{1}{79\,(-9+20\,g)\,(5+y4)}\left(20\left(4835-3700\,g-158\,L+2\sqrt{6310900+4410000\,g^2-399740\,L+6241\,L^2+200\,g\,(-52130+1659\,L)}\right)\right)\Big\},$$

$$\left\{0,\ 0,\ d,\ -\frac{100\ (1-g)+\frac{20\left(\frac{1}{4}-g\right)\left(4835-3700\,g-158\,L+2\sqrt{6310900+4410000\,g^2-399740\,L+6241\,L^2+200\,g\,(-52130+1659\,L)}\right)}{79\,(-9+20\,g)}}{4\left(100+\frac{20\left(4835-3700\,g-158\,L+2\sqrt{6310900+4410000\,g^2-399740\,L+6241\,L^2+200\,g\,(-52130+1659\,L)}\right)}{79\,(-9+20\,g)}\right)},\right.$$

$$\frac{4\left(100\ (1-g)+\frac{20\left(\frac{1}{4}-g\right)\left(4835-3700\,g-158\,L+2\sqrt{6310900+4410000\,g^2-399740\,L+6241\,L^2+200\,g\,(-52130+1659\,L)}\right)}{79\,(-9+20\,g)}\right)}{100+\frac{20\left(4835-3700\,g-158\,L+2\sqrt{6310900+4410000\,g^2-399740\,L+6241\,L^2+200\,g\,(-52130+1659\,L)}\right)}{79\,(-9+20\,g)}},$$

$$-d,\ 0\Big\},$$

$$\Big\{0,\ -d,\ -\frac{d}{4},\ -\frac{y4}{5+y4},\ -d+g,\ \frac{1}{16}-\frac{d}{4},\ -2\,d+\frac{1}{79\,(-9+20\,g)\,(5+y4)^2}\Big(20\left(4835-3700\,g-158\,L+2\sqrt{6310900+4410000\,g^2-399740\,L+6241\,L^2+200\,g\,(-52130+1659\,L)}\right)y4\Big)-\frac{1}{79\,(-9+20\,g)\,(5+y4)}\left(20\left(4835-3700\,g-158\,L+2\sqrt{6310900+4410000\,g^2-399740\,L+6241\,L^2+200\,g\,(-52130+1659\,L)}\right)\right)\Big\}\Big\}$$

```
eigen = Eigenvalues[ma]
```

$$\left\{-2\,d,\ \frac{-500+530\,g-25\,g^2-20\,L+121\,g\,L-105\,g^2\,L}{2000-2200\,g+100\,g^2+400\,L-820\,g\,L+420\,g^2\,L},\right.$$
$$(-500-4000\,d+530\,g+4400\,d\,g-25\,g^2-200\,d\,g^2-20\,L-800\,d\,L+121\,g\,L+$$
$$1640\,d\,g\,L-105\,g^2\,L-840\,d\,g^2\,L)\,/\,(2000-2200\,g+100\,g^2+400\,L-820\,g\,L+420\,g^2\,L),$$
$$\frac{1}{2\,(-100+100\,g)}\,(100+400\,d-200\,g-400\,d\,g+105\,g^2+400\,L-840\,g\,L+441\,g^2\,L-$$
$$\sqrt{(10000-61000\,g^2+82000\,g^3-30975\,g^4-80000\,L+328000\,g\,L-500200\,g^2\,L+336000\,g^3\,L-$$
$$83790\,g^4\,L+160000\,L^2-672000\,g\,L^2+1058400\,g^2\,L^2-740880\,g^3\,L^2+194481\,g^4\,L^2)}),$$
$$\frac{1}{2\,(-100+100\,g)}\,(100+400\,d-200\,g-400\,d\,g+105\,g^2+400\,L-840\,g\,L+441\,g^2\,L+$$
$$\sqrt{(10000-61000\,g^2+82000\,g^3-30975\,g^4-80000\,L+328000\,g\,L-500200\,g^2\,L+336000\,g^3\,L-$$
$$83790\,g^4\,L+160000\,L^2-672000\,g\,L^2+1058400\,g^2\,L^2-740880\,g^3\,L^2+194481\,g^4\,L^2)}),$$
$$\frac{1}{2\,(-100+100\,g)}\,(100-200\,g+105\,g^2+400\,L-840\,g\,L+441\,g^2\,L-$$
$$\sqrt{(-100+200\,g-105\,g^2-400\,L+840\,g\,L-441\,g^2\,L)^2-$$
$$4\,(-100+100\,g)\,(100\,g-205\,g^2+105\,g^3-400\,L+1240\,g\,L-1281\,g^2\,L+441\,g^3\,L)}),$$
$$\frac{1}{2\,(-100+100\,g)}\,(100-200\,g+105\,g^2+400\,L-840\,g\,L+441\,g^2\,L+$$
$$\sqrt{(-100+200\,g-105\,g^2-400\,L+840\,g\,L-441\,g^2\,L)^2-$$
$$\left.4\,(-100+100\,g)\,(100\,g-205\,g^2+105\,g^3-400\,L+1240\,g\,L-1281\,g^2\,L+441\,g^3\,L)}\right)\Big)\Big\}$$

$$E1=\frac{-500+530\,g-25\,g^2-20\,L+121\,g\,L-105\,g^2\,L}{2000-2200\,g+100\,g^2+400\,L-820\,g\,L+420\,g^2\,L}$$

$$\frac{-500+530\,g-25\,g^2-20\,L+121\,g\,L-105\,g^2\,L}{2000-2200\,g+100\,g^2+400\,L-820\,g\,L+420\,g^2\,L}$$

```
V1 = Solve[E1 == 0, g] // Simplify
```

$$\left\{\left\{g\to\frac{530+121\,L+\sqrt{230900-83740\,L+6241\,L^2}}{50+210\,L}\right\},\ \left\{g\to\frac{530+121\,L-\sqrt{230900-83740\,L+6241\,L^2}}{50+210\,L}\right\}\right\}$$

B7 Overall plots from AUTO and analytical results of two-compartment model

```
graphd002 = Show[Plot[(530 + 121 L + Sqrt[230900 - 83740 L + 6241 L^2])/(50 + 210 L), {L, 0, 200},
  AxesStyle -> Automatic, PlotRange -> {0, 1}, AxesLabel -> {"L", "gamma"}],
 Plot[(530 + 121 L - Sqrt[230900 - 83740 L + 6241 L^2])/(50 + 210 L), {L, 0, 200}, AxesStyle -> Automatic,
  PlotRange -> {0, 1}, AxesLabel -> {"L", "gamma"}], Plot[20 L/(5 + 21 L), {L, 0, 200},
  AxesStyle -> Automatic, PlotRange -> {0, 1}, AxesLabel -> {"L", "gamma"}],
 Plot[(1545.` - 195.5` Sqrt[-11.219742779922962` + L] Sqrt[-4.585883818542511` + L] + 384.5` L)/
  (145.` + 609.` L), {L, 0, 200}, AxesStyle -> Automatic, PlotRange -> {0, 1}, AxesLabel -> {"L", "gamma"}],
 Plot[(1545.` + 195.5` Sqrt[-11.219742779922962` + L] Sqrt[-4.585883818542511` + L] + 384.5` L)/
  (145.` + 609.` L), {L, 0, 200}, AxesStyle -> Automatic, PlotRange -> {0, 1}, AxesLabel -> {"L", "gamma"}],
 Plot[20/21, {L, 0, 200}, AxesStyle -> Automatic, PlotRange -> {0, 1},
  AxesLabel -> {"L", "gamma"}], Plot[1/(2625.` + 11025.` L)
   (1743.3333333333333` + 10822.` L + ((0.20998684164914555` - 0.3637078786572405` I)
       (-6.0589`*^6 + 580440.` L - 933156.` L^2))/
     (-2.8642651`*^10 + 1.43179344`*^10 L + 1.457093988`*^10 L^2 + 1.802857392`*^9 L^3 +
       7.655317152062684`*^9 Sqrt[-1.6410941204500646` + L] (0.23809523809523808` + L)
        Sqrt[12.709661892350022` + 4.5239705972721085` L + L^2])^(1/3) -
    (0.13228342099734997` + 0.22912160616643376` I)
     (-2.8642651`*^10 + 1.43179344`*^10 L + 1.457093988`*^10 L^2 + 1.802857392`*^9 L^3 +
       7.655317152062684`*^9 Sqrt[-1.6410941204500646` + L] (0.23809523809523808` + L)
        Sqrt[12.709661892350022` + 4.5239705972721085` L + L^2])^(1/3)), {L, 0, 200},
 AxesStyle -> Automatic, PlotRange -> {0, 1}, AxesLabel -> {"L", "gamma"}],
 Plot[1/(2625.` + 11025.` L) (1743.3333333333333` + 10822.` L +
    ((0.20998684164914555` + 0.3637078786572405` I) (-6.0589`*^6 + 580440.` L -
       933156.` L^2))/(-2.8642651`*^10 + 1.43179344`*^10 L + 1.457093988`*^10 L^2 +
       1.802857392`*^9 L^3 + 7.655317152062684`*^9 Sqrt[-1.6410941204500646` + L]
        (0.23809523809523808` + L) Sqrt[12.709661892350022` + 4.5239705972721085` L + L^2])^
    (1/3) - (0.13228342099734997` - 0.22912160616643376` I)
     (-2.8642651`*^10 + 1.43179344`*^10 L + 1.457093988`*^10 L^2 + 1.802857392`*^9 L^3 +
       7.655317152062684`*^9 Sqrt[-1.6410941204500646` + L] (0.23809523809523808` + L)
        Sqrt[12.709661892350022` + 4.5239705972721085` L + L^2])^(1/3)), {L, 0, 200},
 AxesStyle -> Automatic, PlotRange -> {0, 1}, AxesLabel -> {"L", "gamma"}],
```

```
Plot[1/(2625.` + 11025.` L) (1743.3333333333333` + 10822.` L +
    (2.5445785497360155`*^6 - 243769.52473366002` L + 391900.96241190005` L^2)/
     (-2.8642651`*^10 + 1.43179344`*^10 L + 1.457093988`*^10 L^2 + 1.802857392`*^9 L^3 +
       7.655317152062684`*^9 Sqrt[-1.6410941204500646` + L] (0.23809523809523808` + L)
        Sqrt[12.709661892350022` + 4.5239705972721085` L + L^2])^(1/3) +
    0.26456684199469993` (-2.8642651`*^10 + 1.43179344`*^10 L +
       1.457093988`*^10 L^2 + 1.802857392`*^9 L^3 +
       7.655317152062684`*^9 Sqrt[-1.6410941204500646` + L] (0.23809523809523808` + L)
        Sqrt[12.709661892350022` + 4.5239705972721085` L + L^2])^(1/3)),
  {L, 0, 200}, AxesStyle -> Automatic, PlotRange -> {0, 1}, AxesLabel ->
   {"L", "gamma"}],
 Plot[0.6, {L, 0, 200}, AxesStyle -> Automatic,
  PlotRange -> {0, 1},
  AxesLabel -> {"L", "gamma"}],
 Plot[0.4, {L, 0, 200}, AxesStyle -> Automatic,
  PlotRange -> {0, 1},
  AxesLabel -> {"L", "gamma"}]]
```

Plot::plnr : $\frac{530 + 121\,L + \sqrt{230900 - 83740\,L - 6241\,L^2}}{50 + 210\,L}$ is not a machine-size real number at L = 8.11339831458316`.

Plot::plnr : $\frac{530 + 121\,L + \sqrt{230900 - 83740\,L + 6241\,L^2}}{50 + 210\,L}$ is not a machine-size real number at L = 3.949634152604036`.

Plot::plnr : $\frac{530 + 121\,L + \sqrt{230900 - 83740\,L + 6241\,L^2}}{50 + 210\,L}$ is not a machine-size real number at L = 3.891379285226266`.

General::stop : Further output of Plot::plnr will be suppressed during this calculation.

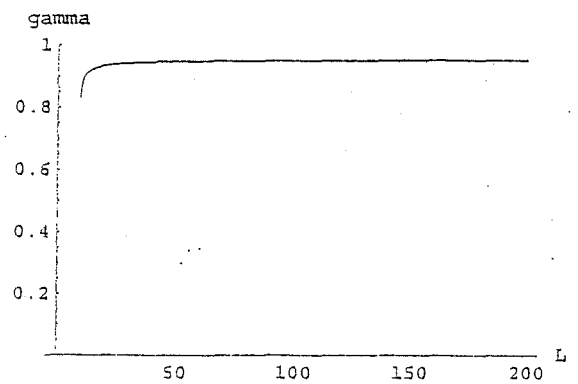

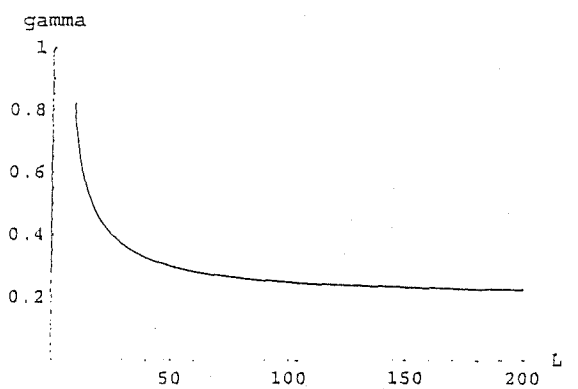

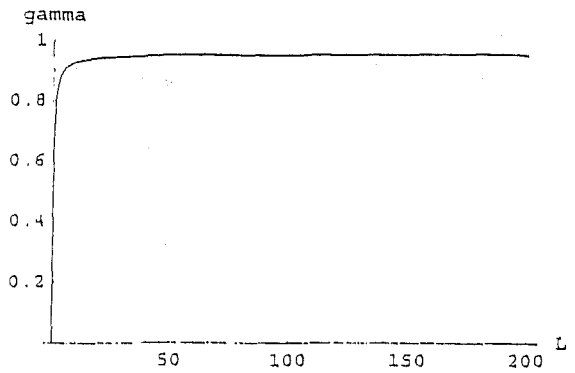
gamma
1
0.8
0.6
0.4
0.2
50
100
150
200
L

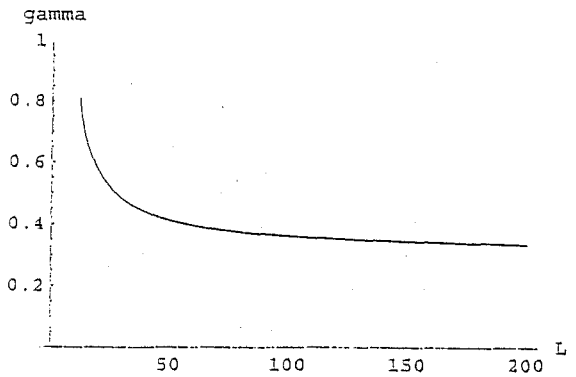
gamma
1
0.8
0.6
0.4
0.2
50
100
150
200
L

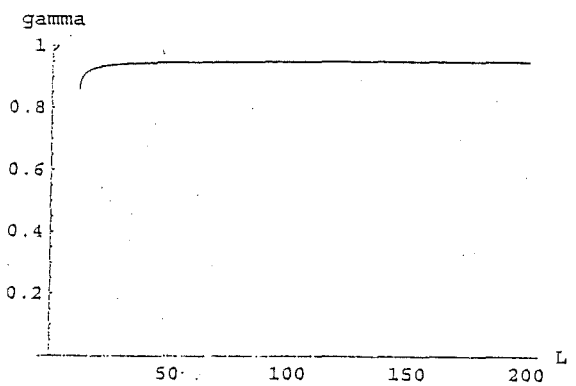
gamma
1
0.8
0.6
0.4
0.2
50
100
150
200
L

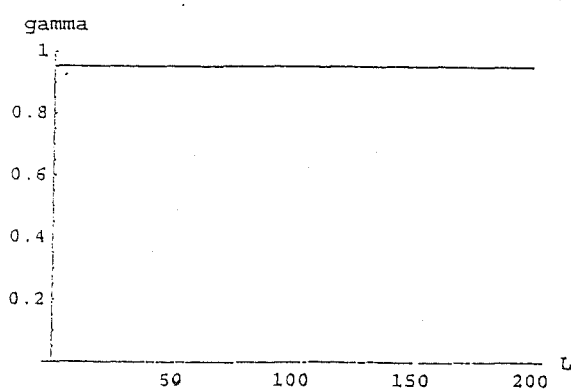
gamma
1
0.8
0.6
0.4
0.2
50
100
150
200
L

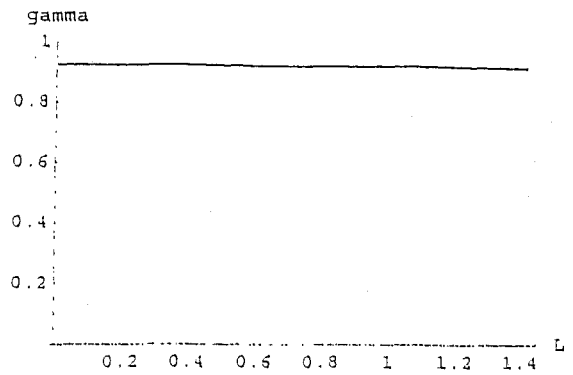
gamma
1
0.8
0.6
0.4
0.2
0.2 0.4 0.6 0.8 1 1.2 1.4
L

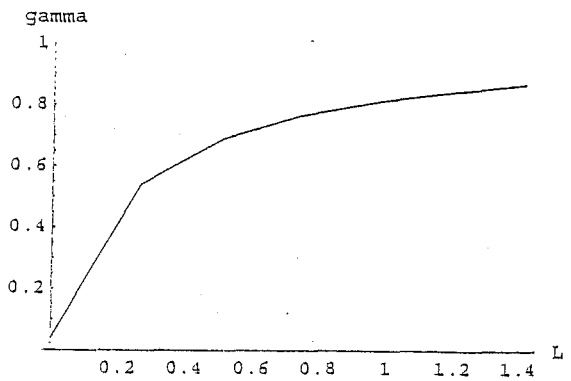
gamma
1
0.8
0.6
0.4
0.2
0.2 0.4 0.6 0.8 1 1.2 1.4
L

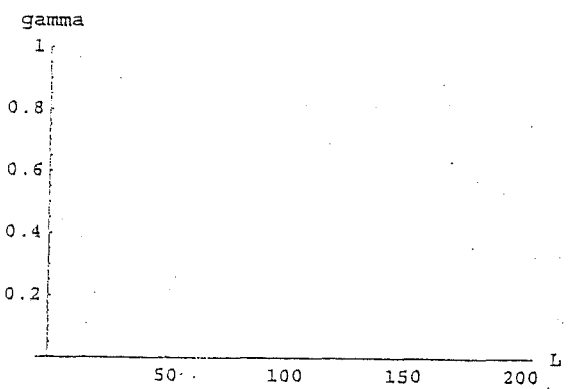
gamma
1
0.8
0.6
0.4
0.2
50 100 150 200
L

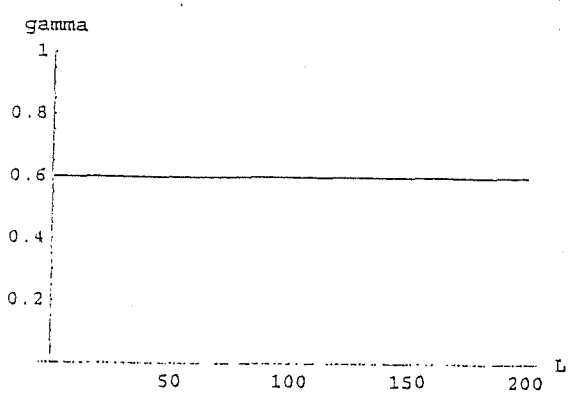
gamma
1
0.8
0.6
0.4
0.2
50 100 150 200
L

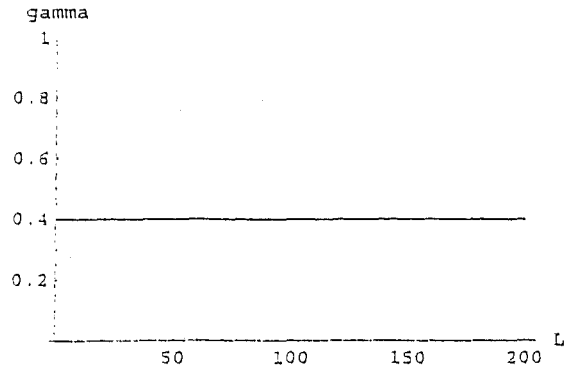

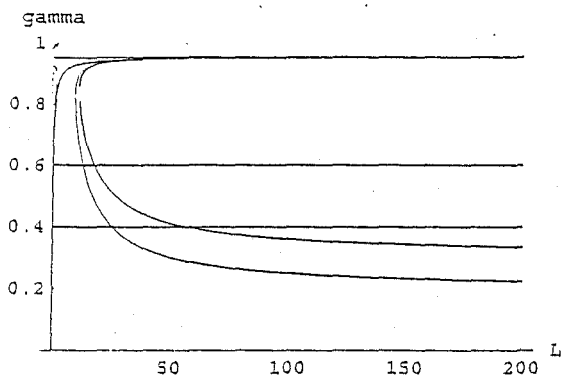

- Graphics -

```
LPd002 = {{20.87, 0.4405}, {21.06, 0.4369}, {21.35, 0.431}, {21.84, 0.42},
   {22.66, 0.4}, {23.56, 0.3763}, {25.41, 0.3254}, {27.88, 0.2553},
   {30.47, 0.1812}, {33.08, 0.1057}, {35.71, 0.02967}, {38.34, -0.0468}}
```

```
{{20.87, 0.4405}, {21.06, 0.4369}, {21.35, 0.431}, {21.84, 0.42},
 {22.66, 0.4}, {23.56, 0.3763}, {25.41, 0.3254}, {27.88, 0.2553},
 {30.47, 0.1812}, {33.08, 0.1057}, {35.71, 0.02967}, {38.34, -0.0468}}
```

```
LPgrd002 = ListPlot[LPd002, PlotRange → {0, 1}, PlotJoined → True]
```

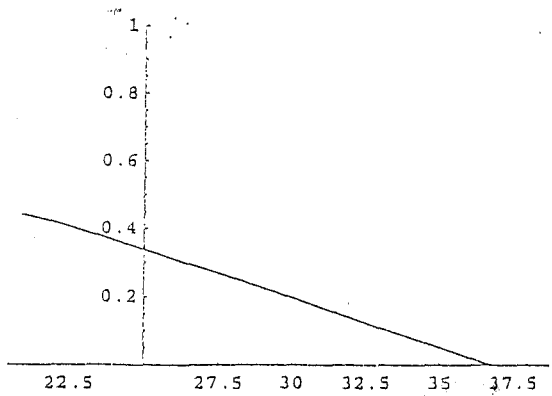

- Graphics -

```
HB1d002 = {{46.81, 0.8079}, {39.88, 0.8073}, {33.71, 0.8063}, {27.42, 0.8043},
   {21.26, 0.7993}, {15.88, 0.7785}, {15.18, 0.7089}, {17.07, 0.6295},
   {19.39, 0.5506}, {21.85, 0.4721}, {24.16, 0.4}, {26.5, 0.3281}, {29.06, 0.2501},
   {31.63, 0.1733}, {34.21, 0.09442}, {36.8, 0.01665}, {39.39, -0.06109}}
```

```
{{46.81, 0.8079}, {39.88, 0.8073}, {33.71, 0.8063}, {27.42, 0.8043},
 {21.26, 0.7993}, {15.88, 0.7785}, {15.18, 0.7089}, {17.07, 0.6295},
 {19.39, 0.5506}, {21.85, 0.4721}, {24.16, 0.4}, {26.5, 0.3281}, {29.06, 0.2501},
 {31.63, 0.1733}, {34.21, 0.09442}, {36.8, 0.01665}, {39.39, -0.06109}}
```

```
HB1grd002 = ListPlot[HB1d002, PlotRange → {0, 1}, PlotJoined → True]
```

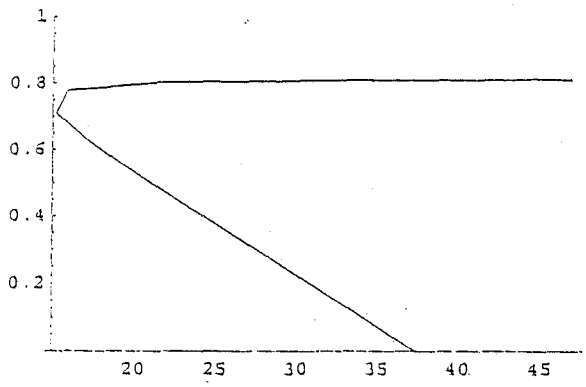


```
- Graphics -
```

```
HB2d002 = {{200.2, 0.4733}, {191.5, 0.4733}, {170.3, 0.4733}, {159.7, 0.4732},
   {149.1, 0.4732}, {138.5, 0.4732}, {127.9, 0.4732}, {117.3, 0.4731},
   {106.7, 0.4731}, {96.06, 0.473}, {85.45, 0.4728}, {74.85, 0.4725}, {64.25, 0.472},
   {53.67, 0.4709}, {43.11, 0.468}, {32.87, 0.4555}, {28.07, 0.4}, {28.99, 0.3137},
   {30.95, 0.2346}, {33.2, 0.1559}, {35.58, 0.07754}, {38.04, -0.0006871}}
```

```
{{200.2, 0.4733}, {191.5, 0.4733}, {170.3, 0.4733}, {159.7, 0.4732},
 {149.1, 0.4732}, {138.5, 0.4732}, {127.9, 0.4732}, {117.3, 0.4731},
 {106.7, 0.4731}, {96.06, 0.473}, {85.45, 0.4728}, {74.85, 0.4725}, {64.25, 0.472},
 {53.67, 0.4709}, {43.11, 0.468}, {32.87, 0.4555}, {28.07, 0.4}, {28.99, 0.3137},
 {30.95, 0.2346}, {33.2, 0.1559}, {35.58, 0.07754}, {38.04, -0.0006871}}
```

```
HB2grd002 = ListPlot[HB2d002, PlotRange → {0, 1}, PlotJoined → True]
```

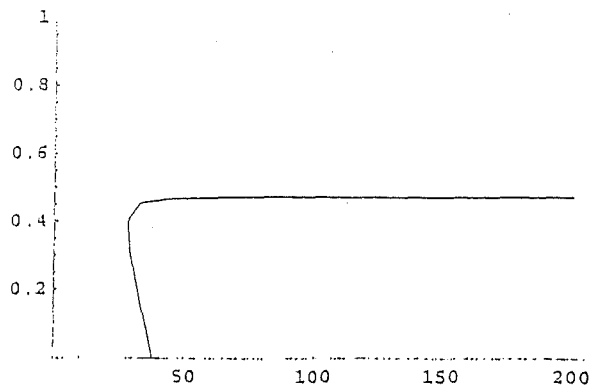


```
- Graphics -
```

```
combineplotd002 = Show[graphd002, LPgrd002, HB1grd002, HB2grd002,
  AxesStyle → Thickness[0.005], PlotRange → {0, 1}, AxesLabel → {"L", "gamma"}]
```

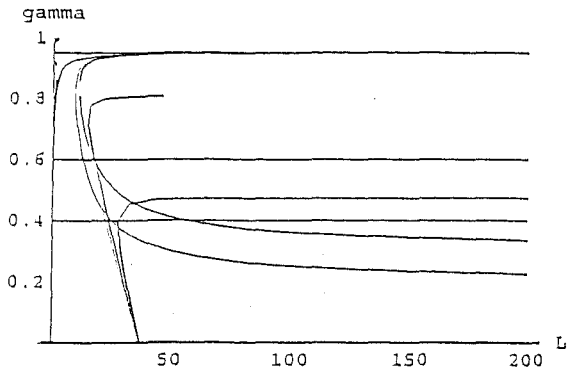

- Graphics -

```
graphd0026 =
 Show[Plot[(8055.` - 974.5` √(-11.73059276144144` + L) √(-4.800961881965436` + L) + 2045.5` L)/(755.` + 3171.` L),
   {L, 0, 60}, AxesStyle → Automatic, PlotRange → {0, 1}, AxesLabel → {"L", "gamma"}],
  Plot[(8055.` + 974.5` √(-11.73059276144144` + L) √(-4.800961881965436` + L) + 2045.5` L)/(755.` + 3171.` L),
   {L, 0, 60}, AxesStyle → Automatic, PlotRange → {0, 1}, AxesLabel → {"L", "gamma"}]]
```

Plot::plnr : $\frac{8055. - \text{<<1>>} + 2045.5\,L}{755. + 3171.\,L}$ is not a machine-size real number at L = 5.088527991562421`.

Plot::plnr : $\frac{8055. - \text{<<1>>} + 2045.5\,L}{755. + 3171.\,L}$ is not a machine-size real number at L = 4.923986528621818`.

Plot::plnr : $\frac{8055. - \text{<<1>>} + 2045.5\,L}{755. + 3171.\,L}$ is not a machine-size real number at L = 4.832111204207404`.

General::stop : Further output of Plot::plnr will be suppressed during this calculation.

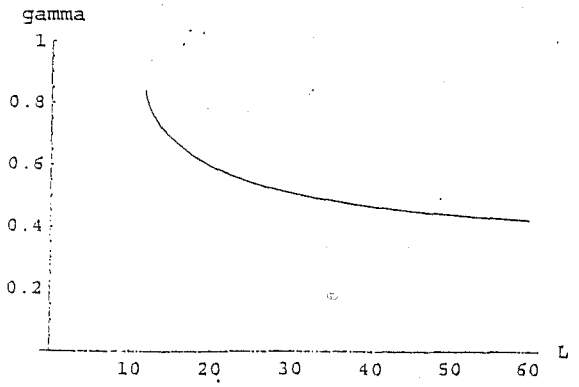

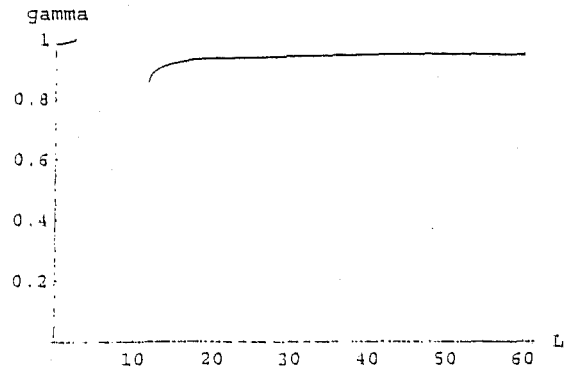

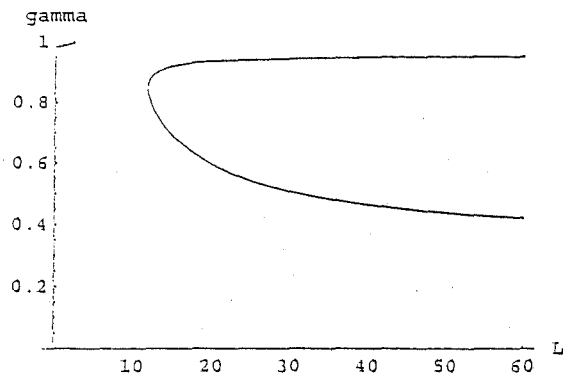

- Graphics -

```
graph3 = Show[graph1, graphd002, graphd0026,
  AxesStyle → Thickness[0.005], PlotRange → {0, 1}, AxesLabel → {"L", "gamma"}]
```

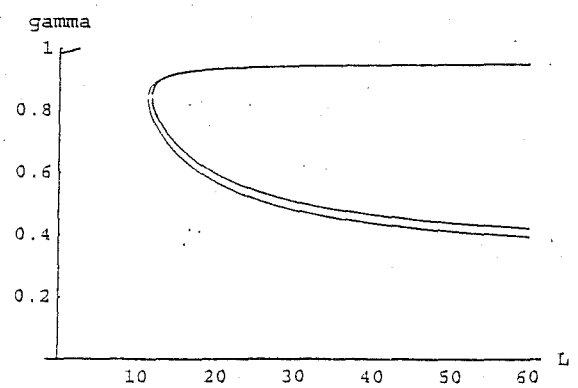

- Graphics -

$$\text{graphd0026E3} = \text{Show}\left[\text{Plot}\left[\frac{530 + 121\,L + \sqrt{230900 - 83740\,L + 6241\,L^2}}{50 + 210\,L}, \{L, 0, 60\},\right.\right.$$
$$\text{AxesStyle} \to \text{Automatic}, \text{PlotRange} \to \{0, 1\}, \text{AxesLabel} \to \{\text{"L"}, \text{"gamma"}\}\Big],$$
$$\text{Plot}\left[\frac{530 + 121\,L - \sqrt{230900 - 83740\,L + 6241\,L^2}}{50 + 210\,L}, \{L, 0, 60\},\right.$$
$$\left.\text{AxesStyle} \to \text{Automatic}, \text{PlotRange} \to \{0, 1\}, \text{AxesLabel} \to \{\text{"L"}, \text{"gamma"}\}\right],$$
$$\text{Plot}\left[\frac{8055.` - 974.5` \sqrt{-11.73059276144144` + L}\ \sqrt{-4.800961881965436` + L} + 2045.5` L}{755.` + 3171.` L},\right.$$

```
  {L, 0, 60}, AxesStyle → Automatic, PlotRange → {0, 1}, AxesLabel → {"L", "gamma"}],
 Plot[(8055.` + 974.5` √(-11.73059276144144` + L) √(-4.800961881965436` + L) + 2045.5` L)/
  (755.` + 3171.` L),
  {L, 0, 60}, AxesStyle → Automatic, PlotRange → {0, 1},
  AxesLabel → {"L", "gamma"}], Plot[1/(131250.` + 551250.` L)
   (87691.66666666666` + 543305.` L + ((0.20998684164914555` - 0.3637078786572405` i)
        (-1.4737868125`*^10 + 3.00794025`*^9 L - 3.015657225`*^9 L²)) /
      (-3.39504916446875`*^15 + 2.64637526225625`*^15 L + 2.17605279913875`*^15 L² +
        3.3120963302175`*^14 L³ + 1.3303069591613528`*^15 √(-1.2463068255518803` + L)
         (0.23809523809523808` + L) √(10.222623885007133` + 3.3425344486869135` L + L²))^
       (1/3) - (0.13228342099734997` + 0.22912160616643376` i) (-3.39504916446875`*^15 +
        2.64637526225625`*^15 L + 2.17605279913875`*^15 L² + 3.3120963302175`*^14 L³ +
        1.3303069591613528`*^15 √(-1.2463068255518803` + L) (0.23809523809523808` + L)
         √(10.222623885007133` + 3.3425344486869135` L + L²))^(1/3)), {L, 0, 40},
  AxesStyle → Automatic, PlotRange → {0, 1}, AxesLabel → {"L", "gamma"}],
 Plot[1/(131250.` + 551250.` L)
   (87691.66666666666` + 543305.` L + ((0.20998684164914555` + 0.3637078786572405` i)
        (-1.4737868125`*^10 + 3.00794025`*^9 L - 3.015657225`*^9 L²)) /
      (-3.39504916446875`*^15 + 2.64637526225625`*^15 L + 2.17605279913875`*^15 L² +
        3.3120963302175`*^14 L³ + 1.3303069591613528`*^15 √(-1.2463068255518803` + L)
         (0.23809523809523808` + L) √(10.222623885007133` + 3.3425344486869135` L + L²))^
       (1/3) - (0.13228342099734997` - 0.22912160616643376` i) (-3.39504916446875`*^15 +
        2.64637526225625`*^15 L + 2.17605279913875`*^15 L² + 3.3120963302175`*^14 L³ +
        1.3303069591613528`*^15 √(-1.2463068255518803` + L) (0.23809523809523808` + L)
         √(10.222623885007133` + 3.3425344486869135` L + L²))^(1/3)),
  {L, 0, 40}, AxesStyle → Automatic, PlotRange → {0, 1},
  AxesLabel → {"L", "gamma"}],
 Plot[1/(131250.` + 551250.` L) (87691.66666666666` + 543305.` L +
   (6.189516760420728`*^9 - 1.2632557459336822`*^9 L + 1.2664966723483531`*^9 L²) /
    (-3.39504916446875`*^15 + 2.64637526225625`*^15 L + 2.17605279913875`*^15 L² +
      3.3120963302175`*^14 L³ + 1.3303069591613528`*^15 √(-1.2463068255518803` + L)
       (0.23809523809523808` + L) √(10.222623885007133` + 3.3425344486869135` L + L²))^
     (1/3) + 0.26456684199469993` (-3.39504916446875`*^15 + 2.64637526225625`*^15 L +
      2.17605279913875`*^15 L² + 3.3120963302175`*^14 L³ +
      1.3303069591613528`*^15 √(-1.2463068255518803` + L) (0.23809523809523808` + L)
       √(10.222623885007133` + 3.3425344486869135` L + L²))^(1/3)),
  {L, 0, 40}, AxesStyle → Automatic, PlotRange → {0, 1},
  AxesLabel → {"L", "gamma"}],
 Plot[20 L/(5 + 21 L), {L, 0, 40},
  AxesStyle → Automatic,
  PlotRange → {0, 1},
  AxesLabel → {"L", "gamma"}]]
```

Plot::plnr : $\frac{530 + 121\,L + \sqrt{230900 - 83740\,L + 6241\,L^2}}{50 + 210\,L}$ is not a machine-size real number at L = 5.088527991562421`.

Plot::plnr : $\frac{530 + 121\,L + \sqrt{230900 - 83740\,L + 6241\,L^2}}{50 + 210\,L}$ is not a machine-size real number at L = 4.440717792946121`.

Plot::plnr : $\frac{530 + 121\,L + \sqrt{230900 - 83740\,L + 6241\,L^2}}{50 + 210\,L}$ is not a machine-size real number at L = 4.094139549943254`.

General::stop : Further output of Plot::plnr will be suppressed during this calculation.

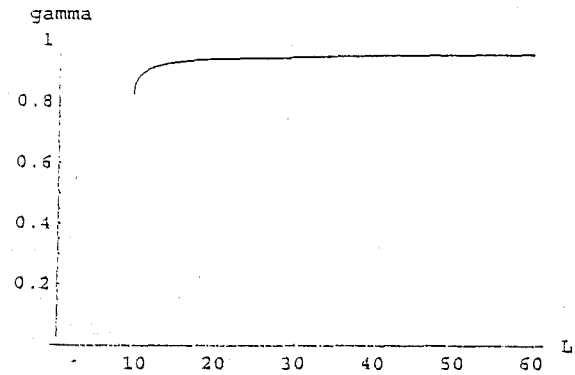

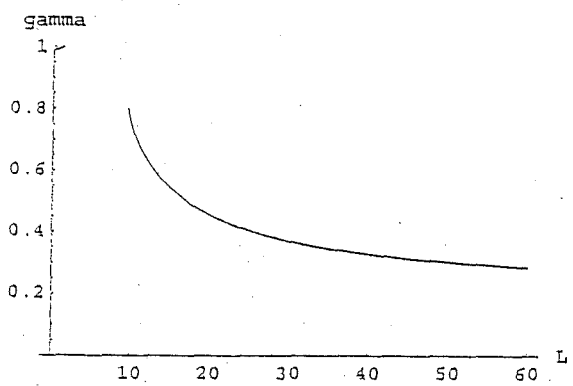

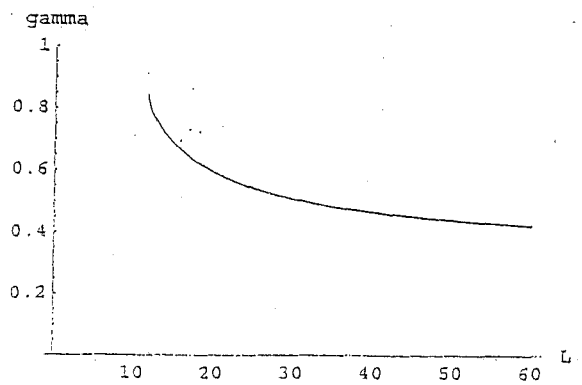

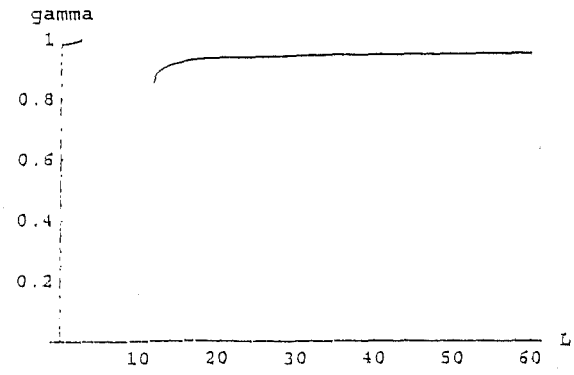
gamma
1
0.8
0.6
0.4
0.2
10
20
30
40
50
60
L

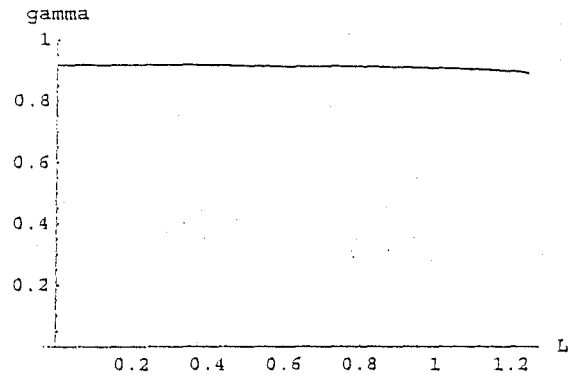
gamma
1
0.8
0.6
0.4
0.2
0.2
0.4
0.6
0.8
1
1.2
L

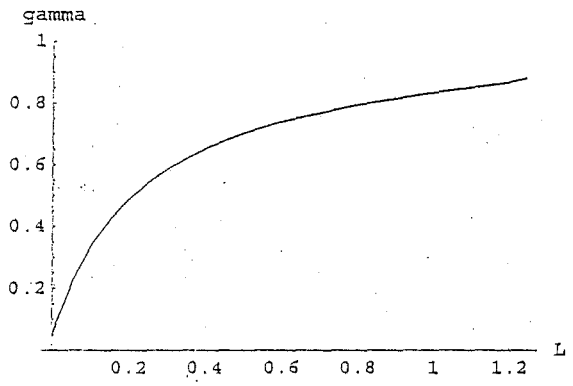
gamma
1
0.8
0.6
0.4
0.2
0.2
0.4
0.6
0.8
1
1.2
L

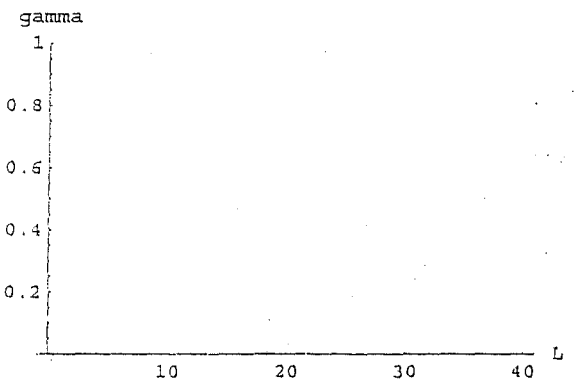
gamma
1
0.8
0.6
0.4
0.2
10
20
30
40
L

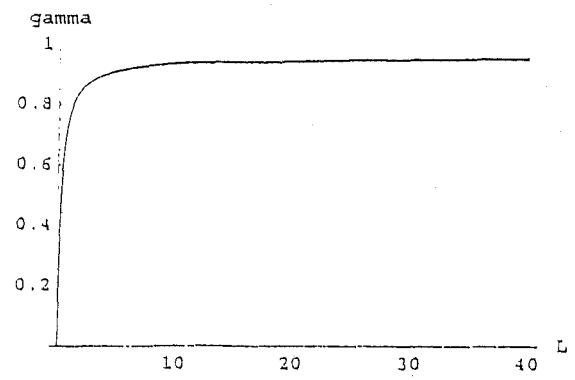
gamma
1
0.8
0.6
0.4
0.2
10
20
30
40
L

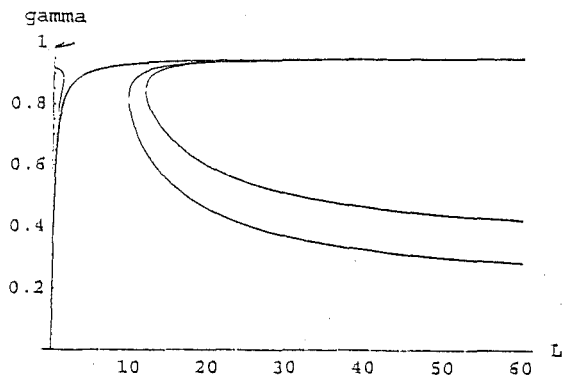
gamma
1
0.8
0.6
0.4
0.2
10
20
30
40
50
60
L

- Graphics -

APPENDIX C

TABLES

C1: The Biological and nutrient parameters and their values

Parameter	Definition	Value	Dimensions
μ_{max}	Maximum growth rate of phytoplankton	2	day^{-1}
L	Light (Irradiance)	50	$\mu Einst.m^{-2}s^{-1}$
L_H	Half Saturation light (irradiance) constant	50	$\mu Einst.m^{-2}s^{-1}$
μ	Light saturated growth rate of phytoplankton	1	day^{-1}
h	Half saturation of total free nitrogen	5	$mgN\ m^{-3}$
Q	Minimum phytoplankton N quota	0.05	$mgN\ mgC^{-1}$
R	Maximum phytoplankton N quota	0.25	$mgN\ mgC^{-1}$
$\hat{C}$	Half saturation constant for zooplankton uptake of phytoplankton carbon	100	$mgC\ m^{-3}$
U	Maximum phytoplankton uptake rate per unit biomass	1	$mgN\ mgC^{-1}\ day^{-1}$
Γ	Maximum zooplankton grazing rate	1	$mgN\ mgC^{-1}\ day^{-1}$
γ_1	Zooplankton loss rate	0.25	day^{-1}
γ_2	Nitrogen quotas of zooplankton	0.25	$mgNmgC^{-1}$

Note:

i) The maximum growth rate of phytoplankton μ_{max} of the diatom *Thalassiosira pseudonana* under the conditions of nitrogen in the laboratory of 1.7-1.9 day^{-1} is given by Thompson et al. (1989). This is compares with values of 1.22 day^{-1} for *Thalassiosira Fluviatilis* and 2.48 day^{-1} for *Chlorrella Pyrenoidosa* found by Laws & Bannister (1980) in the laboratory. We shall use an estimate of 2.0 day^{-1}.

ii) The light and the half saturation light constant L_H, is estimated by Law and Bannister (1980) to be ~60 $\mu Einst.m^{-2}s^{-1}$ and Thompson et al. (1989) to be ~40 $\mu Einst.m^{-2}s^{-1}$. We choose a value of ~50 $\mu Einst.m^{-2}s^{-1}$.

iii) Thus, the light saturated growth rate of phytoplankton μ is given by $\mu = \mu_{max}\left(\frac{L}{L+L_H}\right)$ i.e. $\mu = 1\ day^{-1}$.

iv) The mean of the half saturation of total free nitrogen h is found by Caperon & Meyer (1972) to be 4.2 $mgN\ m^{-3}$. We choose a whole number value of 5.0 $mgN\ m^{-3}$.

v) The minimum phytoplankton N quota Q is takes the value of 0.05 $mgN\ mgC^{-1}$ by Tett & Droop (1986), Laws & Bannister (1980) and Caperon & Meyer (1972).

vi) The maximum phytoplankton N quota Q is estimated to be 0.05 $mgN\ mgC^{-1}$ by Tett & Droop (1986).

vii) The half saturation constant for zooplankton uptake of phytoplankton carbon $\hat{C}$ is estimated to be 100 $mgC\,m^{-3}$. Estimates of ~200 $mgC\,m^{-3}$ and ~100-200 $mgC\,m^{-3}$ for Acartia tonsa based on the data of Kiorboe et. al. (1985) and Libourel Hiode & Roman (1987) respectively.

viii) Caperon Meyer (1972) found the maximum phytoplankton uptake rate per unit biomass U for a number of different species in the range 0.2-2.64 $mgN\,mgC^{-1}\,day^{-1}$, with a means of 1.2. We use a whole number 1.0 $mgN\,mgC^{-1}\,day^{-1}$.

ix) The maximum grazing rate Γ is taken to be 1.0 $mgN\,mgC^{-1}\,day^{-1}$. Kiorboe et. al. (1985) measured the maximum grazing rate of *Acartia tonsa* feeding on a mixed culture of *Isochrysis galbana* and *Rhodomanas baltica* to be 1.8 $mgN\,mgC^{-1}\,day^{-1}$.This compares with a measured range of 0.21-0.32 for *Acartia tonsa* feeding on small diatoms by Libourel Houde & Roman (1987).

x) The zooplankton loss rate is estimated by Kiorboe et al. (1985) to be in the range of 0.19-0.49 day^{-1}. We choose a value of 0.25 day^{-1}.

xi) Redfield estimated the nitrogen quota of zooplankton to be 0.15 $mgNmgC^{-1}$ in response to the temperature. We choose 0.25 $mgNmgC^{-1}$, a higher value since Brunei is an equatorial climate and having 12hours per day of light the nitrogen quota is presumably higher.

C2a: The various bifurcation points λ for a one compartment model executed by AUTO (numerical result)

γ	BP1	BP2	LP	HB
0.4	0.1724	25.17	22.66	24.16
0.45	0.2132	20.21		22.55
0.5	0.2631	16.93		20.96
0.6	0.4053	12.91		17.91
0.7	0.6604	10.66		15.34
0.8	3.333	11.67		21.82

C2b: The bifurcation point 1 (BP1) for a one compartment model executed by MATHEMATICA (analytical result)

$$\text{Table}\left[\left\{g, \frac{5g}{20-21g}\right\}, \{g, 0, 1, 0.1\}\right]$$

```
{{0,0},{0.1,0.027933},{0.2,0.0632911},{0.3,0.109489},{0.4,0.1724
14},{0.5,0.263158},{0.6,0.405405},{0.7,0.660377,{0.8,1.25},{0.9,
4.09091},{1.,-5.}}
```

C2c: The bifurcation point 2 (BP2) for a one-compartment model executed by MATHEMATICA (analytical result)

$$\text{Table}\left[\left\{g, \frac{25}{5g-1} + \frac{5g}{20-21g}\right\}, \{g, 0, 1, 0.1\}\right]$$

```
{{0,-25},{0.1,49.9721},{0.2,ComplexInfinity},{0.3,50.1095},
{0.4,25.1724},{0.5,16.9298},{0.6,12.9054},{0.7,10.6604},{0.8,9.5
8333},{0.9,11.2338},{1.,1.25}}
```

C3a: The various bifurcation points λ for a two compartment model executed by AUTO (numerical result)

γ	BP1	BP2	LP	HB1	HB2
0.4	0.1724	25.17	22.66	24.16	28.07
0.45	0.2132	20.21		22.55	31.4
0.5	0.2631	16.93		20.96	
0.6	0.4053	12.91		17.91	
0.7	0.6604	10.66		15.34	

C3b: The bifurcation point 1 (BP1) denoted by V_5 and V_6 for a two compartment model executed by MATHEMATICA (analytical result)

$$\text{Table}\left[\left\{g, \frac{5g}{20-21g}\right\}, \{g, 0, 1, 0.1\}\right]$$

```
{{0,0},{0.1,0.027933},{0.2,0.0632911},{0.3,0.109489},{0.4,0.172
414},{0.5,0.263158},{0.6,0.405405},{0.7,0.660377},{0.8,1.25},{0
.9,4.09091},{1.,-5.}}
```

C3c: The bifurcation point 1 (BP2) denoted by V_1 for a two compartment model executed by MATHEMATICA (analytical result)

$$\text{Table}\left[\left\{g, -\frac{5\,(100 - 106\,g + 5\,g^2)}{20 - 121\,g + 105\,g^2}\right\}, \{g, 0, 1, 0.1\}\right]$$

$$\{\{0, -25\}, \{0.1, -49.9721\}, \{0.2, 2.22365\times10^{17}\}, \{0.3, 50.1095\}, \{0.4, 25.1724\},$$
$$\{0.5, 16.9298\}, \{0.6, 12.9054\}, \{0.7, 10.6604\}, \{0.8, 9.58333\}, \{0.9, 11.2338\}, \{1., 1.25\}\}$$

C4a: The bifurcation points for a three compartment model (equal growth parameter of the phytoplankton i.e. $\mu_1 = \mu_2 = \mu_3 = 1$ executed by AUTO (numerical result) for section 4.3

μ_1	μ_2	μ_3	d_1	d_2	d_3	BP1	BP2	LP	HB1 (s)	HB2 (u)	uf BP	uf LP	uf HB
1	1	1	0.02	0.02	0.02	0.1724	25.17	22.66	24.16		30.45 37.21	23.25 24.02	24.56 25.23 28.34
1	1	1	0.01	0.02	0.02	0.1724	25.17	22.66	24.16	28.07			
1	1	1	0.03	0.02	0.02	0.1724	25.17	22.66	24.16				
1	1	1	0.04	0.02	0.02	0.1724	25.17	22.66	24.16				
1	1	1	0.02	0.01	0.02	0.1724	25.17	22.66	24.16				

C4b: The bifurcation points for a three compartment model (different growth parameter of the phytoplankton and equal diffusion parameter d executed by AUTO (numerical result) for section 4.4

μ	μ_1	μ_2	d	d_1	d_2	BP1	BP2	LP1	LP2	HB1 (s)	HB2 (u)	uf BP	uf LP	uf HB
0.5	1	1	0.02	0.02	0.02	0.1494	12.01	23.63	23.34	24.78	31.19	36.13	26	29.4
1	0.5	1	0.02	0.02	0.02	0.1494	12.01	23.63	23.34	24.78	31.19	36.13	26	29.49
1	1	0.5	0.02	0.02	0.02	0.1494	12.01	23.63	23.34	24.78	31.19	36.13	26	29.49

C4c: The bifurcation points for a three compartment model (one different growth parameter of the phytoplankton and one different diffusion parameter executed by AUTO (numerical result) for section 4.5

μ	μ_1	μ_2	d	d_1	d_2	BP1	BP2	LP1	LP2	HB1	HB2	ufBP	ufLP	ufHB
1	1	0.5	0.04	0.02	0.02	0.1831	12.01	23.63	23.34	24.78		36.13	26	29.49
1	1	0.5	0.02	0.04	0.02	0.186	13.1	23.43	23.43	24.93	37.76	44.97	30.17 31.55 30.25	
1	1	0.5	0.02	0.02	0.04	0.186	13.1	23.43	23.43	24.93	37.76	44.97	30.17 31.55 30.25	

C4c: The bifurcation points for a three compartment model (one different growth parameter of the phytoplankton and one different diffusion parameter executed by AUTO (numerical result) for section 4.5 – continuation

μ	μ_1	μ_2	d	d_1	d_2	BP1	BP2	LP1	LP2	HB1	HB2	ufBP	ufLP	ufHB
0.5	1	1	0.04	0.02	0.02	0.186	13.1	23.43	23.43	24.93	37.76	44.97	31.55 30.25	
0.5	1	1	0.02	0.04	0.02	0.1831	12.01	23.63	23.34	24.78		36.13	26	29.49
0.5	1	1	0.02	0.02	0.04	0.186	13.1	23.43	23.43	24.93	37.76	44.97	31.55 30.25	

μ	μ_1	μ_2	d	d_1	d_2	BP1	BP2	LP1	LP2	HB1	HB2	ufBP	ufLP	ufHB
1	0.5	1	0.04	0.04	0.02	0.186	13.1	23.43	23.43	24.93	37.76	44.97	30.17 30.25 31.55	
1	0.5	1	0.02	0.04	0.02	0.186	13.1	23.43	23.43	24.93	37.76	44.97	30.17 30.25 31.55	
1	0.5	1	0.02	0.02	0.04	0.1831	12.01	23.63	23.34	24.78		36.13	26	29.49

APPENDIX D

XPP AND AUTO PROGRAMS

D1 Program for the one-compartment model

```
# Simple nutrient-phytoplankton-zooplankton model 8 march 2000

init C_p=1 N_p=0.2 C_z=1

par lamda=5,g_p=0.25,U_nmax=1,F_nh=5,Q_pmax=0.25,Q_off=0.01,g_zmax=1,

par C_hp=100, mu_max=2,Q_pmin=0.05,L_h=50,g_z=0.05,Q_z=0.25, a_L=50, b_L=0

L= max(0,a_L-b_L*sin(2*pi*t))

Q_p=N_p/C_p

F_n=lamda-N_p-(Q_z*C_z)

U_n=U_nmax*C_p*(F_n/(F_n+F_nh))*(1/(1+exp((Q_p-Q_pmax)/Q_off)))

gamma_z=g_zmax*C_z*C_p/(C_p+C_hp)

mu=mu_max*C_p*max(0,(1-Q_pmin/Q_p))*L/(L+L_h)

dN_p/dt=U_n - g_p*N_p -gamma_z*Q_p

dC_p/dt=mu - g_p*C_p -gamma_z

dC_z/dt=(Q_p/Q_z)*gamma_z-g_z*C_z

aux Ratio=C_p/N_p

@ BOUND=1e+12

@ NJMP=1

@ TOTAL=1000

@ XP=T,YP=C_p

@ BELL=off

@ MAXSTOR=1500000
```

D2 Program for the two-compartment model

```
# Simple nutrient-phytoplankton-zooplankton model

# 25 September 2002

init C_p1=1 N_p1=0.2 C_z1=1 C_p2=10 N_p2=1 C_z2=4 F_n2=10


par lamda=5,g_p=0.4,D=0.02,mu_maxe=1,mu_max=0.5,U_nmax=1,F_nh=5,

par Q_pmax=0.25,Q_off=0.01,g_zmax=1,Q_pmin=0.05, g_z=0.25,C_hp=100,

par Q_z=0.25


Q_p1=N_p1/C_p1

Q_p2=N_p2/C_p2

F_n1=(2*lamda)-N_p1-(Q_z*C_z1)-F_n2-N_p2-(Q_z*C_z2)


U_n1=U_nmax*C_p1*(F_n1/(F_n1+F_nh))*(1/(1+exp((Q_p1-Q_pmax)/Q_off)))

U_n2=U_nmax*C_p2*(F_n2/(F_n2+F_nh))*(1/(1+exp((Q_p2-Q_pmax)/Q_off)))


gamma_z1=g_zmax*C_z1*C_p1/(C_p1+C_hp)

gamma_z2=g_zmax*C_z2*C_p2/(C_p2+C_hp)


mu_1=mu_max1*C_p1*max(0,(1-Q_pmin/Q_p1))

mu_2=mu_max2*C_p2*max(0,(1-Q_pmin/Q_p2))
```

```
dN_p1/dt=U_n1 - g_p*N_p1 -gamma_z1*Q_p1-D1*(N_p1-N_p2)

dC_p1/dt=mu_1 - g_p*C_p1-gamma_z1-D1*(C_p1-C_p2)

dC_z1/dt=(Q_p1/Q_z)*gamma_z1-g_z*C_z1-D1*(C_z1-C_z2)


dN_p2/dt=U_n2 - g_p*N_p2 -gamma_z2*Q_p2-D1*(N_p2-N_p1)

dC_p2/dt=mu_2 - g_p*C_p2 -gamma_z2-D1*(C_p2-C_p1)

dC_z2/dt=(Q_p2/Q_z)*gamma_z2-g_z*C_z2-D1*(C_z2-C_z1)

dF_n2/dt=g_p*N_p2 + g_z*C_z2*Q_z-U_n2 – D1*(F_n2-F_n)


aux Ratio=C_p1/N_p1

aux Ratio=C_p2/N_p2

aux F_n1+N_p1+(Q_z*C_z1)+F_n2+N_p2+(Q_z*C_z2)=2*lamda


@ BOUND=1e+12

@ NJMP=1

@ TOTAL=1000

@ XP=T,YP=C_p1

@ BELL=off

@ MAXSTOR=1500000

done
```

D3 Program for the three-compartment model

```
# Simple nutrient-phytoplankton-zooplankton model
#       29 December 2002

init C_p1=1 N_p1=0.2 C_z1=1 C_p2=10 N_p2=1 C_z2=4 F_n1=10
init C_p3=10 N_p3=1 C_z3=4 F_n3=10

par lamda=15,g_p=0.4,D1=0.02,mu_max1=0.5,D2=0.02,D3=0.02,mu_max2=1,
par mu_max3=1, U_nmax=1,F_nh=5,Q_pmax=0.25,Q_off=0.01,g_zmax=1,
par Q_pmin=0.05,g_z=0.25,C_hp=100,Q_z=0.25

Q_p1=N_p1/C_p1
Q_p2=N_p2/C_p2
Q_p3=N_p3/C_p3

F_n2=(3*lamda)-N_p2-(Q_z*C_z2)-F_n1-N_p1-(Q_z*C_z1)-F_n3-N_p3-(Q_z*C_z3)

U_n1=U_nmax*C_p1*(F_n1/(F_n1+F_nh))*(1/(1+exp((Q_p1-Q_pmax)/Q_off)))
U_n2=U_nmax*C_p2*(F_n2/(F_n2+F_nh))*(1/(1+exp((Q_p2-Q_pmax)/Q_off)))
U_n3=U_nmax*C_p3*(F_n3/(F_n3+F_nh))*(1/(1+exp((Q_p3-Q_pmax)/Q_off)))

gamma_z1=g_zmax*C_z1*C_p1/(C_p1+C_hp)
```

gamma_z2=g_zmax*C_z2*C_p2/(C_p2+C_hp)

gamma_z3=g_zmax*C_z3*C_p3/(C_p3+C_hp)

mu_1=mu_max1*C_p1*max(0,(1-Q_pmin/Q_p1))

mu_2=mu_max2*C_p2*max(0,(1-Q_pmin/Q_p2))

mu_3=mu_max3*C_p3*max(0,(1-Q_pmin/Q_p3))

dN_p1/dt=U_n1 - g_p*N_p1 -gamma_z1*Q_p1-D1*(N_p1-N_p2)-D3*(N_p1-N_p3)

dC_p1/dt=mu_1 - g_p*C_p1 -gamma_z1-D1*(C_p1-C_p3)-D3*(C_p1-C_p3)

dC_z1/dt=(Q_p1/Q_z)*gamma_z1-g_z*C_z1-D1*(C_z1-C_z3)-D3*(C_z1-C_z3)

dF_n1/dt=g_p*N_p1 + g_z*C_z1*Q_z-U_n1 - D1*(F_n1-F_n3)-D3*(F_n1-F_n3)

dN_p2/dt=U_n2 - g_p*N_p2 -gamma_z2*Q_p2-D1*(N_p2-N_p1)-D2*(N_p2-N_p3)

dC_p2/dt=mu_2 - g_p*C_p2 -gamma_z2-D1*(C_p2-C_p1)-D2*(C_p2-C_p3)

dC_z2/dt=(Q_p2/Q_z)*gamma_z2-g_z*C_z2-D1*(C_z2-C_z1)-D2*(C_z2-C_z3)

dN_p3/dt=U_n3 - g_p*N_p3 -gamma_z3*Q_p3-D3*(N_p3-N_p1)-D2*(N_p3-N_p2)

dC_p3/dt=mu_3 - g_p*C_p3 -gamma_z3-D3*(C_p3-C_p1)-D2*(C_p3-C_p2)

dC_z3/dt=(Q_p3/Q_z)*gamma_z3-g_z*C_z3-D3*(C_z3-C_z1)-D2*(C_z3-C_z2)

dF_n3/dt=g_p*N_p3 + g_z*C_z3*Q_z-U_n3 -D3*(F_n3-F_n1)-D2*(F_n3-F_n2)

aux Ratio=C_p1/N_p1

aux Ratio=C_p2/N_p2

```
aux Ratio=C_p3/N_p3

aux F_n1+N_p1+(Q_z*C_z1)+F_n2+N_p2+(Q_z*C_z2)+F_n3+N_p3+
        (Q_z*C_z3)=3*lamda


@ BOUND=1e+12

@ NJMP=1

@ TOTAL=1000

@ XP=T,YP=C_p1

@ BELL=off

@ MAXSTOR=1500000

done
```

REFERENCES

[1] Andersen, V. and Nidal, P. 1989. Modelling of phytoplankton population dynamics in an enclosed water column. *J. Mar. Biol. Assoc. U. K.* **69**, 625-646

[2] Busenberg. S., Kumar, S.K., Austin, P. and Wake, G. 1990. The dynamics of a model of a plankton-nutrient interaction. *Bull. Math. Biol.* **52**, 677-696

[3] Balakrisnan, E. 1996. Numerical Study of Thermal Ignition in the new variables. PHD Thesis, Massey university.

[4] Caperon, J. W. and Meyer, J. 1972. Nitrogen-limited growth of marine phytoplankton I. Changes in population characteristics with steady state growth rate. *Deep-sea Res.* **19**, 601-618

[5] Caperon, J. W. and Meyer, J. 1972. Nitrogen-limited growth of marine phytoplankton II. Uptake kinetics and their role in nutrient-limited growth of phytoplankton. *Deep-sea Res.* **19**, 619-632

[6] Collins, C.D. 1980. Formulation and validation of a mathematical model of phytoplankton growth. *Ecology* **61**, 639-649

[7] De Angelis, D. L. 1992. *Dynamics of nutrient Cycling and Food Webs*, Chapman & Hall, New York

[8] De Brujin, N, G. 1981. *Asymptotic methods in analysis*, Dover, New York

[9] Droop, M.R. 1974. The nutrient status of algae cells in continuous culture. *J. Marine Biol. Asso. U.K.* **54**, 825-855

[10] Doedel, E.J. 1981. AUTO: A program for the automatic bifurcation analysis of autonomous systems. *Congressus Numerantium* **30**, 265-284

[11] Doedel, E., Wang, X. & Fairgrieve, T. 1994. AUTO: Software for continuation and bifurcation problems in ordinary differential equations. *Applied Mathematics Reports*, California Institute of Technology

[12] Doedel, E., Wang, X., Champneys, A. R., Kuznetsov, Y. A., Sandstede, B. & Fairgrieve, T. 1998. AUTO 97: Continuation and Bifurcation Software for ordinary differential equations. *Applied Mathematics Reports*, California Institute of Technology

[13] Dugdale, R.C. 1967. Nutrient limitation in the sea: Dynamics, identification and significance. *Limnol. Oceanogr.* **12**, 685-695

[14] Edelstein-Keshet, L. 1988. *Mathematical models in Biology*, Random House, New York

[15] Ermentrout, B. 1997. XPPAUT 3.0: the differential equations tool. Xppaut manual.

[16] Evans, G.T. and Parlow, J.S. 1985. A model of annual plankton cycles, *Biol. Oceanogr.* **3**, 327-427

[17] Frost, B.W. 1987. Grazing control of phytoplankton stock in the open sub-arctic Pacific Ocean. A model assessing the role of mesozooplankton, particularly the large calanoid copepods neocalanus. *Mar. Ecol. Ser.* **39**, 49-68

[18] Fuhs, G. W. 1969. Phosphorus content and rate of groth in the diatoms Cyclotella nana and Thalassiorira fluviatilis, *J. Phycol.* **5**, 312-321

[19] Grover, J.P. 1991. Resource competition in a variable environment-phytoplankton growing according to the variable-internal stores model. *Am. Nat.* **138**, 811-835

[20] Grover, J.P. 1992. Constant and variable yield models of population growth-Responses to environmental variability and implications for competition. *J. Theoret. Biol.* **158**, 409-428

[21] Guikenheimer, J. & Holmes, P. 1983. *Nonlinear Oscillations, Dynamical Systems, and Bifurcations of Vector fields.* Springer-Verlag, New York.

[22] Hale, J. & Kocak, H. 1991. *Dynamics and Bifurcations*, Springer-Verlag, New York

[23] Hethcote, H.W. 1976. Qualitative analysis of communicable disease models. *Math. Biosci.* **28**, 335-356

[24] Jang, S. 2000. Dynamics of variable-yield nutrient-phytoplankton-zooplankton models with nutrient recycling and self-shading, *J. Math. Biol.* **40**, 229-250

[25] Kearns, E.A. and Folsome, C. E. 1981. Measurements of biological activity in materially closed microbial ecosystems. *Biosystems* **14**, 205-209

[26] Ketchum, B.H. 1939. The absorption of phosphate and nitrate by illuminated cultures of Nitzschia Clsterium. *Amer. J. Botany* **26**, 399-407

[27] Khan, Q.J.A, Balakrishnan and Wake, G. 2004. Analysis of a predator-Prey System with Predator Switching. *Bulletin of Mathematical Biology*, **66**, 109-123

[28] King, M. 1997. Fisheries Biology: Assessment and Management. Blackwell Science ltd., United Kingdom.

[29] Kuenzler, E.J. and Ketchum, B.H. 1962. Rate of phosphorus uptake by phaeodactylum tricornutum, *Biol. Bull. Marine Biol. Lab., Woods, Hole* **123**, 134-145

[30] Lange, K. and Oyarzun, F. J. 1992. The attractiveness of the Droop equations. *Math. Biosci.* **111**. 261-278

[31] Lehman, J.T., Botkin, D.B., Likens, G.E. 1975. The assumptions and rationales of a computer model of phytoplankton population dynamics. *Limnol. Oceanogr.* **20**, 343-364

[32] Marsden, J.E. & Mc. Cracken, M. 1976. *The Hopf bifurcation and its applications, Applied Mathematical Sciences vol. 19*, Springer-Verlag, New York

[33] May, R.M. 1973. Mass and energy flow in closed ecosystems: a comment. *J. Theoret. Biol.* **39**, 15-163

[34] Monod, J. 1942. *Recherches sur la croissance des cultures bacteriennes*, Herman, Paris

[35] Nisbet, R.M., McKinstry, J. and Gurney, W.S. 1983. A "strategic" model of material cycling in a closed ecosystem. *Math. Biosci.* **11**, 319-335

[36] Odell, G.M. 1980. *Qualitative theory of systems of ordinary differential equations, including phase plane analysis and the use of the Hopf bifurcation theorem. In L. A Siegel, ed., Mathematical Models in Molecular and Cellular Biology.* Cambridge University Press, Cambridge

[37] Perko, L. 1996. *Differential Equations and dynamical systems (2^{nd} edition)*, Springer Verlag.

[38] Rand, R.H., Upadhyaya, S.K., Cooke, J.R. and Storti, D.W. 1981. Hopf bifurcation in a stomatal oscillator, *J. Math. Biol.* **12**, 1-11

[39] Rhee, G.Y. 1973. A continuous culture study of phosphate uptake, growth rate and polyphosphate in Scenedesmus sp. *J. Phycol.* **9**, 495-506

[40] Riley, G.A., H. Stommel and D.P. Burrpus. 1949. Qualitative ecology of the phytoplankton of the Western North Atlantic. *Bull. Bingh. Ocean. Coll.* **12**, 1-169

[41] Ross, A.H. et. al. 1993. A strategic simulation model of a fjord ecosystem, *American Society of limnology and oceanography inc.* **38(1)**, 128-153

[42] Ross, A.H. et. al. 1994. A comparative study of the ecosystem dynamics of four fjords, 39(2), 318-343. *American Society of limnology and oceanography inc.* **39(2)**, 318-343

[43] Smith, H.L. and Waltman, P. 1994. Competition for a single limiting resource in continuous culture: The variable-yield model. *SIAM Appl. Math.* **54**. 1113-1131

[44] Steele, J.H. 1974. *The Structure of Marine Ecosystems*. Oxford: Blackwell Scientific

[45] Steele, J.H. and Frost, B.W. 1977. The structure of plankton communities. *Phil. Trans. R. Soc. Lond.* **B280**, 485-534

[46] Steele, J.H. and Henderson, E.W. 1981. A simple plankton model. *Am. Nat.* **117**, 676-691

[47] Steele, J.H. and Henderson, E.W. 1992. The role of predation in plankton models. *J. Plank. Res.* **14**, 157

[48] Taylor, A. J. 1988. Characteristic properties of model for the vertical distributions of phytoplankton under stratification. *Ecol. Modelling* **40**, 175-199

[49] Tett, et.al. 1986. Physical exchange and the dynamics of phytoplankton in Scottish sea lochs, p. 205-218. In S. Skreslet [ed.] The role of freshwater outflow in coastal marine ecosystems. NATO ASI Ser. G. V. 7. Springer-Verlag, New York

[50] Wroblewski, J.S., Sarmeinto, J.L. and Fliel, G.R. 1988. An ocean basin scale model of plankton dynamics in the North Atlantic. Solutions for the climatological oceanographic condition in May. *Global Biogeochem. Cycles* **2**, 199-218

[51] http://www.acm.caltech.edu/~redrod/auto2000/distribution/

[52] http://www.math.pitt.edu/~bard/xpp/xpp.html